MOLECULAR RECOGNITION IN WATER: DESIGN, SYNTHESIS, AND CHARACTERIZATION OF RIGID MOLECULAR RECEPTORS AND ENZYMATIC MECHANISTIC PROBES

by

Robert William Hoppe

A Dissertation Submitted in

Partial Fulfillment of the

Requirements for the Degree of

Doctor of Philosophy

in Chemistry

at

The University of Wisconsin-Milwaukee

August 2016

ABSTRACT

MOLECULAR RECOGNITION IN WATER: DESIGN, SYNTHESIS, AND CHARACTERIZATION OF RIGID MOLECULAR RECEPTORS AND ENZYMATIC MECHANISTIC PROBES

by

Robert William Hoppe

The University of Wisconsin-Milwaukee, 2016
Under the Supervision of Alan W. Schwabacher

Molecular recognition can be defined as a selective and reversible binding between two or more molecules through non-covalent interactions. Multiple weakly attractive intermolecular forces work in concert to achieve selectivity in association. Such discrimination is critical to the physiological processes of catalysis, transport, antigen recognition, and storage. To better understand this phenomenon, acyclic synthetic molecular receptors also known as "molecular tweezers" were made to study the inclusion of small molecule guests from water. Three anionic tweezers derivatives with *syn*- cofacial orientation were constructed from a 1,2:4,5-*bis*-Tröger's Base skeleton that differed in the amount and distribution of negative charge about the receptors. These binding isomers were found to undergo self association to form dimers in solution by inclusion of the naphthalene wall of one tweezers into the cleft of another. Small molecule binding was evaluated at different ionic strengths and under concentration regimes in which either the desired monomeric tweezers or the dimeric complex predominated.

Small molecules were also created in order to probe the mechanisms by which enzymes facilitate their transformations. Cinnamylidene pyruvate and fluorinated pyruvate derivatives were synthesized to better understand why SbADC, an ezyme classified as an acetoacetate decarboxylase, demonstrates aldolase activity.

Enduracidinine is an unsaturated amino acid found in the potent antibiotics mannopeptimycin, teixobactin, and enduracidin. To investigate the biosynthesis of this amino acid, a new preparation of L-vinylglycine was devised. L-vinylglycine is a potential general precursor to the formation β,γ-unsaturated amino acids. Conditions were identified in which such unsaturated amino acids are formed by olefin metathesis of protected L-vinylglycine and alkenes including allylamine derivatives.

© Copyright by Robert William Hoppe, 2016
All Rights Reserved

TABLE OF CONTENTS

List of Figures x

List of Tables xvii

List of Abbreviations xviii

Acknowledgements xxi

PART ONE: DESIGN, SYNTHESIS, AND CHARACTERIZATION OF RIGID MOLECULAR RECEPTORS

I. INTRODUCTION

A. Molecular Recognition 1

B. Precidented Natural and Synthetic Molecular Hosts. 2
1. Cyclic Molecular Receptors. 2
2. Acyclic (non-macrocyclic) Molecular Receptors 6

C. Tröger's Base and *bis*-Tröger's Base 9

D. Rationale and Design of Target *bis*-Tröger's Base Molecular Receptor 14

II. RESULTS AND DISCUSSION

A. Formation of the key intermediate N,N'-di-t-Boc-2,5-diaminoterephthaldehyde. 16
1. Synthesis of Dimethyl 2,5-diaminocyclohexa-1,4-diene-1,4-dicarboxylate 16
2. Synthesis of Dimethyl 2,5-bis((tert-butoxycarbonyl)amino)terephthalate 17
a. Diaryl amine formation 18
b. Exploration on mechanism of diarylamine formation 21
3. Synthesis of Di-tert-butyl (2,5-bis(hydroxymethyl)-1,4-phenylene)dicarbamate 22
4. Synthesis of N,N'-di-t-Boc-2,5-diaminoterephthaldehyde 23
a. Over oxidation from MnO_2 and alternate Cu(I) catalyzed oxidation 24

B. Synthesis of acyclic *bis*-Tröger's Base Molecular Receptor 27
1. Preparation of *bis*-imines 27
2. Synthesis *bis*-α-aminophosphonates. 30
3. Trögerization Affording Molecular Receptors Isomers. 38
4. Reactions to Generate Water Soluble Molecular Receptors. 45

C. Characterization of Molecular Receptor Isomers. 49

D. Dimerization of Water Soluble Receptor Isomers in Water 52
1. Analysis by ^{1}H NMR Spectroscopy 52
2. Analysis by Fluorescent Spectroscopy. 56

3. Analysis by UV-VIS Spectroscopy 64

E. Binding Studies of Molecular Receptor by Small Molecule Titration 66
1. Carbethoxy tetra anion isomers 23 and 24. 68
2. Methyl phosphonate tetra anion isomers 25 and 26. 71
3. Hexa-anionic isomers 27 and 28 79

F. Quinolone Synthesis for Functionalized Walls for *bis*-Tröger's Base Molecular Receptors . 83
1. Preparation of 7-Amino-4-oxo-1,4-dihydro-quinoline-2-carboxylic acid ethyl ester . . 85
a. From (3-Amino-phenyl)-carbamic acid tert-butyl ester Route. 85
b. From N-(3-aminophenyl)-2,2,2-trifluoroacetamide Route. 87
c. From 3-nitroaniline Route. 88
2. Preparation of 6-Amino-4-oxo-1,4-dihydro-quinoline-2-carboxylic acid ethyl ester . . 92

III. CONCLUSION 92

PART TWO: SMALL MOLECULE SYNTHESIS FOR ENZYMATIC MECHANISTIC PROBES

IV. SMALL MOLECULE PROBES FOR EVALUATING SbADC ALDOLASE ACTIVITY 97

A. SbADC Background Information. 97

B. Rational for SbADC Molecular Probes. 98

V. RESULTS AND DISCUSSION 101

C. Formation of Cinnamylidenepyruvate and 4-NO_2 Cinnamylidenepyruvate Salts. 101

D. Difluoropyruvate Synthesis. 104

VI. SMALL MOLECULE PROBES FOR MppR AND MppP 108

A. Enduracididine and Enduracidin Background Information. 108

B. Roles of MppP and MppR 111

C. Attempts to Make Guanidiniumacetaldehdye for MppR Evaluation 116

D. Towards β,γ-dehydroarginine for MppP Evaluation. 118
1. L-Vinylglycine Synthesis 122
a. L-Selenomethionine selenoxide Route. 124
b. L-Methinonine sulfoxide Route. 126
i. Gas Phase Pyrolysis 126
ii. *in situ* Thermolysis. 128

iii. Addition and Distillation Method. 129
2. Olefin Cross Metathesis of L-Vinylglycine Derivatives 139
a. Background on Olefin Metathesis. 139
b. Synthesis and Screening of Allylamine Derivatives for Cross Metathesis 146
c. Cross Metathesis of L-Vinylglycine Derivatives and Selected Allylamine Derivatives. 153

VII. CONCLUSION 156

VIII. EXPERIMENTAL SECTION 159

Dimethyl 2,5-diaminocyclohexa-1,4-diene-1,4-dicarboxylate (1). 160

Dimethyl 2,5-*bis*((tert-butoxycarbonyl)amino)terephthalate (2) 161

Dimethyl 2,5-diaminoterephthalate (3). 162

Tetramethyl 5,5'-azanediyl*bis*(2-((tert-butoxycarbonyl)amino)terephthalate) (4) 163

Dimethyl 2-amino-5-(p-tolylamino)terephthalate (5) 164

Dimethyl 2,5-*bis*(p-tolylamino)terephthalate (6) 165

Di-*tert*-butyl (2,5-*bis*(hydroxymethyl)-1,4-phenylene)dicarbamate (7) 166

N,N’-di-t-Boc-2,5-diaminoterephthaldehyde (8) 167

Ethyl 6-amino-2-naphthoate (12). 169

Diethyl 6,6'-((1E,1'E)-((2,5-*bis*((*tert*-butoxycarbonyl)amino)-1,4-phenylene)*bis*(methanylylidene))*bis*(azanylylidene))*bis*(2-naphthoate) (13) 170

Diethyl 6,6'-(((1R,1'S)-(2,5-*bis*((*tert*-butoxycarbonyl)amino)-1,4-phenylene)*bis*((dimethoxyphosphoryl)methylene))*bis*(azanediyl))*bis*(2-naphthoate) (16) 172

Diethyl 6,6'-(((1S,1'S)-(2,5-bis((tert-butoxycarbonyl)amino)-1,4-phenylene)bis((dimethoxyphosphoryl)methylene))bis(azanediyl))bis(2-naphthoate) (17). 173

C-Me, P-Me *rac*-tweezers (18) 174

C-Me, P-Me *meso*-isomer (19) 176

rac- carbethoxy tetra acid tweezers (23) 178

meso- carbethoxy tetra acid isomer (24). 179

rac-methylphosphonate tetra anionic tweezers (25). 180

meso-methylphosphonate tetra anionic isomer (26). 181

rac-hexa anionic tweezers (27) 182

meso-hexa anionic isomer (28) 183

tert-butyl (3-aminophenyl)carbamate (29). 184

2-(3-*tert*-Butoxycarbonylamino-phenylamino)-but-2-enedioic acid diethyl ester (30). 185

7-Amino-4-oxo-1,4-dihydro-quinoline-2-carboxylic acid ethyl ester (31) 186

Ethyl 5-amino-4-oxo-1,4-dihydroquinoline-2-carboxylate (32). 187

Diethyl 2-((3-(2,2,2-trifluoroacetamido)phenyl)amino)fumarate (34) 187

Ethyl 4-oxo-7-(2,2,2-trifluoroacetamido)-1,4-dihydroquinoline-2-carboxylate (35). 188

Ethyl 4-oxo-5-(2,2,2-trifluoroacetamido)-1,4-dihydroquinoline-2-carboxylate (36). 189

Diethyl 2-((3-nitrophenyl)amino)fumarate (37) 190

Ethyl 7-nitro-4-oxo-1,4-dihydroquinoline-2-carboxylate (38). 191

Ethyl 5-nitro-4-oxo-1,4-dihydroquinoline-2-carboxylate (39). 192

Diethyl 2-((4-nitrophenyl)amino)fumarate (40) 193

Ethyl 6-nitro-4-oxo-1,4-dihydroquinoline-2-carboxylate (41). 193

Ethyl 6-amino-4-oxo-1,4-dihydroquinoline-2-carboxylate (42). 194

Potassium (3E,5E)-2-oxo-6-phenylhexa-3,5-dienoate (45) 195

Potassium (3E,5E)-6-(4-nitrophenyl)-2-oxohexa-3,5-dienoate (46) 197

Sodium trifluoropyruvate (47) 198

5-methyl-2-(2,2,2-trifluoroacetyl)furan (50). 199

5-methyl-2-(2,2-difluoroacetyl)furan (51). 200

Methyl difluoropyruvate methyl hemiacetal (52). 201

Sodium difluoropyruvate hydrate (53) 202

N,N'-Di-Boc-N"-(2,2-dimethoxy-ethyl)-guanidine (54). 203

N-Allyl-N',N''-Di-Boc-guanidine (55). 203

N-allyl guanidinium trifluoracetate (57) 204

2-Amino-5-hydroxy-4,5-dihydro-3H-imidazolium chloride (58) 205

L-Selenomethionine methyl ester hydrochloride (62). 206

N-Boc-L-Selenomethionine methyl ester (63). 207

N-Boc-L-Selenomethionine oxide methyl ester (64). 208

L-Methionine methyl ester hydrochloride (66). 208

N-Boc-L-Methionine methyl ester (67) 209

N-Boc-L-Methionine sulfoxide methyl ester (68) 210

L-Methionine sulfoxide (70) 211

L-Vinylglycine (71) 212

(S)-2-((R)-2-((((9H-fluoren-9-yl)methoxy)carbonyl)amino)propanamido)but-3-enoic acid (72) 213

(*S*)-2-((((9H-fluoren-9-yl)methoxy)carbonyl)amino)but-3-enoic acid (73) 214

(*S*)-2-((*tert*-butoxycarbonyl)amino)but-3-enoic acid (74) 215

Dicyclohexyl ammonium 2-((*tert*-butoxycarbonyl)amino)but-3-enoate (75). 216

Allylammonium chloride (76). 217

tert-butyl allylcarbamate (78). 217

(9H-fluoren-9-yl)methyl allylcarbamate (79) 218

N-allyl-2,2,2-trifluoroacetamide (80). 219

3-azidoprop-1-ene (81). 219

(*Z*)-di-*tert*.-butyl but-2-ene-1,4-diyldicarbamate (82) 220

(*E*)-di-*tert*.-butyl but-2-ene-1,4-diyldicarbamate (83) 221

(*E*)-*bis*((9H-fluoren-9-yl)methyl) but-2-ene-1,4-diyldicarbamate (84) 221

(*E/Z*)-N,N'-(but-2-ene-1,4-diyl)*bis*(2,2,2-trifluoroacetamide) (85) 222

(*E*)-oct-4-enedioic acid (86) 223

(*S,E*)-2,5-*bis*((tert-butoxycarbonyl)amino)hept-3-enoic acid (87). 223

(*S,E*)-5-((((9H-fluoren-9-yl)methoxy)carbonyl)amino)-2-((*tert*-butoxycarbonyl)amino)pent-3-enoic acid (88) 224

(*S,E*)-2-((*tert*-butoxycarbonyl)amino)hept-3-enoic acid (89). 225

IX. REFERENCES 227

X. APPENDIX 239

A. Characterization Data for Selected Compounds 239

XI. CURRICULUM VITAE 441

LIST OF FIGURES

Figure 1: Equilibrium for association between a molecular receptor (host, H) and an associating molecule (guest,G) in solution to form a complex (C). 2

Figure 2: Example of a cyclodextrins. 3

Figure 3: Cyclic polyether, 18-crown-6, drawn with a potassium ion bound into its cavity. 4

Figure 4: Depiction of an unoriented host adopting a binding conformation before guest inclusion 4

Figure 5: Koga's macrocycle. 5

Figure 6: Whitock's caffeine based molecular tweezers and a molecular tweezers constructed by Zimmerman 7

Figure 7: *bis*-Kagan's ether (left) and Harmata's molecular tweezers based on a *bis*-Kagan's ether architecture 8

Figure 8: Examples of a moleclar tweezers (left) and a molecular clip (right) generated by Klärner 9

Figure 9: Formation of the two Tröger's Base isomers from *p*-toluidine and formaldehyde. . . . 10

Figure 10: A Wilcox molecular tweezers based on Tröger's Base that binds pyrimidin-2-amine 11

Figure 11: Precidented 1,2:4,3-*bis*-Tröger's Base isomer and desired 1,2:4,5- *bis*-Tröger's Base. 12

Figure 12: Retro-synthetic scheme for modular construction of the desired water soluble *bis*-Tröger's Base molecular tweezers 14

Figure 13: 1,2;4,5-*bis*-Tröger's Base molecular tweezer with naphthalene walls illustrating their offset nature 15

Figure 14: Overall synthetic sequence to produce key intermediate dialdehyde 8. 16

Figure 15: Synthesis of *bis*-enamine 1 from dimethyl succinyl succinate 16

Figure 16: Scheme for aromatization and di-Boc protection of *bis*-enamine 1 17

Figure 17: Deprotection of 2 to afford aromatic diamine 3 20

Figure 18: Compound 4, the diaryl amine side product formed from condensation of 2 20

Figure 19: Mono- and *bis*- diarylamine formation from *bis*-enamine 21

Figure 20: Reduction of aromatic diester 2 to desired diol 7. 22

Figure 21: Selective oxidation of diol 7 to desired dialdehyde 8 23

Figure 22: Selecive oxidation to dialdehyde with MnO_2 24

Figure 23: Over oxidation of DA to mono-aldehyde mono-carboxylic acid with MnO_2 24

Figure 24: Selective oxidation to DA with Cu(I) catalyst 26

Figure 25: General scheme for *bis*-imine formation from dialdehyde 8 27

Figure 26: Optimized condition for synthesis of *bis*-imine 13 28

Figure 27: Formation *bis*-α-aminophosphonates 14 and 15 from *bis*-imine 13 30

Figure 28: General "one pot" reaction scheme for *bis*-aminophosphonate formation. 32

Figure 29: Proposed mechanism for dimethyl methylphosphonate formation with $P(OMe)_3$ 32

Figure 30: Proposed mechanism for reaction of $P(OMe)_3$ with THF in the presence of $Yb(OTf)_3$. 33

Figure 31: "One pot" *bis*-aminophosphonate synthesis with $HPO(OMe)_2$ 33

Figure 32: Use of BSA to shift $HPO(OMe)_2$ equilibrium and to prevent methyl transfer. 36

Figure 33: Trogerization to form desired *rac*-(18) and conrol *meso*- (19) molecular receptors isomers 38

Figure 34: "One pot" molecular twezers synthetic scheme using $HPO(OMe)_2$ 39

Figure 35: "One pot" molecular twezers synthetic scheme using diethyl phosphite. 40

Figure 36: "One pot" tweezers synthesis starting from *bis*-imine 41

Figure 37: Scheme for the synthesis of tetraBoc derivative of 13 43

Figure 38: "One pot" synthesis of molecular tweezers using dimethyl phosphite 44

Figure 39: TMSBr deprotection of tweezers isomers to afford carbethoxy tetra acids derivatives 45

Figure 40: Saponification of tweezers isomers to form the methyl phosphonate tetra anion derivatives 47

Figure 41: Hexa-anionic tweezers isomers formed by saponification of the TMSBr dealkylated derivatives 48

Figure 42: Space filling models for the fully esterified binding *rac*- isomer (left) and the non-binding *meso*- isomer (right). 49

Figure 43: ^{1}H NMR dilution of the fully esterified *rac*- tweezers 18 in $CDCl_3$ 50

Figure 44: Equation used for the non-linear least squares fit for the dimerization of the fully esterified *rac*- tweezers utilizing NMR chemcial shifts (top) and fit using chemical shift proton A (bottom). 51

Figure 45: Chemical shifts, coupling constants, and NOESY correlations for the full esterified binding *rac*- isomer 18 in $CDCl_3$ at $3x10^{-3}$M concentration. 51

Figure 46: ^{1}H NMR spectrum of the fully esterified non-binding *meso*- tweezers isomer 19. 52

Figure 47: Comparison of the ^{1}H NMR spectra of *rac*- carbethoxy tetra anionic tweezers 23 in D_2O and 50% TFA/$CDCl_3$ versus the non-binding *meso*- isomer 24 in D_2O 53

Figure 48: Comparison of the ^{1}H NMR spectra of *rac*- methyl phosphonate tetra anionic tweezers 25 in D_2O and 50% TFA/$CDCl_3$ versus the non-binding *meso*- isomer 26 in D_2O. 54

Figure 49: Comparison of the ^{1}H NMR spectra of *rac*- hexa anionic tweezers 27 in D_2O and 50% TFA/CDCl3 versus the non-binding *meso*- isomer 28 in D_2O 55

Figure 50: Derivation of the equation used to determine K_{dim} for the dimerization of the binding *rac*- tweezers by fluorescence spectroscopy. 57

Figure 51: Plot of fluorescent emission (445nm) versus concentration for *rac*- carbethoxy tetra anion 23 tweezers using 300nm excitation. 58

Figure 52: Fluorescence of *rac*- methyl phosphonate tweezer displaying fine structure at 300nm excitation. 59

Figure 53: Fluorescent emssion and plot of fluorescence (430nm) versus concentration for *rac*- methyl phosphonate tetra anion tweezers 25. 60

Figure 54: Plot of concentration vs. fluorescence for *meso*- methyl phosphonate isomer 26 61

Figure 55: Fluorescent emission of control *meso*- methyl phosphonate tetra anion 26 at various excitation wavelengths plotted to include excitation wavelengths. 62

Figure 56: Fluorescent emission and plot of emission (405nm) vs. concentration for *rac*- hexa anionic tweezers using 345nm excitation 63

Figure 57: Plot of fluorescent emission (405nm) versus concentration for the control *meso*- hexa anion isomer using 345nm excitation 64

Figure 58: Plot of wavelength vs. epsilon for the binding 25 (left) and the control 26 (right) methyl phosphonate tetra anion isomers. 65

Figure 59: Plot of concentration vs. epsilon for 25 fit by non-linear least squares. 66

Figure 60: Derivation of equation used to determine K_d in small molecule binding titrations where H=host, G=guest, and C=complex 67

Figure 61: Stern-Volmer equation where I_o= intial fluorescence, I= fluorescene with quencher present, k=quencher rate coefficient, and t=lifetime of the exicted state of the emitting molecule 67

Figure 62: Titration of *rac*- and *meso*- carbethoxy tetraanion isomers with L-Tyr Et ester HCl 69

Figure 63: Titration of *rac*- and *meso*- carbethoxy tetraanion isomers with methyl viologen 70

Figure 64: Fluorescent emission of tetra anion tweezers 25 with varying excitation wavelength plotted to include excitation wavelengths. 72

Figure 65: Titration of binding *rac*- and *meso*- methyl phosphonate isomers with 1-Me nicotinamide chloride in nanopure water 74

Figure 66: 1:1 binding and Stern-Volmer plot for titration of *rac*- methyl phosphonate tweezers 25 with 1-Me nicotinamide chloride in nanopure water 75

Figure 67: 1:1 binding and Stern-Volmer plot for titration of control *meso*- methyl phosphonate tetra anion isomer with 1-Me nicotinamide chloride in nanopure water. 76

Figure 68: ^{1}H NMR comparison of the aromatic region of free *meso*- methyl phopshonate tetra anion 26, free 1-Me nicotinamide chloride, and a 1:1 mixture of the two at $1.8x10^{-2}$M concentration. 77

Figure 69: Comparison of K_d for binding 25 and control 26 isomer to 1-Me nicotinamide chloride in nanopure water and 150mM NaCl, 10mM pH7 phosphate buffer 78

Figure 70: Comparison of fluorescent emissions of the binding *rac*- hexa anionic tweezers (top) and the non-binding *meso*- control isomer (bottom). Stern-Volmer plot also included for binding isomer 27. 81

Figure 71: Titration of hexa anionic tweezers 27 with disodium 2-naphthylphosphate 82

Figure 72: 7-Amino-4-oxo-1,4-dihydro-quinoline-2-carboxylic acid ethyl ester and its resulting *bis*-Tröger's Base tweezer 83

Figure 73: 6-Amino-4-oxo-1,4-dihydro-quinoline-2-carboxylic acid ethyl ester and the possible combinations of bis-Tröger's Base tweezers 84

Figure 74: General scheme for aminoquinolone synthesis. 84

Figure 75: Synthetic route to produce 7-amino-2-carboxy from 1,3-diaminobenzene 85

Figure 76: Synthetic route for quinolone production from mono-trifluoroacetyl protected 1,3-diaminobenzene. 87

Figure 77: Proposed hydrogen bonded intermediate responsible for regioselective cyclization. 88

Figure 78: Quinolone synthetic scheme starting from 3-nitroaniline 88

Figure 79: Synthetic scheme for production of 6-amino-2-carboxy-4-oxoquionlone ethyl ester. 92

Figure 80: 1,2:4,5-*bis*-Troger's Base tweezer scheme displaying desired quinolones for future inclusion 96

Figure 81: Proposed use of trifluoropyruvate and difluoropyrubate for mechanistic determination of SbADC aldol pathway. 99

Figure 82: An example synthetic scheme in formation of difluoropyruvate analogues. 100

Figure 83: Formation of cinnamylidene pyruvate sodium salt. 101

Figure 84: Formation of 4-nitrocinnamylidene pyruvate sodium salt. 102

Figure 85: General scheme for isolating sodium pyruvate free cinnamylidene pyruvate analogues 102

Figure 86: ^{1}H NMR spectra of 4-nitrocinnamylidene pyruvate over the course of sodium pyruvate removal. 103

Figure 87: Scheme for sodium trifluoropyruvate hydrate 104

Figure 88: Proposed synthetic route for simplifed difluoropyruvate formation. 104

Figure 89: Desired E2 elimination of O,O-(bis-trimethylsilyl) ethyl trifluoropyruvate 105

Figure 90: Proposed E2 elimination of O,O-(*bis*-trimethylsilyl) ethyl trifluoropyruvate that occurred 106

Figure 91: Literature based synthesis for ozonolysis precursor. 106

Figure 92: Ozonolysis scheme for synthesis of methyl difluoropyruvate methyl hemiacetal 106

Figure 93: Enduracididine (left) and allo-enduracididine (right) 110

Figure 94: Enduracidin A (R=H) and Enduracidin B (R=CH_3). Image provided by Dr. Nicholas Silvaggi. 111

Figure 95: Proposed biosynthesis for enduracididine. 112

Figure 96: Aldol condensation and dehydration product of imidazole carboxaldehyde and sodium pyruvate formed by MppR. 113

Figure 97: Literature route to γ-OH arginine 114

Figure 98: γ-OH arginine synthesis from epichlorohydrin 115

Figure 99: Retro-synthetic analysis for dehydro-L-Arginine by Aldol reactions route 116

Figure 100: Guanidinylation of aminoacetaldehyde dimethyl acetal 54. 116

Figure 101: Formation of 2-aminoimidazole from guanidinylated aminoacetaldehyde dimethyl acetal upon acidic hydrolysis. 117

Figure 102: Desired oxidative cleavage of guanidinylated allylamine. 118

Figure 103: Model reactions to test conditions for oxidative cleavage of an alkene with K_2OsO_4 119

Figure 104: Proposed stabilized complex that prevents dihydroxylation by osmium tetroxide 119

Figure 105: Cyclized hemiaminal generated upon treatment of allylguanidinium trifluoroacetate with osmium tetroxide. 120

Figure 106: Synthethis diBoc protected cyclic hemiaminal from diBoc protected allylguanidine 121

Figure 107: Reaction of di-Boc cyclic hemiaminal 59 with sodium pyruvate 122

Figure 108: α ,β -unsaturated ketone formation by arylselenoxide elimination and desired elimation of a methyl selenoxide to form vinylglycine 124

Figure 109: Synthetic scheme of N-Boc-L-vinylglycine methyl ester synthesis from L-selenomethionine. 125

Figure 110: Synthesis of L-vinylglycine methyl ester form L-methionine 126

Figure 111: Illustration of apparatus constructed for gas phase pyrolysis 127

Figure 112: NMR spectra of isolated materials from *in situ* thermolysis of silylated L-methionine 128

Figure 113: Synthetic scheme for L-vinylglycine formaton by in situ silylation followed by thermolysis with distillation 132

Figure 114: L-Vgy derivatization and HPLC trace demonstrating retention of desired stereocenter 135

Figure 115: Reaction conditions in which L-vinylglcyine methyl ester will or will not isomerize 136

Figure 116: Fmoc- and Boc- protection of L-vinylgycine. 138

Figure 117: Examples of intramolecular olefin metathesis with amino acid derivatives. 139

Figure 118: Successful metathesis after saponification of a lactone. 140

Figure 119: Homodimer formation due to isomerization of vinyl sidechain. 140

Figure 120: From left to right Schrock's, Grubb's 1st gen, and Grubb's 2nd gen metathesis catalysts. 141

Figure 121: Afforded yields of cross metathesis product as steric hindrance around olefin increases 141

Figure 122: Effects of increasing steric hindrance on rate of metathesis 142

Figure 123: Hoveyda-Grubbs's 2nd generation metathesis catalyst 144

Figure 124: Ring closing yields using water soluble Hoveyda-Grubbs 2nd gen catalysts. 146

Figure 125: General scheme for homodimer formation via olefin metathesis. 148

Figure 126: Homodimer formation via olefin metathesis of Boc protected allyl amine 152

Figure 127: Example olefin cross metathesis using Hoveyda-Grubbs 2nd generation catalyst. 153

Figure 128: Future direction for dehydroarginine synthesis 158

LIST OF TABLES

Table 1: *bis*-aminophosphonate disastereomers afforded from deactivated silica gel chromatography. 35

Table 2: Observed dissociation constants from the titration of the proposed *rac*- carbethoxy tetra anionic tweezers 23 dimer 68

Table 3: Apparent K_d values for small molecules titrated with binding *rac*- methyl phosphonate tetra anion tweezers 73

Table 4: Apparent K_d values substrate association to binding *rac*- hexa anionic tweezers at $5.0x10^{-6}$ M concentrations. 80

Table 5: Quinolone mol ratios with varying substituents and reaction conditions 90

Table 6: Parameters and results in thermolysis of N-Boc-L-selenomethionine oxide methyl ester 125

Table 7: Experimental parameters in screening *in situ* thermolysis for L-vinylglycine formation. 129

Table 8: Results fom tested conditions *in situ* thermolysis parameters in L-vinylglycine synthesis 129

Table 9: Experimental parameters from *in situ* thermolysis with distillation. 130

Table 10: Experimental results from in situ thermolysis with distillation. 131

Table 11: Pseudo- first order kinetic data for the isomerization of L-vinylglycine derivatives. All reactions conducted at 22°C and in $CDCl_3$. 137

Table 12: Synthesis of allyl amine derivatives for homodimerization screening 146

Table 13: Alkene reactivities for homodimer formation. 150

Table 14: Summary of results for combinations of metathesis substrates. 156

LIST OF ABBREVIATIONS

1.	AcOH	Acetic acid
2.	Ar	Aryl
3.	b	Broad (NMR)
4.	Boc	*t*-Butyloxycarbonyl
5.	BSA	*bis*-(trimethylsilyl)acetamide
6.	CM	Cross metathesis
7.	Cy	Cyclohexyl
8.	d	Day
9.	d	Doublet (NMR)
10.	dd	Doublet of doublets (NMR)
11.	DEHP	*bis*-(2-ethylhexyl)phthalate
12.	DIPEA	N,N-Diisopropyl ethyl amine
13.	DMAP	4-Dimethylaminopridine
14.	DME	1,2-dimethoxyethane
15.	DMSO	Dimethylsulfoxide
16.	DUIS	Duel ionization source (MS)
17.	EDTA	Ethylenediaminetetraacetic acid
18.	EI	Electron impact (MS)
19.	eq.	Equivalents
20.	ESI	Electron Spray Ionization
21.	EtOAc	Ethyl acetate

22. EtOH	Ethyl alcohol
23. eV	Electron volt (MS)
24. Fmoc	9-Fluorenylmethoxycarbonyl
25. H.G. II	Hoveyda-Grubbs 2nd generation metathesis catalyst
26. HMDS	Hexamethyldisiloxane
27. h	Hour
28. Hz	Hertz (NMR)
29. IpOH	Isopropyl alcohol
30. IR	Infra-red
31. J	Coupling constant (NMR)
32. m	Multiplet (NMR)
33. MeOH	Methyl alcohol
34. Mes	Mesityl
35. min	Minute
36. mp	Melting point
37. MS	Mass spectrometry
38. “n-methylnicotinamide”	1-Methylnicotinamide chloride
39. Nap	Naphthyl
40. NMR	Nuclear magnestic resonance
41. NOESY	Nuclear Overhauser effect spectroscopy
42. NP Water	Nanopure (18MΩ water)
43. OM	Olefin metathesis

44. Pd-C	Palladium on carbon
45. Ph	Phenyl
46. PhMe	Toluene
47. ppm	Parts per million (NMR)
48. q	Quartet (NMR)
49. R_f	Retention factor
50. RT	room temperature
51. s	Second
52. s	Singlet (NMR)
53. t	time
54. t	Triplet (NMR)
55. TFA	Trifluoroacetic acid
56. THF	Tetrahydrofuran
57. TLC	Thin layer chromatography
58. TMSBr	Bromotrimethylsilane
59. TMSCl	Chlorotrimethylsilane
60. TOF	Time of flight
61. UV	Ultra-violet
62. Vgy	Vinylglycine

ACKNOWLEDGEMENTS

I would like to thank first and foremost the University of Wisconsin-Milwaukee for providing an institution with faculty and facilities that provided me the opportunity to develop my intellect and skills. I will forever be grateful for its existence and the service it provides to members of the local community like myself for the ability to pursue an education so that we may better ourselves and others. I would like to acknowledge the guidance and patience of my advisor, Dr.Alan W. Schwabacher, in providing me the tutelage and in my training as a scientist that challenged my intellect and allowed my knowledge in chemistry to flourish. Thanks to Dr. Nicholas Silvaggi for providing another source of opportunity in collaboration to hone my skills by being able to interact frequently another groups of researchers. I would like to acknowledge Samuel Melton as my closest research collaborator. The dedication, skills, and feedback he has provided in the evaluation of dimerization and binding of the molecular receptors as well as the synthesis of L-vinylglycine were invaluable and will forever be in his debt. I wish him the best of luck in his future education. I would also like the thank John Lukesh III, Chris Meyer, and Curtis Jones who were undergraduate collaborators with me when they attended this university. Having gone onto their own scientific careers I am grateful for the sense of accomplishment they give me in the ability to develop their skills at the earliest stages of their training. To my friends Nina Yuan, Lisa Mueller, Karl Koebke, it feels unfortunate that I was not able to know you all earlier but will be forever grateful that I did. You all have provided me with the fellowship and support I needed. To John Kestell, Sarah Oehm, Tyler Fenske, Paul Henning, and all of the other fine people in the Chemistry and Biochemistry department I have learned from and met over the years, interacting with all of you has been a pleasure and will never forget the

ways in which you have helped me large and small. I would like to thank my brothers, Christopher and Phillip Hoppe, as they have made things possible for me that were not. Lastly, I would like to thank my mother Sue Hoppe and father Ken Hoppe for their continued support and dedication to me as their son in my pursuit of this goal. Without them, this along with everything else could not have been possible. I will always be thankful for the sacrifices you have made for me. I only hope to one day to be able to give you the support you have given me.

PART ONE: DESIGN, SYNTHESIS, AND CHARACTERIZATION OF RIGID MOLECULAR RECEPTORS

I. INTRODUCTION

A. Molecular Recognition

Molecular recognition can be defined as a selective and reversible binding between two or more molecules through non-covalent interactions. Multiple weakly attractive intermolecular forces work in concert to achieve selectivity and thus makes it substantially more difficult to predict than the formation of covalent chemical bonds. Intercalaction of a smaller molecule into the cavity of a larger molecule often describes the mode of action in which two molecules bind together. While net forces like van der Waals attractions or the hydrophobic effect[1], which is a property of the solvent, are primer movers in this phenomenon other electrostatic interactions like dipole-dipole, aromatic stacking[2], the cation-π effect[3], ion pairing[4],and hydrogen bonding[5] in arrays[6], and ditopic coordination[7] provide the means for exceptionally strong affinities and substrate discrimination in binding.

Molecular recognition also known as Host-Guest chemistry[8] is critical to the physiological processes of catalysis, transport, antigen recognition, and storage. In studying what can lead to selective and strong binding these powerful capabilities demonstrated by nature could be replicated. For theses reasons the concepts of molecular recognition have been applied to molecular acuators[9], drug discovery[10], and the self assembly of molecular capsules.[11]

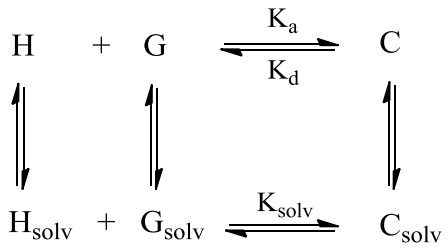


Figure 1: Equilibrium for association between a molecular receptor (host, H) and an associating molecule (guest,G) in solution to form a complex (C)

The strength of the binding interactions is described in terms of an equilibrium constants as either the forward direction of the association of components in complex formation (K_a in units L/mol) or the backwards direction of the dissociation of the complex to the individual compounds (K_d in units mol/L). However as these associations occur in a solvent there exists another equilibrium for the solvation of the host and guest molecules individually to come together to form a solvated complex. The strength of the association to form this solvated complex depends upon solvation energies, temperature, and ionic strength among many other factors lending to a small change in the energies between the two states. For these reasons, prediciting what molecules will bind together strongly and selectively is difficult and thus requires the use of experimentation to elucidate fundamental principles to understand this interaction.

B. Precidented Natural and Synthetic Molecular Hosts

1. Cyclic Molecular Receptors

Cyclodextrin, a macrocyclic polysaccharide comprised of glucose units, was the first molecule reported to bind another molecule by way of inclusion of elemental iodine into its

cavity.[12] In the decades following many prominent researchers took up investigating this bucker shaped structure and its propensity to intercalate small molcules

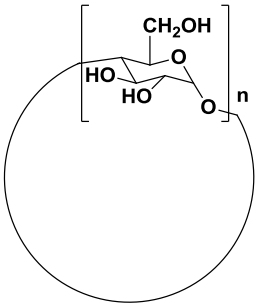


Figure 2: Example of a cyclodextrin: n=6 α-cyclodextrin, n=7 β-cyclodextrin, n=8 γ-cyclodextrin

Cramer and Hettler[13] were among the first to profile complex formation with cyclodextins while researchers like Saenger[14] and Breslow[15] studied the inclusion complexes of derivatized cyclodextrins. Cyclodextrins have also been exploited for pharmaceutical purposes to deliver drugs[16] or release over time to create a continuous dosage.

While naturally occurring substances like cyclodextrins and enzymes hold enormous potential for understand what entails the formation of a complex the creation of synthetic molecular receptors could hold even greater potential. Synthetic receptors would allow for the modification of the binding cavity identify of the specific non-covalent interactions responsible for binding. The first artificial host molecule were macrocyclic polyethers synthesized by Pedersen in 1967.[17] This class of compounds dubbed crown ethers were called so for their ability to “crown” metal cations and thioureas[18] by inclusion into their cavity by ion-dipole interactions.

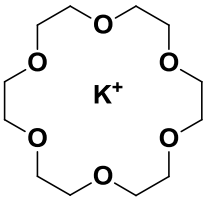


Figure 3: Cyclic polyether, 18-crown-6, drawn with a potassium ion bound into its cavity

These crown ethers, especially 18-crown-6[19], bind cationic substrates with high affinities as all of the oxygens are orientated towards the interior of the macrocycle wereas the alkyl linkers are positioned on the exterior. This demonstrates the concept of "preorganization". Preorganization[8] is the concept that the host and guest molecules bind with the strongest affinites if the functional groups responsible for complexation are orientated in a cooperative fashion prior to the components coming into proximity. An example of this would be in the theortetrical comparison of 18-crown-6 to its acyclic analogue with the assumption that the acyclic version has the capability to bind potassium ion.

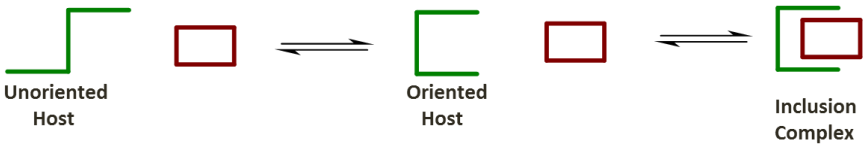


Figure 4: Depiction of an unoriented host adopting a binding conformation before guest inclusion

The acyclic version would not bind the the alkali ion as strongly as 18-crown-6 as it contains many more rotational degrees of freedom and thus contains many conformations unsuitable for complex formation. This would result in s lower ΔG term in the Gibbs Free Energy equation compared to the crown ether as the acyclic version ΔS term would be more positive upon complex formation. This loss of entropy results from the acyclic version having to orient

itself to allow for all six oxyen atoms to coordinate to the cation like the crown ether and overall weaker affinity.

From these concepts, Koga reported the first unambiguous example of a water soluble, macrocyclic synthetic molecular receptor.[20] Comprised of two diamino diphenylmethanes with two n-butyl alkyl chains linking connecting the amino groups the macrocyle was found to dissolve in aqueous media below pH2.

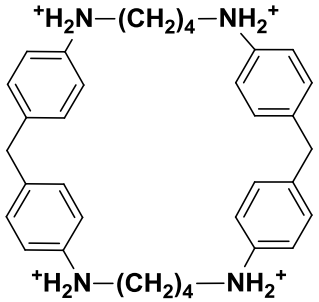


Figure 5: Koga's macrocycle

This host molecule was able to fuly include hydrocarbons like durene, naphthalene, and *p*-xylene. A dissociation constant for 8-anilino-1-naphthalene sulfonic acid (K_d= 1.6x10^{-4} M) was determined by fluorescent emission and the orientation of 2,7-dihydroxynaphthalene bound into the cavity was determined using ^{1}H NMR. In using these spectroscopic techniques, Koga was able to demonstrate the utility of these techniques and were widely adopted afterwards. This work went on to inspire others in the study of small molecule binding with significant contributions made by Diedertich and Dougherty. Diederich focused on making macrocyclic receptors that were soluble in water at pH7[21] that were capable of binding hydrophobic moieties like pyrene and facilitating their transport through aqueous media.[22] He was also able to correlate the binding affinities in electron donor-acceptor interactions with electron poor naphthalene derivatives bidning stronger to the electron rich macrocycle.[23] Dougherty too

focused on synthetic macrocycles soluble in neutral water. He reported[24] that his receptor was able to form inclusion complexes wth quaternary ammonium ions. He later went on to show that binding can not only be driven by the hydropobic effect but by the attraction of the cation to the π electrons in the aromatic walls of the macrocycle.[25] This interaction, coined the cation-π effect, was found to be so favorable that it orientated the quaternary ammonium to the interior of the cavity while the hydrophobic part of the ammonium salt was left exposed to the aqueous environment.[26]

2. Acyclic (non-macrocyclic) Molecular Receptors

Acyclic, synthetic molecular receptors were dubbed "molecular twezers" by Whitlock in the first known publication of this architecture in 1978.[27] Molecular tweezers are usually characterized by two aromatic walls that are approximately parallel to one another in a syn-cofacial configuration and held apart by a rigid linker. This initial design was intended to act as a *bis*-intercalater for DNA that was restricted to a single strand of DNA. Whitlock constructed his tweezers by alkylating caffeine molecules with a rigid diyne linker and prove that it was able to associate to 2,6-dihydroxybenzoate by binding between the aromatic walls to form a sandwich complex by π-π stacking. From this elegant design the next iteration of molecular recognition studies was birthed. Early designs utilized diphenyl glycourils[28] or a derivatized Kemp's triacid[29] the work provided by Zimmerman provided foundational examples in constructing molecular tweezers. His motif displays a high degree of preorganization with an aromatic linker and a syn-cofacial arrangement of acridine walls connected in the 9- position.[30]

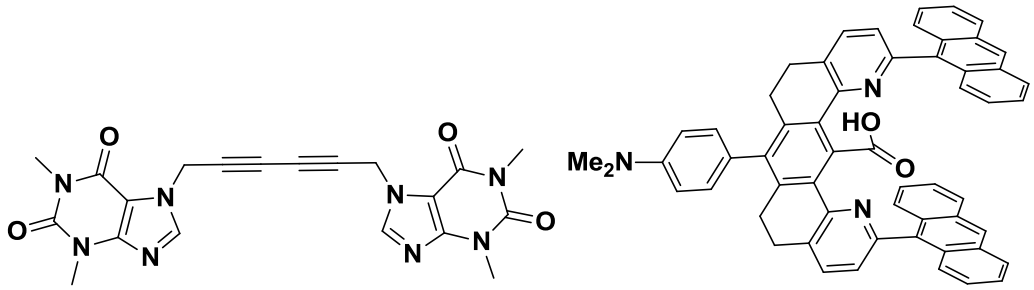


Figure 6: Whitock's caffeine based molecular tweezers and a molecular tweezers constructed by Zimmerman

With the anthracenes twisted out of conjugation due to steric hinderance they can rotate until to walls achieve a conformation until the walls are parallel and approximately 7Å apart so that they can bind a flat, aromatic guest. The import of the rigid spacer was demonstrated in a later publication where Zimmer substituted the rigid linker for a butyl linker to connect the anathcene sized walls and found that the binding affinity towards 2,4,7-trinitrofluorene decreased by a factor at least 40. He also demonstrated that binding affinities can be greatly enhanced through the use of cooperative non-covalent interactions.[31] When a carboxylic acid group was incorporated into the spacer the combination of π-π interactions and hydrogen bonding the tweezer was able to bind 9-propyladenine with high affinity (K_d = 4.0x10^{-5} M) in $CDCl_3$. When the carboxylic acid was converted to a methyl ester the binding affinity diminished precipitously with no detectable binding was observed by ^{1}H NMR when 9-propyladenine was added to the tweezers in up top four fold stoichiometric excess.

The next contribution in the development of molecular tweezers come from Harmata. His methodology progessed from the synthesis of asymmetric Kagan's ethers[32] to symmetrical *bis*-Kagan's ethers.[33] Kagan's ether[34] is a diaryl, [6.6.1] bicyclic ether with the oxygen atom bridging the two rings while a *bis*-Kagan's ether is two of these structures connected by a common benzene ring. This structure is more preorganized than Zimmerman's tweezers as the

aromatic walls are enforced into being parallel and are precluded from rotating by being incorporated into the cyclic ether.

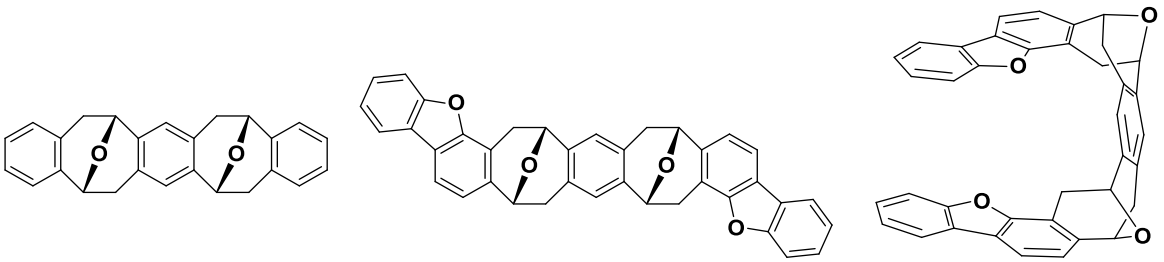


Figure 7: *bis*-Kagan's ether (left) and Harmata's molecular tweezers based on a *bis*-Kagan's ether architecture

However, this structure was not able to bind electron poor, aromatic molcules due to the small aromatic surface area in the cavity. When the benzene walls were replaced with dibenzofuraqns an X-ray crystal structure was obtained with 1,3,5-trinitrobenzene bound into the 7Å cavity forming the classic sandwich complex to corroborating the function f the desired shape.[35] The use of bicyclic polyethers[36] and dibenzofuran sized derivatives as walls[37] have seen continued use since Harmata's publication to bind quaternary ammonium ions and aromatic guests respectively.

The molecular tweezers developed by Klärner[38] utilized a scheme which employed Diels-Alder reactions to attach a dimethylhydroquinone norbornen derivative to an aromatic norborndiene. If one Diels-Alder reaction occurs then a U-shaped molecular tweezers is afforded, if done twice then a C-shaped molecular clip is produced. In each of these cases is was found that these structures were able to intercalate eletron poor, armomatic small molecules into their cavities.[39]

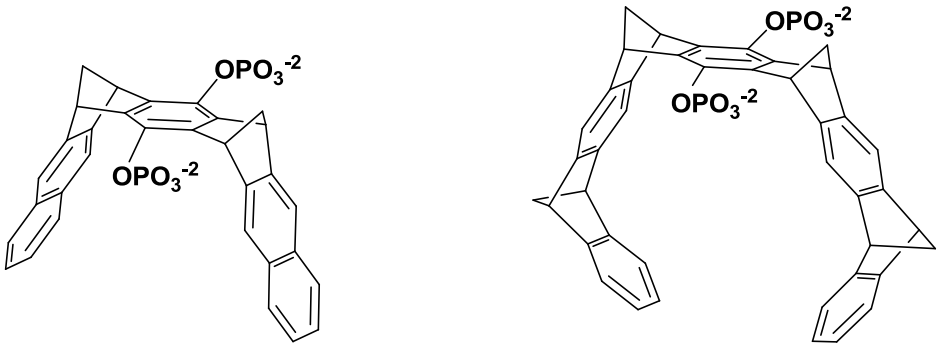


Figure 8: Examples of a moleclar tweezers (left) and a molecular clip (right) generated by Klärner

While initially confined to organic solvents, these structures were given water solubility by converting the dimethylhydroquinone ethers to *bis*-phosphates and *bis*-methyl phosphonates which allowed for the binding of thiazolium salts in aqueous media.[40] These receptors were studied further and found to inhibit enzyme activity in a novel fashion: alcohol dehydrogenase by binding its cofactor NAD^+ [41] and G6PD by binding to $NADP^+$.[42] In binding to flavium salts[43] Klärner observed a spectroscopic response in the UV-Vis region which demonstrates the potential for molecular tweezes to be useful a molecular sensors. To date, this class of water soluble molecular tweezers has shown the most robust utility small molecule complex formation.[44]

C. Tröger's Base and *bis*-Tröger's Base

While the previously detailed works into molecular tweezers were being published, a parallel strategy was being developed using an easier to synthesize moiety that also generated a well defined cleft for molecular binding. Tröger's Base, composed of two aromatic amines and three formaldehyde equivelants, was chosen was chosen by Wilcox to suite these criteria. First synthesized by Julius Tröger in 1887[45] Tröger's Base is a chiral compound formed from *p*-toluidine and formalin in the presence of concentrated hydrochloric acid. The chirality in this

structure comes not from chiral carbons but from the sterogenic nitrogens in the bicyclic ring system which cannot undergo inversion. If inversion where to occur the bridging methylene unit would have to pass through to the other face of the ring system, ring would place the atoms in the same plane in the process, but the energetic barrier provided by steric hinderence and bond angle strain prevent this.

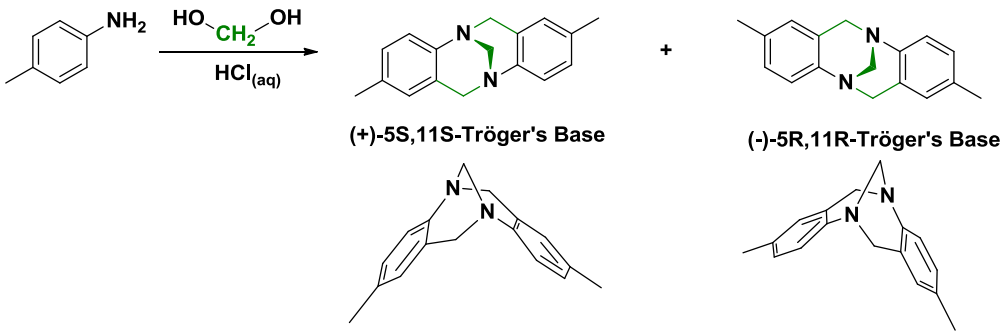


Figure 9: Formation of the two Tröger's Base isomers from *p*-toluidine and formaldehyde

Since its discovery, Tröger's Base was subject of intensive investigation into its structure, mechanism of formation, and origin of its chiral nature. Wganer probed the mechanism of formation by generating Tröger's Base from intermediates isolated along the synthetic pathway[46] wereas, Spielman was able to confirm the structure of Tröger's Base through its degradation products.[47] Prelog and Wieland were the first to report the separation of the isomers[48] the assignment of the absolute configuration of these chiral partners was not conducted until 1967 where circular dichroism was used to analyze the (+)- and (-)- isomers.[49] From these experiments it was concluded that the (+)- isomer was of the 1R, 3R configuration while the (-)- isomer was 1S, 3S. Later studies however contradicted these assignments with the acquisition of an X-ray crystal structure[50] and isomeric resolution utilizing a chiral Brønsted acid.[51] It wasn't until 2000 that the initial assignment were unambiguously refuted and the true

configuration of the chiral Tröger's Base isomers were determined as the (+)- being 1S, 3S and the (-)- isomer being 1R, 3R.[52]

Among the first to take advantage of the shape of Tröger's Base to generate molecular tweezers was Wilcox.[53] In taking advantage of the fact the the aromatic faces in Tröger's Base are in the range of 92 to 104° apart, 9,10-dihydro-9,10-ethenoanthracen-2-amine was condensed with formaldehyde to generate a molecular receptor which was found to have two ethanol molecules in its cavity via X-Ray crystallographic analysis.[54]

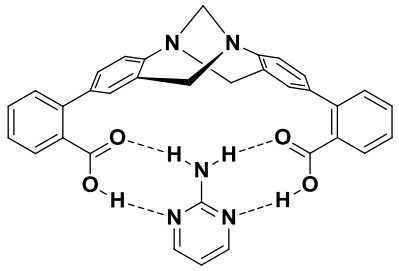


Figure 10: A Wilcox molecular tweezers based on Tröger's Base that binds pyrimidin-2-amine

He later developed a molecular tweezers utilizing a *bis*-carboxylic acid motif to bind to 2-aminopyrimidine through hydrogen bonding[55] which later elucidated the influence of water included in the active site on binding affinities.[56] His work demonstrated that the rigid, well defined structure of Tröger's Base was of utility in constructing rigid molecular frameworks that could be incorporated in architectures ranging from metallo-macrocycles[57] to colorometric sensors for anion recognition.[58]

Analogous to Harmata's *bis*-Kagan's ether tweezers and the recognition of the perpendicular nature of the aromatic elements in Tröger's Base, 2001 saw the introduction of a *bis*-Tröger's Base into the catalogue of molecular tweezers.[59] Starting with a Tröger's Base

derived from *p*-toluidine and 4-nitroaniline Pardo *et. al.* was able to synthesize a diastereomeric mixture of *bis*-Tröger's Bases via Friedel-Crafts alkylation. This process was only able to proceed under the fairly harsh conditions of anhydrous ethanol and concentrated hydrochloric acid at 90°C for 24h and resulted in regio-selective cyclization with a 29% overall yield affording the 1,2; 4,5 isomer in a 4:1 ratio of the *syn*-cofcial isomer to the *anti*- isomer.

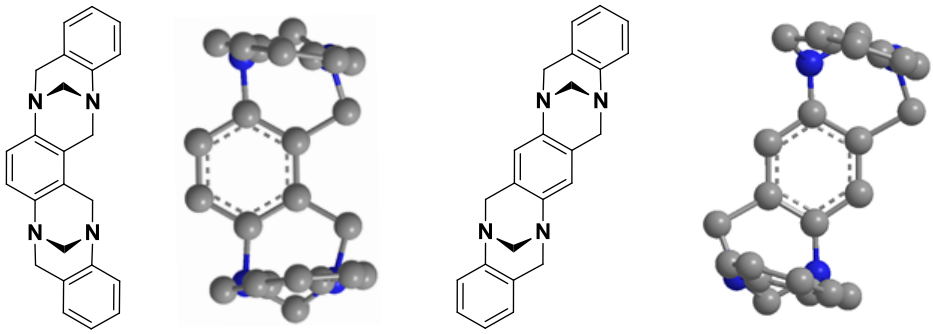


Figure 11: Precidented 1,2:4,3-*bis*-Tröger's Base isomer and desired 1,2:4,5- *bis*-Tröger's Base

This nomenclature is derived from the substitution pattern around the around the cental benzene spacer. The 1 and 4 numbers denote the position of the amino groups in the benzene while the 2 and 3 number describe the positions in that benzene ring where Friedel-Cratfs alkylation occurred. The observed ratios invites intruging questions. What was the reason for the favorablility of the *syn*- isomer, the one with the aromatic walls on the same side of the spacer unit, over the *anti*- isomer, the one with the walls on the opposite sides of the linker? What was the origin of the regio-selecitivity in cyclization to form the *bis*-Tröger's Base? To address the first question, the Pardo group subjected the *anti*- isomer to the previously described cyclization conditions and recovered the same 4:1 ratio of *syn*- : *anti*- isomers. They attributed this ratio to the *syn*- isomer being more thermodymacially favorable due to the π-stacking interactions of the parallel aromatic walls. While this may be true, I propose it to be a

more complicated mechanism. Under the acidic conditions and isomerization concentrations, this *bis*-Tröger's Base is able is able to isomerize freely between the two isomers with the *syn*-isomer able to associate with iself, albeit weakly, to form a dimer by π-π stacking interactions. This would remove the self associating *syn*- isomer from the equilibrium and by the Le Châtelier's Principle would drive its continued formation.

With regards to the regioselectivity of Friedel-Crafts alkylation, the Pardo group expected a statistical formation of the 1,2:4,5 isomer alongside the 1,2:4,3 isomer but as satated before observed the latter exclusively. They postulated that even though the 1,2:4,3 isomer is more sterically hindered it was formed preferentially due to the π-stacking of the aromatic walls. This however seems unlikely as the cavity, like the *bis*-Kagan's ether, is approximately 7Å apart in either configuration.

In a later synthesis of *bis*-Tröger's Base starting from *p*-phenlenediamine, the 1,2:4,3 isomer was also afforded exclusively.[60] To overcome this regioselectivity, the cyclization to the 1,2:4,5 isomer was enforced by using 1,4-diamino-2,5-dimethylbenzene as the spacer unit.[61] The isolated yield of the cavity shaped *syn*- isomer was 7% en route to generating linear oligio-Tröger's Bases. Dolenskŷ would later go on to incorporate naphthalene sized walls into a *bis*-Tröger's Base tweezers synthesis of the 1,2:4,3 isomer[62] in order to provide enough aromatic surface area to potentially bind small molecules. The synthetic procedure was improved to utilize a one-pot procedure but only afforded *bis*-Tröger's Bases in low yield (8-13%). To date, there are no know examples of a 1,2:4,5 *bis*-Tröger's Base tweezers without substitution on the core benzene linker to compel the Friedel-Crafts alkylation into this pattern.

D. Rationale and Design of Target *bis*-Tröger's Base Molecular Receptor

Inspired by the design of Harmata's tweezers, the desired 1,2;4,5 *bis*-Tröger's base molecular receptor has the same connectivity to afford parallel naphthalene sized walls held approximately 7Å apart by a rigid spacer. In reviewing the previous syntheses of *bis*-Tröger's Bases a common feature held in common was the occuranace of the Friedel-Crafts on the central benzene spacer generating the 1,2:4,3- isomer preferentially. The designed spacer unit for desired *bis*-Tröger, the tweezers core, depicted below will circumvent. By already possessing the bonding required for the 1,2:4,5 isomer on the spacer units Trögerization should occur unambiguously to said isomer. This tweezers core not only allows for modular synthesis by condensation with a wide range of aromatic amines but could also facilitate others in their studies of *bis*-Tröger's Base molecular receptors as convenient starting compounds are not readily available.[63]

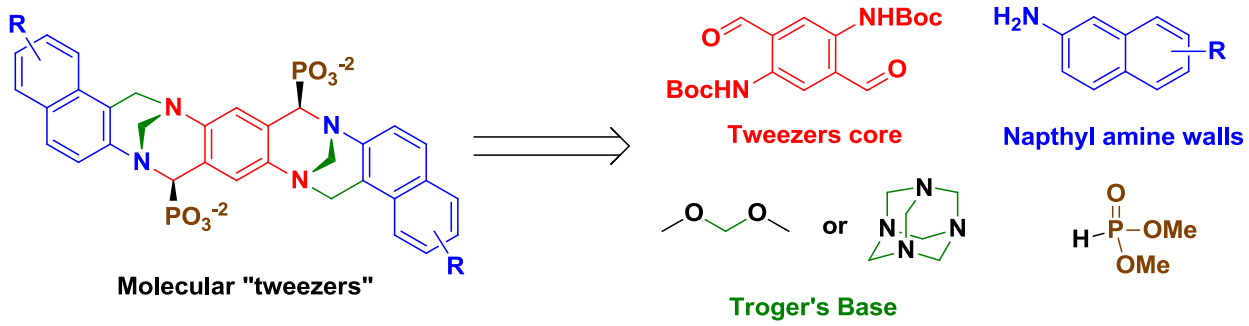


Figure 12: Retro-synthetic scheme for modular construction of the desired water soluble *bis*-Tröger's Base molecular tweezers

Water solubility is installed into the molecular tweezers by the transformation of the imine into an α-amino phosphonate which will then be dealkylated subsequently. Although this functionality provides significant water solubilization it also introduces a not insignificant amount of steric bulk. The consequence of this is that upon cyclization to form the *bis*-Tröger's

Base, the stereochemistry of the bridging methylene is determined by the stereochemistry of the α-aminophosphate to generate the *syn*- cofacial or *anti*- isomersin an expected 1:1 ratio. These orientations cannot be interconverted under acidic conditons as seen in previous *bis*-Tröger's bases as its formation is sensitive to steric interactions.[64] The alternative to generating a statistical mixture of *syn*-cofacial and *anti*- isomers and isolate more of the desired binding syn- isomer would be to either build in water solubilizing functional groups into the walls of the molecule or employ a stereoselective method of forming the α-amino phosphonate.

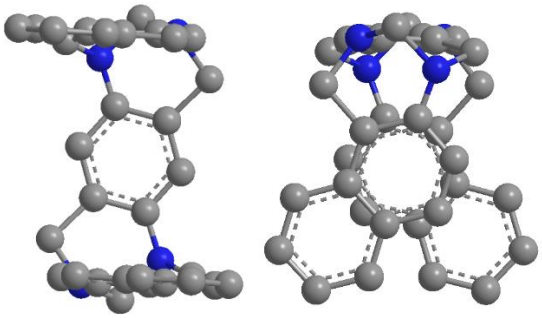


Figure 13: 1,2;4,5-*bis*-Tröger's Base molecular tweezer with naphthalene walls illustrating their offset nature

In contrast to the 1,2;4,3- isomer, inclusion of naphthalene sized hydrocarbons for the walls in the 1,2;4,5- leads to them existing in an offset orientation mimicking the pattern observed in the crystal structure of benzene.[65] This feature should facilitate easier inclusion of aromatic guest molecules in the cavity compared to the 1,2;4,3- isomer which has its walls directly over one another.

II. RESULTS AND DISCUSSION

A. Formation of the key intermediate N,N'-di-t-Boc-2,5-diaminoterephthaldehyde

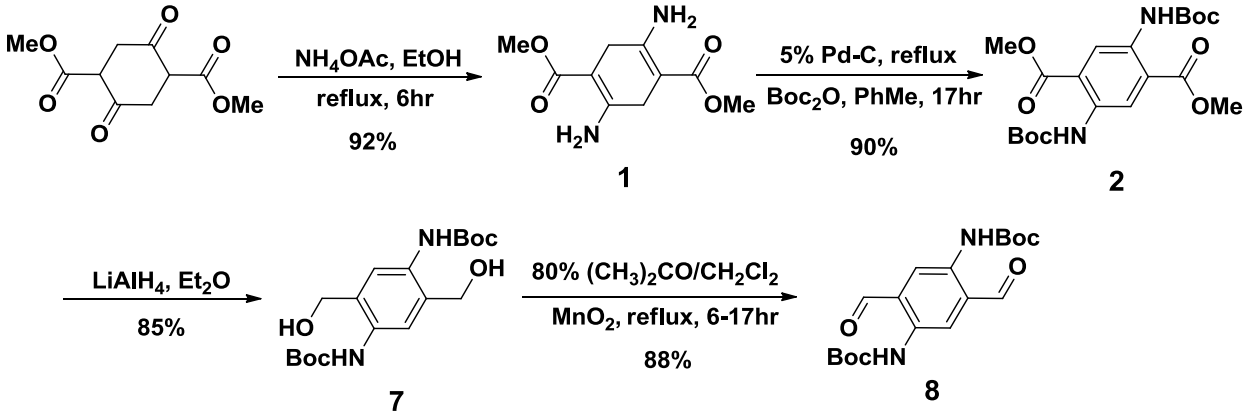


Figure 14: Overall synthetic sequence to produce key intermediate dialdehyde 8

1. Synthesis of Dimethyl 2,5-diaminocyclohexa-1,4-diene-1,4-dicarboxylate

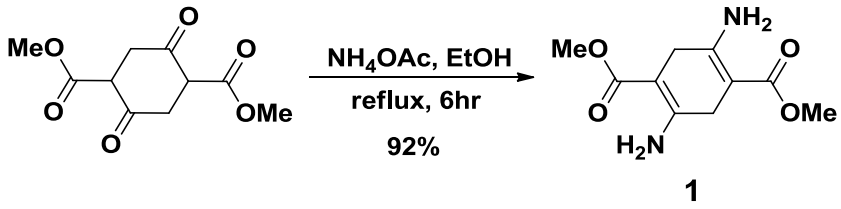


Figure 15: Synthesis of *bis*enamine 1 from dimethyl succinyl succinate

Succinyl succinate diester derivatives have been condensed with amines for over 100 years utilizing molten NH_4OAc[66] and NH_3 in ethanol[67]. However, neat alkyl amines[68] and NH_4OAc in solution[69] provide for more facile methods to the desired *bis*-enamines. In a method initaly developed by Kanchan Tiwari[70], she chose to go the route of NH_4OAc in ethanol as we needed the primary enamine. Baeyer describes uses ten equivalents of NH_4OAc, but she found that reducing it to five equivalents was sufficient with 95% yield on a one gram scale of

dimethyl succinyl succinate (DMSS). Use of ethanol as the solvent allowed **1** to crystallize from the reaction medium eliminating the need for subsequent purification. In scaling the reaction up to 55g scale, the equivalents of NH_4OAc were reduced to three and four equivalents with each producing yields of 87% and 88% respectively and identical melting points of 212-214˚C. On this scale addition of DMSS needs to be added in portions to the refluxing ethanol to ensure it dissolves.

2. Synthesis of Dimethyl 2,5-*bis*((tert-butoxycarbonyl)amino)terephthalate

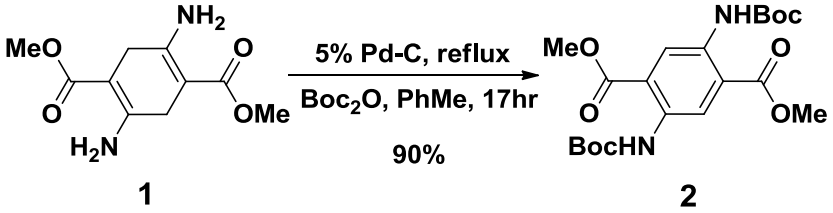


Figure 16: Scheme for aromatization and di-Boc protection of *bis*-enamine 1

Use of Pd-C has been demonstrated to be able to oxidize heterocycles[71] and cyclic enamines[72] to the corresponding anilines, but required the use of a sacrificial oxidant to prevent disproportionation of the enamine. Fortunately, refluxing in toluene for 13hr with 30% by weight 10% Pd-C afforded the aromatized **1** in 98% yield with no reduced **1** observed. Boc protection of both amines was accomplished in 66% yield by Kanchan Tiwari in boiling toluene with 5% Pd-C with 4eq Boc_2O followed by 2eq Boc_2O after 4hr. Boc_2O was added in several portons because it is unstable under the reactions conditions and **1** does not acylate until it has been aromatized. This was taken into consideration when increasing the scale of **1** production.

Under my direction, John Lukesh III increased the initial concentration of **1** by a factor of two on a 1g scale. This was considered feasible as **2** is more soluble in boilng toluene than is **1**.

A greater concentrations of Boc_2O (7eq, added in two portions) was utilized with complete conversion to **2** was observed after 22hr. He was able to acquire a 92% yield of the desired product in four crops from recrystallization from CH_2Cl_2/hexanes. In further testing conditions for scale up, the concentration of **1** was increased further in efforts to decrease the amount of the most expensive reagent, Boc_2O, required for conversion to **2**. Coupled with the aromatization of **1** before the addition of Boc_2O, this alteration to the synthetic methodology was considered to be beneficial. However, this was not the case with side product formation observed. This complication is described subsequently.

a. Diarylamine formation

In the effort to make **8** on a large scale so attempted was **2** but with isolated yields of only ~50%. In the small scale preparations of **2**, Pd-C and Boc_2O were added concurrently to **1** but as Boc_2O thermally decomposes it was thought prudent to aromatize **1** to **3** beforehand. On testing these changes desirable for large scale reaction, it was observed that TLC did not indicate complete reaction over the same time scale. Aromatization initially occurred in distilling toluene to azeotropically remove residual water or ethanol from **1** to prevent it from later reacting with Boc_2O. This resulted in a yellow-green distillate and a pungent smelling vapor being produced that was basic to pH paper. Due to the composition of the mixture and the odor of the gas, it was concluded that ammonia was being produced and was taking as the first evidence that another transformation was occuring.

A potential source of ammonia was residual NH_4OAc in the **1**. This was ruled out by washing with H_2O and EtOH, and use of pure 1 with a melting point of 212-214˚C. With

exogenous ammonia ruled out, hydrolysis of the *bis*-enamine was considered the next most likely mechanism. After isolating **2** from the mixture by crystallization, its mother liquor was analyzed by ^{1}H NMR and observed to be a mixture of DE, Boc_2O, and an unidentified side product that was not mono Boc protected **2**. The excess Boc_2O present suggested that the amine functionality was lost and replaced with something that would not reaction with the Boc_2O, possibly a hydroxyl group. To test the phenol hypothesis, 6g of the concentrated mother liquor was dissolved in CH_2Cl_2 and extracted with sat. Na_2CO_3. The aqueous phase was removed, acidified to pH6, and extracted with CH_2Cl_2. After drying the organic phase and concentrating to dryness 1.8mg of material was afforded that identified as not the side product by ^{1}H NMR. This did not fully rule out the phenol as the side product as the phenoxide may not have been able to be partitioned into water.

To rule out hydrolysis, a portion of **1** was split into two portions for a side by side reaction. The first portion was not azeotropically dried by distillation of toluene and heated at reflux without 5% Pd-C for 3hr with no change in pH paper observed above the condenser. 5% Pd-C was then added and after 12min pH Hydrion paper indicated pH11 vapor above the condenser. After heating at reflux for 18hr, no pH change was observed above the condenser as testing with pH paper. The second portion of **1** was dried azeotropically by distillation of toluene and heated at reflux for 3hr with no observed change in pH paper before the addition of Pd-C. After 5min the pH paper changed to pH9-10. The products from each of the portions were isolated and analyzed by ^{1}H NMR to afford identical spectra containing **3**.

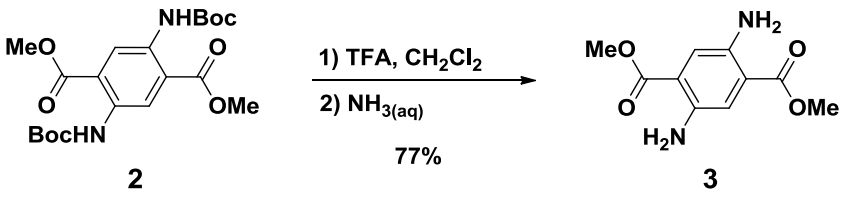


Figure 17: Deprotection of 2 to afford aromatic diamine 3

To corroborate the signals, a very pure sample of authentic aromatic diamine **3** is was synthesized in 77% overall yield from the TFA deprotection **2** and subsequent deprotonation in 75% conc. $NH_{3(aq)}$. No side product was produced with this method. The ^{1}H NMR spectrum matched that of the aromatic **3** described above. **3** was also exposed to 5% Pd-C in refluxing toluene with no change in composition as observed by TLC. This also ruled out the possibility of **3** reacting with itself to evolve ammonia. It was shown that if the previous protocol of concurrent addition of Pd-C and Boc_2O was used **2** was generated in 88% yield after recrystallization form toluenen. **2** was also made from **3** with a 92% yield with no observation of **4** in the isolated product.

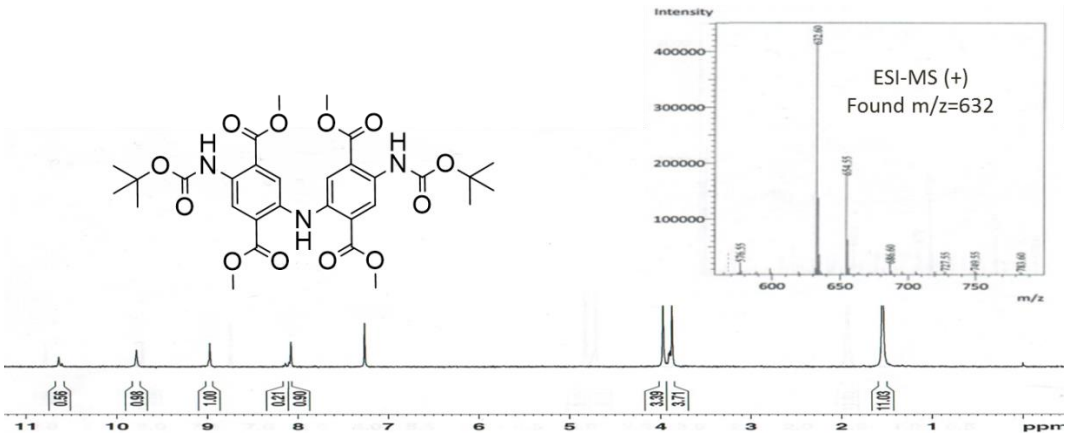


Figure 18: Compound 4, the diaryl amine side product formed from condensation of 2

Mass spectrometric analysis of the mother liquor from a synthesis of **2** in which side product formed proved that the side product was not a phenol. The signals produced had a m/z of 442 (**2**+Na^+) and 632 which is a consistent with **4**. This data ruled out hydrolysis as a mechanism of side product formation. This mixture was purified by flash chromatography in which diarylamine **4** was isolated and characterized by ^1H NMR and ESI-MS confirmed to be the side product generated by Pd-C oxidation. With this diarylamine in hand, it was hypothesized that en route to being aromatized by Pd-C, condenses with itself to form the diaryl amine in the absence of Boc_2O which resulted in the evolution of NH_3. This surprising results raised the question of when the coupling occurred. The most plausible pathway for condensation would be the transamination of the aromatic amine **3** with the imine form of **2**. As this process is expected to be acid catalyzed it was checked to see if this process could be inhibited by the use of base washed catalyst and glassware. What was determined was that it had no effect in decreasing diarylamine formation.

b. Exploration on mechanism of diaryl amine formation

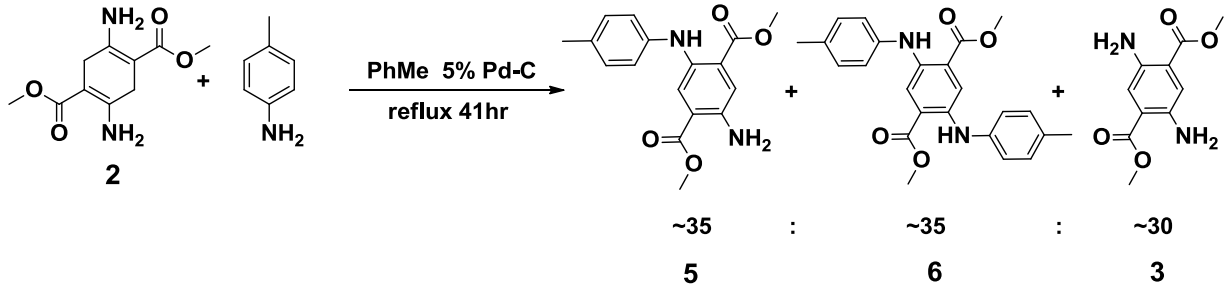
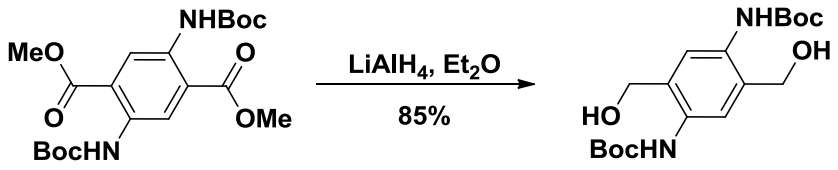


Figure 19: Mono- and *bis*- diarylamine formation from *bis*-enamine

To further elucidate this process, **1** and *p*-toluidine were heated in refluxing toluene together without Pd-C. No change was observed by TLC over 17h. Upon addition of 5% Pd-C however, two new spots were observed and after 16-41hr of reflux **5** and **6** were isolated by

flash chromatography in a 1:1 molar ratio with 71% conversion of **1** into the mono- and bis-variants. To ensure exchange of the amine was not due to acid catalysis, the 5% Pd-C was washed with 15% NaOH and rinsed with nanopure water until the filtrate was neutral. Following above procedure, **5** and **6** were observed to be in a 2.3:1 molar ratio respectively with 63% mol conversion of **1** into the desired products. In obtaining compounds **5** and **6**, the hypothesis of having an aniline condense with **1** en route to aromatization was confirmed.

3. Synthesis of Di-tert-butyl (2,5-*bis*(hydroxymethyl)-1,4-phenylene)dicarbamate



2 **7**

Figure 20: Reduction of aromatic diester 2 to desired diol 7

$LiBH_4$ in CH_3OH or IpOH was utilized initially by Kanchan Tiwari reduced diester **2** to afford only trace amoounts of diol **3**. When the solvent was switched to THF, a 63% yield by NMR with complete reaction after 4h even though **2** was still only moderately soluble. She observed that if pH7 buffer was not used in the workup of the $LiBH_4$ the crude product was contaminated with a *bis*-cyclic urethane from the addition of the benzyl alchol in the the carbonyl of the Boc group. The solubility issues of **2** in the reduction medium were ultimately overcome by a two solvent method employing $LiAlH_4$.

$LiAlH_4$ has been used to reduce a vast array of organic compounds[73] but we were leery of its use with its ability to reduce the Boc group. This concern did not come to fruition however as deprotonation of the Boc protected NH preserved the protecting group. As $LiAlH_4$ is soluble in Et_2O but not in CH_2Cl_2 and **2** is readily soluble in CH_2Cl_2 but not in Et_2O a solution was made of

each in the appropriate solvent. **2** in solution was then added to refluxing $LiAlH_4$ to produce the desired diol in ~2hr over the scale of 0.5g to 27g scale with 71-88% yield. (22g scale, 79% yield, mp 162-166; 27g scale, 82% yield mp 154-157. Most pure product 6g scale, 86% yield, mp 177-180 extracted quenched rxn mix/celite cake with CH_2Cl_2 only)

4. Synthesis of N,N'-di-*t*-Boc-2,5-diaminoterephthaldehyde

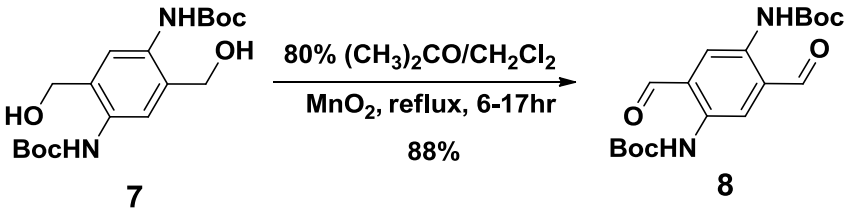


Figure 21: Selective oxidation of diol 7 to desired dialdehyde 8

MnO_2 has been shown to be a mild oxidant[74] for selective oxidation of benzylic of vinylic alcohols after systematic testing [75] and although documented to have difficulty[76] in oxidizing ortho- amino benzyl alcohols, it was not the case for our particular substrate. Although its chemioselectivity is desired, MnO_2 has many complicating factors in its use. First is that it must be freshly synthesized, usually by the Attenburrow[77] method, and generates a fine solid that requires a large investment in time to collect by filtration and washed. Its activity also varies based upon its method of production[78] and to what extent it is dried. If applicable, Goldman[79] has found that wet MnO_2 can be stored for extended periods of time without precipitous loss in activity which greatly reduces the time in preparing the oxidant. Another issue in MnO_2 oxidation is that it requires a large stoichiometric excess which translates to a large volume of solid and can make efficient stirring tricky although recent work[80] has found that

substoiciometric "active" MnO_2 from Sigma-Aldrich has been used under an atmosphere of O_2 to circumvent some of these concerns.

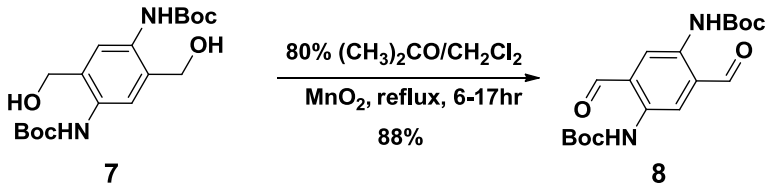


Figure 22: Selecive oxidation to dialdehyde with MnO_2

Oxidation of diol **7** to dialdehyde **8** was reliable when carried out using MnO_2 prepared by the Attenburrow procedure and dried in an oven at 110˚C with periodic mixing until a free flowing powder resulted. When the oxidation was conducted in refluxing CH_2Cl_2 yields averaged 40%, which was attributed to the inability of the diol and mono-aldehyde to desorb from the MnO_2 surface. Yields inproved to 85-95% when the oxidation was carried out in 20% CH_2Cl_2 in acetone. However care needs to be taken in the order of addition of the solvent. If **7** and MnO_2 were mixed together as solid, the addition of a flammable solvent first resulted in ignition of the materials. Combination of the mixed solids with CH_2Cl_2, followed by acetone avoided combustion.

a. Over oxidation from MnO_2 and alternate Cu(I) catalyzed oxidation

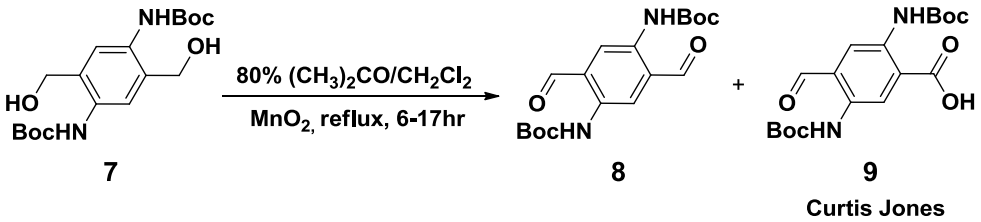


Figure 23: Over oxidation of DA to mono-aldehyde mono-carboxylic acid with MnO_2

Scale up of the oxidation commenced with MnO_2 synthesized via the Attenburrow procedure using newly purchased reagents. Yields of the dialdehyde unexpectantly dipped to a 38% and 53%. Extraction of the MnO_2 from the reaction with 50% CH_3OH/CH_2Cl_2 produced a new solid. Analysis by ^1H NMR in DMSO-d_6 and ESI in negative ion mode confirmed that the reaction with MnO_2 somehow produced the mono carboxylic acid, mono aldehyde **9** by generating m/z= 370 ($M\text{-}H^+$, 100%) and singlet integrating to 2H at 13ppm. Even though the MnO_2 is described in the literature needing to be alkaline for the reaction to proceed, it was postulated that excess hydroxide or other water soluble contaminents like $KMnO_4$ were present.

A new batch of MnO_2 was made and washed with water until the filtrate was colorless and neutral to pH Hydrion paper. Reaction with 25eq MnO_2 at 17hr reflux and 35eq MnO_2 at reflux for 24hr produced 58% **8** with 21% mono acid mono aldehyde and 43% **8** with 34% mono acid mono aldehyde **9** respectively. To rule out potential oxidation by Fe^{+3} or other dissolved metal ions from the metal instruments used in the synthesis of MnO_2 ceramic tools with analogous results as described above. Yield improved to 74-87% when the MnO_2 synthesized was washed with hot 0.6M pH7 phosphate buffer. CH_3OH was added to the system to decrease adsorbtion of **7** to MnO_2 in hopes of limiting the chance of over oxidation. However with a combination of 10% CH_3OH/ 20% CH_2Cl_2/70% acetone the reaction was incomplete over 2d at reflux and 75eq. MnO_2. The carboxylic acid side product began to form after 3d and incomplete transformation of **7** observed.

An alternative method to MnO_2 attracted our attention which would be to make an "active" MnO_2 layer deposited on the surface of activated carbon[81]. The solid was easily

filtered. Its washing with water until the filtrate was neutral took a fraction of the time compared to the Attenburrow method.Use of a 12 MnO_2-C : 1 **7** mass ratio was used in 80% THF/CH_2Cl_2 resulted in trace dialdehyde formation after 24h at refluxing temperature. This method was no longer explored proving impractical for our purposes and should not be taken as an indictment of this clever technique. As Carpino noted in his work that the activated carbon employed came from the J.T. Baker company and other sources of activated carbon produced minimally active or non-reactive MnO_2 on C.

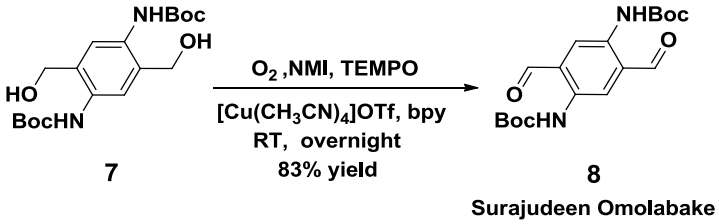


Figure 24: Selective oxidation to DA with Cu(I) catalyst

As the MnO_2 made did not have consistent chemical reactivity over its many preparations coupled with the days required for 100+g scale preparation it was determined to not be worth the effort or the sacrifice of diol. Although the Swern oxidation is known to selectively oxidize an alcohol to an aldehyde and has been optimized[82], it was not attempted due to concerns of solubility of the diol at the low temperature required. In collaboration with Surajudeen Omolabake we found an aerobic oxidation utilizing Cu(I)[83] the ideal for **7**. Complete conversion occurred overnight when exposed to the atmosphere at room temperature with rapid stirring. It was accidentally discovered that the oxidation was able to occur in the absence of 2,2'-bipyridyl with 50% mol ratio NMI as opposed to the 20% prescribed by the literature. Yields in the 80% range were average with crystallization of the product from the reaction medium occurring if CH_3CN was used as the solvent.

B. Synthesis of acyclic *bis*-Tröger's Base Molecular Receptor

1. Preparation of *bis*-imines

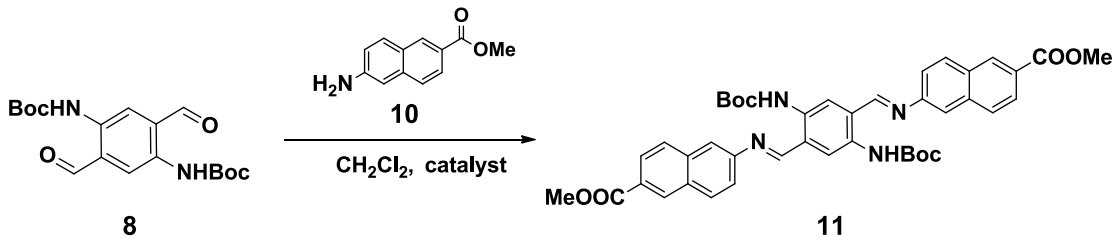


Figure 25: General scheme for *bis*-imine formation from dialdehyde 8

With the key intermediate dialdehyde in hand, construction of the molecular tweezers began by condensation of a naphthyl amine with it to form a *bis*-imine was first conducted in collaboration with Nzagi Nyakirangani[84]. The naphthyl amine initially chosen was methyl 6-amino-2-naphthoate which was prepared in 94% yield (mp 154-157˚C) by refluxing 6-amino-2-naphthoic acid in dry CH_3OH for 2h using 18M H_2SO_4 as the acid catalyst. The dialdehyde was combined with excess **10** in boiling toluene using a Dean-Stark trap to drive the reaction to completion by azeotropic removal of water. Over the course of 17h the dialdehyde was no longer detectable by TLC and an orange solid formed. This orange solid was also observed by Nzagi Nyakirangani who had also had difficulties in identifying this material. This solid was insoluble in ethanol, DMSO, and sparingly soluble in $CDCl_3$ in which a ^1H NMR spectrum was acquired. From the spectrum the material was speculated to be composed of **10**, the mono imine, and the *bis*-imine but was sufficiently complicated to prohibit confident assignment. The synthesis was conducted again with an acid catalyst, the hydrochloride salt of **10** as well as a chemical dehydrating agent, *bis*-(trimethylsilyl)acetamide (BSA), were employed in an effort to completely form the desired *bis*-imine. After mixing at room temperature overnight a greater

amount of the orange solid was produced, which was sufficiently insoluble to prevent NMR analysis. In order to rule out the possibility that the orange solid was some kind of polymer derived from **8**, a similar reaction was carried out in the absence of naphthylamine **10**. No orange solid was formed, as no new spots were observed by TLC.

The insoluble orange solid was treated in glacial acetic acid with trimethyl phosphite for if the orange solid was indeed the desired *bis*-imine these reagents would be able to convert it into the corresponding *bis*-α-aminophosphonates. After 10d of vigorous stirring at room temperature, the desired aminophosphonates were formed, confirming that the organe solid was indeed the *bis*-imine. The crystallinity of the *bis*-imine was was exploited subsequently to drive its formation and eliminate the need for removal of water. Use of CH_2Cl_2 as a solvent and glacial acetic used the acid catalyst gave **11** in 88% yield.

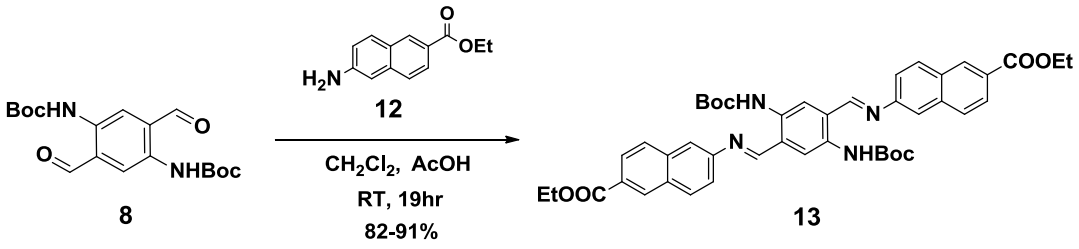


Figure 26: Optimized condition for synthesis of *bis*-imine 13

Ethyl 6-amino-2-naphthoate **12** was made by Fischer esterification in anhydrous ethanol using concentrated sulfuric acid as the catalyst. After complete esterification and partitioning between CH_2Cl_2 and saturated aqueous $NaHCO_3$, yields ranged from 62-97. The purity of the material typically afforded after isolation is usually good enough to carry on without purification. **13** was first made by the condensation of **8** with a slight excess of the two equivalents of **12** needed in CH_2Cl_2 in the presence of $Yb(OTf)_3$. The lanthanide catalyst was

used to develop conditions later used in a one pot synthesis of the *bis*-aminophosphonates. After 4hr at room temperature **8** was no longer seen by TLC, and a large amount of orange solid was seen in the reaction volume. After collecting by vacuum using ethyl acetate or methanol to transfer, **13** was afforded in 63% and 82% yield respectively. Synthesis was optimized using CH_2Cl_2 and glacial acetic acid on a 1.6g scale of the **8** to give the *bis*-imine in 91% yield in two crops with a melting point of 282-286°C of the first crop when allowed to stir at room temperature overnight and washed with EtOAc. After many preparations it was correlated that a purer crude product was produced after prolonged time stirring at room temperature. Due to its highly crystalline nature and the small amount of the *bis*-imine that can go into solution it is able to selectively complex with itself and enriching the solid in the desired material. *Bis*-imine **13**, with ethyl esters instead of methyl esters, was soluble enough in $CDCl_3$ to be characterized by ^{1}H, a ^{13}C NMR and MS. In the ^{1}H NMR spectrum, a singlet is observed at δ11.8 ppm which was attributed to the N-H of the Boc protected amine which is intramolecularly hydrogen bonded to the imine nitrogen. The consequence of this would be to lock all atoms participating in this six membered ring into a planar conformation that enhances crystallinity.

Solvents screened to determine not only a good solvent for recrystallization but a good solvent to put **13** into solution for reaction. The best solvents for dissolving **13** were as follows: THF ≈ CH_2Cl_2 >> EtOAc, toluene, Et_2O >> CH_3CN, DMSO, hexane.

2. Synthesis *bis*-α-aminophosphonates

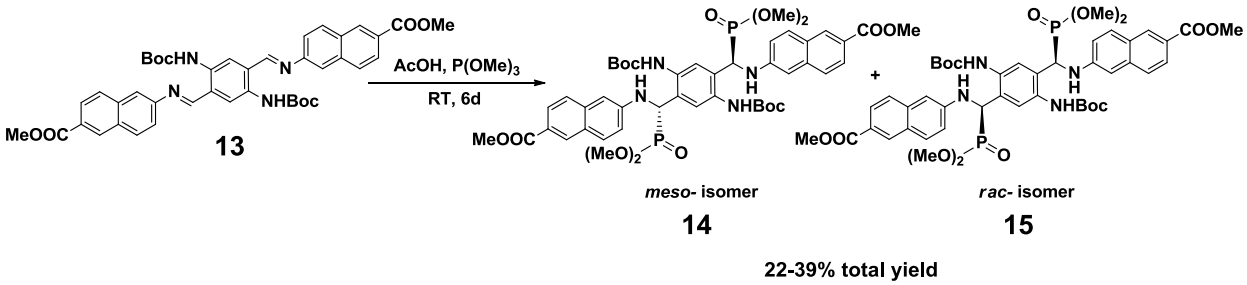


Figure 27: Formation *bis*-α-aminophosphonates 14 and 15 from *bis*-imine 13

The first attempt to improve *bis*-α-aminophosphonate, elevated temperature to shorten reaction times and to increase the solubilty of *bis*-imine **13** were investigated. However, at temperatures above 80˚C, the Boc protecting groups were removed. With degradation at higher temperatures and room temperature consigning reaction times to prohibitively long periods, investigation into altering the phosphite and catalyst species was conducted. It has been demonstrated in the literature that metal catalysts based on indium[85], scandium[86], and ytterbium[87] facilitate α-aminophosphonate formation from imines with dialkylphosphites. Of these, ytterbium was chosen by Nzagi Nyakirangani and used by myself due to its ability to catalyze condensation of amines and ketones or aldehydes in β-enamino synthesis[88], its use in one pot preparations as it poorly catalyzes the dialkyl phosphite addition to the aldehyde[89], and its future potential for asymmetric aminophosphonation using chiral ligands[90,91,92]. To confirm that a dilakyl phosphite would not add to **8** in the presence of an ytterbium catalyst a mixture of **8**, $Yb(OTf)_3$, and dimethyl phosphite in $CDCl_3$. This was monitored by NMR spectroscopy over the course of a day with no changes observed in the ^{1}H or ^{31}P resonances for the components.

Introduction of $P(OMe)_3$ however readily added to aldehyde at room temperature, so should only be used if the *bis*-imine is preformed.

When **8**, **10**, $Yb(OTf)_3$, and $HPO(OMe)_2$ were combined in either CH_2Cl_2 or CH_3CN, only trace amounts of the *bis*-aminophosphonates were formed after 4d at room temperature. This lack of activity was attributed to the poor solubility of **11** in either solvent which reduces concentrations below those that rapidly react. When done in neat $HPO(OMe)_2$ at 50°C for 18h 47% of the *meso*- diastereomer **14** and 31% of the *rac*- diastereomer **15** were isolated after silica gel flash chromatography with Nzagi Nyakirangani initially isolating only the *meso*- isomer. The diastereomers were readily separated on silica as they have marked different R_f values. We tentatively assigned the *meso*- isomer **14** as the faster moving isomer with higher R_f. Presumably, phosphonate group association with silica will dominate chromatographic retention, being most strongly retained when both phosphonates contact the surface While free rotation about the single bond allows placement of phosphonate on either face of the central benzene ring, there must be a lowest energy conformation. In the *rac*- diastereomer **15**, with the same chirality at each of the aminophosphonate centers, both phosphonates will be on the same face in the lowest energy conformation. If formation of **14** and **15** was conducted in neat $HPO(OMe)_2$ at 90°C the desired materials were not produced.The isolated material resembled neither the starting material nor the products but with apparent loss of the Boc protecting groups. This preliminary data reinforced the idea that the insolubility of the *bis*-imine is the major impediment to reactivity that needs to be overcome.

Bisaminophosphonate synthesis from dialdehyde

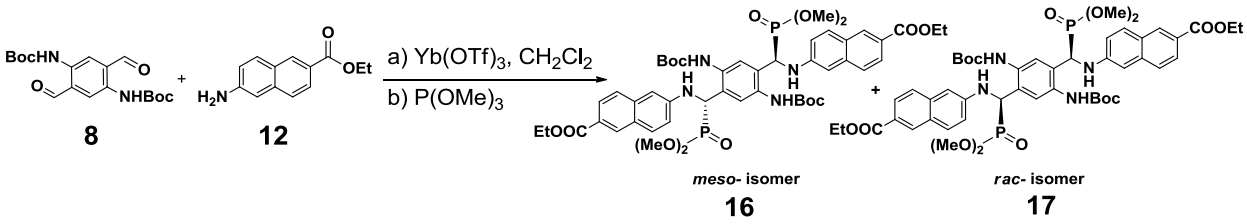


Figure 28: General "one pot" reaction scheme for *bis*-aminophosphonate formation

Investigation into forming **16** and **17** efficiently starting by formation of *bis*-imine **13** *in situ* first using CH_2Cl_2 and glacial AcOH, followed by the addition of $P(OMe)_3$. The rationale behind this was to determine if the lanthanide catalyst could be omitted and then later used in developing asymmetric phosphonation. What was found though was that even with circa 10x stoichiometric excess of $P(OMe)_3$ in the presence of acid and at room temperature did not facilitate quantitative transformation. When $Yb(OTf)_3$ was introduced and the mixture heated to 60°C for 3h the reaction was complete. Analysis by ^1H NMR showed that the Boc groups remained intact but ^{31}P NMR showed signatures for the remaining trimethylphosphite, the *bis*-aminophosphonate diastereomers, and a new signal at δ34 ppm which is attributed to dimethyl methylphosphonate, believed to be formed by the following mechanism:

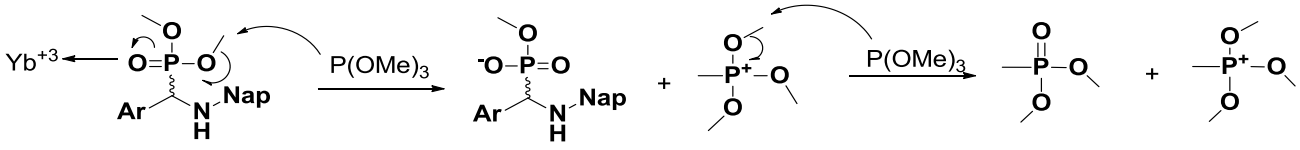


Figure 29: Proposed mechanism for dimethyl methylphosphonate formation with $P(OMe)_3$

When the solvent was changed to THF using 60°C temperature, the reaction time decreased to 14h but unfortunately $P(OMe)_3$ was still too reactive and not only formed dimethyl methylphosphonate but reacted with this solvent in the presence of ytterbium (III)

triflate. A side product was tentatively assigned as dimethyl (4-hydroxybutyl)phosphite which was formed, presumably by ring opening of lantanide corrodinated to THF.

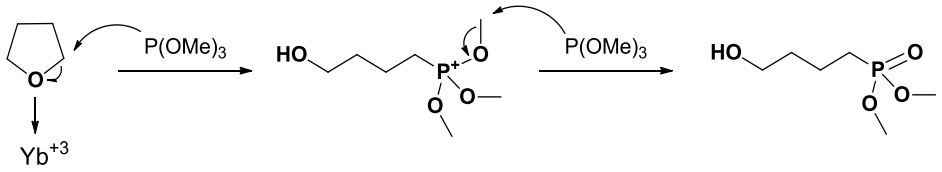


Figure 30: Proposed mechanism for reaction of $P(OMe)_3$ with THF in the presence of $Yb(OTf)_3$

After silica gel flash chromatography the *bis*-aminophosphonates were afforded in an estimated 50% total yield that were not separated from the methyl dimethylphosphate or the dimethyl (4-hydroxybutyl)phosphite. From these results continued use of trialkyl phosphites were put aside due to its demonstrated propensity to form side products at the expense of the desired compounds and focus shifted to conditions in which dialkyl phosphites could be employed.

<u>Bisaminophosphonate Formation using $HPO(OMe)_2$</u>

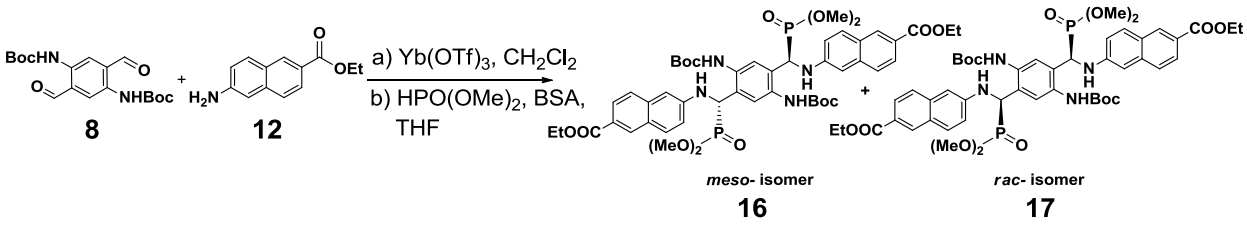


Figure 31: "One pot" *bis*-aminophosphonate synthesis with $HPO(OMe)_2$

Its been shown in the literature that transformation of an imine to an aminophosphonate with a dialkylphosphite and a catalyst as a homogeneous mixture occurs over the range of 0.5 to 4h[93] with a wide range of compatible aldehydes and amines. Building off of the previous work done by Nzagi Nyakirangani, prospecting began using the “one pot”

method for *bis*-aminophosphonate formation. *Bis*-imine **13** was formed first in the presence of $Yb(OTf)_3$ with 4.5eq dimethyl phosphite in CH_2Cl_2 for 4d to give 34% yield (28% *meso*- **16**, 6% *rac*- **17**) after silica gel chromatography. This contrasted greatly from the 1:1 diastereomeric ratio observed in the NMR of the crude product before purification. Resolution suffered as the remaining dimethyl phosphite interfered with chromatography. Analysis of the diastereomers by ^{1}H and ^{31}P NMR showed clean isolation of products from the dimethyl phosphite, but the *rac*- portion contained more than one signal in the ^{31}P spectrum and lower integration ratio of the phosphoesters in ^{1}H spectrum. From this it was surmised that degradation of the aminophosphonates was occurring on silica gel by the lack of mass balance after this purification technique and the retention of color on the silica. As the ratio of aminophosphonate diasteromers formed should be 1:1 as the conditions for aminophosphonation are unselective, the *rac*- isomer was being degraded to a greater degree as it was isolated in a significantly lower amount. Put forward here is a mechanism by which degradation occurs which seems feasible as it is similar to the removal of a methyl phosphonate ester by excess trimethyl phosphite and provides and explanation as to why the *rac*- isomer is affected disproportionately. The longer contact time with the slower migrating racemic isomer **17** may explain the greater degree of degradation.

If the silica gel acidity was the problem, neutralization may avoid it. The first protocol employed was to expose silica gel to gaseous ammonia. To do this a sample of silica gelwas exposed to the vapor over a container holding concentrated aqueous ammonia for one week with periodic mixing over that time. When this silica gel was used for chromatographic separation it indeed significantly decreased the polarity of the eluent needed but caused the

diastereomers to collute. However, if the silica gel that was treated in this manner was left exposed to the atmosphere for a day with periodic mixing the separation was accomplished with the *meso*- isomer being eluted with 40% CH_3CN/CH_2Cl_2 instead of 80% CH_3CN/CH_2Cl_2 and the *rac*- isomer was eluted with 80-100% CH_3CN/CH_2Cl_2 instead of 10% CH_3OH/CH_2Cl_2. Use of the silica gel also produced a lesser degree of degradation upon separation of the diasteromers. Although encouragingwe chose not to follow up on this due to questions of reproducibility. With quantitation in mind though, deactivated silica gel was prepared by exposure of silica gel to well defined amounts of Et_3N in CH_2Cl_2 as a slurry. Mixtures of 2.5% and 5% allowed for sufficient deactivation while still affording separation. The 2.5% mixture behaved analogously to the gaseous ammonia exposed silica while the 5% mixture produced the largest disparity in eluents needed to elute the products with the *meso*- isomer being collected with 10% CH_3CN/CH_2Cl_2 and the *rac*- isomer being collected with 100% CH_3CN. Deactivation of the silica indeed afforded a greater amount of the *rac*- isomer but still failed to completely prevent degradation.

% by mass NEt_3/silica	Yield **16**	Yield **17**	Total Yield
0%	28%	6%	34%
2.5%	39%	19%	58%
5%	32%	21%	53%

Table 1: *bis*-aminophosphonate disastereomers afforded from deactivated silica gel chromatography

With the anemic activity of the dimethyl phospite and the use of trimethyl phosphite producing side products a species of intermediate activity was desired. Dimethyl phosphite is in

equilibrium with its trivalent tautomer but the equilibrium heavily favors that of the pentavalent form. This can be shifted though by the introduction of a silylating agent. BSA was chosen not only for its two equivalents of silylating group per molecule but also acts as a base to facilitate proton transfer in isomerization.

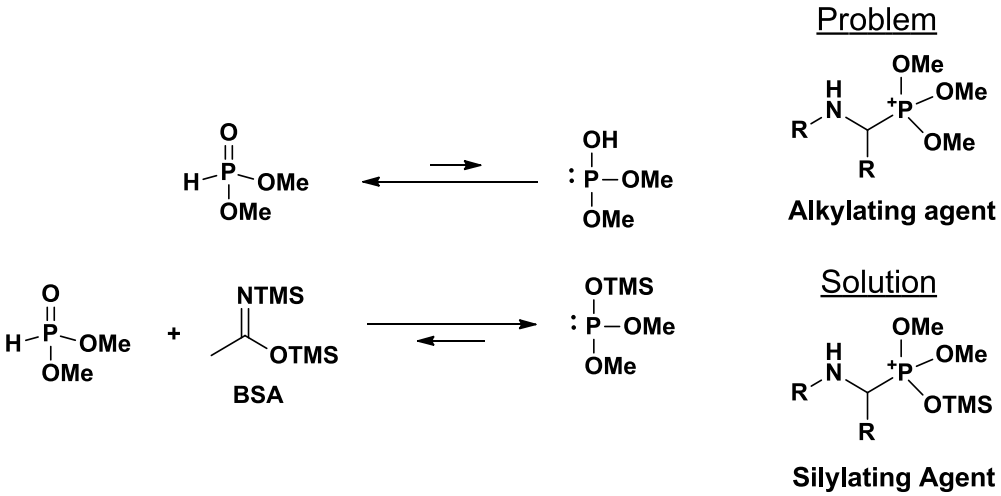


Figure 32: Use of BSA to shift $HPO(OMe)_2$ equilibrium and prevent to methyl transfer

Dimethylphosphite was combined with BSA and monitored by 31P NMR over the course of a day over which time the signal at δ15 ppm from $HPO(OMe)_2$ decreased and a new signal grew in at δ129 ppm. As this new resonance was similar in chemical shift to $P(OMe)_3$ (δ141 ppm) this was taken as evidence of the desired conversion to dimethyl trimethylsilylphosphite[94]. Along with this change another modification to the synthetic procedure was introduced in order to still utilize the large excesses of dimethyl phosphite required but allow it to be removed as this cannot be easily done by simple evaporation. It well known that use of I_2 in pyridine and water can oxidize dimethyl phosphite to a phosphinic acid[95] which could then be removed by washing with aqueous base. When the dialkyl phosphite was injected with an equimolar amount of BSA reaction times averaged 18-30h at room

temperatures with yield increasing to a consistent 50% of the diastereomeric mixture after silica gel chromatography. It was discovered that quenching of the silylating agent was paramount by addition alcohol prior to being exposed to the I_2/ aqueous pyridine mixture for if this was not done then only trace amounts of the desired products were isolated. This could possibly be attributed to I^- demethylating the methyl phosphonates too quickly under aprotic conditions.

It wasn't until much later that the oxidative workup was suspected to be in participating in the dealkylation of the phosphonates in **16** and **17** even after quenching the BSA. This was tested by taking a crude mixture of the diastereomers, splitting it into two portions, and treating one of the halves. Analysis of the untreated half when viewed with ^{31}P NMR showed signals for the excess dimethyl phosphite and the two desired *bis*-aminophosphonates wereas the treated half had the resonances of the products along wth an array of singals upfield confirming the removal of the phosphomethyl esters. The mechanism of dealkylation is suspected to be by S_N2 reaction with I^-. This avenue of excess phosphite removal was abandoned as subsequently developed methodologies do not utilize chromatographic separation.

With the susceptibility of the dimethyl phosphonates to degradation on silica gel established the phosphonating agent was switched to diethyl phosphite in order to slow the rate of ethyl phosphonate ester S_N2 cleavage. This approach was validated by isolation of 73% total yield of the *bis*-aminophosphonates after chromatographic separation. From this result it was deemed worthy to carry forward with diethyl phosphite as the phosphonating agent as

well as pursuing tweezers synthesis without isolation of the *bis*-aminophosphonates which will be discussed in a later section.

3. Trögerization Affording Molecular Receptors Isomers

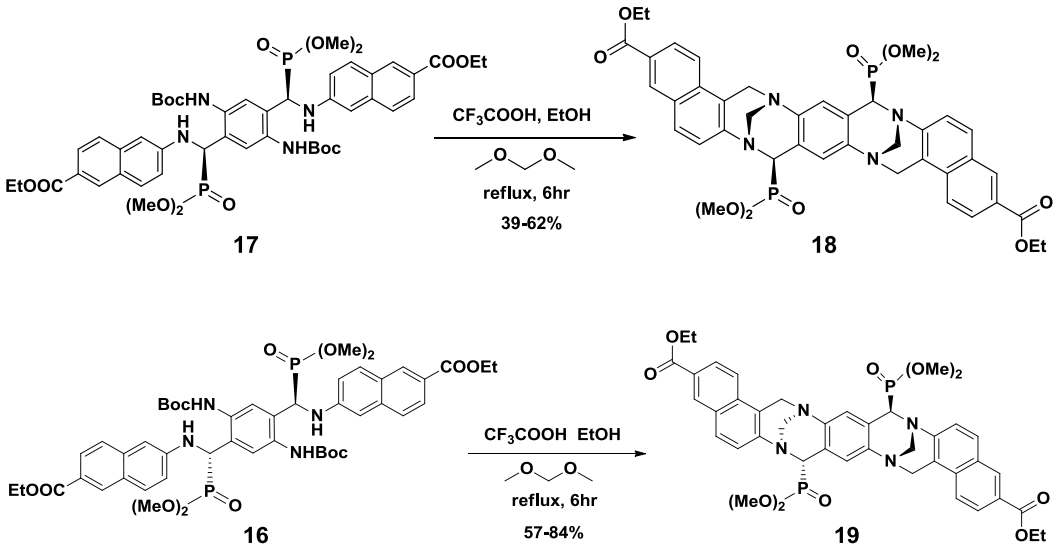


Figure 33: Trogerization to form desired *rac*-(18) and control *meso*- (19) molecular receptors isomers

With isolated **17** and **16** on hand cyclization to form the *bis*-Tröger's base tweezers commenced. The acid chosen, trifluoroacetic acid (TFA), and the formaldehyde equivalent, dimethoxymethane (DMM), were chosen for Trögerization as both of these required reagents are volatile so that when used in excess remaining amounts of them can be removed under reduced pressure. In using these two as reactive solvents two things were observed: that a reflux temperature at 60°C or above was required to drive Tröger's base formation to completion and that polyformaldehyde was generated as a side product. The polyformaldehyde was not separated from the desired product through silica gel flash chromatography but was able to be removed only after extensive washing with a saturated $NaHCO_{3(aq)}$ solution. Fortunately it was found that the addition of either methanol or ethanol as a cosolvent

prevented polyformaldehyde formation by condensing with the formaldehyde equivalent as well as elevating the reflux temperature of the mixture. Additonally crude **17** was cyclized in the presence of dimethyl phosphite, dimethyl methylphosphonate, and dimethyl (4-hydroxybutyl)phosphonate with no observable interference in Tröger's base formation. **18** and **19** molecular tweezers isomers displayed similar behavior on silica gel as its *bis*-aminophosphonate counterparts with regards to degradation occurring over the course of flash chromatography, albeit to a lesser degree. Although these tweezers isomers were not still not separated from the phosphite derivatives they were stil able to be identified by ^{1}H NMR and provided samples for monitoring their formation by TLC.

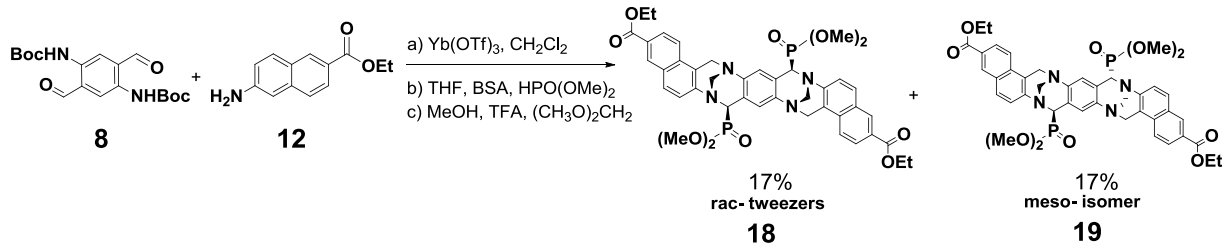


Figure 34: "One pot" molecular tweezers synthetic scheme using $HPO(OMe)_2$

Synthesis to form the desired molecular tweezers built upon the previous procedure in which the bisimine **13** was formed *in situ* followed by the introduction of the aminophosphinating reagents followed by exposure to condition to form the *bis*-Tröger's base skeleton. Synthesis proceeded in one flask starting with **8** and **12**. The formation of the intermediates **13, 16**, and **17** were followed by TLC until the desired products were completely formed. When the desired compound was formed the mixture was concentrated by rotary evaporation and exposured to the next set of reaction conditions without removal of $Yb(OTf)_3$. This proved to be detrimental as the more stable *meso*- isomer **19** was afforded in only 17% yield but a 17% yield the *rac*- isomer **18** was also obtained. Even though this sequence did not

produce an overall increase in yield of the **18** after chromatographic isolation, it did provide an amount of material on par with the protocol utilizing chromatographic isolation in each synthetic step. When the lanthanide was removed prior to cyclization conditions with an EDTA/$NaHCO_3$ solution, yields did not substantially increase.

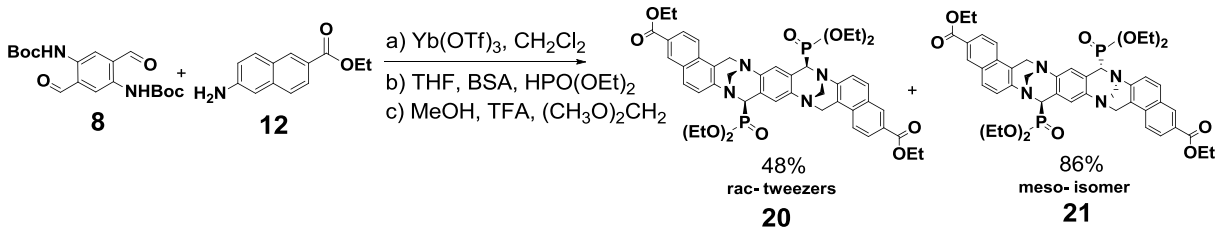


Figure 35: "One pot" molecular twezers synthetic scheme using diethyl phosphite

With the increased stability of the ethyl phosphonate esters previously demonstrated exploration of the “one pot” synthetic method was conducted using diethyl phosphite with removal of the lanthanide before Trögerization. The resulting tweezers isomers were were separated by flash chromatography to afford a substantial increase in yield compared to the dimethyl phosphonate analogues with an average yield of 76% for the *meso*- isomer **21** and 58% average yield for the desired *rac*- isomer **20**. The *meso*- and *rac*- isomers exhibited dramatically different physical properties. For example, the *meso*- isomer was isolated as a crystalline white solid with a fairly high melting point range of 299-303°C while the binding *rac*- isomer is a semi-solid with a low melting point range of 50-60°C.

From these observations and with an appreciable amount of the two isomers now in hand we set about a separation by crystallization. The solubilites of the two were then screened against a panel of solvents. While the *rac*- isomer, **20**, was found to be soluble in all the solvents tested save for hexanes, **21** on the other hand proved to be insoluble or sparingly soluble in

CH_3CN, toluene, ethanol, and EtOAc and could be recrystallized from any of these solvents. When a mixture of **20** and **21** was triturated with EtOAc, toluene, or CH_3CN the *meso*- isomer remained solid and was isolated by vacuum filtration while the desired *rac*- isomer remained in the supernatents. Most attempts to recrystallize the *rac*- isomer failed: addition of hexanes to a solution of **20** in any of the solubilizing solvents caused oiling out. What was found to be an effective method to solidify **20** was to take a solution in toluene (56mL/g) and add it dropwise to ten volumes of stirring hexanes.

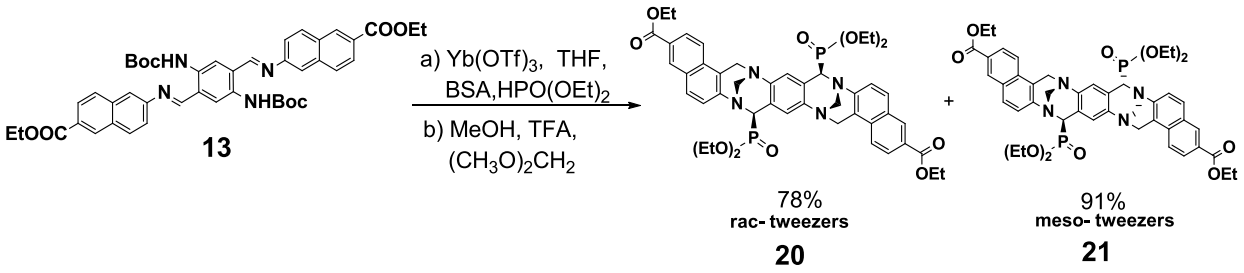
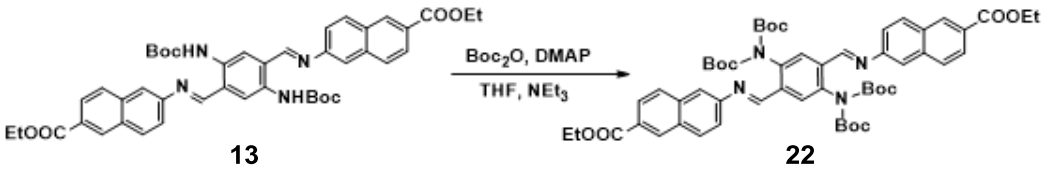


Figure 36: "One pot" tweezers synthesis starting from *bis*-imine

Scale up of the molecular tweezers synthesis was now conducted with an optimized "one pot" procedure and a method of non-chromatographic separation. The synthetic protocol began with the easily isolated and recrystallized *bis*-imine **13** as opposed to forming it *in situ*. This avoids formation of Tröger's base derivative formed from **12**, which required silica gel chromatography for removal. After aminophosphonation, extractive removal of the lanthanide catalyst, and cyclization to form the *bis*-Tröger's bases, the volatiles were removed by rotary evaporation before neutralization. The resulting crude solid was then triturated with hexanes to remove any remaining diethyl phosphite before being triturated with EtOAc to leave behind **21** as a white solid. The EtOAc supernatents were concentrated to dryness, dissolved in toluene, and added dropwise to stirring hexanes to generate the solidified **20**. In the end, an 84% yield

of non-binding *meso*- isomer **21** and a 72% yield of the desired binding *rac*- isomer **20** were afforded. This process was repeated several times to give yields of **21** averaging 86% and **20** averaging 75%.

When this synthesis was done on a 1g scale or above of the *bis*-imine **13** using the developed methodology the transformation to the corresponding *bis*-aminophosphonates was not complete after the usual 18hr time period. Instead, it required three days and additional portions of $Yb(OTf)_3$, diethyl phosphite, and BSA reaching these final concentrations and ratios: $Yb(OTf)_3$= 0.39eq, $7x10^{-3}$M; $HPO(OEt)_2$ = 99eq, 1.8M; BSA = 49eq, 0.9M. This change in behavior was attributed to the increased purity and thus the increased crystallinity of the **13** used as well as a diminishing in the activity of the lanthanide catalystover time. As mentioned previously, the chemical literature thoroughly demonstrates rapid aminophosphonation on time scales up to hours in length. This implies that the catalyst if active in this time frame. Undergraduate Angel Corona added various ligands and attempted to study varying catalyst compositions and stoichiometries to maximize reaction rate. He found a dependence on order of ligand addition and irreproducible rates. Sometimes *bis*-imine **13** was solubilized in minutes, with apparent completion of reaction by TLC in that time. Unfortunately, identical conditions required days for completion if the starting imine did not quickly dissolve. We interpret these results to say that a transient lanthanide complex acts as a much more active catalyst before diminishing over time.



13 22

Figure 37: Scheme for the synthesis of tetraBoc derivative of 13

In an attempt to circumvent the insolubility of the *bis*-imine **13** formation of the tetraBoc derivative was prepared. The reason for this is that the *bis*-imine is a flat, aromatic molecule with a large amount of surface area that allows for a multitude of π-π interactions. If this could be inhibited by reducing its planarity, it would make a poor crystal and more easily dissolve. Addition of another Boc group on the Boc protected nitrogen would eliminate the intramolecular hydrogen bond that enforces the shape. Use of DMAP and Boc_2O in CH_3CN has been shown to accomplish this.[96] The described conditions did not facilitate additional Boc protection which was attributed again to the poor solubility of **13** in CH_3CN. When the solvent was switched to THF, and triethylamine was added, the desired tetraBoc compound was completely formed after 17hr and isolated in 89% yield of **22** by silica gel chromatography. This material was then exposed to the aminophosphonation conditions as a homogeneous solution with the derivative *bis*-imine being consumed after 4hr. Analysis of the mixture by ^{31}P NMR however did not show just the two signals anticipated for the aminophosphonate disastereomers but instead contained ten major peaks in the chemical shift range of the desired materials (δ25-30ppm). This multitude of signals could have arisen from the transfer of a Boc groups from the phenylamine to the naphthylamine. If this were the case it should not prohibit cyclization as the trifluoroacetic acid in the next reaction step would remove the Boc groups. This technique seems promising for efficient conversion of the **13** on a large scale and should be investigated by future researchers. However, due to the number of the signals and ambiguity in interpretation this avenue was not followed up.

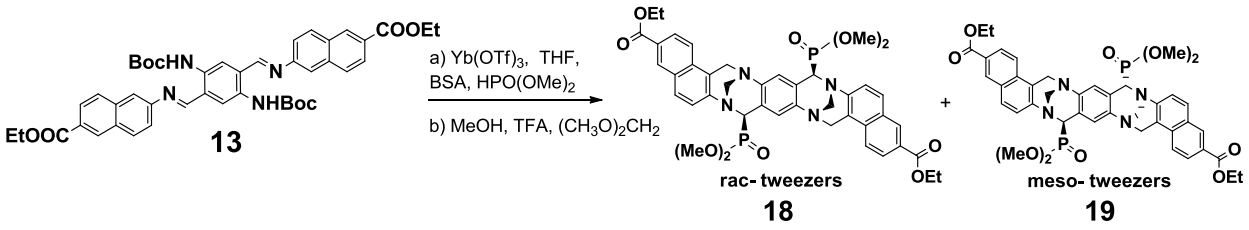


Figure 38: "One pot" synthesis of molecular tweezers using dimethyl phosphite

With a developed "one pot" protocol and the ability to separate the isomers non-chromatographically it was decided to go back to the dimethylphosphonate version of the molecular tweezers. The reason for this would be a simpler ^{1}H NMR spectrum which would allow for unambiguous interpretation when evaluating conditions for phosphonate ester removal. The ^{1}H NMR spectrum for the dimethyl phosphonates exist as two doublets as each of the diastereotopic methyl groups is coupled to the phosphoros nucleus. On the other hand the splitting pattern of the diethyl phosphonates is substantially more complex. Each of the two diastereotopic ethyls has a pair of diastereotopic hydrogens that couple each other, are doubled by the ^{31}P, and coupled into a quartet by the meighboring methyl, yielding 4 sets of ddq for 64 peaks in a 0.2ppm spectral range. The carbethoxy group also has a nearby quartet.

Transformation of **13** on a 1.6g scale to **16** and **17** required the same prolonged reaction time; 11d and four addtions of $Yb(OTf)_3$. The tweezers isomers were separated non-chromatographically using toluene to afford an average yield of 86% **19** and 83% **18**. The desired *rac*- isomer was purified by dissolving in minimal 1,4-dioxane and precipitating by addition of eight volumes hexanes. It was observed that the *rac*- isomer **18** needs to be kept in cold storage as the material appears to degrade if kept at room temperature. This was concluded when old samples of **18**, which were kept at room temperature from four months to

one year were combined with toluene which produced a heterogeneous mixture. The degraded material was able to be separated from intact **18** by vacuum filtration as the degraded material was not soluble in toluene. Investigation into the composition of this degraded material was not pursued as proper storage and separation techniques were indentified, but S_N2 attack at the phosphonate methyl is plausible.

4. Reactions to Generate Water Soluble Molecular Receptors

To turn the molecular tweezers into a water soluble form, the esters need to be removed. Detailed below are the formations of three different water soluble derivatives that vary in the amount and distribution of negative charge on the molecular tweezers. Known synthetic methods were employed to take advantage of the selectivity in ester cleavage based on the atom the ester is connected to. These techniques were also used to make water soluble version of the *meso*- tweezers isomers to serve as a negative control in small molecule titration to evaluate complex formation with the desired *rac*- binding isomer.

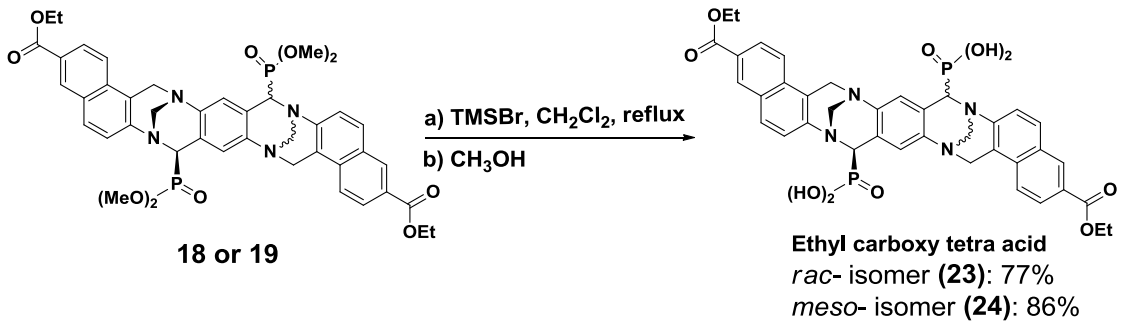


Figure 39: TMSBr deprotection of tweezers isomers to afford carbethoxy tetra acids derivatives

Bromotrimethylsilane (TMSBr) was first described in 1977[97] to selectively cleave alkyl phosphonate esters in the presence of carboxylate esters swiftly at room temperature in high yield. For this reason this method has been used subsequently[98] with demonstrated tolerance

for a multitude of functional groups.[99] The conversion of **18** to the desired carbethoxy tetraacid compound was done with large excesses (10x stoichiometric) of TMSBr in CH_2Cl_2 at reflux for 1.5 to 16h or at room temperature over 22hr without apparent degradation or side reactions. However, this is dependent upon the purity of the TMSBr. If the TMSBr is colorless or a *faint* yellow color removal of the phosphoesters occurred without complication. If the TMSBr was orange in color or darker, which is indicative of Br_2 from HBr formed, the afforded material could not be identified and was concluded to have been degraded. Complete removal of the P-Me esters was determined by NMR spectroscopy when doublets in ^1H at δ4.04 and 3.98ppm disappeared and signals in ^{31}P converged to δ17ppm. After this the volatiles were removed by vacuum in an anhydrous environment to prevent HBr formation until a solid remained after which it was exposed to methanol to remove trimethylsilyl esters. Dealkylation of the *meso*-isomer **19** required refluxing temperature to go to compeletion in a reasonable amount of time but could also be accomplished in 7d at room temperature if time is not a factor. Both of the isomers were purified by dissolving in boiling EtOH, cooling to room temperature, and precipitation with hexanes to yield 77% **23** and 86% **24** respectively.

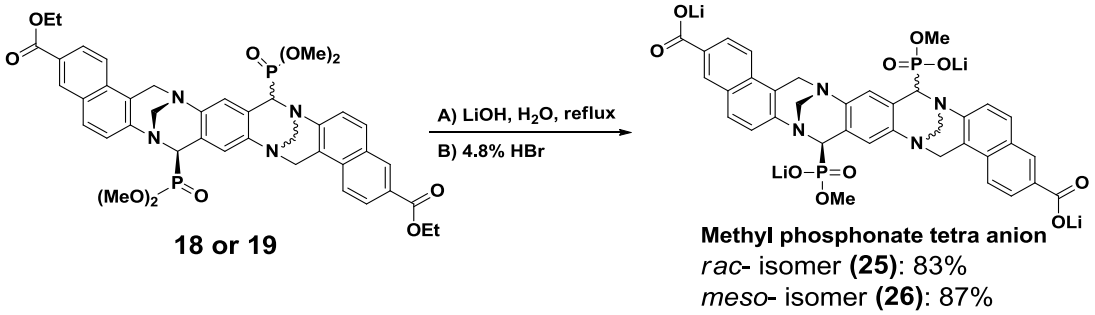


Figure 40: Saponification of tweezers isomers to form the methyl phosphonate tetra anion derivatives

Another water soluble derivative was made when the tweezers isomers were exposed to aqueous hydroxide to saponify the carboxylic esters and selectively remove a single phosphonate methyl ester on each of the phosphonates. Rabinowitz demonstrated this selectivity[100] in dealkylation utilizing aqueous hydroxide at refluxing temperatures over the course of 16h resulting in high yield. The origin of this selectivity is attributed to coulombic repulsion of subsequent hydroxide after the first equivalent breaks the first P-O bond through an addition elimination mechanism.

The saponification procedure was developed using **19** as it was in abundance. Lithium hydroxide was chosen as even though it is the weakest of the alkali hydroxides it can be used in excess as it is readily removed after neutralization with HBr: LiBr is soluble in THF. **19** was mixed with a four fold excess of LiOH in a combination of 1,4-dioxane and D_2O so progress could be monitored by ^1H NMR spectroscopy. TLC analysis would not be able to distinguish the degree of ester removal over time. After 15h all of the desired esters were removed and the absence of the benzyl hydrogen in the aminophosphonate was noted. When submitted to mass spectrometry analysis a m/z of 743 in the negative ion mode and a m/z of 745 were observed suggesting a molar mass of the resulting compound as 744 g/mol. This molar mass is two mass units higher than that of the tetracid form of the saponified *meso*- tweezers which is what seen in MS analysis due to the use of formic acid as the modifier. From this mass increase and lack of signal in the NMR it was determined that H/D exchange occurred on that benzyl position under the aqueous basic conditions before cleavage of the phosphonate ester. This was proved when saponification was performed in H_2O and no loss of benzyl signal was seen and no increase in mass in spectrometric analysis.

The desired saponified tweezers isomers are formed and stable in the refluxing hydroxide solution after 15h after which it is concentrated to dryness to remove the dioxane as to not react with the hydrobromic acid. After redissolving in water, neutralizing to pH7 with 4.8% HBr, and trituration with THF **25** was afforded in 83% yield and **26** was afforded in 87% yield.

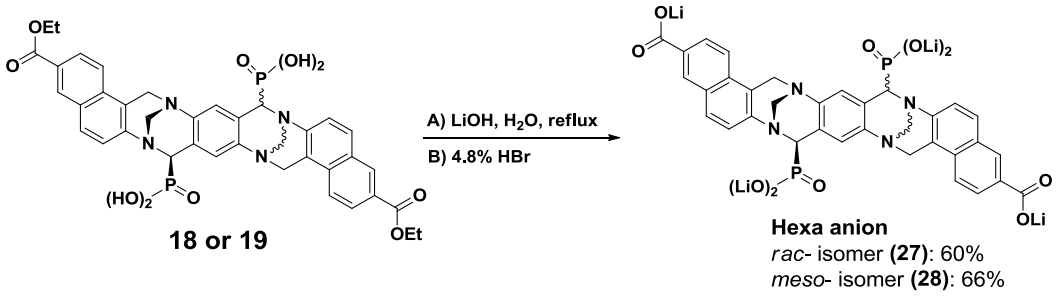


Figure 41: Hexa-anionic tweezers isomers formed by saponification of the TMSBr dealkylated derivatives

The fully deprotected hexa-anionic tweezers were produced by saponification of the bromotrimethylsilane dealkylated water soluble tweezers **18** and **19**. The LiOH saponification protocol described previously was used with saponification complete after 6hr at reflux in the aquoues hydroxide. Neutralization with HBr and trituration with THF afforded **27** in 61% yield and **28** in 66% yield.

C. Characterization of Molecular Receptor Isomers

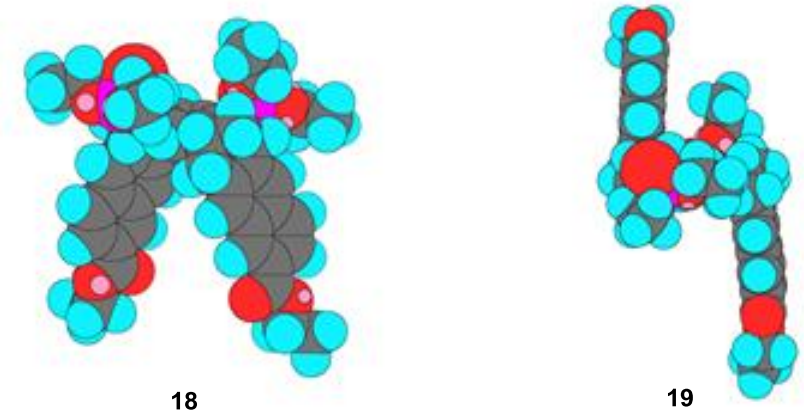


Figure 42: Space filling models for the fully esterified binding *rac*- isomer (left) and the non-binding *meso*- isomer (right)

Isomers **18** and **19** displayed markedly different behaviors when analyzed by ^{1}H NMR spectroscopy. The fully esterified *rac*- isomer **18** was initially difficult to identify as the resonances seen were very broad but at least were in chemical shifts regions consistant for the chemical bonds for the hydrogen atoms in the desired material. In contrast, the *meso*- isomer **19** gave sharp signals in the same region. To test whether the broading is due to binding, dimerization only of **18**, we acquired ^{1}H NMR spectra at various concentrations from 10^{-2}M down to $1.4x10^{-4}$M, roughly the detection limit for the 300MHz Bruker NMR for 30min acquisition time. Over the course of the dilution, the aromatic hydrogens in the naphthalene walls shifted downfield while the aromatic signals in the benzene core shifted upfield with no more apparent movement at concentrations of $3.4x10^{-4}$M and below. This behavior is consistent with the binding, *rac*- form of the molecular receptors self association by the formation of a dimer the inclusion of the naphthalene wall of one molecule of the tweezers into the cavity of another molecule of the tweezers. In dimer formation by this mechanism the

delocalized electrons in the aromatic naphthalene walls from the tweezers would shield the hydrogens on the other copy of the tweezers while the benzene hydrogens would be deshielded by the edge on interaction with the naphthalene quadrupole.

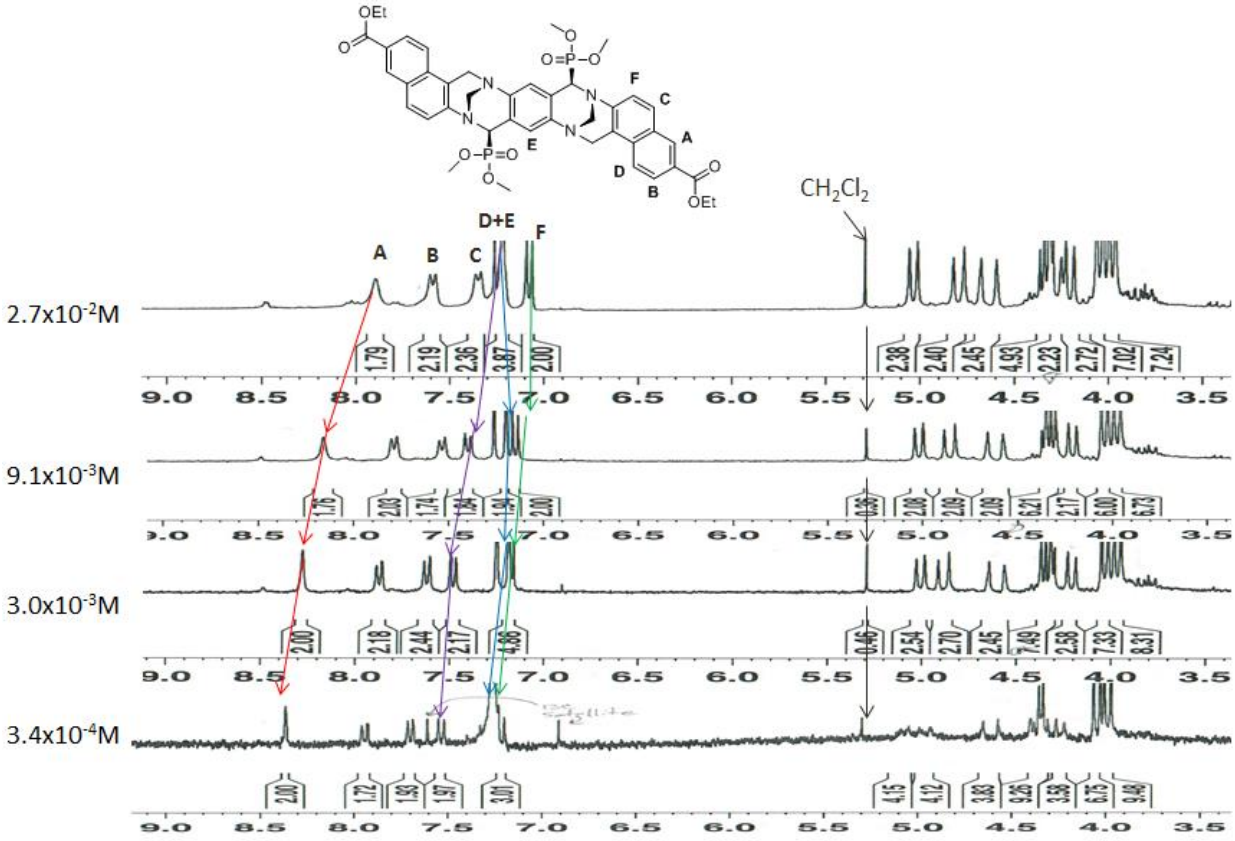


Figure 43: ^{1}H NMR dilution of the fully esterified *rac*- tweezers 18 in $CDCl_3$

From the NMR dilution study the chemical shifts of the naphthalene hydrogens versus concentration were plotted and analyzed via non-linear least squares fit via the derived equation below to see whether the changes are consistent with dimerization and to determine the dimerization constant of **18** in $CDCl_3$. The value calculated from this data was $1.5x10^{-1}$M but it should be stressed that this value is just an estimate based on the number of data points (4) used in the analysis and at least ten data points are required to garner an accurate estimate.

$$H + H \underset{K_{dim}}{\overset{K_a}{\rightleftharpoons}} C \qquad [H_o] = [H] + 2[C]$$

H_o = initial host concentration

$$[C] = ((4[H_o] + K_{dim}) - \sqrt{(8[H_o] * K_{dim} + K_{dim}{}^2)})/8$$

$$\delta_{obs} = \delta_{Ho}\left(\frac{H}{H_o}\right) + \delta_c\left(\frac{2C}{H_o}\right)$$

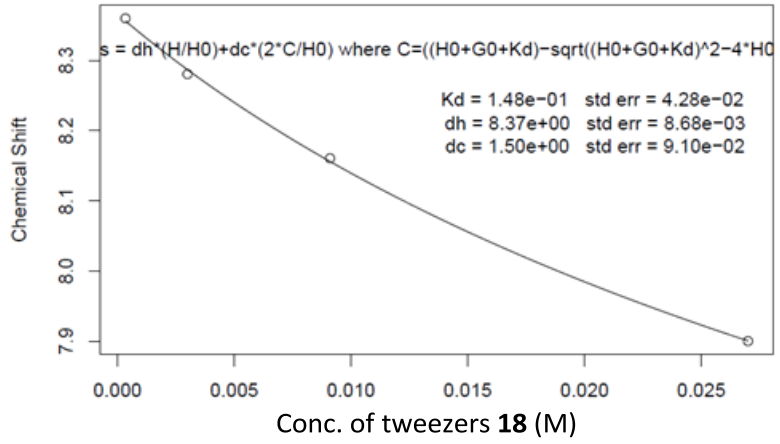


Figure 44: Equation used for the non-linear least squares fit for the dimerization of the fully esterified *rac*-tweezers utilizing NMR chemcial shifts (top) and fit using chemical shift proton A (bottom)

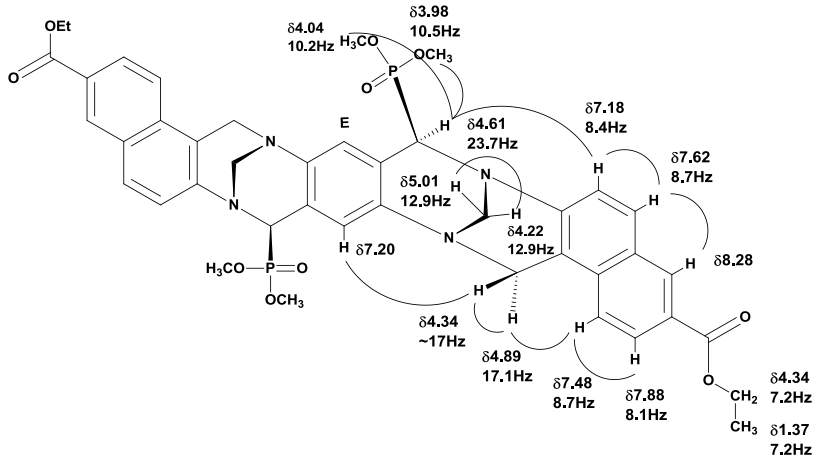


Figure 45: Chemical shifts, coupling constants, and NOESY correlations for the full esterified binding *rac*- isomer 18 in $CDCl_3$ at $3x10^{-3}$M concentration

When at a concentrations that were monomeric the hydrogen signals of *rac*- isomer **18** in the *bis*-Tröger's base skeleton were able to be distinguished by their distinct coupling

constants. The hydrogens on the methylene bridging the two nitrogens had a coupling constant of 13Hz, the hydrogens on the methylene connecting the naphthalene wall exhibited a coupling constant of 17Hz, and the benzyl hydrogen in the aminophosphonate displayed a signal with 23Hz due to its coupling with the phosphorous.

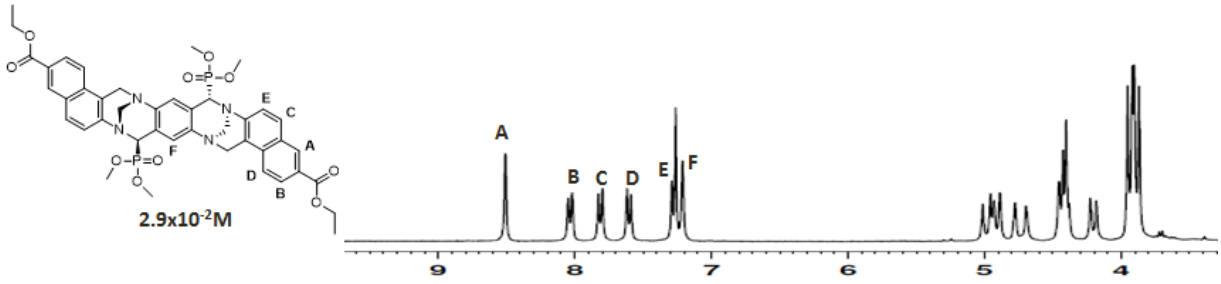


Figure 46: ^{1}H NMR spectrum of the fully esterified non-binding *meso*- tweezers isomer 19

When the ^{1}H NMR spectrum was acquired for the control *meso*- isomer **19** no broadening of the hydrogen signals were observed at concentrations where that phenomenon was seen in the *rac*- isomer. From this it was concluded that *meso*- isomer was not associating with itself while in solution, consistent with our design.

D. Dimerization of Water Soluble Receptor Isomers in Water

1. Analysis by ^{1}H NMR Spectroscopy

All of the water soluble derivatives of the binding *rac*- isomer also showed the propensity for self assembly in aqueous enviornments. This made inital characterization of all of these compounds difficult as in the case of carbethoxy tetra anion **23**, which produced a ^{1}H NMR spectrum containing ill defined singals over broad chemical shift ranges.

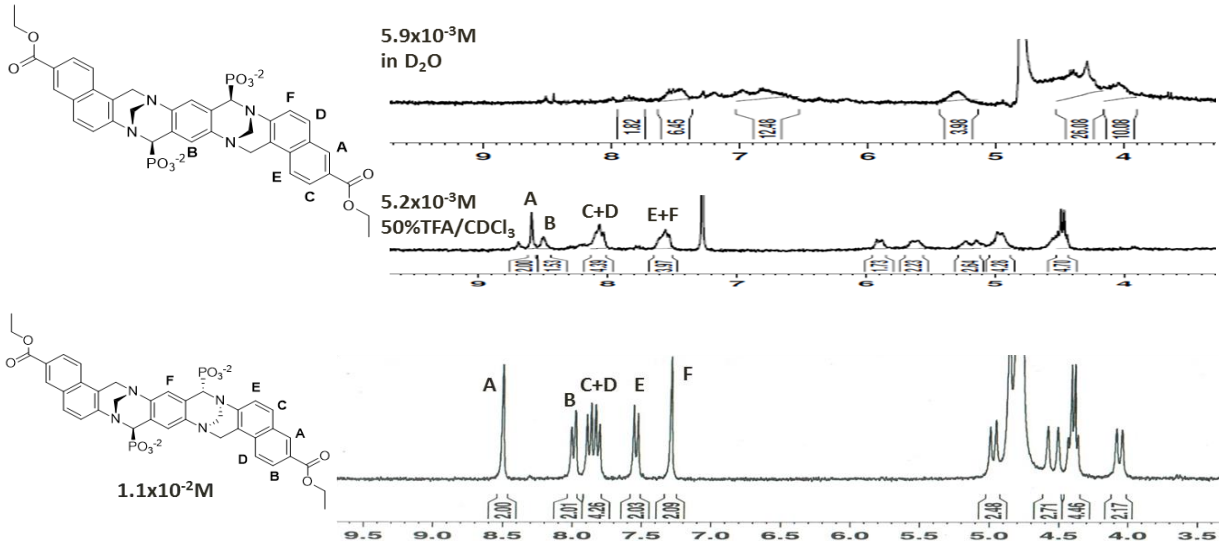


Figure 47: Comparison of the ^{1}H NMR spectra of *rac*- carbethoxy tetra anionic tweezers 23 in D_2O and 50% TFA/$CDCl_3$ versus the non-binding *meso*- isomer 24 in D_2O

The sample in D_2O was exposed to temperatures ranging from 274K to 313K in hopes of increasing the resolution of the peaks by either increasing or decreasing the rate of exchange of the tweezer molecules in dimer formation but this was not observed. This suggests that rapid exchange on an NMR scale is not accessible at a reasonable temperature. Pyridine-d_5 was used as a solvent in effort to produce monomeric species by insertion into the cavity and did seem to work when the concentration of the *rac*- tweezers **23** was around $5x10^{-4}$M but the signals from the residual solvent and their ^{13}C satellite peaks obscured the majority of the aromatic region. DMSO-d_6 was successful in producing a spectrum with resolved aromatic signals but a broad singlet was seen in the spectrum in the 3 to 4ppm range which is in the area needed to evulate if the P-Me esters are absent. What did produce the best results for characterization was dissolving the initially isolated tetra acid **23** in a mixture of 50% TFA in $CDCl_3$. Although not as well resolved as the *meso*- isomer **24**, it produced data sufficient for accurate integration and assignment of the hydrogens. The lack of doublets at δ4ppm with J=10Hz confirms the absence of methyl phosphonates and the efficiency of the TMSBr dealkylation method. The control

meso- carbethoxy tetra anion isomer **24**, like the full esterified form, gave sharp peaks which was interpreted as no self association in D_2O at concentrations ranges equal to or greater than those where the binding *rac*- isomer **23** appears to do so.

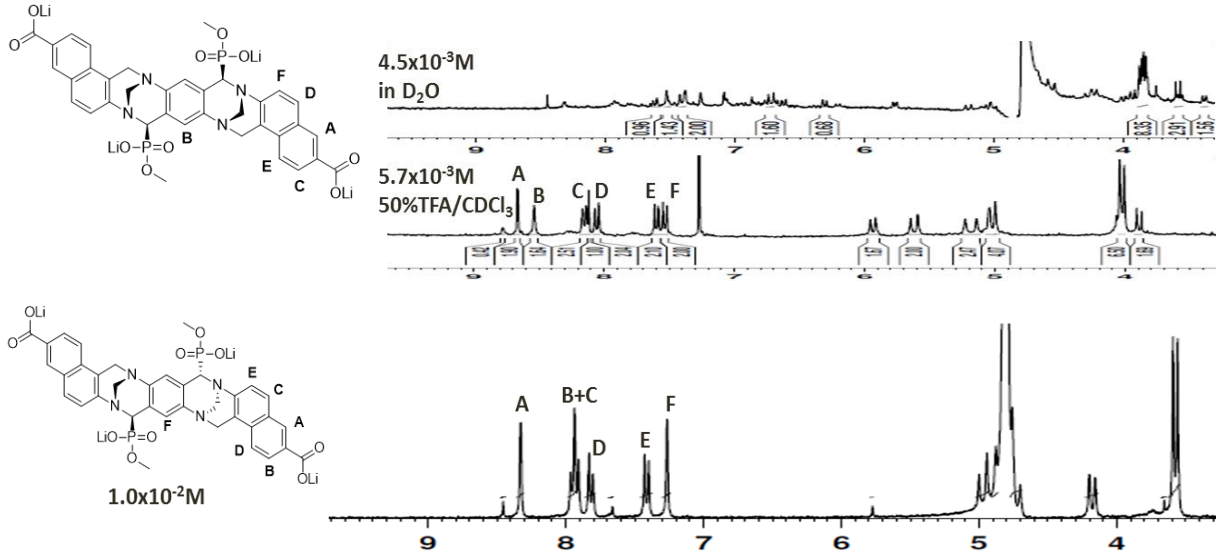
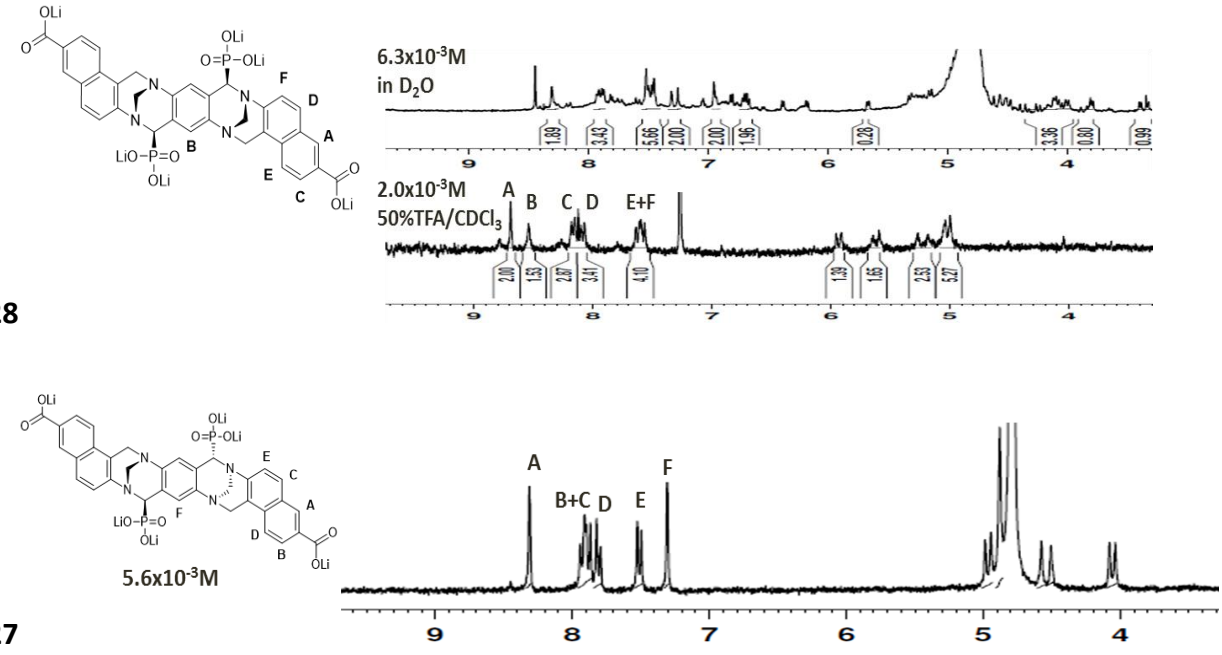


Figure 48: Comparison of the ^{1}H NMR spectra of *rac*- methyl phosphonate tetra anionic isomer 25 in D_2O and 50% TFA/$CDCl_3$ versus the non-binding *meso*- isomer 26 in D_2O

As opposed to **23**, the *rac*- methyl phosphonate tetra anionic tweezers **25** when in D_2O did not produce broad signals but an array of signals presumed to be a mixture of species that are exchanging with each other in solution. This presumably is able to occur as this saponified form of the molecular tweezers has an energentic barrier to dimerization from the negatively charged carboxylates on the edges of the naphthalene. The ^{1}H NMR is consistent with the desired cleavage by hydroxide having taken place. The ^{1}H NMR simplified slightly upon dilution in D_2O but not to the point of producing a single set of signals. Use of 50% TFA/$CDCl_3$ in NMR analysis was able to produce a well resolved set of signals that allowed for characterization of **25**. It appears that the molecule is not stable to strongly acidic conditions: an impurity forms

showing a doublet at δ3.9ppm with J=11Hz in proximity to the methyl phosphonate signal. This may be due to partial transformation of the Tröger's Base skeleton.

This phenomenon also occurs for the *meso*- isomer **26** in 50% TFA/$CDCl_3$ but it is not required as like the other control isomers affords well resolved NMR spectra at mM concentratons. The residual solvent signal in D_2O however does reside in the same chemical shift range of the Tröger's base signals and 50% TFA/$CDCl_3$ is needed to see these resonances as the residual solvent signals in this mixture do not mask them. After replicating the saponification procedure for both isomers multiple times the intregrity of the Tröger's base skeleton remained intact under the alkaline conditions with the TFA/$CDCl_3$ needed only to absolutely confirm the structure.



28

27

Figure 49: Comparison of the ^{1}H NMR spectra of *rac*- hexa anionic tweezers 27 in D_2O and 50% TFA/CDCl3 versus the non-binding *meso*- isomer 28 in D_2O

The binding *rac*- **(27)** and control *meso*- **(28)** isomers for the fully deprotected hexa anionic derivative exhibited the same behavior in D_2O and 50% TFA/$CDCl_3$ as their other water soluble counterparts. The set of signals in D_2O were less braod than that of the methyl phosphonate tetra anion and did seem to coalesce to a single set between $6.3x10^{-4}$ and $6.3x10^{-5}$M but a sufficient signal to noise ratio required to assign the peaks could not be achieved.

2. Analysis by Fluorescent Spectroscopy

BACKGROUND AND GENERAL PROCEDURES

As ^{1}H NMR spectroscopy could not be used at sufficiently low concentrations to determine a dimerization constant for the water soluble tweezers varieties, fluorescent spectroscopy was used. This technique would allow for the dilution of the tweezers to concentrations below the level of detection of NMR by monitoring its fluorescent emission. It is expected that the dimerized complex and the free monomeric species would emit differently to allow to for a way to identify the concentration in which dimerization occurs. A deviation from linearity in fluorescent emission upon dilution of the tweezers would provide evidence of association. If a single species exists in solution its fluorescence will decrease proportionally with concentration with a constant excitation wavelength as described by the Beer-Lambert Law.

$$H + H \underset{K_{dim}}{\overset{K_a}{\rightleftharpoons}} C \qquad [H_o] = [H] + 2[C] \qquad [C] = \frac{1}{2}([H_o] - [H])$$

H_o = initial host concentration

$$[H] = [Ho] - 2[C]$$

$$K_{dim} = \frac{[H][H]}{[C]} = \frac{([H_o] - [C])([H_o] - [C])}{[C]}] = \frac{[H_o]^2 - 4[H_o][C] + 4[C]^2}{[C]}$$

$$= 4[C]^2 - [C](4[H_o] + Kdim) + [H_o]^2 = 0$$

$$[C] = ((4[H_o] + K_{dim}) - \sqrt{(8[H_o] * K_{dim} + K_{dim}^2)})/8$$

$$I = Ih([Ho] - 2[C]) + Ic[C]$$

Figure 50: Derivation of the equation used to determine K_{dim} for the dimerization of the binding *rac*- tweezers by fluorescence spectroscopy

Correction of fluorescencefor screening of exciting light was used. In cases where the absorbance of the tweezers isomers were above a value of 0.1 the intensity of the fluorescent emission was corrected using the equation of I=I*10^(A/2). The term of A/2 was used to compensate for the dimunition of emission produced at a point halfway through the sample where fluorescence is monitored. This correction factor was used only for absorbance values between 0.1 and 0.2 as values corrections exceeding 0.2 will be inconsequential.

Carbethoxy tetra acid tweezers 23

The Ocean Optics SD2000 was initially used in trying to determine monomeric concentrations of the *rac*- carbethoxy tetra anion tweezers **23** which was irradiated with broadband light centered at 365nm. A 7.2×10^{-2}M solution in 10mM pH7 phosphate buffer was serially diluted by a factor of 2 until a final concentration of 7.0×10^{-5}M was reached. Linear decrease in fluorescent emisson was observed from 2.25×10^{-3}M and lower by monitoring the emission maximum (495nm) of the tweezers. Fluorescence was non-linear in range of 7.2×10^{-2} to 2.25×10^{-3}M with fluorescence increasing upon dilution. This linearized using our screening

correction of the exciting light and not from dimer to monomer transition. The Fluorolog-3 fluorimeter was used subsequently to test concentraton ranges below the level of detection of the Ocean Optics, with more control of excitation wavelength.

23 was dissolved in an aqueous solution containing 150mM NaCl and 10mM pH7 phosphate buffer and serially diluted by factors of 1/3 from an intial concentration of 2.50×10^{-5} to a final concentration of 2.89×10^{-7}M. Spectra were acquired using an excitation wavelength of 300nm. A broad emission centered at 445nm was seen down to 10^{-7}M. A plot of tweezers concentration versus fluorescent emission at 445nm showed a linear correlation in the decrease in emission.

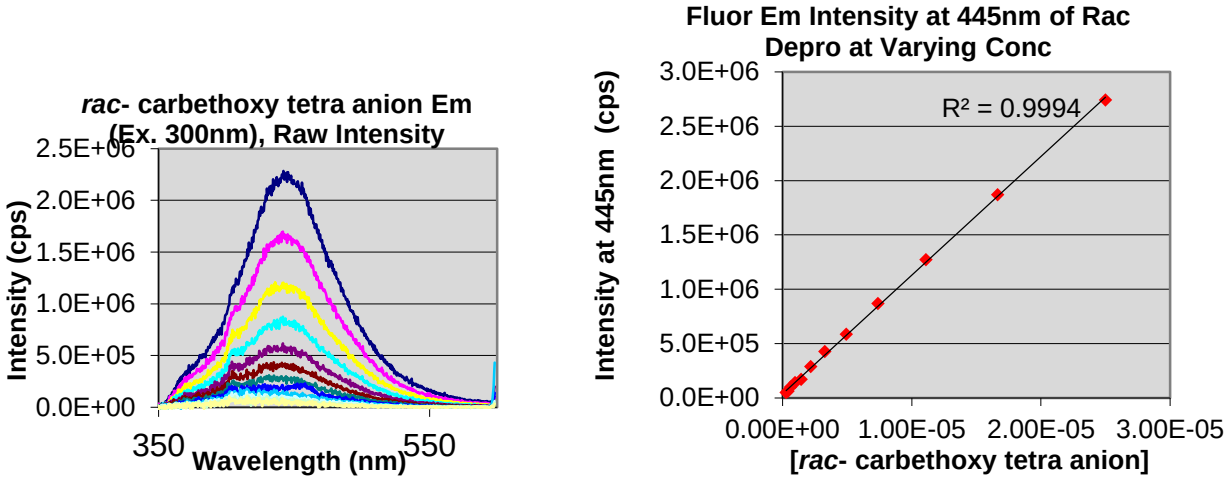


Figure 51: Plot of fluorescent emission (445nm) versus concentration for *rac*- carbethoxy tetra anion 23 tweerzers using 300nm excitation

This is consistent with a single species present over this concentration range, either monomer or a dimeric. **23** is expected to dimerize most strongly and if it is dimeric, the $K_{dim} < 3 \times 10^{-7}$M the limit of detection for this compound with the Fluorolog fluorimeter.

Methyl phosphonate tetra anion isomers 25 and 26

It is expected that the methyl phosphonate tweezers, bearing carboxylate anions on their walls, should not dimerize as readily. To keep ionic strength roughly constant an aqueous solution of 150mM NaCl and 10mM pH7 phosphate buffer was used in the dilution studies. Dimerization behavior was again evaluated using deviation from linearity in fluorescent emission with dilution. Using 300nm excitatation the emission spectrum of the binding isomer displayed a fine structure with emission maxima at 405 and 430nm. The *rac*- methyl phosphonate tetra anion isomer **25** was diluted from $2.5x10^{-5}$M to $4.3x10^{-7}$M. A plot of fluorescence at 405nm versus tweezers concentration made made and analyzed using the non-linear least squares fit to determine K_{dim}. Although it converged it produced error of equal value to the dimerization constant (K_{dim} = $1.9x10^{-4}$M ± $2.1x10^{-4}$M) which makes sense as the plot of fluorescence vs. concentration appeared to have only a slight curvature to it, and dimer would be mostly dissociated even at the highest concentration.

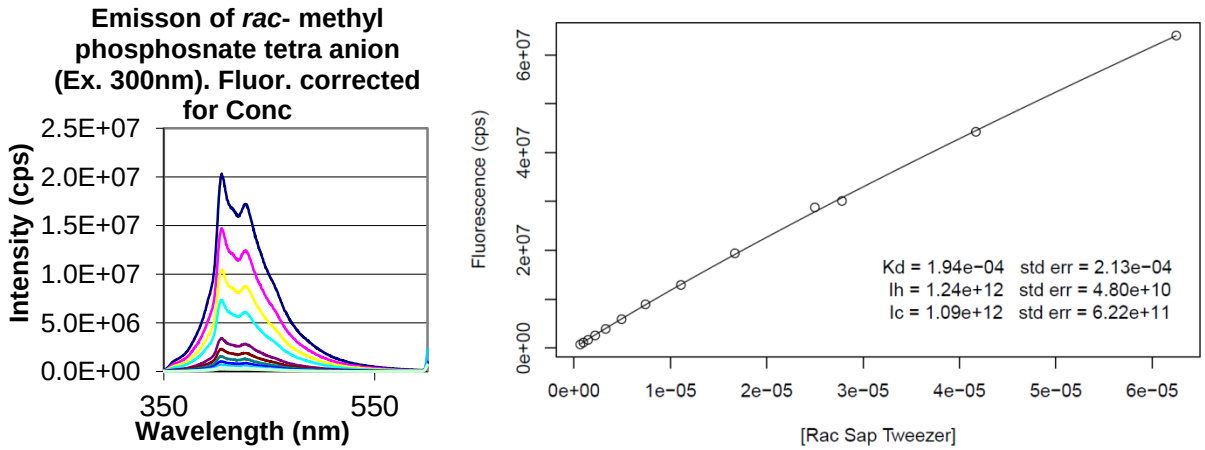


Figure 52: Fluorescence of *rac*- methyl phosphonate tweezer displaying fine structure at 300nm excitation

This result from the concentration range tested again is suggestive of a single species in solution while being diluted. Using 300nm excitation, concentrations above $2.5x10^{-5}$M could not be studied because of screening of light. Dilution was repeated using the ionic solution over the range of $2.5x10^{-4}$ to $1.5x10^{-5}$M which was anticipated to be a regime in which dilution would facilitate the change from dimer to monomer. The plot of fluorescent emission at 430nm versus *rac*- isomer concentration produced a line with slightly more curvature resulting in a K_{dim} of $4.5x10^{-4}$M ± $9.8x10^{-5}$M with the standard error being satisfactory for the value for K_{dim}. This suggests a significant association of the tweezers to form a dimer, overcoming a substantial amount of coulombic repulsion in the process.

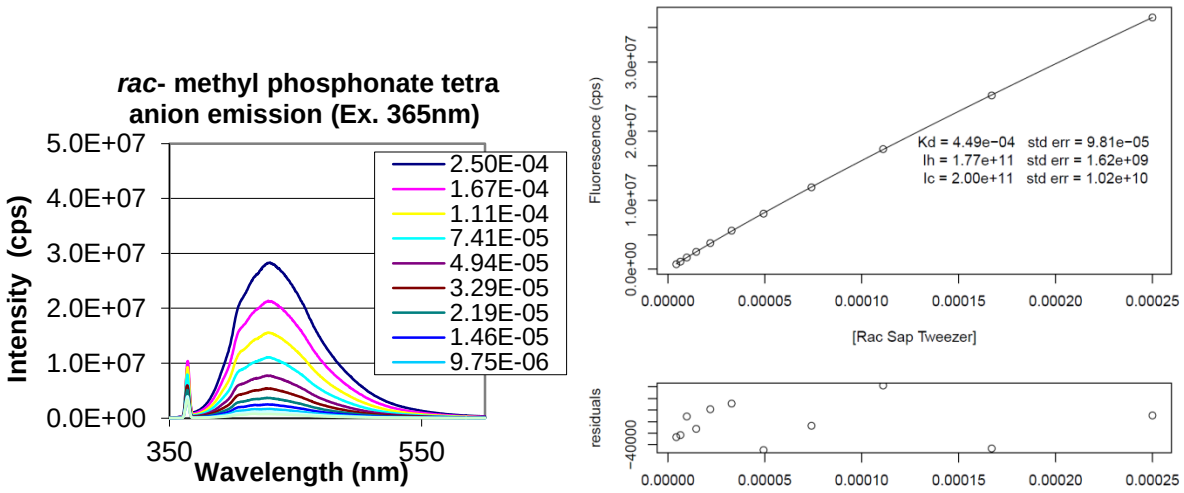


Figure 53: Fluorescent emssion and plot of fluorescence (430nm) versus concentration for *rac*- methyl phosphonate tetra anion tweezers 25

From these data it appears that fluorescence spectroscopy is limited in its ability to determine a dimerization constant with low standard error using 300 and 365nm light. 345nm excitation light however may be just right if this dilution is to be repeated as it might allow for solutions of high enough concentration to contain predominantly dimer but not have the rapidly diminishing emission upon dilution so that concentrations lower than $1.5x10^{-5}$M can be

investigated. The ideal concentration range to study dimerization would span from 80% dimer to 80% monomer, but this method is limited to 50% dimer. Dimerization was subsequent investigated by UV-Vis spectroscopy and will be discussed in a later section

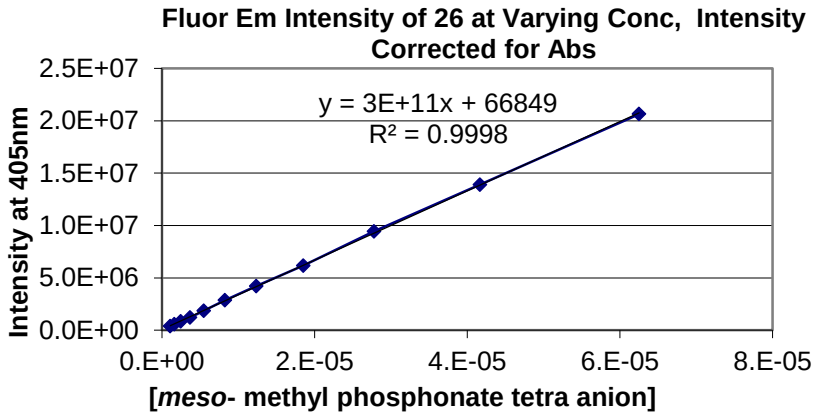


Figure 54: Plot of concentration vs. fluorescence for *meso*- methyl phosphonate isomer 26

The control isomer, *meso*- methyl phosphonate tetra anion **26**, was diluted form 2.5×10^{-4}M to 4.3×10^{-6}M but only data from 6.25×10^{-5}M and below were used in the plot of emission at 405nm vs. concentration as absorbance values for concentrations above that were above 0.2 using 300nm excitation. As anticipated the resulting plot was linear and was able to converge when fit to a non-linear least squares model producing a K_{dim} of 1.9×10^{-7}M $\pm$ 6.8×10^{-6}M. The enormous error range indicates that this behavior is not appropriately modeled by dimerization. The standard amount of error was an order of magnitude larger than the derived value and linear decrease of fluorescence are consistent with the behavior.

To confirm that the *meso*- isomer was not self associating, the fluorescent emission with variable excitation of a 1.8×10^{-4}M solution of the control *meso*- isomer was monitored. As seen previously with the *rac*- isomer **25**, different excitation wavelengths produced different shapes in the fluorescent emission spectrum due to the differences in the absorbance of either the

dimer or monomer. If only a single species is present then a change in fluorescent intensity would be expected with no change in the shape of the emission spectrum.

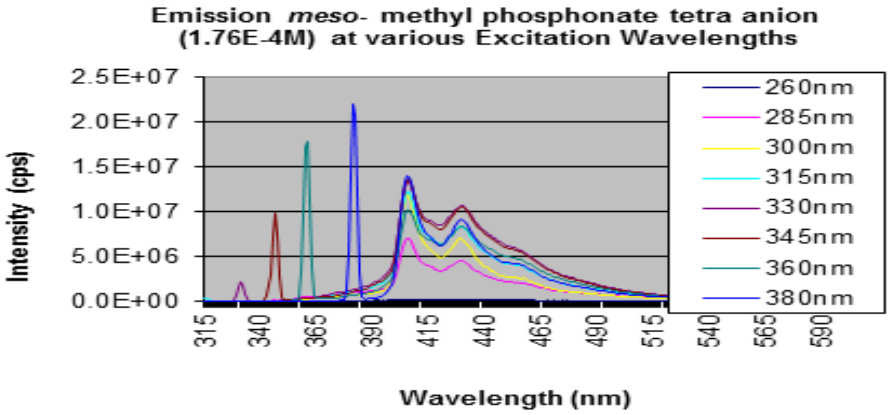


Figure 55: Fluorescent emission of control *meso*- methyl phosphonate tetra anion 26 at various excitation wavelengths plotted to include excitation wavelengths

This is exactly what was observed. Fluorescence increase from 260 to 315nm as screening of the light went away and fluorescent intensity diminished with the longer wavelengths supporting what was observed with NMR that the control *meso*- isomer is not dimerizing when in solution.

Hexa-anions 27 and 28

The final water soluble derivative, the fully de-esterified hexa-anion **27** is expected to dimerize the weakest. It was diluted in the same manner to determine the dimerization equilibrium contrant. Using the solution of 150mM NaCl and 10mM pH7 phosphate buffer to dilute to mitigate the change in ionic strength the *rac*- hexa anion was diluted from $2.5x10^{-4}$M to $1.7x10^{-7}$M using 345nm excitation. The emission at 405nm versus tweezers concentration produced the greatest deviation from linearity in the plot and when fit to the dimerization equation it produced a $K_{dim} = 1.2x10^{-4}M \pm 9.0x10^{-6}M$.

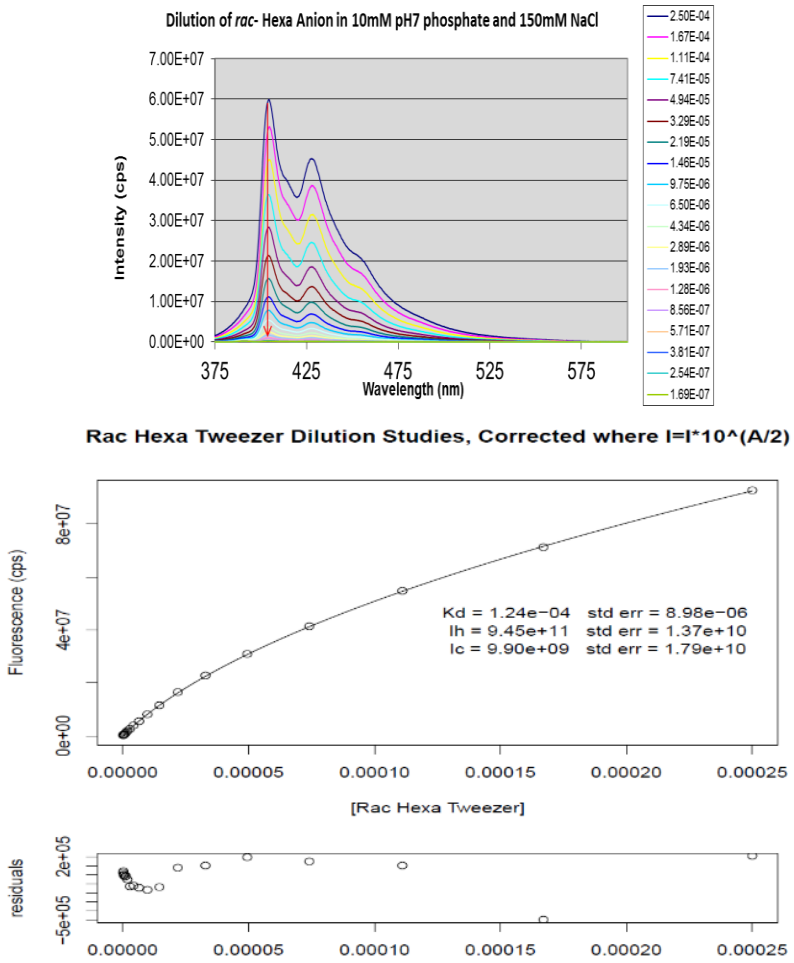


Figure 56: Fluorescent emission and plot of emission (405nm) vs. concentration for *rac*- hexa anionic tweezers using 345nm excitation

From the small error in the K_{dim} value it shows that the model is appropriate in describing the observed phenomenon. The binding *rac*- hexa anion **27** also has the weakest K_{dim} of the three due to the not only the carboxylates on the edge of the tweezers providing the coulombic barrier but also from having the greatest amount of negative charge per tweezers molecule. The average amount of negative charge per hexa- anion in solution at pH7 is presumably that of a penta-anion when comparing it to other *bis*-aminophosphonic acids.[101] Overcoming coulombic repulsion to dimerize a penta-anion at 10^{-4}M implies a significant association.

The control *meso*- isomer **28** was evaluated using the same protocol for dilution monitored by fluorescent emission as the *rac*- isomer. When the plot of emission at 405nm versus *meso*- isomer concentration was fit it was able to converge but produced a value or error greater in magnitude for the calculated K_{dim}. This again demonstrated that dimerization is a poor model for characterzing the decrease in fluorescence and that the control *meso*- isomer does not complex with itself in aqueous media.

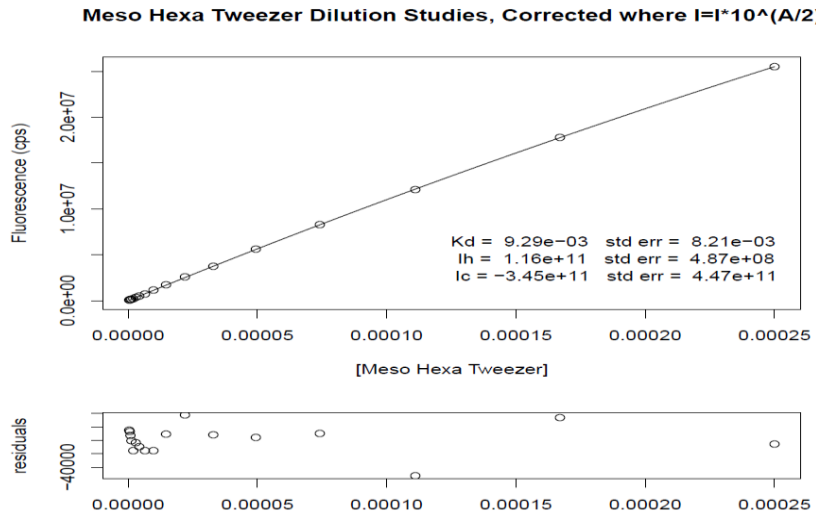


Figure 57: Plot of fluorescent emission (405nm) versus concentration for the control *meso*- hexa anionic isomer using 345nm excitation

3. Analysis by UV-VIS Spectroscopy

<u>Methyl phosphonate tetra anion 25 and 26</u>

In the effort to find a more convienient alternative to fluorescence for determing dimerization UV-Vis absorbance was investigated. Absorbace spectra for the binding *rac*- **(25)** and control *meso*- **(26)** isomers were monitored over a concentration range of$4.4x10^{-4}$M to $3.4x10^{-6}$M using water containing 150mM NaCl and 10mM pH7 phosphate buffer as the diluent.

Exctinction coeffiencts were calculated for each wavelength by dividing the absorbance spectrum by the concentration of the sample. Plots of wavelength versus these epsilon values at each concentration were constructed. What was seen from this was that at 297nm there were deviation in epsilon for the *rac*- isomer whereas no deviation was seen in the *meso*-isomer at the same wavelength providing another spectroscopic example a difference in behavior for the binding *rac*- isomer **25** and control *meso*- isomer **26**.

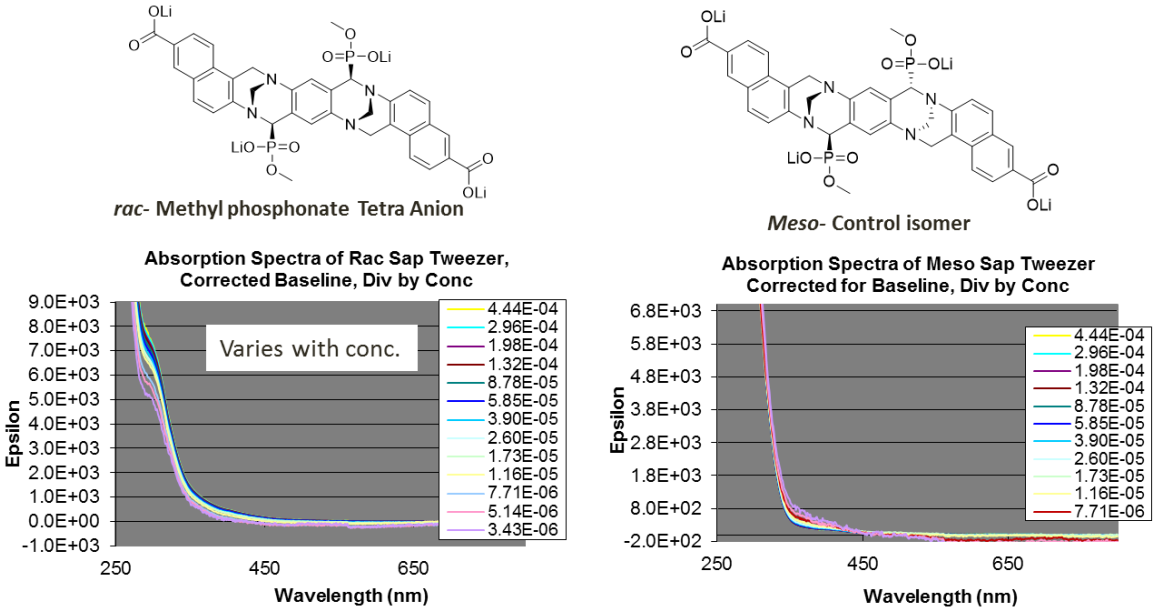


Figure 58: Plot of wavelength vs. epsilon for the binding 25 (left) and the control 26 (right) methyl phosphonate tetra anion isomers

The concentraton **25** versus calculated epsilon was plotted and fit using non-linear least squares. The equation used was the same as that for determining K_{dim} using NMR except epsilon values were used instead of chemical shifts. Unfortunately, when fit it produced errors larger than the K_{dim} value but this is not due to dimerization being a poor model. When analyzing the fit, it showed that the majority of the data did not fall on the actual curvature which is required for an accurate calculation. If this dilution study were to be repeated,

absorbance data at concentrations below $7x10^{-6}$M need to be acquired to collect more data points and to get closer to the predicted K_{dim} value.

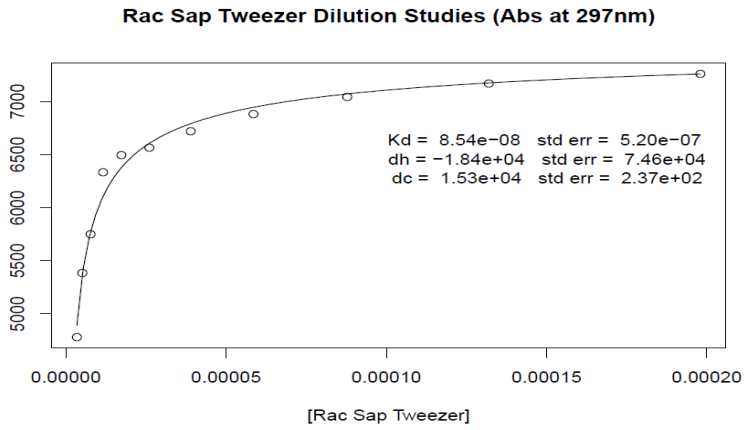


Figure 59: Plot of concentration vs. epsilon for 25 fit by non-linear least squares

E. Binding Studies of Molecular Receptor by Small Molecule Titration

Titration of the water soluble *rac*- binding molecular tweezers and the *meso*-nonbinding control isomer were carried out by fluorescence spectroscopy, monitoring the decrease in fluorescent emission of the tweezers isomer upon titration of the small molecule guest. Guest solutions contained the tweezers isomer at the same concentration as the solution of tweezers isomer being evaluated as not to dilute the tweezers isomer upon addition of the titrant. Fluorescent emission of the host was monitored at a particular wavelength with increasing guest concentration and fit to the equation below which models a 1:1 binding interaction and fit using non-linear least squares to determine the dissociation constant (K_d) of the complex. Adherence to this model would be consistant with decrease in fluorescence by static (intramolecular) quenching. This could be confirmed with fluorescence lifetime

measurements of the host as the fluorescence lifetime of the complex will not change with increasing concentration of the small molecule.

$$H + G \underset{K_d}{\overset{K_a}{\rightleftharpoons}} C$$

$$K_d = \frac{[H][G]}{[C]}$$

$$H_o = [H] + [C]$$

$$G_o = [G] + [C]$$

$$I = I_o[H] + I_c[C]$$

$$K_d = \frac{[H_o - C][G_o - C]}{[C]} \rightarrow [H_o][G_o] - ([H_o] + [G_o])[C] + [C]^2 = K_d[C]$$

$$[C] = \frac{([H_o] + [G_o] + K_d) - \sqrt{([H_o] + [G_o] + K_d)^2 - 4[H_o][G_o]}}{2}$$

$$I = I_o([H_o] - [C]) + I_c[C] = I_o[H_o] - I_o[C] + I_c[C] = I_o[H_o] + (I_c - I_o)[C]$$

$$\rightarrow I_o[H]_o + \frac{Ic - Io}{2}([H_o] + [G_o] + K_d) - \sqrt{([H_o] + [G_o] + K_d)^2 - 4[H_o][G_o]})$$

Figure 60: Derivation of equation used to determine K_d in small molecule binding titrations where H=host, G=guest, and C=complex

The fluorescent data were also fit to the Stern-Volmer equation which models dynamic (intermolecular) quenching of fluorescence with adherence to this model is taken as evidence of intermolecular quenching. Use of fluorescent lifetime measurements could be used if required to confirm dynamic quenching as the fluorescent lifetime of the host molecule will decrease with increasing concentration of the small molecule.

$$\text{Stern-Volmer Equation} \qquad \frac{I_o}{I} = 1 + kt[Q]$$

Figure 61: Stern-Volmer equation where I_o= intial fluorescence, I= fluorescene with quencher present, k=quencher rate coefficient, and t=lifetime of the exicted state of the emitting molecule

1. Carbethoxy tetra anion isomers 23 and 24

The titrations of **23** with the small molecules described below were conducted using an Ocean Optics SD2000 fiber optic spectrometer. The titrations of the water soluble tweezers were conducted at concnetrations ($5x10^{-5}$ and $1x10^{-5}$M where the self associated dimer predominates. As a consequence, the titrants are presumably in competition with the binding pocket of the dimer .

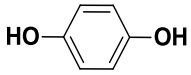
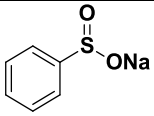
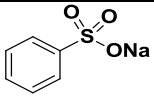
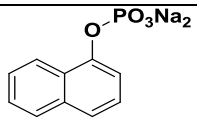
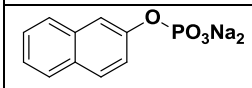
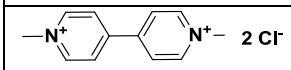
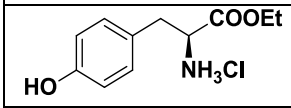
Substrate	Apparent K_d (M) (Titration Medium)
	$2.3x10^{-2}$± $1.6x10^{-3}$ (10mM pH7 phosphate buffer)
	$3.7x10^{-2}$± $1.6x10^{-2}$ (10mM pH7 phosphate buffer)
	>$5.5x10^{-2}$ (10mM pH7 phosphate buffer) $3.2\ x10^{-2}$± $1.2x10^{-1}$ (10mM pH7 phosphate buffer)
	$1.2\ x10^{-3}$± $3.5x10^{-4}$ (10mM pH7 phosphate buffer) $1.4x10^{-3}$± $4.8x10^{-4}$ (10mM pH7 phosphate buffer)
	$8.3\ x10^{-4}$± $3.3x10^{-4}$ (10mM pH7 phosphate buffer) $2.6x10^{-3}$± $7.0x10^{-4}$ (10mM pH7 phosphate buffer)
	$3.6x10^{-3}$± $3.0x10^{-4}$ (10mM pH7 phosphate buffer) $2.4x10^{-3}$± $2.7x10^{-4}$ (10mM pH7 phosphate buffer)
	$3.0x10^{-3}$± $7.0x10^{-4}$ (100mM pH7 phosphate buffer)

Table 2: Observed dissociation constants from the titration of the proposed *rac*- carbethoxy tetra anionic tweezers 23 dimer

Hydroquinone and sodium benzenesulfonate were determined to not bind with the dimer. It was concluded that hydroquinone was not able to bind strongly enough into the molecular tweezers to compete with the dimer as evidenced by its adherence to Stern-Volmer behavior. The sodium benzensulfonate was speculated to not bind because it has too much

steric bulk in proximity to the benzene group. Results from sodium benzenesulfinate titration are suggestive as being able to intecalate into the binding cavity as it did not display a Stern-Volmer relationship but the calculated dissociation constant had fifty percent error. The naphthylphosphates and methyl viologen both appear to bind as they both fit to the binding equation and both deviate from Stern-Volmer behavior. Interestly enough, both of these substrates have dissociation constant on par with one another yet they are oppositely charged supporting the hypothesis that the carbethoxy tetra anion binding isomer is dimeric.

The preliminary study was continued by selecting the cationic guests, methyl viologen and L-tyrosine ethyl ester hydrochloride, and performing titrations with the *meso*- nonbinding control isomer **24** to determine if the differences in fluorescent quenching would demonstrate binding behavior in the *rac*- binding isomer.

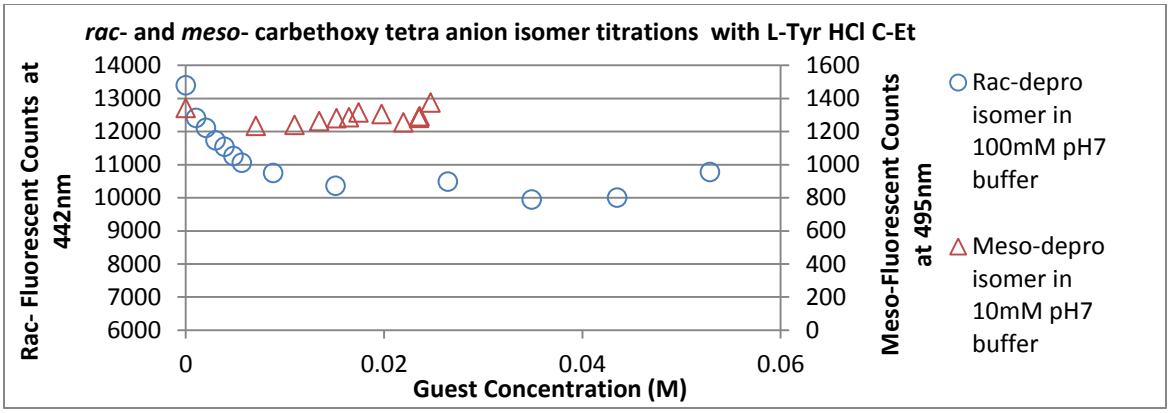


Figure 62: Titration of *rac*- and *meso*- carbethoxy tetraanion isomers with L-Tyr Et ester HCl

When the concentration of L-Tyr ethyl ester hydrochloride versus fluorescent intensity of the tweezers isomers were plotted on the same graph **23** seemed to exhibit binding behavior by the curvature in decrease in fluorescence and its deviation from linearity in the Stern-Volmer plot. From the results of later titrations with cationic guests and the methyl

phosphonate form of the molecular tweezers it was concluded that the guest molecule was likely to be associated with the dimer coulombically not being inserted into the binding isomer's cavity. The fluorescence of **24** stayed fairly constant but increased with increasing concentration of the titrant. It also did not exhibit Stern-Volmer behavior as the value of I_0/I decreased, not increased, with increasing guest concentration. This behavior is counterintuitive as this data suggests that addition of L-Tyr ethyl ester HCl is able increase the fluorescence of the *meso*- isomer by some mechanism as the guest does not emit at the excitation wavelength used to irradiate the non-binding isomer. It is speculated that the *meso*- isomer **24** is not complexing with the guest molecule but the results unfortunately do not provide the evidence for it.

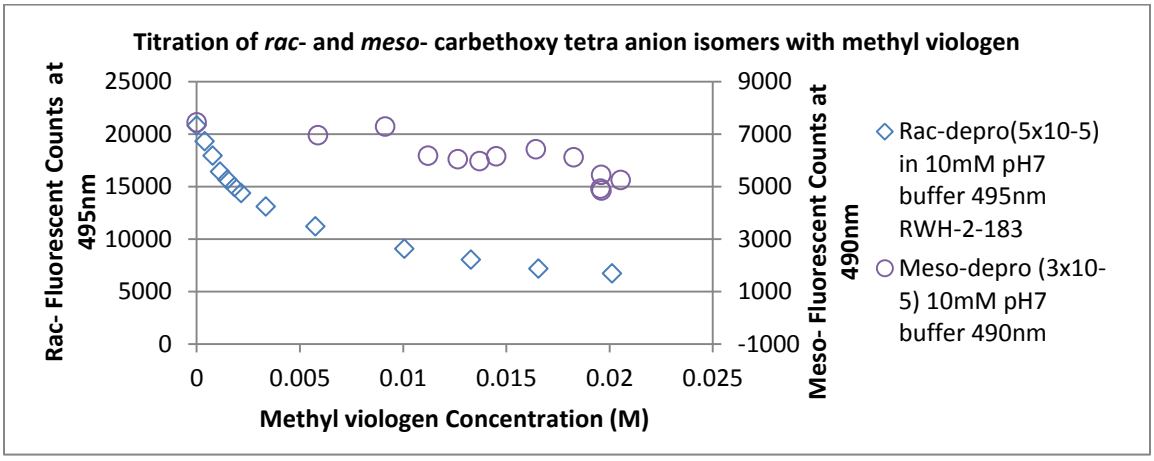


Figure 63: Titration of *rac*- and *meso*- carbethoxy tetraanion isomers with methyl viologen

Titration of the *rac*- and *meso*- carbethoxy tetra-anionic isomers displayed similar fluorescent behavior when titrated with methyl viologen. *Rac*- tweezers **23** appears to be binding methyl viologen by fitting to the 1:1 binding equation and not following Stern-Volmer behavior. However, the quenching of fluorescence for the binding isomer appears to be extrapolating to zero with increasing quest concentration. This is rationalized by having not only

the intramolecular form of quenching occurring but also the quenching of of the fluorescence of the complex by intermolecular collision and can be seen in the later half of the titration by an apparent linear decrease in emission. What was expected to be seen on binding however would be a shift in fluorescent emission by formation of a charge transfer complex between the two but this phenomenon was not observed. This suggests that the methyl viologen is associating tightly to the exterior of the tweezers dimer in the low ionic strength of the titration medium to form a complex that is an ion pair. The control isomer **24**'s behavior was consistent with its structure by an overall linear decrease in fluorescence, non-convergance to the binding isotherm, and adherence to the Stern-Volmer relationship. Interestingly when compared to the *meso*- control of the methyl phosphonate tetra-anion, whose decrease in fluorescent emission when titrated with cationic guests mimicked binding, the *meso*- carbethoxy analogue did not. There is no explaination for the difference in the behavior at this time.

As the binding affinities afforded from the titrations were of the same approximate value, it was concluded that the guests were not binding into the cavity of the tweezers.

2. Methyl phosphonate tetra anionic isomers 25 and 26

Fluorescent titrations where conducted on a Fluorolog-3 Model FL3-22 by Horiba Jobin-Yvon using nanopure water as the titration medium. Concentrations used for titration for the *rac*- binding and *meso*-control isomers were either 5.0×10^{-6} or 5.0×10^{-7}M which were assumed to be predominated by monomeric species. This assumption was supported by observing the fluorescent emission of **25** at various excitation wavelengths. If a single species is present,

change in excitation wavelength should change the intensity of the emission but not change the shape of the emission profile which is what was observed.

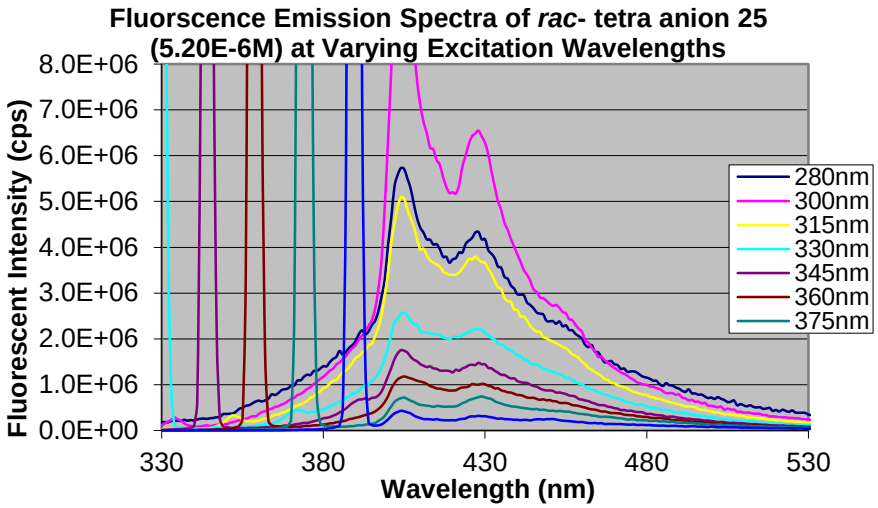


Figure 64: Fluorescent emission of tetra anion tweezers 25 with varying excitation wavelength plotted to include exication wavelengths

All of the small molcules screened were fit by non-linear least squares to a 1:1 binding equation and did not adhere to intermolecular quenching as described by the Stern-Volmer equation. Titration of neutral and anionic small molecule appeared to bind weakly with K_d's on the order of 10^{-2}M which was attributed to the small amount of aromatic surface in the benzene sized substrates. For this reason it was expected that 1-naphthylacetic acid would bind stronger than sodium phenylacetate but appeared to bind with the same affinity. This was attributed to the sparing solubility of the 1-naphtlyacetic acid in nanopure water which prohibited a solution of sufficient concentration to follow probe the guest. If this material were to be titrated in the future it is suggested to form a salt of the 1-naphtylacetic acid to circumvent the limitation in solubility. The cationic guests afforded dissociation constants on average of an order of magnitude stronger when compared to the other titrants for 1-Me nicotinaminium choride and 100x stronger for methyl viologen.

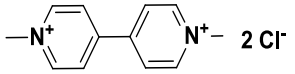
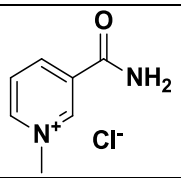
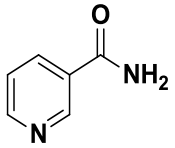
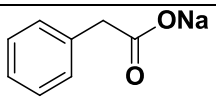
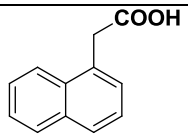
Substrate	Apparent K_d (M)(Titration Medium)
	$5.9x10^{-2}$±$3.8x10^{-3}$ (NP Water)
	$2.1x10^{-4}$±$1.6x10^{-5}$ (NP Water)
	$3.6x10^{-3}$±$1.2x10^{-4}$ (NP Water) $2.5x10^{-3}$±$1.4x10^{-4}$ (NP Water) $6.0x10^{-3}$±$5.0x10^{-4}$ (150mM NaCl, 10mM pH7)
	$3.8x10^{-2}$± $2.2x10^{-2}$ (NP Water)
	$1.8x10^{-2}$± $3.1x10^{-3}$ (NP Water)
	$4.3x10^{-2}$± $4.5x10^{-2}$ (NP Water)

Table 3: Apparent K_d values for small molecules titrated with binding *rac*- methyl phosphonate tetra anion tweezers 25

These results were less encouraging when the small molecules were evaluated against the control isomer **26**. For the non-cationic guests, the shape of the plot of decreasing fluorescence versus titrant cocnetration and the total decrease in fluorescence were eerily similar save for the last few data points were they began to diverge at the highest concentrations. The plots of **26** had the same slight curvature as the plots for the binding isomer **25** did and for this reason were able to fit to the 1:1 binding equation. These control isomer plots were analyzed for a Stern-Volmer relationship and showed inconsistent behavior. Sodium phenylacetate and nictotinamide showed Stern-Volmer correlation where pyridine did not. With conflicting data for the behavior of **26** in acting as a negative control and noisy data from the minimal response in quenching of fluorescence in the concentration ranges tested for

the small molecules the behaviors between the two isomers could not be distinguished from one another with any confidence. This could possibly be accomplished by future reseaches with increasing the concentrations of titrant solutions as well as increasing the ionic strength of the titration medium.

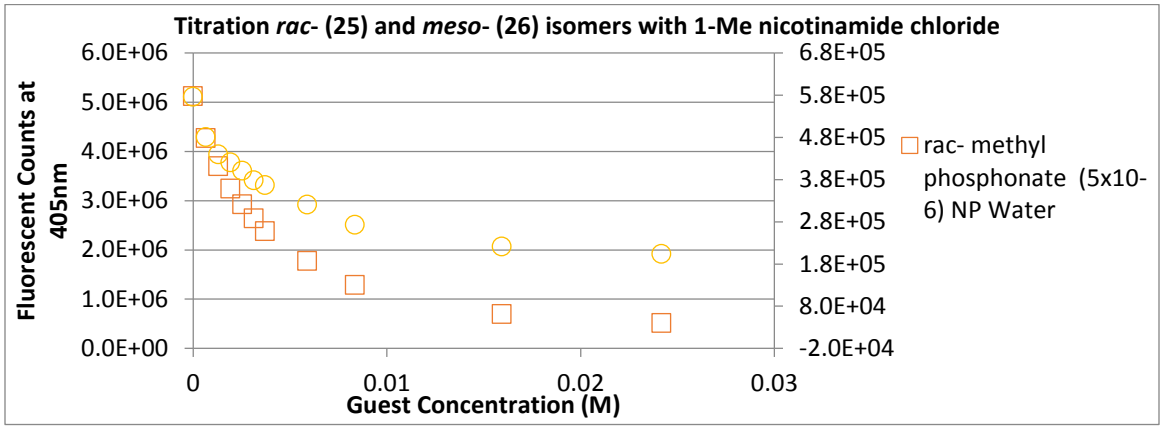


Figure 65: Titration of binding *rac*- and *meso*- methyl phosphonate isomers with 1-Me nicotinamide chloride in nanopure water

In tritrations using the cationic guests methyl viologen and 1-Me nicotinamide chloride the binding *rac*- isomer **25** and the control *meso*- isomer **26** looked to be behaving in the same manner as if binding was occurring in both cases. For titrations with methyl viologen both isomers deviated from linearity when modeled by the Stern-Volmer and both converged to the binding equation with 2.1×10^{-4}M ± 1.6×10^{-5}M and 6.2×10^{-4}M ± 8.7×10^{-5}M for the binding *rac*- isomer and the control *meso*- isomer respectively. Shown below is the data from the titration of the binding *rac*- methyl phosphonate tetra anion tweezers with 1-Me nicotinamide chloride in nanopure water.

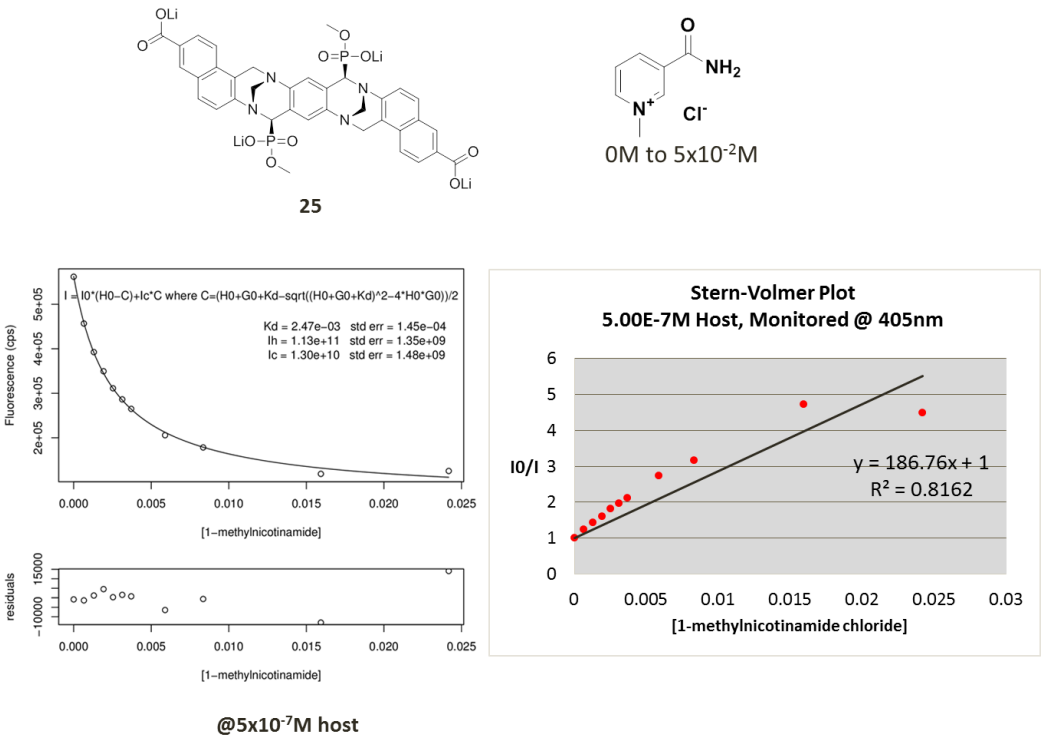


Figure 66: 1:1 binding and Stern-Volmer plot for titration of *rac*- methyl phosphonate tweezers 25 with 1-Me nicotinamide chloride in nanopure water

The small amount of error and the even distribution of errors as plotted by the residuals in the 1:1 binding fit show that this is a good description for binding interaction of the gueswt molecule. The curvature of the I_o/I values with increasing guest concentration when compared to the linear regression for the Stern-Volmer plot demonstrate that the decrease in fluorescence observed is not described well by an intermolecular quenching model.

When the negative control *meso*- isomer **26** was titrated with the same protocol it quenched fluorescence in an apparent non-linear fashion but produced errors equal to the calculated K_d when fit to the binding isotherm demonstrating that intramolecular quenching is not a good model as expected for the isomer that lacks the cavity to allow intercalation of a small molecule. However, when the data was evaluated by the Stern-Volmer relationship it demonstrated the same behavior was the binding isomer. It was from the culmination of these

results in titrating cationic guest that the ionic strength of the titration medium was thought to be of import when trying to demonstrate the differences in the isomers of the molecular receptors. In the very low ionic strength condition of nanopure water it was postulated that the cationic guest would be able to mimic the spectroscopic profile of static (intramolecular) quenching by forming a tight ionic pair with the tetra anionic host which would be interesting as the coulombic attraction between the charged species would be more stable than the solvated ion in water.

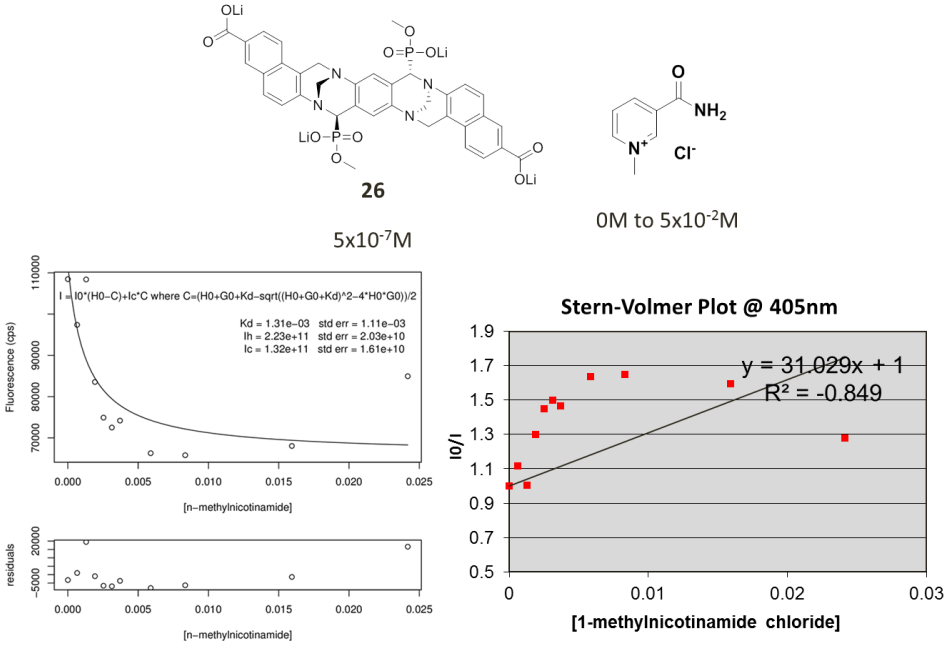
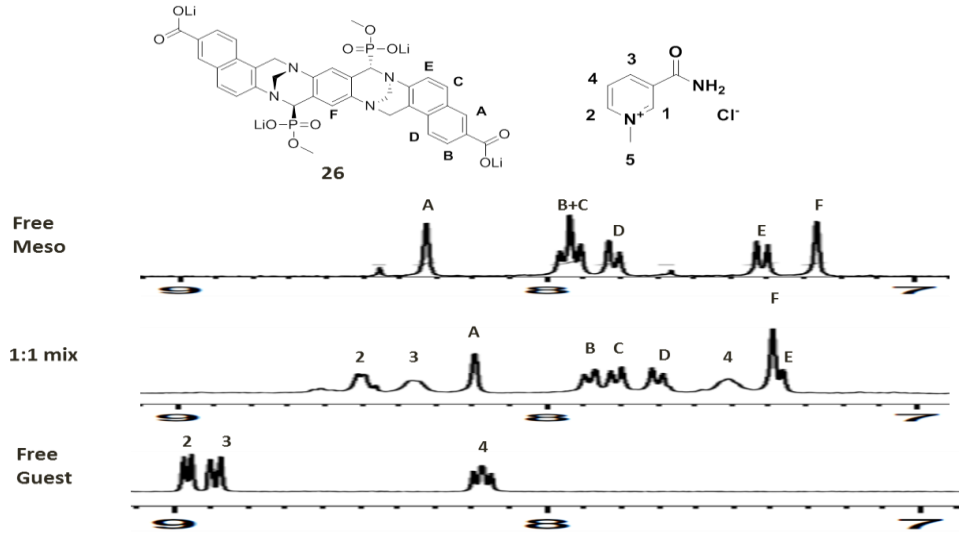


Figure 67: 1:1 binding and Stern-Volmer plot for titration of control *meso*- methyl phosphonate tetra anion isomer with 1-Me nicotinamide chloride in nanopure water

This association was explored using ^{1}H NMR spectroscopy to compare the chemical shifts of free **26**, free 1-Me nicotinamide chloride, and a 1:1 mixture of the two at a concentration similar to the end points of the titration condition in pure D_2O and D_2O of increased ionic strength. The ionic strength of the D_2O was modified by addition NaCl to

160mM concentration which was approximation of the 150mM NaCl, 10mM pH7 phosphate buffer used in subsequent titration.

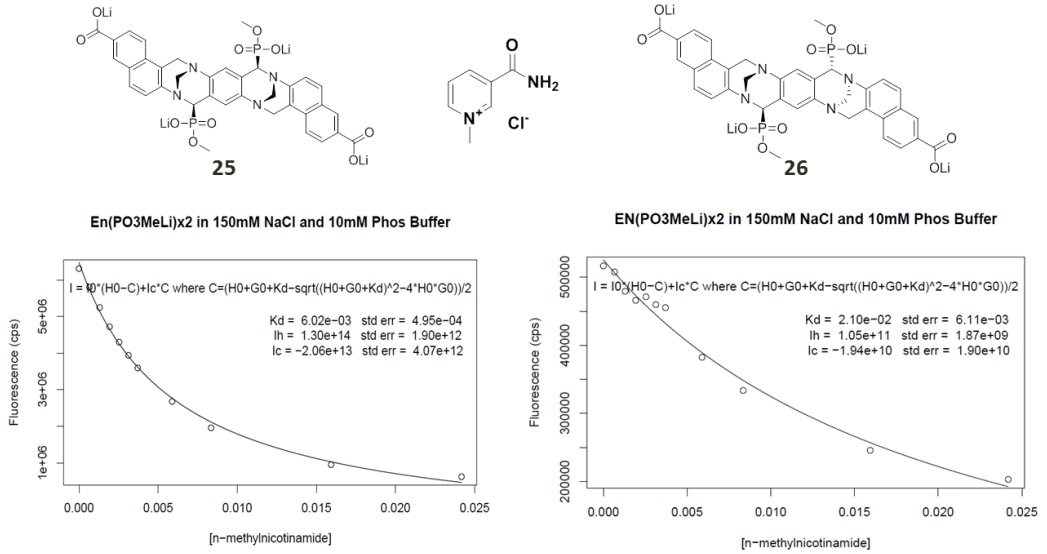


	Free Guest (δ,ppm)	1:1 in D_2O (δ,ppm)	Δδ (ppm)	@160mM NaCl (δ,ppm)	Δδ (ppm)
1	9.28	-		-	
2	8.97	8.50	0.47	8.56	0.41
3	8.89	8.36	0.63	8.43	0.56
4	8.13	7.51	0.62	7.59	0.54
5	4.47	4.17	0.30	4.22	0.25

Figure 68: ^{1}H NMR comparison of the aromatic region of free *meso*- methyl phopshonate tetra anion 26, free 1-Me nicotinamide chloride, and a 1:1 mixture of the two at 1.8x10^{-2}M concentration

When the components were comined in a 1:1 ratio in pure D_2O large upfield shifts were observed in the 1-Me nicotinamide Cl and all but one of the signals in the aromatic region of the *meso*- control. Upon mixing it was also observed that while the *meso*- isomer's signals remained sharp while those of the nicotinamide became broadened, consistent with its associating. From the upfield shifts of the hydrogens in the naphthyl wall of the *meso*-compound along with the concurrent down field shift of hydrogen F that resides on the central benzene ring it is proposed that the nicotinamide salt is associated on the face of the

naphthylene on the opposite side of the phosphonate moiety and perpendicular to the benzene ring. The 1-Me nicotinamide Cl would need to be on the opposite face was when the complex was made using molecular models the 1-Me nicotinamide Cl would not be be in proximity to the hydrogens on the benzene core. The ionic strength of the mixture was then adjusted to 160mM strength by the addition of NaCl with only minor downfield shifts for the 1- Me nicotinamide chloride in the ^{1}H spectrum which shows that even with increased ionic strength the cationic guest and the tetra anionic isomer are still closely associated.



Solvent	K_d
Nanopure H_2O	$3.6x10^{-3} \pm 1.2x10^{-4}$
150mM NaCl, 10mM buffer	$6.0x10^{-3} \pm 5.0x10^{-4}$

Solvent	K_d
Nanopure H_2O	$4.2x10^{-3} \pm 6.7x10^{-4}$
150mM NaCl, 10mM buffer	$2.1x10^{-2} \pm 6.1x10^{-3}$

Figure 69: Comparison of K_d for binding 25 and control 26 isomer to 1-Me nicotinamide chloride in nanopure water and 150mM NaCl, 10mM pH7 phosphate buffer

The titration of the methyl phosphonate tetra anion isomer with 1-Me nicotinamide chloride was conducted again but now in aqueous 150mM NaCl, 10mM pH7 phosphate buffer so that the ionic strength of the medium would not appreciable change over the course of the

experiment. What was found was in this solution the dissociation constant for the binding *rac*-isomer decreased by a factor of 1.7 and for the control *meso*- isomer decreased by a factor of 5 which is evidence for the binding isomer forming an inclusion complex with the guest. If the association of the binding isomer was strictly coulombic it would be expected to have its apparent K_d value diminished by the same amount as the control *meso*- isomer. When the K_d values of the binding and control isomer where compared to one another under the new ionic conditions the binding isomer was able to associate with the 1-Me nicotinamide Cl 3.5x stronger wereas in nanopure water the two isomers associated with the guest molecule with the same affinity. This too was taken as evidence as a demonstration of the difference in behavior of the binding isomer **25** and the control isomer **26**.

3. Hexa-anionic isomers 27 and 28

The best chance of binding a small molecule into the cavity of the *bis*-Tröger's Base tweezers would be with the hexa-anionic derivative. As this form has a dimer that is held together the weakest, it can it be titrated at concentrations where ne is confident that the tweezers exists as a monomer. In pH9 borate buffer, 1-Me nicotinamide chloride appeared to associate with approximately the same affinity to the hexa anion **27** (K_d =8.2x10^{-3} M) as it did to the *rac*- methyl phosphonate tetra anion tweezers under the same ionic strength regime. Borate buffer was used to ensure that the hexa-anionic tweezers were fully deprotonated so there was no ambiguity to the charge on the host molecule.

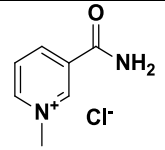
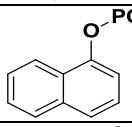
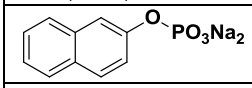
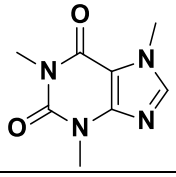
Substrate	Apparent K_d (M) (Titation Medium)
	$8.2x10^{-3} \pm 1.0x10^{-3}$ (150mM NaCl, 10mM pH9 borate buffer)
	$7.2x10^{-3} \pm 4.4x10^{-3}$ (150mM NaCl, 10mM pH7 phosphate buffer)*
	ambiguous
	$4.2x10^{-4} \pm 4.2x10^{-5}$ (150mM NaCl, 10mM pH9 borate buffer)

Table 4: Apparent K_d values substrate association to binding *rac*- hexa anionic tweezers at $5.0x10^{-6}$ M concentrations. *K_d generated by fitting the curvature in the data to the 1:1 binding equation

Titrations of the *rac*- tweezers **27** and the *meso*- non-binding control **28** with caffeine provided the best evidence for the descrimination between the two. Upon addition, the fluoresence of the binding isomer decreased sharply initially and appeared to reach and asymptotic value. This data did not exhibit Stern-Volmer behavior and when fit this data was fit to the non-linear least squares fit it converged to generate a K_d of $4.2x10^{-4}$ M which is similar to binding affity reported by other synthetic acyclic receptors.[44] In contrast, when the *meso*- hexa anionic **28** was exposed to increasing concentrations of caffeine its fluorescent emission vacillated around a constant value before decreasing, increased at the end of the addition, and did converge when fit to the 1:1 binding equation. This increase in fluorescence is not understood at the present time as the absorbance of caffeine at 365nm is 0.002 and thus should not lead to emission form the guest. However, as their beaviors are so different one can be confident that **27** is actually binding to caffeine presumably via intercalation between its naphthalene walls.

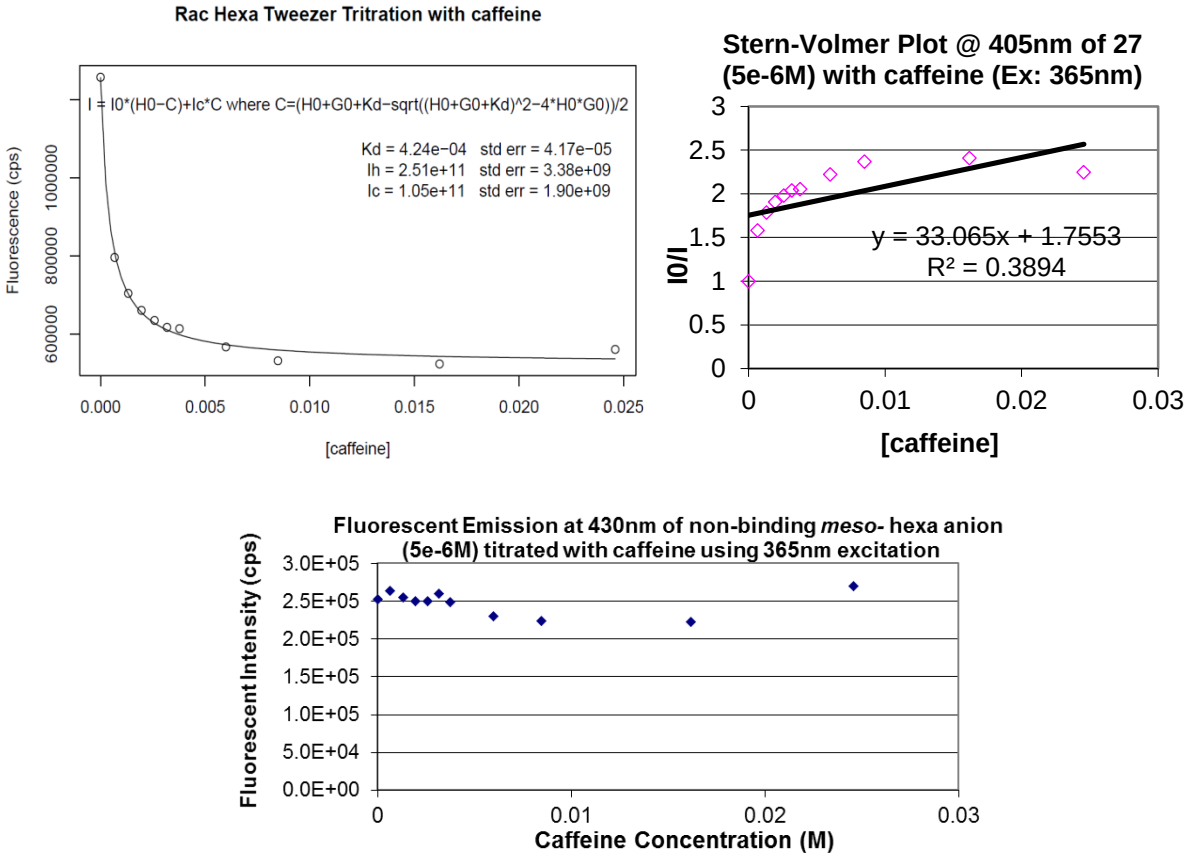


Figure 70: Comparison of fluorescent emissions of the binding *rac*- hexa anionic tweezers (top) and the non-binding *meso*- control isomer (bottom). Stern-Volmer plot also included for binding isomer 27

When titrations of **27** were carried out in water containing 10mM pH7 phosphate buffer, 150mM NaCl with 1- or 2-naphthylphosphate disodium salt the data acquired by fluorescent titrations were ambiguous to stay the least. When the 1-naphthylphosphate analogue was titrated with the binding isomer its fluorescent emission increased upon the first addition of guest then fluctuated up and down until 0.06M concentration of the guest was reached. Upon increasing the concentration, the fluorescence of the tweezers decreased to 66% of its initial value before increasing in value after 0.016M of the guest. Then the data points corresponding to the curvature was analyzed with the 1:1 binding model a K_d of 7.2×10^{-3}M was produced after convergence. With regards to the 2-naphthylphosphate, it too

increased in fluorescent emission with the first addition of guest before leveling off until 0.004M of the guest was achieved. After that, fluorescence decreased in a curve before reaching an apparent minimum before increasing with the last addition. When the data in the curvature were analyzed with the 1:1 binding model it did not converge presumably due to the lack data points. These fluorescent data from the naphthylphosphate guest molecules suggests the the mechanism of binding may be either more complexed than initially estimated or that the phenomenon responsible for the increase in emission signature cannot be fully understood at the present time. Due these observations, titrations of the control isomer **28** were not conducted with the phosphate salts.

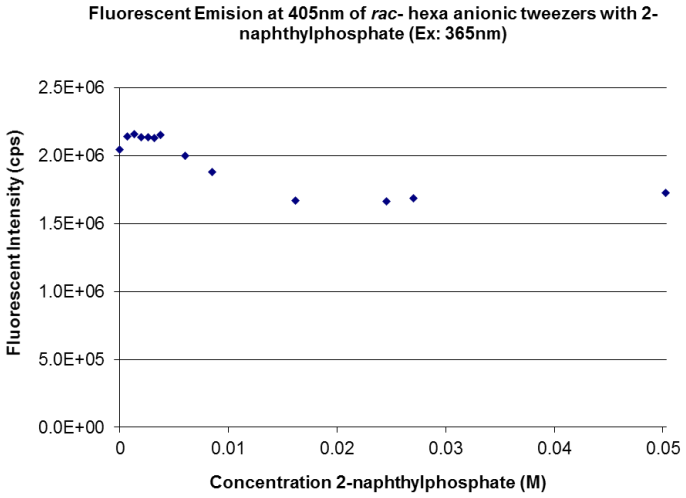


Figure 71: Titration of hexa anionic tweezers 27 with disodium 2-naphthylphosphate

F. Quinolone Synthesis for Functionalized Walls for *bis*-Tröger's Base Molecular Receptors

Quinolones have been reported as therapeutic agents ranging in use from the treatment of Herpes Simplex Type I[102] (HSV-1), as an antitumor agent[103] for Burkitt's lymphoma, as iron coordinating compounds to inhibit Factor Inhibiting Hypoxia-inducible factor[104], an antifilarial chemotherapy agent[105], and an inhibitor to the binding of Nerve Growth Factor p75 to diminish neural apoptosis[106]. Although these properties may prove beneficial for specific recognition in the future, the rational in synthesizing the quinolones described below would be to exploit the differences in reactivity of its functional groups to allow for selective instillation of a wide range function groups. The consequence is this would be multiple non-covalent interactions leading to selectivity in substrate binding and could potentially produced catalytic acitvity. However, the dipole moments of the cavity induced by the quinolones in the *bis*-Tröger's base tweezers and its inherent fluorescent properties to monitor binding by fluorescence or absorbance are of immediate interest.

7-Amino-4-oxo-1,4-dihydro-quinoline-2-carboxylic acid ethyl ester when exposed to cyclization conditions should cyclize in the 8 position of the quinolone exclusively yielding a single orientation of tweezers.

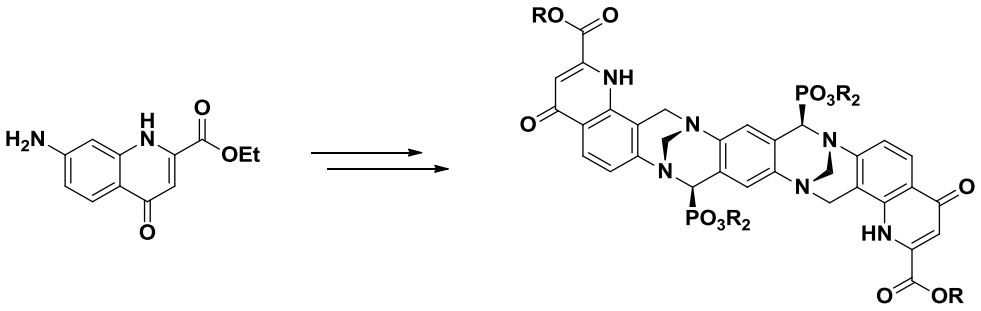


Figure 72: 7-Amino-4-oxo-1,4-dihydro-quinoline-2-carboxylic acid ethyl ester and its resulting *bis*-Tröger's Base tweezer

However when incorporating 6-amino- derivative into the tweezer's architecture there is a question of regioselectivity and could undergo Friedel-Crafts alkylation on the 5 or 7 position of the quinolone to produce a mixture of differently bonded molecular receptors in which some will not have the correct shape to intercalate substrates.

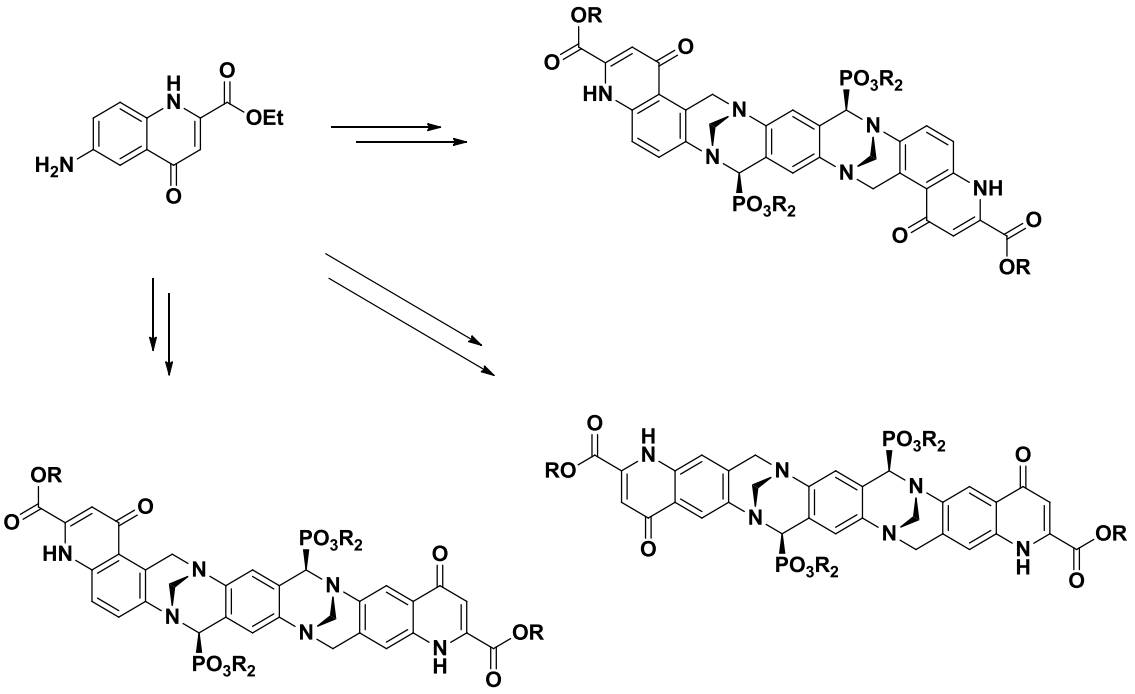


Figure 73: 6-Amino-4-oxo-1,4-dihydro-quinoline-2-carboxylic acid ethyl ester and the possible combinations of bis-Tröger's Base tweezers

Below is a general scheme envisioned for the transformations needed to produce the quinolones:

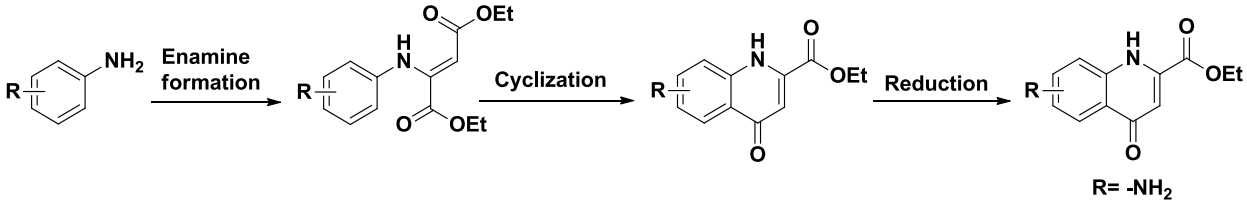


Figure 74: General scheme for aminoquinolone synthesis

Diethyl oxaloacetate was first used[107] and is commonly used to generate the 2-carboxy-4-oxo-quinolone variety along with diethyl acetylenedicarboxylate which can form enamines even with less reactive or sterically hindered anilines[108]. Although the reactivity of diethyl acetylenedicarboxylate is greater than that of diethyl oxaloacete, so is its price leading to the use of diethyl oxaloacetate. Quinolone synthesis has been reported in the literature as early as 1887[109] by Conrad and Limpach reporting the formation of 4-oxoquinolone formation under high temperature conditions which have been modified overtime to induced thermal cyclization[110,111]. Before 1946 it was contended that cyclizing an enamine made from an aniline and diethyl oxaloacetate generated either a 2-oxo quinolone isomer or the 7- substituted 4-oxo isomer cleanly before Surrey and Hammer demonstrated that the resulting material generated upon thermolysis was that of a mixture of 7- and 5- substituated 4-oxo-quinlones[112] and occurs even in the gas phase[113]

1. Preparation of 7-Amino-4-oxo-1,4-dihydro-quinoline-2-carboxylic acid ethyl ester

a. From (3-Amino-phenyl)-carbamic acid tert-butyl ester Route

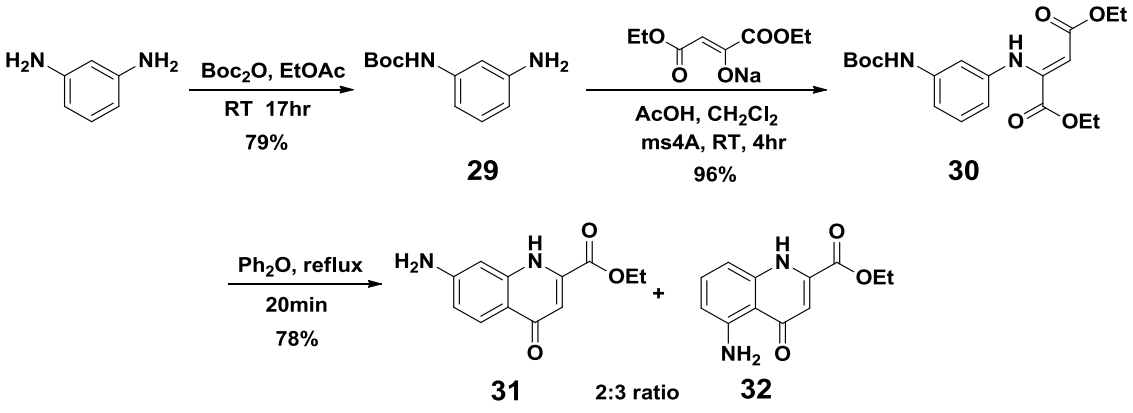


Figure 75: Synthetic route to produce 7-amino-2-carboxy from 1,3-diaminobenzene

Mono-Boc protection of 1,3-diaminobenzene to generate **29** was afforded in 79% yield by using a 100% excess of the diamine over Boc_2O. Utilizing the ability to partition the diamine into water to remove its excess and recrystallization from hexane to remove the diBoc protected side product gave a pure product. Formation of the enamine **30** from the sodium salt of diethyl oxaloacetate in glacial acetic acid cleanly generated the enamine in 4h if 4Å molecular sieves were used to drive the equilibrium by physical removal of water. The excess diethyl oxaloacete was removed by partitioning the reaction mixture between hexane and sat. Na_2CO_3 to produce the enamine in 96% yield as an orange oil. Diphenyl ether (258˚C) was used due to its chemical stability at high temperatures. Refluxing the enamine oil in diphenyl ether for 20min facilitated quinolone formation as well as Boc protecting group removal. Analysis of the quinolone mixture by ^1H NMR spectroscopy revealed a 2:3 ratio of **31** to **32**. This was determined by the ratio of integrations of the doublet of doublets signal at δ6.69ppm for the 7-NH_2 isomer and the triplet at δ7.24ppm indicative of the 5-NH_2 compound. From this data it was hypothesized that when the Boc group was removed and the resulting amino group was able to direct the Fridel-Crafts acylation ortho- to it. The installation of a thermally stable protecting was deemed necessary and thus cyclization with a trifluoroacetyl protecting group was investigated.

b. From N-(3-aminophenyl)-2,2,2-trifluoroacetamide Route

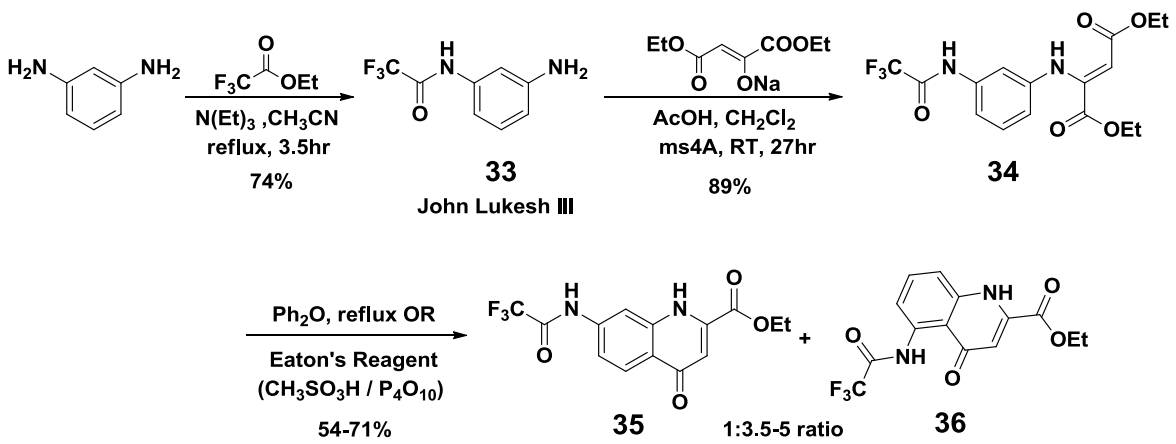


Figure 76: Synthetic route for quinolone production from mono-trifluoroacetyl protected 1,3-diaminobenzene

The mono-trilfuoroacetyl 1,3-diaminobenzene **(33)** used was synthesized, isolated, and purified by John Lukesh III which was then condensed using the glacial acetic acid, 4Å molecular sieves and workup method to generate the enamine **34** cleanly in 89% yield as a lime green oil. After exposuring the enamine to refluxing diphenyl ether, analysis of the crude product with ^{1}H NMR spectroscopy revealed a mol ratio of 1:5 for the 7-trifluoroacetyl quinolone **35** to 5-trifluoroacetyl quinolone **36** and a 1:3.5 mol ratio of **35**:**36** when the experiment was replicated. As an alternative to thermal cyclization, strongly acidic conditions were also known to facilitate cyclization. Published by Eaton in 1973[114] demonstrated that Eaton's reagent (1:10 solution by weight of P_4O_{10}:CH_3SO_3H) not only induced ring closure but sidestepped the difficulties with the physical properties of polypohsphoric acid and thus has been used since then as an alternative.[115] Unfortunately when Eaton's reagent was used the ratio increased even more in favor of the **36** to a 6.7:1 mol ratio compared to the desired **35**. Ring formation using $POCl_3$ was also used but appeared to produce **36** as the major product. Quinolone formation was attempted with the enamine adsorbed to either silica gel or basic alumina which was placed

into a thermal well in refluxing diphenyl ether which afforded incomplete conversion of the starting material and low mass recovery off of the solid support. From these results it was postulated that this seeming regioselectivity could be due to the formation on an intramolecular hydrogen bond upon the formation of the ketene intermediate.

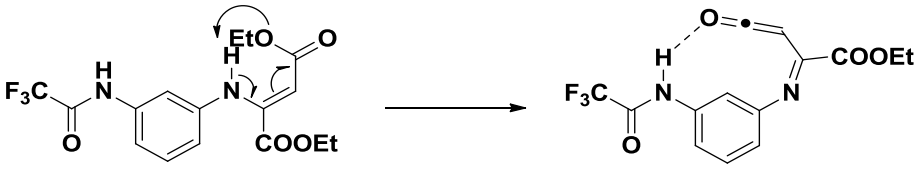


Figure 77: Proposed hydrogen bonded intermediate responsible for regioselective cyclization

If this mechanism were true, then eliminating the ability to hydrogen bond should prevent ortho- direction. This informed the change to a nitro group which would be subsequently reduced to the amine functionality to generate the 7-Amino-4-oxo-1,4-dihydro-quinoline-2-carboxylic acid ethyl ester.

c. From 3-nitroaniline Route

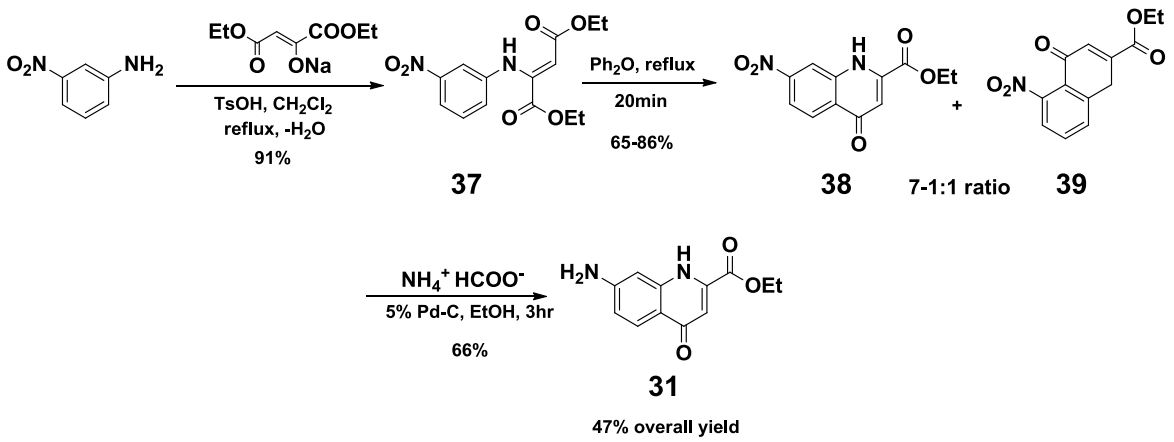


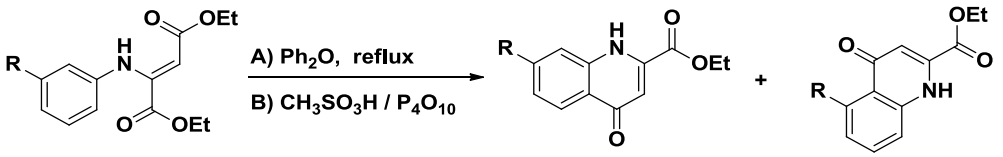
Figure 78: Quinolone synthetic scheme starting from 3-nitroaniline

Enamine formation was first attempt with the glacial acetic acid, 4Å molecular sieves method but only afforded the desired enamine **37** in 54% yield. This was presumably due to the

inductive effect of the nitro reducing the nucleophilicity of the amineand thus requiring harsher conditions to increase yield. Condensation of the 3-nitroaniline and sodium diethyl oxaloacetate was driven then by elevated temperature and physical removal of water via azeotrope with a distilling solvent returned via Dean-Stark trap. It was discovered that choice of solvent was not trivial as use of toluene (b.p. 110˚C) or 1,2-dichloroethane (b.p. 84˚C) lead to substantial formation of a crystalline, orange side product. This material was not fully characterized but evidence ^{1}H NMR gave speculation that it was likely produced by condensation of two 3-nitroanilines by reaction of the amine functionality with a protonated nitro group. Dicholoromethane (b.p. 40˚C) was employed next due to its lower boiling point and ability to azeotropically remove water albeit poor. It was due to this poor azeotrope (99 CH_2Cl_2:1H_2O) that reaction times were extended considerably to ranges of overnight to several days. It was later discovered that on the synthetic scale that this transformation was attempted that the water removed by the dichloromethane was not able to quantitatively separate and allowed for return of water back into the reaction mixture. If however the heavier than water Dean Stark trap was packed with 4Å molecular sieves atop a loosely fit plug of cotton the reaction could be reliably completed overnight. On larger scales though replacing of the sieves may be required to thoroughly remove all of the water generated from the reaction.

37 was then subjected to the thermolytic cyclization protocol of 20min exposure in refluxing diphenyl ether and unfortunately still produced the mixture of 7-NO_2 isomer **38** and 5-NO_2 isomer **39**. In replicating this transformation many times it was observed that although the mol ratio of the quinolone mixture improved with regards to 7-NO_2 to 5-NO_2 isomers it was inconsistent, ranging from 7:1 to 1:1, with no correlation able to be determined for this

observed behavior. Jackie Koch developed a procedure the exploited the greater crystallinity of the quinolone **38** to isolate it exclusively via recrystallization using a mixture of ethanol and toluene and is described in detail in the experimental section. She also found that if only ethanol was used, **38** could still be separated but the amount of material recovered decreased significantly. Interestingly enough when the enamine **37** was cyclized using Eaton's reagent at 110˚C the mol ratio of the resulting quinolone mixture was observed to be 2.3:1 in preference of the 5-NO_2 isomer. From these results it appears that although neither the **39** or **38** isomer can be made exclusively there is at least some ability in directing ring closure by either substituent effects or cyclization conditions.



R	Conditions	Mol Ratio	
BocHN-	A	2	3
$CF_3(CO)HN$-	A	1	3.5-5
$CF_3(CO)HN$-	B	1	6.7
O_2N-	A	7-1	1
O_2N-	B	1	2.3

Table 5: Quinolone mol ratios with varying substituents and reaction conditions

Reduction of the nitro group was first attempted on a mixture of the **38** and **39** using ammonium formate (NH_4O_2CH), 5% Pd-C, and methanol as a solvent. Ammonium formate is attractive as the reducing agent because in the presence of Pd-C it decomposes to produce a concentration of hydrogen gas *in situ* which corresponds to a high pressure of H_2 over the reaction volume. This eliminates the necessity for a specialized high pressure apparatus and the

safety concerns that come with it. Transformation to the amino group occurred as expected but under these conditions trans-esterification with the alcohol solvent occurred resulting in the methyl ester of the corresponding aminoquinolones. Although unexpected in retrospect should not have been wholly unanticipated due to the weakly acidic nature of the ammonium formate. When repeated with ethanol as the solvent the desired aminoquinolone **31** was afforded in 66% yield after isolation by flash chromatography and an average 47% overall yield from the starting 3-nitroaniline.

Attempts to isolate **31** non-chromatographically proved to be problematic. When the starting quinolone **38** was observed to be absent by TLC analysis the mixture was filtered to which CH_2Cl_2 was added to the filtrate to decrease the solvent polarity to cause an unreacted ammonium formate to precipitate. Although precipitation of the salt did occur the removal of the ammonium formate was not quantitative. Reducing the volume of the filtrate or concentrating to dryness resulted in the formation of solid aminoquinolone which was not separated from the excess salt. It was observed that if left to stir for excessive time in the presence of Pd-C the ammonium formate is able to be converted to into insoluble ammonium carbonate however with no way to conveniently monitor this conversion it was not considered as a method of separation. It was later found that use of $H_{2(g)}$ is not detrimental to the rate of reaction and will be discussed subsequently.

2. Preparation of 6-Amino-4-oxo-1,4-dihydro-quinoline-2-carboxylic acid ethyl ester

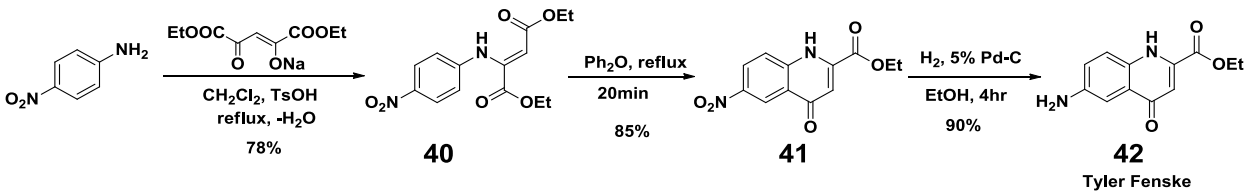


Figure 79: Synthetic scheme for production of 6-amino-2-carboxy-4-oxoquionlone ethyl ester

With a developed methodology in hand, formation of **42** proceeded smoothly especially without question of regioselectivity in ring closure. A major contribution in the reduction step was provided by Tyler Fenske who observed that use of $H_{2(g)}$ reduced the nitro group at the same rate as that of the ammonium formate and in 90% yield with effortless removal of the excess, gaseous reducing agent.

III. CONCLUSION

The dialdehyde **8** was afforded in a 50% overall yield starting from the dimethyl ester of succinyl succinate without chromatography and the most of the intermediates being able to crystallize from the reaction mixture, eliminating the need for subsequent purification steps. The diarylamino side products were demonstrated to be formed from the bisenamine **2** in the absence of Boc_2O with bis-aryl amino derivatives able to be produced from the corresponding anilines with the mono-substituted version predominating. This opens up a different route by which acridones can be synthesized as well as the possibility for asymmetric quinacridones.

The desired hexa-methyl ester of 1,2:4,5-*bis*-Tröger's Base stereoimsomer was afforded as a diastereomeric mixture of the *syn*-cofacially oriented *rac*- isomer and the control *meso*-isomer in 69% overall yield from the key intermediate dialdehyde **8**. This proceeded through

the *bis*-imine formation from the core dialdehyde, transformation into α-aminophosphonates, then cyclization to the final *bis*-Tröger's Base. Each of these isomers was then converted into water soluble analogues via selective dealkylation protocols employing combinations of bromotrimethylsilane and aqueous lithium hydroxide. Two tetra anionic molecular tweezers derivatives were afforded each with a different distribution of charge across its surface along with a fully deprotected hexa anionic receptor.

Each of the organic and water soluble forms of the *rac*- and *meso*- 1,2;4,5-*bis*-Tröger's Bases were characterized using spectroscopic techniques and spectrometric techniques to confirm their identity. It was shown that the desired binding *rac*- isomers underwent self-association to presumably form a dimeric complex in solution wereas the non-binding control *meso*- isomers did not. ^{1}H NMR analysis of the fully esterified *rac*- isomer in $CDCl_3$ produced broad resonances what sharped and shifted downfield upon dilution, which is behavior consistant with the interpretation dimer formation. The water soluble derivatives were not able to produce unambiguous spectra upon dilution in D_2O but were able to generate well resolved spectra in a mixture of 50% TFA/$CDCl_3$ to allow for their identification. In contrast, the non-binding *meso*- isomers produced well resolved spectra in all cases even at sample concentrations greater than those were dimerization was observed with the *rac*- isomers. This demonstrated the desired lack of self association for the non-binding *meso*- isomers so that it may serve as a negative control for dimeration and titration studies.

Equilibrium constants for dimer formation were determined for the *rac*- isomers using a combination of ^{1}H NMR and fluorescence spectroscopy and analyzed using a dimeration equation fit using a non-liner least squares method. K_{dim} for the fully esterified tweezers was

calculated to be $1.5x10^{-1}$ M in $CDCl_3$ but this is just an estimate based upon the low number of data points acquired in the NMR dilution experiment. Deviation from Beer's Law in fluorescent emission upon dilution was used to determine the strength of self association for the water soluble molecular tweezers. The *rac*- hexa anionic tweezers formed the weakest dimer with a K_{dim} value of $1.2x10^{-4}M \pm 9.0x10^{-6}M$. The tetra anions formed progressively stronger dimers with the *rac*- methyl phosphonate analogue producing $K_{dim}= 4.5x10^{-4}M \pm 9.8x10^{-5}M$ and the TMSBr dealylated *rac*- carbethoxy $K_{dim} < 4.4x10^{-7}M$. In the case of the *rac*- carbethoxy tweezers a linear decrease in fluorescence was observed upon dilution down the $4.4 x10^{-7}M$, which was the limit of detection for this compound and prevented fitting to the dimerization model.

Each of the water soluble binding *rac*- and control *meso*- *bis*-Trögers Base derivatives were titrated with small molecules monitoring the decrease in fluorescent emission to acquire the data to be fit to the 1:1 binding model which describes intra-molecular (static) quenching. Data was also fit the Stern-Volmer equation, which models inter-molecular (dynamic) quenching, as a way to discriminate between the binding and non-binding isomers. The *rac*- carbethoxy tetra anion similar dissocation constants (K_d) across a range of guest molecules reinforcing the notion that it exhists as a dimer at $10^{-5}M$ concentration regime the titrations were conducted at. The ionic strength of the aqueous media was also observed to be of import with regards to distinguishing between the binding and non-binding isomers during small molecule titrations. In a low ionic strength environment, like nanopure water, it appeared that both the *rac*- methyl phosphonate and control *meso*- methyl phosphonate tetra anions exhibited binding behavior in the presence of cationic guest molecules like 1-Me nicotinamide chloride. When ionic strength was increased so that the water contained 150mM NaCl and

10mM pH7 phosphate buffer, both isomers were still able to converge to the 1:1 binding model when titrated with 1-Me nicotinamide chloride. However, the calculated K_d diminished by a factor of 5 for the control *meso*- isomer between the low and high ionic strength conditions wereas the K_d for binding *rac*- isomer diminished only by a factor of 1.7.

From this it was concluded that the cationic guest molecule was associating to the control isomer through coulombic attraction which in retrospect is not surprising. To confirm that the nicotinamide salt was indeed forming a pair, ^{1}H NMR was used to analyze a mixture of the 1-Me nicotinamide chloride with the control *meso*- isomer. What was observed was a significant upfield shift and broadening of the guest's resonances along with minor upfield shift in the naphthyl signature of the *meso*- isomer. When the ionic strength was increased to 160mM NaCl the peaks for the 1-Me nicotinamide chloride shifted only slightly back downfield and still appeared to be significantly associated to the control *meso*- isomer. Titration with charge neutral guest like pyridine or nicotinamide, or anionic guests like sodium phenylacetate did not sufficiently quench either isomer upon addition. This prohibited confidently distinguishing between the modes of intra- or inter-molecular quenching between the two isomers.

The *rac*- hexa anionic tweezers provided the best data with regards to small molecule titrations using cationic or neutral guest. Ionic strength of the aqueous media was accounted for by containing 150mM NaCl and 10mM pH9 borate buffer which ensures that the hexa anionic tweezers fully deprotonated. Titration of the binding *rac*- isomer with 1-Me nicotinamide chloride resulted convergence of the 1:1 binding model, negative Stern-Volmer correlation, and a K_d value of 8.2×10^{-3}M ± 1.0×10^{-3}M. This value is similar to the dissocation

constant afforded by the *rac*- methyl phosphonate tetra anion tweezers. Titration with caffeine resulted in the same spectroscopic behavior and yielded a K_d value of $4.2x10^{-4}M \pm 4.2x10^{-5}M$.

The future diection of this work should continue small molecule titration with the binding *rac*- hexa anionic tweezers to determine the scope and trends in its ability to intercalacte guest molecules. As it appears that quenching of fluorescence it not adequate in order to determine dissociation constants in some cases it is recommended that the walls of the molecular tweezers be modified to a potentially more responsive moiety.

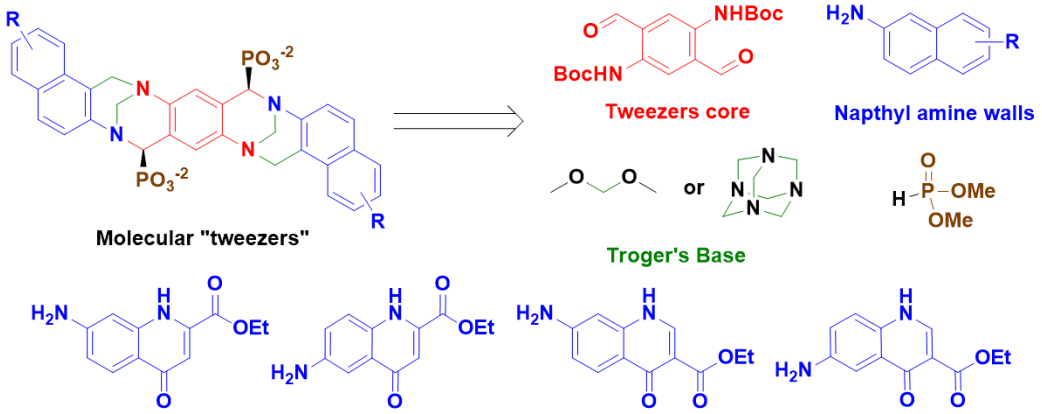


Figure 80: 1,2:4,5-*bis*-Troger's Base tweezer scheme displaying desired quinolones for future inclusion

This can be accomplished by incorporating the syntheized amino-quinolone derivatives, 7-Amino-4-oxo-1,4-dihydro-quinoline-2-carboxylic acid ethyl ester (47% overall yield) and 6-Amino-4-oxo-1,4-dihydro-quinoline-2-carboxylic acid ethyl ester (60% overall yield), into the modular tweezers synthetic scheme. These structures would provide a different fluorescent signature to monitor binding as well a potentially upon up the range of small molecules the tweezers may bind by the presence of dipole-dipole interactions in the cavity.

IV. SMALL MOLECULE PROBES FOR EVALUATING SbADC ALDOLASE ACTIVITY

A. SbADC Background Information

S. Bingchenggensis Acetoacetate Decarboxylase (SbADC) is a tetrameric enzyme first isolated from *Streptomyces Bingchenggensis* from Harbin, China and having sequence homology to that of Group V acetoacetate decarboxylases. However, SbADC does not display the same properties of its brethren and instead was discovered to catalyze Aldol Condensation and Aldol Dehydration as well as the retro variants of these reactions with α-keto acids. It was discovered in the Silvaggi lab that it reacted preferentially with pyruvate and various aldehydes. The purpose of the enzyme for its native species is as of yet unknown but characterization of its aldolase functionality was conducted.

The mode of active site catalysis for SbADC was studied by stop flow, steady state, and inhibition kinetics as well as X-ray crystallography conducted by Lisa Mueller to achieve kinetic parameters in intermolecular interactions in the active site to determine which residues are involved in the transformations. When allowed to react with benzaldehyde; pyruvate and acetoacetate were the only nucleophiles to react with catalytic SbADC action with rates of 2.112μM s^{-1} and 0.012 μM s^{-1} rate where as glyoxylate had non-enzymatic reaction and 2-oxobutyrate did not react leading to the conclusion that pyruvate was the preferred α-keto substrate. Aldehyde substrates were then screened with *trans*-cinnamaldehyde observed to the bind the stongest (42-48μM) with $k_{cat}/K_m = 3.9x10^5$ $M^{-1}s^{-1}$. Soaking with hexanal produced no reaction and imidazole-2-carboxaldehyde reacted but did not turn over. Inbetween these

results with increasing reactivity: benzaldyhde < *trans*-2-hexenal, *trans*-2,4-heptadienal < *trans*-2-octenal leading to the conclusion that an α,β-unsaturated aldehyde with required and if steric bulk is in an aldehyde (like a benzyl group) it has to be at least two carbons away from the aldehyde. *Trans*-cinnamaldehyde analogues were screened. Ortho substitution proved detrimental to binding (o-methoxy K_d=185μM) while hydrogen bonding substituents in the para position enhanced binding (o-methoxy K_d= 21.5μM, o-nitro K_d=7.6μM)

When SbADC was soaked with sodium pyruvate and the X-ray crystal structure was acquired it appeared as a hemiaminal in three of the four active sites and a Schiff base in the last. However when SbADC had the active site mutation of Y252F and soaked with cinnamylidine pyruvate it was observed to be the Schiff base in all four active sites leading to the speculation that Y252 is needed for the retro Aldol activity as it hydrogen bonds to a water molecule and orients to close to the α-keto moiety. α-Keto acid enones and dieneones have been synthesized from pyruvate for almost one hundred years[116] utilizing silyl enol ethers and Lewis acids[117], two carbon ethylene homologation[118], and base catalyzed Aldol Condensation and Dehydration[119,120]. For evaluating the X-ray crystal structures of benzylidine pyruvate, cinnamylidine pyruvate, 4-nitrocinnamylidine pyruvate with SbADC the dieneones used were mixtures with pyruvate. For the kinetic studies these substrates were purified to be 98-99% pyruvate free to obtain accurate enzymatic parameters.

B. Rational for SbADC Molecular Probes

In the attempt to elucidate the reason why SbADC does not facilitate the decarboxylation of pyruvate to acetaldehyde, SbADC was to be soaked with various

combinations of substrates to study X-ray crystal structures. This series of X-ray crystal structures when viewed in sequence would produce a “molecular” movie which would show the position of the enzyme’s active site residues, their proximity to substrate functionalities, and thus their role in the catalyzing Aldol reactions. Shown below is the schematic for the desired “molecular movie” showing the steps in the reaction that would be of interest.

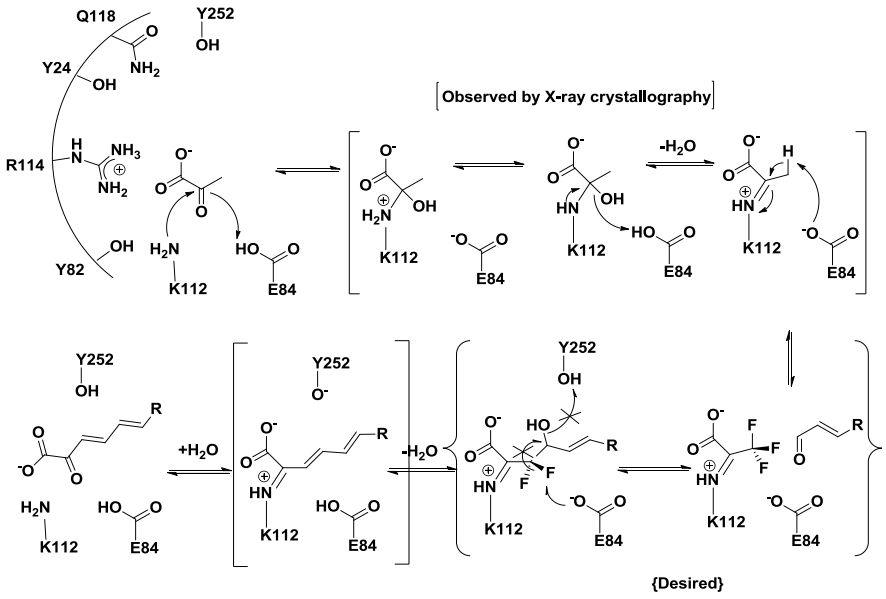


Figure 81: Proposed use of trifluoropyruvate and difluoropyrubate for mechanistic determination of SbADC aldol pathway

The structures in square brackets are the combinations that are already observed by X-ray crystallography while the ones in curly brackets are the ones desired to be produced. For these trifluoropyruvate and difluoropyruvate were synthesized. The purpose of the trifluoropyruvate would be to soak the enzyme with a substrate that cannot undergo Aldol condensation. Trifluoropyruvate would be concurrently soaked with cinnamaldehyde to see the proximity of the substrates to one another and the positions of the active site residues that would be getting into bonding distance of the substrates. Difluoropyruvate would be employed as it is able to undergo aldol condensation but not aldol dehydration. This attenuated reactivity

would also allow for the identification of which side chains participate in Aldol dehydration reaction by their proximity to the Aldol product.

Ethyl trifluoropyruvate is commercially available so the sodium salt of the hydrate of trifluoropyruvate can be made by acidic hydrolysis and neutralization. This method minimizes the presence of excess hydroxide which would denature the enzyme being studied. Ethyl difluoropyruvate is not commercially available so it or an analogue is needed to be made so its salt can be used.

Of the literature examples for synthesizing difluorocompounds, only a few seemed attractive for difluoropyruvate. One of these was as follows:

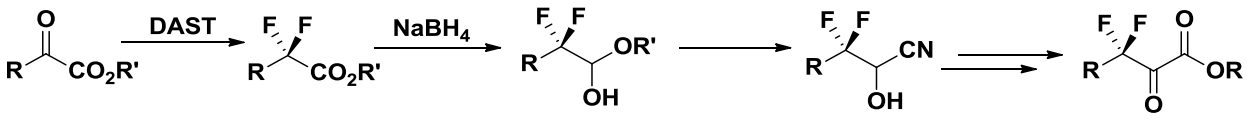


Figure 82: An example synthetic scheme in formation of difluoropyruvate analogues

This method[121] used (diethylamino)sulfur trifluoride (DAST) to make β,β-difluoro compounds by reaction with the α-keto carbonyl and subsequently regenerating it by reduction of the ester to to the aldehyde level followed by substitution with cyanide, oxidation, then acid hydrolysis. This method worked well for cases when R was either alkyl or aryl substituents. No examples of R=H were reported, leading one to believe that it may be unsuccessful with the method. The other route was the Mg^0 promoted mono-defluorination[122] of trifluoromethyl ketones. This simple preparation was attempted with ethyl trifluoropyruvate even though there was no precedent for an α-keto trifluoromethyl moiety to get to difluoropyruvate directly. The most reliable route and the one ultimately used was trifluoroacetylation of 2-methylfuran by

Friedel-Crafts acylation then Mg^0 promoted monodefluorination[123] followed by ozonolysis of the resulting 5-difluoroacetyl-2-methylfuran[124].

V. RESULTS AND DISCUSSION

C. Formation of Cinnamylidenepyruvate and 4-NO_2 Cinnamylidenepyruvate

The sodium benzylidene pyruvate, sodium and potassium cinnamylidene pyruvate salts, and sodium and postassum 4-nitrocinnamylidene pyruvate salts were synthesized from their corresponding aldehydes using the base catalyzed aldol chemistry. Preliminary studies began with the synthesis of sodium benzylidene pyruvate to determine an appropriate method for cinnamylidiene preparation. Benzylidene pyruvate was prepared from benzaldehyde and sodium pyruvate with sodium hydroxize as described[5] and isolated in 34% purified yield. The initial precipitate from the reaction mixture was isolated and determined to be a mixture of the condensation and dehydration product in ~1:2 molar ratio and free of pyruvate. The mixture was purified from aqueous media and acidified to pH1 with the desired dieneone precipitating from solution. Acidification shifts the α-hydrogen from δ6.9ppm to δ7.6ppm.

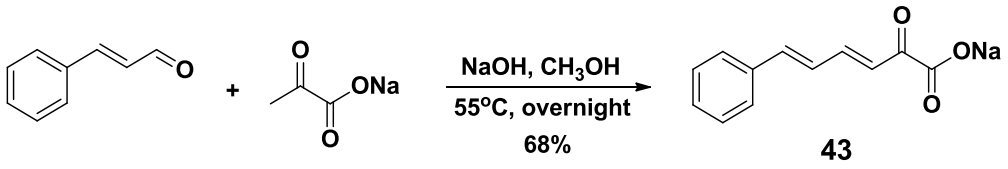


Figure 83: Formation of cinnamylidene pyruvate sodium salt

43 was synthesized using the same method, but at 55˚C with a yellow solid precipitating from the reaction mixture in 68% crude yield as mixture of the desired dieneone and pyruvate (27% by mass of the mixture). The mixture was made pyruvate free by the same precipitation

method from acidic aqueous media with a 42% yield and exhibited the same large change in chemical shift of the hydrogen α to the ketone in either the salt or acid form. However the dieneone was reactive to aqueous acid. Extraction of the supernatant of EtOAc afforded a yellow oil in 36% crude mass that was a mix of the desired acid (74% by mass), ethyl acetate, and what was hypothesized to be the Aldol condensation product form by hydration of the dienone. Total estimated yield from the precipitate and extract is ~60%.

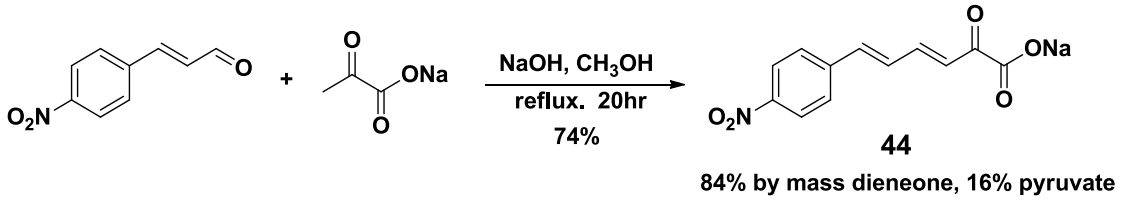


Figure 84: Formation of 4-nitrocinnamylidene pyruvate sodium salt

The 4-NO_2 analogue **44** was synthesized with the previous methods and placed through the same workup protocol but to pH2. This dienone however proved to be very sensitive to aqueous acid and afforded none of the desired material. Synthesis without acidic workup but with precipitation of the salts with isopropyl alcohol afforded a 74% yield of the product as a mixture that was 84% by mass **44** and 14% by mass sodium pyruvate.

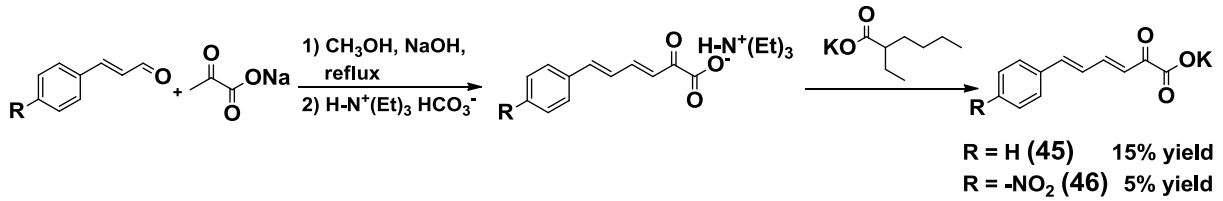


Figure 85: General scheme for isolating sodium pyruvate free cinnamylidene pyruvate analogues

The acid sensitivity of **45** and **46** prevented straightforward extraction to remove contaminating pyruvate. However compounds **45** and **46** could be extracted from their aqueous solutions in triethylammonium bicarbonate into CH_2Cl_2. Evaporation yielded the oily

triethylammonium salts. The crystallize potassium salts were obtained by dissolution in ethyl acetate and precipitated upon addition of a solution of potassium 2-ethylhexanoate[125] generating 15% yield **46** and 5% yield **46** with 1-2% by mass pyruvate as determined by ^{1}H NMR spectroscopy. The desired products were able to be isolated pure as when the triethyl ammonium salt acquired from extraction when exposed to ethyl acetate the large majority of it did not dissolve. The resulting supernatant was decanted from the undissolved oil and mixed with a solution of potassium 2-ethylhexanoate in ethyl acetate precipitating the dieneone salt. When the insoluble oil, which was dissolved in CH_2Cl_2, was mixed with potassium 2-ethylhexanoate no precipitate was formed even when the salt was just in large excess. Analysis of the EtOAc insoluble oil by ^{1}H NMR showed that the doublet characteristic of the hydrogen α to the ketone of the dieneone were reduced to 75% signal intensity relative to the dieneone and instead had a new set of signals from δ3.5 to δ3.2 that appeared to be a triplet and a doublet.

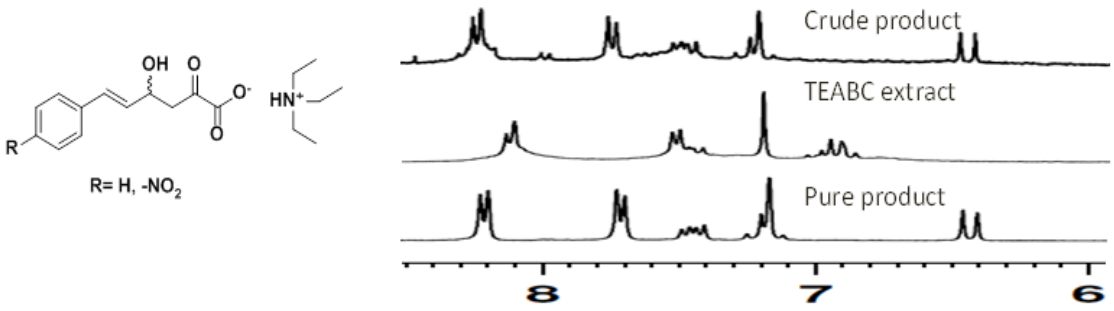


Figure 86: ^{1}H NMR spectra of 4-nitrocinnamylidene pyruvate over the course of sodium pyruvate removal

A ^{1}H NMR spectrum was acquired of the triethyl ammonium bicarbonate extract and looked the same as the EtOAc insoluble oil. From this data it was concluded that the dieneones still undergo hydration to form the Aldol product even under these mild conditions. Attempts

to minimize hydration by raising the pH of the reaction mixture to 12 from 8 by bubbling in of CO_2 before exposure to triethylammonium bicarbonate did not mitigate the amount of product degradation. The cinnamylidene pyruvate derviatives containing 1-2% pyruvate were then used by Lisa Mueller to obtain kinetic parameters for SbADC by monitoring the retro Aldol reactions in stop flow experiments.

D. Difluoropyruvate Synthesis

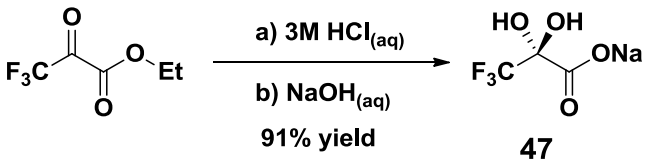


Figure 87: Scheme for sodium trifluoropyruvate hydrate

Ethyl trifluoropyruvate hydrolysis was monitored by ^{1}H NMR to ensure complete hydrolysis by watching the ester quartet turn to that of the quartet of ethanol. ^{1}H NMR was deemed necessary for evaluating the reaction mixture as ethyl trifluoropyruvate readily hydrates, analogous to that of hexafluoroacetone, and was unclear if it could migrate upon silica gel for TLC analysis. After overnight reflux with a pyruvate concentration of 0.37M gave a 93% yield of **47** after neutralization with NaOH.

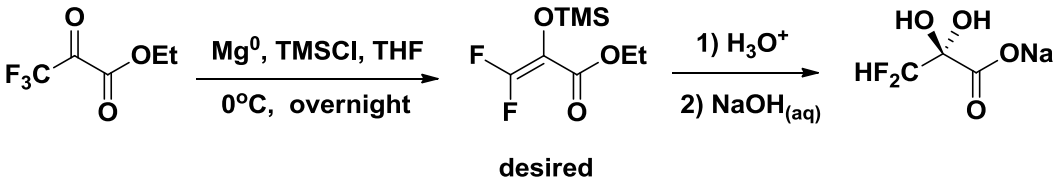


Figure 88: Proposed synthetic route for simplifed difluoropyruvate formation

If Mg^0 reduction and mono defluorination proceeds as for CF_3COAr[123], this has the potential to provide a succinct route to difluorpyruvates. When ethyl trifluoropyruvate was

exposed to the mono-defluorination conditions reduction occurred but afforded a mixture of the E and Z isomers of *bis*-silyl enol ether **48** without elimination of fluoride. This material exposed to a range of conditions in efforts to produce ethyl difluoropyruvate **(49)** by the most succinct route known. The first was exposure to aqueous hydrochloric acid. The purpose of this admittedly was not to yield difluoropyruvate but confirm the identity of the product afforded from the monodefluorination reaction. Upon addition of acid the quartet indicative of the ethyl ester of trifluoropyruvate was observed as well as the quartet seen of the alpha hydrogen in ethyl trifluorolactate. The second condition was addition of $(Bu)_4NF$ in portions over time. The goal in using this organic soluble fluoride was to react in an E_2 fashion kicking out fluoride by making trimethylsilyl fluoride in the following fashion:

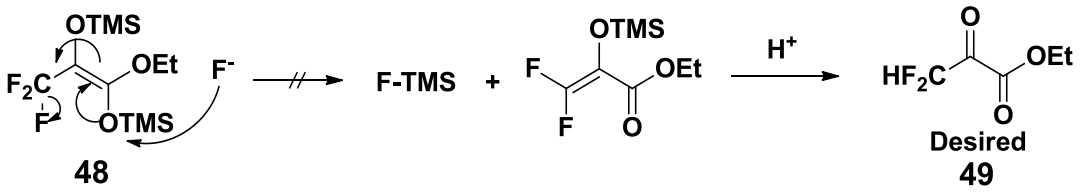


Figure 89: Desired E2 elimination of O,O-(bis-trimethylsilyl) ethyl trifluoropyruvate

After 20hr with 6eq of $(Bu)_4NF$ added over that time, trifluoroacetic acid was added was to remove the trimethylsilyl groups and to see if a triplet at 6ppm would be produced. This singal is indicative of the desired difluorocompound but no change in the ^1H NMR spectrum observed. If the removal of the silyl groups by fluoride did not occur, then the combination of ethyl trifluoropyruvate and ethyl trifluorolactate would be observed after protonation. The resonances for the compounds were also not seen in the NMR. From this data, it was postulated that the E_2 elimination occurred but the resulting difluoroalkene also acted as a

Michael acceptor which condensed with the *bis*-silylenol ether precursor. The proposed mechanism is diagramed below:

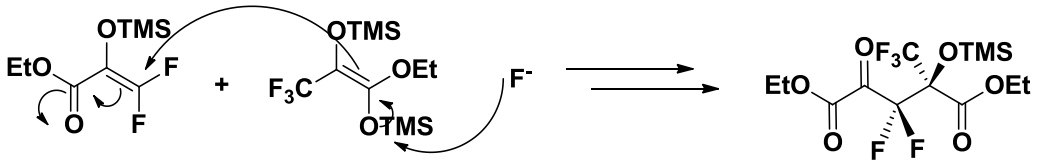


Figure 90: Proposed E2 elimination of O,O-(*bis*-trimethylsilyl) ethyl trifluoropyruvate that occured

With the limited success using ethyl trifluoropyruvate the ozonolysis scheme was pursued by way of an ozone generator on loan with many thanks to Dr. Tysoe.

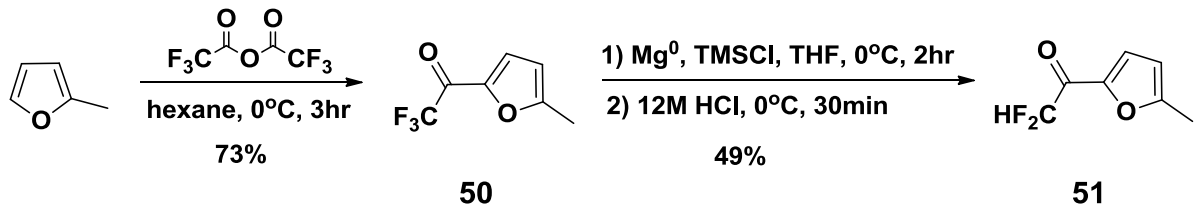


Figure 91: Literature based synthesis for ozonolysis precursor

Trifluoroacetylation of 2-methylfuran with trifluoroacetic anhydride was conducted by the literature procedure to afford **50** in 73% yield followed by the magnesium facilitated mono-defluorination in 44% purified yield after vacuum distillation of **51**.

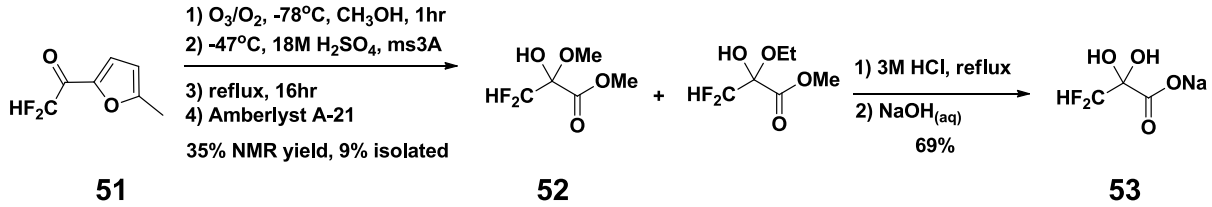


Figure 92: Ozonolysis scheme for synthesis of methyl difluoropyruvate methyl hemiacetal

In the end, ozonolysis of the difluorofuran does produce the methyl ester **52**. Katagiri, Ozaki, and Tanaka[124] describe ozonolysis "until a green color is formed" which proved to be

problematic in reproducing what they accomplished. We found bubbling of gas into the reaction mixture until a yellow-green color was apparent to produce a mixture of methyl difluoropyruvate hydrate, **52**, and unreacted difluoroacetylmethyl furan. We found if ozone was bubbled into the reaction mixture when the greenish color formed, and then disappeared, the conversion of **51** to **52** was complete.

Separation of **52** from contaminating CF_2HCO_2H was described by passage through silica gel.[124] Repeated attempts at chromatographic separation on silica failed, using various CH_3OH/CH_2Cl_2 or CH_3CN/CH_2Cl_2 eluents. Acidic byproducts were successfully removed by passage through a column of Amberlyst A-21, a polystyrene supported tertiary amine ion exchange resin. This treatment successfully removed the acidic components but elution with ethanol caused exchange with the methyl hemiacetal of the desired product to produce a mixture of the ethyl and methyl hemiacetals of methyl difluoropyruvate. Using the same methodology for the formation of **47**, compound **53** was afforded in 69% yield after acidic hydrolysis and neutralization.

Soaking SbADC crystals with 50mM **53** did not produce sufficient electron density in the active site to conclude that it was complexed in the cavity. This is more than likely due to the propensity of the difluoropyruvate to hydrate and not have enough of the keto form present to form an imine with the active site lysine. As 50 to 150mM pyruvate was used to generate 1.5Å resolution images, a concentration of 150mM or greater would probably be needed to the **53** to form a Schiff Base with the enzyme. When **47** and cinnamaldehyde were soaked with SbADC concurrently no electron density was observed in the active site. This result was not expected for if the pair would not occupy the active site at least the Schiff base of **47** was expected to be

seen. The reason for this remains unknown but conducting the soaks at various concentrations of the two components might generate the desired crystallographic structure.

VI. SMALL MOLECULE PROBES FOR MppR AND MppP

A. Enduracididine and Enduracidin Background Information

Second to vaccines, antibiotics seem to be the most effective means to treat disease and illness. Unfortunately, this boon is being combated by the organisms we eliminate by their evolution of antibiotic resistance. Infectious agents now exist that are either resistant or immune to our most potent substances like vancomycin or methicillin. The mode of action of these last resort antibiotics, like vancomycin, impede the growth of these bacteria by inhibiting the expansion of their cell walls upon growth causing the cells to lyse in the process due to internal osmotic pressure. Antibiotics such as ramoplanin, enduracidin, and mannopeptimycin[126] prohibit growth in much the same way but seem to exhibit a peculiar ability to not be adapted against.

All three of these structures are similar in their construction and anitibiotic potency. In 2002, Cudic *et. al.* investigated the mechanism of ramoplanin[127] to inhibit the late stage glycosyltransferase reactions necessary for bacterial growth. Different from the recognition of the N-acyl-D-Ala-D-Ala moiety like vancomycin, Somner and Reynold postulated that it was inhibition of Lipid I to Lipid II conversion that stopped the glycosyltransference.[128,129] Testing of this hyposthesis was problematic for some time as acquisition of pure murG, the enzyme that facilitates transglycosylation, and assay soluble version of Lipid I and II were not available until 1998 when the Walker labs synthesized a biomimetic analogue that was water soluble to test

the activity of the murG enzyme.[130] It was also stated in this paper that murG has no human equivalent and that the muramyl-pentapeptide moiety is unique to bacterial organisms. Their work continued[131] by following the accumulation of radiolabelled Lipid II in increasing amounts of ramoplanin present to suggest a new mechanism of action for the antibiotic: binding to Lipid II by ramoplanin to prevent its polymerization and thus prevent cell wall biosynthesis. These two modes were tested later in 2006 to confirm which one of these pathways was taken.[132] Using inhibition kinetics and binding assays it was demonstrated that Lipid II binds approximately ten times stronger to enduracidin and ramoplanin than Lipid I but was only favored in competition experiments by a factor of five. Although capture of Lipid II is slightly favorable both of these pathways appear to happen equally. It is this that makes these antibiotics so resistant to adaptive mutation in that they target and disrupt a process so fundamental to the bacteria's survival that in order to evolve against it would require an alternate method to construct its cellular membranes.

Enduracidin was first observed from *Strepomyces fungicidicus* from the soil of Nishinomia, Japan and found to have potent antibiotic activity against gram-positive bacteria and moderate activity against acid-fast and phytopathogenic organisms while having no activity against gram-negative bacteria, fungi, or yeasts tested.[133] Later in the year enduracidin was isolated and characterized[134] demonstrating its most potent activity against antibiotic resistant strains of *S. aureus* with minimum inhibition concentrations (MIC) ranging from 0.1-0.2µg/mL.

The antibiotic's efficacy was demonstrated[135] *in vitro* and *in vivo* when administered intravenously, intraperitoneally, and subcutaneously but not orally against *S. aureus*, *S. pyogenes*, and *D. pneumonia*. Digestion of enduracidin in 6M HCl yielded nine types of known

amino acids along with two as of then unidentified residues. In a follow up publication[136] the structures of the known amino acids were determined and called enduracididine and allo-enduracididine, the enantiomer of enduracididine.

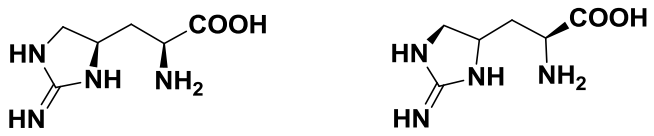


Figure 93: Enduracididine (left) and allo-enduracididine (right)

The origin of enduracididine was investigated by feed experiments of *S. fungicidicus* with radiolabelled amino acids.[137] For these it was concluded that aspartic acid, threonine, serine, glycine, alanine, ornithine, and citrullene were directly incorporated into the cyclic polypeoptide whereas the 4-hydroxyphenyl and 3,5-dichloro-4-hydroxyphenyl glycine residues were derived from tyrosine. For enduracididine it was presumed that either arginine or histidine was the precursor to enduracididine but with this study it shows that the radiolabelled arginine was the amino acid used to make enduracididine providing solid evidence that arginine was the precursor.

B. Roles of MppP and MppR

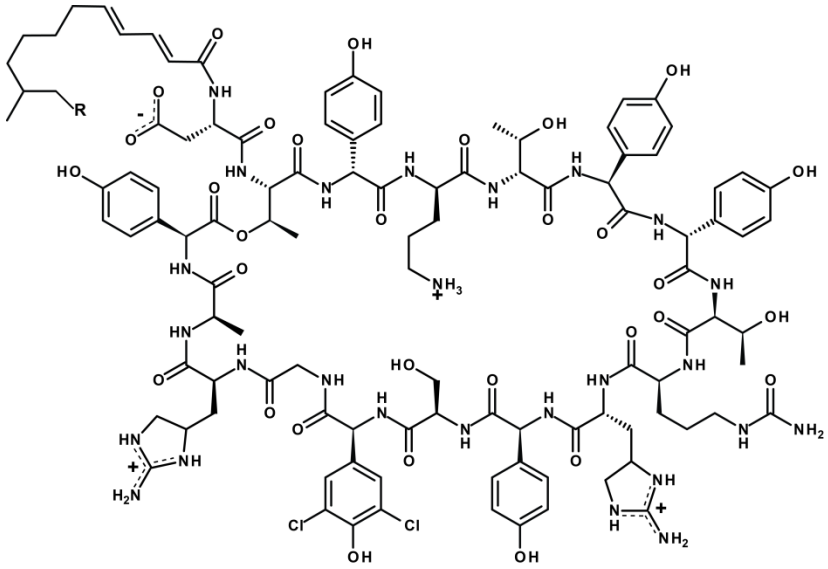


Figure 94: Enduracidin A (R=H) and Enduracidin B (R=CH_3). Image provided by Dr. Nicholas Silvaggi

Using *Streptomyces eurocidius* Eguchi[138] uncovered more detail as to the specific transformations arginine undergoes along the metabolic pathway to enduracididine when looking at the role of argainine in the biosynthesis of 2-nitroimidazole. When the bacteria was heated at 50˚C the production of 2-aminoimidazole, the precursor to 2-nitroimidazole, ended. When arginine was administered to the bacteria followed by 50˚C heat treatment a guanidine positive material was seen to accumulate. Exposure of the guanidine positive fraction to H_2O_2 to decarboxylate the amino acids present afforded 3-hydroxy-4-guanidino-butyric acid implying that γ-OH-arginine was the material that was building up. Pyridoxal phosphate (PLP) and oxygen were also confirmed as necessary to the reaction for if the cofactor was omitted and the reaction was conducted under an inert atmosphere 2-aminoimidaxzole production was not seen.

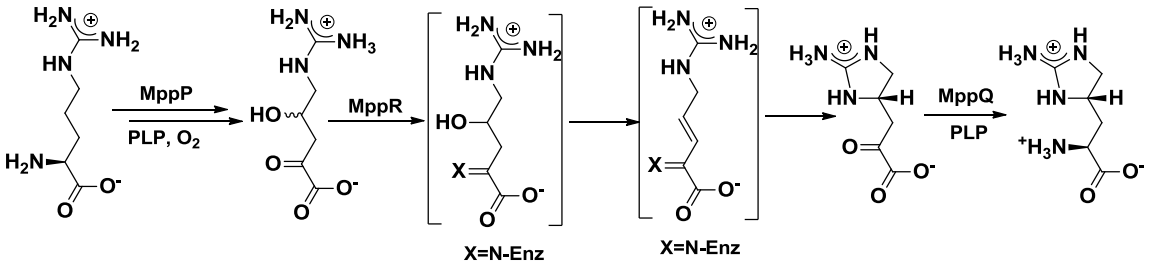


Figure 95: Proposed biosynthesis for enduracididine

The proposed biosynthetic pathway was the oxidation of arginine followed by loss of pyruvate from the oxidized arginine's α-keto analogue to produce 2-aminoimidazole for conversion to the 2-nitroimidazole antibiotic. When given arginine and its cofactors, pyridoxal phosphate and molecular oxygen, 2-aminoimidazole production proceeded. However if deprived of these or if the enzyme was heated to 50°C 2-aminoimidazole was not formed but instead a guanidine positive material accumulated. When this accumulated fraction was treated with H_2O_2 to induce decarboxylation 3-hydroxy-4-guanidinobutyric acid was found as the product implying that the guanidine positive substance was γ-hydroxy-arginine which underwent transamination to the α-keto acid then decarboxylated. Interestingly enough, when γ-OH-arginine was given to the enzyme in the absence of pyridoxal phosphate and/or molecular oxygen 2-aminoimidazole was formed along with an equal amount of pyruvate. Although not identified, it was postulated that an aldolase type enzyme would be required to affect the transformation decribed above.

Genetic sequencing and experimentation with cloned variants lead to the identification of the 17 amino acid gene cluster for the production of enduracididine.[139] It was found that both *S. enduricidicus* and *S. hygroscopius* contained the three gene operon for antibiotic EndP, EndQ, EndR and MppP, MppQ, MppR for the biosynthesis of enduracidin and mannopeptimycin respectively. They also held in common a non-heme based oxygenase that utilized 2-oxo-

glutarate that does not hydroxylate arginine but instead hydroxylates enduracididine in the β position.[140] MppP and MppQ were both shown to be pyridoxal based aminotransferases with the role of MppR still undetermined.

The structural and functional capability of it was later reported[141] demonstrating its activity as an aldolase and confirming the previous hypothesis that an aldolase is needed to be present as was postulated by the feed experiments of *S. eurocidius.* Bioinformatic analysis shows that MppR has a low but significant sequence homology to that of a previously uncharacterized group of acetoacetate decarboxylase family with the similarity notably occurring in the active site. X-ray crystallography of MppR crystallized from HEPES buffer showed a HEPES molecule bound in the active site with the sulfonyl group hydrogen bonded to the active site lysine L156. Treatment of MppR with sodium pyruvate either as a soak or being present during crystallization covalently bonded to L156 as a Schiff base with no coordinated water proximal to the former α-keto functionality probably due to the hydrophobic nature of the active site itself.



Figure 96: Aldol condensation and dehydration product of imidazole carboxaldehyde and sodium pyruvate formed by MppR

Encouraged by this observation, imidazole-2-carboxalyde was soaked with MppR and sodium pyruvate with the resulting crystal structure showing the Aldol product between the two, however, with no enzymatic turnover. HPLC analysis with UV/VIS detection showed none of the enone in the supernatant. To test the role of MppR in the biosynthesis of enduracididine it was treated with 2-oxo-γ-OH-arginine which resulted from the exposure of 4(R/S)-hydroxy-

2(S)-arginine with an L-amino acid oxidase (LAAO) from *C. atrox*. Over time this produced the 2-oxo derivative of enduracididine with the same stereochemistry at C4 as seen in mannopeptimycins and making the same intermolecular interactions with the active site residues as pyruvate did.

(2S,4R)-2-amino-5-guanidino-4-hydroxypentanoic acid, colloquially known as γ-OH-arginine, was first isolated from the sea cucumber *Polycheira rufescens*. [142] Identification of the amino acid was derived from material isolated after reaction of treated extract with an L-arginase and comparing the compounds to synthetically produced γ-OH ornithine and γ-OH-arginine.

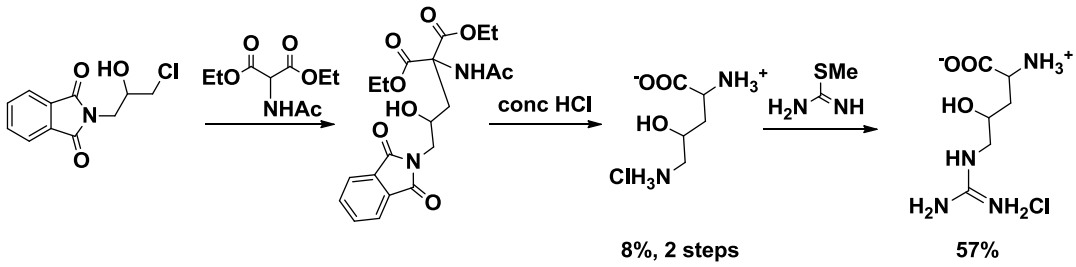


Figure 97: Literature route to γ-OH arginine

γ-OH-arginine was made in 4.6% overall yieldby first making γ-OH ornithine which was then treated with S-methylthioisourea to install the guanidine group. The stereochemistry of the γ-OH-arginine isolated from *P. rufescens* was published by Fujita year later[143] as the S chirality on the hydroxyl containing carbon and R as the chirality of the amino bearing carbon. A later report[144] altered the route used by Fujita by first reacting epichlorohydrin with sodium diethyl malonate instead of phthalamide.

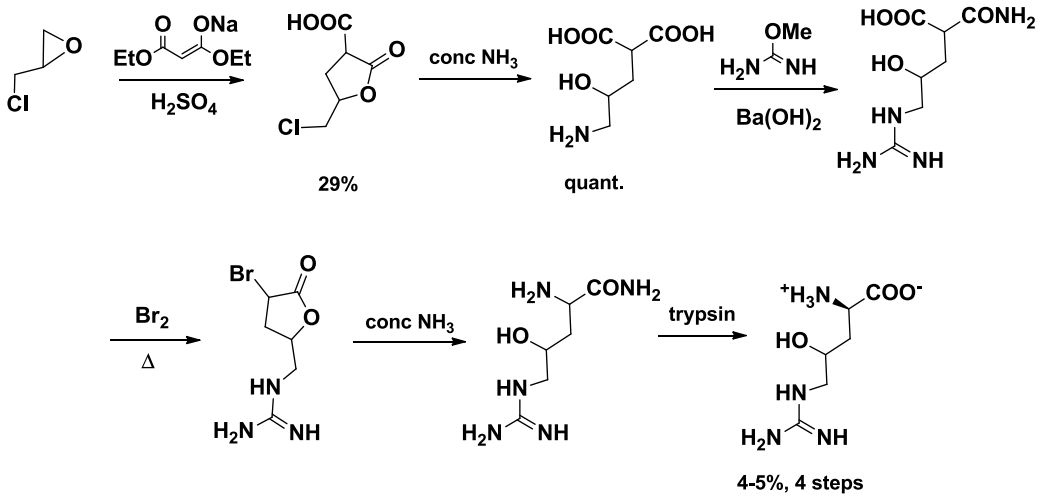


Figure 98: γ-OH arginine synthesis from epichlorohydrin

After treatment with ammonia the guanidine was formed from OMe isourea. Reaction with bromine, then ammonia, then trypsin give the desired product in 1.3% yield as a mixture of the R and S hydroxyl diastereomers with no isolation of the intermediates after formation of the epichlorohydrin malonate adduct. The low yield was attributed to the multitude of side reactions undoubtedly produced by reaction with bromine as well as trypsin hydrolyzing only two of the four total diastereomers present. They also replicated Fujita's method using OMe isourea but did not report a yield however it was stated that use of an acidic eluent for ion exchange chromatography drove the γ-OH-arginine to lactone formation.

More recent methodologies focus on stereoselectivity to increase yield of the (2S,4R) isomer to study the biosynthesis of enduracidin,[145] synthesis of a fully protected, organic soluble enduracididine in 3-8% overall yield[146] using a single enantiomer of a key aziradine intermediate,[147] and synthesis of β-OH enduracididine derivatives to generate modified mannopeptimycins via peptide coupling.[148] Synthesis of γ-OH-arginine and its dehydro analogue were undertaken to more thoroughly explore MppR as well as to open a pathway to make

modified enduracididines which would hopefully be incorporated into the biosynthesis resulting in modified enduracidins to fight antibiotic resistant bacteria in the future.

C. Attempts to Make Guanidiniumacetaldehdye for MppR Evaluation

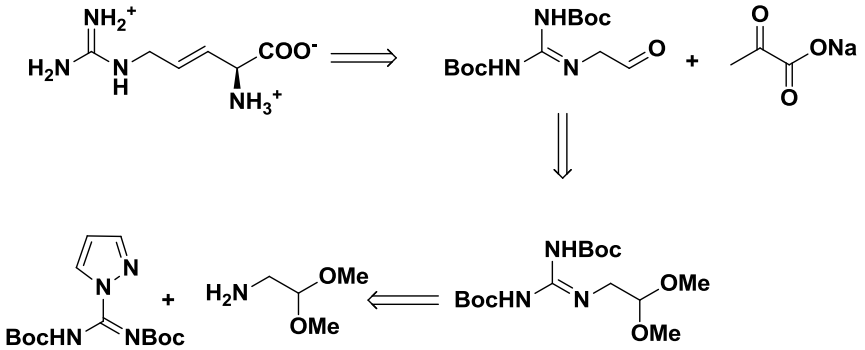


Figure 99: Retro-synthetic analysis for dehydro-L-Arginine by Aldol reactions route

The above retrosynthetic analysis shows that the most expedient route to γ-hydroxy-arginine or dehydro-arginine would be through Aldol Condensation of sodium pyruvate with guanidinoacetaldehyde. Good reagents have been developed for installing guanidino functionality on imines[149] but Drake, Petel, and Lebl have made an extremely convenient and efficient guanidinylating agent[150] (used exclusively from here on in) and if reacted with the dimethyl acetal of amino acetaldehyde acidic hydrolysis would provide the desired material.

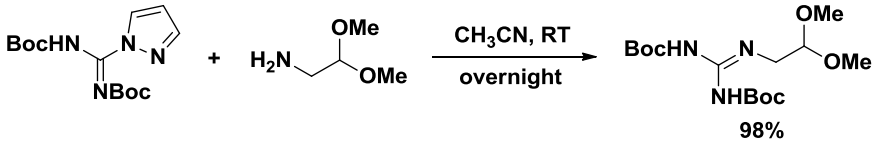


Figure 100: Guanidinylation of aminoacetaldehyde dimethyl acetal 54

When the dimethyl acetal was exposed to the pyrazolyl diBoc-carboxamidine the resulting guanidine was afforded in an average of 98% yield with two degree melting point range due to the easy removal of pyrazole side product due to its volatility.

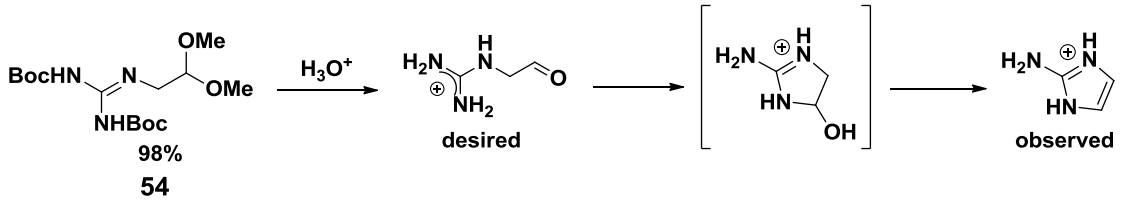
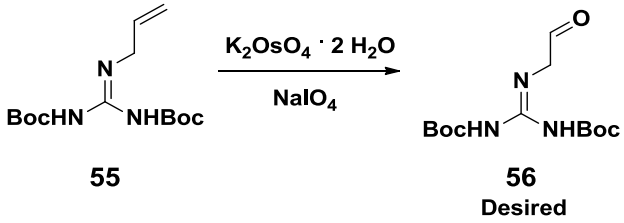


Figure 101: Formation of 2-aminoimidazole from guanidinylated aminoacetaldehyde dimethyl acetal upon acidic hydrolysis

Hydrolysis of dimethyl acetal **54** in 11M trifluoroacetic acid in deuterium oxide was monitored by ^{1}H NMR with complete removal of the Boc groups after 20min when data was first acquired. When the spectrum of the sample was obtained a second time 18hr later, only singlets corresponding to methanol and 2-aminoimidazole were present. As acid hydrolysis resulted in cyclization and aromatization, removal of the Boc groups to generate the guanidinium salt was conducted in hopes to prevent cyclization. When the acetal was combined with two equivalents of methanesulfonic acid at -78°C and warmed to 0°C no removal of the Boc groups was observed. It was only after warming to room temperature that removal of only one Boc group occurred as determind by ^{1}H NMR. Even after 46hr at room temperature no change was observed from the now monoBoc guanidine. Hydrolysis was undertaken again but with 12M HCl at 0°C and followed by no D NMR. Complete conversion of the substrate to 2-aminoimidazole occurred in ≤ 48min. Under these conditions it was deemed an unsuitable method for formation of the guanidinoacetaldehyde as cyclization and aromatization could not be prevented. In all of these cases the characteristic resonance of an aldehyde in ^{1}H NMR was not observed, even transiently.

D. Towards β,γ-dehydroarginine for MppP Evaluation

With acidic hydrolysis of the dimethyl acetal demonstrated to not be a viable route to make guanidinoacetaldehyde an alternative method was adopted. Oxidative cleavage of the appropriate alkene precursor to produce the aldehyde first while keeping the Boc groups intact to prevent cyclization was the rationale for the new approach. Guanidinylation of allyl amine to afford **55** averaged yields of 97% with two degree melting point range. Its been shown that generation of OsO_4 *in situ* with $NaIO_4$ can be used to convert an alkene to a diol which then is cleaved by $NaIO_4$ to the corresponding carbonyl compounds can be performed conveniently and in decent yield.[151] When di-Boc allylguanidine was exposed to these conditions only unreacted starting material was recovered in 83%, even after 35hr time and was not observed anymore on TLC analysis. The reaction was performed again with none of the desired aldehyde **56** obsevered even after 3days. However, after three days a new signal was observed by ^1H NMR at δ 6.7ppm and interpreted to be the diBoc derivative of 2-aminoimidazole and present in only as minor amount.



55 **56** **Desired**

Figure 102: Desired oxidative cleavage of guanidinylated allylamine

Perplexed by this lack of activity on what appeared to be a suitable substrate the quality of the reagents were tested by way of reaction with a different allyl compound.

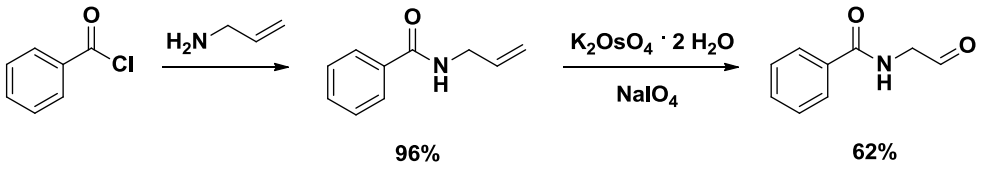


Figure 103: Model reactions to test conditions for oxidative cleavage of an alkene with K_2OsO_4

N-Benzoyl allylamine was synthesized in 96% yield and exposed to the oxidation regime to produce the corresponding aldehyde in 62% yield. In comparing the structure of the di-Boc allylguanidine and the benzoyl allylamine it was hypothesized that the benzoyl analogue was able to react was that the lone pair of electons on the nitrogen were involved in resonance were as the lone pair on the allyl moiety were sitting as a free lone pair which can coordinate to the osmium when the osmate ester is formed preventing diol formation by either occupying a required coordination site by chelation preventing the ligand transfer needed for the oxidative regeneration of the osmium. The hypothesis was tested by deprotection of **55** in refluxing 50% CF_3COOH/CH_2Cl_2 for 1hr. Elevated temperature was needed as exposure to the acid at room temperature only removed one of the Boc groups which is agreement with previous observations as a di-cation would need to be made to remove the second Boc group.

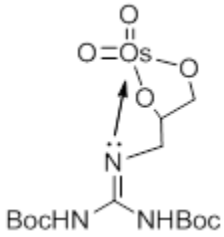


Figure 104: Proposed stabilized complex that prevents dihydroxylation by osmium tetroxide

The resulting trifluoroacetate salt **57** was treated with the oxidation reagents in a mixture of D_2O and CD_3OD and monitored by ^1H NMR.

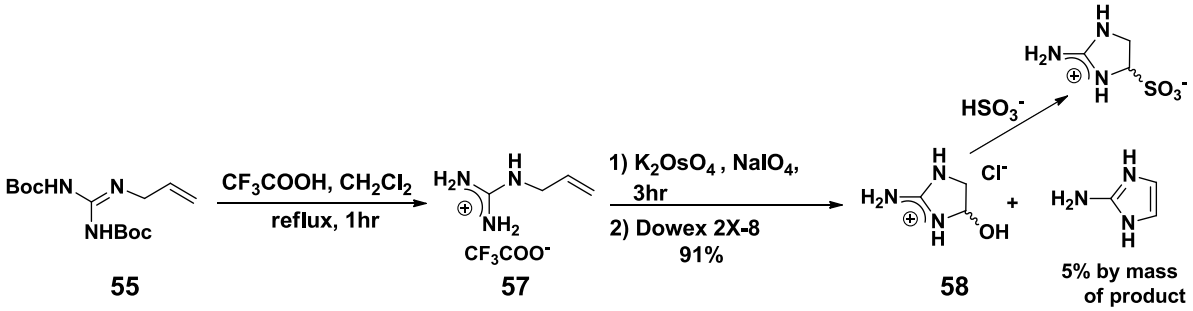


Figure 105: Cyclized hemiaminal generated upon treatment of allylguanidinium trifluoroacetate with osmium tetroxide

After 3.5hr the alkene resonances were no longer observed but neither was that of the desired aldehyde. Instead signals of δ5.6, δ3.9, δ3.5 were seen, each as a doublet of doublets. From this it was concluded that the aldehyde did form but cyclized to hemiaminal **58** even with the protonated guanidine at neutral pH due to the germinal coupling constants. Also observed in the reaction mixture was formalin, corroborating that the oxidative cleavage took place. 2-aminoimidazole was also produced but in trace amounts which implies that **58** is the kinetic product, and aromatization to the imidazole occurs over time.

The reaction mixture was split into two portions to which was added hydroxylamine to one and sodium bisulfite added to the other. Each was added to react with the aldehyde in a manner that could be reversed and to keep it acyclic so it could not aromatize. Exposure to hydroxylamine hydrochloride did not produce the desired oxime but instead catalyzed the transformation to 2-aminoimidazole completely. Addition of 20eq of sodium bisulfite on the other hand did not aromatize the hemiaminal and made the sulfonate of the hemiaminal proving that elimination to the aromatic species is avoidable. After accounting for these two compounds another doublet of doublets was seen but wasn't enough to confirm the presence of the acyclic bisulfite adduct. The splitting pattern, chemical shift, and coupling constants of the cyclic sulfonate shifted upfield to δ5.3 for methyne hydrogen and downfield shifts of δ5.0

and δ4.9 for the methylene hydrogens. Since the identity of the corresponding anion from the reaction may oxidize MppR when exposed to it the reaction was repeated and the hemianimal was purified to the chloride salt via ion exchange chromatography with Dowex 2X-8 resin.

As hemiaminal **58** had to be produced by cyclization of the guanidine group into an aldehyde, there presumably some mechanism by which the equilibrium can be perturbed so that the aldehyde can be present. Even if it could not open back up, it could lose a hydroxyl group to form an iminium ion which could go on to react with pyruvate in an aldol manner. Based on these possibilities, the Silvaggi group combined **58**, sodium pyruvate, and MppR. Unfortunately, they found that no reaction between the components was observed.

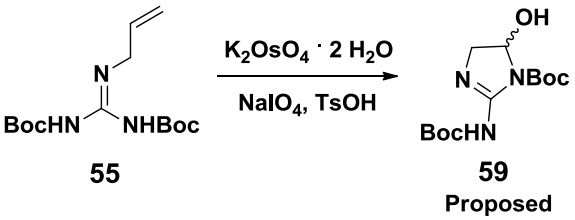


Figure 106: Synthethis diBoc protected cyclic hemiaminal from diBoc protected allylguanidine

With the lone pair hypothesis validated, the di-Boc allylguanidine was treated with K_2OsO_4 and $NaIO_4$ again but this time in the presence of 1eq *p*-toluenesulfonic acid to determine if protonation would be a viable way to oxidize the allyl group while keeping the guanidine Bocs intact. By ^1H NMR it was unable to be determined if the cyclized hemiaminal was a salt or became deprotonated to become neutral but the alkene signals went away and resonances similar to that of **58** were seen. As the mixture was taken in $CDCl_3$ it was presumed to be the neutral species. The mixture was partitioned against water to remove the inorganic salts and concentrated before being allowed to react with sodium pyruvate as per the cinnamylidine method to produce **59**.

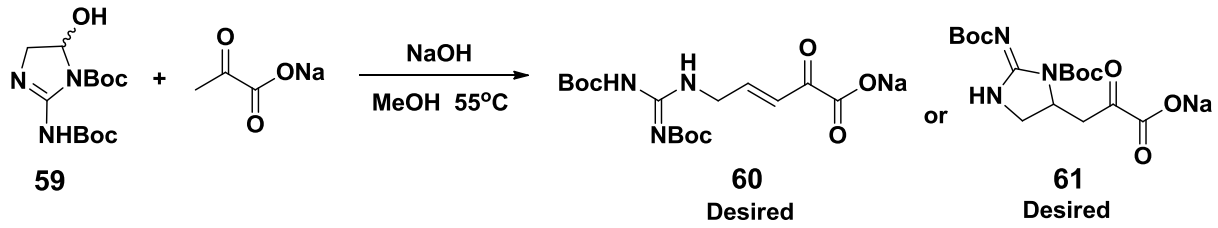


Figure 107: Reaction of di-Boc cyclic hemiaminal 59 with sodium pyruvate

After 17hr at 55°C **59** was longer seen by TLC. Analysis by ^{1}H NMR in D_2O showed no Boc signals present nor any other the alkene signals anticipated for the Aldol product. The crude product was extracted from triethylammonium bicarbonate with CH_2Cl_2 to isolate the desired product if present. What was observed by ^{1}H NMR did not have signals correlating to the alkene **60** and the starting material **59** was not isolated. One thought would be that the Boc protected nitrogen in the guanidine could Michael add into the enone product to cyclize to **61**. This was considered a possibility as demonstrated by the guanidine's propensity for cyclization but based on the ambiguity of the ^{1}H NMR spectrum, and the low amount of material recovered, it was deemed an unattractive method to make the dehydroarginine. However, more investigation should be undertaken to conclude if the material generated was indeed α-keto enduracididine as the methodology used would provide a succinct path for its synthesis.

1. L-Vinylglycine Synthesis

Vinylglycine[152] is a simple chiral substance allowing transformation of each of the three groups bonded to the chiral center.[153] It has become even more valuable since the development of efficient olefin metathesis catalysts that can convert it to other unsaturated amino acids. The unsaturation diverts pyridoxal-mediated transformations, leading to suicide substrate behavior of substituted vinylglycines with several pyridoxal based enzymes.[154,155,156] A

GABA transaminase irreversible inhibitor has also been prepared by a similar means.[157] Even in the absence of pyridoxal, the α-proton of vinylglycine ester is considerably more acidic than that of saturated amino acid esters: in mild base β-γ unsaturation of vinylglycine esters is rapidly converted to α-β unsaturation. Even in neutral D_2O, vinylglycine esters α-deuterate and gradually isomerize.[158] This obviously limits the conditions and procedures appropriate for preparation and transformation of such unsaturated amino acids.

Vinylglycine has been prepared by a variety of methods[159,160] including sulfoxide or selenoxide elimination from methionine derivatives,[161,162,163,164,165,166] oxidative decarboxylation of glutamic acid,[167] asymmetric allylic substitution and subsequent transformation,[168] vinyl Grignard reaction with an α-bromoglycine,[169] and an interesting route involving Neber rearrangement.[170] All these procedures yield vinylglycine in a protected or racemic form, from which L-vinylglycine itself can be isolated by deprotection and/or enzymatic resolution.

Perhaps the most common route is that reported by the Rapoport group in 1980 involving vapor-phase thermolysis of the Cbz protected methyl ester of methionine sulfoxide.[92,171] Contamination with isomerization products and variable yields encouraged modifications of conditions over the years, leading ultimately to a 79% yield of 95% pure protected vinylglycine.[96] Deprotection of chromatographically-isolated Cbz vinylglycine ester in refluxing hydrochloric acid allows subsequent transformation.[161] However, the gas phase reaction limits reaction scale, and requires careful control of conditions inconvenient with standard laboratory glassware. Attempts to increase throughput by solution phase approaches met with difficulties.[93] Despite this procedure, and the significant number of papers and patents describing vinylglycine and its use,[172,173] vinylglycine is not readily available commercially.

We report here a modification to the Rappoport approach to unprotected vinylglycine that allows convenient reaction at larger scale using standard apparatus and short reaction times. We have replaced two protection steps, thermolysis, chromatographic purification of protected vinylglycine, and deprotection, with a single simpler process using *in situ* protection, more convenient thermolysis, and a simple workup that effects deprotection and isolation of crystalline vinylglycine without chromatography. We have optimized for convenience rather than yield: conversion of methionine into pure crystalline vinylglycine requires two simple operations.

a. L-Selenomethionine selenoxide Route

The mildest procedures leading to vinylglycines appear to involve phenylselenoxide elimination.[174] A succinct method would be the by β,γ-syn elimination of the selenoxide analogue of L-Methionine with the chemical literature demonstrating that the α,β- elimination to form enones occurs rapidly, usually with no ability to isolate the corresponding selenoxide.

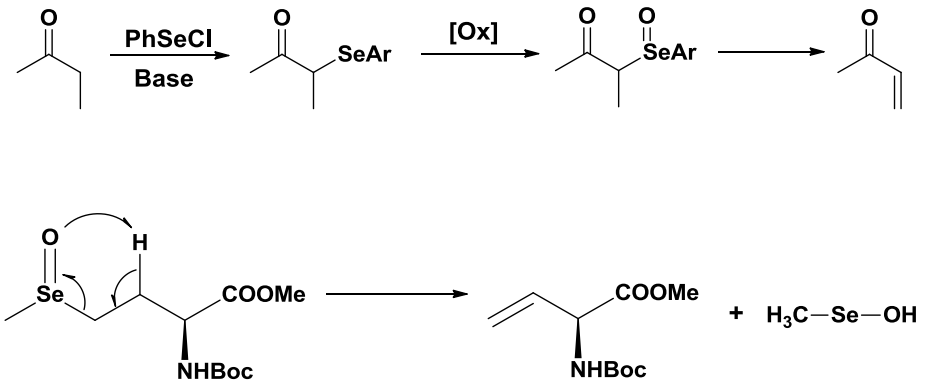


Figure 108: α ,β -unsaturated ketone formation by arylselenoxide elimination and desired elimation of a methyl selenoxide to form vinylglycine

While not as facile as the α,β- elimination, the β,γ-elimination was deemed feasible. L-selenomethionine was converted to the methyl ester **62**, N-Boc protected to **63**, and oxidized

the the selenoxide **64** using standard protocols. While the α,β- elimination can occur between -78°C and 0°C, elevated temperature were employed in investigation of the β,γ-elimination to generated the vinylglycine derivative **65**.

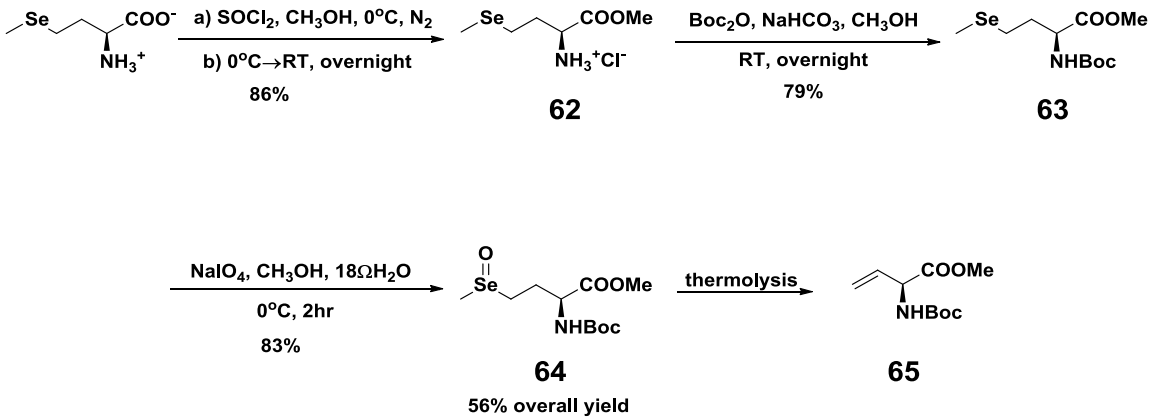


Figure 109: Synthetic scheme of N-Boc-L-vinylglycine methyl ester synthesis from L-selenomethionine

It has been previously reported[106] that a derivative of L-Selenomethionine oxide reduces back to its L-Selenomethionine derivative in acetone over 7d at room temperature in the absence of light. What was surprising was not the extent of this conversion in our experimental observations but the rapidity at which this transformation took place. Tabulated below are the experimental parameters and results from the β,γ-elimination of **64**:

Entry	Conc SeO	Conc $P(OMe)_3$	Temp(°C)	Time	Solvent	χ(vinyl:Se)	%yield(NMR)
1	$1.0e^{-2}$ M	-	138	2h	p-xylene	1 : 4	10
2	$1.0e^{-2}$ M	-	81	2h	CH_3CN	0 : 1	39 L-MetSe
3	$9.0e^{-3}$ M	0.09 M	110	20min	Toluene	1 : 2.5	50⟶0
4	$8.0e^{-3}$ M	0.10 M	110	20min	Toluene	1 : 1.8	41
5	$4.0e^{-3}$ M	-	111	25min	$P(OMe)_3$	-	0
6	$1.0e^{-2}$ M	3.60 M	reflux	25min	Hexane	1 : 10	15
7	$2.0e^{-2}$ M	0.27 M	110	40min	Toluene	0 : 1	97 L-MetSe
8	$1.5e^{-2}$ M	-	110	20min	Toluene	1 : 2.5	36

Table 6: Parameters and results in thermolysis of NBoc-L-selenomethionine oxide methyl ester

In our hands the methyl selenoxide **64** eliminated less well: only low yields (10-41%) of **65** were obtained on thermolysis. The major product was the precedented reduction to selenide.[175] Poor results were found at various temperatures, even in the presence of excess periodate, though it helped in a related phenylselenoxide case[176].

b. L-Methinonine sulfoxide Route

i. Gas Phase Pyrolysis

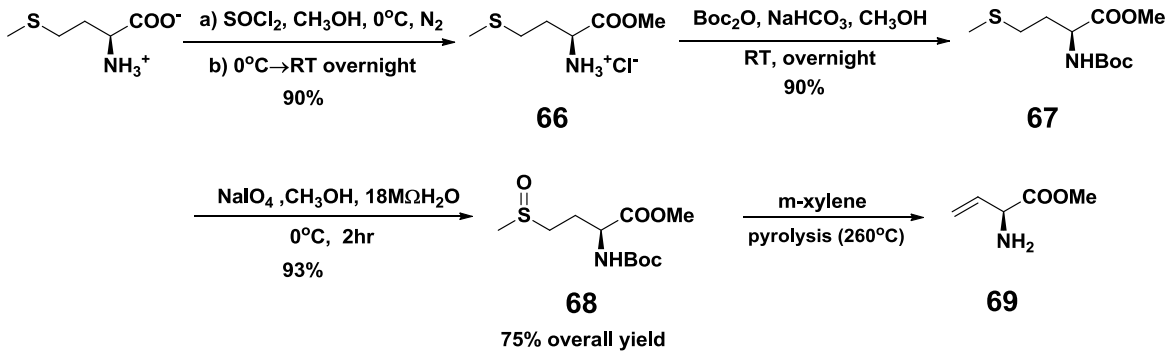


Figure 110: Synthesis of L-vinylglycine methyl ester form L-methionine

With the failure to produce vinyl glycine by β,γ-elimination from **64** in appreciable amounts, we turned to the harsh sulfoxide elimination procedure using the N-Boc methyl ester derivative of methionine sulfoxide, as reported by Rich[164] which provided the most detail for pyrolysis as well as an attractive yield before Rappoport's report and thus this method was chosen.[161] L- methionine was converted to **68** using the same protocols in the derviatization of L-selenomethione to **64**. Vapor or aerosol introduction of **68** in xylene to a hot tube at 266˚C led in our hands to variable yields (2-18%) of vinylglycine methyl ester with loss of Boc protection and on average 50% recovery of **68.** Pyrolysis was successful on one account affording a 59% yield of **69** as estimated by NMR a mixture with DEHP. The capricious behavior was attributed

to the low volatility of starting material and to lability of product, as isomerization of desired vinylglycine to α-β unsaturated side product was also observed.

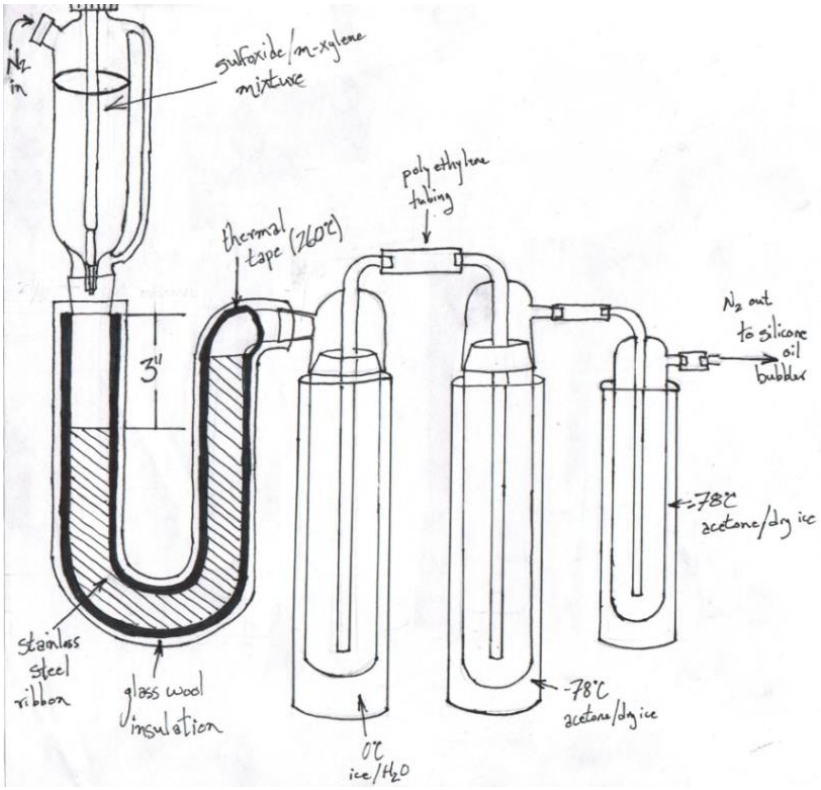


Figure 111: Illustration of apparatus constructed for gas phase pyrolysis

The thermal Boc removal is not entirely unwelcome, as its removal would be the next step in our sequence, but consideration of other protecting groups led to a useful modification. Protection of methionine sulfoxide in an organic soluble and more volatile form is needed, as we found pyrolysis of L-methionine sulfoxide **(70)** itself does not lead to L-vinyglycine **(71)**. As stocks of **68** were depleted, pyrolysis of a different protected form of L-Methionine sulfoxide was performed we chose trimethylsilyl groups to protect both the acid and the amine functionality, partly to increase volatility, and partly because both groups could be added before and removed after elimination as one procedure. Vapor phase thermolysis proceeded in a similar efficiency as before, though exposure of product to water caused complete

deprotection to free vinylglycine. Previous solution phase thermolyses led to problems because of decomposition of products on longer high temperature exposure times.[162] Pyrolysis proved successful and reproducible with the silylated methionine sulfoxide. The parameter that determined reproducibility was not only the temperature of pyrolysis, but the position of the stainless steel packing material in the pyrolysis tube.

ii. *in situ* Thermolysis

As the silylated methionine sulfoxide solution was able to be transformed into vinyl glycine by pyrolysis and vinyl glycine was recovered from the packing material at temperatures up to 310°C, it was hypothesized that the reaction could be performed in solution with the high boiling solvent diphenyl ether. The thermolysis was performed with variable amount of time with the solution at reflux. The table below details the distribution of materials was identified by ^{1}H NMR

	Molar Ratio of Compounds in Crude Product	
t (reflux)	Vinyl glycine	Side product
4 min	1.0	0.17
5 min	1.0	0.36
8 min	1.0	0.39
16 min	1.0	1.66

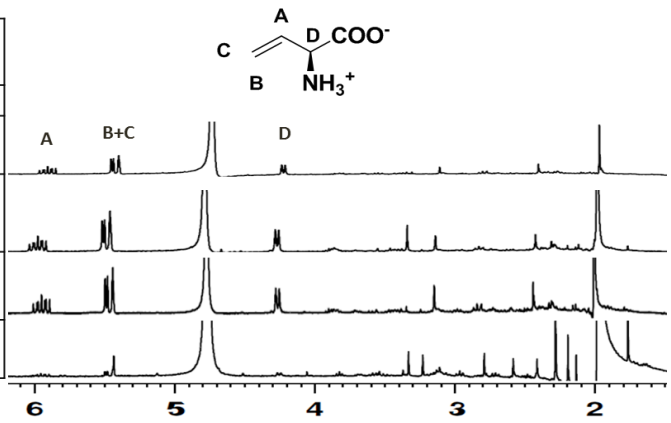


Figure 112: NMR spectra of isolated materials from *in situ* thermolysis of silylated L-methionine

Aqueous workup of the 5min trial afforded a 34% NMR yield of vinyl glycine. Encouraged, thermolysis of non-silylated **70** was done for 3.5min in refluxing diphenyl ether. Undetermined degradation products were produced as determined by NMR with signals observed that did not correspond to L-Methionine sulfoxide, vinyl glycine, or the side product, concluding that vinyl glycine cannot be produced without the presence of N,O-(bistrimethylsilyl)acetamide. Thermolysis of the silylated L-Methionine sulfoxide was scaled up and replicated with experimental parameters and results tabulated below:

Entry	Conc. L-MetSO	Conc. BSA	Mol Ratio L-Met SO:BSA	BSA:Ph_2O (v:v)	Time to Reflux	Time at Reflux
1	0.09 M	0.39 M	1 : 4.3	1 : 11	4 min	1 min
2	0.10 M	0.37 M	1 : 3.6	1 : 10	3 min	2 min
3	0.15 M	0.59 M	1 : 4.0	1 : 6	3 min	3 min
4	0.28 M	0.91 M	1 : 3.3	1 : 3.5	2 min	3 min

Table 7: Experimental parameters in screening *in situ* thermolysis for L-vinylglycine formation

	% by mass of the crude product				
Entry	Vinyl Gly	Acetamide	Side Product	L-Met SO	Estimated NMR yield L-Vgy
1	49	37	7	7	68%
2	52	37	11		54%
3	43	39	7	11	68%
4	15	65	20		30%

Table 8: Results fom tested conditions *in situ* thermolysis parameters in L-vinylglycine synthesis

iii. Addition and Distillation Method

Because of the expected substantially greater volatility of trimethylsilyl derivatives, we tried solution-phase heating of the silylated methionine sulfoxide. This provides a dramatic operational simplification.

Simply stirring L-methionine sulfoxide[177] in N,O-*bis*(trimethylsilyl)acetamide (BSA) caused gradual dissolution as the zwitterionic starting material was converted to the trimethylsilyl ester and likely the N-trimethylsilyl derivative as well.[178]

Surprisingly the material in the still pot after aqueous workup was determined by ^{1}H NMR to contain trace amounts of vinyl glycine with the majority being the unidentified side product and other degradation products accounting for 15% of the theoretical mass. Analysis of the distillate showed the presence of the silylated vinyl glycine. After aqueous workup the crude product was determined to be 3% by mass side product, 50% by mass acetaminde, and 47% by mass vinyl glycine corresponding to a 48% yield by NMR and the cleanest crude product seen to date. The experiment was replicated with similar success. The tables below are the parameters and results for the subsequent trails:

Entry	Conc SO (M)	Conc. BSA (M)	Ratio BSA:Ph_2O(mols)	Time to Reflux	Distill Time
136	0.16	0.56	1:3.5	5.5 min	4 min
138	0.12	0.43	1:3.6	8 min	6 min
130	0.30	0.67	1:2.2	10 min	9 min
140	0.27	1.92	1:7.1	7 min	5 min
142	0.18	0.72	1:4	15 min	4 min

Table 9: Experimental parameters from *in situ* thermolysis with distillation

		% by mass of the crude product			
Entry	Amount Distilled	L-vinylglycine	Acetamide	Side Product	% yield
136	2/3 rxn V	47	50	3	48
138	4/5 rxn V	45	52	3	51
130	To 246°C head temp	16	80	4	22
140	To 246°C head temp	22	73	5	36
142	175-253°C head temp	34	62	4	44

Table 10: Experimental results from in situ thermolysis with distillation

Thermolysis with distillation has consistently lead to the best molar ratios of vinyl glycine to unknown side product (on average 1:0.04 as determined by ratio of vinyl integrals to the triplet at 3.86ppm). Fractions can be collected during the course of distillation to obtain a purer crude product with the head temperature range of 175-246°C containing all of the vinyl product. However, the head temperature range of 175-200°C does contain vinyl glycine it only averages ~1% by mass and ~1% by mass side product with the remainder of the mass being acetamide. Interestingly, a large excess of BSA did not lead to an increased yield of vinyl glycine and corresponded to an increased amount of acetamide. The current hypothesis is that not only does amount of BSA correspond to the best yield but the ratio of volumes of BSA and diphenyl ether. This is presumably due to the time at which the reaction volume reaches the boiling temperature of diphenyl ether.

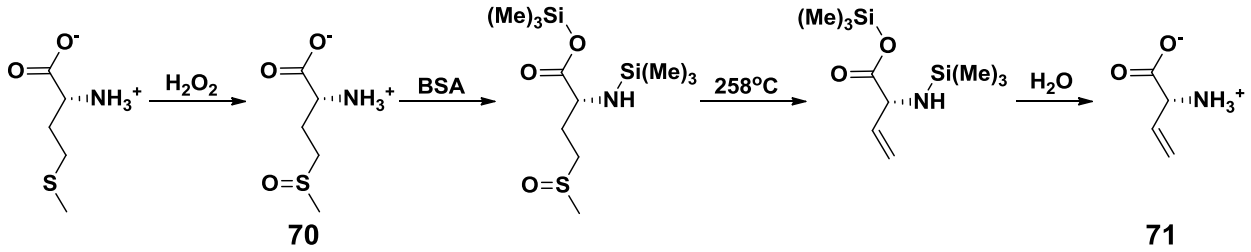


Figure 113: Synthetic scheme for L-vinylglycine formaton by in situ silylation followed by thermolysis with distillation

Though promising the *in situ* silylation and distillation method has the drawback of scale. A volume ratio of diphenyl ether to N,O-(*bis*-trimethylsilyl)acetamide (BSA) of 6:1 was determined to be optimal and therefore the reaction volume increases rapidly with scale. To circumvent this limitation the silylated methionine sulfoxide was added to distilling diphenyl ether. This method proved to be successful in maintaining decent yield along with bringing the silylated mixture to boiling Ph_2O temperature quickly, something not obtainable with lower than 6:1 Ph_2O:BSA . The *In situ* thermolyses where the ratio of Ph_2O to BSA was less than 6:1(v/v) a greater proportion of side product were observed in the isolated material.

Heating caused direct distillation of silylated vinylglycine from the reaction mixture. The addition of the silylated L-methionine sulfoxide mixture via Hirschberg constant addition funnel allowed for the production of vinyl glycine with low amounts of side product (estimated 1%-4% by mass across scale up) while going down to a ratio of Ph_2O:BSA of 2.3:1 (v/v). This protocol was used for reaction scales of 1.4g, 10.6g, 20.1g, 36.0g, and 50.4g with an average yield of vinylglycine of 38%. Of these, the 1.4g scale reaction proved to be anomalous in the fact that no side product was observed in the isolated crude by NMR and would obviously be the ideal method of preparation. The workup procedure was identical across the reactions with regards to hydrolysis and precipitation protocol. In this case, the silylation vessel was flame dried, N_2

flushed, silylated mixture diluted by about half with Ph_2O prior to addition, the pot temperature minimum was 254°C and 40% of the combined volumes used was collected as distillate. This result may be anomalous, as the only factors not carried on throughout the scale were flame dried glassware which was N_2 flushed and only distilling 40% of the combined volumes.

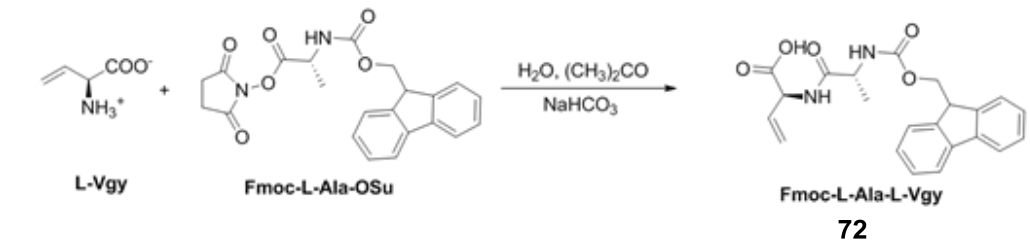
The other concern with scale up, especially with the 50g reaction, is the length of time needed to do the reaction. In this case the addition occurred over 54min at which time almost all Ph_2O was distilled with 92% of the combined volumes being collected as the distillate. Although dilution with Ph_2O does not seem to be needed with smaller scales (1-10g), it is recommended to dilute it with Ph_2O to ensure the distillation pot does not go dry. This also opens up the opportunity to use smaller glassware or work with larger scale as the Ph_2O being distilled is being replaced. Overall, the addition is robust enough with increasing scale while still use standard glassware. The problem of consistently not producing the side product during synthesis remains as well as a way to separate it from the desired product.

The initial isolation of **71** by precipitation of the aqueous phase with CH_3CN was still used, but done twice with scales greater than 20g. At the 20g scale, the crude product was determined to be 28% by mass acetamide which produced a sticky semisolid, whereas if the first precipitate was redissolved in water and precipitated again with acetonitrile, the average mass contribution was 3%. This protocol, although convenient and used for expediency, probably used more water than required to dissolve and thus increased the required amount of acetonitrile to precipitate. If time is not a factor, it is recommended to precipitate once and dry under vacuum overnight followed by triteration of the crude product in boiling ethanol to limit the use of acetonitrile.

Since this method of vinylglycine synthesis appears to the be the most succinct when compared to the literature and employs H_2O while still using standard synthetic glassware, exploration of the silylation conditions were carried out to make the overall procedure more amiable to industrial scale up. First, the typical heat treatment was monitored over time with ^1H NMR. The spectra showed from room temperature to 81°C over the course of 100min the α-hydrogen shifted upfield by 0.3ppm and the CH_3 signal transform from a doublet to a singlet. From 125min to 18hr of heating the spectrum did not change from the 100min spectrum and was determined that silylation was complete at 100min. Second, temperatures above 80°C were investigated. Heating at reflux for 2hr and 100°C produced identical spectra which were different from the 80°C and afforded 12% and 6% yield of vinylglycine with an estimated 5:2 and 2:1 molar ratio of vinylglycine to sideproduct. Lastly, cooler temperatures were employed. L-Methionine sulfoxide was silylated at 80°C until the mixture was homogeneous followed by room temperature stirring overnight or stirring at room temperature overnight. These two methods produced NMR spectrum like that of the 80°C overnight silylated product.

However, as slow heating caused starting material decomposition to form side products, and prolonged heating also destroyed the product, we settled upon dropwise addition to distilling diphenyl ether (258˚C), which caused rapid heating, elimination, and carryover of product. Hydrolysis, partitioning between water and hexane, and addition of acetonitrile to the aqueous layer caused precipitation of free vinylglycine in 95% purity. This protocol was used for reaction scales of 1-50g, with a 38% average yield of purified vinylglycine with reaction times ranging from 11-54min. No epimerization was apparent as determined by

HPLC separation of the dipeptide diastereomers prepared by reaction of vinylglycine with Fmoc-L-Ala-OSu and Fmoc-D-Ala-OSu.



72

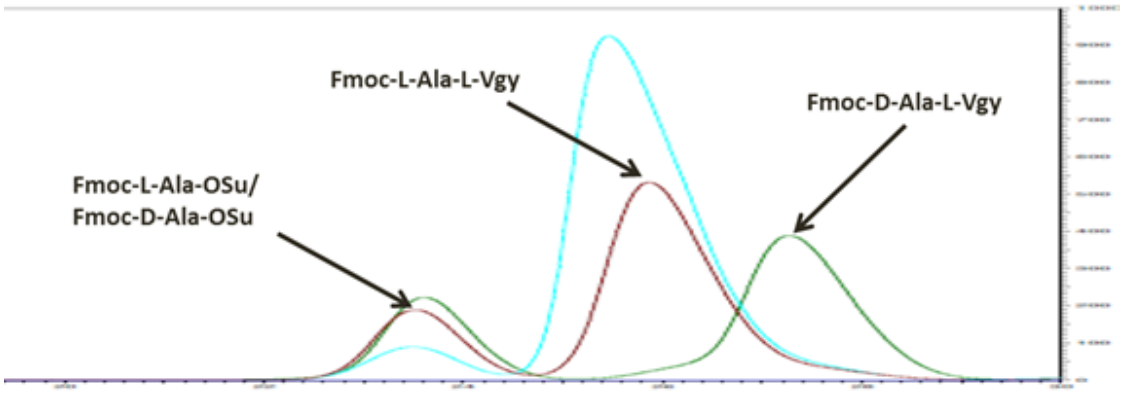


Figure 114: L-Vgy derivatization and HPLC trace demonstrating retention of desired stereocenter

Using these much less careful conditions, we have found effective elimination to vinylglycine without isomerization or epimerization. When N-Cbz vinylglycine methyl ester is used in thermolysis there had been substantial difficulties which are avoided by very short contact times with high temperatures. We wondered which features in our case allowed the simpler reaction conditions. The free acid is, as expected, quite resistant to isomerization compared to the ester: in contrast to the Boc protection of the free acid, bicarbonate in methanol causes complete isomerization during Boc protection of vinylglycine methyl ester in under 4h. In contrast, dissolution of vinylglycine methyl ester in BSA and triethylamine led to no detectable isomerization, even after 50 h. In order to separate effects of ester, and N-substituent on isomerization rates, we carried out the following studies.[179]

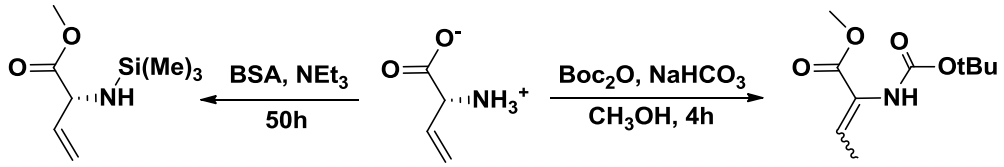


Figure 115: Reaction conditions in which L-vinylglcyine methyl ester will or will not isomerize

Comparison of N-Boc with N-TMS groups was made by dissolution of Boc-vinylglycine or free vinylglycine 1 in BSA, followed by addition of Et_3N. Boc vinylglycine TMS ester isomerized with a half time of ca. 1.6h, while the N-TMS derivative had an isomerization half-time of ca. 10^3h, demonstrating that the N protecting group is a substantial part of the difference. We compared TMS with H: vinylglycine methyl ester hydrochloride, on exposure to Et_3N, isomerized with a half time of ca 5.4h while vinylglycine exposed to TMSCl and Et_3N isomerized considerably more slowly, with a half time of ca. 1.7×10^2h. While N-Boc facilitates isomerization, it appears the N-TMS group slows it down compared to the N-H material, though the ester also changed. In comparing methyl ester with TMS ester, each in BSA solution, we found that in comparison to the N-TMS TMS carboxy ester half time of ca. 10^3h, the N-TMS methyl ester showed no detectable isomerization in that sample after 50h exposure to Et_3N, corresponding to a half time $>2 \times 10^3$h. Consequently, the faster isomerization of NH, methyl ester *vs* NTMS, TMS ester substrate is not due to the ester.

While the low isomerization tendency of silylated vinylglycine may not be critical to the success of the preparation, it is gratifying that this medium is less conducive to isomerization.

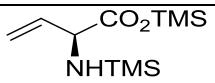
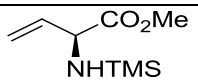
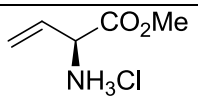
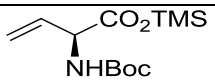
Substrate	Conditions	Solvent	[vinyl] (M)	[S.agent] (M)	[Net_3] (M)	Time (hr)	Mol Ratio (vinyl:enamine)	t ½ (hr)
	BSA/NEt_3	$CDCl_3$ (77%)	0.092	0.31	1.05	64.5	1 : 0.045	$1.0x10^3$
						92.5	1 : 0.06	$1.1x10^3$
	TMSCl/NEt_3	$CDCl_3$ (75%)	0.141	0.91	0.99	18	1 : 0.09	$1.4x10^2$
						108	1 : 0.73	$1.4x10^2$
	BSA/NEt_3	$CDCl_3$ (81%)	0.004	0.25	1.50	50	1 :<0.02	$>2.3x10^3$
	TMSCl/NEt_3	$CDCl_3$ (75%)	0.136	0.88	0.96	69	1 : 0.33	$1.7x10^2$
	NEt_3	$CDCl_3$ (86%)	0.094	0	0.99	19	1 : 6.7	6.4
						42.5	<1 : 28	<8.7
	BSA/NEt_3	$CDCl_3$ (62%)	0.03	0.95	0.90	1	1 : 2	0.63
						5	<1: 22	<1.2
	TMSCl/NEt_3	$CDCl_3$ (75%)	0.075	0.91	0.99	1.5	1 : 7	0.3
						18.5	<1 : 33	<3.6

Table 11: Pseudo- first order kinetic data for the isomerization of L-vinylglycine derivatives. All reactions conducted at 22°C and in $CDCl_3$

Boc group installation attempted on the C-Me L-Vgy HCl with Boc_2O in CH_3OH in the presence of $NaHCO_3$ to yield a mixture of the enamine isomers exclusively after 4h as observed by TLC and confirmed by ^1H NMR. Properties of derivatives of vinylglycine appropriate to peptide coupling have not been described in the literature, despite the report that incorporation from the Fmoc derivative was superior to incorporation of a phenylselenide followed by elimination: an uncharacterized Fmoc derivative was used.[180] Fmoc vinylglycine (**73)** prepared and characterized. The Boc derivative **74** is an oil at room temperature, so it was converted into its crystalline dicylohexylammonium salt **75**.

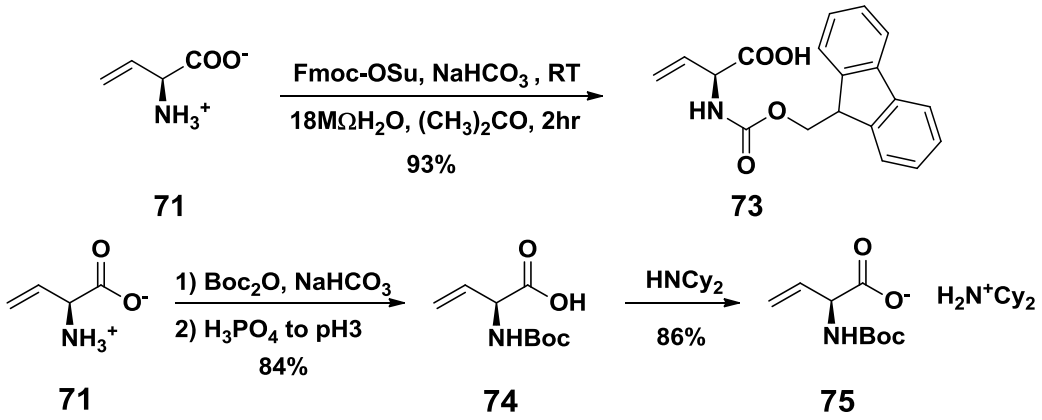


Figure 116: Fmoc- and Boc- protection of L-vinylgycine

Olefin methathesis (OM) can convert vinylglycine into other unsaturated amino acids, though steric hindrance prevents its homodimerization. Olefin metathesis in the presence of a more reactive alkene can lead to crossmetathesis.[181] Most examples of efficient vinylglycine and vinyl amine olefin metathesis involves intramolecular reaction.[182,183] Intermolecular reactions of vinyl glycine derivatives[100,103,184,185] and related substances[186] are reported, but some attempts have led to other products.[187] As we hoped to prepare unsaturated substances related to arginine for mechanistic studies[188] we screened several allyl derivatives for OM cross coupling to vinylglycine.

While simple terminal alkenes react under olefin metathesis conditions to cross couple with less reactive alkenes such as vinylglycine, the pairing of less reactive alkenes is problematic. Early attempts to cross couple protected allyamine with vinylglycine failed, even in an intramolecular case.[118]

2. Olefin Cross Metathesis of L-Vinylglycine Derivatives

a. Background on Olefin Metathesis

The net transformation of olefin metathesis is to cleave the strongest (double) bond, and reconnect the fragments. It proceeds by reversible cycloaddition of metallocarbenes to olefins forming a metallocyclobutane. It has become a powerful and versatile tool in the pursuit of sp^2 C-C bond formation. These metal catalysts are either molybdenum or ruthenium based, with each containing a metal carbene bonded to their metal center which serves as the driving force for olefin metathesis.

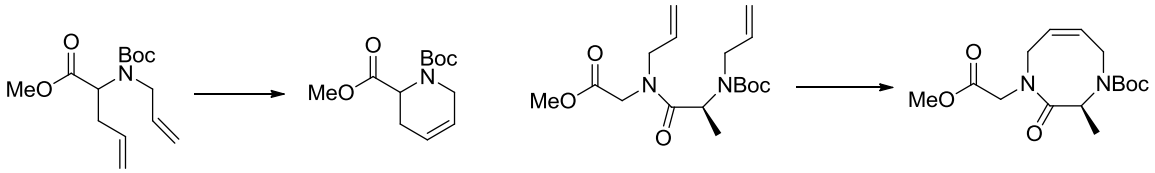


Figure 117: Examples of intramolecular olefin metathesis with amino acid derivatives

Some of the earlier examples of metathesis on amino acid or peptide scaffolds were attempts to perform ring closing metathesis on side chains containing allyl functionalites to make cyclic peptides[189] which remain a topic of interest as cyclic peptides provide a physiologically novel structures.[190] However when one of the allyl groups was for a vinyl group, intramolecular ring closure was prevented.[191]

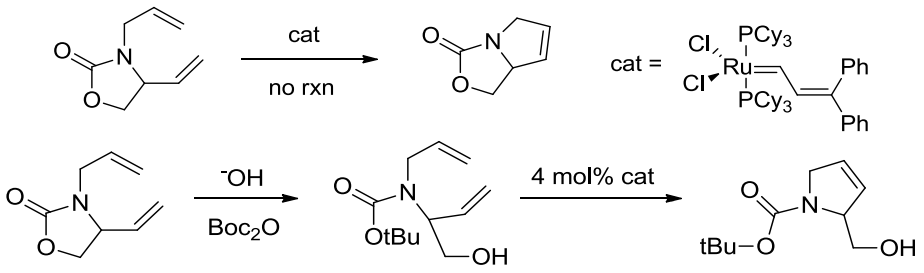


Figure 118: Successful metathesis after saponification of a lactone

Once the lactone was saponified, ring closing metathesis occurred in 95% yield. Whether this was due to steric hinderence or the pre-Grubbs 1st generation catalyst not being active enough was unknown at the time. Another attempt at ring closing metathesis was an N-allyl derivative of N-Boc-vinylglycine methyl ester.[192] While this did not have the previous constraint of being cyclic, instead of cyclizing with 5mol% catalyst at 25°C, the vinyl side chain isomerized to the α,β-unsaturated side chain and cross metathesized with itself to form a homodimer.

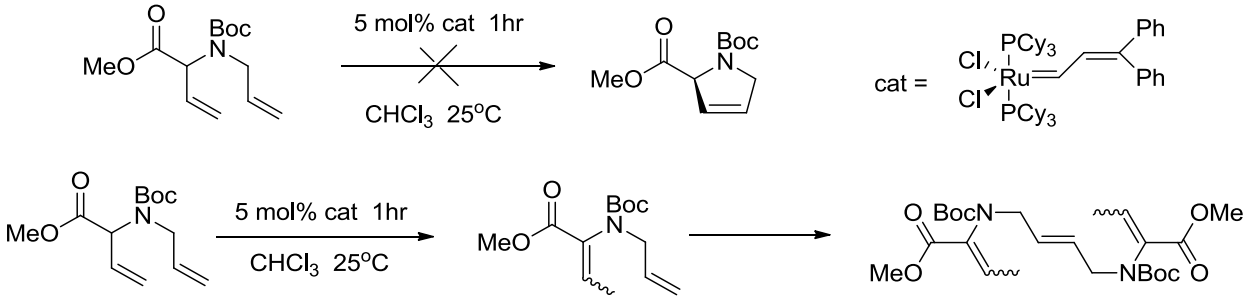


Figure 119: Homodimer formation due to isomerization of vinyl sidechain

The Schrock metathesis catalyst which can have difficulties performing cross metathesis if the substrates are not reactive enough[193] was employed a year later to perform cross metathesis on N-Cbz-vinylglycine methyl ester without isomerization to the α,β-unsaturated sidechain.[194] The cross metathesis product between the vinyl moiety and allyl trimethylsilane

was accomplished by use of a more reactive alkene, but it is limited in application due to the Schrock catalyst's need anhydrous and anerobic reaction conditions.

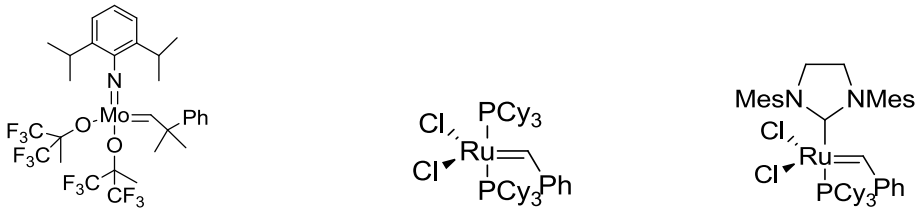


Figure 120: From left to right Schrock's, Grubb's 1st gen, and Grubb's 2nd gen metathesis catalysts

The Grubbs 1st generation catalyst, made by substitution to a styrenyl carbene, was used to perform cross metathesis on unsaturated α-amino acids to systematically test the parameters of C-ester steric hindrance as well as proximity of the olefin to the amino acid backbone with regard to the ability to perform cross metathesis.[195] N-Boc homoallylgycine was used as a model compound to evaluate ester sterics when metathesized with styrene or hexene. The esters were methyl, benzyl, t-butyl, and one instance of the free acid ranged from 52-66% yield showing no appreciable effect from increasing steric bulk at this carbon chain length. The contributing factor that affected the propensity towards cross metathesis was the proximity of the double bond to the amino acid's chiral center: the yield of the desired product decreased as it approached the α-amino carbon. When cross metathesis was conducted using hexene with homoallylglycine, allyglycine, and vinylglycine yields dropped as bulk increased from 66% to 45% to 7% respectively.

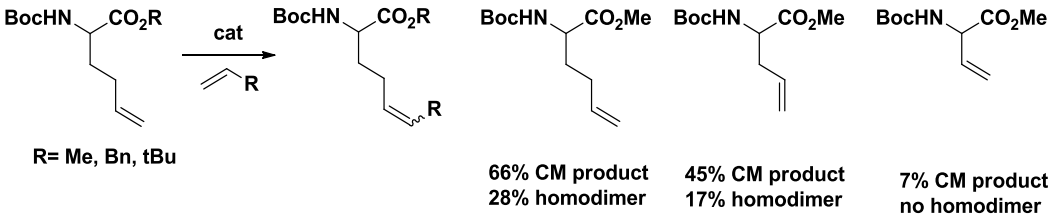


Figure 121: Afforded yields of cross metathesis product as steric hindrance around olefin increases

The sensitivity to sterics for the 1st generation Grubbs catalyst was quantified by the rate of metathesis with increasing encumberance around the α-carbon to the olefin.[196]

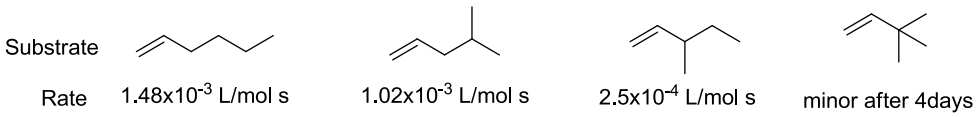


Figure 122: Effects of increasing steric hindrance on rate of metathesis

If hydrogens were substituted for methyl groups β- to the olefins (or presumably even further away) the rate decreased slightly from 1.48 to $1.02x10^{-3}$ L/mol·s. When this same change in substituents took place α- to the alkene, resulting in a 3° carbon, the rate dropped by an order of magnitude to $2.5x10^{-4}$ L/mol·s had only trace amounts of metathesis product observed after 4 days if 4° carbon was in proximity. The electronic characteristics were also correlated to a rate which increased by an overall factor of four when changed from p-NO_2 styrene to p-Me styrene to p-OMe styrene, suggesting electron rich species react faster.

Over the course of these studies it was observed that the E isomers were isolated or formed preferentially over the Z isomer. A paper on a new methodology for cross metathesis with Grubbs 1st generation catalyst for greater E selectivity demonstrated homodimerization of terminal olefins before cross metathesis occurred but at the cost of an overall lower yield of the cross metathesis product.[197] The 2nd generation Grubbs catalyst also shares this tendency[198] towards formation of the E isomer. Compatibility with aliphatic alcohol, ester, or ether containing functionalities was no problem affording yields on average of 70% and E:Z ratios ranging from 3-10:1. The only detriment to homodimerization in these cases was reaction temperature. If the temperature were to exceed that of the boiling point of dichloromethane

the yield would decrease, which was attributed to the decomposition of the metathesis catalyst.

The tolerance of alkenes with nitrogen substituents towards metathesis were also studied. Though not as widely explored, the examples of Boc protected allyl amine and amides in peptides did not interfere with cross coupling. What did prevent facile metathesis were amides alpha to the terminal olefin. When metathesis was attempted on N-methoxy-N-methyl-acrylamide, a Weinreb amide, it gave a low yield of 17% and the low E:Z ratio of 1.9:1.This lack of reactivity was speculated to be due to intramolecular coordination of the amide to the ruthenium center when it became attached as a carbene to stabilize it as an intermediate and interrupt the catalytic cycle.

In the year 2000 Hoveyda advanced metathesis technology with his modification to the Grubbs catalyst by replacing the initial styrenyl carbene with an intramolecular coordinating isoproxystyrene[199] increasing the reactivity of the catalyst, as well as stabilizing it, allowing for a more robust set of experimental conditions in which metathesis may be conducted. This ruthenium carbene complex is known as the Hoveyda-Grubbs 2nd generation catalyst. Substrates previously unresponsive to cross metathesis with previous catalysts were now able to be reevaluated for these purposes. N-Boc-2-vinyl-pyrrolidine was able to do metathesis with methyl 3-butenoate[200] in 31% yield in a 10:1 E:Z ratio under conditions where the 1st generation Grubbs catalyst could not perform and N-benzyl-N-Boc-ethenamine with methyl 3-butenoate in 60% yield. The 1st generation Hoveyda-Grubbs catalyst, in which the tricyclohexylphosphine ligand was replaced with an N,N'-*bis*-mesitylimidazole carbene, is also able to effectuate

vinylglycine metathesis due to the enhanced reactivity of the metal afforded by the additional carbene moiety.

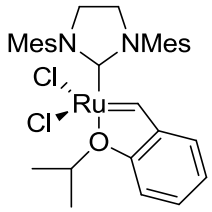


Figure 123: Hoveyda-Grubbs's 2nd generation metathesis catalyst

In the synthesis of D-glycosyl-asparagines, α- or β- allyl glycosides were coupled with vinylglycine derivatives containing different combinations of N-protecting groups and carboxy esters.[201] What was found from the Orlando group was that metathesis of α- or β- positions displayed slight preference towards the α- position due to the lesser degree of steric interaction. Neither N-Cbz, N-Boc, N-Fmoc nor C-Me, C-Bn- or C-tBu esters altered the yields of the desired glycoside metathesis product substantially. However, when the alkene on the glycoside was change to vinyl from allyl no cross metathesis was observed. Isomerization of the vinyl group in the vinylglycine derivative to the α,β-unsaturated alkene was observed when exposed to refluxing CCl_4 (76˚C) and 1,2-dichloroethane (84˚C).

Cross metathesis of protected vinylglycines was also used to make other biologically important molecules like diaminopimelic acid,[202] a component in peptidoglycan biosynthesis in gram-negative bacteria as well as in the synthetic route to make the natural products Syringolin A and B.[203] Syringolin A and B have been identified as a proteasome inhibitor which act as Michael receptors for conjugate addition to N-terminal threonine residues, acting as virulence factors for plant pathogens was well as a potential therapeutic for human neuroblastoma.

Early in the sequence 4-bromobutene was coupled with a vinylglycine analogue in 69% yield using 10mol% catalyst over two additions and five hours of reaction time.

As these catalysts are non-polar and conducting olefin metathesis in physiological media has become of interest, water soluble varieties of the Hoveyda-Grubbs catalyst have been synthesized and determining their limitations in metathesis has been undertaken. One of the first attempts involved attaching a polyethylene glycol chain to the imidazole ligand in the Hoveyda-Grubbs 2nd generation catalyst which resulted in an average molar mass of 5000g/mol.[204] This was able to perform ring closing metathesis on a range of substrates and cross metathesis on allyl alcohol but failed to produce homodimers of acrylic acid or allyl ammonium chloride. Altering the pH of the aqueous media did not perturb the reactivity of the catalyst to either induce metathesis on the unreactive substrates or prohibit the metathesis of the successful species.

The other water solubilizing changes made to the Hoveyda-Grubbs 2nd gen. catalyst were quaternary ammomiums on the iospropoxy styrene ligand[205] or use of a solvent mixture consisting of water and an organic cosolvent[206] in which the main drawback was the low maximum concentration of the Hoveyda-Grubbs 2nd gen catalyst. Ring closing was able to be performed on secondary ammonium chlorides to form five and six member rings and tertiary amines to close to a five member ring in good yield if the amine was a trifluoroamide or tosylamide. The cases were ring closure did not occur were if quaternary ammoniums were present or if the nitrogen was replaced with a diphenyl silane suggesting that the steric bulk around these moieties hindered metathesis.

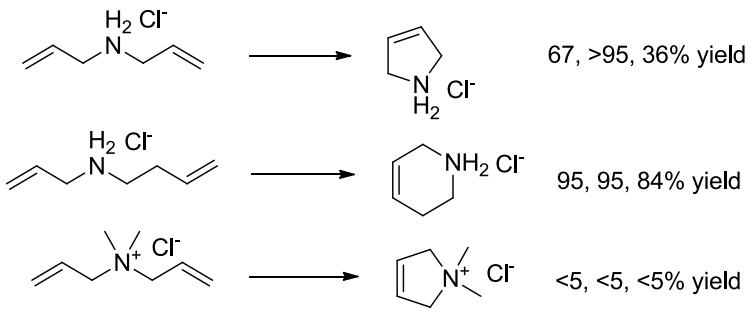


Figure 124: Ring closing yields using water soluble Hoveyda-Grubbs 2nd gen catalysts

b. Synthesis and Screening of Allylamine Derivatives for Cross Metathesis

Our metathesis experimentation began with evaluating the ability of desired alkenes to homodimerize in the presence of Hoveyda-Grubbs 2nd generation catalyst to screen for substrates suitable to perform cross-metathesis on an analogue of vinylglycine. Allyl amine was tried first and when combined with 11mol% of the catalyst in CH_2Cl_2. Upon addition of the amine the color of the solution changed from an emerald green to a brown color and after refluxing for 17hr no metathesis was observed. This was attributed to the coordination of the amine to the ruthenium, inactivating the metal towards metathesis. This observation prompted the creation of a series of derivatives.

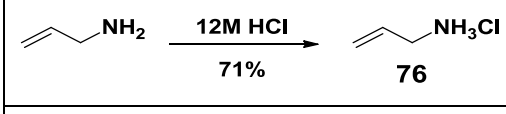
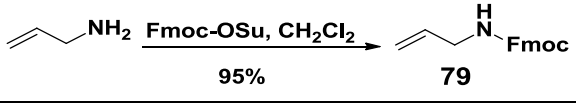
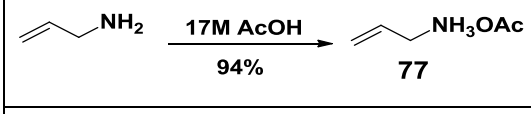
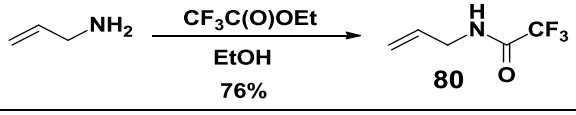
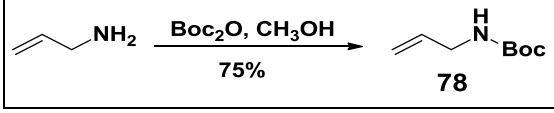
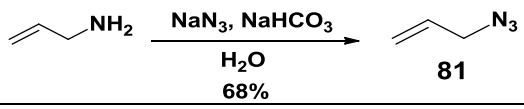
	
	
	

Table 12: Synthesis of allyl amine derivatives for homodimerization screening

The duo of protonated allyl amines, allyl ammonium chloride and allyl ammonium acetate, were made by combining with 12M HCl and glacial acetic acid respectively. After concentration with rotary evaporation, azeotropic drying by evaporation of toluene, and exposure to vacuum to remove residual solvent, 71% yield of **76** and 94% yield of **77** were obtained. Synthesis of acyl analogues proceeded next. Boc protection of allyl amine occurred quite rapidly using Boc anhydride and excess of allyl amine in methanol at room temperature. Mixing of the two produced a large exotherm and effervescence upon mixing and complete conversion after 20min as seen by TLC (silica, $KMnO_4$, 5% CH_3OH/CH_2Cl_2, R_f amine= 0.0, R_f Boc amine= 0.78). The white solid afforded after workup corresponded to 75% yield **78** and had a melting point range of 28-34˚C. **78** was also observed to be volatile which was discovered after leaving a previous preparation under vacuum overnight to remove residual solvent to find it had evaporated away. This implies that sublimation should be employed in future preparations to purify this substance.

Fmoc protection used the N-hydroxy succinimide ester of fluorenyl methyloxycarbonyl with an excess of allyl amine in CH_2Cl_2 to produce **79** in 95% yield with 121-122˚C melting point in one hour. **80** was created by treating allyl amine with two equivalents ethyl trifluoroacetate, a volatile trifluoroacetylating agent that does not require base to be present. Mixing at room temperature in ethanol produced a large exotherm and complete reaction after 15min (silica gel, 40% EtOAc/hexane, $KMnO_4$ visualized, R_f product= 0.55). Isolation of the desired product became troublesome as its boiling point was lower than that of either ethanol or ethyl trifluoroacetate meaning that removal of the solvent or excess reagent came at the expense of the yield as the small scale prohibited convenient distillation. From this procedure, the

trifluoroacetate **80** was afforded in 76% yield. Allylamine is the lowest in boiling point of the combination so subsequent syntheses should employ it in excess coupled with its slow addition to ethyl trifluoroacetate in an ice bath using neat conditions.

The final derivative made was **81**. $NaHCO_3$, as an extra precaution to prevent the formation of hydrazoic acid, was dissolved in water along with NaN_3 before the addition of allyl bromide as per the literature.[207] A biphasic mixture resulted with the organic layer on the bottom. After 30min of stirring at room temperature, the organic phase switched positions with the aqueous phase and is an indication that the reaction is proceeding, but not a sign of complete reaction. After 4hr though TLC showed complete conversion to the allyl azide (silica, 10% EtOAc/hexane, $KMnO_4$, R_f amine= 0.57, R_f azide= 0.64). As with **80** and **78**, isolation was problematic due to its volatility. Previous preparations utilized ethyl ether to partition the allyl azide away from the aqueous layer, but use of rotary evaporation or vacuum to remove the solvent also evaporated allyl azide resulting in negligible mass. It was determined then to separate **81** neat and pass it over a column of $MgSO_4$ in pasteur pipet to give the desired material in 68% yield.

Homodimer Formation

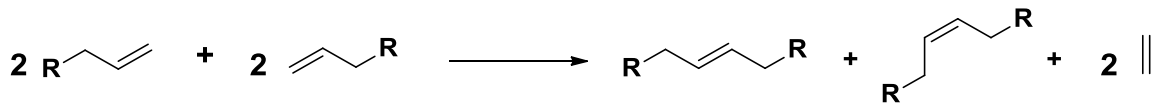


Figure 125: General scheme for homodimer formation via olefin metathesis

Cross metathesis with the vinylglycine moiety is predicated upon the formation of a metathesis homodimer with the allylamine derivatives. This is due to the fact that the allyl

functionalities have a lesser amount of steric hinderence about the olefin compared to the vinyl and thus will undergo metathesis first. As a result, selectivity in cross metathesis can be achieved by having the allyl homodimer then react with the vinyl group. Cross metathesis of L-vinylglycine is desirable as it would provide the most direct route to dehydroarginine. Allylammonium salts and aqueous cosolvent conditions were used as described by the Raines publication[206] to investigate metathesis. A solution of **76** in D_2O as added to a solution of the Hoveyda-Grubbs 2nd generation catalyst (5mol%) in 1,2-dimethoxyethane (DME) which caused some of the catalyst to precipitate. The mixture was stirred at room temperature over the course of five days while being periodically monitored by ^{1}H NMR with no change observed in the spectra over that time. The same results were seen with **77** in CH_2Cl_2 and H_2O/acetone solvent systems with 10mol% catalyst at reflux and 55°C respectively over the course of 24hr. The mixtures were allowed to sit for an additional 12d at room temperature in the hopes of seeing metathesis proceed, but to no avail. Lack of metathesis was determined to be due to the proximity of the positive charge to the allyl functionality and not the chloride ion.

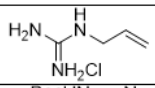
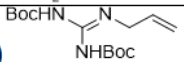
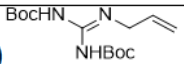
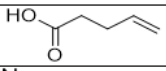
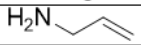
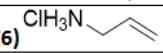
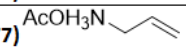
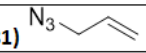
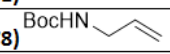
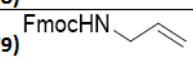
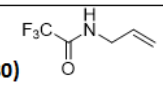
Alkene	Solvent	Temp (˚C)	Cat.(mol%)	Time	Result
	H_2O/ acetone	reflux	12	18h	No metathesis
 **(55)**	$CDCl_3$	RT	11	72h	No metathesis
 **(55)**	CH_2Cl_2/ AcOH	reflux	13	48h	No metathesis
	CH_2Cl_2	reflux	9	18h	quant. (TLC) 88% isolated
	CH_2Cl_2	reflux	11	19h	No metathesis
 **(76)**	H_2O/DME	RT	5	96h	No metathesis
 **(77)**	CH_2Cl_2	reflux	9	21h	No metathesis
 **(81)**	CH_2Cl_2	reflux	8→13	43h	40% yield (NMR)
 **(78)**	CH_2Cl_2	reflux	12	18h	75% isolated
 **(79)**	CH_2Cl_2	reflux	10	4h	quant. (TLC) 47% isolated
 **(80)**	CH_2Cl_2	reflux	12	17h	quant. (TLC) 43% isolated

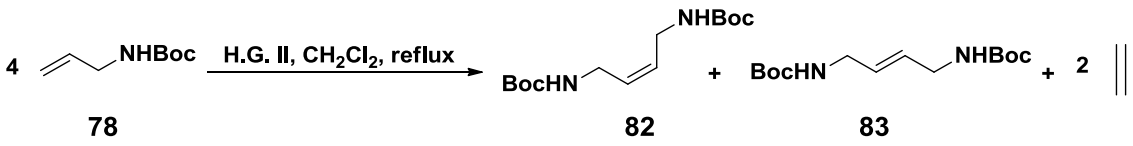
Table 13: Alkene reactivities for homodimer formation

Allyl guanidinium chloride was investigated next with the thought that maybe a more delocalized cation would not be an impediment. The reaction appeared to proceed with 12mol% catalyst in 20% H_2O/acetone at reflux for 17hr at which time the ^1H spectrum was taken and showed a lack of the starting alkene signals. The mixture was washed with CH_2Cl_2 and the aqueous phase concentrated to give a 68% crude yield. The crude product was analyzed by ESI-MS to give a peak at m/z=307.5 which would correspond to a vapor phase complex between the desired homodimer and allyl guanidinium chloride with a bridging chloride between them and further evidence that metathesis had occurred. However, an M+2 peak at 25% intensity indicative of the ^{37}Cl isotope was absent. Comparison its NMR spectrum to that of the homodimer formed from **78** showed a similar set of signals. The resonances of this homodimer were broad singlets at δ5.62, δ4.57, and δ3.72 and those of the allylguanidinium homodimer were broad singlets at δ5.74, δ5.30, δ4.20, δ4.12 but these signals were only a

fraction of the signals present or their intensities. From these data, metathesis of this substrate appears to occur but is sufficiently ambiguous to prevent a definitive conclusion.

As the cationic allyl amines proved stagnant to homodimerization, **55** was tried next with 11mol% metathesis catalyst in $CDCl_3$ at room temperature. This mixture was monitored by ^1H NMR over 22.5hr with no appreciable change in the spectral signatures of the catalyst or the starting olefin. Although initially perplexing, recalling the coordination of the imine lone pair to the osmium tetroxide to attempt oxidative cleavage of the alkene and how it prevented reaction could explain this lack of metathesis reactivity. If the lone pair on the guanidine could be occupied by being protonated it could it could facilitate olefin metathesis much like the case of oxidative cleavage to proceed to form **59.** The experiment was replicated with 13mol% catalyst and 10 eq glacial acetic acid and heated at 40°C in CD_2Cl_2. After heating overnight this mixture only starting materials were observed to be present. The reaction volume was vented with a slow stream of N_2 to the atmosphere and set back to reflux for another 24hr. ^1H NMR analysis showed no ethylene present or starting materials and TLC did show new spots which were isolated with flash chromatography. These spots were then submitted for ESI-MS analysis but did not give any peaks corresponding to the molecular ion of the desired homodimer product. The conclusion from this experiment that as the neutral compound the imine lone pair prevented metathesis by coordination to the ruthenium and trying to circumvent this by protonation also prohibited homodimerization for the same reason as the allyl ammonium compounds, the proximity of the formal positive charge.

Being cationic and sterically bulky has been demonstrated to be detrimental to olefin metathesis allyl azide was exposed to metathesis conditions next. The metathesis catalyst was added at reflux in $CDCl_3$ with allyl azide in two portions up to a total of 13mol% over the course of two days which resulted in a 1:3 molar ratio of the homodimer to the monomer. The solution changed from a green to a dark brown color upon reaching reflux similar to the attempted metathesis of allyl amine which was assumed to correlate to catalyst decomposition. However when conducted at room temperature with 20mol% catalyst added in two portions over two days a 1:6 molar ratio of homodimer to monomerwas produced. Allyl azide also seems to be a poor substrate for olefin metathesis under these conditions.



78 82 83

Figure 126: Homodimer formation via olefin metathesis of Boc protected allyl amine

Thankfully not all of the allyl amine derivatives were unreactive. The acyl derivatives were able to homodimerize but with reactivity dependent on solvent observed. In the case of Boc protected **78** use of 30% H_2O/DME resulted in no metathesis while reflux in CH_2Cl_2 afforded complete metathesis in 16hr in a 75% yield in a 1:1.6 ratio of Z:E isomers **82** and **83**. Fmoc derivative **79** underwent complete conversion in refluxing dichloromethane with 10mol% catalyst in 1.5hr. 58% yield of this homodimer **84** was afforded but mass was only acquired from the crystalline material from the reaction mixture, the E isomer. A more quantitative yield can be generated by utilizing flash chromatography on the crude product but was deemed unnecessary, as looking for metathesis activity was the primary goal.

N-allyl-trifluoroacetamide also underwent complete homodimer formation overnight with 12mol% catalyst in refluxing CH_2Cl_2 even though the color of the mixture changed to a dark brown upon reaching reflux temperature. A 43% yield of homodimer **85** was analyzed by ESI-MS (-ion mode) and produced ions corresponding to M-H^+, M+$HCOO^-$, and M+CF_3COO^- confirming that metathesis occurred. As expected the less hindered alkene 4-pentenoic acid, underwent olefin metathesis smoothly to form homodimer **86** in 88% isolated yield.

c. Cross Metathesis of L-Vinylglycine Derivatives and Selected Allylamine Derivatives

Even with the lack of precedence of cross metathesis between two ammonium bearing olefins, the metathesis of vinylglycine hydrochloride with allyl guanidinium chloride was attempted to make the dehydroarginine directly. Using conditions described by Raines[206], no change was observed in the composition of the mixture by ^{1}H NMR over the course of 89hr. The next attempt at cross metathesis was done with allyl ammonium acetate **(77)** and N-Boc-L-vinylglycine **(74)** in 28% D_2O/DME with 6mol% catalyst. Even though it seems unlikely as the allyl ammonium acetate did not form a homodimer, it may be possible with a cationic and neutral olefin as opposed to bringing two cationic species together to metathesize into a dicationic species. After heating at 55˚C for 24hr the ^{1}H spectrum remain unchanged. The mixture was brought to room temperature and monitored sporatically over the course of 13d with still no change seen in the resonances.

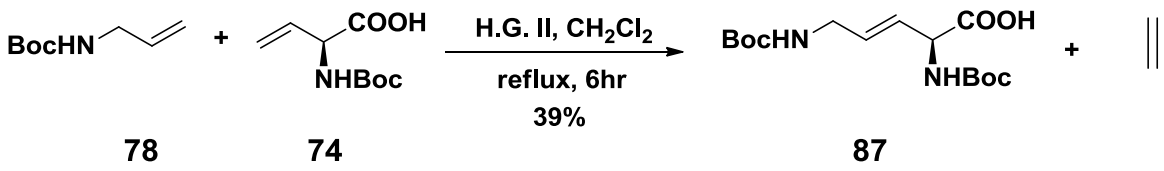


Figure 127: Example olefin cross metathesis using Hoveyda-Grubbs 2nd generation catalyst

Effort was then shifted from the charged olefins to neutral, organic soluble derivatives with the first combination being **78** and **74**. Utilizing 11mol% catalyst and refluxing CH_2Cl_2 only partial reaction was observed over 18hr. The mixture was none the less concentrated, redissolved in EtOAc, and extacted with 29% $NH_{3(aq)}$ to give a crude product that was partially separated by flash chromatography. The fraction containing the largest mol fraction of the cross metathesis product **87** was subjected to ESI-MS (- ion) analysis and produced peaks of m/z= 329 ($M\text{-}H^+$) and 530 (M^-+ **74** vapor complex). Accounting for the unreacted **74** a 17% yield based on conversion was isolated. This low yield could be attributed to the low partitioning of the desired product into aqueous ammonia as well as the incomplete reaction. Recommendations in improving the yield of the cross metathesis product can be done by increasing the ratio of 4:1 **78**: **74**, increasing the amount of catalyst to 20mol% in two portions, and chromatography of the reaction mixture should be done in future preparations.

The Fmoc derivatives of vinylglycine coupled to the Boc allyl amine **(78)** is desirable as cross metathesis would generate a product containing orthogonal protecting groups. This will allow for installation of the guanidine functionality unambiguously on the resulting side chain amine. The dicyclohexylammonium salt of Fmoc-L-vinylglycine was prepared and mixed with 6eq Boc allyl amine with 20mol% catalyst in refluxing CH_2Cl_2 for 24hr with no change as seem by TLC. An additional 20mol% calatyst was added and left at reflux for 4d before analysis of the mixture by TLC was done again and still looked like the starting materials. The proton spectrum confirmed that it was still reactants along with the NBoc allyl amine homodimers **82** and **83**. The steric hindrance around the vinylglycine olefin was too bulky to effectuate metathesis.

73 was employed next with Boc allyl amine under similar metathesis conditions but with only 20mol% catalyst. After 4d at reflux no new spots by TLC or a molecular ion from ESI-MS analysis of the reaction mixture was observed.

This continued reticence Fmoc vinylglycine towards metathesis prompted the swapping of the protecting groups on the coupling partners to Fmoc allyl amine and N-Boc-L-vinylglycine **(74)**. A minimum of two equivelents Fmoc allyl amine **(79)** and 25mol% metathesis catalyst were left in refluxing CH_2Cl_2 for 4d before TLC analysis which showed the absence of **74**. The reaction, though complete, has yet to have the cross metathesis product **88** isolated. Extraction with ammonia did not partition the product into the aqueous phase, using silica gel flash chromatography with 10% AcOH/CH_2Cl_2, or ion exchange chromatography with Dowex 2X-8 (quaternary ammonium, strong anion exchanger) failed to generate materials that produced the desired molecular ion with ESI-MS. Use of chromatography before any separation should be used subsequently in attempts to isolate the product and should not be abandoned as a possibility.

Metathesis between N-allyl trifluoroacetamide **(80)** and **74** was able to be done with 6eq of **80** and 18mol% catalyst added in two portions in refluxing CH_2Cl_2 over two days. The product was attempted to be isolated by extraction with pH9 water but was not able to partition it into the water and confirmed by lack of molecular ion when analyzed by ESI-MS. This product should be isolated by chromatography.

Success was also found in the coupling of 4-pentenoic acid and **74** with 6eq of the acid and 15mol% metathesis catalyst added in two portions over two days in refluxing CH_2Cl_2 to

genereate cross metathesis product. Isolation of the cross metathesis product was accomplished by trifluoroacetic acid removal of the Boc group, dissolving the resulting salt in water, followed by washing with EtOAc to afford **89** in 58% yield.

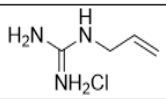
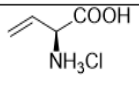
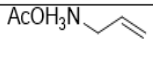
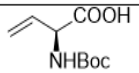
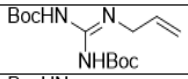
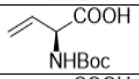
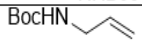
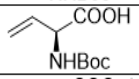
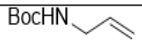
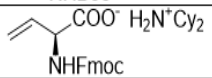
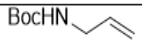
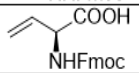
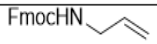
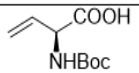
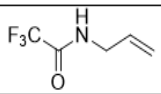
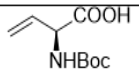
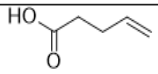
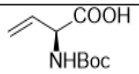
Entry			Solvent	mol% catalyst	Temp	Time	Result
1			D_2O/ $(CD_3)_2CO$	22	reflux	89h	No cross metathesis
2			28% D_2O/DME	6	55˚C→RT	1d→14d	No cross metathesis
3			CD_2Cl_2	16→40	reflux	6d	No cross metathesis
4			CH_2Cl_2	11	reflux	18h	Cross metathesis
5			CH_2Cl_2	20→42	reflux	5d	No cross metathesis
6			CH_2Cl_2	11	reflux	18h	No cross metathesis
7			CH_2Cl_2	20	reflux	18h	Cross metathesis
8			CH_2Cl_2	12→18	reflux	2d	Cross metathesis
9			CH_2Cl_2	9→15	reflux	2d	Cross metathesis 43% est. yield

Table 14: Summary of results for combinations of metathesis substrates

VII. CONCLUSION

Cinnamylidene pyruvate and (4-nitro)cinnamylidene pyruvate salts were synthesized in a facile manner that allowed subsequent reserchers to generate more material and additional pyruvate adducts to further probe the reactivity of SbADC. Triethylammonium bicarbonate extraction of the cinnamylidiene pyruvates allowed of the removal of excess sodium pyruvate for kinetic stop flow experiments but at the cost of a large amount of the desired pyruvate

adducts with most of the desired diene reverting back to the Aldol condensation product by hydration of the diene.

The method for sodium difluoropyruvate synthesis was improved on from the described literature methods by detailing ozonolysis conditions that does not generate a mixture of furan starting material and desired difluoropyrvate ester as well as employing an anion exchange resin to simply the removal of acidic byproducts. Unfortunately the limited amount of material that could be made under the time constraints did not yield solutions of a sufficient concentration to occupy the active site of SbADC to afford unambiguous x-ray cryallography data.

A synthetic route that affords L-vinylglycine in two steps that can be conducted on a 50g scale utilizing conventional laboratory glassware in an average 39% yield was also developed. This method proved to be a dramatic simplification from the literature in the amount of material that could be generated with regard to time invested. Utilizing relatively inexpensive reagents, easily obtainable temperature, and standard laboratory techniques researchers in need of this material are stronger encouraged to use this methodology.

The L-vinylglycine made was derivatized with Boc and Fmoc protecting and made into a crystalline dicyclohexylammonium salt so that it could be used in subsequent screening for olefin metathesis reaction conditions en route to forming β,γ-dehydroarginine. It was found that Boc-L-vinylgylcine was able to undergo cross metathesis with Boc protected allyl amine, Fmoc protected allyl amine, trifluoroacetyl allylamine, and 4-pentenoic acid opening up the potential to for other non-canonical dehydro amino acids.

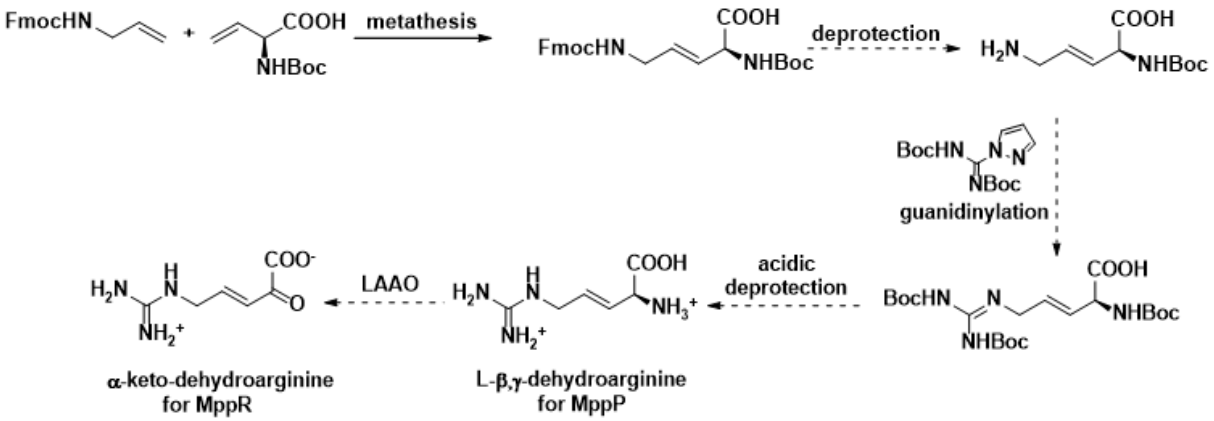


Figure 128: Future direction for dehydroarginine synthesis

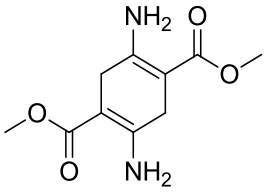
Future researchers who pick up this almost completed project are suggested to follow the route shown above as it is know that cross metatheis between Fmoc allyl amine and Boc-L-vinylglycine is able to go to completetion with the presence of the desired product confirmed by ESI-MS. This cross metathesis product is the most desirable as its protecting groups are orthogonal allowing for the Fmoc group to be removed while retaining the Boc group allowing for unambiguous guanidinylation. However, the desired material is yet to be isolated from the reaction mixture with silica gel and reverse phase flash chromatography proving to be ineffective in this task. It is suggested to use preparative HPLC for initial isolation of the desired cross metathesis product followed by development of a method to separate it from the Fmoc allylamine homodimer. The remaining steps in the sequence are well known and described in detail for analogous compounds in the experimental.

VIII. EXPERIMENTAL SECTION

General Procedures:

Reagents and solvents purchased from suppliers were used as received unless otherwise noted in experimental procedures. ^{1}H NMR spectra were collected on a 300MHz Brucker DPX 300 NMR unless otherwise noted. Chemical shifts (δ) are reported as downfield in parts per million of tetramethylsilane. Coupling constants (J) are reported in Hertz and splitting patterns denoted as singlet (s), doublet (d), doublet of doublets (dd), triplet (t), quartet (q), multiplet (m),and broad (b). ^{13}C NMR spectra were ^{1}H decoupled and collected on a 300 MHz Brucker DPX 300 NMR with chemical shifts (δ) reported as downfield of tetramethylsilane. The ^{31}P NMR spectra were ^{1}H decoupled, and collected on a 300MHz Brucker DPX 300 spectrometer with chemical shifts (δ) reported downfield of an 85% H_3PO_4 external standard.Low resolution mass spectrometry data was collected on a Hewlett-Packard 5985 B GC-mass spectrometer and a Shimadzu LCMS-2020 Single Quadrupole. High resolution mass spectrometry data was acquired with a Shimadzu LCMS-IT-TOF. Infrared sprectroscopy was performed on a Shimadzu IRAffinity-1S FTIR. Elemental analysis was conducted on a Perkin-Elmer 240C carbon, hydrogen, and nitrogen analyzer. Melting points were determined using a MEL-TEMP II apparatus without correction. HPLC analysis was performed on Agilent Technologies 1220 Infinity LC. UV-Vis absorption data was collected on a Perkin Elmer Lambda 650 using quartz absorbance cells. Fluorescent measurements were collected using right angle scattering on a Fluorolog-3 Model FL3-22 by Horiba Jobin-Yvon using quartz fluorescent cells or an Ocean Optics SD2000 dual channel fiber optic spectrometer. Analytical TLC was conducted on Merck silica gel 60 F_{254}

plates and visualized using shortwave ultraviolet light unless noted otherwise. Flash chromatography employed Sorbent Technologies silica gel 60Å, 32-63µm Standard Grade.



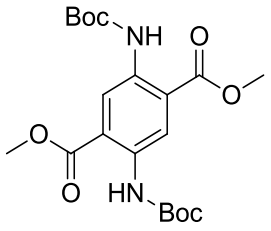
Dimethyl 2,5-diaminocyclohexa-1,4-diene-1,4-dicarboxylate (**1**)

70.82g (0.9969mol) NH_4OAc was combined with 2.0L anhyd. EtOH, placed under an atmosphere of N_2, and heated to reflux. 54.93g (0.2407mol) dimethyl 2,5-dioxocyclohexane-1,4-dicarboxylate was added to the boiling solution in three equal portions, waiting for the previous portion to dissolve before the next addition with 400mL anhyd. EtOH added with the last portion. The mixture continued to heat at reflux for 2.5h before TLC showed the reaction to be complete (10% CH_3CN/CH_2Cl_2, silica, $R_{f\ SM} = 0.76$, $R_{f\ BE} = 0.38$) over which time orange crystals formed on the side of the reaction flask. The mixture was allowed to cool to room temperature slowly before being placed into an ice bath for 1h. The resulting orange solid was collected by vacuum filtration and washed with 500mL cold anhyd. EtOH. After drying under vacuum to remove residual solvent overnight 47.72g (88% yield, mp = 212-214˚C) of a cream orange colored solid.

^{1}H NMR (300MHz, $CDCl_3$): δ3.71 (s, 6H); 3.13 (s, 4H)

^{13}C NMR (300MHz, $CDCl_3$): δ169.3; 155.6; 86.8; 50.8; 30.4

ESI-MS (DUIS, + ion): 268 (M + CH_3CNH^+, 100%); 227 (M + H^+, 98%)



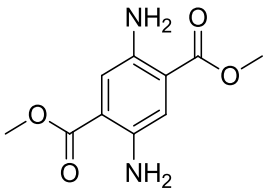
Dimethyl 2,5-bis((tert-butoxycarbonyl)amino)terephthalate (**2**)

3.708g (16.39mmol) **1** was suspended in 180mL toluene, heated to boiling, and had 80mL toluene removed via distillation. 22.11g (101.3mmol) Boc_2O dissolved in 40mL toluene was added to the reaction mixture followed immediately by 0.409g 5% Pd-C and heated at reflux for 15h before the addition of 3.917g (17.95mmol) Boc_2O dissolved in 8mL toluene. The mixture was allowed to reflux for an additional 8h before the addition of 8.229g (37.71mmol) Boc_2O dissolved in 12mL toluene. With an additional 20h reflux time, TLC showed the reaction to be complete (10% CH_3CN/CH_2Cl_2, silica, $R_{f\ product} = 0.72$). The boiling mixture was filtered over a pad of Celite and rinsed with boiling toluene until the filtrate appeared colorless (90mL). The filtrate was boiled down to 75mL total volume, allowed to cool to room temperature slowly, and placed in an ice bath for 30min. The resulting solid was collected by vacuum filtration, rinsed with three 10mL portions cold toluene, and placed under vacuum overnight to remove residual solvent to yield 6.146g (88% yield, mp = 248.5-250˚C) of a lemon yellow solid.

^{1}H NMR (300MHz, $CDCl_3$): δ 9.96 (s, 2H); δ 9.03 (s, 2H); δ 3.94 (s, 6H); δ 1.52 (s, 18H)

^{13}C NMR (300MHz, $CDCl_3$): δ 167.8; 152.8; 135.2; 120.9; 119.2; 80.6; 52.7; 28.2

ESI-MS (DUIS, + ion): 448 (M + CH_3CN + Na^+, 31%); 442 (M + NH_4^+, 100%); 310 (56%); 266 (M - 2Boc + CH_3CNH^+, 30%)



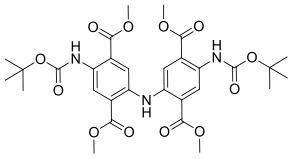
Dimethyl 2,5-diaminoterephthalate (**3**)

0.4165g (0.9813mmol) **2** was dissolved in 15mL CH_2Cl_2 to which was added 10mL CF_3COOH. The mixture was placed under an atmosphere of nitrogen before it was heated at reflux for 5min at which time TLC showed the deprotection was complete (R_f: 0.62, silica, shortwave UV, 25% CH_3CN/CH_2Cl_2). The reaction mixture was concentrated with rotary evaporation to dryness before being placed under vacuum overnight to remove residual solvent to afford 0.3746g of a yellow solid. The resulting solid was combined with 75% conc. $NH_{3(aq)}$ upon which created a suspension and a color change of yellow to orange in the visible solid. After stirring rapidly for 5min the solid was collected by vacuum filtration, washed with two 10mL potions RT DI H_2O followed by 10mL RT EtOH. (**Note:** Upon EtOH rinse, filtrate turned orange, don't use EtOH to wash away water) The orange solid was placed under vacuum for 1h to remove residual solvent to yield 0.1708g (78% overall yield) of the desired diamine as an orange tinged yellow solid.

^1H NMR (300MHz, $CDCl_3$): δ7.28 (s, 2H); 4.97 (s, 4H); 3.88 (s, 6H)

ESI-MS (DUIS, + ion): 266 ($M + CH_3CNH^+$, 100%); 225 ($M + H^+$, 93%)

Tetramethyl 5,5'-azanediylbis(2-((tert-butoxycarbonyl)amino)terephthalate) (**4**)

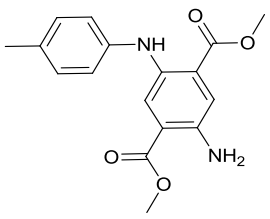


4.541g of the concentrated mother liquor from recrystallization of **2** was combined with 1.085g (14.46mmol) L-Glycine, 4.027g (47.94mmol) $NaHCO_3$, and 95mL CH_3OH. The mixture was left to stir at room temperature for 17h before the remaining solid was removed by vacuum filtration and rinsed with CH_2Cl_2 until the filtrate ran colorless (150mL). The filtrate was concentrated to dryness with rotary evaporation and placed under vacuum overnight to remove residual solvent to afford 5.199g of a pale orange solid. 5.153g of the resulting solid was boiled in 200mL toluene for 5min before filtering remaining solid with vacuum filtration. The filtrate was washed with three 100mL portion sat. $NaHCO_3$, dried over $MgSO_4$, concentrated to dryness with rotary evaporation, and placed under vacuum overnight to remove residual solvent to yield 2.727g of a light orange solid which was determined to be 33% by mass **2** and 67% by mass **4** by ^{1}H NMR. 0.4081g of the new crude product was purified by flash chromatography (8" silica, 2"/min flow rate, 10mL fraction, eluted with 200mL CH_2Cl_2 then 200mL 5% CH_3CN/CH_2Cl_2) to afford 0.1755g **4**.

^{1}H NMR (300MHz, $CDCl_3$): δ10.64 (s, 1H); 9.78 (s, 2H); 8.97 (s, 2H); 8.10 (s, 2H); 3.97 (s, 6H); 3.90 (s, 6H); 1.54 (s, 18H)

ESI-MS (DUIS, + ion): 654 ($M + Na^+$, 54%); 632 ($M + H^+$, 100%)

HRMS (IT-TOF-ESI, + ion): Calc'd for $C_{30}H_{37}N_3O_{12}$: 632.2450. Found: 632.2451



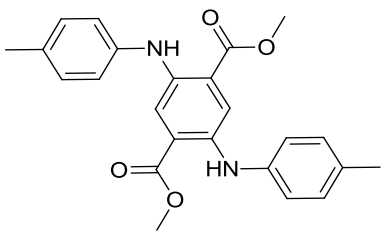
Dimethyl 2-amino-5-(p-tolylamino)terephthalate (**5**)

0.2764g (1.222mmol) **1** and 1.920g (17.92mmol) *p*-toluidine were combined with 100mL toluene. 30mL toluene was distilled off before the addition of 0.0568g 5% Pd-C. The mixture was then allowed to heat at reflux for 41h (**Note:** pH paper neutral when placed above the condenser periodically over the course of the reaction) after which the boiling reaction mixture was filtered over a pad of Celite and rinsed with boiling toluene until the filtrate was observed to be colorless (75mL). The filtrate was then washed with two 100mL portion pH5 $AcOH_{(aq)}$ followed by two 100mL pH3 $AcOH_{(aq)}$. (**Note**: use 4x100mL pH3 portions instead) The organic phase was then removed, dried over $MgSO_4$, filtered, rinsed with 30mL toluene, concentrated with rotary evaporation, and placed under vacuum overnight to afford 0.335g or a reddish-orange solid (87% crude yield). 0.321g of the crude product from purified via flash chromatography (20mm column, 2in/min flow rate, 10mL fraction, 7.75" silica, 50mL CH_2Cl_2, then 100mL 5% CH_3CN/CH_2Cl_2, 50mL 10% CH_3CN/CH_2Cl_2, then 50mL 100% CH_3CN) Fracs 7-10 5% + Frac 1-3 10% afforded 0.140g **5**.

^{1}H NMR (300MHz, $CDCl_3$): δ7.86 (s, 1H); 7.35 (s, 1H); 7.11 (d, J=8.1, 2H); 7.05 (d, J=8.4, 2H); 3.89 (s, 3H); 3.83 (s, 3H); 2.32 (s, 3H)

ESI-MS (DUIS, + ion): 356 (M + CH_3CNH^+, 100%); 315 (M + H^+, 46%)

HRMS (IT-TOF-ESI, + ion): Calc'd for $C_{17}H_{18}N_2O_4$: 315.1339. Found: 315.1340



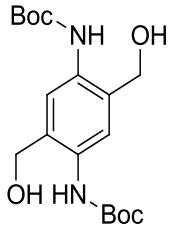
Dimethyl 2,5-bis(p-tolylamino)terephthalate (**6**)

0.2764g (1.222mmol) **1** and 1.920g (17.92mmol) *p*-toluidine were combined with 100mL toluene. 30mL toluene was distilled off before the addition of 0.0568g 5% Pd-C. The mixture was then allowed to heat at reflux for 41h (**Note:** pH paper neutral when placed above the condenser periodically over the course of the reaction) after which the boiling reaction mixture was filtered over a pad of Celite and rinsed with boiling toluene until the filtrate was observed to be colorless (75mL). The filtrate was then washed with two 100mL portion pH5 $AcOH_{(aq)}$ followed by two 100mL pH3 $AcOH_{(aq)}$. (**Note**: use 4x100mL pH3 portions instead) The organic phase was then removed, dried over $MgSO_4$, filtered, rinsed with 30mL toluene, concentrated with rotary evaporation, and placed under vacuum overnight to afford 0.335g or a reddish-orange solid (87% crude yield). 0.321g of the crude product from purified via flash chromatography (20mm column, 2in/min flow rate, 10mL fraction, 7.75" silica, 50mL CH_2Cl_2, then 100mL 5% CH_3CN/CH_2Cl_2, 50mL 10% CH_3CN/CH_2Cl_2, then 50mL 100% CH_3CN) Fracs 5-8 100% CH_2Cl_2 + f1 5% afforded 0.170g **6**.

^{1}H NMR (300MHz, $CDCl_3$): δ8.66 (s, 2H); 7.92 (s, 2H); 7.14 (d, J=8.1Hz, 4H); 7.08 (d, J=8.4Hz, 4H); 3.84 (s, 6H); 2.33 (s, 6H)

ESI-MS (DUIS, + ion): 405 ($M + H^+$, 100%); 446 ($M + CH_3CNH^+$, 19%)

HRMS (IT-TOF-ESI, + ion): Calc'd for $C_{24}H_{24}N_2O_4$: 405.1809. Found: 405.1810

N, N'-di-t-Boc-1,4-diamino-2,5-bis-(hydroxymethyl)benzene (**7**) 

13.99g (368.6mmol) $LiAlH_4$ was combined with 750mL anhydrous Et_2O and heated at reflux for 30min before the addition of 21.95g (51.72mmol) of **2** dissolved in 730mL CH_2Cl_2. The diester solution was added as quickly as possible while still having the color of the solution disappear upon addition. **Note: Evolution of H_2 gas at this scale can produce increases of pressure that need to be taken into consideration** The reaction was heated at reflux for 1.5h before TLC showed the reaction was complete (R_f = 0.79 diester, R_f = 0.14 diol 10% CH_3CN/CH_2Cl_2). The mixture was removed from the heat and quenched by sequential, **dropwise**, addition of 14mL DI H_2O, 14mL 15% $NaOH_{(aq)}$, then 42mL DI H_2O. The mixture was filtered over Celite with the filter pad being removed, boiled in 400mL 50% Et_2O/CH_2Cl_2, for 2min before being filtered over Celite again. The filtrates were combined, dried over MgSO4, filtered, concentrated to dryness with rotary evaporation, and placed under vacuum overnight to yield 15.00g (79% yield) of **7** as a white solid (mp = 162-166˚C)

^{1}H NMR (300MHz, $CDCl_3$): δ 7.78 (s, 2H); 7.59 (s, 2H); 4.67 (s, 4H); 1.92 (s, 2H); 1.51 (s, 18H)

^{13}C NMR (300MHz, $CDCl_3$): δ 153.7; 133.2; 129.7; 121.7; 80.6; 64.2; 28.5

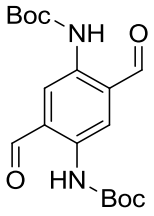
MS (EI, 70eV): 368 (M^+, 43%); 312 (M^+ - C_4H_8, 30%); 256 (312 - C_4H_8, 100%); 221 (M^+ - $C_5H_{10}O_2$, 30%); 212 (256 - CO_2, 48%); 194 (212 - H_2O, 76%); 150 (194 - CO_2, 88%); 132 (150 - H_2O, 32%)

ESI-MS (DUIS, - ion): 367(M - H^+, 90%); 293(M - 2Boc + CF_3COO^-, 100%)

HRMS (IT-TOF-ESI, + ion): Calc'd for $C_{18}H_{28}N_2O_6 + NH_4^+$; 386.2291. Found: 368.2288

IR (KBr pellet): IR (KBr pellet):3384cm$^-$ (N-H); 3195cm$^-$ (O-H); 3011 cm$^-$, 2979 cm$^-$, 2931 cm$^-$, 2856 cm$^-$(C-Hs); 1686 cm$^-$, 1677 cm$^-$ (C=O); 1537 cm$^-$(aromatic C-H); 1167 cm$^-$ (C-O)

Elem. Anal.: Calc'd for $C_{18}H_{28}N_2O_6$: C, 58.68; H, 7.66; N, 7.60. Found C, 58.54; H, 7.73; N, 7.52

N,N'-di-t-Boc-2,5-diaminoterephthaldehyde (**8**) 

MnO_2 method

3.018g **7** (8.194mmol) was placed into a 500mL round bottom flask along with 42.47g (488.5mmol) freshly prepared, dried in a 135° C oven until powdry with periodic grinding, MnO_2. 90mL CH_2Cl_2 was added to the reaction vessel **before** the addition of 210mL acetone. The reflux apparatus was placed under an N_2 atmosphere and heated to reflux while stirring rapidly. After 15h, the reaction was incomplete by TLC (R_f **8** = 0.85, R_f monoaldehyde intermediate = 0.60 10% CH_3CN/CH_2Cl_2) and an additional 4.519g (51.98mmol) 1 day old MnO_2 was added to the reaction and set back to reflux. After an additional 5h TLC showed the reaction was complete. The reaction was filtered hot over a pad of Celite and rinsed with CH_2Cl_2 until the filtrate ran clear (200mL). The MnO_2/Celite pad was placed into a 500mL beaker along with 100mL CH_2Cl_2, 100mL THF, and 100mL MeOH, stirred rapidly, and boiled for ~1-2min before filtering over a pad of Celite. This process was repeated once more. The filtrates were

combined, dried over $MgSO_4$, filtered, concentrated with rotary vacuum, and dried over high to remove residual solvent overnight to yield 2.831g **8** (95% yield). 1.015g crude **8** recrystallized from 45mL CH_3CN (44.3mL CH_3CN / g **8**) (58% recovery, mp = 219-221° C) this recovery is not typical though after multiple recrystallizations.

[Cu(MeCN)$_4$]OTf method

0.3036g (0.8240mmol) **7** was combined with 0.0325g (0.0883mmol) [Cu(I)(MeCN)$_4$]OTf, 0.0013g (0.0083mmol) bpy, 13.4µL (0.168mmol) NMI, 0.0013g (0.0083mmol) TEMPO, and dissolved in 30mL CH_3CN. The mixture was set to stir rapidly open to the air at room temperature for 23h at which time TLC showed incomplete reaction. 0.0130g (0.0832mmol) TEMPO dissolved in 2mL CH_3CN and 20µL (0.251mmol) NMI were added along with 8mL CH_2Cl_2 to rinse the walls of the vessel. The mixture was set to stir rapidly open to the air for 18h at which time TLC showed complete reaction then filtered over a plug of silica (4.5cm dia., 0.75cm tall) and rinsed with CH_2Cl_2 until the filtrate ran clear (30mL). The filtrate was diluted with 20mL CH_3OH (to prevent bumping), concentrated to dryness with rotary evaporation, and placed under vacuum for 2h to afford 0.286g **8** (95% yield, mp 212-217˚C). 0.2641g of crude **8** was recrystallized from 10mL CH_3CN, cooled, and placed in a -20˚C freezer overnight to yield 0.2191g (83% recovery, mp = 218-220˚C) as orange needles. The mother liquor was concentrated, dissolved in 1.5mL CH_2Cl_2, and diluted with 12mL hexane. The mixture was boiled down to ½ volume, cooled, and placed in a -20˚C freezer overnight to afford 0.0101g DA as yellow plates. **8** afforded in 83% purified yield in two crops from recrystallization.

^{1}H NMR (300MHz, $CDCl_3$): δ 10.11 (s, 2H); 10.01 (s, 2H); 8.88 (s, 2H); 1.55 (s, 18H)

^{13}C NMR (300MHz, $CDCl_3$): δ 195.6; 153.2; 135.3; 126.0; 125.2; 81.5; 28.4

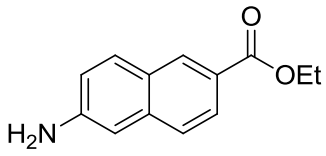
MS (EI, 70eV): 364 (M^+, 35%); 308 (M^+ - C_4H_8, 39); 252 (308 - C_4H_8, 84%); 208 (252 - CO_2, 48%); 191 (252 - CH_3NO_2, 33%); 164 (208 - CO_2, 100%); 136 (164 - CO, 27%); 108 (136 - CO, 25%)

ESI-MS (DUIS, - ion): 458 (54%); 431 (M^- + Na^+ + $HCOO^-$, 78%); 363 (M - H^+, 100%)

HRMS (IT-TOF-ESI, + ion): Calc'd for $C_{18}H_{24}N_2O_6$ + NH_4^+: 382.1978. Found: 382.1973

IR (KBr pellet): 3314cm$^-$ (N-H); 3003cm$^-$, 2976 cm$^-$, 2933cm$^-$ (methyl C-H); 2886cm$^-$ (aldehyde C-H); 1724cm$^-$ (amide C=O); 1674cm$^-$ (aldehyde C=O); 1550cm$^-$ (aromatic C-H); 1148cm$^-$ (C-O)

Elem. Anal. Calc'd for $C_{18}H_{24}N_2O_6$: C, 59.33; H, 6.64; N, 7.69. Found: C, 56.68; H, 6.42; N, 7.22

<u>*Ethyl 6-amino-2-naphthoate*</u> (**12**) 

0.9425g (5.035mmol) 6-amino-2-naphthalene-2-carboxylic acid was combined with 24mL anhyd. ethanol to which was added 1.3mL conc. H_2SO_4, causing a purplish brown solid to precipitate from the mixture. This mixture was placed under and atmosphere of N_2 and heated to reflux, which causing the mixture to become homogeneous. After 2h TLC showed the reaction to be complete. The mixture was then allowed to cool slightly before it was poured into a seperatory funnel containing 50mL CH_2Cl_2 and 50mL sat. $NaHCO_3$. The organic layer was removed and washed with 50mL sat. $NaHCO_3$. Another portion of 50mL CH_2Cl_2 was used to countercurrently extract the two aqueous phases. The organic portions were combined, dried over $MgSO_4$, filtered, concentrated with rotary evaporation, and placed under vacuum

overnight to remove residual solvent to afford 1.054g (97%, m.p = 68-71°C) of the desired product as a purple hued brown solid.

^{1}H NMR (300MHz, $CDCl_3$): δ 8.45 (s, 1H), 7.94 (dd, J = 8.6 Hz; 1.5Hz, 1H), 7.75 (d, J = 9.3Hz, 1H), 7.58 (d, J = 8.6Hz, 1H), 6.96 (dd, J = overlapped, 1H), 6.95 (d, J = overlapped, 1H), 4.41 (q, J = 7.1Hz, 2H), 3.94 (bs, 2H), 1.42 (t, J = 7.1Hz, 3H)

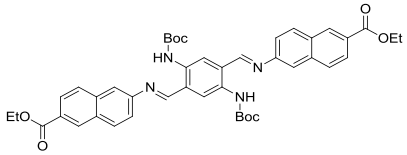
^{13}C NMR (300MHz, $CDCl_3$): δ 167.2, 146.6, 137.6, 131.1, 131.0, 126.8, 126.1, 125.8, 124.3, 118.8, 108.0, 60.9, 14.9

MS (EI, 70eV) 215 (M^+, 100%), 187 (M^+ - C_2H_4, 38%), 170 (M^+ - C_2H_5O, 79%), 142 (M^+ - $C_3H_5O_3$), 115 (142 - CHN, 31%)

IR (KBr pellet): Peaks showed the following functional groups: 3431 cm^-, 3349 cm^- (NH_2), 1690 cm^- (C=O); 1294cm^- (C-O)

Elem. Anal. Calc'd for $C_{13}H_{13}NO_2$: C, 72.54; H, 6.09; N, 6.51. Found C, 71.82; H, 6.13; N, 6.36

Diethyl 6,6'-((1E,1'E)-((2,5-bis((tert-butoxycarbonyl)amino)-1,4-phenylene)bis(methanylylidene))bis(azanylylidene))bis(2-naphthoate) (**13**)



1.003g (2.752mmol) **8** and 1.192g (5.536mmol) **7** were dissolved in 30mL distilled CH_2Cl_2 before the addition of 1.35mL (23.58mmol) glacial acetic acid. The mixture was set to stir at room temperature under an atmosphere of N_2 21h at which time TLC was used to confirm the reaction was complete. Over the course of the reaction it became heterogeneous while orange

solid. The reaction mixture was concentrated to ca. 1/3 volume before diluting with 20mL EtOAc and collecting the orange solid by centrifugation. The supernatant was decanted and the orange solid was combined thoroughly with 20mL EtOAc before centrifuging, decanting and drying the solid under vacuum overnight. 1.792g (86%, mp = 280-282°C) **13** was afforded as a bright orange solid. The supernatants were combined, concentrated with rotary evaporation, diluted with 10mL EtOAc, and centrifuged to collect another portion of orange solid. The supernatant was decanted, washed with 7mL EtOAc, centrifuged, supernatant decanted, and dried under vacuum for 5h to afford 0.1086g (5%) **13** as an orange solid for a total of 1.900g (91% yield)

^{1}H NMR (300MHz, $CDCl_3$): δ11.84 (s, 2H); 8.85 (s, 2H); 8.77 (s, 2H); 8.63 (s, 2H); 8.12 (d, J=8.7Hz, 2H); 8.04 (d, J=9Hz, 2H); 7.92 (d, J=8.7, 2H); 7.72 (s, 2H); 7.56 (d, J=8.7Hz, 2H); 4.47 (q, J=7.2Hz, 4H); 1.59 (s, 18H); 1.47 (t, J=7.2Hz, 6H)

^{13}C NMR (300MHz, $CDCl_3$): δ166.8; 163.2; 153.8; 149.3; 136.4; 135.0; 131.7; 131.0; 130.9; 128.4; 128.0; 126.3; 124.2; 123.2; 121.7; 118.7; 80.6; 61.3; 28.6; 14.6

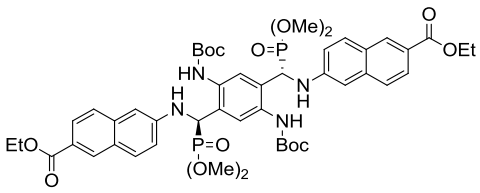
IR (KBr pellet) 3410cm^{-}; 2975 cm^{-}; 2359 cm^{-}; 2341 cm^{-}; 1713 cm^{-}; 1273 cm^{-}, 1241 cm^{-}

ESI-MS (DUIS, + ion): 759 ($M + H^{+}$, 100%)

HRMS (IT-TOF-ESI): Calc'd for $C_{44}H_{46}N_4O_8 + H^{+}$: 759.3388 Found: 759.3381

Elem. Anal.: Calc'd for $C_{44}H_{46}N_4O_8$ C: 69.64; H: 6.11; N: 7.38. Found C: 67.45; H: 6.16; N: 6.80

Diethyl 6,6'-(((1R,1'S)-(2,5-bis((tert-butoxycarbonyl)amino)-1,4-phenylene)bis((dimethoxyphosphoryl)methylene))bis(azanediyl))bis(2-naphthoate) (**16**)



0.1072g (0.4981mmol) **12**, 0.0865g (0.2374mmol) **8**, and 0.0543g (0.0875mmol) $Yb(OTf)_3$ were combined and dissolved in 5mL CH_2Cl_2 under an atmosphere of N_2. After 2.75h TLC showed that NEDA fully formed. The mixture was made homogeneous with the addition of 7mL CH_2Cl_2 before the addition of 0.25mL (4.240mmol) $P(OMe)_3$. After 21h, the mixture was observed to be homogenous but with the monoamine, mono-aminophosphonate still present so 0.20mL (1.696mmol) $P(OMe)_3$ was added. After stirring for 21h the reaction appeared complete by TLC. The mixture was poured into a sep. funnel containing 50mL 80% sat.Na_2CO_3 and 25mL CH_2Cl_2. The organic layer was countercurrently washed with 50mL 80% sat.Na_2CO_3. A 40mL portion CH_2Cl_2 run through the countercurrent extraction apparatus before the organic layers were combined, dried over $MgSO_4$, filtered, concentrated with rotary evaporation, and placed under vacuum to remove residual solvents to afford **16** and **17** (0.2337g, 100%) as a brown solid. Purified by flash chromatography (100mL 10% CH_3CN/CH_2Cl_2, 200mL 40% CH_3CN/CH_2Cl_2, 200mL CH_3CN) to afford **16** (0.0377g, 32%) as an off white solid.

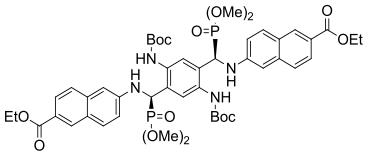
^{1}H NMR (300MHz, $CDCl_3$): δ 8.39 (s, 2H); 7.86 (dd, J=8.6;1.6, 2H); 7.77 (bs, 2H); 7.72 (d, J=8.7, 2H); 7.59 (bs, 2H); 7.38 (d, J=8.7, 2H); 6.99 (dd, J=8.8;2.3, 2H); 6.54 (nd, J=1.9, 2H); 5.13 (dd, J=22.1; 5.4, 2H); 4.99 (dd, J=10.2;5.7, 2H); 4.39 (q, J=7.1, 4H); 3.67 (d, J=10.5, 6H); 3.61 (d, J=10.3, 6H); 1.51 (s, 18H); 1.41 (t, J=7.1, 6H)

^{13}C NMR (300MHz, $CDCl_3$): δ 167.1, 154.0, 137.4, 134.3, 130.9, 130.8, 128.6, 127.1, 126.1, 126.0, 125.8, 124.6, 118.7, 106.2, 80.5, 60.9, 55.5, 53.8, 53.0, 51.1, 28.6, 14.1

^{31}P NMR (300MHz, $CDCl_3$): δ 24.94

ESI-MS (DUIS, + ion): 997 ($M + H^+$, 100%)

Diethyl 6,6'-(((1S,1'S)-(2,5-bis((tert-butoxycarbonyl)amino)-1,4-phenylene)bis((dimethoxyphosphoryl)methylene))bis(azanediyl))bis(2-naphthoate) (**17**)



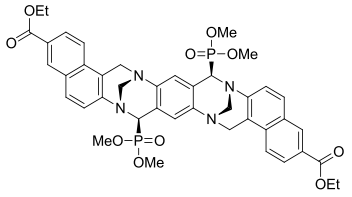
0.1072g (0.4981mmol) **12**, 0.0865g (0.2374mmol) **8**, and 0.0543g (0.0875mmol) $Yb(OTf)_3$ were combined and dissolved in 5mL CH_2Cl_2 under an atmosphere of N_2. After 2.75h **13** fully formed. The mixture was made homogeneous with the addition of 7mL CH_2Cl_2 before the addition of 0.25mL (4.2402mmol) $P(OMe)_3$. After 21h, the mixture was observed to be homogenous but with the monoamine, mono-aminophosphonate still present so 0.20mL (1.696mmol) $P(OMe)_3$ was added. After stirring for 21h the reaction appeared complete by TLC. The mixture was poured into a sep. funnel containing 50mL 80% sat.Na_2CO_3 and 25mL CH_2Cl_2. The organic layer was countercurrently washed with 50mL 80% sat.Na_2CO_3. A 40mL portion CH_2Cl_2 run through the countercurrent extraction apparatus before the organic layers were combined, dried over $MgSO_4$, filtered, concentrated with rotary evaporation, and placed under vacuum to remove residual solvents to afford **16** and **17** (0.2337g, 99.7%) as a brown solid. Purified by flash chromatography (100mL 10%CH_3CN/CH_2Cl_2, 200mL 40% CH_3CN/CH_2Cl_2, 200mL CH_3CN) to afford EDPB (0.0344g, 29%) as an tan solid.

^{1}H NMR (300MHz, $CDCl_3$): δ 8.38 (s, 2H), 8.00 (bs, 2H), 7.87 (dd, J = 8.6;1.6, 2H), 7.77 (s, 2H), 7.69 (d, J = 8.8, 2H), 7.44 (d, J = 8.6, 2H), 6.96 (dd, J = 8.8;2.2, 2H), 6.65 (s, 2H), 5.08 (dd, J = 2.94;6.7), 4.99 (d, J = 7.0, 2H), 4.39 (q, J = 7.1, 4H), 3.58 (d, J = 10.5, 2H), 1.46 (s, 18H), 1.41 (t, J = 7.1, 6H)

^{13}C NMR (300MHz, $CDCl_3$): δ 167.1, 153.8, 145.7, 145.5, 137.3, 134.1, 130.8, 130.8, 127.1, 126.5, 126.1, 124.6, 118.7, 106.5, 80.5, 60.9, 54.7, 54.2, 52.5, 28.5, 14.5

^{31}P NMR (300MHz, $CDCl_3$): δ 25.65

ESI-MS (DUIS, - ion): 977 ($M - H^+$, 100%)



<u>*C-Me, P-Me rac- tweezers*</u> (**18**)

0.1107g (0.1122mmol) EDPB was combined with 3mL (74.064mml) MeOH and 1.5mL (16.932mol) methylal and placed under an atmosphere of N_2 before the addition of 7mL (90.861mmol) CF_3COOH. The mixture was heated at reflux for 22hr before concentration over rotary evaporation. The mixture was poured into a sep. funnel containing 55mL 80% sat. Na_2CO_3 and 30mL CH_2Cl_2 and 15mL sat. NaCl. The organic layer was removed and countercurrently washed with 55mL 80% sat. Na_2CO_3 and 15mL sat. NaCl 20mL CH_2Cl_2 run through the extraction apparatus before the organic portions were combined, dried over $MgSO_4$, filtered, concentrated with rotary evaporation, and placed under vacuum to remove residual solvents to afford 0.0835g **18** (90% yield) as a tan solid. Purified by flash chromatography (silica, 75% CH_3CN/CH_2Cl_2, 10% $MeOH/CH_2Cl_2$).

Largest Scale:

1.886g (1.927mmol) of the 1:1 mixture of **16** and **17** was combined with 14.0mL anhyd. ethanol, 14.0mL methylal (90mmol), and 34.0mL CF_3COOH. The mixture was placed under an atmosphere of N_2 and heated at reflux for 20hr after which it was cooled to room temperature, diluted with 30mL toluene and concentrated to dryness with rotary evaporation. The concentrate was dissolved in 100mL CH_2Cl_2 and washed with two 50mL portions sat. $NaHCO_3$. The aqueous washes were combined and back extracted with two 30mL portions CH_2Cl_2. The organic extracts were combined, dried over $MgSO_4$, filtered, concentrated to dryness with rotary evaporation and placed under vacuum overnight to remove residual solvent to afford 1.6862g of a beige solid. 0.577g of the crude product was combined with 30mL boiling toluene, concentrated to 25mL total volume, cooled to room temperature, and placed on ice for 15min. The resulting mixture was filtered and rinsed with 15mL toluene. The filtrate was concentrate to dryness with rotary evaporation, dissolved in 10mL 1,4-dioxane and precipitate using 100mL hexane. The solid was collected by centrifugation, washed with 40mL hexane, and placed under vacuum overnight to remove residual solvent to afford 0.2253g (81% yield, mp = 308˚C (s), 320˚C (d)) of the light tan solid **18**.

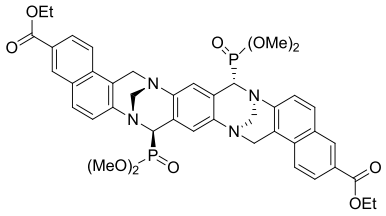
1H NMR (300MHz, $CDCl_3$, at $3x10^{-3}$M): δ8.28 (s, 2H); 7.88 (d, J=7.8Hz, 2H); 7.62 (d, J=8.7Hz, 2H); 7.48 (d, J=8.7, 2H); 7.20 (s, 2H); 7.18 (d, J=8.4Hz, 2H); 5.01 (d, J=12.0Hz, 2H); 4.89 (d, J=17.1Hz, 2H); 4.61 (d, J=23.7Hz, 2H); 4.36 (d, overlapped, 2H); 4.34 (q, J=7.2Hz, 4H); 4.22 (d, J=13.0Hz, 2H); 4.04 (d, J=10.2Hz, 6H); 3.98 (d, J=10.5Hz, 6H); 1.34 (t, J=7.2Hz, 6H)

^{13}C NMR (300MHz, $CDCl_3$): δ166.7; 166.5; 147.9; 133.6; 133.2; 131.5; 131.1; 130.2; 129.9; 129.4; 126.8; 126.5; 126.1; 125.6; 124.9; 124.7; 123.3; 122.3; 121.3; 64.4; 63.6; 62.3; 61.25; 61.20; 56.4; 55.3; 53.2; 28.2; 14.5

^{31}P NMR: δ23.8

ESI-MS (DUIS, + ion): 868($M + CH_3CNH^+$, 100%); 827($M + H^+$, 42%)

HRMS (IT-TOF-ESI, + ion): Calc'd for [$C_{42}H_{44}N_4O_{10}P_2 + H^+$] 827.2605 Found: 827.2610



<u>*C-Me, P-Me meso- isomer*</u> (**19**)

0.1501g (0.1521mmol) **16**, 1.2mL (13.545mmol) methylal, and 2.5mL MeOH (61.720mmol) were combined under an atmosphere of N_2 before 4mL (341.36mmol) CF_3COOH was added. The mixture was heated at reflux for 21hr concentrating the mixture with rotary evaporation. 10mL CH_2Cl_2 was to the concentrate and countercurrently washed with 50mL 80% sat. Na_2CO_3 in the first sep. funnel and 50mL 80% sat. Na_2CO_3 and 30mL sat. NaCl in the second sep.funnel. 60mL CH_2Cl_2 run through the extraction apparatus before the organic portions were combined, dried over $MgSO_4$, filtered, concentrated with rotary evaporation, and placed under high vacuum to afford **19** (0.1062g, 84%) as a solid. Crude product is purified by flash chromatography (40% CH_3CN/CH_2Cl_2, 5% $MeOH/CH_2Cl_2$, and 10% $MeOH/CH_2Cl_2$ if not eluted out in the 5% portion).

Largest Scale:

1.886g (1.927mmol) of the 1:1 mixture of **16** and **17** was combined with 14.0mL anhyd. ethanol, 14.0mL methylal (90mmol), and 34.0mL CF_3COOH. The mixture was placed under an atmosphere of N_2 and heated at reflux for 20hr after which it was cooled to room temperature, diluted with 30mL toluene and concentrated to dryness with rotary evaporation. The concentrate was dissolved in 100mL CH_2Cl_2 and washed with two 50mL portions sat. $NaHCO_3$. The aqueous washes were combined and back extracted with two 30mL portions CH_2Cl_2. The organic extracts were combined, dried over $MgSO_4$, filtered, concentrated to dryness with rotary evaporation and placed under vacuum overnight to remove residual solvent to afford 1.6862g of a beige solid. 0.577g of the crude product was combined with 30mL boiling toluene, concentrated to 25mL total volume, cooled to room temperature, and placed on ice for 15min. The resulting mixture was filtered with 15mL toluene used to rinse the collected solid which was then placed under vacuum overnight to afford 0.241g (84% yield, mp = 322˚C (s), 338˚C (d)) of the *meso*-isomer **19**.

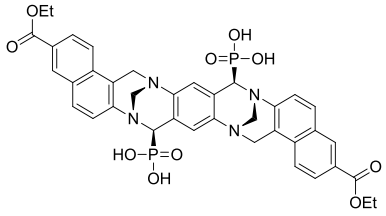
^{1}H NMR (300MHz, $CDCl_3$): δ8.52 (s, 2H); 8.05 (d, J=8.7Hz, 2H); 7.84 (d, J=9.0Hz, 2H); 7.61 (d, J=9.0Hz, 2H); 7.31 (s, 2H); 7.28 (d, overlapped, 2H); 5.07 (d, J=16.8Hz, 2H); 5.00 (d, J=13.8Hz, 2H); 4.75 (d, J=24.3Hz, 2H); 4.45 (d, overlapped, 2H); 4.43 (q, overlapped, 4H); 4.25 (d, J=12.9Hz, 2H); 3.94 (d, J=10.5Hz, 6H); 3.85 (d, J=10.8Hz, 6H); 1.43 (t, J=7.2Hz, 6H)

^{13}C NMR (300MHz, $CDCl_3$): δ166.8; 133.7; 131.6; 130.3; 129.8; 127.1; 126.5; 125.8; 124.9; 123.5; 122.2; 121.4; 64.4; 63.6; 62.3; 61.2; 57.1; 55.2; 53.3; 14.5

^{31}P NMR (300MHz, $CDCl_3$): δ23.7

ESI-MS (DUIS, + ion): 827 ($M + H^+$, 100%); 424 ((M + $2H^+$)/2, 40%); 270 (26%)

HRMS (IT-TOF-ESI, + ion): Calc'd for [$C_{42}H_{44}N_4O_{10}P_2 + H^+$] 827.2605 Found: 827.2600



<u>*rac*-carbethoxy tetra acid tweezers</u> (**23**)

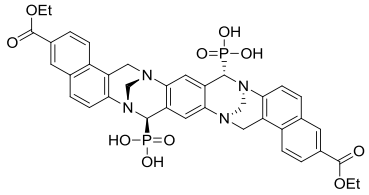
0.121g (0.146mmol) *rac*- napthyl tweezers was dissolved in 6mL CH_2Cl_2 (distilled from CaH_2) and placed under an atmosphere of N_2 before the addition of 0.80mL (6.0mmol) bromotrimethylsilane. The mixture was stirred at room temperature for 16hr before the mixture was concentrated to dryness with vacuum. The crude product was dissolved in 10mL boiling ethanol and cooled to room temperature before the addition of 40mL hexane causing a solid to precipitate and stored overnight at -20˚C. The solid was collected by centrifugation, washed with 15mL hexane, and placed under vacuum overnight to remove residual solvent to afford 0.087g (77% yield, mp = 350˚C (d)) **23**.

^{1}H NMR (1:1 dTFA/$CDCl_3$): δ8.58 (s, 2H); 8.49 (s, 2H); 8.07 (d, J=9.3Hz, 2H); 8.04 (d, J=9.6Hz, 2H); 7.58 (d, J=9.0Hz, 2H); 7.53 (d, J=9.0, 2H); 5.89 (d, J=11.4Hz, 2H); 5.62 (d, J=15.0Hz, 2H); 5.19 (d, J=25.5Hz, 2H); 4.94 (overlapped, 4H); 4.47 (q, J=6.9Hz, 4H); 1.45 (t, J=7.2Hz, 6H)

^{31}P NMR (300MHz, DMSO-d_6): δ17.2

ESI-MS (DUIS, - ion): 769 ($M + H^+$, 100%)

HRMS (IT-TOF-ESI, + ion): Calc'd for $C_{38}H_3N_4O_{10}P_2 + H^+$: 771.1979 Found: 771.1975



meso- carbethoxy tetra acid isomer (**24**)

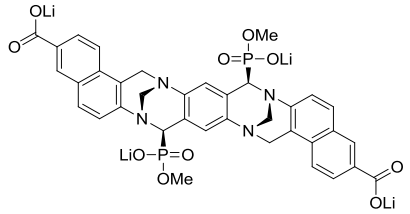
0.212g (0.1256mmol) **19** was suspended in 10mL CH_2Cl_2 (distilled from CaH_2) and placed under an atmosphere of N_2 before the addition of 0.90mL (6.8mmol) bromotrimethylsilane. The mixture was heated at reflux for 18hr after which time none of the starting material was seen by TLC (R_f =0.35, 10% CH_3OH/CH_2Cl_2, silica). The reaction mixture was concentrated to dryness under vacuum. The 16mL boiling ethanol was added to the crude product, allowed to cool to room temperature, diluted with 25mL hexane, and stored overnight at -20˚C. The solid was collected by centrifugation, washed with 15mL hexane, and placed under vacuum overnight to remove residual solvent to yield 0.170g (86% yield, mp = 340˚C (darkens), 380˚C (shrinks), >400˚C) of **24**.

^{1}H NMR (300MHz, D_2O): δ8.50 (s, 2H); 7.99 (d, J=8.4Hz, 2H); 7.88 (d, J=8.7Hz, 2H); 7.82 (d, J=8.7Hz, 2H); 7.54 (d, J=9.0Hz, 2H); 7.29 (s, 2H); 4.98 (d, J=12.3Hz, 2H); 4.9-4.7 (obscured by HOD, 4H); 4.55 (d, J=21.3Hz, 2H); 4.40 (q, J=6.9Hz, 4H); 4.07 (d, J=11.7Hz, 2H); 1.40 (t, J=7.2Hz, 6H)

31P NMR (300MHz, D_2O): δ18.2

ESI-MS (DUIS, - ion): 770 (M - H^+, 100%); 384 (M - $2H^+$, 40%)

HRMS (IT-TOF-ESI, + ion): [Calc'd for $C_{38}H_3N_4O_{10}P_2 + H^+$] 771.1979 Found: 771.1970



<u>*rac*-methyl phosphonate tetra anionic tweezers</u> (**25**)

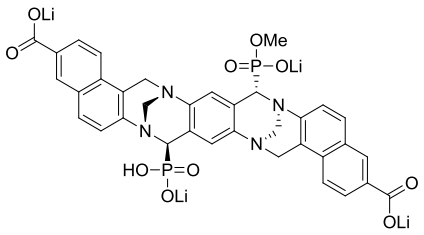
0.076g (0.0.092mmol) **18** was dissolved in 2mL 1,4-dioxane to which was added 0.018g (0.752mmol) LiOH in 5.5mL 18Ω H_2O and heated at reflux for 22hr. The mixture was allowed to cool to room temperature, concentrated to dryness with rotary evaporation, dried azeotropically by the evaporation of 50mL toluene, and placed under vacuum overnight to yield 0.0734g of a mixture that was 87% by mass **25**. 0.0491g of the crude solid was dissolved in 10mL 18Ω H_2O, titrated to pH7 with 4.8% HBr (0.89M), concentrated to dryness with rotary evaporation, dissolved in 12mL 18Ω H_2O, and concentrated to dryness again. 10mL THF was added to the solid and swirled periodically over the course of 20min after which the THF was removed. This process was repeated with a 20mL portion THF then followed by a 6mL portion THF before being placed under vacuum for 3d to remove residual solvent to afford 0.0401g of **25** (96% by mass, 90% recovery) as a mixture with THF.

^{1}H NMR (1:1 TFA:$CDCl_3$): δ8.67 (s, 2H); 8.52 (s, 2H); 8.16 (d, J=8.7Hz, 2H); 8.06 (d, J=9.0Hz, 2H); 7.60 (d, J=9.0Hz, 2H); 7.54 (d, J=8.7Hz, 2H); 5.94 (d, J=11.7Hz, 2H); 5.63 (d, J=17.1Hz, 2H); 5.19 (d, J=25.8Hz, 2H); 5.02 (overlapped, 4H); 4.14 (d, J=10.8Hz, 6H)

^{31}P NMR (1:1 TFA:$CDCl_3$): δ17.2

ESI-MS (- ion mode): 748 ($M - 2H^+ + Li^+$, 50%); 741 ($M - H^+$, 100%)

HRMS (IT-TOF-ESI, + ion): Calc'd for $C_{36}H_{32}N_4O_{10}P_2 + H^+$: 743.1666 Found: 743.1671



<u>*meso*-methylphosphonate tetra anionic isomer</u> (**26**)

0.095g (0.115mmol) **19** was suspended in 15mL 1,4-dioxane to which was added 0.025g (1.03mmol) LiOH in 4.5mL 18Ω H_2O. The mixture was placed under an atmosphere of N_2 and heated at reflux for 29hr. The mixture was concentrated to dryness with rotary evaporation, combined with 4mL 18Ω H_2O, and filtered through a plug of Celite. The filtrate was concentrated to dryness with rotary evaporation, dried azeotropically by the evaporation of 25mL toluene, and placed under vacuum for 3d for yield 0.0889g of **26** in 86% yield as an 85% by mass mixture with LiOH. 0.0125g of the crude product was dissolved in 10 mL 18Ω H_2O and titrated to pH7 with 4.8% HBr (0.89M). The mixture was concentrated to dryness with rotary evaporation and triturated with 10mL THF by period swirling over 20min. The THF was decanted and the process was repeated one more time before the solid was placed under vacuum overnight to remove residual solvent to afford 0.011g **26** (100% recovery)

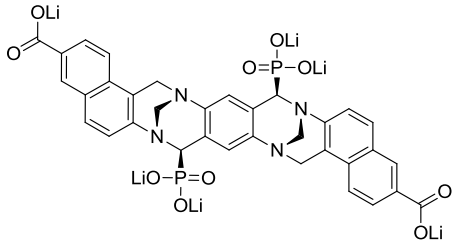
^{1}H NMR (300MHz, D_2O): δ8.46 (s, 2H); 7.94 (d, overlapped, 2H); 7.94 (d, overlapped, 2H); 7.82 (nd, J=7.2Hz); 7.42 (d, J=8.7Hz, 2H); 7.27 (s, 2H); 4.97 (d, J=16.5Hz, 2H); 4.95-4.55 (obscured by HOD, 6H); 4.18 (d, J=12.0Hz, 2H); 3.56 (d, J=9.0Hz, 6H)

^{13}C NMR (300MHz, D_2O): δ176.1; 146.8 (d); 143.5; 133.6; 132.8; 130.7; 130.4; 130.1; 127.2; 126.2; 125.6; 125.2; 122.5; 121.9; 65.1; 63.0 (d); 56.8; 53.1

^{31}P NMR (300MHz, D_2O): δ16.9

ESI-MS (DUIS, - ion): 747($M - H^+ - Li^+$, 100%); 741($M - H^+$, 58%)

HRMS (IT-TOF-ESI): Calc'd for $C_{36}H_{32}N_4O_4P_2 + H^+$: 743.1666 Found: 743.1666



<u>*rac-hexa anionic tweezers*</u> (**27**)

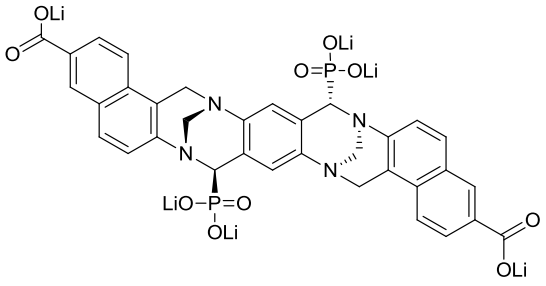
0.041g (0.053mmol) **23** was combined with 0.024g (0.994mmol) LiOH and 8mL 18Ω H_2O. The mixture was heated at reflux for 24hr after which time the mixture was allowed to cool to room temperature and brought to pH7 by dropwise addition of 4.8% HBr (0.89M). The mixture was concentrated to dryness with rotary evaporation, dissolved in 10mL 18Ω H_2O**,** and concentrated to dryness again. The crude product was combined with 11mL THF, mixed thoroughly, centrifuged, and THF decanted. This process was repeated twice more before the solid was placed under vacuum for 2d to remove residual solvent to afford 0.0276g ***27*** as a 90% by mass mixture (62% yield) with THF.

^{1}H NMR (300MHz, 50% TFA/$CDCl_3$): δ8.69 (s, 2H); δ8.54 (s, 2H); δ8.16 (d, J=8.1Hz, 2H); δ8.08 (d, J=7.8Hz, 2H); δ7.62 (d, J=8.1Hz, 2H); δ7.58 (d, J=9.3Hz, 2H); δ5.93 (d, J=12.9Hz, 2H); δ5.62 (d, J=14.1Hz, 2H); δ5.22 (d, J=25.2Hz, 2H); δ5.02 (d, overlapped, 4H)

^{31}P NMR (50% TFA/$CDCl_3$): δ17.6

ESI-MS (DUIS, - ion): 713 (M - H^+, 85%); 473 (100%)

HRMS (IT-TOF-ESI, + ion): Calc'd for $C_{34}H_{28}N_4O_{10}P_2$ + H^+: 715.1353 Found: 715.1357



<u>*meso-hexa anionic isomer*</u> (**28**)

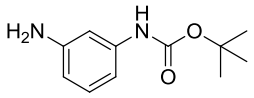
0.079g (0.103mmol) **24** was combined with 0.050g (0.2.07mmol) LiOH in 10mL 18Ω H_2O and heated at reflux for 25hr after it was allowed to cool to room temperature and neutralized to pH7 with 4.8% HBr (0.89M). The mixture was concentrated to dryness with rotary evaporation, redissolved in 10mL 18Ω H_2O, and concentrated to dryness again. The crude solid was mixed thoroughly with 10mL THF, centrifuged, and THF was decanted. This process was repeated twice more before being placed under vacuum overnight to afford 0.0517g (66% yield) of the *meso*-hexa anion tweezer as a pale yellow solid.

^{1}H NMR (50% TFA/$CDCl_3$): δ8.80 (s, 2H); 8.28 (d, obscured, 2H); 8.27 (s, 2H); 8.17 (d, J=8.7Hz, 2H); 7.80 (d, J=8.4Hz, 2H); 7.58 (d, J=8.7Hz, 2H); 5.87 (d, J=12.6Hz, 2H); 5.61 (d, J=15.9Hz, 2H); 5.20 (d, J=22.5Hz, 2H); 5.11 (d, J=16.2Hz, 2H); 4.97 (d, J=12.3Hz, 2H)

^{31}P NMR (50% TFA:$CDCl_3$): δ16.0

ESI-MS (DUIS, - ion): 713 (M - H^+, 100%); 473 (89%)

HRMS (IT-TOF-ESI, + ion): Calc'd for $C_{34}H_{28}N_4O_{10}P_2 + H^+$: 715.1353 Found: 715.1398

tert-butyl (3-aminophenyl)carbamate (**29**) 

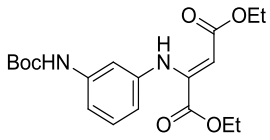
2.064g 1,3-diaminobenzene (19.09mmol) was dissolved in 15mL of EtOAc at room temperature to which as added 2.033g Boc_2O (9.315mmol) dropwise under an atmosphere of N_2. After 90min, the starting diamine and mono Boc material observed by TLC. At 120min the diacylated product started to show by TLC (50% EtOAc/CH_2Cl_2, silica, short UV,R_f diamine= 0.34 R_f mono Boc = 0.72, R_f DiBoc= 0.92). The reaction mixture was diluted with 50mL of CH_2Cl_2 and washed with eight 250mL portion DI H_2O. The organic layer was removed, dried over $MgSO_4$, concentrated over rotary vacuum, and dried over vacuum overnight to yield 1.528g **29** (79% yield) as a smokey white solid. Recrystallized from hexanes using hot filtration to afford white crystals (mp = 108-109°C).

^{1}H NMR (300MHz, $CDCl_3$): δ7.32 (t, J=8.0Hz, 1H); 6.92 (1H, s); 6.56 (ddd, J=7.3; 1.8; 0.6, 1H); 6.56 (s, 1H); 6.33 (ddd, J=7.9; 2.1; 0.7, 1H); 3.23 (bs, 2H); 1.51 (s, 9H)

^{13}C NMR (300MHz, $CDCl_3$): δ152.6; 147.2; 139.3; 129.6; 109.8; 108.5; 105.0; 80.2; 28.3

MS (EI, 70eV): 208 (M^+, 25%); 152 (M^+ - C_4H_8, 100%); 108 (152 - CO_2, 78%); 57 ($C_4H_9^+$, 84%)

2-(3-tert-Butoxycarbonylamino-phenylamino)-but-2-enedioic acid diethyl ester (**30**)

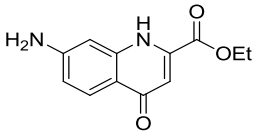


0.9982g (4.794mmol) tert-butyl (3-aminophenyl)carbamate **29** and 2.192g (10.43mmol) sodium diethyl oxaloacetate were added to 11mL CH_2Cl_2 and 8.9mL glacial AcOH. The mixture was stirred until homogeneous before the addition of 4Åms (25% reaction volume). The mixture was swirled periodically over 4h at which time TLC showed the reaction was done (25% EtOAc/CH_2Cl_2, silica, short UV, R_f amine=0.5, R_f enamine=0.9). The mixture was poured into 125mL sat. Na_2CO_3 and 100mL hexanes. The organic phase was removed and the aqueous player was extracted with an addition two 100mL portions hexanes. The organic extracts were combined, washed with four 100mL portions DI H_2O then 60mL pH2 phosphate buffer before drying over $MgSO_4$. After drying the mixture was filtered, concentrated with rotary evaportation, and placed under vacuum overnight to yield the 1.558g (96% yield) desired enamine **30** as an orange oil.

^{1}H NMR (300MHz, $CDCl_3$): δ9.61 (s, 1H); 7.15 (unresolved, 2H); 6.95 (dd, J=6.7 Hz; 1.4 Hz, 1H); 6.57 (dd J=6.9 Hz; 2.0 Hz, 1H); 6.42 (s, 1H); 5.37 (s, 1H); 4.20 (q, J=7.1 Hz, 4H); 1.51 (s, 9H); 1.32 (t, J=7.1Hz, 3H); δ1.15 (t, J=7.1Hz, 3H)

^{13}C NMR (300MHz, $CDCl_3$): δ169.8; 164.7; 152.7; 148.6; 141.4; 139.6; 129.7; 115.6; 114.2; 111.2; 94.5; δ81.0; 62.5; 60.3; 28.6; 14.7; 14.0

MS (EI, 70eV): 378 (M^+, 18%); 322 (M^+ - C_4H_8, 22%); 249 (322 - $C_3H_5O_2$, 39%); 203 (249 - C_2H_6O, 68%); 185 (203 - H_2O, 36%); 159 (203 - CO_2, 100%); 132 (159 - CO, 32%)



7-Amino-4-oxo-1,4-dihydro-quinoline-2-carboxylic acid ethyl ester (**31**)

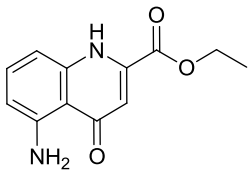
0.0326g (0.1243mmol) **38** and 0.0109g 5% Pd-C were suspended in 10mL anhyd. EtOH to which was added 0.1930g (3.061mmol) ammonium formate. The mixture was stirred rapidly for 3h before TLC showed the absence of starting material (50% EtOAc/CH_2Cl_2, silica, short UV R_f nitro= 0.39, R_f amino= 0.08). The mixture was filtered through Celite, rinsed with 40mL anhyd. EtOH, and concentrated to dryness with rotary evaporation. The crude was dissolved in 5.5mL EtOH and diluted with 30mL CH_2Cl_2 causing NH_4O_2CH to precipitate which was removed by filtration. The filtrate was concentrated to dryness with rotary evaporation and purified by flash chromatography (5% IpOH/CH_3CN) to yield 0.019g (66% yield) of **31**.

^{1}H NMR (300MHz, DMSO-d_6): δ11.40 (s,1H); 8.03 (d, J=8.7Hz, 1H); 6.81 (d, J=1.8Hz, 1H); 6.64 (dd, J=8.8; 2.1Hz, 1H); 6.42 (d, J=2.1Hz, 1H); 6.03 (s, 2H); 4.41 (q, J=7.1Hz, 2H); 1.42 (t, J=7.1Hz, 3H)

^{13}C NMR (300MHz, DMSO-d_6): δ162.8; 153.1; 142.8; 137.1; 126.4; 117.7; 114.4; 110.6; 110.0; 98.1; 62.6; 14.3

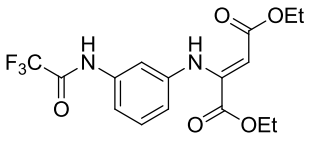
MS (EI, 70eV): 232 (M^+, 49%); 158 (M^+ - $C_3H_5O_2$, 10%); 130 (158 - CO); 104 (130 - C_2H_2, 27%); 57 ($C_3H_5O^+$, 56%)

ESI-MS (DUIS, + ion): 465 (2M + H^+, 28%); 291 (M + 59, 38%); 233 (M + H^+, 100%)

Ethyl 5-amino-4-oxo-1,4-dihydroquinoline-2-carboxylate (**32**) 

^{1}H NMR (300MHz, DMSO-d_6): δ11.52 (s, 1H); 7.51 (bs, 2H); 7.23 (t, J=8.8Hz, 1H); 6.86 (dd, J=7.3; 0.8Hz, 1H); 6.40 (d, J=1.9Hz, 1H); 6.20 (dd, J=7.4; 0.7Hz, 1H); 4.40 (q, J=7.1Hz, 2H); 1.35 (t, J=7.1Hz, 3H)

^{13}C NMR (300MHz, DMSO-d_6): δ181.9; 162.4; 151.1; 142.7; 137.2; 133.6; 112.7; 110.7; 107.0; 103.7; 62.8; 14.3

Diethyl 2-((3-(2,2,2-trifluoroacetamido)phenyl)amino)fumarate (**34**) 

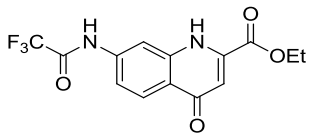
0.154g (0.753mmol) N-(3-aminophenyl)-2,2,2-trifluoroacetamide **(33)** and 0.404g (1.92mmol) sodium diethyl oxaloacetate were dissolved in 5mL CH_2Cl_2 and 0.3mL glacial AcOH. After homogeneous 0.709g 4Åms were added to the mixture and swirled periodically over the course of 27h at which time the reaction was observed to be complete by TLC (1:1:1 EtOAc/CH_2Cl_2/NEt_3, silica, short UV R_f amine=0.54, R_f enamine=0.82). The reaction volume was poured into 20mL sat. Na_2CO_3 and 100mL hexanes. The organic phase was removed and the aqueous layer was extracted with an addition two 50mL portions hexanes. The organic extracts were combined, washed with 20mL sat. Na_2CO_3, dried over $MgSO_4$, filtered, concentrated with rotary evaporation, and placed under vacuum overnight to remove residual solvent to yield 0.252g (89% yield) of **34** as a yellow green oil.

^{1}H NMR (300MHz, $CDCl_3$): δ9.61 (s, 1H); 8.15 (s, 1H); 7.26(obscured, 1H); 7.24 (t, J=8.0Hz, 1H); 7.14 (d, J=8.2Hz, 1H); 6.73 (d, J=7.8Hz, 1H); 5.47 (s, 1H); 4.24 (q, J=7.2Hz, 4H); 1.30 (t, J=7.1Hz, 3H); 1.18 (t, J=7.1Hz, 3H)

^{13}C NMR (300MHz, $CDCl_3$): δ169.3; 164.2; 154.8; 147.3; 141.0; 136.2; 129.5; 118.0; 115.7; 115.5; 112.7; 95.4; 62.4; 60.8; 14.1; 13.5

MS (EI, 70eV): 374 (M^+, 12%); 301 (M^+ - $C_3H_5O_2$, 13%); 255 (301 - C_2H_6O, 100%); 228 (256 - CO, 18%)

Ethyl 4-oxo-7-(2,2,2-trifluoroacetamido)-1,4-dihydroquinoline-2-carboxylate (**35**)



Thermolysis method

0.0526g (0.1405mmol) diethyl 2-((3-(2,2,2-trifluoroacetamido)phenyl)amino)fumarate (**34**) was combined with 25mL Ph_2O and heated at reflux under an atmosphere of N_2 for 20min after which it was cooled to room temperature below the addition of 170mL hexane. The mixture was stored in a 0˚C refrigerator with crystals being collected by vacuum filtration the following day. After rinsing with hexanes and residual solvent removed 0.0249g (54% yield) quinolones afforded in a 1:3.5 mol ratio of the 7- : 5-trifluoroacetyl isomers.

Eaton's Reagent method

0.149g (0.394mol) **34** was dissolved in 10mL Eaton's Reagent and heated at 116˚C for 50min after which the reaction volume was poured into 20mL CH_2Cl_2 to which was added sat.

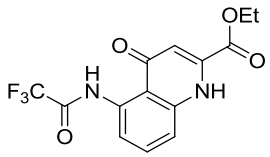
Na_2CO_3 until no more effervescence was observed. The organic layer was removed and the aqueous phase was extracted with two 60mL portions CH_2Cl_2. The organic layers were combined, dried over $MgSO_4$, filtered, concentrated with rotary evaporation, and placed under vacuum to remove residual solvent yield 0.105g (81% yield) of the quinolones in a 1:7 mol ratio of the 7- : 5-trifluoroacetyl isomers.

^{1}H NMR (300MHz, DMSO-d_6): δ12.26 (s, 1H); 11.64 (s, 1H); 8.13 (d, J=8.9Hz, 1H); 7.96 (d, J=2.0Hz, 1H); 7.52 (dd, J=9.0; 2.1Hz, 1H); 6.89 (s, 1H); 4.47 (q, J=7.1Hz, 2H); 1.39 (t, J=7.1Hz, 3H)

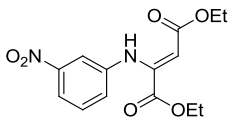
^{13}C NMR (300MHz, DMSO-d_6): δ168.7; 165.3; 161.4; 155.1; 140.5; 138.9; 131.9; 127.1; 123.5; 115.8; 114.2; 107.3; 62.3; 14.2

MS (EI, 70eV): 328 (M^+, 100%); 299 (M^+ - C_2H_5, 25%); 256 (299 +H - CO_2, 34%); 203 (256 + H - C_3H_2O, 16%); 157 (256 - H - C_2HF_3O, 22%); 132 (157 + H - C_2H_2, 40%); 69 (CF_3^+, 45%)

Ethyl 4-oxo-5-(2,2,2-trifluoroacetamido)-1,4-dihydroquinoline-2-carboxylate (**36**)



^{1}H NMR (300MHz, $CDCl_3$): δ14.79 (s, 1H); 9.26 (s, 1H); 8.57 (d, J=8.1Hz, 1H); 7.69 (t, J=8.3Hz, 1H); 7.23 (d, J=8.4; 0.9Hz, 1H); 6.96 (s, 1H); 4.52 (q, J=7.1Hz, 2H); 1.45 (t, J=7.1Hz, 3H)

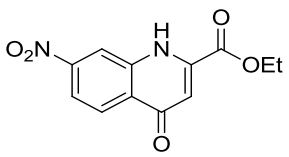
Diethyl 2-((3-nitrophenyl)amino)fumarate (**37**) 

1.024 (7.417mmol) m-nitroanaline, 3.118g (14.84mmol) sodium diethyl oxaloacetate, 2.982g $TsOH \cdot H_2O$(15.68mmol) were combined in 60mL of CH_2Cl_2, fitted with a heavier than water Dean-Stark Trap and heated to reflux overnight. After the starting aniline had been seen to be consumed (silica,1:1:1 EtOAc: CH_2Cl_2: NEt_3, short UV R_f aniline=0.65, R_f enamine=0.83) the reaction mixture was poured into 50mL of hexane and washed with 200mL of a 0.1M K_3PO_4 solution. The organic phase was then washed with 200mL of DI H_2O, dried over $MgSO_4$, filter, concentrated over rotary vacuum, and placed on high vacuum to removal residual solvent to yield 2.085g (92% yield) of the desired enamine as a yellow oil.

^{1}H NMR (300MHz, $CDCl_3$): δ9.77 (s, 1H); 7.92 (dd, J=8.1; 1.5Hz, 1H); 7.72 (t, J=2.1Hz, 1H); 7.44 (t, J=8.1Hz, 1H); 7.20 (dd, J=8.0; 2.1Hz, 1H); 5.62 (s, 1H); 4.24 (q, J=7.2Hz, 4H); 1.32 (t, J=7.1Hz, 3H); 1.21 (t, J=7.1Hz, 3H)

^{13}C NMR (300MHz, $CDCl_3$): δ169.2; 163.5; 148.7; 146.3; 141.8; 129.8; 126.2; 118.3; 115.0; 97.6; 62.5; 60.5; 14.3; 13.8

MS (EI, 70eV): 308 (M^+, 18%); 235 (M^+ - $C_3H_5O_2$, 28%); 189 (235 - C_2H_6O, 100%); 162 (189 - CO, 23%); 143 (189 - NO_2, 24%); 89 ($C_3H_7NO_2^+$, 23%); 76 ($C_6H_4^+$, 49%)



Ethyl 7-nitro-4-oxo-1,4-dihydroquinoline-2-carboxylate (**38**)

Thermolysis

0.282g (0.916mmol) **37** was dissolved in 80°C 40mL Ph_2O. The reaction mixture was degassed and backfilled with N_2 three time, placed under an atmosphere of N_2, and heated at reflux for 21min before the mixture was allowed to cool to room temperature over which time a yellow solid precipitated. 50mL hexanes were added to ensure complete precipitation before the solid was collected by vacuum filtration, washed with an additional 100mL hexane, and dried under vacuum overnight to remove residual solvent to generate 0.194g (81%) of the quinolones in a mol ratio of 4:1 of the 7-NO_2 : 5-NO_2 isomers.

Eaton's Reagent

0.273g (0.886mmol) **37** to which was added 5mL Eaton's Reagent. The mixture was placed under a N_2 atmosphere and heated at 110°C 3h over which time it changed color to a dark red color and was removed from the heat. After 20h at room temperature the mixture was poured into 50mL CH_2Cl_2 and 60mL sat. Na_2CO_3. The organic layer was removed and the aqueous phase was extracted with an addition two 40mL portions CH_2Cl_2. The organic extracts were combined, dried over $MgSO_4$, filtered, concentrated with rotary evaporation, and placed under vacuum overnight to remove residual solvent to yield 0.254g (109% yield) of the quinolones in a mol ration of 1:2.3 of the 7-NO_2 : 5-NO_2 isomers.

Recrystallization procedure developed by Jackie Koch

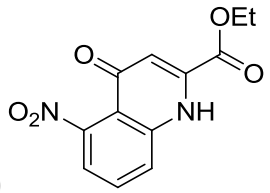
0.1006 g of a 2.6:1 mol ratio 7-NO_2 : 5-NO_2 quinolone isomers mixture was suspended in 8mL boiling EtOH for 3 min to which was added 10mL boiling toluene and continued to heat at boiling for 9 min. The mixture was placed on ice for 15 min with the resulting solid collected by centrifugation. It was then washed with 20mL hexanes and placed under vacuum overnight to afford 0.0639 g of the **38** in 88% recovery (mp = 308-310°C)

^{1}H NMR (300MHz, DMSO-d_6):δ12.47 (s, 1H); 8.87 (d, J=2.2Hz, 1H); 8.29 (d, J=8.9, 1H); 8.09 (dd, J=8.9; 2.2Hz, 1H); 6.79 (s, 1H); 4.44 (q, J=7.1Hz, 2H); 1.38 (t, J=7.1, 3H)

^{13}C NMR (300MHz, DMSO-d_6): saturated solution too dilute to acquire all signals

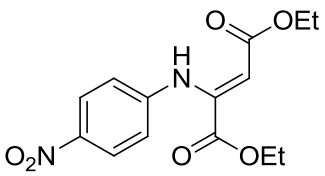
Signals observed: δ161.8; 149.6; 128.5; 127.0; 117.5; 111.1; 62.8; 13.9

MS (EI, 70eV): 262 (M^+, 67%); 188 (M^+ - $C_3H_6O_2$, 98%); 142 (188^+ - NO_2); 114 (142^+ - CO, 75%); 88 (114^+ - C_2H_2, 61%); 75 ($C_3H_7O_2^+$, 100%); 62 (88^+ - C_2H_2, 58%)



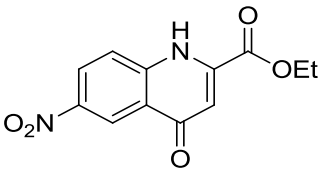
Ethyl 5-nitro-4-oxo-1,4-dihydroquinoline-2-carboxylate (**39**)

^{1}H NMR (300MHz, DMSO-d_6): δ14.86 (1H, s); 8.19 (d, J=8.5, 1H); 7.86 (1H, t, J=7.9Hz); 7.62 (1H, d, J=7.4Hz); 6.69 (1H, s); 4.47 (2H, q, J=6.8Hz); 1.40 (3H, t, J=7.4Hz)

Diethyl 2-((4-nitrophenyl)amino)fumarate (**40**) 

0.6405g (4.637mmol) p-nitroaniline, 1.951g (9.282mmol) sodium diethyl oxaloacetate, 1.855g (9.752mmol) $TsOH \cdot H_2O$, and 50mL CH_2Cl_2 were combined in heated at reflux with a heavier than water Dean-Stark trap with 0.596g loosely packed cotton contained within. After 3d the aniline was no longer seen by TLC (1:1:1 EtOAc:CH_2Cl_2:NEt_3, silica, shortUV, R_f aniline=0.37, R_f enamine=0.86) and the mixture was allowed to cool to room temperature before being poured into 120mL hexanes. The mixture was washed with three 200mL portions sat. Na_2CO_3. The aqueous phase was back extracted with 200mL hexane. The organic extracts were combined, dried over $MgSO_4$, filtered, concentrated with rotary evaporation, and placed under vacuum overnight to yield 1.216g of the desired product as a mixture with the starting aniline. The desired enamine **40** was present in a 92:8 mol ratio to provide an NMR yield of 78%

^{1}HNMR (300MHz, $CDCl_3$): δ9.82 (s,1H); 8.15 (d, J=9.0Hz, 2H); 6.90 (d, J=9.0Hz, 2H); 5.69 (1H, s); 4.27 (q, J=7.1Hz, 2H); 4.23 (q, J=7.1Hz, 2H); 1.31 (q, J=7.1Hz, 3H); 1.23 (q, J=7.1Hz, 3H)

Ethyl 6-nitro-4-oxo-1,4-dihydroquinoline-2-carboxylate (**41**) 

1.112g (3.607mmol) **40** was combined with 25mL Ph_2O, placed under an atmosphere of N_2, and heated at reflux for 20min. The mixture was cooled to room temperature, diluted with 250mL hexanes, and left to sit overnight. The resulting precipitate was collected by vacuum

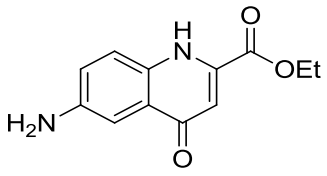
filtration and placed under vacuum overnight to afford 0.807g (85% yield) of the desired quinolone **41**.

^{1}H NMR (300MHz, DMSO-d_6): δ12.54 (s, 1H); 8.80 (d, J=2.6Hz, 1H); 8.48 (dd, J=9.2; 2.6Hz, 1H); 8.11 (d, J=9.2Hz, 1H); 6.76 (s, 1H); 4.44 (q, J=7.1Hz, 2H); 1.38 (q, J=7.1Hz, 3H)

^{13}C NMR: δ177.1; 161.7; 143.8; 143.1; 139.2; 126.5; 124.7; 121.4; 121.2; 111.3; 62.9; 13.8

MS (EI, 70eV): 262 (M^+, 96%); 216 (M^+ - C_2H_6O, 25%); 188 (216 - CO, 100%); 142 (188 - NO_2, 40%)

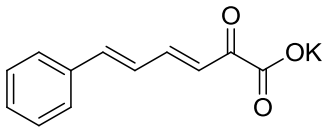
Ethyl 6-amino-4-oxo-1,4-dihydroquinoline-2-carboxylate (**42**)



0.1075g (0.4100mmol) **41**, 0.6093g (9.577mmol) NH_4O_2CH, 0.0282g 5% Pd-C, and 5mL anhyd. EtOH were combined under an atmosphere of N_2. The mixture was mixed at a rapid pace for 6d at which time the mixture was filtered over Celite and rinsed with 60mL anhyd. EtOH. The filtrate was concentrated to dryness with rotary evaporation and placed under vacuum for 10d to generate 0.096g (100% yield) of the desired product.

^{1}H NMR (300MHz, $CDCl_3$): δ9.01 (s, 1H); 7.55 (d, J=2.6, 1H); 7.29 (d, J=8.8Hz, 1H); 7.09 (dd, J=8.7; 2.6Hz, 1H); 6.91 (s, 1H); 4.47 (q, J=7.1Hz, 2H); 3.91 (s, 2H); 1.43 (t, J=7.1Hz, 3H)

MS (EI, 70eV): 232 (M^+, 73%); 186 (M^+ - C_2H_6O, 9%); 158 (186 - CO, 100%); 130 (158 - CO, 17%); 104 (130 - C_2H_2, 16%)

Potassium (3E,5E)-2-oxo-6-phenylhexa-3,5-dienoate (**45**) 

3.292g (24.91mmol) cinnamaldehyde, 2.804g (25.48mmol) sodium pyruvate, and 0.1123g (2.808mmol) NaOH were combined with 25mL CH_3OH before being placed under an atmosphere of N_2 and heated to reflux for 17h. The volume was observed to be heterogeneous with yellow solid but TLC showed that the starting aldehyde was still present (25% CH_3CN/CH_2Cl_2 R_f: 0.85) and concentrated to dryness with rotary evaporation. 0.4030g (10.08mmol) NaOH and 46mL CH_3OH were placed into the reaction vessel and heated at reflux for 3h before the starting aldehyde was no longer visible by TLC. The yellow solid was collected by vacuum filtration, rinsed with two 100mL portions CH_3OH, and placed under vacuum overnight to afford 2.083g (37% crude yield). CO_2 was bubbled into the filtrate until it reached pH 8 before being concentrated to dryness with rotary evaporation before being combined with 150mL 18Ω H_2O and 75mL triethylamine (TEA). CO_2 was bubbled into the mixture while on ice until it became homogeneous before being extracted with five 50mL CH_2Cl_2. The organic portions were combined, dried over $MgSO_4$, filtered, concentrated with rotary evaporation, and placed under vacuum overnight to yield 2.050g of an auburn oil. The oil was combined with 100mL EtOAc, heated to boiling, decanted from the remaining undissolved semisolid, and cooled to room temperature. The supernatant was combined with 1.643g (9.013mmol) potassium 2-ethylhexanoate (K-2EHA) dissolved in 30mL EtOAc which produced a precipitate. The solid was collected by centrifugation, washed with two 30mL portions EtOAc, and placed under vacuum overnight to remove residual solvent to afford 0.433g of crude **45** as a yellow solid. 2.045g of the initially isolated yellow solid was dissolved in 185mL 2.4M

triethylammonium bicarbonate (TEABC) and extracted with four 50mL portions CH_2Cl_2. The organic extracts were combined, dried over $MgSO_4$, filtered, concentrated with rotary evaporation, and placed under vacuum overnight to yield 1.0963g of an auburn oil. The oil was combined with 50mL EtOAc and stirred at room temperature before the supernatant was decanted and mixed with 0.8073g (4.429mmol) K-2EHA producing a solid upon mixing. The solid was collected by centrifugation, washed with three 30mL portions EtOAc, and dried under vacuum to afford 0.7836g of crude **45** as a yellow solid. 1.118g of crude **45** was recrystallized from 55mL CH_3OH and 100mL EtOAc and boiled down to 1/3 of the total volume and stored in a -10˚C freezer overnight. The resulting solid was collected by centrifugation and dried under vacuum to yield 0.914g **45** as a yellow solid (15% yield, 99.4% **45**, 0.6% by mass pyruvate, mp = 204˚C (darkens to tan), 228˚C (shrinks, darkens to brown), 260˚C (d)

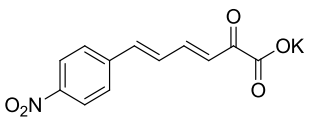
^{1}H NMR (300MHz, D_2O): δ7.63 (d, J=8.1Hz, 2H); 7.51 (q_{AB}, J=15.6Hz, 9.6Hz, 1H); 7.48-7.41(m, 3H); 7.20-7.07 (m, J=15.6Hz; 8.7Hz, 2H); 6.40 (d, J=15.6Hz, 1H)

^{13}C NMR (300MHz, D_2O): δ198.3; 173.0; 151.7; 144.7; 136.4; 130.6; 129.7; 128.4; 127.4; 126.0

ESI-MS (DUIS, + ion): 519 ($2M + K^+$, 100%); 279 ($M + K^+$, 96%)

ESI-MS (DUIS, - ion): 441 ($2M^- + K^+$, 89%); 201 (M^-, 100%)

UV-VIS: λ_{max}=335nm; ε=38868 L mol^- cm^-

Potassium (3E,5E)-6-(4-nitrophenyl)-2-oxohexa-3,5-dienoate (**46**) 

1.456g (8.222mmol) 4-nitrocinnamaldehyde and 1.351g (12.28mmol) sodium pyruvate were suspended in 25mL. 0.1133g (2.832mmol) NaOH was dissolved in 25mL CH_3OH, added to the reaction mixture, and quantitatively transferred with 10mL CH_3OH. The mixture was placed under an atmosphere of N_2 and heated at reflux for 3.5h before the starting aldehyde was no longer visible by TLC (25% CH_3CN/CH_2Cl_2 R_f: 0.87). The mixture was allowed to cool to room temperature, concentrated with rotary evaporation, and placed under vacuum overnight to afford 2.133g of a brown solid. 2.132g of the crude product was added to 120mL 18Ω H_2O and 100mL TEA. CO_2 was bubbled into the mixture until it became homogeneous, extracted with six 100mL portions CH_2Cl_2. The organic extracts were combined, dried over $MgSO_4$, filtered, concentrated with rotary evaporation, and placed under vacuum to yield 2.372g of a dark brown solid. 1.539g of the dark brown solid was mixed with 140mL EtOAc and heated to boiling before the supernatant was decanted, cooled to room temperature. 1.357g potassium 2-ethylhexanoate dissolved in 50mL EtOAc was added to the supernatant, producing a precipitate. The solid was collected by centrifugation, washed with two 40mL portions EtOAc, and dried under vacuum to produce 0.2123g of the crude product which was recrystallized from 12mL CH_3OH and 15mL EtOAc. After concentrating to 10mL total volume the mixture brought to room temperature and placed on ice for several minutes before collecting the solid by centrifugation and drying under vacuum to yield 0.1257g (5% yield) **46** (98% pure, 2% pyruvate mp = 198˚C (darkens from brown to dark brown), > 400˚C

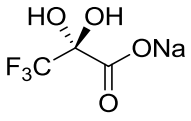
^{1}H NMR (300MHz, D_2O): δ8.21 (d, J=8.4Hz, 2H); 7.72 (d, J=8.7Hz, 2H); 7.46 (q_{AB}, J=15.3Hz, 8.4Hz, 1H); 7.20 (m, 2H); 6.46 (d, J=15.6Hz, 2H)

^{13}C NMR (300MHz, D_2O): δ198.9; 173.6; 150.9; 149.0; 144.1; 142.4; 132.3; 129.9; 129.0; 125.8

MS (DUIS, + ion): 324 ($M + K^+$, 89%), 150 ($C_8H_7NO_2 + H^+$, 100%)

MS (DUIS, - ion): 531 ($2M^-+K^+$, 65%); 493 ($2M^-+H^+$, 69%); 246 (M^-, 38%); 202 ($M^- - CO_2$, 100%);

UV-VIS: λ_{max}=356nm; ε=16922 L mol^- cm^-



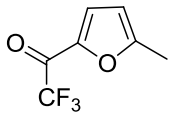
Sodium trifluoropyruvate (**47**)

3.760g ethyl trifluoropruvate was combined with 50mL 1.2M HCl and heated at reflux for 21h at which time hydrolysis appeared complete by TLC (R_f ester= 0.22, R_f prod=0.0, 10% CH_3CN/CH_2Cl_2, DNP stain). The reaction mixture was concentrated to dryness with rotary evaporation, redissolved in 50mL 18Ω H_2O, and concentrated to dryness with rotary evaporation again. The crude product was dissolved in 30mL 18Ω H_2O neutralized to pH7 with $NaOH_{(aq)}$, concentrated to near dryness with rotary evaporation, and azeotropically dried by evaporation of toluene. The **47** was placed under vacuum overnight to generate 3.542g (91% yield, mp = 206˚C(d)) as a white solid.

^{1}H NMR (300MHz, D_2O): no signals observed

^{13}C NMR (300MHz, D_2O): δ 171.1; 122.4 (q); 92.2 (q)

ESI-MS (DUIS, - ion): 227 (M + HCO_2^-, 41%); 159 (M^- (hydrate), 100%); 141 (M^- (keto form), 85%)

<u>*5-methyl-2-(2,2,2-trifluoroacetyl)furan*</u> (**50**) 

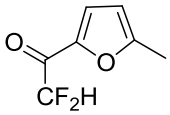
8.0mL 2-methylfuran (88.67mol) and 60mL hexane were combined in a 200mL round bottom flask. The reaction mixture was placed under an atmosphere of N_2 and submerged into an ice bath and stirred for 20min to allow for thermo-equilibration. 8.25mL (59.35mmol) trifluoroacetic anhydride was then injected into the reaction mixture dropwise and stirred rapidly at 0°C for 2.5h.The reaction mixture was concentrated with rotary evaporation to 1/6 volume before being poured into a separatory funnel containing 150mL 0°C sat.$NaHCO_3$ and 30mL Et_2O. The organic layer was removed with the aqueous phase being countercurrently extracted with three 30mL portions of Et_2O. The organic phases were combined, dried over $MgSO_4$, filtered, rinsed with 10mL Et_2O, and concentrated with rotary evaporation to afford 12.439g (118% crude yield) of a free flowing orange liquid. The crude product was purified by vacuum distillation with the following parameters:

Pressure: 20torr Fraction 1 collected with 80°C head temp and oil bath temp 119-126°C

Pressure: 20torr Fraction 2 collected with 80°C head temp and oil bath temp 128-139°C

Fraction 1: 6.7228g Fraction 2: 1.0354g were both **50** to generate a 74% purified yield

^{1}H NMR (300MHz, $CDCl_3$): δ7.45 (d, bs, 1H); 6.33 (d, J=3.6Hz, 1H); 2.48 (s, 3H)

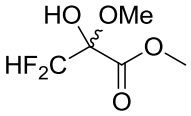
5-methyl-2-(2,2-difluoroacetyl)furan (**51**) 

1.354g Mg^0 (55.71mmol) was crushed with a mortar and pestle, placed into a 250mL round bottom flask, and placed under an atmosphere of N_2. 110mL THF (distilled, Na^0/benzaophenone) and 14mL (110.3mmol) TMSCl were placed into the reaction vessel before being submerged in an ice bath while stirring rapidly. A solution of 5.004g (28.09mmol) **50** in 28mL THF was added dropwise at the rate of 1drop/5sec. After 1h the reaction mixture darkened to a blackish blue. 30min after all of the **50** solution was added the reaction mixture was filtered. The crude yellow liquid was combined with 20mL THF and added to rapidly stirring 4.4mL conc. HCl on an ice bath. The mixture was stirred at 0°C for 30min before being poured into a seperatory funnel containing 30mL Et_2O and 35mL sat. $NaHCO_3$. The organic layer was removed and the aqueous phase was extracted with two 30mL portions of Et_2O. The organic portions were combined, dried over $MgSO_4$, filtered, concentrated with rotary evaporation, and placed under vacuum to remove residual solvent for 30s to afforded 3.838g (85% crude yield) of a yellow liquid. ^1H NMR analysis determined the crude product was 88% by mass for afford a corrected mass to be 3.3889g (75% NMR yield). The reaction mixture was concentrated to 1/8 total volume with rotary evaporation before diluting with 300mL hexane, causing a white solid to precipitate. The white solid was removed via filtration over Celite. The filtrate was concentrated with rotary evaporation and placed under vacuum to remove residual solvent for 30s to afford 5.200g (80% crude yield) of a yellow liquid. Crude **51** purified by vacuum distillation with the following parameters: Pressure: 20torr Fraction 1: 96-105°C head temp,

130-140°C oil temp, Pressure: 20torr Fraction 2: 105-103°C head temp, 140-160°C oil temp. 64% yield of pure **51**

^{1}H NMR (300MHz, $CDCl_3$): δ7.39 (bs, 1H); 6.24 (d, J=3.6Hz, 1H); 6.12 (t, J=53.7Hz, 1H); 2.40 (s, 3H)

<u>*Methyl difluoropyruvate methyl hemiacetal*</u> (**52**)

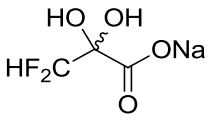


0.518g (3.237mmol) **51** was combined with 16mL CH_3OH in a 50mL round bottom flask was placed under a nitrogen atmosphere and submerged in a -78°C bath. After stirring for 3min a mixture of O_3/O_2 was bubbled into the reaction mixture with the following parameters: A2Z O_3 generator Model#A2Z5-5GLAB, 0.56Amp on meter(100% production), 13PSI O_2 from the regulator, 0.5L/min bubble flow rate. After 25min of bubbling the reaction mixture was observed to be faint greenish yellow in color and after 35min of bubbling, the reaction mixture became colorless. After 1h, the O_3/O_2 bubbling was ceased and N_2 then bubbled through the reaction mixture for 18min. The reaction vessel was then moved to a -47°C bath (m-xylene/$N_{2(l)}$) for 2min before the dropwise addition of 0.07mL conc. H_2SO_4 and 0.2126g 3Å molecular sieves. After warming to room temperature the mixture was heated at reflux for 16h. The reaction mixture was concentrated to ~4mL total volume with rotary evaporation. The H_2SO_4 was removed by passing over a column (49mmx24mm) silica gel and eluted with 10% CH_3OH/CH_2Cl_2 collecting 2.5mL fractions. Desired product collected in fractions 5-16 with ^{1}H NMR yield of the 35% of the desired product as a mixture with CF_2HCOOH. (Note: Use ionic exchange technique only)

Removal of the acidic side product via ion exchange chromatography by the following method: 10.2231g Amberlyst A-21 (swollen with 18.1MΩ H_2O) was used to make a 10.25" tall by 10mm wide column. 300mL 5M NH_3 was passed through the column followed by 18.1Ω H_2O until the effluent was neutral to pH Hydron paper then 150mL MeOH. The reaction concentrate was loaded on top of the column and eluted with MeOH. Seventeen 3mL fraction were collected at a rate of ~1drop/s. Eight 5mL fraction were then collected at a rate of ~2drops/s. Fractions 3-19 contained the desired product was visualized by $KMnO_4$ stain on silica.

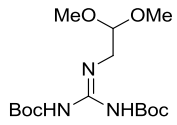
^{1}H NMR (300MHz, $CDCl_3$): δ5.81 (t, J=54.9Hz, 1H); 3.94 (s, 3H); 3.34 (s, 3H)

<u>*Sodium difluoropyruvate hydrate*</u> (**53**)



0.0652g (0.4178mmol) mixture of **52** and the ethyl hemiacetal derivative were dissolved in 20mL 3M HCl, placed under an atmosphere of N_2, and heated to reflux for 17h being cooled to room temperature. The reaction mixture was filtered (as specks of brown solid formed in the mixture overnight), concentrated with rotary evaporation, and dried azeotropically with CH_3CN and toluene, and placed under vacuum to remove residual solvent for 2h to afford 0.0464g (78% crude yield) of a yellow solid (difluoropyruvic acid). The crude product was dissolved in 15mL 18.1MΩ H_2O and titrated to neutrality with a solution of NaOH. The mixture was concentrated with rotary evaporation, dried azeotropically with CH_3CN and toluene, and placed under vacuum overnight to remove residual solvent to afford 0.0470g (69%crude yield) of a tannish solid.

^{1}H NMR (300MHz, D_2O): δ5.94 (t, J=55.2Hz, 1H)

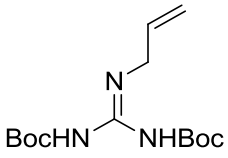
N,N'-Di-Boc-N"-(2,2-dimethoxy-ethyl)-guanidine (**54**) 

0.253g (0.816mmol) N,N'-Di-Boc-1H-pyrazole-1-carboxamidine was placed under an atmosphere of N_2 before being dissolved in 4.1mL CH_3CN. The mixture was set to stir before the addition of 0.27mL (2.48mmol) aminoacetaldehyde dimethyl acetal. The mixture was allowed to stir for 1.5h before TLC showed only the presence of the desired product (0.43 25% EtOAc/CH_2Cl_2, silica). The mixture was concentrated with rotary evaporation and placed under vacuum overnight to remove residual solvent to afford 0.218g **54** (99% yield, mp = 101-104˚C) as a white solid.

^{1}H NMR (300MHz, $CDCl_3$): δ11.46 (s, 1H); 8.48 (s, 1H); 4.48 (t, J=5.4Hz, 1H); 3.59 (q_{AB}, J=5.4Hz, 2H); 3.40 (s, 6H)

^{13}C NMR (300MHz, $CDCl_3$): δ163.6; 156.4; 153.1; 102.0; 83.2; 79.4; 54.1; 42.3; 28.4; 28.2

MS (EI, 70eV): 347 (M^+, 100%); 290 (M^+ - C_4H_8, 30%); 236 (35%)

N-Allyl-N',N''-Di-Boc-guanidine (**55**) 

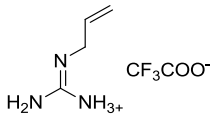
0.159g (0.512mmol) N,N'-Di-Boc-1H-pyrazole-1-carboxamidine was dissolved in 3mL CH_3CN before 0.12mL (1.600mmol) allyl amine was added to the reaction mixture and subsequently

placed under an inert atmosphere. The mixture was allowed to stir at room temperature for 3h before the reaction mixture was concentrated with rotary evaporation and placed under vacuum overnight to remove residual solvent to afford 0.147g (96% yield) of off-white solid **55**.

^{1}H NMR (300MHz, $CDCl_3$): δ11.52 (s, 1H); 8.41 (s, 1H); 5.89 (m, J= 15.9; 10.2; 5.1Hz, 1H); 5.24 (d, J= 17.1; 1.2Hz, 1H); 5.17 (d, J= 10.2Hz, 1H); 4.08 (dd, J= 5.4; 1.2Hz, 2H); 1.50 (s, 18H)

^{13}C NMR (300MHz, $CDCl_3$): δ163.7; 156.2; 153.4; 133.4; 116.9; 83.7; 79.5; 43.4; 28.4; 28.2

MS (CI): 299 (M^+, 10%); 243 (M- $C_3H_7N+H^+$, 17%); 188 (M^+-111, 100%)

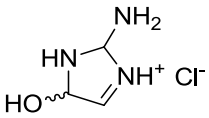
N-allyl guanidinium trifluoracetate (**57**) 

0.106g (0.355mmol) **55** was dissolved in 3.0mL CH_2Cl_2 before the addition of 1.0mL CF_3COOH. The reaction mixture was set to stir and heated at reflux for 3h. The reaction mixture was allowed to cool to room temperature, concentrated by rotary evaporation, and dried azeotropically via evaporation of toluene. After being placed under vacuum overnight to remove residual solvent afforded 0.0819g (108%) **57**.

^{1}H NMR (300MHz, D_2O): δ5.86 (m, 1H); 5.28 (dd, J= 12.3; 0.9Hz, 1H); 5.23 (dd, overlapped, 2H); 3.83 (d, J= 4.8Hz, 2H)

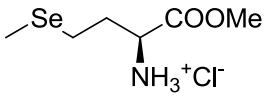
^{13}C NMR (300MHz, CD_3CN): δ158.8; 133.6; 117.3; 44.2

ESI-MS (DUIS, + ion): 100 (M - CF_3COO^-, 100%)

2-Amino-5-hydroxy-4,5-dihydro-3H-imidazolium chloride (**58**) 

0.0331g (0.1459mmol) 1-allylguanidinium trifluoroacetate and 0.0856g (0.4002mmol) $NaIO_4$ were combined in a 25mL pear bottom flask along with 0.08mL CD_3OD. 0.0037g (0.0100mmol) $K_2OsO_4 \cdot 2H_2O$ was dissolved in 0.50mL D_2O, injected into the reaction mixture, and quantitatively transferred with 0.50mL D_2O. The mixture was allowed to stir at room temperature. Shortly after mixing, a white solid was observed to precipitate from the reaction mixture. The reaction was allowed to mix for 2.5 h before being analyzed by ^1H NMR at which point the reaction was determined to be complete. The reaction mixture was filtered, rinsed with 6mL CH_3OH, and combined with NMR sample. Dowex 2-X8 ion exchange resin was swelled with 3M HCl. A column 28cm tall and 2cm wide was constructed with the resin and rinsed with 300mL 3M HCl. 18.1Ω H_2O was run through the column until the effluent was neutral to pH Hydron paper(180mL) followed by 150mL CH_3OH. The methanolic solution was loaded on the column and eluted with CH_3OH. Twenty 10mL fractions were collected at the rate of 10mL/min. All fractions were negative to starch iodide paper with TLC showing the majority of the material collected in fractions 3-8. All fractions were combined, concentrated with rotary evaporation, dried azeotropically by evaporation of toluene, and placed under vacuum overnight to remove residual solvent to afford 0.0254g (128% crude yield). ^1H NMR analysis in D_2O showed the product to be 92% by mass **58**, 5% by mass 2-aminoimidizole, and 3% by mass toluene.

^1H NMR (300MHz, D_2O): δ5.57 (dd, J= 6.9; 1.5Hz, 1H); 3.89 (dd, J= 11.7; 6.9Hz, 1H); 3.52 (dd, J= 11.7; 1.5Hz, 1H)



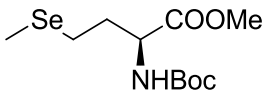
L-Selenomethionine methyl ester hydrochloride (**62**)

12.0mL anhyd. CH_3OH was placed into a flame dried 25mL round bottom flask placed into an ice/salt bath, allowed to thermoequilibrate before the dropwise addition of 1.0mL (13.71mmol) $SOCl_2$. 0.5242g (2.673mmol) L-Selenomethionine added to the mixture, placed under an atmosphere of N_2, sceptum wired on, and allowed to warm to room temperature in the air while stirring for 22h. TLC was take and showed the reaction to be complete (4:1:1 nBuOH:AcOH:H_2O, silica, KMnO4, R_f a.a: 0.65, R_f ester: 0.38) Note: Mixture should be concentrated with rotary evaporation to dryness and dissolved in CH_3OH before precipitation. The reaction mixture was quantitatively transferred to a beaker with 5.0mL distilled CH_3OH before the addition of 150mL cold, anhyd. Et_2O. The beaker was placed into an ice bath for 5 min before the collection of the white solid that formed by vacuum filtration and dried under vacuum overnight 0.4598g (70% yield, mp = 158-161˚C) **62** as a white solid.

^{1}H NMR (300MHz, D_2O): δ4.29 (t, J=6.3, 1H); 3.86 (s, 3H); 2.67 (t, J=6.9Hz, 2H); 2.23 (m, 2H); 2.02 (s, 3H)

^{13}C NMR (300MHz, D_2O): δ176.3; 59.5; 58.4; 24.7; 9.1

ESI-MS (DUIS, + ion): 253 (M^+ + CH_3CN, 57%); 212 (M^+, 100%); 210 (M^+ (^{78}Se), 56%)



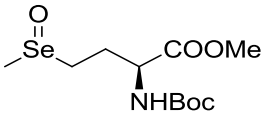
N-Boc-L-Selenomethionine methyl ester (**63**)

0.4078g (1.6538mmol) **62** and 0.4644g (5.529mmol) $NaHCO_3$ were combined in 5.0mL distilled CH_3OH. 0.6652g (3.048mmol) Boc_2O was dissolved in 3.0mL distilled CH_3OH, injected into the reaction mixture, and quantitatively transferred using 2.0mL distilled CH_3OH. The mixture was placed under an atmosphere of N_2 and stirred at room temperature for 15h at which time TLC was taken and showed the reaction to be complete (4:1:1 nBuOH:AcOH:H_2O, silica, $KMnO_4$ visualized R_f SM: 0.44, R_f prod: 0.94). 0.1131g (1.507mmol) glycine was added to the reaction mixture and stirred for 1h before the reaction mixture was filtered and concentrated with rotary evaporation before being diluted with 20mL CH_2Cl_2 and poured into a separatory funnel containing 50mL sat. $NaHCO_3$ and 20mL CH_2Cl_2. The organic layer was removed and the aqueous phase was extracted with two 25mL portions CH_2Cl_2. The organic portions were combined, dried over $MgSO_4$, filtered, concentrated with rotary evaporation, and placed under vacuum overnight to remove residual solvent to afford 0.4046g (79% yield) of the desired product **63** as a pale yellow oil.

^{1}H NMR (300MHz, $CDCl_3$): δ5.09 (s, 1H); 4.41 (s, 1H); 3.76 (s, 3H); 2.55 (t, J=8.1Hz, 2H); 2.20 (m, 1H); 2.00 (m, 1H); 2.00 (s, 3H); 1.45 (s, 9H)

^{13}C NMR (300MHz, $CDCl_3$): δ172.7; 155.2; 79.7; 53.4; 52.2; 33.1; 28.2; 20.3; 4.0

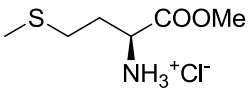
ESI-MS (DUIS, + ion): 312 ($M + H^+$, 33%); 253 ($M + H^+$ - COOMe, 54%); 212 ($M + H^+$-Boc, 100%)



N-Boc-L-Selenomethionine oxide methyl ester (**64**)

0.3192g (1.029mmol) **63** was dissolved in 13mL distilled CH_3OH, diluted with 7.0mL 18Ω H_2O, and submerged in an ice bath. The mixture was allowed to thermoequilibrate before the addition of 0.2347g (1.097mmol) $NaIO_4$. The mixture was set to stir rapidly in the ice bath for 2h before it was confirmed to be complete by TLC (4:1:1 nBuOH/AcOH/H_2O, silica, $KMnO_4$ R_f Se: 0.94, R_f SeO: 0.60). The reaction mixture was filtered, rinsed with 10mL distilled CH_3OH, and concentrated with rotary evaporation to remove the methanolic portion before it was diluted with 13mL 80% sat. NaCl. The aqueous phase was then countercurrently extracted with three 40mL portions EtOAc. The organic portions were combined, dried over $MgSO_4$, filtered, concentrated with rotary evaporation, and placed under vacuum overnight to afford 0.2335g of a pale yellow oil that was 4.6% by mass EtOAc to yield 0.2247g (67% yield) **64**.

^{1}H NMR (300MHz, $CDCl_3$): δ5.57 (d, J=6.6Hz, 1H); 4.41 (m, 1H); 3.78 (s, 3H); 2.95 (m, 1H); 2.79 (m, 1H); 2.54 (s, 3H); 2.27 (m, 1H); 2.13 (m, 1H); 1.45 (s, 9H)



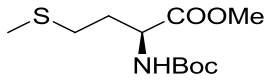
L-Methionine methyl ester hydrochloride (**66**)

12.0mL CH_3OH (distilled from Mg^0/I_2) was placed into a 25mL flame dried round bottom flask. The vessel was submerged in an ice/salt bath (-12°C) and allowed to thermoequilibrate before the dropwise addition of 2.5mL (34.27mmol) $SOCl_2$. 1.003g (6.721mmol) L-Methionine was then added to the methanolic mixture, placed under an atmosphere of N_2, sceptum wired

on, and allowed to warm to room temperature in air for 17h. TLC was then taken, showing the reaction to be complete. (4:1:1 nBuOH/AcOH/H_2O, silica, $KMnO_4$, L-Met R_f a.a.: 0.35, R_f ester:0.45) Note: Reaction mixture should be concentrated with rotary evaporation to dryness and dissolved in MeOH before continuing The reaction mixture was cooled to 0°C before the addition of 150mL cold Et_2O, causing a white solid to precipitate. The white solid was collected by vacuum filtration and dried under vacuum overnight (1st crop). White solid was observed to have formed in the filtrate which was collected by vacuum filtration and dried under vacuum overnight (2nd crop). The two crops were combined to afford 1.215g **66** (90% yield) as a white solid.

^{1}H NMR (300MHz, D_2O); δ4.29 (t, J=6.3Hz, 1H); 3.86 (s, 3H); 2.69 (t, J=7.2Hz, 2H); 2.26 (m, 2H); 2.12 (s, 3H)

N-Boc-L-Methionine Methyl Ester (**67**)

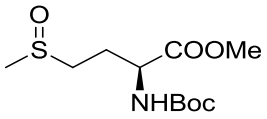


0.7251g (3.631mmol) **66** and 0.7234g (8.613mmol) $NaHCO_3$ were combined with 5.0mL distilled CH_3OH. 1.083g (4.963mml) Boc_2O was dissolved in 3.0mL distilled CH_3OH, injected into the reaction mixture, and quanitatively transferred using 2.0mL distilled CH_3OH. The mixture was placed under an atmosphere of N_2, and stirred rapidly at room temperature for 18h. TLC was taken, showing only the presence of **67** (4:1:1 nBuOH:AcOH:H_2O, silica, $KMnO_4$ visuallized R_f SM: 0.49, R_f prod: 0.93). 0.1828g (2.435mmol) glycine was added to the reaction mixture and stirred at room temperature for 3h before the mixture was filtered, concentrated with rotary evaporation to near dryness, diluted with 20mL CH_2Cl_2 and poured into a seperatory funnel containing 20mL CH_2Cl_2 and 50mL sat. $NaHCO_3$. The organic layer was removed and the

aqueous phase was extracted with two 25mL portions CH_2Cl_2. The organic portions were combined, dried over $MgSO_4$, filtered, concentrated with rotary evaporation, and placed under vacuum overnight to remove residual solvent to afford 0.8652g (90% yield) of **67** as a pale yellow oil.

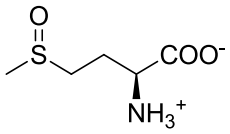
^{1}H NMR (300MHz, $CDCl_3$): δ5.11 (s, 1H); 4.41 (s, 1H); 3.76 (s, 3H); 2.54 (t, J=7.8Hz, 2H); 2.10 (s, 3H); 2.10 (m, 1H); 1.94 (m, 1H); 1.45 (s, 9H)

<u>*N-Boc-L-Methionine sulfoxide Methyl Ester*</u> (**68**)



0.5496g (2.087mmol) **67** was dissolved in 7.0mL distilled CH_3OH to which was added 4.0mL 18Ω H_2O. The mixture was submerged in an icebath and stirred rapidly for 3min to thermoequilibrate before the addition of 0.4712g (2.203mmol) $NaIO_4$. The mixture was stirred rapidly for 1.5h during which a white solid formed in the reaction volume. After 1.5h TLC showed the reaction to be complete (4:1:1 nBuOH:AcOH:H_2O, silica, $KMnO_4$ visuallized S R_f: 0.93, SO R_f: 0.58). The reaction mixture was filtered and concentrated with rotary evaporation to near dryness before being diluted with 15mL 80% sat. NaCl. The aqueous phase was countercurrently extracted with four 40mL portions of EtOAc. The organic phases were combined, dried over $MgSO_4$, filtered, concentrated with rotary evaporation, and placed under vacuum overnight to remove residual solvent to afford 0.6495g of a pale yellow oil which was determine to be 16.9% by mass EtOAc to yield 0.5397g (93% yield) **68**.

^{1}H NMR (300MHz, $CDCl_3$): δ5.27 (s, 1H); 4.43 (m, 1H); 3.78 (s, 3H); 2.79 (t, J=7.8, 2H); 2.57 (s, 3H); 2.35 (m, 1H); 2.14 (m, 1H); 1.45 (s, 9H)



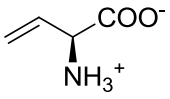
L-Methionine sulfoxide (**70**)

3.005g (20.14mmol) L-Methionine was suspended in 10mL DI H_2O in a 25mL round bottom flask. 2.2mL 30% H_2O_2 was added to the suspension in the following manner: 0.36mL over the course of 2min, dropwise with 5min of stirring until 1.44mL total volume of 30% H_2O_2 was added. At this point the mixture became homogeneous. The mixture was allowed to stir for 1.5h (Note:Does not appear to be necessary). After this time 0.36mL 30% H_2O_2 followed by a 0.40mL 30% H_2O_2 portion added to the reaction in the same manner as described above. After 1.2h of stirring at RT, TLC showed all of the starting material consumed. 150mL 200proof EtOH was then added to the aqueous solution causing a white solid to precipitate. The mixture sat at room temperature for 30min before the white solid was collected by vacuum filtration, rinsed with 20mL 200proof EtOH, and dried under vacuum overnight to remove residual solvent to afford 3.096g **70** (93% yield, mp = 254˚C(d)) as a white solid.

^{1}H NMR (300MHz, D_2O): δ3.87 (q, J=6.3Hz, 1H); 3.02 (m, 2H); 2.74 (s, 3H); 2.33 (q, J=7.2Hz, 2H)

^{13}C NMR (300MHz, D_2O): δ173.8; 54.0; 48.9; 37.1; 24.4

ESI-MS (DUIS, + ion): 188 ($M + Na^+$, 100%); 166 ($M + H^+$, 14%)



L-Vinylglycine (**71**)

20.09g (0.1216mol) L-Methionine sulfoxide was combined with 120mL (0.4872mol) *bis*-(trimethylsilyl)acetamide and set to stir in a 25-80˚C oil bath for 19h after which it was diluted with 80mL Ph_2O. The mixture was added to 300mL boiling Ph_2O over the course of 33.5min. Distillate was collected with pot temperature not dropping below 250˚C and a head temperature range of 238-248˚C. The 275mL EtOH and 30mL H_2O was poured into the distillate (417mL). The resulting mixture thickened and required being shaken by hand periodically over 20min. Volatiles were removed by rotary evaporation before the addition of 20mL H_2O and 150mL hexane. The mixture was shaken well and allowed to separate before the removal of the organic phase. The aqueous phase was washed with another 150mL hexane before the addition of 400mL CH_3CN which caused a tan solid to precipitate. The solid was collected by vacuum filtration, rinsed with 40mL CH_3CN, and placed under vacuum overnight to remove residual solvent to afford 7.672g. 7.267g of the crude product was triturated with 155mL boiling anhyd. EtOH for 5min before being collected by vacuum filtration, rinsed with 20mL cold EtOH, and dried under vacuum overnight to yield 4.568g **71** (37% yield, 95% purity as estimated by NMR, mp = 216˚C(d)) (35% yield overall).

^{1}H NMR (300MHz, D_2O): δ5.97 (ddd, J=10.2; 6; 4.5Hz, 1H); 5.48 (d, J= 10.2Hz, 1H); 5.48 (d, J=6.3Hz, 1H); 4.27 (d, J=4.5Hz, 1H)

^{13}C NMR (300MHz, D_2O); δ173.5; 130.8; 122.0, 57.7

ESI-MS (DUIS, + ion): 102 ($M + H^+$, 22%)

HRMS (IT-TOF-ESI, + ion): Calc'd $C_4H_7NO_2$ ($M + H^+$): 102.0550. Found: 102.0553

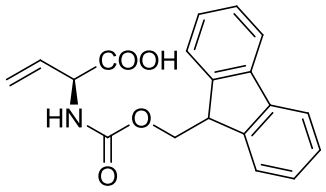
(S)-2-((R)-2-((((9H-fluoren-9-yl)methoxy)carbonyl)amino)propanamido)but-3-enoic acid (**72**)

0.3371g (0.8090mmol) 98% Fmoc-L-Ala-OSu was dissolved in 10mL acetone to which was added 0.1317g (1.568mmol) $NaHCO_3$ dissolved in 5mL H_2O (using 2mL H_2O to quant. trans.) which caused the bicarbonate to precipitate. 0.1144g (1.075mmol) **71** dissolved in 5mL H_2O was then added to the mixture, using 2mL H_2O to quantitatively transfer. Upon addition the mixture became homogeneous and was set to stir at room temperature for 3h at which time TLC showed the reaction to be complete ($R_{f\ OSu}$=0.54, silica, 10% CH_3OH/CH_2Cl_2). The mixture was acidifed to pH1 with 1mL 12M HCl and extracted with three 35mL CH_2Cl_2. The organic portions were combined, washed with three 35mL portions 3M HCl, dried over $MgSO_4$, filtered, concentrated with rotary evaporation, and placed under vacuum overnight to remove residual solvent to afford 0.3131g of the desired dipeptide **72** as a white solid (98% yield, mp = 176˚C (shrinks), 184-188˚C)

^{1}H NMR (300MHz, CD_3OD): δ7.79 (d, J=7.5Hz, 2H); 7.67 (dd, J=7.2Hz, 2H); 7.39 (t J=7.2Hz, 2H); 7.31 (t, J=7.2Hz, 2H); 6.00 (m, J=16.8, 10.5; 4.8Hz 1H); 5.38 (d, J=16.8Hz, 1H); 5.25 (d, J=10.2Hz, 1H); 4.98 (d, J=5.1Hz, 1H); 4.36 (t, J=6.9Hz, 2H,; 4.22 (d, J=6.6Hz, 1H,; 4.22 (d, J=6.6Hz, 1H); 1.37 (d, J=7.2Hz, 3H)

^{13}C NMR (300MHz, CD_3OD): δ175.3; 173.1; 158.3; 145.4; 145.2; 142.6; 133.5; 128.8; 128.2; 126.3; 120.9; 117.9; 68.0; 56.0; 51.8; 18.2

HRMS (IT-TOF-ESI, -ion): Calc'd ($C_{22}H_{22}N_2O_5$): 393.1456. Found: 393.1458



(S)-2-((((9H-fluoren-9-yl)methoxy)carbonyl)amino)but-3-enoic acid (**73**)

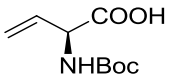
1.024g (2.974mmol) Fmoc-OSu was dissolved in 13mL acetone to which was added 0.3344g (3.143mmol) **71** dissolved in 11mL H_2O and 0.5330g (6.344mmol) $NaHCO_3$ dissolved in 9mL H_2O. Upon addition, the vinylglycine precipitated out. The mixture was heated at 65˚C for 1h before the mixture was observed to be homogeneous. The mixture was removed from the heat and stirred at room temperature for 26h at room temperature at which time TLC did not show Fmoc-OSu (R_f =0.73, silica, 10% CH_3OH/CH_2Cl_2). The mixture was then acidified to pH1 with 1mL 12M HCl and extracted with three 35mL portions CH_2Cl_2. The organic phases were combined, washed with three 35mL portions 4M HCl, dried over $MgSO_4$, filtered, rinsed with 20mL CH_2Cl_2, concentrated with rotary evaporation, and placed under vacuum overnight to remove residual solvent to afford 0.876g of the desired product as an off-white solid (91% yield, mp = 146-149˚C) 0.0484g of the crude product was dissolved in 0.6mL EtOAc and diluted with 14mL hexane producing a cloudy white mixture which was allowed to sit at room temperature for 1h to produce crystals. The solid was collected by centrifugation, washed with 10mL hexane, and dried under vacuum to remove residual solvent to afford 0.0448g **73** (93% recovery, mp = 160-161˚C).

^{1}H NMR (300MHz, CD_3OD): δ7.80 (d, J=7.5Hz, 2H); 7.68 (d, J=6.9Hz, 2H); 7.39 (t, J=7.5Hz, 2H); 7.31 (t, J=7.5Hz, 2H); 6.01 (ddd, J=16.8; 10.2, 5.7Hz, 1H); 5.36 (d, J=17.4Hz, 1H); 5.26 (d, J=10.2Hz, 1H); 4.78 (d, J=5.4Hz, 1H); 4.36 (m, 2H); 4.24 (t, J=7.2Hz, 1H)

^{13}C NMR (300MHz, CD_3OD): δ145.3; 145.2; 133.9; 128.8; 128.2; 128.2; 126.5; 120.9; 117.8; 68.1; 57.8; 48.4

MS (DUIS, - ion): 322 ($M - H^+$, 100%)

HRMS (IT-TOF-ESI, - ion): Calc'd $C_{19}H_{17}NO_4$ ($M - H^+$): 322.1085. Found: 322.1091

(S)-2-((tert-butoxycarbonyl)amino)but-3-enoic acid (**74**) 

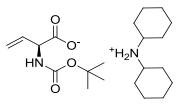
0.1624g L-Vinylglycine (1.542mmol) was combined with 0.5228g (2.428mmol) Boc_2O, 0.6813g (8.112mmol) $NaHCO_3$, and suspended in 12mL CH_3OH. The mixture was set to stir at room temperature for 24h at which time TLC show complete reaction (10% AcOH/CH_2Cl_2 R_f: 0.42). The mixture was filtered and the filtrate was concentrated to dryness with rotary evaporation, and dissolved in 20mL CH_2Cl_2 and 20mL sat. $NaHCO_3$. The organic layer was removed and the aqueous phase was washed with two 20mL CH_2Cl_2 before acidifying to pH3 with conc. H_3PO_4. After extracting with four 20mL portion EtOAc the organic phases were combined, dried over $MgSO_4$, filtered, concentrated with rotary evaporation, diluted with 30mL toluene, concentrated to dryness, and placed under vacuum overnight to remove residual solvent to yield 0.2601g (84%) of a pale yellow oil.

^{1}H NMR (300MHz, CD_3OD): δ5.97 (ddd, J=16.8; 10.8; 4.5Hz, 1H); 5.34 (d, J=17.1Hz, 1H); 5.23 (d, J=10.5Hz, 1H); 4.69 (d, J=4.5Hz, 1H); 1.45 (s, 9H)

^{13}C NMR (300MHz, CD_3OD): δ174.0; 157.7; 134.3; 117.4; 80.7; 57.5; 28.7

ESI-MS (DUIS, - ion): 423 ($2M^- + Na^+$, 52%); 401 ($2M^- + H^+$, 100%); 200 ($M - H^+$, 72%)

HRMS (IT-TOF-ESI, + ion) Calc'd $C_9H_{15}NO_4Na$ ($M+Na^+$): 224.0893. Found 224.0890

Dicyclohexyl ammonium 2-((tert-butoxycarbonyl)amino)but-3-enoate (**75**) 

0.1682g (0.8360mmol) **74** was dissolved in 1.5mL CH_2Cl_2 to which was added 0.20mL (1.006mmol) dicyclohexylamine. The mixture was brought to a boil, diluted with 12mL hexanes added at a rate that kept the mixture boiling, and concentrated to one third total volume. The mixture was allowed to cool to room temperature before being placed into a -20˚C freezer for 1.5h. The solid was collected by centrifugation, washed with 10mL hexane, and placed under vacuum overnight to remove residual solvent to afford 0.2760g (86% yield, mp = 152˚C (d)) of the desired salt **75** as a yellow solid.

^{1}H NMR ($CDCl_3$): δ6.00 (m, J=16.2; 11.1; 6.3Hz, 1H); 5.62 (d, J=17.1Hz, 1H); 5.25 (d, J= 4.8Hz, 1H); 5.09 (d, J= 10.2Hz, 1H); 4.48 (s, 1H); 2.95 (m, cyclohexyl, 2H); 1.99-1.67 (cyclohexyl, 10H); 1.43 (s, 9H); 1.40-1.20 (cyclohexyl, 10H)

^{13}C NMR ($CDCl_3$): δ176.6; 157.2; 137.7; 114.2; 80.2; 59.9; 54.4; 30.6; 28.8; 26.2; 25.5

ESI-MS (DUIS, + ion): 223 (H_2NCy_2 + CH_3CN, 76%); 182 ($HNCy_2$ + H^+, 100%)

ESI-MS (DUIS, - ion): 401 ($2M^-$ + H^+, 44%); 246 (M + $HCOO^-$, 72%); 200 (M - H^+, 100%)

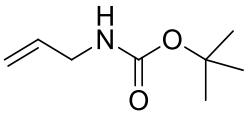
HRMS (IT-TOF-ESI, + ion): calc'd $C_{12}H_{23}N$ ($HNCy_2$ + H^+): 182.9000. Found: 182.9003

HRMS (IT-TOF-ESI, - ion): calc'd ($C_9H_{15}NO_4$ - H^+): 200.0928. Found: 200.0925

Allylammonium chloride (**76**)

3mL (40.02mmol) allyl amine was added to 6mL 12M HCl. The mixture was concentrated to dryness with rotary evaporation, dissolved in 15mL DI H_2O, and concentrated again using 5mL CH_3OH and 15mL toluene to dry by azeotropic evaporation. The resulting white solid was placed under vacuum overnight to yield 2.668g **76** (71% yield).

^{1}H NMR (300MHz, D_2O): δ5.94 (m, 1H); 5.43 (d, J=18.3Hz, 1H); 5.41 (d, J=9.9Hz, 1H); 3.62 (d, J=5.7Hz, 2H)



tert-butyl allylcarbamate (**78**)

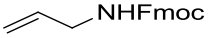
2.096g (9.125mmol) Boc_2O was dissolved in 10mL CH_3OH. The mixture was set to stir rapidly before the slow addition of 0.85mL (11.330mmol) allyl amine. Upon addition the reaction volume became exothermic and evolved gas. After 30min TLC showed the consumption of Boc_2O (5% CH_3OH/CH_2Cl_2 Rf prod= 0.78, R_f Boc_2O= 0.96). The reaction mixture was concentrated to near dryness with rotary evaporation, diluted with 20mL toluene, concentrated to dryness with rotary evaporation, and placed under vacuum for 1.5h to afford 1.075g (75% yield ,mp = 28-34°C) of **78** as a yellow solid.

Note: Product is volatile and will evaporate away if left under vacuum overnight. 1.5h appears to the the amount of time needed at this scale to give the driest product with the best yield.

^{1}H NMR (300MHz, $CDCl_3$): δ5.84 (m, J=17.1; 10.2; 1.5Hz, 1H); 5.18 (dd, J=17.1; 1.5Hz, 1H); 5.11 (dd, J=10.2; 1.2Hz, 1H); 4.60 (s, 1H); 3.75 (nt, unresolved, 2H); 1.45 (s, 9H)

^{13}C NMR (300MHz, $CDCl_3$): δ115.9; 135.0; 115.8; 79.4; 43.2; 28.5

ESI-MS (DUIS, + ion): 315 (2M + H^+, 100%)

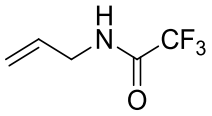
(9H-fluoren-9-yl)methyl allylcarbamate (**79**) 

2.000g (5.810mmol) Fmoc-OSu was dissolved in 20mL CH_2Cl_2 (distilled from CaH_2). 2.0mL (26.12mmol) allyl amine was injected into the mixture was set to stir at room temperature 1h after which time the Fmoc-OSu was not seen by TLC (R_f Fmoc-OSu= 0.16, R_f prod= 0.33). The mixture was filtered with vacuum over a pad of Celite and rinsed with 20mL CH_2Cl_2. The filtrate was washed with four 40mL portions 0.1M $HCl_{(aq)}$. The organic phase was dried over $MgSO_4$, filtered, concentrated with rotary evaporation, and placed under vacuum overnight to remove residual solvent to yield 1.5476g **79** (95% yield, mp = 121-122^oC.) as a white solid.

^1H NMR (300MHz, $CDCl_3$): δ7.77 (d, J=7.2Hz, 2H); 7.60 (d, J=7.5Hz, 2H); 7.40 (t, J=7.2Hz, 2H); 7.31 (t, J=7.5Hz, 2H); 5.84 (m, 1H); 5.18 (d, J=17.4Hz, 1H); 5.14 (d, J=10.2Hz, 1H); 4.82 (t, J=7.5Hz, ,2H); 4.43 (d, J=6.9Hz, 2H); 4.23 (t, J=6.9Hz, 1H); 3.83 (t, unresolved, 2H)

^{13}C NMR (300MHz, $CDCl_3$): δ156.4; 144.1; 141.4; 134.6; 127.8; 125.2; 120.1; 116.2; 66.8; 47.4; 43.6;

ESI-MS (DUIS, + ion): 581 (2M + Na^+, 95%); 334 (M + Na^++CH_3OH, 54%); 302 (M + Na^+, 100%); 297 (M + NH_4^+, 94%); 280 (M + H^+, 65%); 179 (9-methylene-9H-fluorene+H^+, 26%)



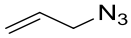
N-allyl-2,2,2-trifluoroacetamide (**80**)

2.0mL (26.66mmol) allyl amine with combined with 2.0mL (54.62mmol) ethyl trifluoroacetamide producing a large exotherm upon addition. (Note: Use no solvent and an excess of allyl amine instead as it is more volatile and add it in portions to stirring ethyl trifluoroacetate stirring in an ice bath) After 15min TLC confirmed that the reaction was complete (silica gel, $KMnO_4$ visualized, R_f product= 0.55 40% EtOAc/hexane). The mixture was concentrated with rotary evaporation and placed under high vacuum for 25min to yield 3.117g (76% yield) of **80** as a light yellow liquid.

^{1}H NMR (300MHz, $CDCl_3$): δ7.52 (s, 1H); 5.77 (m, J=16.2; 10.2; 5.7; 0.9Hz, 1H); 5.18 (dd, J=16.2; 0.9Hz, 1H); 5.15 (dd, J= 10.2; 1.2Hz, 1H); 3.89 (t, J=5.7Hz, 2H)

^{13}C NMR (300MHz, $CDCl_3$): δ157.7 (q, J= 147Hz); 131.9; 117.7; 116.0 (q, J=1143Hz); 42.2

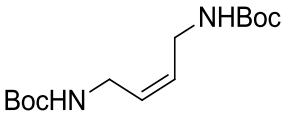
ESI-MS (DUIS, + ion): 329 ($2M + Na^+$, 32%); 231 (69%); 211 (100%)

3-azidoprop-1-ene (**81**) 

0.0872g (1.038mmol) $NaHCO_3$ and 3.078g (47.34mmol) NaN_3 were combined and dissolved in 11mL DI H_2O. 2.5mL (28.89mmol) allyl bromide was then added to the mixture resulting in a biphasic solution. The mixture was set to stir rapidly at room temperature for 30min at which time the aqueous phase was observed to be the bottom layer. TLC of the reaction mixture after 4h showed that it was complete (silica,10% EtOAc/hexane, $KMnO_4$ visualized, R_f allyl bromide= 0.56, R_f product= 0.61). The aqueous phase was removed and the organic phase was passed over a 2cm tall column of $MgSO_4$ in a glass Pasteur pipet to afford

1.6258g (68% yield) of **81** as a yellow liquid. (Note: Do not place product under vacuum for a prolonged period of time as it is volatile and cannot be separated from diethyl ether by means of rotary evaporation even)

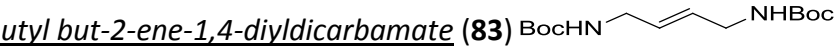
^{1}H NMR (300MHz, $CDCl_3$): δ5.87 (m, 1H); 5.33 (d, J=17.1Hz, 1H); 5.30 (d, J=11.1Hz, 1H); 3.78 (d, J=6Hz, 2H)

(Z)-di-tert.-butyl but-2-ene-1,4-diyldicarbamate (**82**) 

0.0507g (0.3225mmol) **78** was placed into a flame dried, N_2 flushed 25mL round bottom flask to which was added 0.0235g (0.0375mmol) Hoveyda-Grubbs 2nd generation catalyst. The mixture was dissolved in 10mL CH_2Cl_2 (distilled from CaH_2), placed under an atmosphere of N_2, and heated at reflux for 18.5h at which time TLC showed the reaction to be complete (10% CH_3CN/CH_2Cl_2 $R_{f\,SM}$= 0.73, $R_{f\,prod}$= 0.41). The mixture was concentrated with rotary evaporation to dryness and placed under vacuum to remove residual solvent for 30min to yield 0.0897g (194% yield). The crude solid was purified by flash chromatography (silica gel 60, 9" silica, 10mm column, 2'/min flow rate, 5mL fraction, 100mL 10% CH_3CN/CH_2Cl_2, 50mL 20% CH_3CN/CH_2Cl_2) fraction 7-12 10% were combined, concentrated with rotary evaporation, and placed under vacuum overnight to afford 0.0134g **82** as a brown oil (58% yield of *(Z)*- TY)

^{1}H NMR (300MHz, $CDCl_3$): δ5.39 (s, 2H); 4.72 (s, 2H); 3.44 (m, 2H); 3.25 (m, 2H); 1.46 (s, 9H); 1.44 (s, 9H)

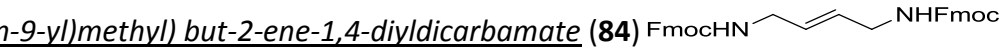
ESI-MS (DUIS, + ion): 309 ($M + Na^+$, 54%); 304 ($M + NH_4^+$, 100%); 287 ($M + H^+$, 42%)

(E)-di-tert.-butyl but-2-ene-1,4-diyldicarbamate (**83**) 

0.0507g (0.3225mmol) **78** was placed into a flame dried, N_2 flushed 25mL round bottom flask to which was added 0.0235g (0.0375mmol) Hoveyda-Grubbs 2nd generation catalyst. The mixture was dissolved in 10mL CH_2Cl_2 (distilled from CaH_2), placed under an atmosphere of N_2, and heated at reflux for 18.5h at which time TLC showed the reaction to be complete (silica, ninhydrin,10% CH_3CN/CH_2Cl_2 $R_{f\,SM}$= 0.73, $R_{f\,prod}$= 0.36). The mixture was concentrated with rotary evaporation to dryness and placed under vacuum to remove residual solvent for 30min to yield 0.0897g (194% yield). The crude solid was purified by flash chromatography (silica gel 60, 9" silica, 10mm column, 2'/min flow rate, 5mL fraction, 100mL 10% CH_3CN/CH_2Cl_2, 50mL 20% CH_3CN/CH_2Cl_2) fraction 13-21 10% were combined, concentrated with rotary evaporation, and placed under vacuum overnight to afford 0.0213g **83** as a tan solid (92% yield of *(E)*- TY)

^{1}H NMR (300MHz, $CDCl_3$): δ5.62 (s, 2H); 4.57 (s, 2H); 3.72 (s, 4H); 1.45 (s, 18H)

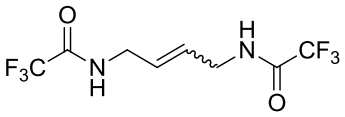
ESI-MS (DUIS, + ion): 309 ($M + Na^+$, 100%); 304 ($M + NH_4^+$, 50%)

(E)-bis((9H-fluoren-9-yl)methyl) but-2-ene-1,4-diyldicarbamate (**84**) 

0.0510g (0.1826mmol) **79** was combined with 0.0115g (0.0184mmol) Hoveyda-Grubbs 2nd generation catalyst and dissolved in 5mL CH_2Cl_2 (distilled from CaH_2). The mixture was placed under an atmosphere of N_2 and reflux for 4h at which time ^{1}H NMR showed consumption of the allyl amine. The mixture was diluted with 6mL hexanes and cooled to -78˚C before the solid present was collected by centrifugation. The supernatant was removed, the white solid was washed with 12mL 50% CH_2Cl_2/hexane, and placed under vacuum overnight to remove residual solvent to afford 0.0229g (47% yield, mp = 191-192˚C) **84** as a white solid.

^{1}H NMR (300MHz, $CDCl_3$): δ7.76 (d, J=7.2Hz, 4H); 7.60 (d, J=7.2Hz, 4H); 7.40 (t, J=7.2Hz, 4H); 7.31 (t, J=7.2Hz, 4H); 5.60 (s, 2H); 4.79 (s, 2H); 4.44 (d, J=6.6Hz, 4H); 4.22 (t, J= 6.0Hz, 2H); 3.80 (s, 2H)

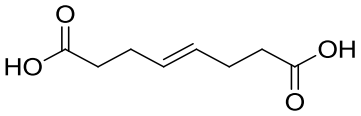
ESI-MS (DUIS, + ion): 553 (M + Na^+, 100%); 548 (M + NH_4^+, 39%)

(E/Z)-N,N'-(but-2-ene-1,4-diyl)bis(2,2,2-trifluoroacetamide) (**85**) 

0.0539g (0.3521mmol) **80** was injected into a solution of 0.0266g (0.0424mmol) Hoveyda-Grubbs 2nd generation catalyst dissolved in 2mL CH_2Cl_2 and quantitatively transferred using two 2mL portions CH_2Cl_2. The mixture was placed under an atmosphere of N_2 and heated at reflux for 18h. 4min after mixing, the color of the mixture darkened to a brownish green color and turned completely brown after 13min when reflux was achieved. After 18h, TLC indicated that the reaction was complete by absence of the starting alkene (silica gel, $KMnO_4$, 40% EtOAc/hexane, R_f SM= 0.55, R_f Z and E products= 0.63 and 0.42).The mixture was concentrated to dryness with rotary evaporation and placed under vacuum overnight to remove residual solvent to yield 0.0478g of **85** (43% yield after subtraction of catalyst mass).

ESI-MS of crude product acquired.

ESI-MS (DUIS, - ion): 391 (M + CF_3COO^-, 47%); 323 (M + $HCOO^-$, 26%); 277 (M - H^+, 100%)

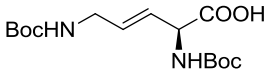


(E)-oct-4-enedioic acid (**86**)

0.05mL (0.4899mmol) 4-pentenoic acid was combined with 0.0273g (0.0436mmol) Hoveyda-Grubbs 2nd generation catalyst dissolved in 10mL CH_2Cl_2 (distilled from CaH_2). The mixture was placed under an atmosphere of N_2 and heated at reflux for 16.5h after which the solution was observed to still be green in color. Analysis of a concentrated aliquot by ^1H NMR in CD_3CN showed no more of the starting alkene. The reaction mixture and NMR sample were combined, dissolved in a combination of 5mL CH_3CN and 15mL CH_2Cl_2, and extracted with 20mL sat. $NaHCO_3$. The aqueous layer was removed and the organic phase was extracted with an additional 20mL sat. $NaHCO_3$. The aqueous phases were combined, washed with two 20mL portions CH_2Cl_2, and acidified to pH1 were 12M HCl. The aqueous phase was extracted with two 35mL EtOAc. The organic extracts were combined, dried over $MgSO_4$, filtered, concentrated with rotary evaporation to dryness, and placed under vacuum overnight to remove residual solvent to yield 0.0185g (44% yield) **86** as an off white solid.

^1H NMR (300MHz, DMSO-d_6): δ12.05 (s, 2H); 5.43 (m, 2H); 2.27-2.18 (m, 8H)

ESI-MS (DUIS, - ion): 387 (35%); 365 ($2M^- + Na^+$, 100%); 343 ($M + M^-$, 86%); 171 ($M - H^+$, 72%)



(S,E)-2,5-bis((tert-butoxycarbonyl)amino)hept-3-enoic acid (**87**)

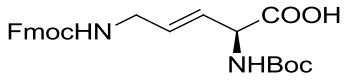
0.0392g (0.2494mmol) **78** dissolved in 2.5mL CH_2Cl_2 was added to 0.0188g (0.0934mmol) **74** and 0.0067g (0.0107mmol) Hoveyda-Grubbs 2nd generation catalyst dissolved in 5mL CH_2Cl_2. The mixture was set to stir heated at reflux under an atmosphere of N_2 for 18h at

which time the mixture was analyzed by ^{1}H NMR revealing that the vinylglycine was almost gone. The reaction mixture was concentrated to dryness wirh rotary evaporation, dissolved in 15mL EtOAc, and extracted with four 7mL portion conc. NH_3. The aqueous extracts were combined, concentrated by rotary evaporation and dried azeotropically by evaporation of 5mL CH_3OH and 15mL toluene. The concentrate was placed under vacuum overnight to yield 0.0333g (102% yield). 0.0144g of the crude product was separation was attempted by flash chromatography (10mm column, 7.5" silica, 2"/min flow rate, 5mL fractions, slurry packed and eluted with 100mL (2.5% AcOH/7.5%IpoH/90%CH_2Cl_2) to afford the desired product **87** as a 3:1 mixture with **74** (0.0043g, 32% yield, 39% based on conversion)

^{1}H NMR (300MHz, $CDCl_3$): δ5.81-5.66 (m, 2H); δ4.65 (d, J=17.7Hz, 1H); 3.65 (d, J=10.2Hz, 2H); 1.44 (s, 9H); 1.43 (s, 9H)

MS (DUIS, -ion): 530 (M^-+NBoc-L-Vgy, 31%); 329 (M-H^+, 100%)

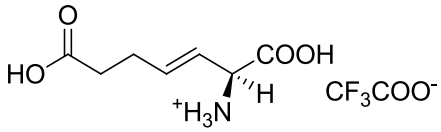
(S,E)-5-((((9H-fluoren-9-yl)methoxy)carbonyl)amino)-2-((tert-butoxycarbonyl)amino)pent-3-enoic acid (**88**)



0.0613g (0.9387mmol) **73** and 0.2622g (0.3047mmol) **79** were combined to which was added 0.0315g (0.0503mmol) Hoveyda-Grubbs 2nd generation catalyst dissolved in 3mL CH_2Cl_2, using two 2mL portions CH_2Cl_2 to quantitatively transfer. The mixture placed under an atmosphere of N_2 and heated at reflux for 21h over which time the initial emerald green color of the solution changed to an orange-green to brown in the first 1h of heating. After 21h TLC showed that the vinylglycine was still present. The mixture was removed from the heat for 24h before the addition of 0.0406g (0.1453mmol) **79**, 0.0150g (0.0239mmol) Hoveyda-Grubbs 2nd

generation catalyst and 3mL CH_2Cl_2 and heated at reflux for another 13h at reflux at which time the NBoc-L-Vgy was no longer seen by TLC (silica, ninhydrin, 10% AcOH/CH_2Cl_2, R_f NBoc-L-Vgy= 0.38, R_f homodimer= 0.56, R_f CM product= 0.20). The mixture was concentrated to dryness with rotary evaporation and placed under vacuum overnight to remove residual solvent to yield 0.4060g crude product (294% yield). 0.1173g of the crude product was dissolved in 20mL CH_2Cl_2 and 10mL toluene and extracted with three 10mL portions sat. $NaHCO_3$. The aqueous portions were combined and washed with 10mL CH_2Cl_2. The aqueous phase was acidifed to pH3 and extracted with three 30mL portions EtOAc. The organic extracts were combined, dried over $MgSO_4$, filtered, concentrated with rotary evaporation, and placed under vacuum overnight to remove residual solvent to afford 0.1200g which was submitted to MS analysis to afford M+NH_4^+ of the desired product.

ESI-MS (DUIS, - ion): 475 (M + Na^+, 98%); 470 (M + NH_4^+, 100%)



<u>*(S,E)-2-((tert-butoxycarbonyl)amino)hept-3-enoic acid*</u> (**89**)

0.1292g (0.6421mmol) **74** was dissolved in 6mL CH_2Cl_2 to which was added 0.20mL (1.956mmol) 4-pentenoic acid followed by 0.0377g (0.0602mmol) Hoveyda-Grubbs 2nd generation catalyst dissolved in 6mL CH_2Cl_2. The mixture was placed under an atmosphere of N_2 and heated to reflux for 24h after which time TLC showed the reaction to be incomplete. 0.20mL 4-pentenoic acid and 0.0259g (0.0413mmol) Hoveyda-Grubbs 2nd generation catalyst were added before resuming reflux for another 21h with a white precipitate forming over the course of the reaction (pentenoic acid homodimer). TLC analysis after this time showed that

starting vinylglycine was no longer present (silica, ninhydrin, 10% AcOH/CH_2Cl_2, R_f NBoc-L-Vgy= 0.35, R_f homodimer= 0.57, R_f product= 0.22). The mixture was filtered to remove the white precipitate, concentrated to dryness with rotary evaporation, and dissolved in 30mL CH_2Cl_2. The solution was extracted with three 10mL portions sat. $NaHCO_3$. The aqueous portions were combined, washed with two 25mL portions CH_2Cl_2, and acidified to pH2 with 85% H_3PO_4, and extracted with three 25mL portions EtOAc. The organic layers were combined, dried over $MgSO_4$, filtered, concentrated with rotary evaporation and placed under vacuum overnight to remove residual solvent to afford 0.1725g (98% crude yield). 0.0465g of the crude product was dissolved in 10mL CH_2Cl_2 and 10mL CF_3COOH and heated at reflux for 1.5h before concentrating with rotary evaporation to dryness. The concentrated crude was dissolved in 30mL EtOAc to which was added 15mL DI H_2O. The aqueous phase was removed and the organic phase was extracted with an addition two 10mL portions H_2O. The aqueous portions were combined, washed with three 20mL portions EtOAc, then concentrated with rotary evapotation to near dryness before being dried azeotropically by evaporation CH_3OH and toluene to afford 0.0290g of **89** as a light tan solid (16% yield, 58% based on amount used)

Boc protected CM product

ESI-MS (DUIS, - ion): 567 ($2M^- + Na^+$, 30%); 545 ($M + M^-$, 75%); 272 ($M - H^+$, 100%)

Deprotected TFA salt of CM product

^{1}H NMR (300MHz, $CDCl_3$): δ6.01 (dt, J=15.6; 6.9Hz, 1H); 5.64 (dd, J= 15.6; 7.5Hz 1H); 4.29 (d, J= 8.1Hz, 1H); 2.52 (t, J= 6.3Hz, 2H); 2.41 (m, J= 14.1Hz; 6.9Hz, 2H)

ESI-MS (DUIS, - ion): 249 ($M-2H^+ + NH_4^+ + AcO^-$, 92%); 172 ($M-H^+$, 100%)

IX. REFERENCES

1. Southall, N.; Dill, K.; Haymet, A.D. *J. Phys. Chem. B.*, **2002**, *106(3)*, 521-533)

2. Newcomb, L.; Gellman, S. *J. Am. Chem. Soc.*, **1994**, *116*, 4993-4994

3. Ma, J.; Dougherty, D. *Chem. Rev.*, **1997**, *97(5)*, 1303-1324

4. Smith, P.; Wilcox, C.S. *J. Org. Chem.*, **1990**, *55*, 5675-5678

5. Kollman, P.; Allen, L.; *Chem. Rev.*, **1972**, *72*, 283-303

6. Murray, T.; Zimmerman, S. *J. Am. Chem. Soc.*, **1992**, *114*, 4010-4011

7. Lee, J.; Schwabacher, A. W. *J. Am. Chem. Soc.*, **1994**, *116*, 8382-8383

8. Cram, D. *Angew. Chem. Int. Ed. Engl.*, **1986**, *25(12)*, 1039-1134

9. Zhang, Z.; Han, M.; Zhang, H.; Liu, Y. *Org. Lett.*, **2013**, *15(7)*, 1698-1701

10. Gschwend, D.; Good, A.; Kuntz, I. *J. Mol. Recogn.*, **1996**, *9(2)*, 175-186

11. Kang, J.; Santamaría, J.; Hilmersson, G. Rebek, Jr., J. *J. Am. Chem. Soc.*, **1998**, *120(29)*, 7389-7390

12. Freudenberg, K.; Meyer-Delius, M. *Ber. Dtsch. Chem. Ges.*, **1938**, *71*, 1596

13. Cramer, F.; Hettler, H. *Die Nayurwissenschaften*, **1967**, *54*, 625

14. Saenger, W. *Angew. Chem. Int. Ed. Engl.*, **1980**, *19*, 344-362

15. Breslow, R. *Acc. Chem. Res.*, **1995**, *28(3)*, 146-153

16. Brewster, M.E.; Loftsson, T. *Adv. Drug Deliv. Rev.*, **2007**, *59(7)*, 645-666

17. Pedersen, C. J. *J. Am. Chem. Soc.*, **1967**, *89(26)*, 7017

18. Pedersen, C. J. *J. Org. Chem.*, **1971**, *36(12)*, 1690-1693

19. Gokel, G.; Cram, D. *J. Org. Chem.*, **1974**, *39(16)*, 2445-2446

20. Odashima, K.; Itai, A.; Iitaka, Y.; Koga, K. *J. Am. Chem. Soc.*, **1980**, *102(7)*, 2504-2505

21. Diederich, F.; Dick, K. *Angew. Chem. int. Ed. Engl.*, **1983**, *22(9)*, 715-716

22. Diederich, F.; Dick, K. *J. Am. Chem. Soc.*, **1984**, *106*, 8024-8036

23. Ferguson, S.; Diederich, F. *Angew. Chem. Int. Ed. Engl.*, **1986**, *25*, 1127-1129

24. Sheppodd, T.; Petti, M.; Dougherty, D. *J. Am. Chem. Soc.*, **1986**, *108*, 6085-6087

25. Petti, M.; Sheppodd, T.; Barrans, Jr., R.; Dougherty, D. *J. Am. Chem. Soc.*, **198**, *110*, 6825-6840

26. Dougherty, D.; Stauffer, D. *Science*, **1990**, *250*, 1558-1560

27. Chen, C. W.; Whitlock, Jr., H. W. *J. Am. Chem. Soc.*, **1978**, *100(15)*, 4921-4922

28. Smeets, J. W.; Sijbesona, R.; Niele, F. G.; Spek, A.; Smeets, W. J. Nolte, R. J. *J. Am. Chem. Soc.*, **1987**, *109*, 928-929

29. Williams, K.; Askew, B.; Bullester, P.; Buhr, C.; Jeong, K.; Jones, S.; Rebek, Jr., J. *J. Am. Chem. Soc.*, **1989**, *111*, 1090-1094

30. Zimmerman, S.; VanZyl, C. *J. Am. Chem. Soc.*, **1987**, *109*, 7894-7896

31. Zimmerman, S.; Wu, W. *J. Am. Chem. Soc.*, **1989**, *111*, 8054-8055

32. Harmata, M. ; Murray, T. *J. Org. Chem.*, **1989**, *54(16)*, 3761-3763

33. Harmata, M.; Barnes, C. *Tet. Lett.*, **1990**, *31(13)*, 1825-1828

34. Kagan, J.; Chen. S.-Y.; Agdeppa, Jr., D.A. *Tet. Lett.*, **1977**, *18(51)*, 4469-4470

35. Harmata, M.; Barnes, C. *J. Am. Chem. Soc.*, **1990**, 112, 5655-5657

36. He, Z.; Yang, X.; Jiang, W. *Org. Lett.*, **2015**, *17*, 3880-3883

37. Legouin, B.; Uriac, P.; Tomasi, S.; Toupet, L.; Bondon, A, van de Weghe, P. *Org. Lett.*, **2009**, *11(3)*, 745-748

38. Klärner, F.-G.; Benkhoff, J.; Boese, R.; Burket, U.; Kameith, M.; Naatz, U. *Angew. Chem. Int. Ed. Engl.*, **1996**, *35(10)*, 1130-1133

39. Klärner, F.-G.; Kahlert, B. *Acc. Chem. Res.*, **2003**, *36*, 919-932

40. Schdrader, T.; Fokkens, M.; Klärner, F.-G.; Polkowska, J.; Bastkowski, F. *J. Org. Chem.*, **2005**, *70*, 10227-10237

41. Talbiersky, P.; Bastkowski, F.; Klärner, F.-G.; Schrader, T. *J. Am. Chem. Soc.*, **2008**, *130*, 9824-9828

42. Kirsch, M.; Talbiersky, P.; Polkowska, J.; Bastkowski, F.; Schaller, T.; de Groot, H.; Klärner, F.-G.; Schrader, T. *Angew. Chem. Int. Ed. Engl.*, **2009**, *48(16)*, 2886-2890

43. Gomes, R.; Parola, A. J.; Bastkowski, F.; Polkowska, J.; Klärner, F.-G. *J. Am. Chem. Soc.*, **2009**, *131(25)*, 8922-8938

44. Klärner, F.-G.; Schrader, T. *Acc. Chem. Res.*, **2013**, *46(4)*, 967-978

45. Tröger, J. *J. prakt. Chem.*, **1887**, *36(2)*, 227

46. Wagner, E.C. *J. Am. Chem. Soc.*, **1935**, *57(7)*, 1296-1298

47. Spielman, M. A. *J. Am. Chem. Soc.*, **1935**, *57*, 583

48. Prelog, V.; Weiland, P. *Helv. Chim. Acta.*, **1944**, *27*, 1127

49. Mason, S. F.; Vane, G. W.; Schofield, K.; Wells, R. J.; Whitehurst, J. S. *J. Chem. Soc. B.*, **1967**, 553-556

50. Larson, S. B.; Wilcox, C. S. *Acta. Cryst.*, **1986**, *C42*, 224-227

51. Wilen, S.; Qi, J. Z.; Willard, P. *J. Org. Chem.*, **1991**, *56*, 485-487

52. Aamouche, A.; Devlin, F. J.; Stephens, P. J *J. Am. Chem. Soc.*, **2000**, *122*, 2346-2354

53. Wilcox, C. S. *Tet. Lett.*, **1985**, *26(47)*, 5749-5752

54. Wilcox, C. S.; Greer, L. M.; Lynch, V. *J. Am Chem. Soc.*, **1987**, *109*, 1865-1867

55. Adrian, Jr., J. C.; Wilcox, C. S. *J. Am. Chem. Soc.*, **1991**, *113*, 678-680

56. Adrian, Jr. J. C.; Wilcox, C. S. *J. Am. Chem. Soc.*, **1992**, *114*, 1398-1403

57. Kiehne, U.; Weilandt, T.; Lutzen, A. *Org. Lett.*, **2007**, *9(7)*, 1283-1286

58. Boyle, E. M.; Comby, S.; Molloy, J. K.; Gunnlaugsson, T. *Org. Lett.*, **2013**, *78*, 8312-8319

59. Pardo, C.; Sesmilo, E.; Gutiérrez-Puebla, E.; Monge, A.; Elguero, J. Fruchier, A. *J. Org. Chem.*, **2001**, *66*, 1607-1611

60. Mas, T.; Pardo, C.; Salort, F.; Elguero, J.; Rosario Torres, M. *Eur. J. Org. Chem.*, **2004**, 1097-1104

61. Dolenskŷ, B.; Valík, M.; Sŷkora, D.; Krâl, V. *Org. Lett.*, **2005**, *7(1)*, 67-70

62. Havlík, M.; Krâl, V.; Kaplânek, R.; Dolenskŷ, B. *Org. Lett.*, **2008**, *10(21)*, 4767-4769

63. Havlík, M.; Krâl, M.; Dolenskŷ, B *Org. Lett.*, **2006**, *8(21)*, 4867-4870

64. Sucholeik, I.; Lynch, V.; Phan, L.; Wilcox, C. S. *J. Org. Chem.*, **1988**, *53*, 98

65. Cox, E.G. *Rev. Mod. Phys*., **1958**, *30*, 159

66. Bogert, M.; Dox, A. *J. Am. Chem. Soc.*, **1905**, *27(10)*, 1302-1305.

67. Sinnreich, J., *Synthesis*, **1980**, *7*, 578-580.

68. Stenger-Smith, J.; Zarras, P.; Merwin, L. *Macromolecules*, **1998**, *31*, 7566-7569.

69. Baeyer *Ber*., **1886**, *19*, 430.

70. Tiwari, K. Synthesis of a versatile building block for binding site preparation, M.S. Thesis, The University of Wisconsin-Milwaukee, December 2006

71. Clark, T.; Sperry, J. *Synlett*, **2012**, *23*, 2827-2829.

72. Cossy, J.; Belotti, D *Org. Lett*, **2002**, *4(15)*, 2557-2559.

73. Nystran, R.; Brown, W. *J. Chem. Soc.*, **1947**, *69(5)*, 1197-1199.

74. Ball, S.; Goodwin, T.; Morton, R. *Biochem. J.*, **1948**, *42(4)*, 516-523.

75. Pratt, E.; van de Castle, J. *J. Org. Chem.*, **1961**, *26(8)*, 2973-2975.

76. Black, D.; Rothnie, N. *Aust. J. Chem.*, **1983**, *36*, 1149-1157.

77. Attenburrow et al, *J. Chem. Soc.*, **1952**, *26(8)*, 1094-1111.

78. Gritter, R.; Dupre, G.; Wallace, T. *Nature*, **1964**, *202(4928)*, 179-181.

79. Goldman, I. *J. Org. Chem.*, **1969**, *34(6)*, 1979-1981.

80. Kamimura, A.; Komatsu, H.; Moriyama, T.; Yuichiro, N. *Tetrahedron*, **2013**, *69*, 5968-5972.

81. Carpino, L. *J. Org. Chem.*, **1970**, *35(11)*, 3971-3972.

82. Perrone, D.; Dondoni, A. *Org. Snth.*, **2000**, *77*, 64.

83. Hoover, J.; Stahl, S., **2013**, *90*, 240-250.

84. Nyakirangani, N. Synthetic Procedures For Molecular Receptors Ph.D. Dissertation, The University of Wisconsin-Milwaukee, December 2009

85. Ranu, B.; Hajra, A.; Jana, U. *Org. Lett.*, **1999**, *1(8)*, 1141-1143).

86. Manabe, K.; Kobayashi, S. *Chem. Commun.*, **2000**, 669-670.

87. Bhagat, S.; Chakraboti, A. *J. Org. Chem.*, **2007**, *72*, 1263-1270.

88. Epifano, F.; Genovase, S.; Cuirihi, M. *Tetrahedron Letters*, **2007**, *48*, 2717-2720.

89. Qian, C.; Huang, T. *J. Org. Chem.*, **1998**, 63, 4125-4128.

90. Ingle, G.; Liang, Y.; Mormino, M.; Li, G.; Fronczek, F.; Antilla, J. *Org. Lett.*, **2011**, *13(8)*, 2054-2057.

91. Joly, G.; Jacobsen, E. *J. Am. Cehm. Soc.*, **2004**, *126*, 4102-4103.

92. Pettersen, D.; Marcolini, M.; Bernardi, L., Fini, F.; Herrera, R.; Sgarzani, V.; Ricci, A. *J. Org. Chem.*, **2006**, *71*, 6269-6272.

93. Bhagat, S.; Chakraborti, A. *J. Org. Chem.*, **2008**, *73*, 6029-6032.

94. Chernyshev, E. A.; Bugerenko, E.F.; Akat'eva, A.S.; Naumov, A.D. *Zhurnal Obshche Khimii*, **1975**, *45(1)*, 242-243

95. Knerr, L.; Paunecouke, X.; Schmitt, G.; Luu, B. *Tetrahedron Letters*, **1996**, *37(29)*, 5123-5126.

96. Grehn, L.; Gunnarsson, K.; Ragnarsson, U. *Acta Chemica Scandinavica B*, **1986**, *40*, 745-750.

97. McKenna, C.; Higa, M.; Cheung, N.; McKenna, M. *Tetrahedron Letters*, **1977**, *2*, 155-158.

98. Norén, J.; Helgstrand, E.; Johansson, N.; Misiorny, A.; Stening, G. *J. Med. Chem.*, **1983**, *26*, 264-270.

99. McKenna, C.; Schmidhauser, J. *J. Chem. Soc. Chem. Commun.*, **1979**, 739.

100. Rabinowitz, R.; *J. Am. Chem. Soc.*, **1960**, *82*, 4564-4567.

101. Van Wazer, J. Phosphorous and Its Compounds, Vol. I New York Interscience Encyclopedias, Inc. 1958.

102. Lucero, B.; Gomes, C.; Frugulhetti, I.; Faro, L.; Alvarenga, L.; Souza, M.; Souza, T.; Ferreira, V. *Bioorganic and Medicinal Chemistry Letters*, **2006**, *16(4)*, 1010-1013.

103. Nakamura, S.; Kozuka, M.; Bastow, K.; Tokuda, H.; Nishino, H.; Suzuki, M.; Tatsuzuki, J.; Natschke, S.; Kuo, S.; Lee, K. *Bioorganic and Medicinal Chemistry Letters*, **2005**, *13*, 4396-4401.

104. Banerji, B.; Conejo-Garcia, A.; McNeill, L.; McDonough, M.; Buck, M.; Hewitson, K.; Oldham, N.; Schofield, C. *Chem. Commun.*, **2005**, 5438-5440.

105. Srivastava, S.; Chauhan, P.; Bhadur, A.; Fatima, N.; Chatterjee, R. *J. Med. Chem.*, **2000**, *43*, 2275-2279.

106. Jean, J.; Laborde, E.; Busch, R.; Caprathe, B.; Sorenson, R.; Fergus, J.; Spiegel, K.; Marks, J.; Dickerson, M.; Davis, R. *J. Med. Chem*., **1995**, *38*, 4439-4445.

107. Kermack, W.; Webster, W. *J. Chem. Soc.*, **1942**, 213-216.

108. Heindel, N.; Bechara, I.; Lemke, L.; Fish, V. *J. Org. Chem.*, **1967**, *32(12)*, 4155-4157.

109. Conrad, M.; Limpach, L. *Ber*., **1887**, *20*, 944.

110. Limpach, L. *J. Am. Chem. Soc.*, **1931**, *64*, 969.

111. Gould, Jr., G.; Jacobs, W. *J. Am. Chem. Soc.*, **1939,** *61*, 2890-2895.

112. Surrey, A. ; Hammer, H. *J. Am. Chem. Soc.*, **1946**, 68, 133-116.

113. Al-Awadi, N.; Abdelhamid, A.; Al-Etaibi, A.; Elnagdi, M. *Synlett*, **2007**, *14*, 2205-2208.

114. Eaton, P.; Carlson, G.; Lee, J. *J. Org. Chem*., **1973**, *38(23)*, 4071-4073.

115. Zewge, D.; Chen, C.; Deer, C.; Dormer, P.; Hughes, D. *J. Org. Chem*., **2007**, *72*, 4276-4279.

116. Reimer, M. *J. Am. Chem. Soc.*, **1931**, *53(8)*, 3147-3149.

117. Sugimura, H.; Yoshida, K. *Bull. Chem. Soc. Jpn.*,**1992**, *65*, 3209-3211.

118. Mahata, P.; Barun, O.; Ila, H.; Junjappa, H. *Synlett*, **2000**, *9*, 1345-1347.

119. Thangavel, V.; Chadta, A. *Tetrahedron*, **2007**, *63*, 4126-4133.

120. Zhu, L.; Meng, Q.; Fan, W.; Xie, X.; Zhang, Z. *J. Org. Chem.*, **2010**, 75, 6027-6030.

121. Parisi, M.; Gattuso, G.; Notti, A.; Raymo, F. *J. Org. Chem.*, **1995**, *60*, 5174-5179.

122. Amii, H.; Kobayashi, T.; Hatamoto, Y.; Uneyama, K. *Chem Commun.*, **1999**, 1323-1324.

123. Takahashi, S.; Jukurogi, T.; Katagari, T.; Uneyama, K. *CrystEngComm*, **2006**, *8*, 320-326.

124. Katagiri, T.; Ozaki, F.; Tanaka, Y. *Journal of Fluorine Chemistry*, **2009**, *130*, 682-683.

125. Raju, R.; Prasad, K. *Tetrahedron*, **2012**, *68*, 1341-1349.

126. He, H.; Willaimson, R.; Shen, B.; Graziani, E.; Yang, H.; Sakya, S.; Petersen, P.; Carter, G. *J. Am. Chem. Soc.*, **2002**, *124*, 9729-9736.

127. Cudic, P.; Kranz, J.; Behenna, D.; Kruger, R.; Tadesse, H.; Wand, A.; Velclich, Y.; Weisel, J.; McCafferty, D. *Proc. Natl. Acad. Sci.*, **2002**, *99(4)*, 7384-7389.

128. Reynold, P.; Somner, E. *Drugs. Exp. Clin. Res.*, **1990**, *16(8)*, 385-389.

129. Reynold, P.; Somner, E. *Antimicrob Agents Chemother.*, **1990**, *34(3)*, 413-419.

130. Men, H.; Park, P.; Ge, M.; Walker, S. *J. Am. Chem. Soc.*, **1998**, *120(10)*, 2484-2485.

131. Lo, M.; Men, H.; Branstrom, A.; Helm, J.; Yao, N.; Goldman, R.; Walker, S. *J. Am. Chem. Soc.*, **2000**, *122(14)*, 3540-3541.

132. Fang,X.; Tiyanont, K.; Zhang, Y.; Wanner, J.; Boger, D.; Walkers. *Mol. BioSyst.*, **2006**, *2*, 69-76.

133. Higashide, E.; Hatano, K.; Shibata, M.; Nakazawa, K. *J. Antibiotics*, **1968**, *21(2)*, 126-137.

134. Asai, M.; Muroi, M.; Sugita, N.; Kawashima, H.; Mizuno, K.; Miyaki, A. *J. Antibitotics*, **1968**, *21(2)*, 138-146.

135. Tsuchiya, K.; Kondo, M.; Oishi, T.; Yamazaki, T. *J. Antibiotics*, **1968**, *21(2)*, 147-153.

136. Horii, S.; Kameda, Y. *J. Antibiotics*, **1968**, *21(4)*, 665-667.

137. Hatano, K.; Nogami, I.; Higashide, E.; Kishi, T. *Agric. Biol. Chem.*, **1984**, *48(6)*, 1503-1508.

138. Nakane, A.; Nakamura, T.; Eguchi, Y *Journal of Biological Chemistry*, **1977**, *252(12)*, 5267-5273.

139. Yin, X.; Zabriskie, T.M. *Microbiology*, **2006**, *152*, 2969-2983.

140. Halti, B.; Tan, Y.; Magarvey, N.; Wagenaar, M.; Yin, X.; Grunstein, M.; Hucul, J.; Zabriskie, T.M. *Chem. Biol.*, **2005**, *12(11)*, 1163-1168.

141. Burroughs, A.; Hoppe, R.; Goebel, N.; Sayyed, B.; Voegtline, T.; Schwabacher, A.; Zabriskie, T.M.; Sivaggi, N. *Biochemistry*, **2013**, *52*, 4492-4506.

142. Fujita, Y. *Bull. Chem. Soc. Japan,* **1959**, *32(5)*, 439-442.

143. Fujita, Y. *Bull. Chem. Soc Japan*, **1960**, *32(10)*, 1379-1381.

144. Rossa, B.A.; Viswanatha, T. *Can. J. Biochem.*, **1968**, *46*, 725-728.

145. Yoon, G.; Zabriskie, T.M. *Journal of Radiolabelled Compounds and Radiopharmaceuticals*, **2008**, *52(2)*, 53-55.

146. Sanière, L.; Leman, L,; Bourguignon, J.; Dauban, P; Dodd, R. *Tetrahedron*, **2004**, *60*, 5889-5897.

147. Leman, L.; Sanière, L.; Dauban, P.; Dodd, R. *ARKIVOC*, **2003**, *(vi)*, 126-134.

148. Schwörer, C.; Oberthür, M. *Eur. J. Org. Chem.*, **2009**, 6129-6139.

149. Frédérick, R.; Charlier, C.; Robert, S.; Wouters, J.; Maserel, B.; Pachet, L. *Bioorganic and Medicinal Chemistry Letters*, **2006**, *16*, 2017-2021.

150. Drake, B.; Patek, M.; Lebl, M. *Synthesis*, **1994**, *6*, 579-582.

151. Behrens, C.; Paquette, L. *Org. Syn. Coll.*, **2004**, *10*, 41.

152. Dardeen, G.; Casimir, J.; Marlier, M.; Larsen, P *Phytochemistry*, **1974**, *13(9),* 1897-1900.

153. Angst, C. *Pure Appl. Chem*., **1987**, *59(3)*, 373-380.

154. Rando, R.; Relyea, N.; Cheng, L. *J. Biol. Chem*.,**1976**, *251(11)*, 3306-3312.

155. Rando, R. *Biochemistry*, **1974**, *13(19)*, 3859-3863.

156. Feng, L.; Kirsch, J. *Biochemistry*, **2000**, *39(10)* , 2436-2444.

157. Brodie, J.; Figueroa, E.; Dewey, S. *Synapse*, **2003**, *50(3)*, 261-265.

158. Goto, Y.; iwaski, K.; torikai, K.; Murakami, H.; Suga, H. *Chem. Commun.*, **2009**, 3419-3421.

159. Friis, P.; Helboe, P.; Larsen, P. *Acta Chemica Scandinavica B*, **1974**, *28*, 317-321.

160. Berkowiz, D.; Charette, B.; Kurukurichi, K.; McFadden, J. *Tet. Assymmetry*, **2006**, *17*, 869-882.

161. Afzali-Ardakani, A.; Rapoport, H *J. Org. Chem*., **1980**, *45*, 4817-4820.

162. Rajenda, G.; Miller, M. *J. Org. Chem*. **1987**, *52(20),* 4471-4477.

163. Itaya, T.; Shimizu, S.; Nakagawa, S.; Morisue, M. *Chem. Pharm. Bull*, **1994**, *42(9)*, 1927-1930.

164. Rich, D.; Tam, J. *J. Org. Chem*., **1977**, *42(24)*, 3815-3820.

165. Kuchenthal, C.; Migenda, J.; Polednia, M.; Maison, W. *Amino Acids*, **2010**, *39(2)*, 443-448.

166. Shirasishi, S., Nomoto, S. *Agric. Biol. Chem*., **1998**, *52 (6)*, 1601-1602.

167. Hanessian, S.; Sahoo, S. *Tetrahedron Letters*, **1984**, *24(14)*, 1425-1428.

168. Berkowitz, D.; Maiti, G. *Org. Lett*., **2004***, 6(16)*, 2661-2664.

169. Biagini, S.; Gibson, S.; Keen, S. *J. Chem. Soc. Perkin Trans. 1*, **1998**, 2485-2499.

170. Hallinan, K.; Crout, D.; Errington, W *J. Chem. Soc. Perkin Trans. 1*, **1994**, 3537-3543.

171. Carrasco, M.; Jones, R.; Kamel, S.; Rapoport, H.; Truong, T., Organic Syntheses, **1998**, Coll. Vol. 9, 63-68.

172. Pirrung, M.; Biswas, G; Ibarra-Rivera, T. *Org. Lett*., **2010**, *12*, 2402–2405.

173. Hoffmann, T.; Waibel, R.; Gmeiner, P. *J. Org. Chem.* **2003**, *68*, 62–69.

174 a. Sharpless, K.; Lauer, R.; Teranishi, A. *J. Am. Chem. Soc.*, **1973**, *95*, 6137-6139.

b. Reich, H.; Renga, J. *J. Org. Chem*., **1975**, *40(22),* 3313-3314.

c. Reich, H.; Renga, J.; Reich, I. *J. Am. Chem. Soc*.,**1975**, *97*, 5434-5447.

175. Walter, R.; Roy, J. *J. Org. Chem*, **1971**, 36(17), 2561-2563.

176. Lebar, M.; Lupoli, T.; Tsukamoto, H.; May, J.; Walker, S.; Kahne, D. *J. Am. Chem. Soc.*, **2013**, *135*, 4632-4635.

177. Bodanszky, M.; Bodanszky, A. The Practice of Peptide Synthesis 1984 Springer-Verlang Berlin New York Tokyo.

178. NMR indicates changes subsequent to dissolution that correlate with higher yields. Possibly this corresponds to a greater degree of N-silylation.

179. In each, base was held constant at 1M triethylamine, and isomerization monitored at 25˚C by ^{1}H NMR. As we did not collect full time course data, and analysis times varied, we have chosen to express half times calculated assuming pseudo first order kinetics and using only 1-2 data points.

180. Kastrinsky, D.B.; Kumar, P.; Marriner, G.A.; Barry, C. E. III, *Synthesis* **2012**; *44*, 3043-3048.

181. Chatterjee, A.K.; Choi, T-L.; Sanders, D.P.; Grubbs,R.H. *J. Am. Chem. Soc.*, **2003**, *125*, 11360-11370.

182. Binder, J.; Blank, T.; Raines, R. *Org. Lett.,* **2007***, 9(23)*, 4885-4888.

183. Huwe, C.; Blechert, S. *Tet. Lett*., **1995**, *36(10)*, 1621-1624.

184. Brümmer, O.; Rückert, A.; Blechert, S. *Chem. Eur. J.,* **1997**, *3(3)*, 441-446.

185. Nolen, E.; Kurish, A.; Wong, K.; Orlando, M. *Tet. Lett*., **2003**, *44(12),* 2449-2453.

186. Vasbinder, M.; Miller, S. *J.Org.Chem.*, **2002**, *67*, 6240-6242.

187. Miller, S.; Blackwell, H.; Grubbs, R. *J. Am. Chem. Soc*., **1996,** *118*, 9606-9614.

188. Han L., Schwabacher, A.W., Moran G.R., Silvaggi N.R. *Biochemistry*, **2015**, *54*, 7029–7040.

189. Miller, S.; Grubbs, R. *J. Am. Chem. Soc.*, **1995**, *117(21)*, 5855-5856.

190. Hoffman, T.; Waibel, R.; Gmeiner, P. *J. Org. Chem.*, **2003**, *68*, 62-69.

191. Huwe, C.; Biechert, S. *Tet. Lett.*, **1995**, *36(10)*, 1621-1624.

192. Miller, S.; Blackwell, H.; Grubbs, R. *J. Am. Chem. Soc.*, **1996**, *118*, 9606-9614.

193. Fu, G.; Grubbs, R. *J. Am. Chem. Soc.*, **1992**, *114*, 5426-5427.

194. Brümmer, O.; Rückert, A.; Biechert, S. *Chem. Eur. J.*, **1997**, *3(3)*, 441-446.

195. Biagini, S.; Gibson, S.; Keen, S. *J. Chem. Soc., Perkin Trans.1*, **1998**, *16*, 2485-2499.

196. Ulman, M.; Grubbs, R. *Organometallics,* **1998**, *17(12)*, 2484-2489.

197. Blackwell, H.; O'Leary, D.; Chatterjee, A.; Washenfelder, R.; Bussman, D.; Grubbs, R. *J. Am. Chem. Soc.*, **2000**, *122(1)*, 58-74.

198. Chatterjee, A.; Grubbs, R. *Org. Lett.*, **1999**, *1(11)*, 1751-1753.

199. Garber, S.; Kingsbury, J.; Gray, B.; Hoveyda, A. *J. Am. Chem. Soc.*, **2000**, *122(34)*, 8168-8179.

200. Vasbinder, M.; Miller, S. *J. Org. Chem.*, **2002**, *67*, 6240-6242.

201. Nolan, E.; Kurish, A.; Wong, K.; Orlando, M. *Tet. Lett.*, **2003**, *44(12)*, 2449-2453.

202. Chowdhury, A.; Boons, G. *Tet. Lett.*, **2005**, *46(10)*, 1675-1678.

203. Pirrung, M.; Biswas, G.; Ibarra-Rivera, T. *Org. Lett.*, **2010**, *12(10)*, 2402-2405.

204. Hong, S.; Grubbs, R. *J. Am. Chem. Soc.*,**2006**, *128(11)*, 3508-3509.

205. Jordan, J.; Grubbs, R. *Angew. Chem. Int. Ed.*, **2007**, *46(27)*, 5152-5155.

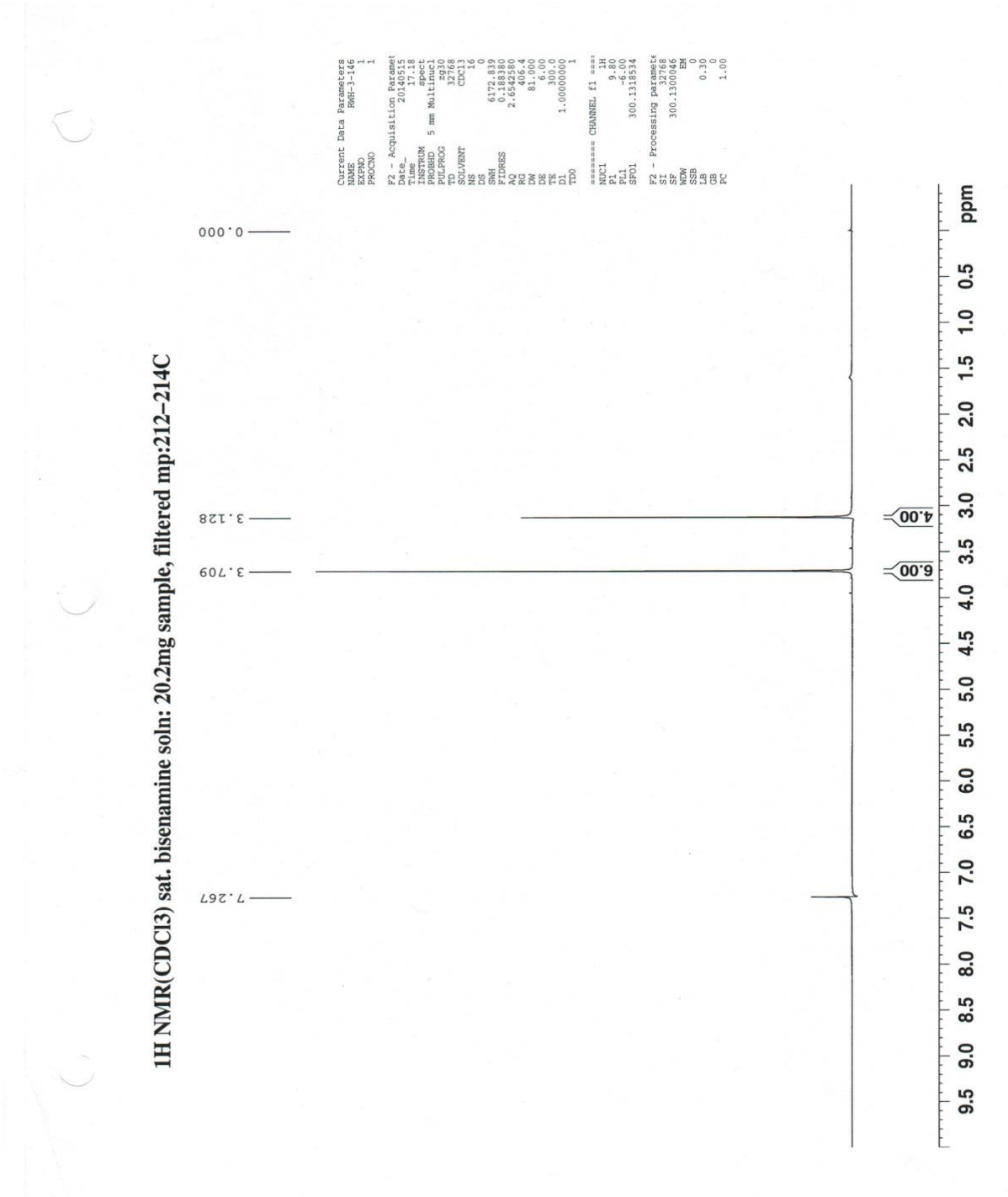
206. Binder, J.; Blank, J.; Raines, R. *Org. Lett.*, **2007**, *9(23)*, 4885-4888.

207. Schwabacher, A.; Lane, J.; Schiesher, M.; Leigh, K.; Johnson, C. *J. Org. Chem.*, **1998**, *63*, 1727-1729.

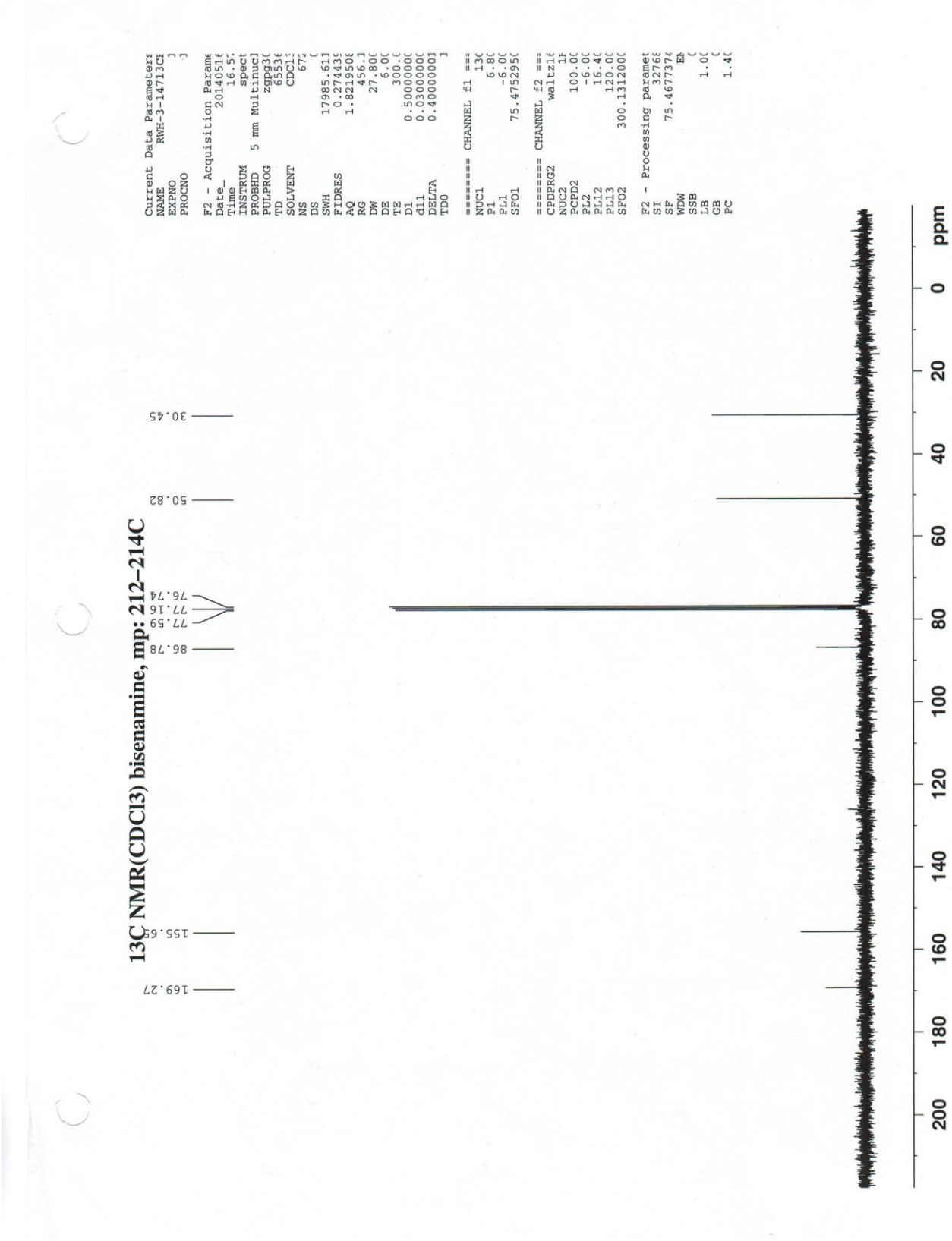
X. APPENDIX

A. Characterization Data for Selected Compounds

^{1}H NMR *Dimethyl 2,5-diaminocyclohexa-1,4-diene-1,4-dicarboxylate* (**1**)



^{13}C NMR <u>*Dimethyl 2,5-diaminocyclohexa-1,4-diene-1,4-dicarboxylate*</u> (**1**)



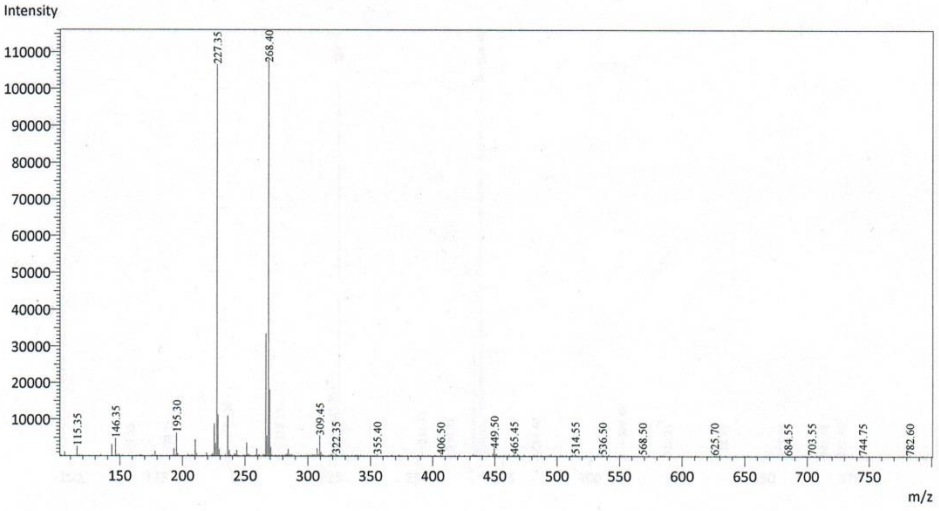
MS *Dimethyl 2,5-diaminocyclohexa-1,4-diene-1,4-dicarboxylate* (**1**)

Shimadzu LCMS-2020 Data Report

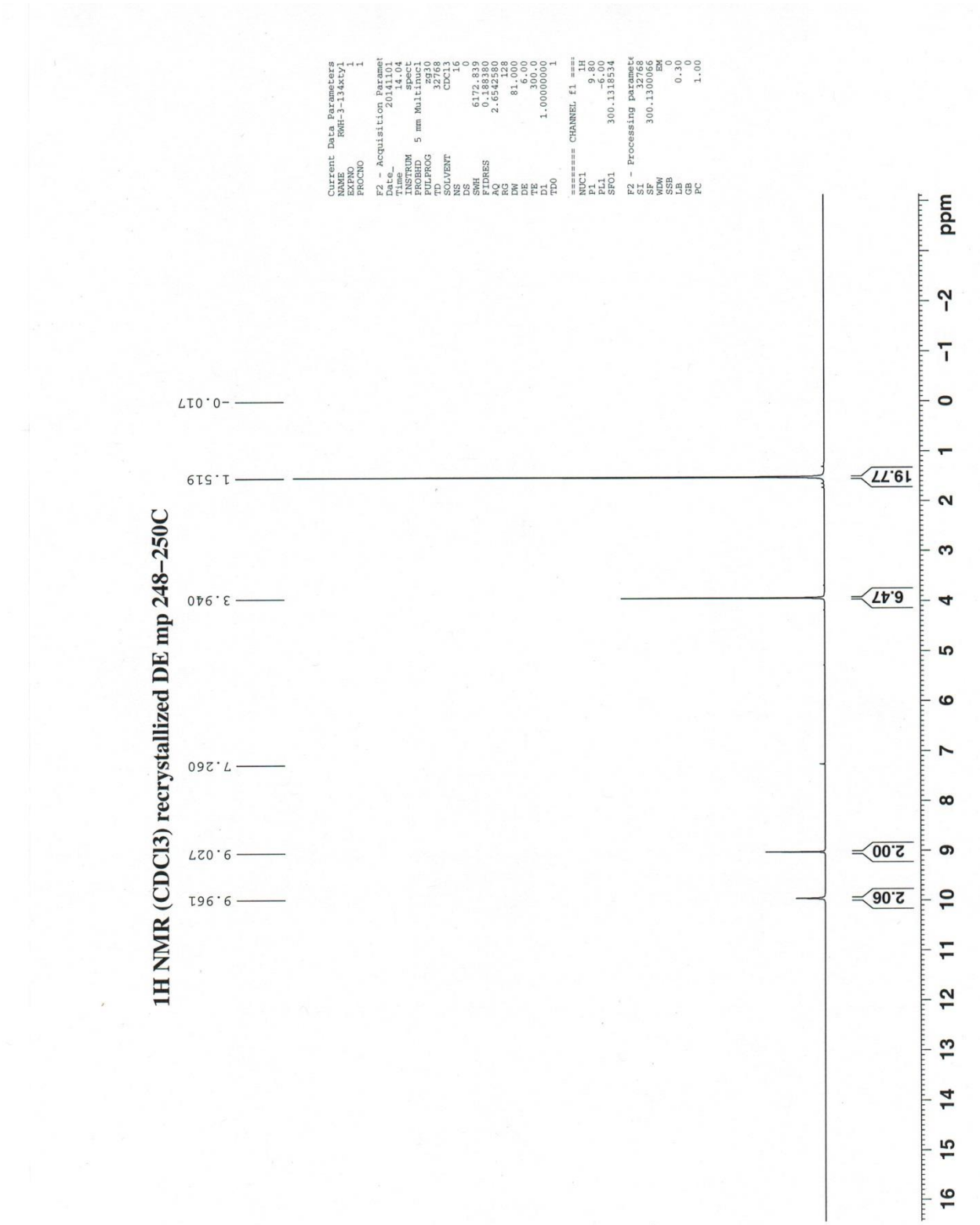
Mass Spectrum for Sample
RWH-3-147 02.lcd

Operator: Mark Wang

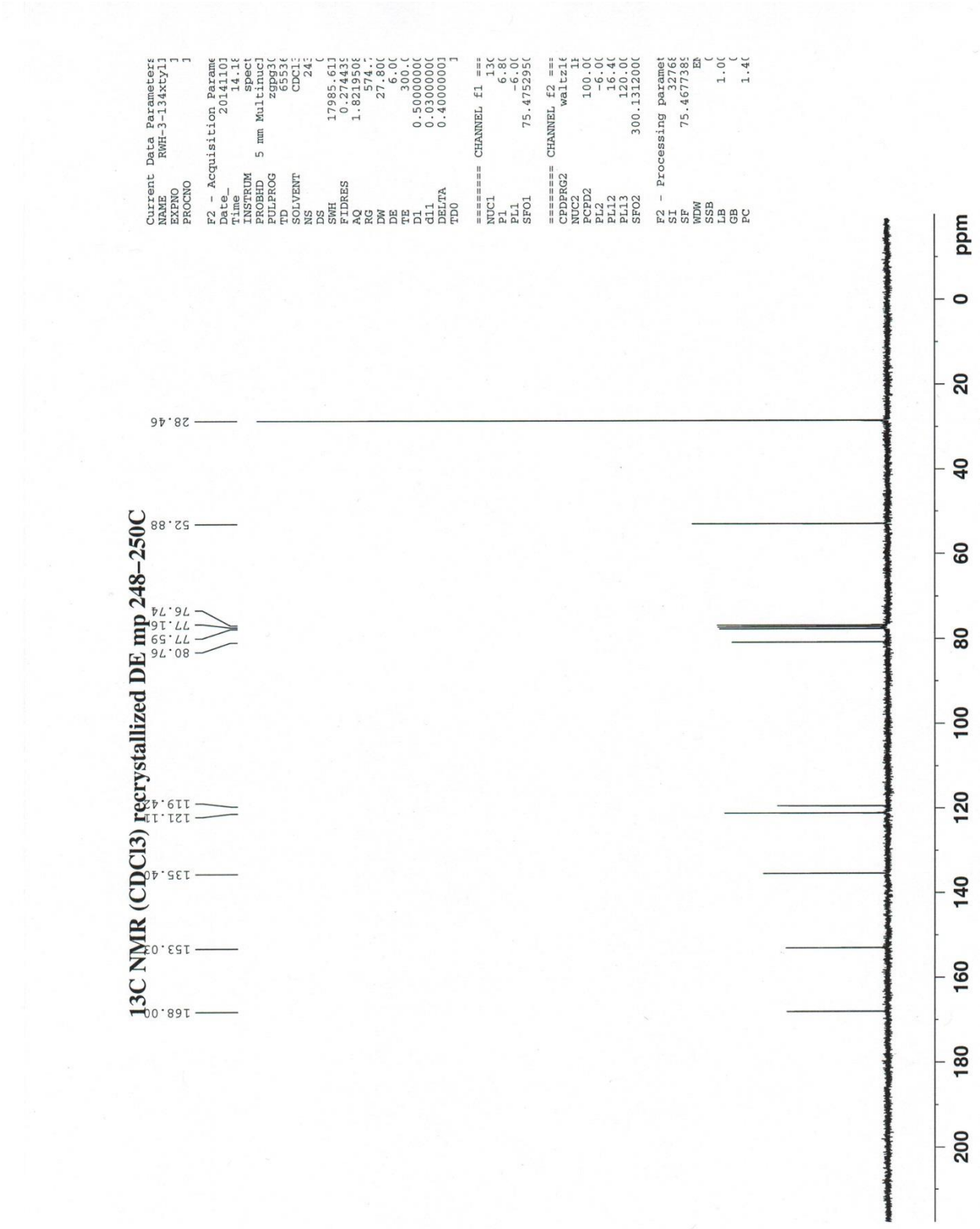
Data Filename: C:\LabSolutions\Data\Schwabacher Alan\RWH-3-147 02.lcd
Spetrum Mode: Averaged
Retention Time: ----
Interface Type (ESI, APCI, DUIS): DUIS
Aquisition Mode: (Scan, SIM, Profife): Scan
Polarity: +



^{1}H NMR *Dimethyl 2,5-bis((tert-butoxycarbonyl)amino)terephthalate* (**2**)



^{13}C NMR *Dimethyl 2,5-bis((tert-butoxycarbonyl)amino)terephthalate* (**2**)



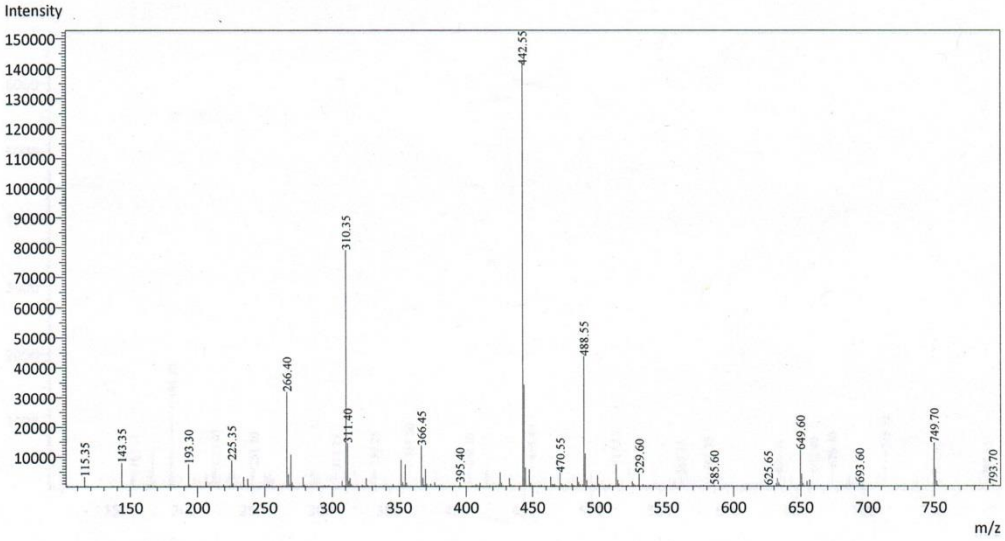
MS *Dimethyl 2,5-bis((tert-butoxycarbonyl)amino)terephthalate* (**2**)

Shimadzu LCMS-2020 Data Report

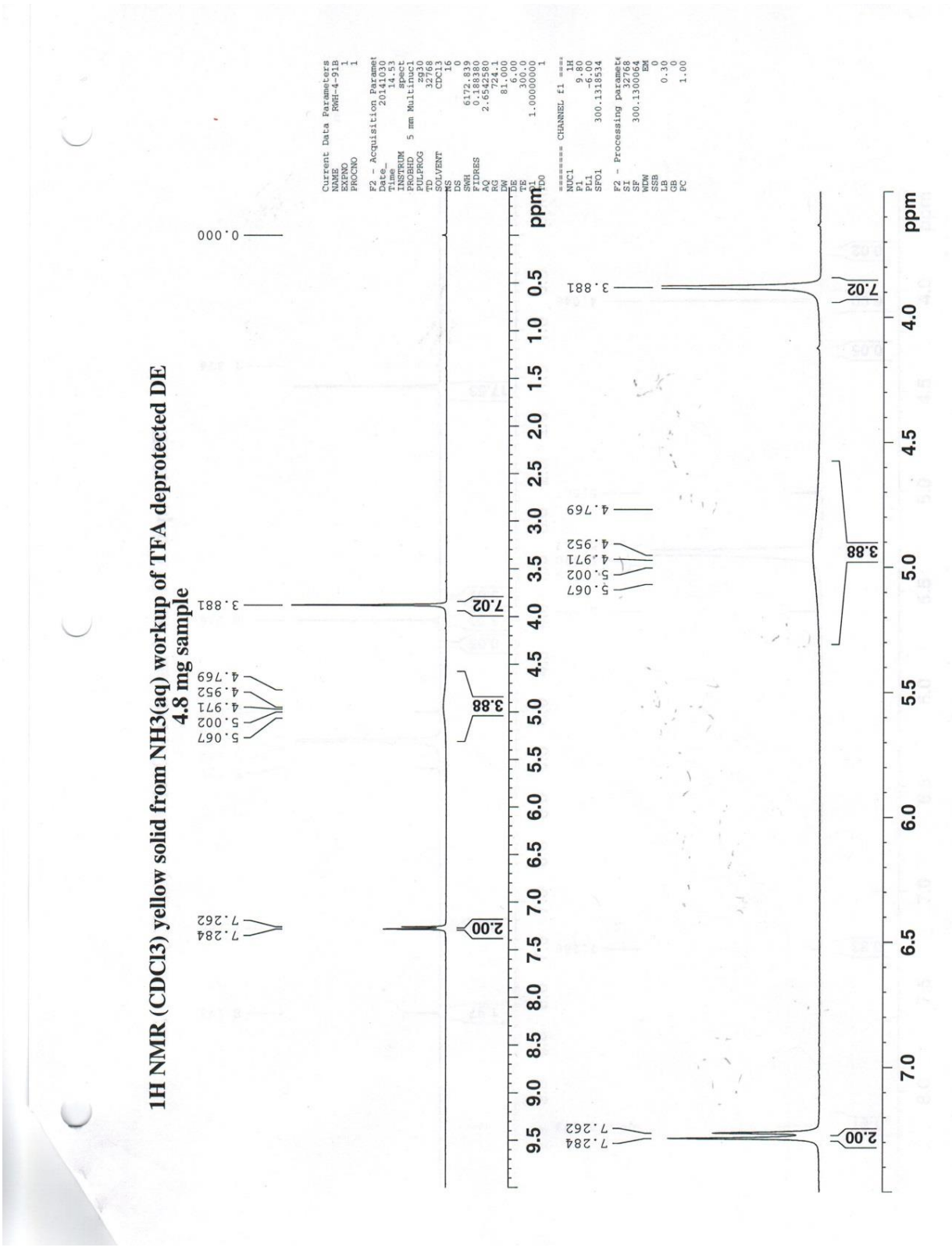
Mass Spectrum for Sample
RWH-3-134 02.lcd

Operator: Mark Wang

Data Filename: C:\LabSolutions\Data\Schwabacher Alan\RWH-3-134 02.lcd
Spetrum Mode: Averaged
Retention Time: ----
Interface Type (ESI, APCI, DUIS): DUIS
Aquisition Mode: (Scan, SIM, Profife): Scan
Polarity: +



^{1}H NMR *Dimethyl 2,5-diaminoterephthalate* (**3**)

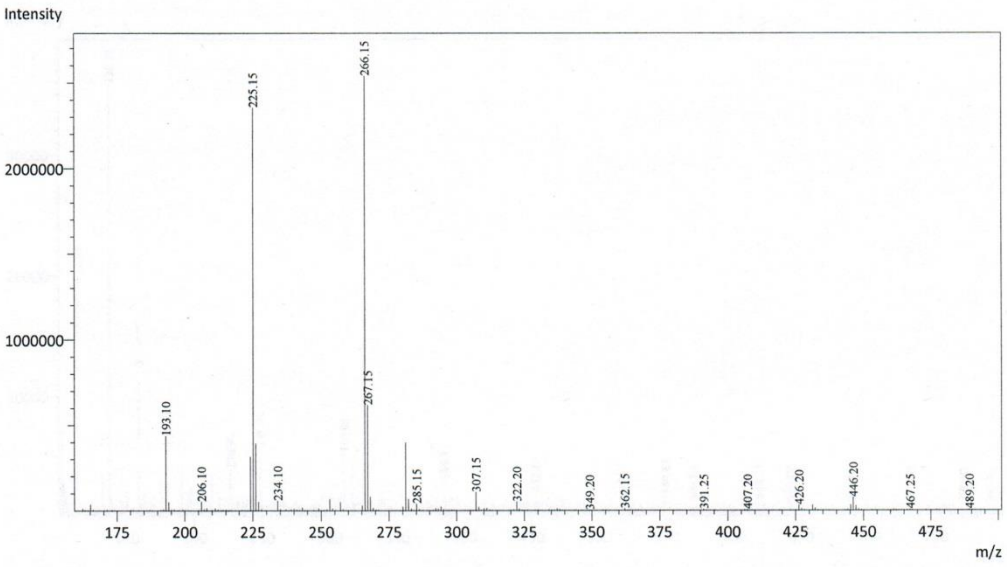


MS *Dimethyl 2,5-diaminoterephthalate* (**3**)

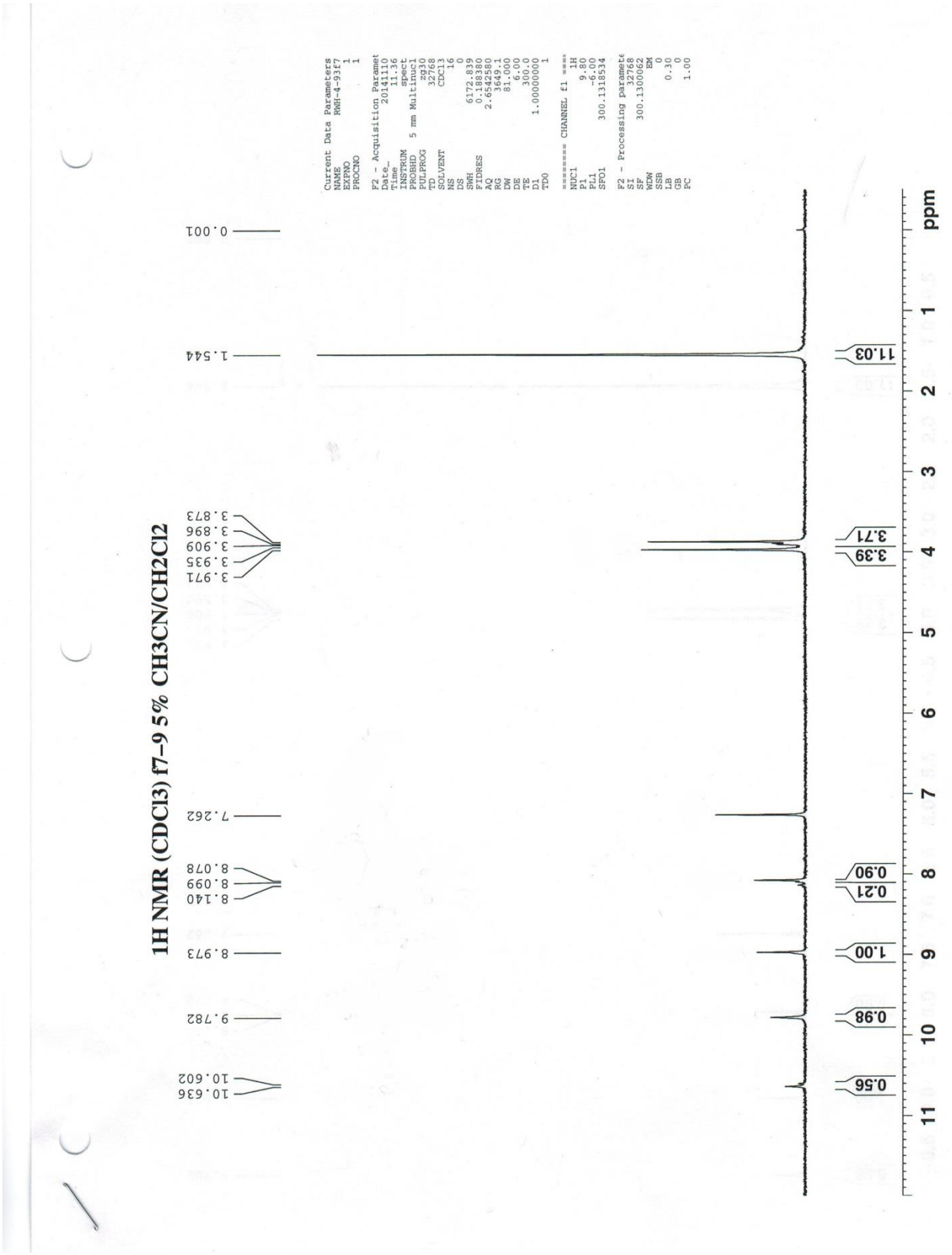
Shimadzu LCMS-2020 Data Report

Mass Spectrum for Sample
RWH-4-91 01.lcd

Operator: Mark Wang
Data Filename: C:\LabSolutions\Data\Schwabacher Alan\RWH-4-91 01.lcd
Spetrum Mode: Averaged
Retention Time: ----
Interface Type (ESI, APCI, DUIS): DUIS
Aquisition Mode: (Scan, SIM, Profife): Scan
Polarity: +



^{1}H NMR *<u>Tetramethyl 5,5'-azanediylbis(2-((tert-butoxycarbonyl)amino)terephthalate)</u>* (**4**)



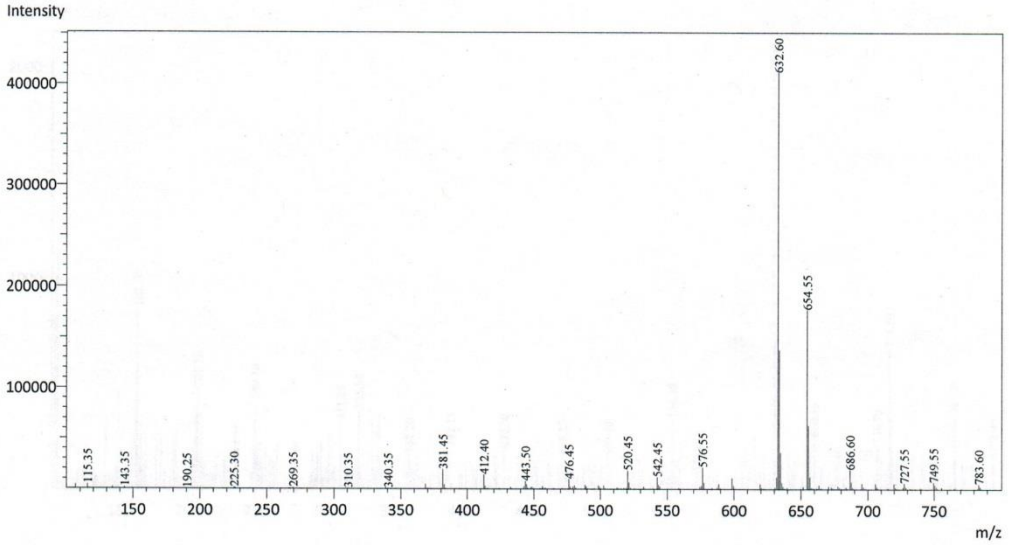
MS *Tetramethyl 5,5'-azanediylbis(2-((tert-butoxycarbonyl)amino)terephthalate)* (**4**)

Shimadzu LCMS-2020 Data Report

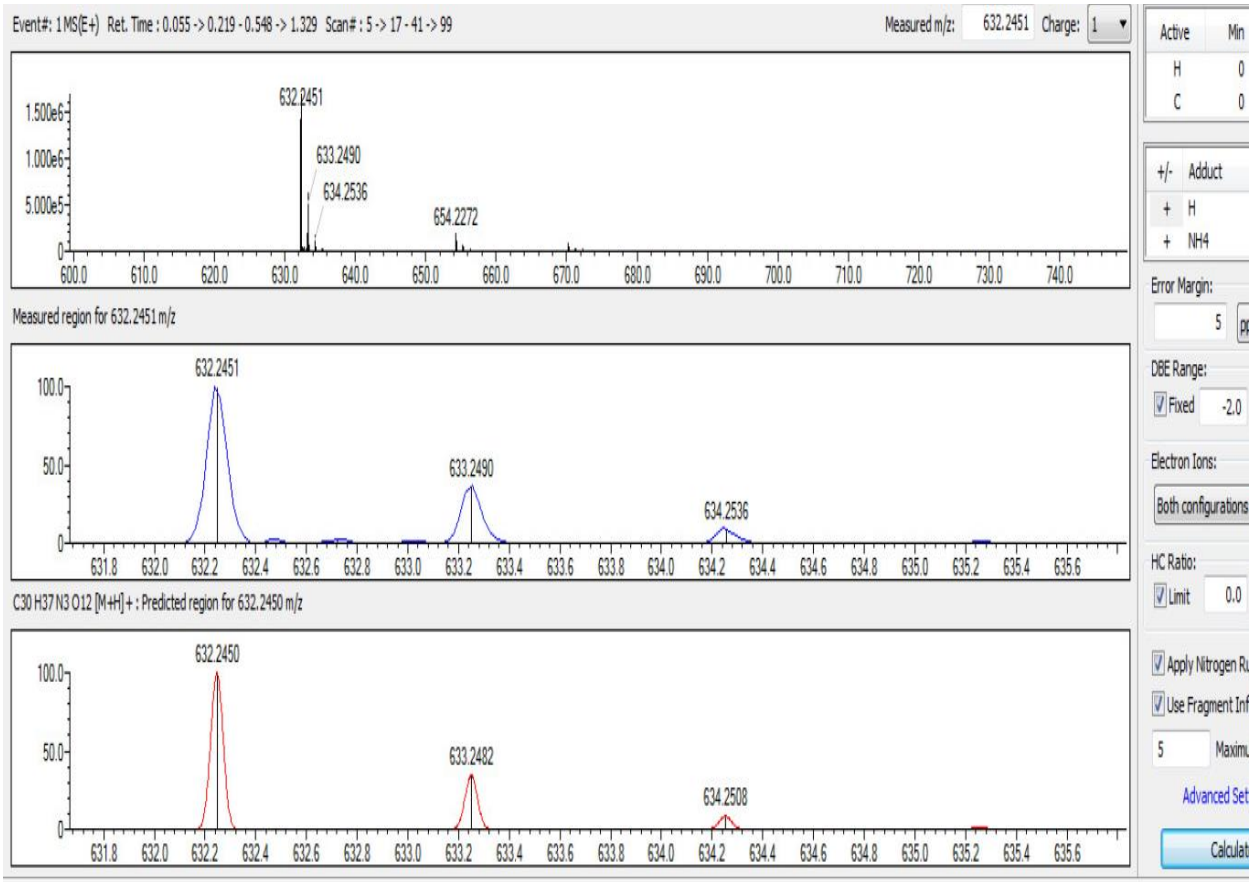
Mass Spectrum for Sample
RWH-4-93.lcd

Operator: Mark Wang

Data Filename: C:\LabSolutions\Data\Schwabacher Alan\RWH-4-93.lcd
Spetrum Mode: Averaged
Retention Time: ----
Interface Type (ESI, APCI, DUIS): DUIS
Aquisition Mode: (Scan, SIM, Profife): Scan
Polarity: +

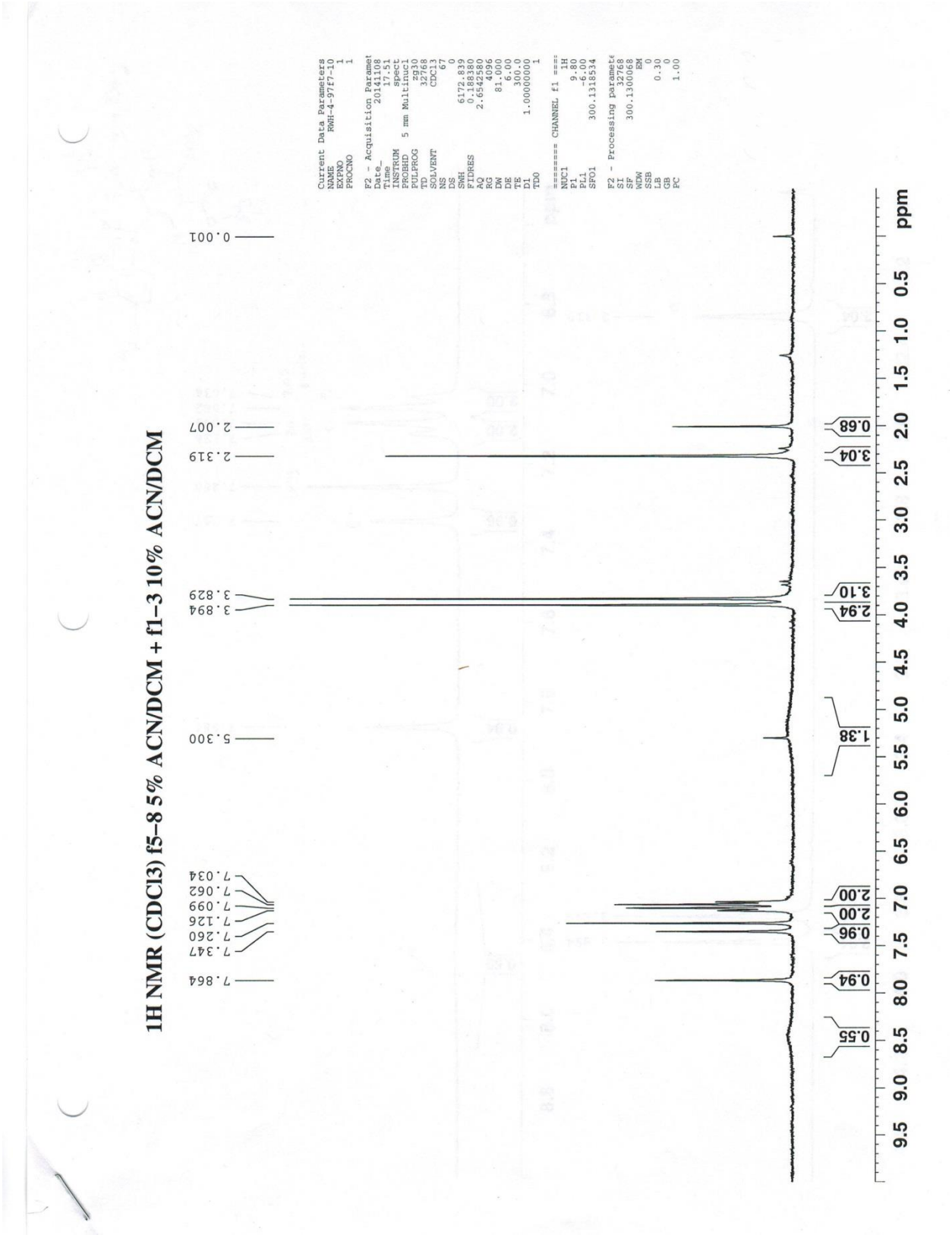


HRMS *Tetramethyl 5,5'-azanediylbis(2-((tert-butoxycarbonyl)amino)terephthalate)* (**4**)



Rank	Score	Formula (M)	Ion	Meas. m/z	Pred. m/z	Diff (mDa)	Diff (ppm)	Iso Score
1	98.91	C30 H37 N3 O12	[M+H]+	632.2451	632.2450	0.1	0.16	98.91
2	97.64	C31 H33 N7 O8	[M+H]+	632.2451	632.2463	-1.2	-1.90	99.89
3	95.00	C28 H25 N17 O2	[M+H]+	632.2451	632.2450	0.1	0.16	95.00
4	91.22	C27 H29 N13 O6	[M+H]+	632.2451	632.2437	1.4	2.21	94.06
5	90.57	C32 H29 N11 O4	[M+H]+	632.2451	632.2477	-2.6	-4.11	98.20

^{1}H NMR *Dimethyl 2-amino-5-(p-tolylamino)terephthalate* (**5**)



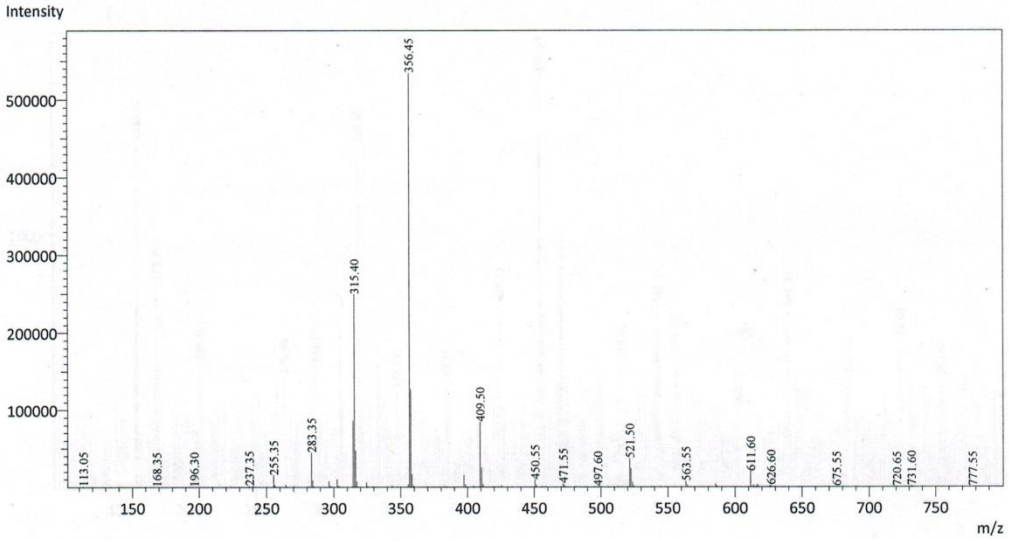
ESI-MS *Dimethyl 2-amino-5-(p-tolylamino)terephthalate* (**5**)

Shimadzu LCMS-2020 Data Report

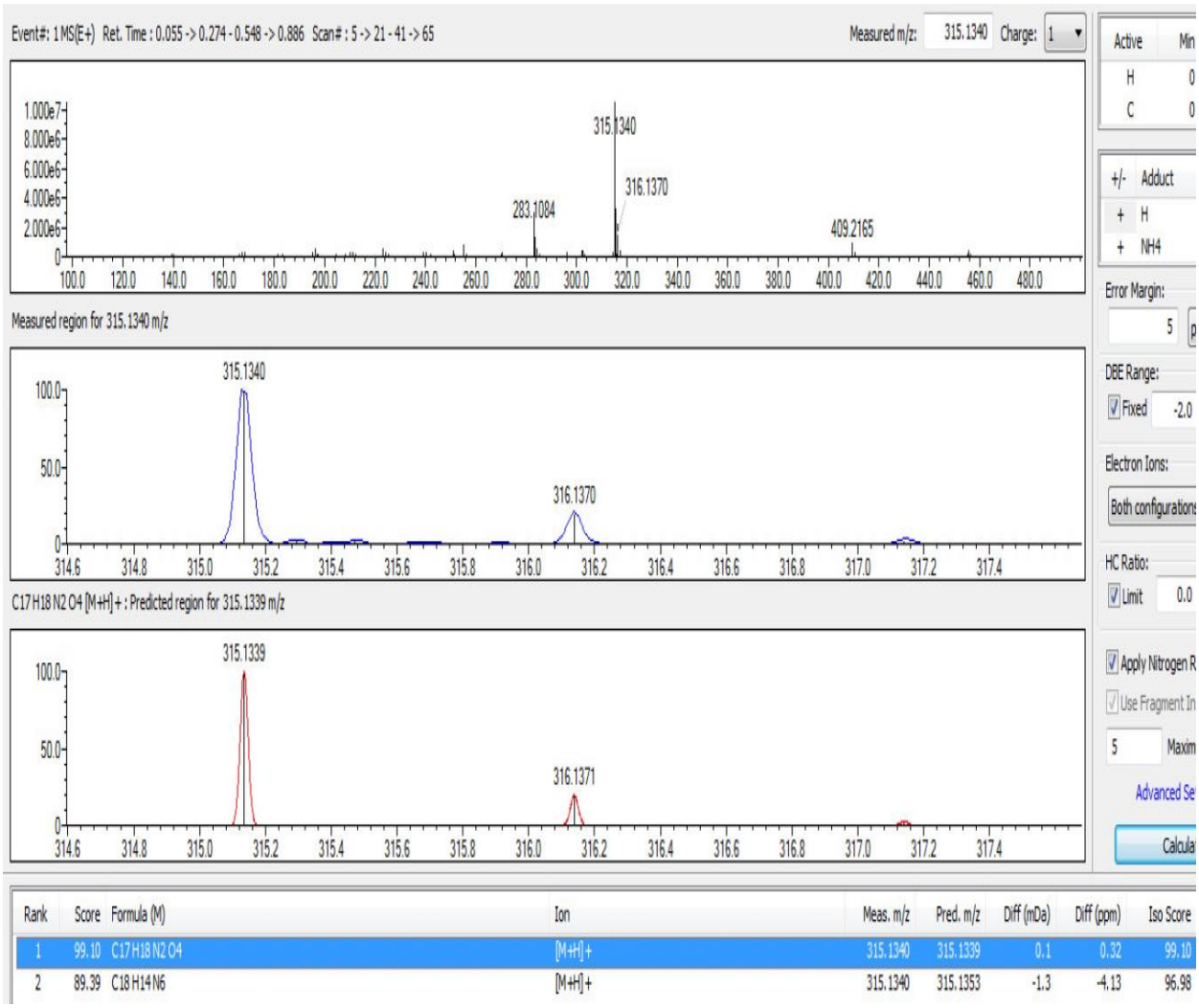
Mass Spectrum for Sample
RWH-4-97f10 01.lcd

Operator: Mark Wang

Data Filename: C:\LabSolutions\Data\Schwabacher Alan\RWH-4-97f10 01.lcd
Spetrum Mode: Averaged
Retention Time: ----
Interface Type (ESI, APCI, DUIS): DUIS
Aquisition Mode: (Scan, SIM, Profife): Scan
Polarity: +

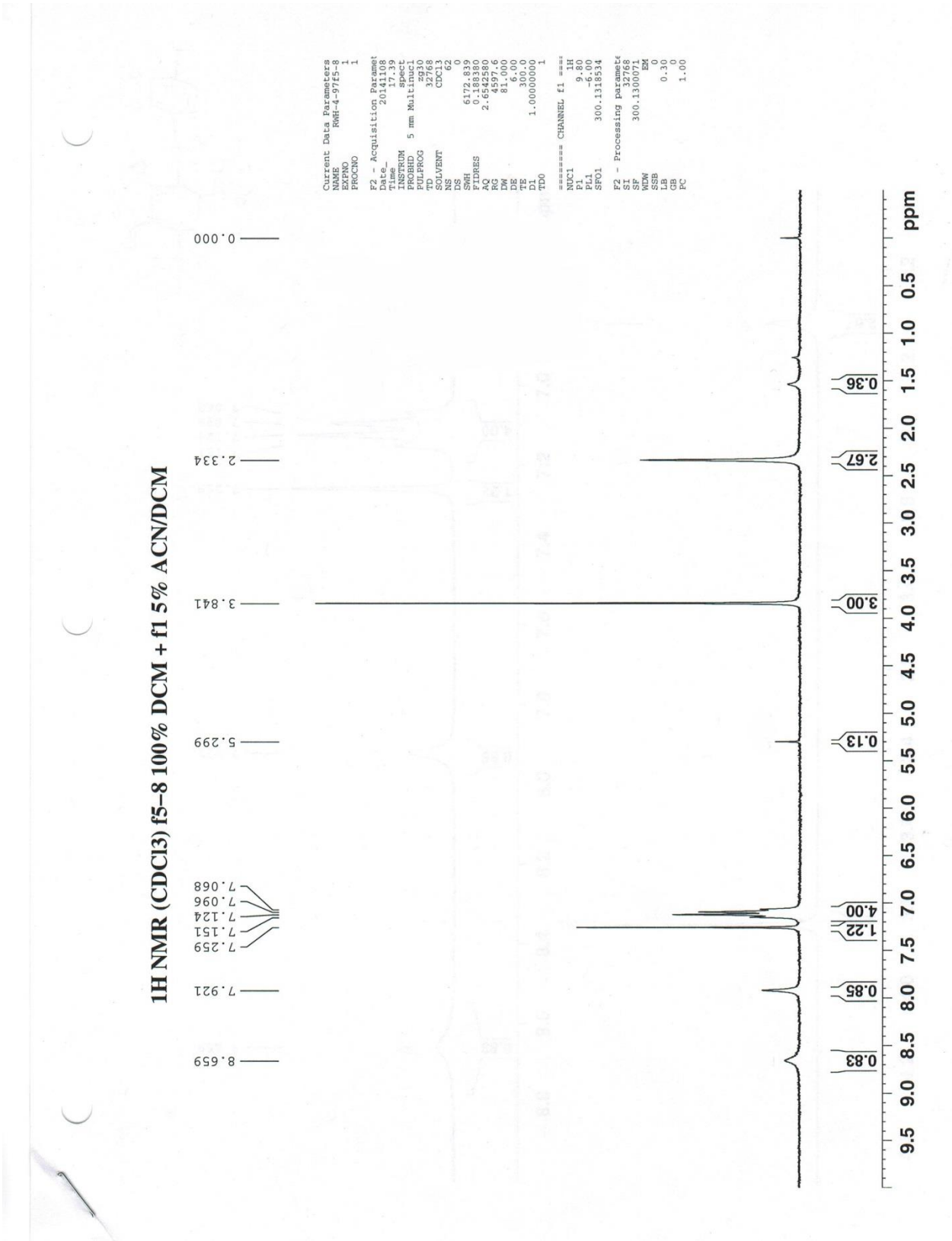


HRMS *Dimethyl 2-amino-5-(p-tolylamino)terephthalate* (**5**)



Rank	Score	Formula (M)	Ion	Meas. m/z	Pred. m/z	Diff (mDa)	Diff (ppm)	Iso Score
1	99.10	C17 H18 N2 O4	[M+H]+	315.1340	315.1339	0.1	0.32	99.10
2	89.39	C18 H14 N6	[M+H]+	315.1340	315.1353	-1.3	-4.13	96.98

^{1}H NMR *Dimethyl 2,5-bis(p-tolylamino)terephthalate* (**6**)



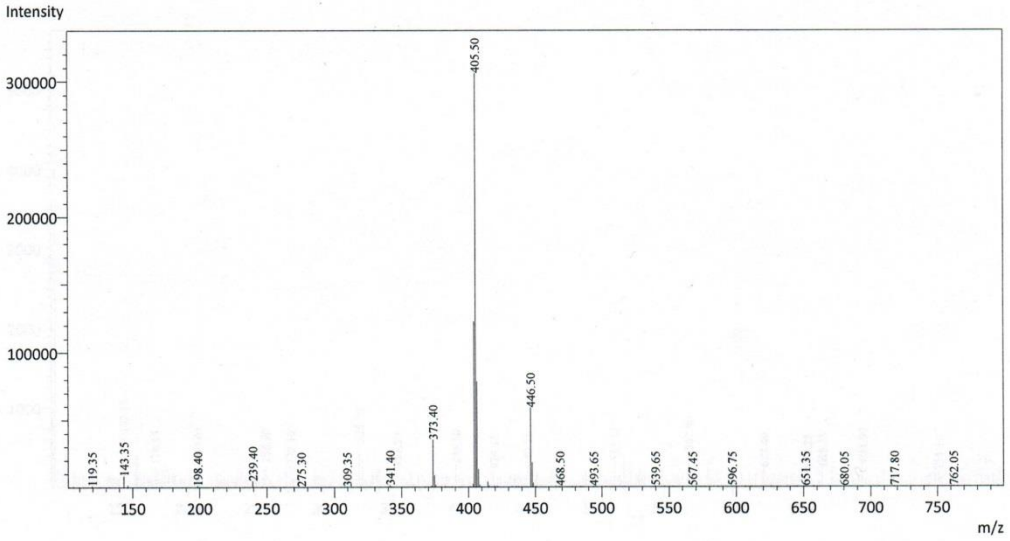
ESI-MS *Dimethyl 2,5-bis(p-tolylamino)terephthalate* (**6**)

Shimadzu LCMS-2020 Data Report

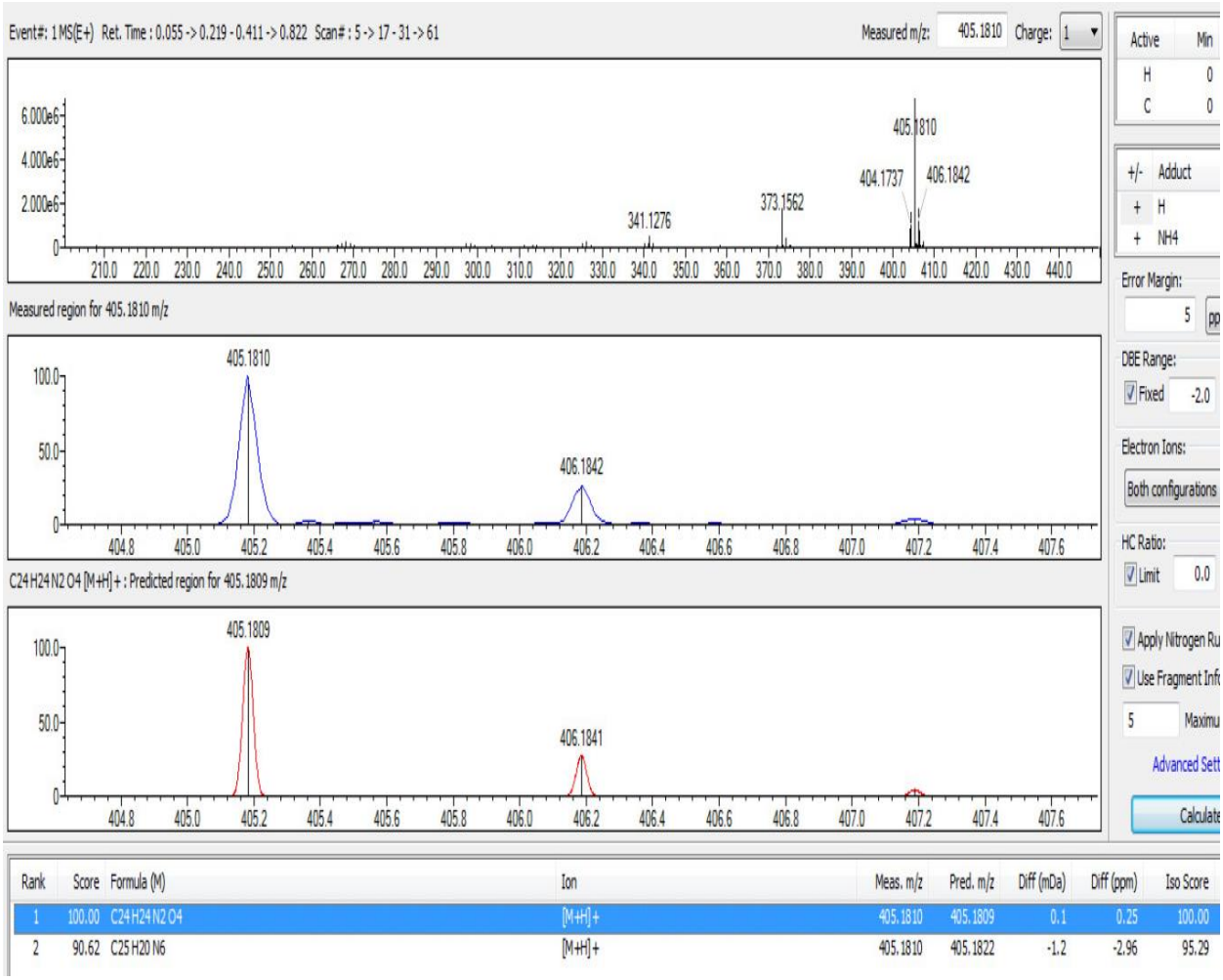
Mass Spectrum for Sample
RWH-4-97f5 01.lcd

Operator: Mark Wang

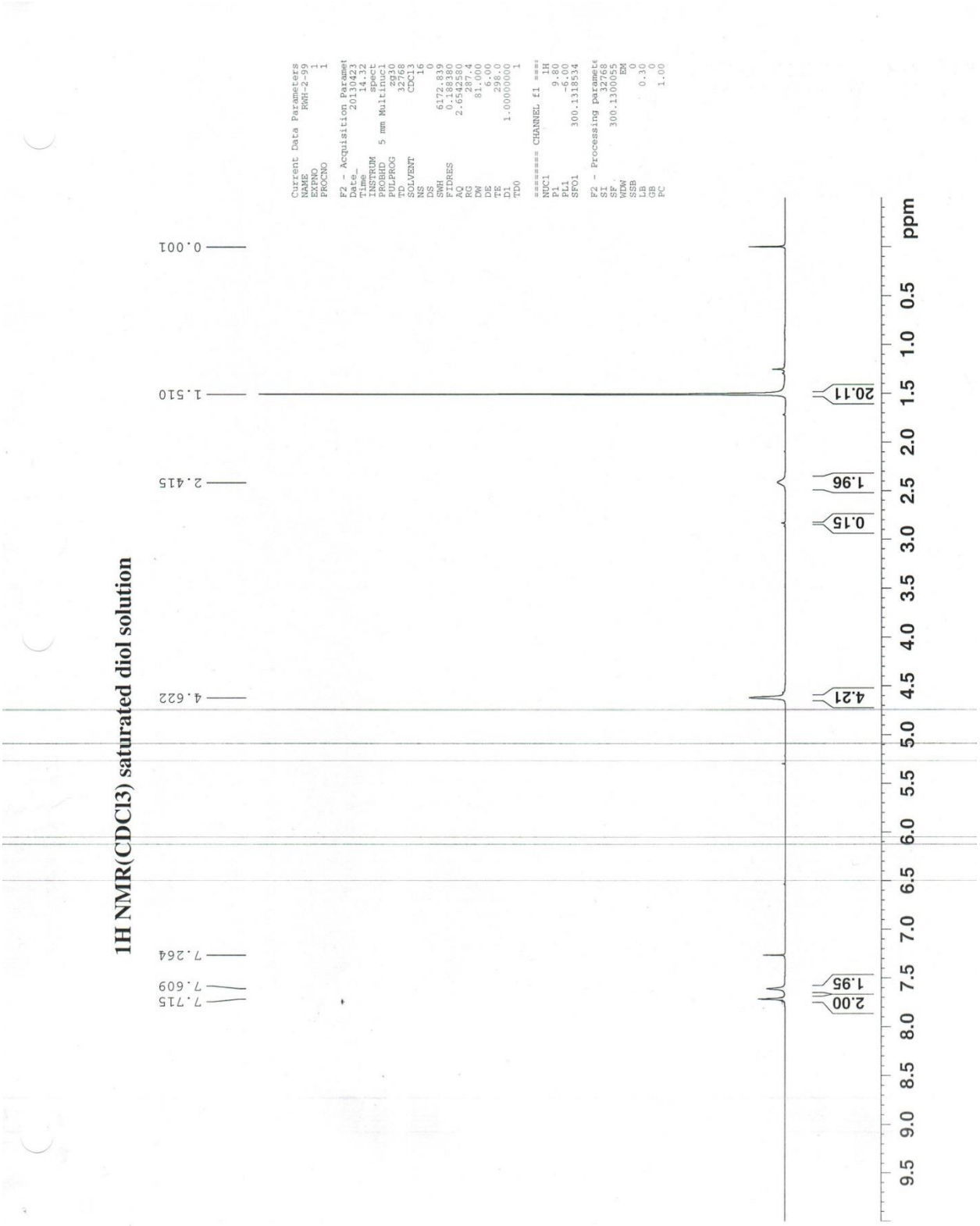
Data Filename: C:\LabSolutions\Data\Schwabacher Alan\RWH-4-97f5 01.lcd
Spetrum Mode: Averaged
Retention Time: ----
Interface Type (ESI, APCI, DUIS): DUIS
Aquisition Mode: (Scan, SIM, Profife): Scan
Polarity: +



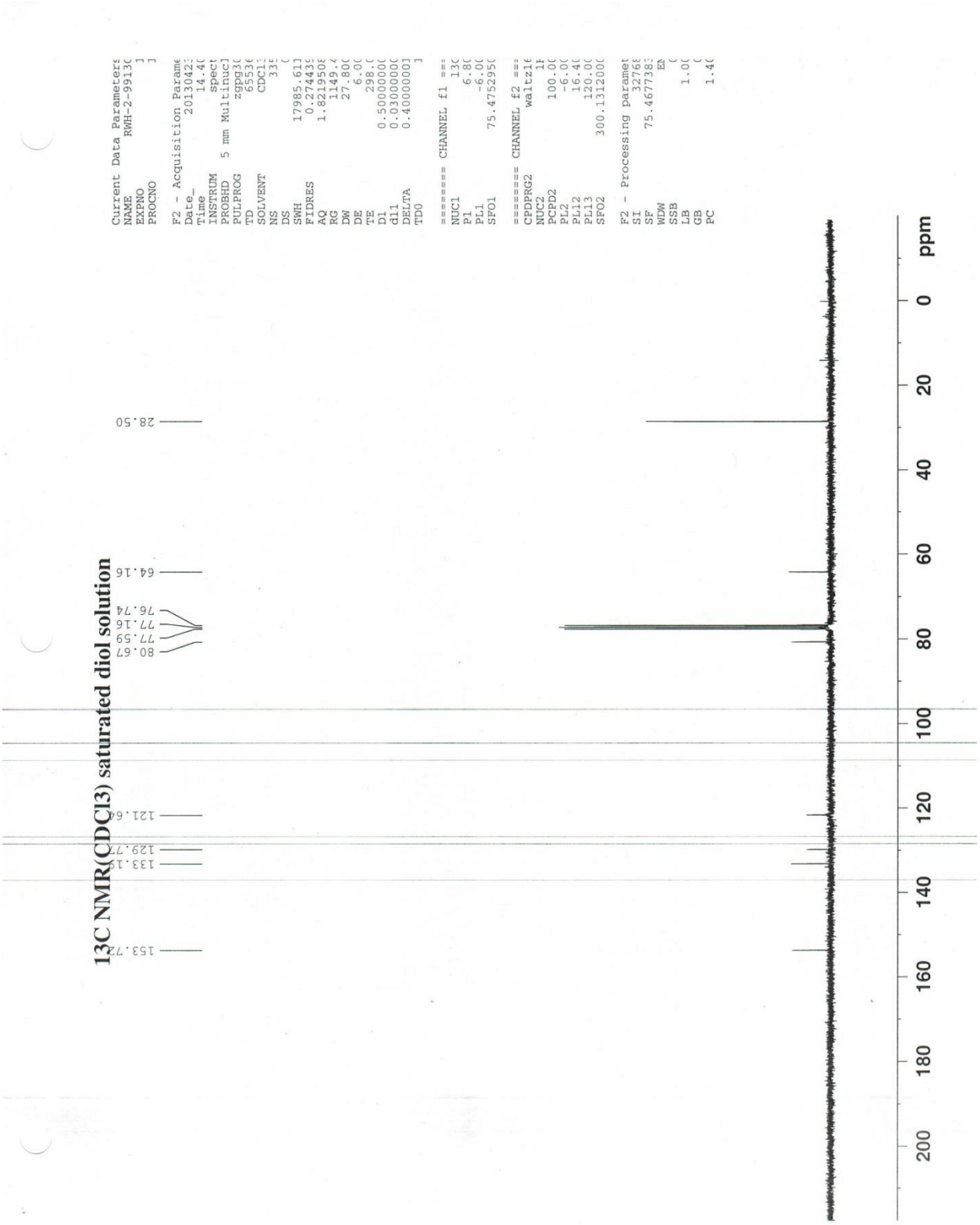
HRMS *Dimethyl 2,5-bis(p-tolylamino)terephthalate* (**6**)



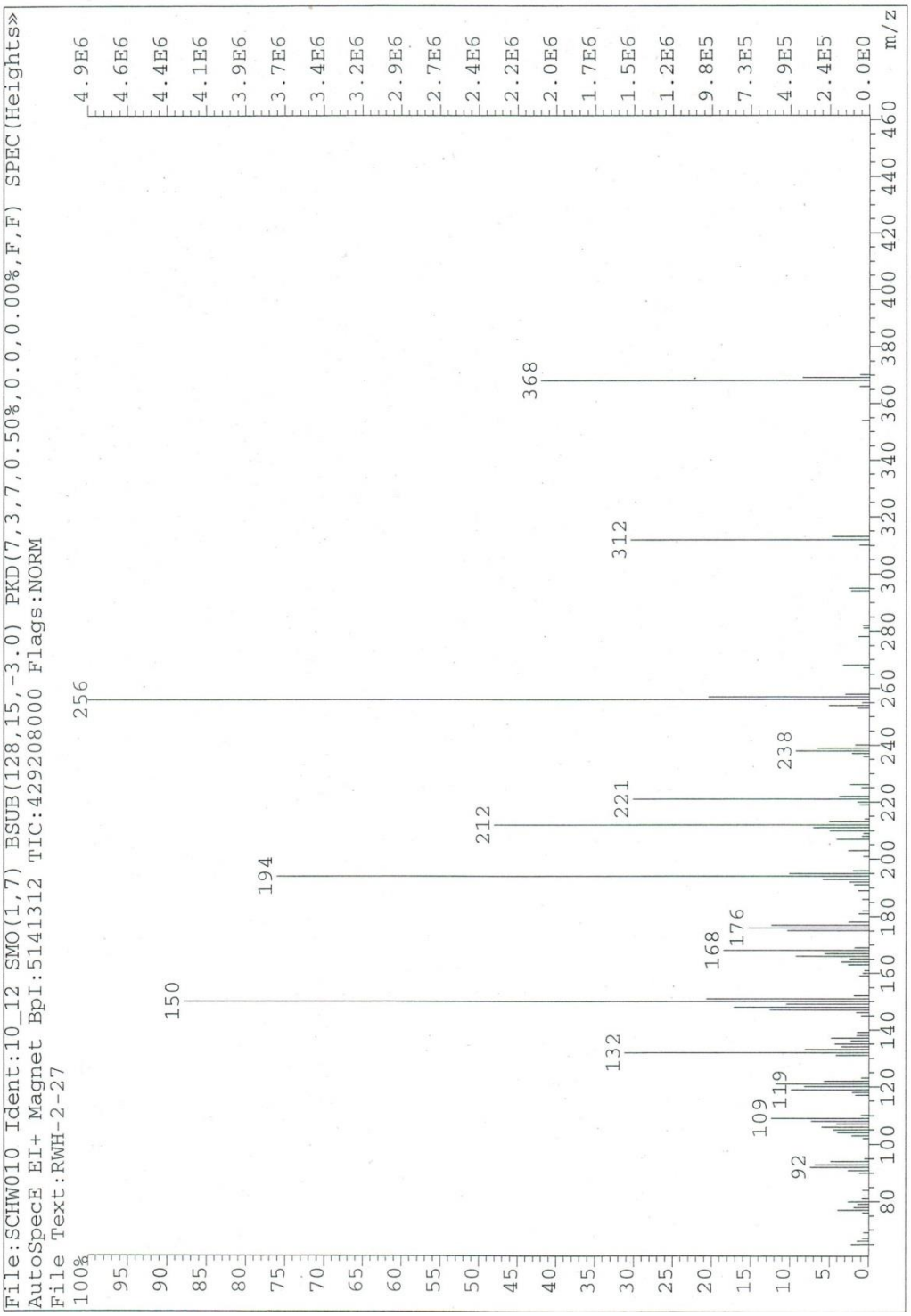
^{1}H NMR *Di-tert-butyl (2,5-bis(hydroxymethyl)-1,4-phenylene)dicarbamate* (**7**)



^{13}C NMR *Di-tert-butyl (2,5-bis(hydroxymethyl)-1,4-phenylene)dicarbamate* (**7**)



MS (EI, 70eV): *Di-tert-butyl (2,5-bis(hydroxymethyl)-1,4-phenylene)dicarbamate* (**7**)



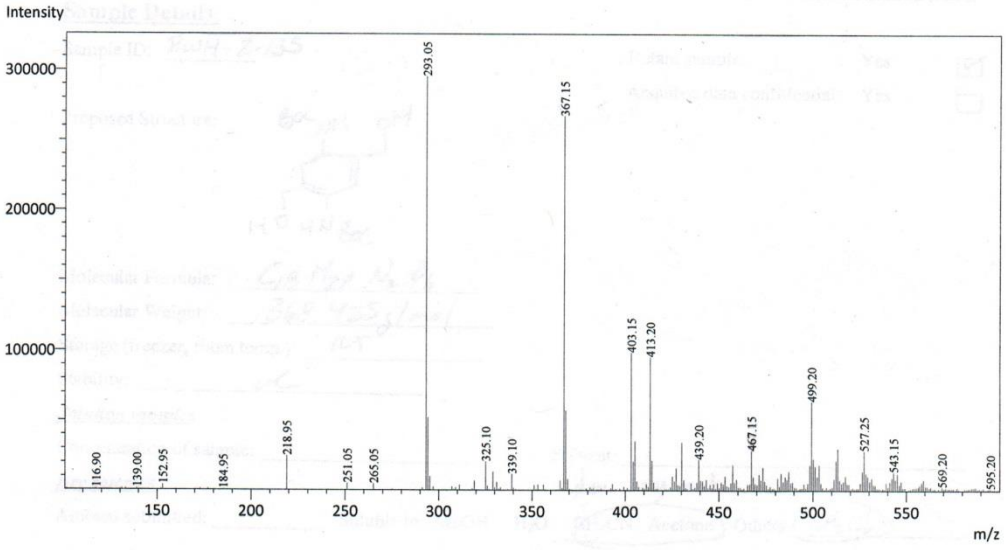
ESI-MS (DUIS, -ion) *Di-tert-butyl (2,5-bis(hydroxymethyl)-1,4-phenylene)dicarbamate* (**7**)

Shimadzu LCMS-2020 Data Report

Mass Spectrum for Sample
RWH-2-135 01.lcd

Operator: Mark Wang

Data Filename: C:\LabSolutions\Data\Schwabacher Alan\RWH-2-135 01.lcd
Spetrum Mode: Averaged
Retention Time: ----
Interface Type (ESI, APCI, DUIS): DUIS
Aquisition Mode: (Scan, SIM, Profife): Scan
Polarity: -



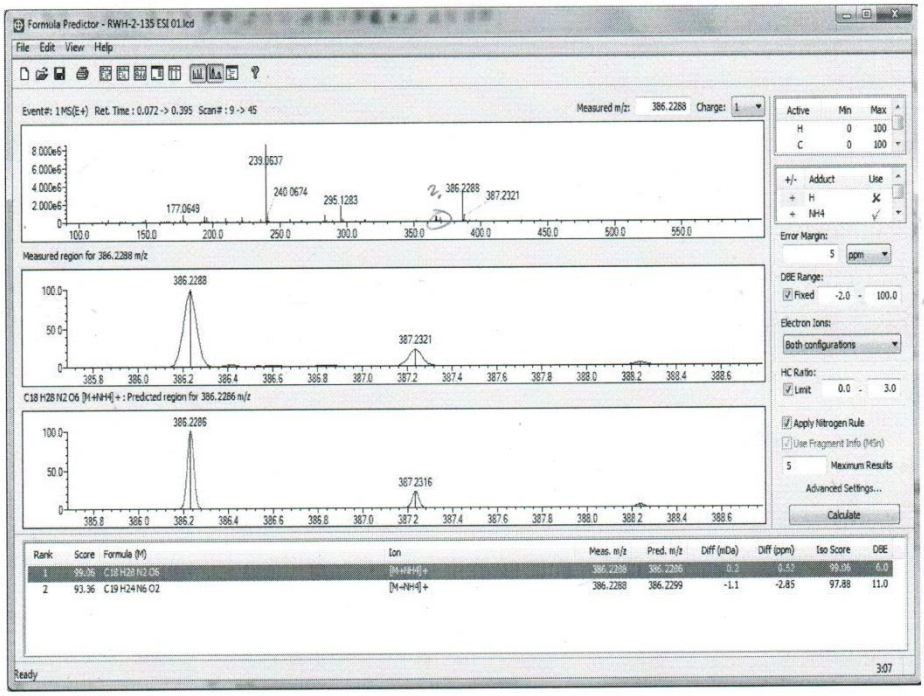
HRMS (IT-TOF) *Di-tert-butyl (2,5-bis(hydroxymethyl)-1,4-phenylene)dicarbamate* (**7**)

Shimadzu LCMS-IT-TOF Analysis Report
Feb 26, 2015

Acquired by : Mark Wang, Department of Chemistry and Biochemistry, UW-Milwaukee

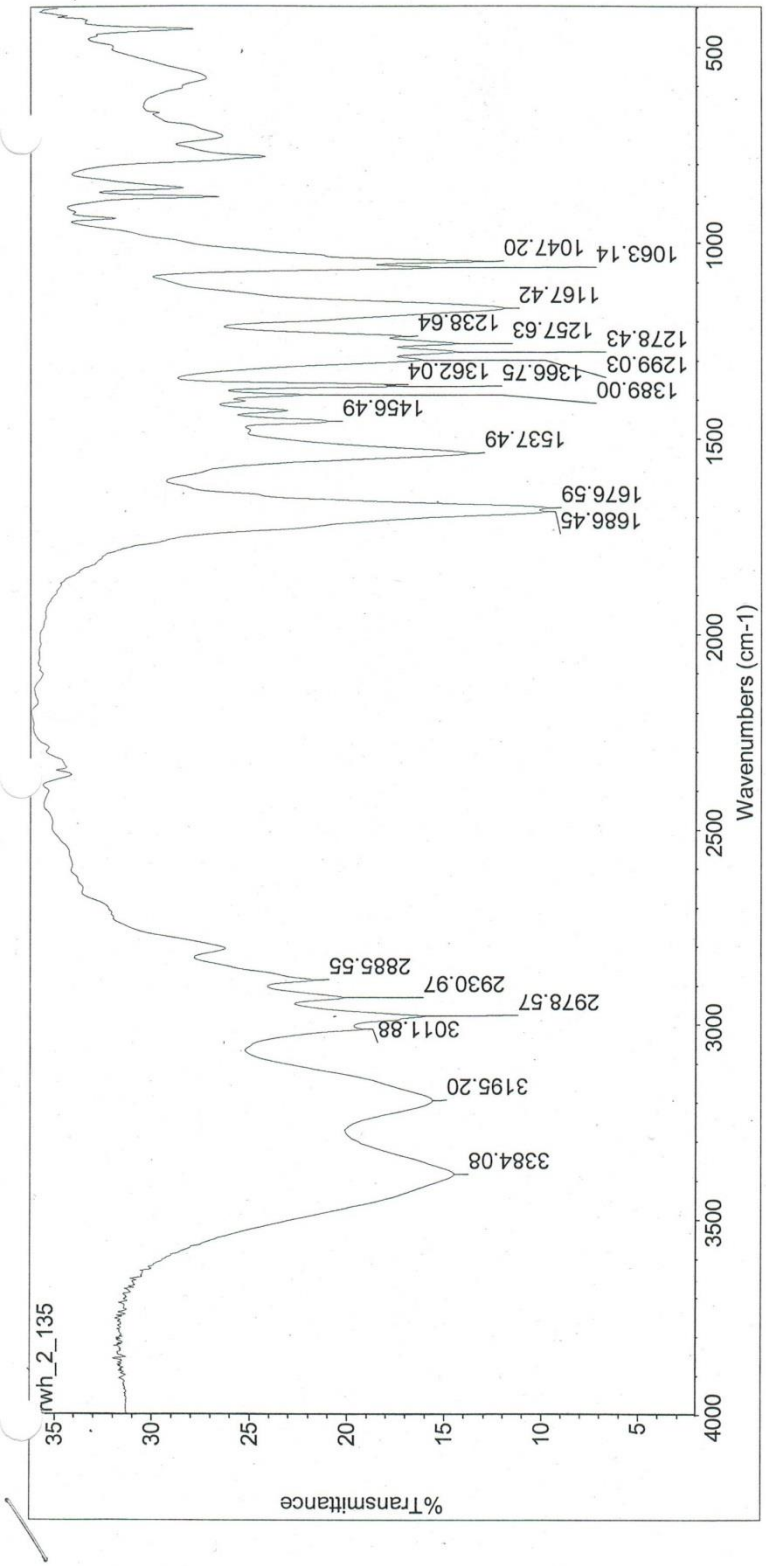
Mass analyzer type: IT-TOF
Ionization method : ESI (Electrospray Ionization)
Sample Name: RWH-2-135 ESI
Sample ID: RWH-2-135 ESI
Vail #: 21
Injection Volume: 5 uL
Data File Name: RWH-2-135 ESI 01.lcd
Method File Name: MW Manual (MS-MS, +, -).lcm
Data Acquired: 2/26/2015 2:48:09 PM
Data Processed: 2/26/2015 2:50:10 PM

Formula Prediction Results



1 / 1

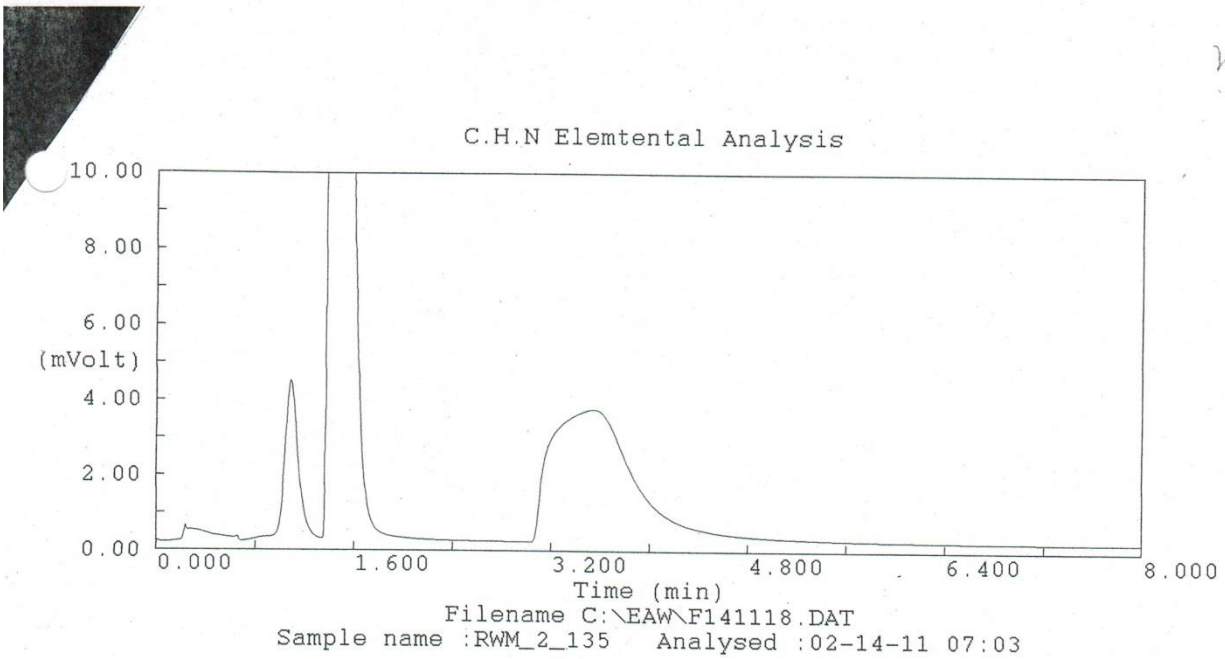
IR *Di-tert-butyl (2,5-bis(hydroxymethyl)-1,4-phenylene)dicarbamate* (**7**)



Wed Jan 26 13:41:18 2011 (GMT-06:00)
FIND PEAKS:
Spectrum: rwh_2_135 (diol)
Region: 4000.00 400.00
Absolute threshold: 22.950
Sensitivity: 70
Peak list:

Position:	1047.20	Intensity:	12.746
Position:	1063.14	Intensity:	15.445
Position:	1167.42	Intensity:	11.920
Position:	1238.64	Intensity:	17.138
Position:	1257.63	Intensity:	14.282
Position:	1278.43	Intensity:	14.368
Position:	1299.03	Intensity:	16.144
Position:	1362.04	Intensity:	17.610

Elem. Anal. *Di-tert-butyl (2,5-bis(hydroxymethyl)-1,4-phenylene)dicarbamate* (**7**)



C.H.N Elemental Analysis

/W version : 1.06
perator ID : Mark Wang
ethod Name : Minute8
nalysed : 02-14-11 07:03

Company Name : UWM Chemistry
Method File : MINUTE8.MTH
Printed : 2/15/2011 03:19

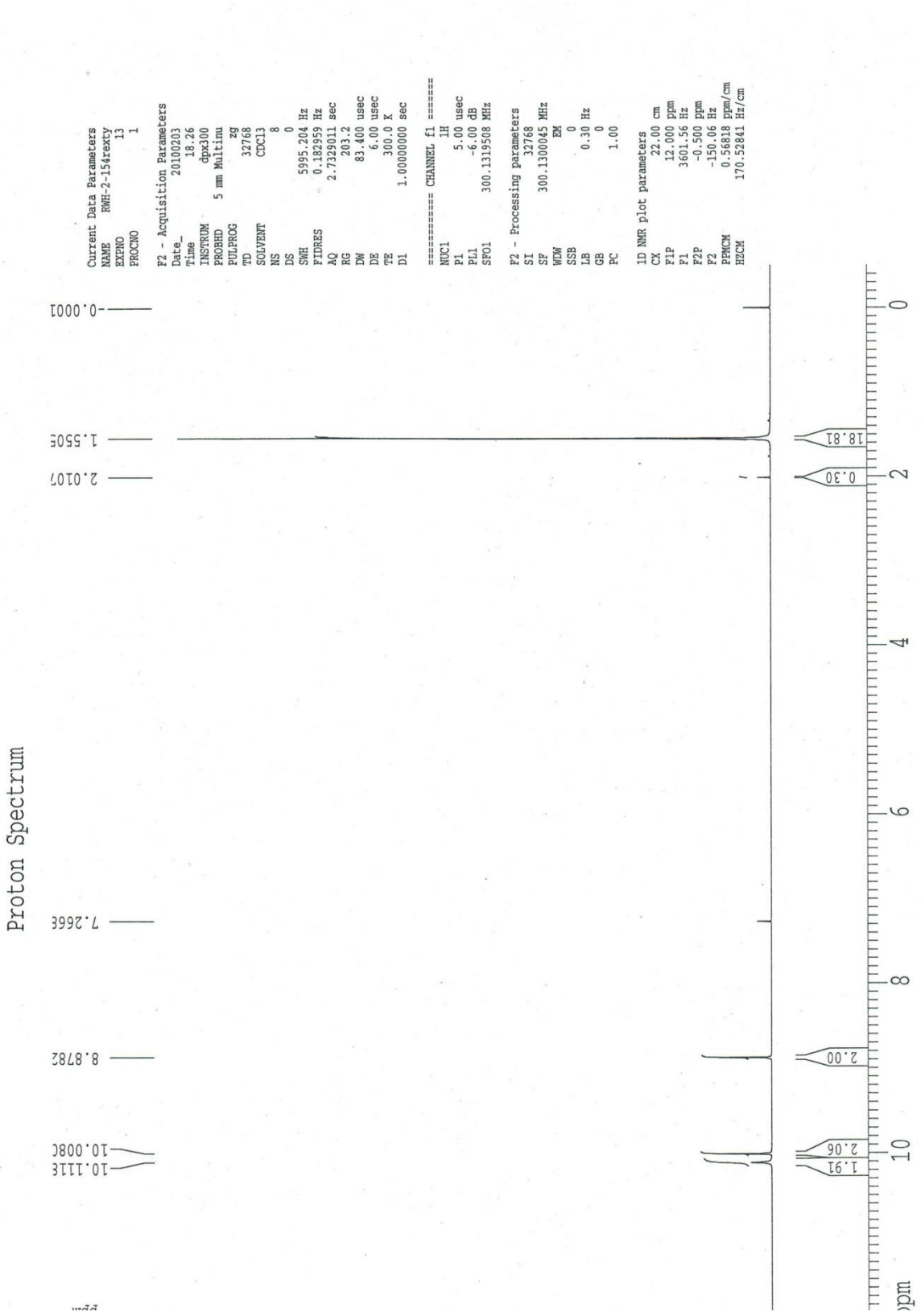
ample ID : RWM_2_135 (# 21)
nalysis Type : UnkNown (Area)
hromatogram : C:\EAW\F141118.DAT

Channel : E.A. Channel A
Sample weight : 1.493

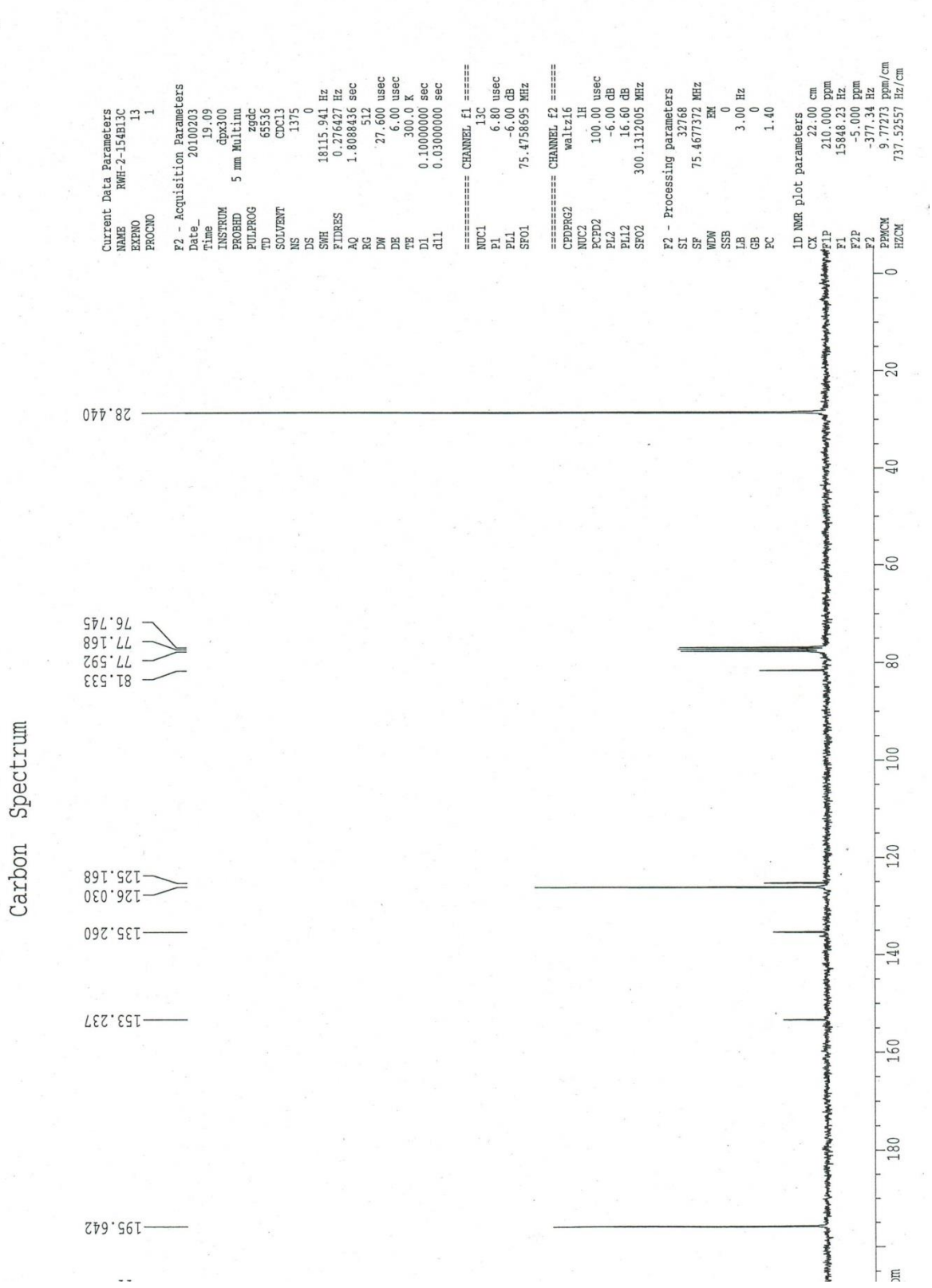
alib. method : using 'K Factors'

Element Name	Element %	Ret.Time	Area	BC	Area ratio	K factor
itrogen	7.5158	1.08	338641	FU	13.853140	.285272E+07
arbon	58.5419	1.41	4691234	FU	1.000000	.535241E+07
ydrogen	7.7307	3.53	1704779	RS	2.751813	.147704E+08

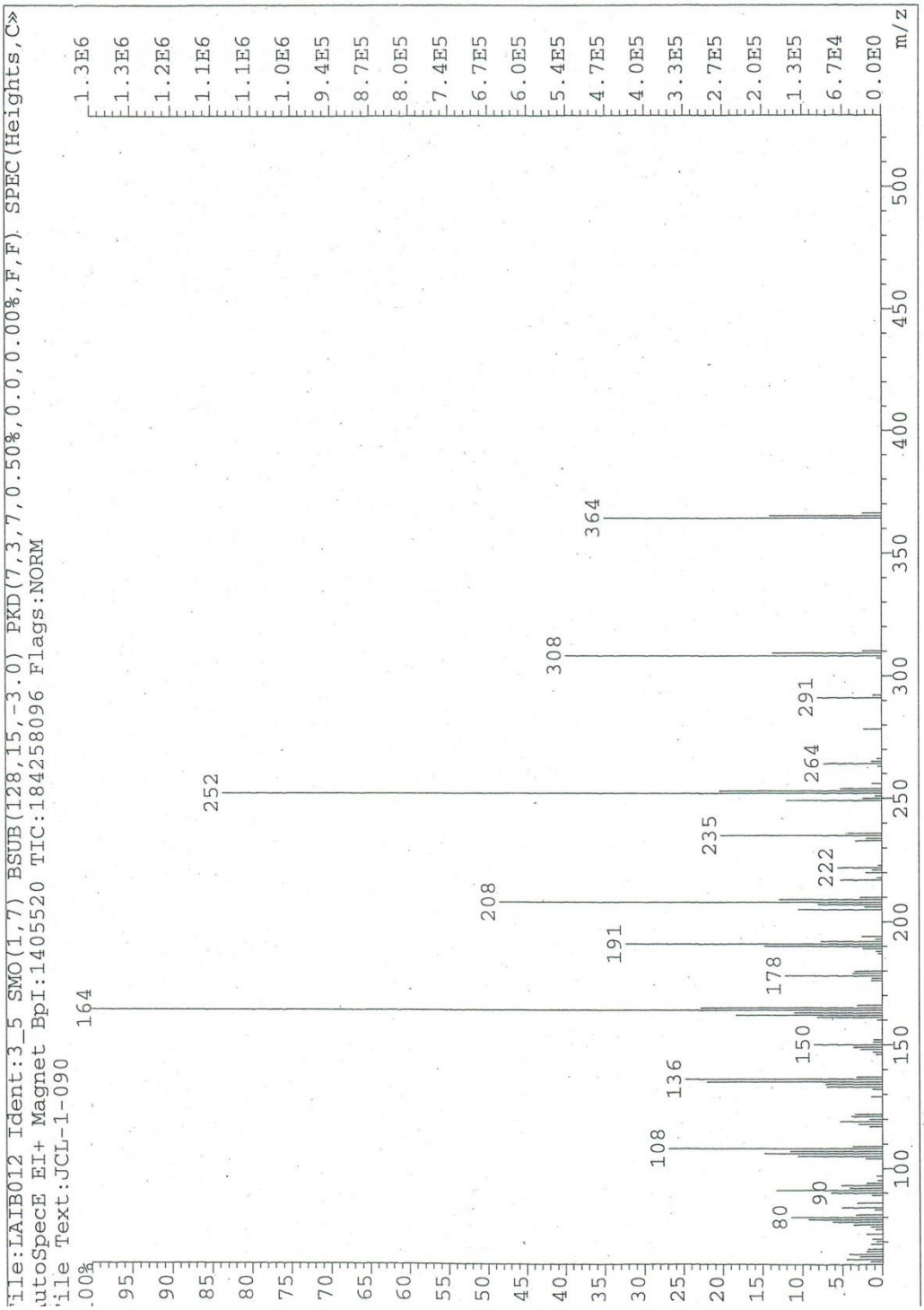
^{1}H NMR *N,N'-di-t-Boc-2,5-diaminoterephthaldehyde* (**8**)



^{13}C NMR *N,N'-di-t-Boc-2,5-diaminoterephthaldehyde* (**8**)



MS (EI, 70eV) *N,N'-di-t-Boc-2,5-diaminoterephthaldehyde* (**8**)



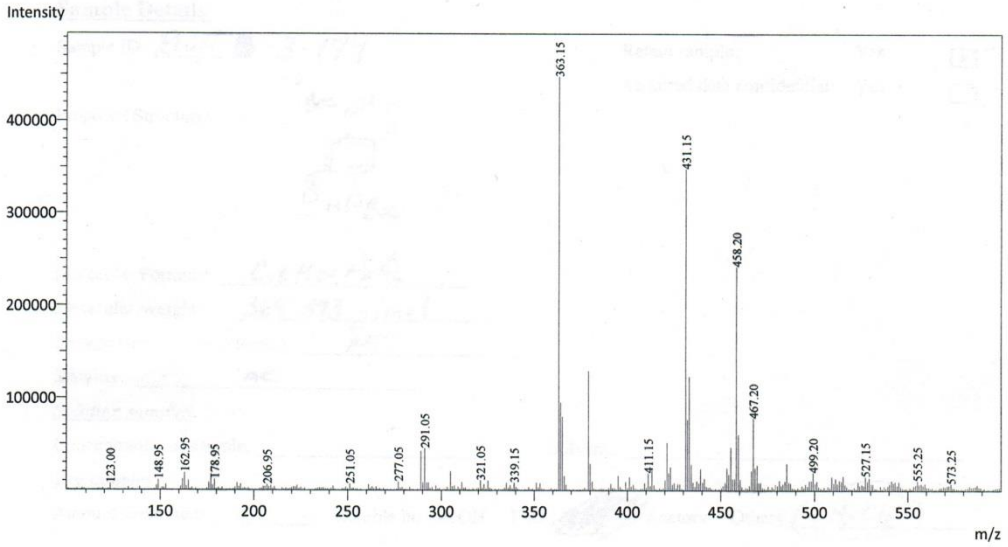
ESI-MS *N,N'-di-t-Boc-2,5-diaminoterephthaldehyde* (**8**)

Shimadzu LCMS-2020 Data Report

Mass Spectrum for Sample
RWH-3-174 01.lcd

Operator: Mark Wang

Data Filename: C:\LabSolutions\Data\Schwabacher Alan\RWH-3-174 01.lcd
Spetrum Mode: Averaged
Retention Time: ----
Interface Type (ESI, APCI, DUIS): DUIS
Aquisition Mode: (Scan, SIM, Profife): Scan
Polarity: -



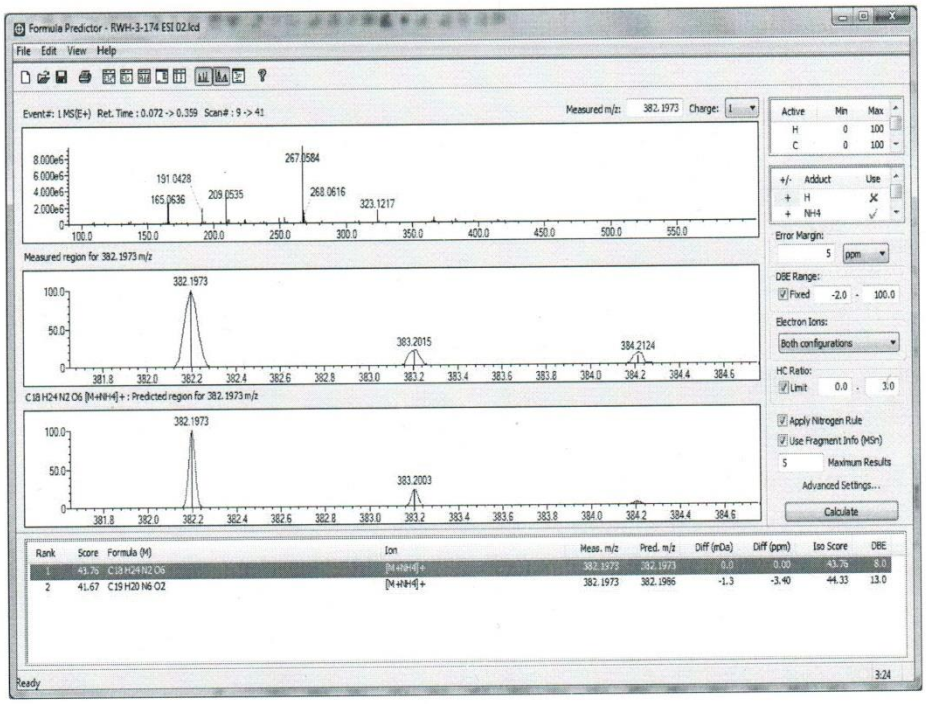
HRMS (IT-TOF) *N,N'-di-t-Boc-2,5-diaminoterephthaldehyde* (**8**)

Shimadzu LCMS-IT-TOF Analysis Report
Feb 26, 2015

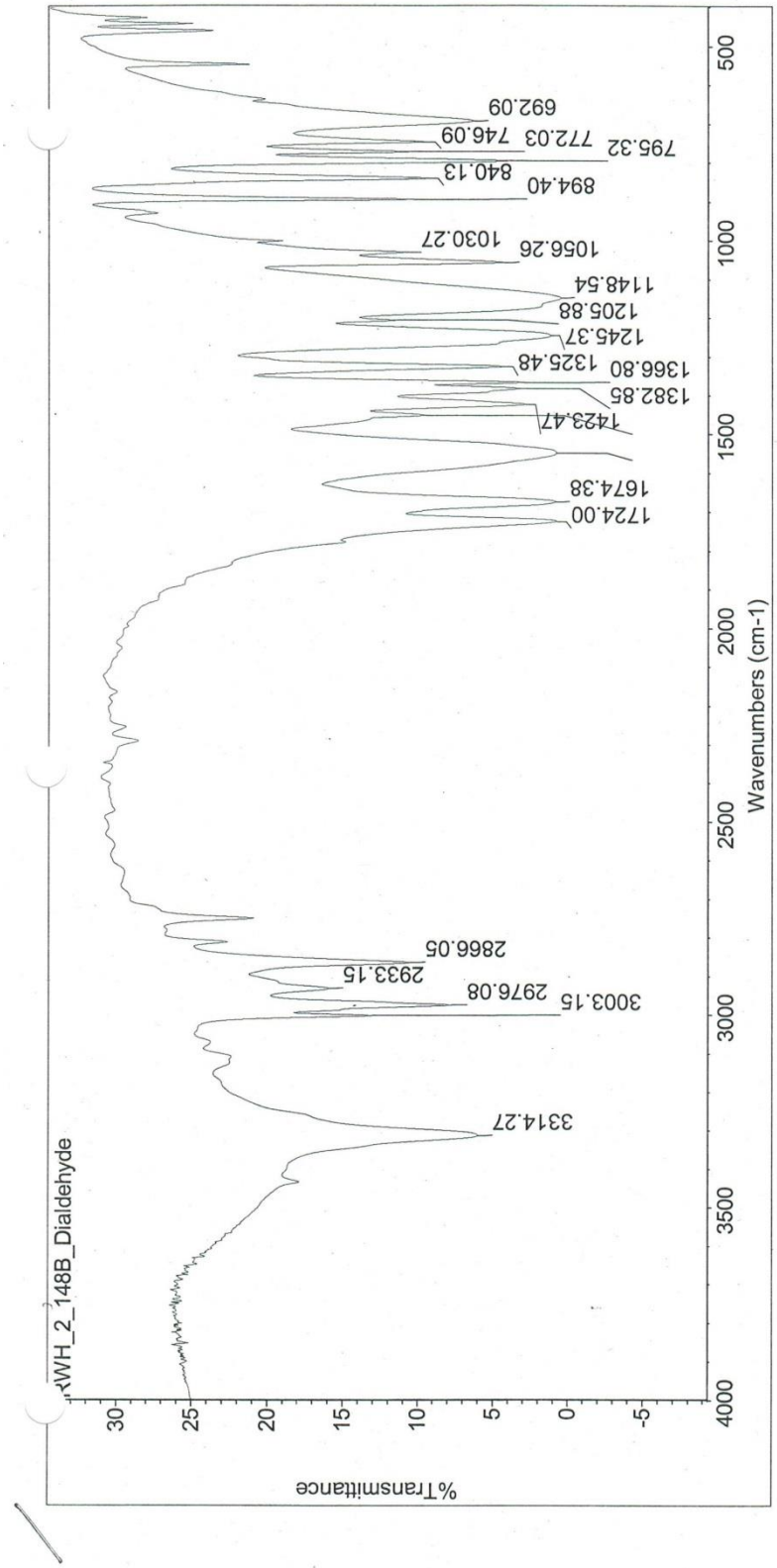
Acquired by : Mark Wang, Department of Chemistry and Biochemistry, UW-Milwaukee

Mass analyzer type: IT-TOF
Ionization method : ESI (Electrospray Ionization)
Sample Name: RWH-3-174 ESI
Sample ID: RWH-3-174 ESI
Vail #: 1
Injection Volume: 5 uL
Data File Name: RWH-3-174 ESI 02.lcd
Method File Name: MW Manual (MS-MS, +, -).lcm
Data Acquired: 2/26/2015 3:20:38 PM
Data Processed: 2/26/2015 3:22:42 PM

Formula Prediction Results



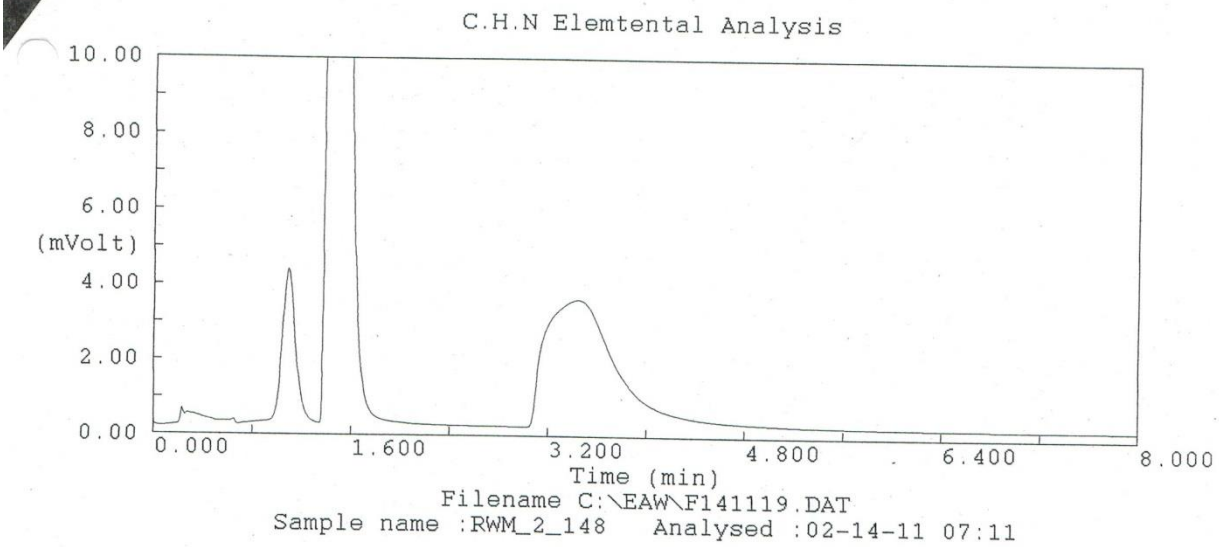
IR (KBr pellet) *N,N'-di-t-Boc-2,5-diaminoterephthaldehyde* (**8**)



Wed Jan 26 14:04:06 2011 (GMT-06:00)
FIND PEAKS:
Spectrum: RWH_2_148B_Dialdehyde
Region: 4000.00 400.00
Absolute threshold: 17.458
Sensitivity: 65
Peak list:

Position:	692.09	Intensity:	6.304
Position:	746.09	Intensity:	9.364
Position:	772.03	Intensity:	10.310
Position:	795.32	Intensity:	3.798
Position:	840.13	Intensity:	9.137
Position:	894.40	Intensity:	9.713
Position:	1030.27	Intensity:	10.776
Position:	1056.26	Intensity:	4.127

Elem. Anal. *N,N'-di-t-Boc-2,5-diaminoterephthaldehyde* (**8**)



C.H.N Elemental Analysis

/w version : 1.06
perator ID : Mark Wang
ethod Name : Minute8
nalysed : 02-14-11 07:11

Company Name : UWM Chemistry
Method File : MINUTE8.MTH
Printed : 2/15/2011 03:21

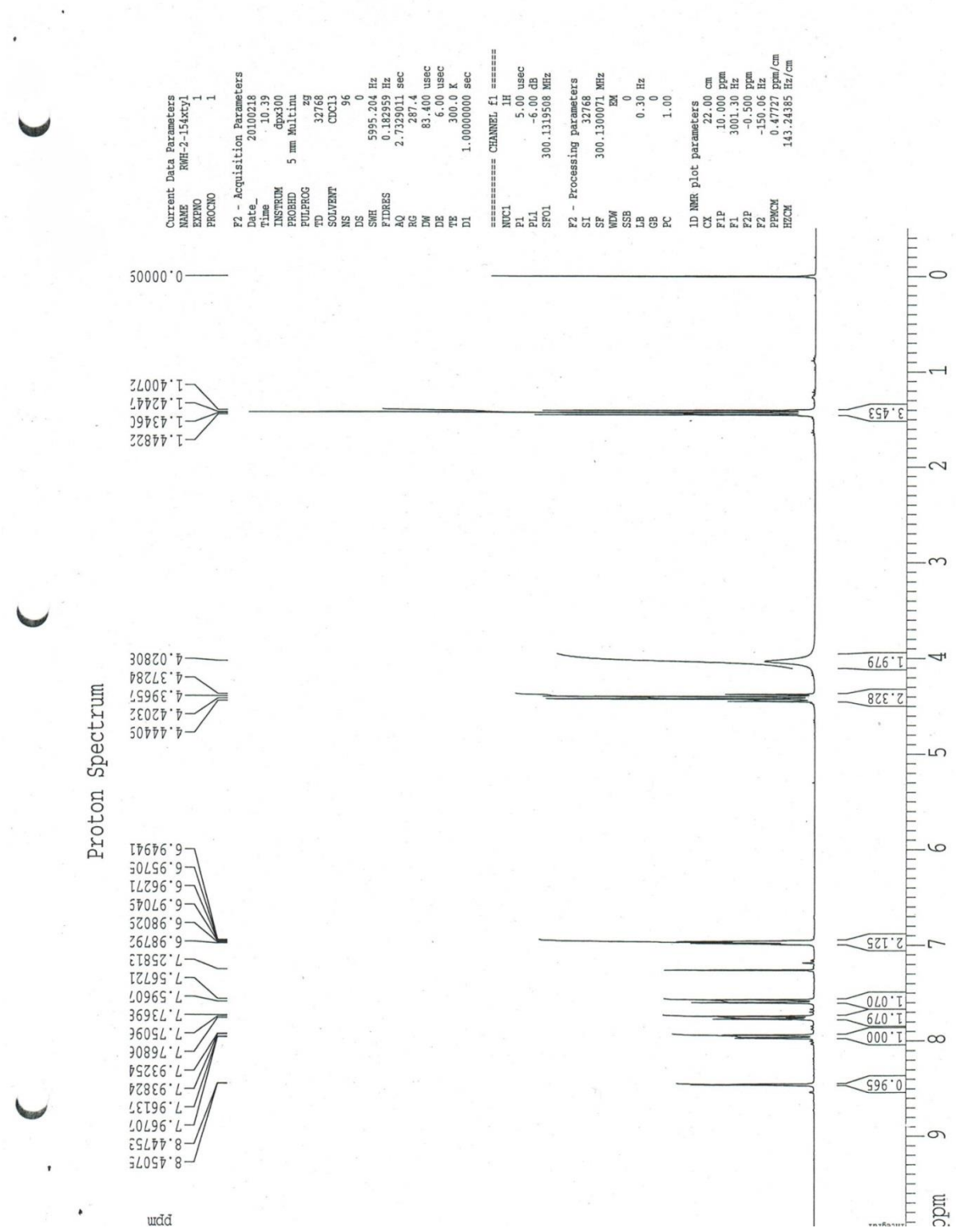
ample ID : RWM_2_148 (# 22)
nalysis Type : UnkNown (Area)
nromatogram : C:\EAW\F141119.DAT

Channel : E.A. Channel A
Sample weight : 1.485

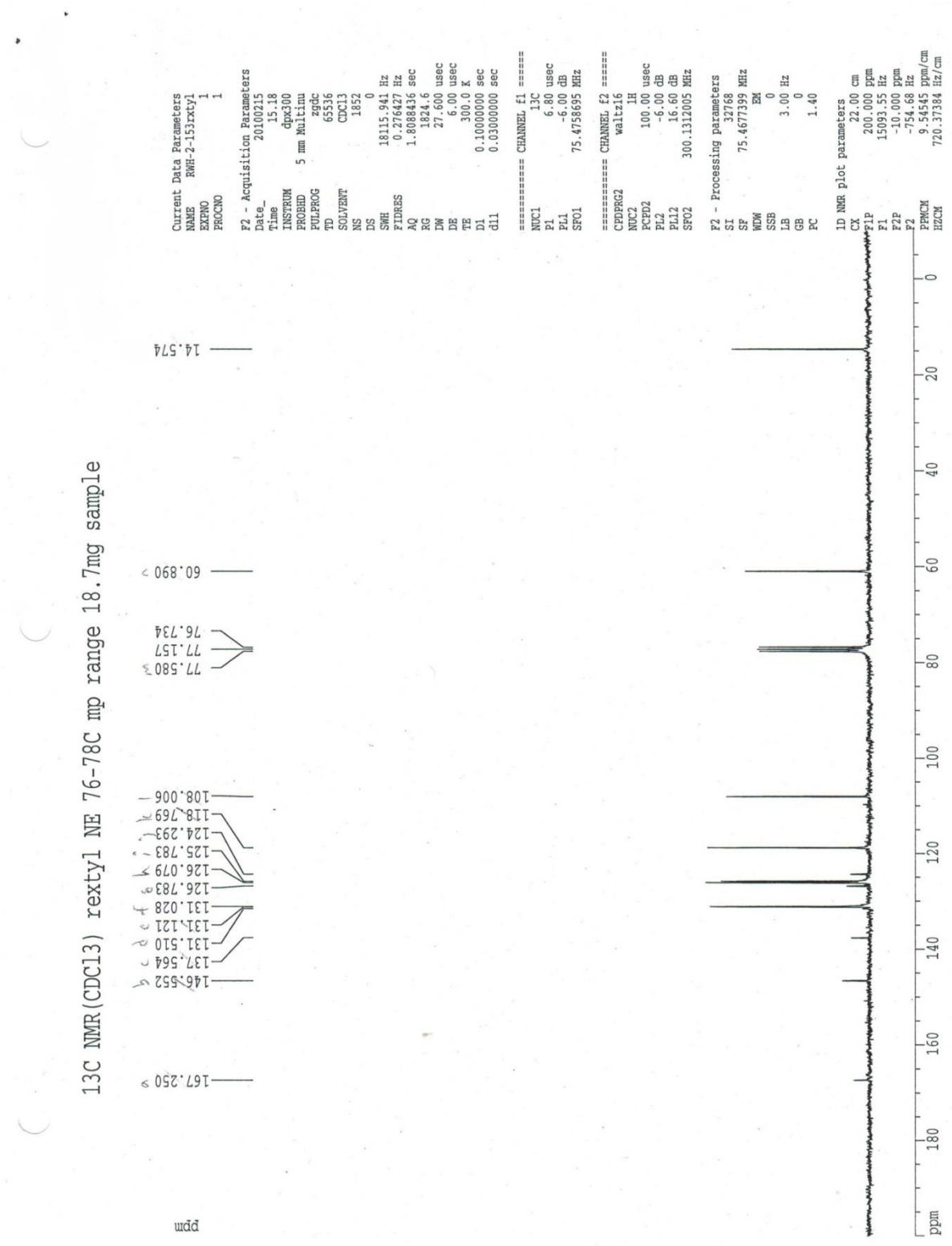
alib. method : using 'K Factors'

Element Name	Element %	Ret.Time	Area	BC	Area ratio	K factor
itrogen	7.2235	1.08	324540	FU	13.923130	.285272E+07
arbon	56.6855	1.42	4518617	FU	1.000000	.535241E+07
ydrogen	6.4252	3.44	1409310	RS	3.206262	.147704E+08

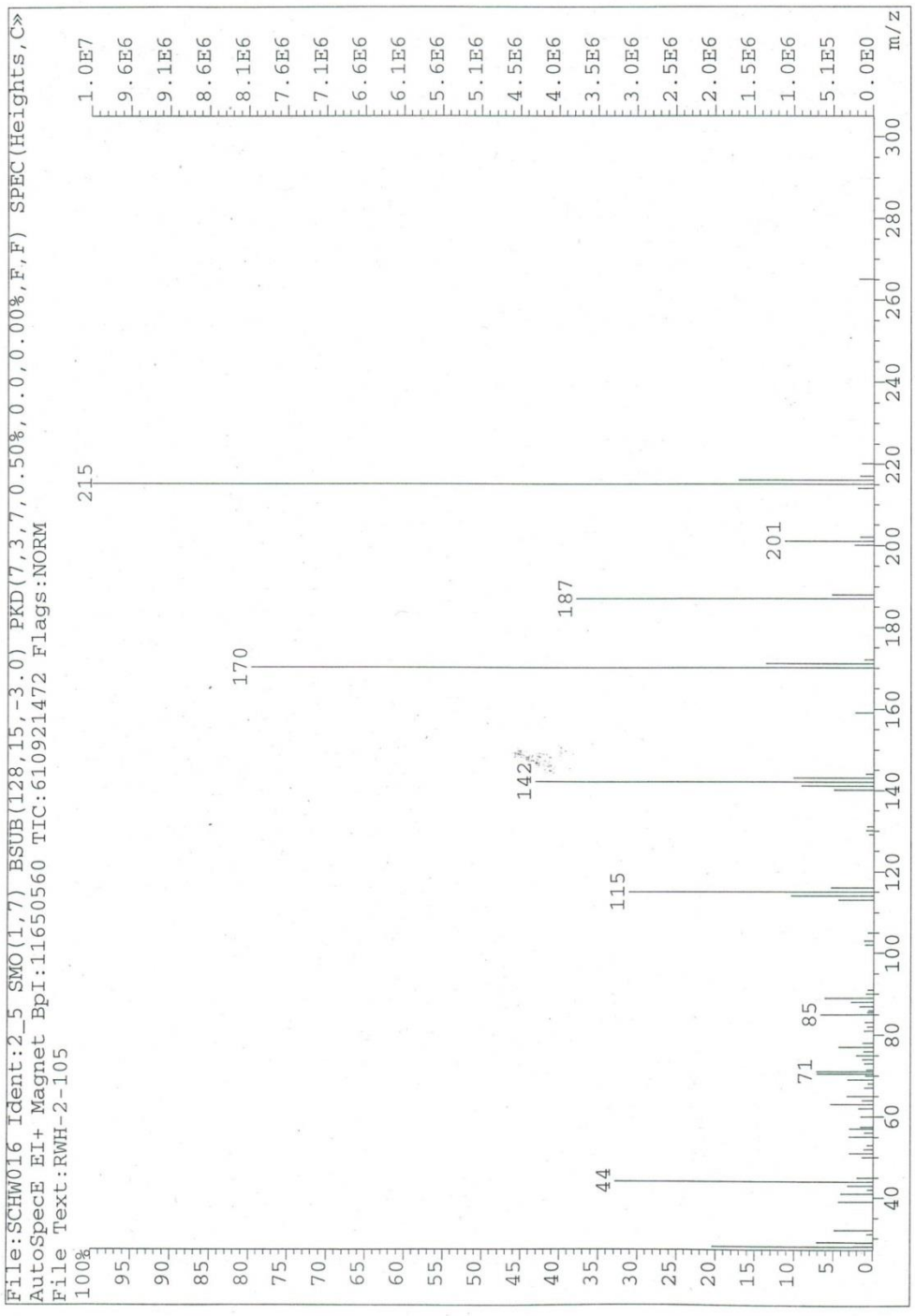
^{1}H NMR *Ethyl 6-amino-2-naphthoate* (**12**)



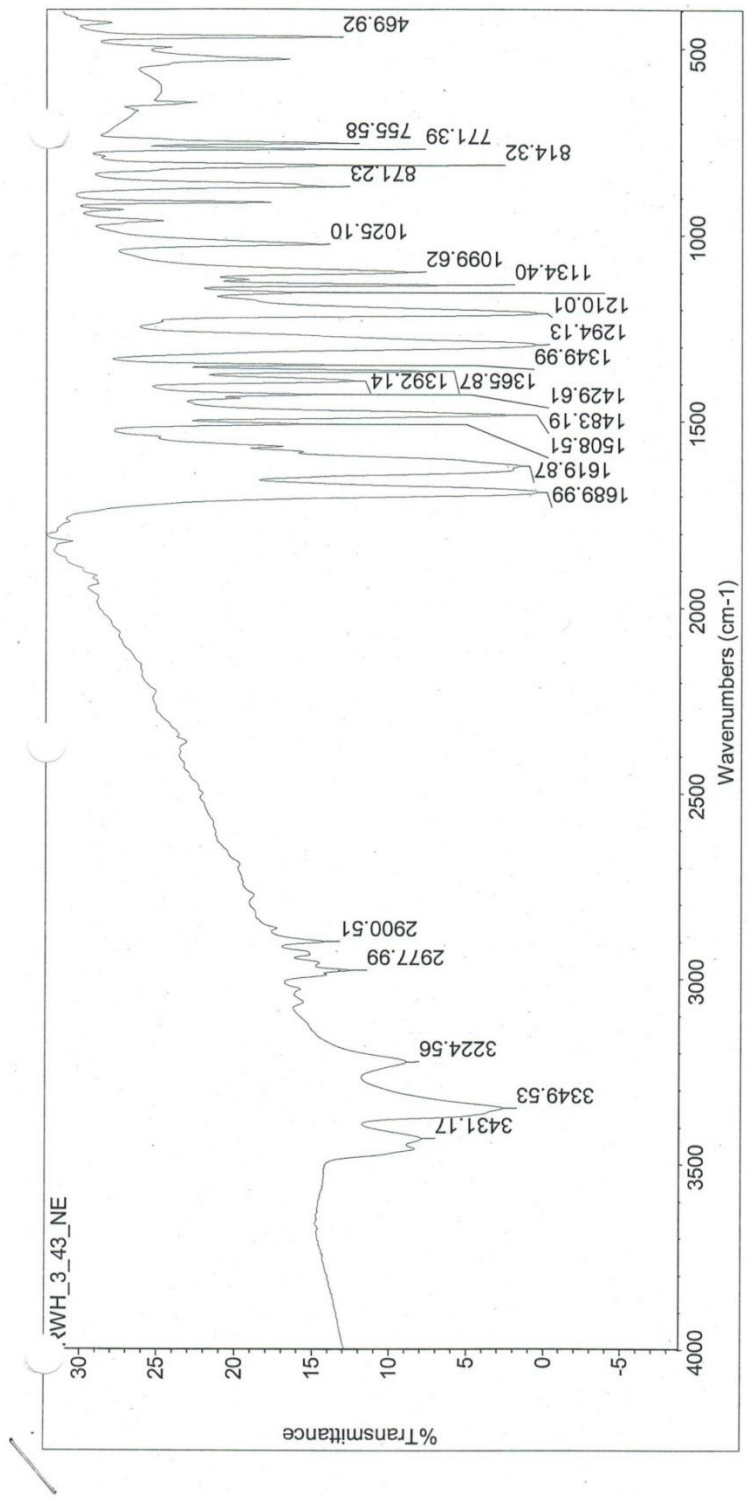
^{13}C NMR *Ethyl 6-amino-2-naphthoate* (**12**)



MS *Ethyl 6-amino-2-naphthoate* (**12**)



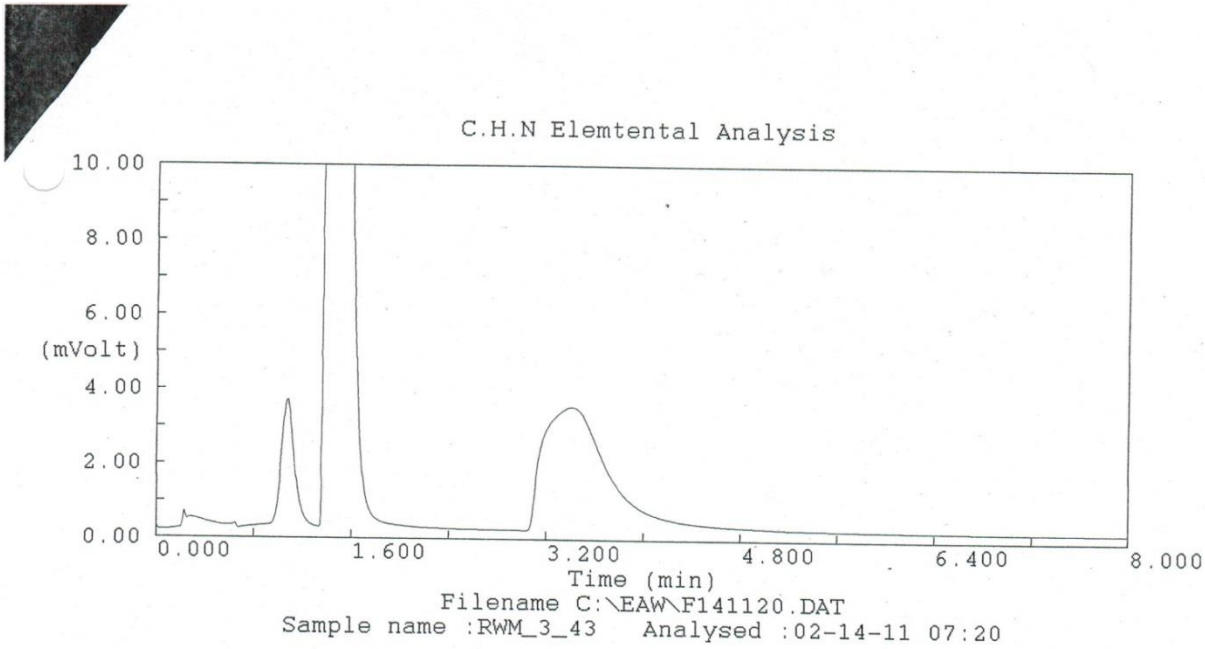
IR *<u>Ethyl 6-amino-2-naphthoate</u>* (**12**)



Wed Jan 26 14:27:26 2011 (GMT-06:00)
FIND PEAKS:
Spectrum: RWH_3_43_NE
Region: 4000.00 400.00
Absolute threshold: 16.295
Sensitivity: 50
Peak list:

Position:	469.92	Intensity:	12.992
Position:	755.58	Intensity:	12.229
Position:	771.39	Intensity:	13.633
Position:	814.32	Intensity:	13.489
Position:	871.23	Intensity:	13.466
Position:	1025.10	Intensity:	14.686
Position:	1099.62	Intensity:	8.575
Position:	1134.40	Intensity:	5.651

Elem. Anal. *Ethyl 6-amino-2-naphthoate* (**NE**)



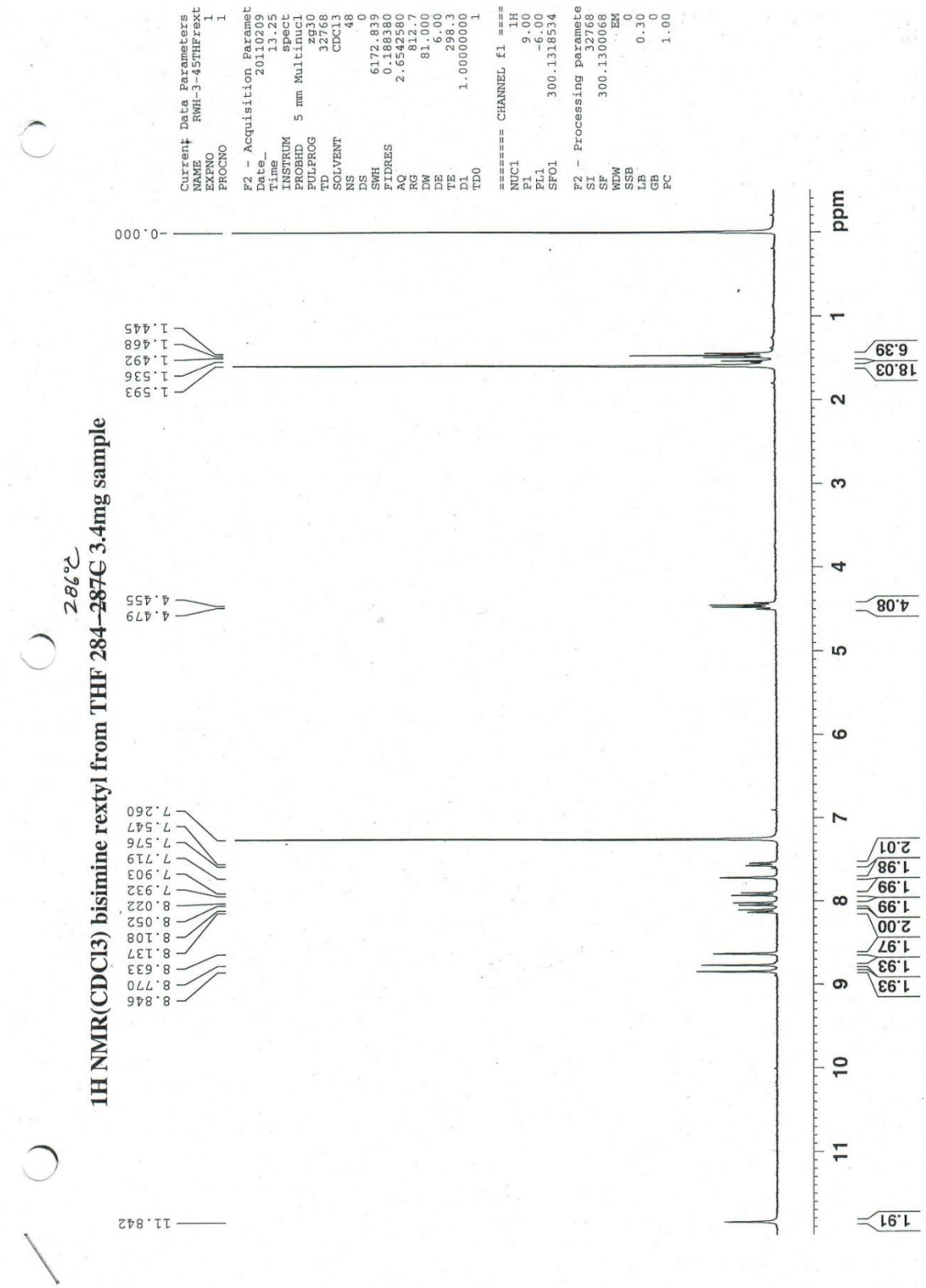
C.H.N Elemental Analysis

S/W version	: 1.06		
Operator ID	: Mark Wang	Company Name	: UWM Chemistry
Method Name	: Minute8	Method File	: MINUTE8.MTH
Analysed	: 02-14-11 07:20	Printed	: 2/15/2011 03:23
Sample ID	: RWM_3_43 (# 23)	Channel	: E.A. Channel A
Analysis Type	: UnkNown (Area)	Sample weight	: 1.436
Chromatogram	: C:\EAW\F141120.DAT		

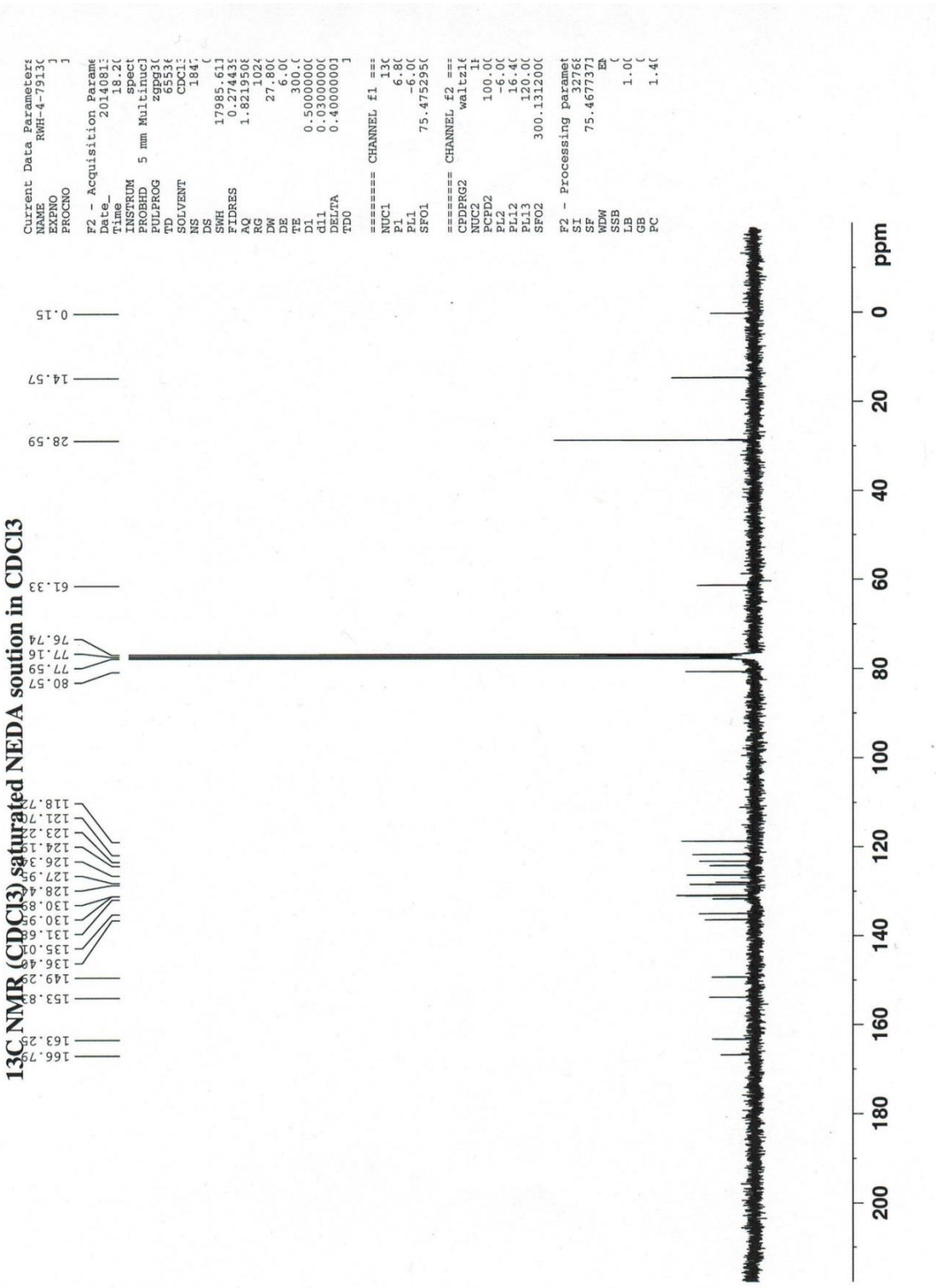
Calib. method : using 'K Factors'

Element Name	Element %	Ret.Time	Area	BC	Area ratio	K factor
Nitrogen	6.3557	1.07	278897	FU	19.840360	.285272E+07
Carbon	71.8228	1.40	5533412	FU	1.000000	.535241E+07
Hydrogen	6.1295	3.41	1300089	RS	4.256179	.147704E+08

^{1}H NMR *Diethyl 6,6'-((1E,1'E)-((2,5-bis((tert-butoxycarbonyl)amino)-1,4-phenylene)bis(methanylylidene))bis(azanylylidene))bis(2-naphthoate)* (**13**)



^{13}C NMR *Diethyl 6,6'-((1E,1'E)-((2,5-bis((tert-butoxycarbonyl)amino)-1,4-phenylene)bis(methanylylidene))bis(azanylylidene))bis(2-naphthoate)* (**13**)



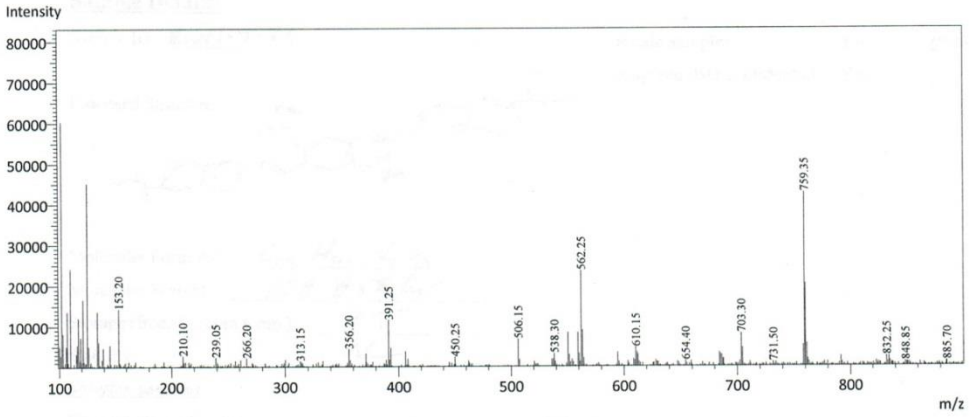
ESI-MS *Diethyl 6,6'-((1E,1'E)-((2,5-bis((tert-butoxycarbonyl)amino)-1,4-phenylene)bis(methanylylidene))bis(azanylylidene))bis(2-naphthoate)* (**13**)

Shimadzu LCMS-2020 Data Report

Mass Spectrum for Sample
RWH-4-80.lcd

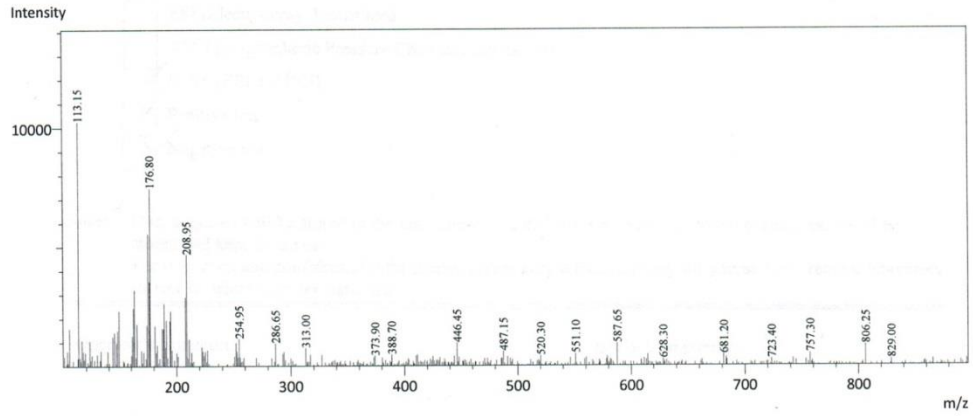
Operator:Tyler Fenske

Data Filename: C:\LabSolutions\Data\Schwabacher Alan\RWH-4-80.lcd
Spetrum Mode: Averaged
Retention Time: ----
Interface Type (ESI, APCI, DUIS): DUIS
Aquisition Mode: (Scan, SIM, Profife): Scan
Polarity: +
H2O/0.1% HCOOH, CH3CN/0.1% HCOOH

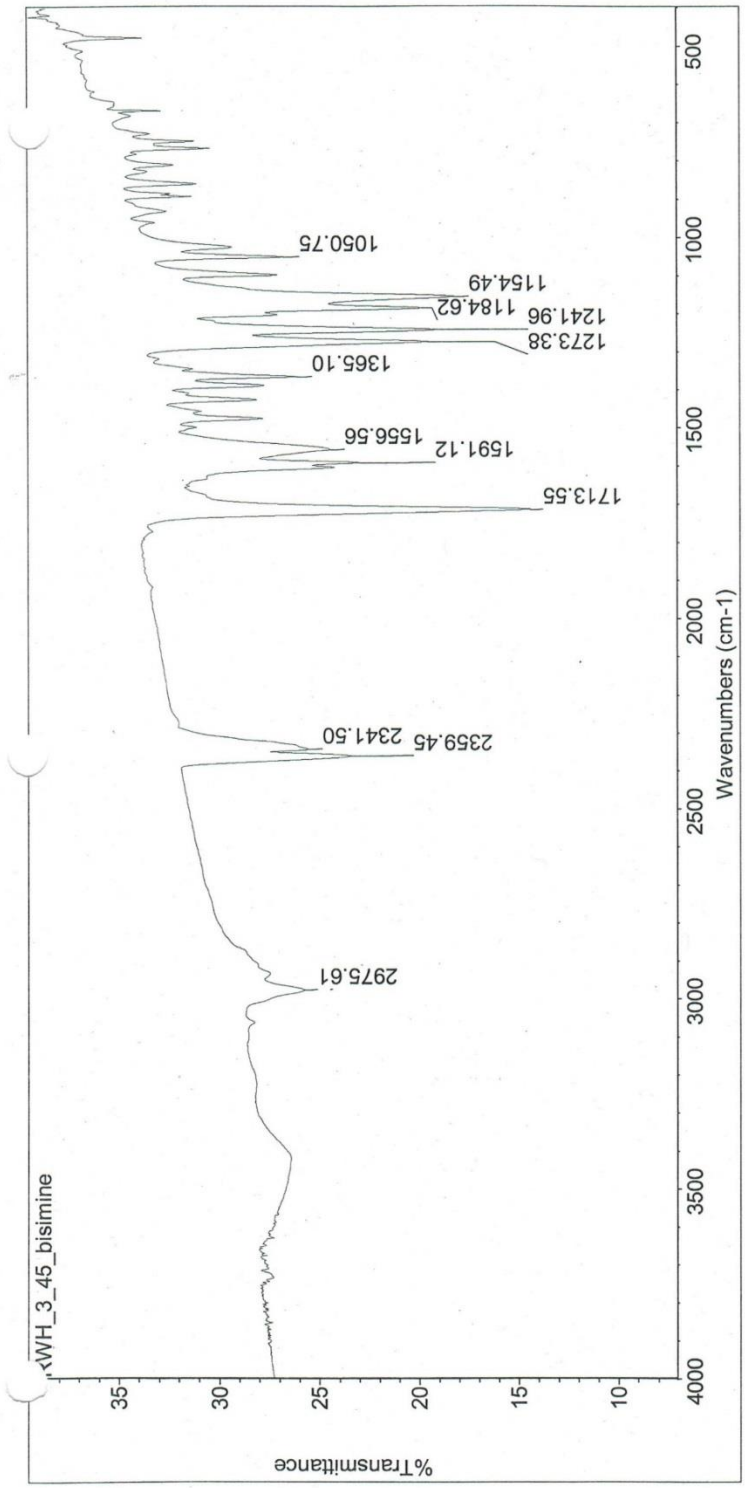


Operator:Tyler Fenske

Data Filename: C:\LabSolutions\Data\Schwabacher Alan\RWH-4-80.lcd
Spetrum Mode: Averaged
Retention Time: ----
Interface Type (ESI, APCI, DUIS): DUIS
Aquisition Mode: (Scan, SIM, Profife): Scan
Polarity: -
H2O/0.1% HCOOH, CH3CN/0.1% HCOOH



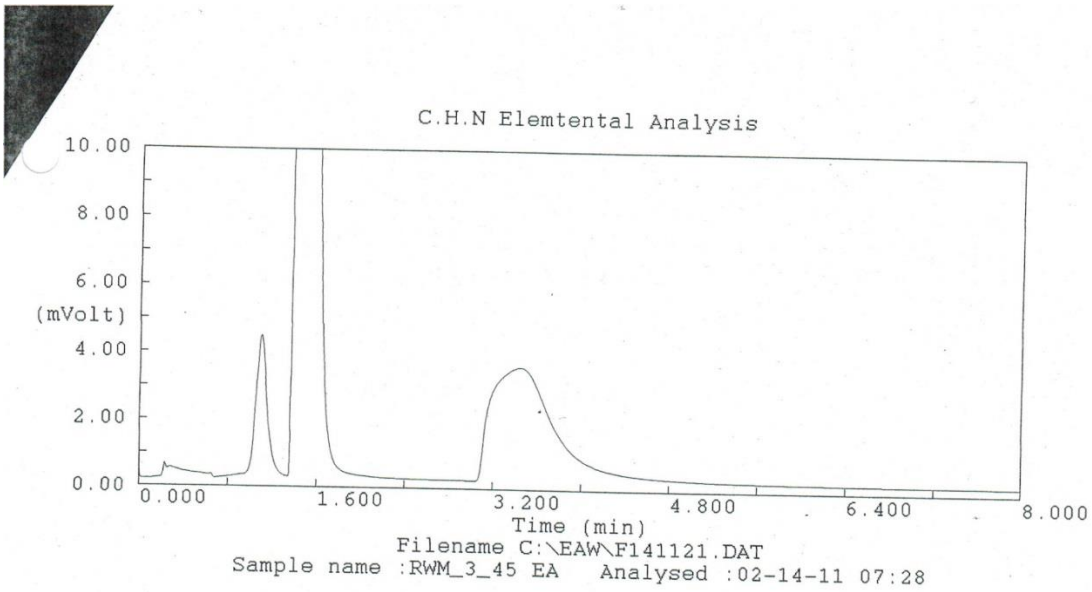
IR *Diethyl 6,6'-((1E,1'E)-((2,5-bis((tert-butoxycarbonyl)amino)-1,4-phenylene)bis(methanylylidene))bis(azanylylidene))bis(2-naphthoate)* (**13**)



Wed Feb 09 14:43:38 2011 (GMT-06:00)
FIND PEAKS:
Spectrum: RWH_3_45_bisimine
Region: 4000.00 400.00
Absolute threshold: 26.926
Sensitivity: 37
Peak list:

Position:	1050.75	Intensity:	26.658
Position:	1154.49	Intensity:	18.146
Position:	1184.62	Intensity:	19.705
Position:	1241.96	Intensity:	19.060
Position:	1273.38	Intensity:	19.369
Position:	1365.10	Intensity:	26.031
Position:	1556.56	Intensity:	24.452
Position:	1591.12	Intensity:	22.840

Elem. Anal. *Diethyl 6,6'-((1E,1'E)-((2,5-bis((tert-butoxycarbonyl)amino)-1,4-phenylene)bis(methanylylidene))bis(azanylylidene))bis(2-naphthoate)* (**13**)



C.H.N Elemental Analysis

/W ersion : 1.06
perator ID : Mark Wang
ethod Name : Minute8
nalysed : 02-14-11 07:28

Company Name : UWM Chemistry
Method File : MINUTE8.MTH
Printed : 2/15/2011 03:25

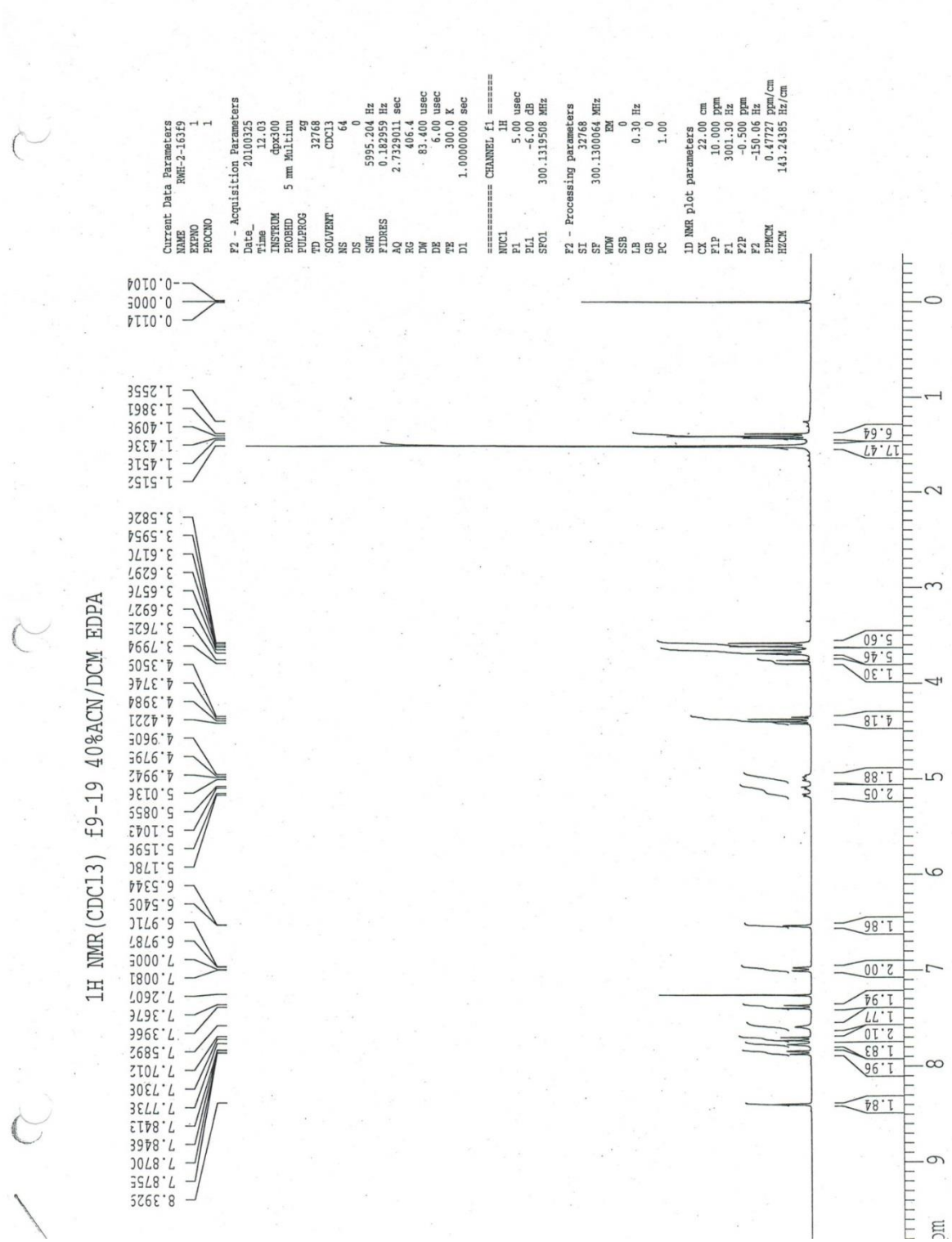
ample ID : RWM_3_45 EA (# 24)
nalysis Type : UnkNown (Area)
hromatogram : C:\EAW\F141121.DAT

Channel : E.A. Channel A
Sample weight : 1.547

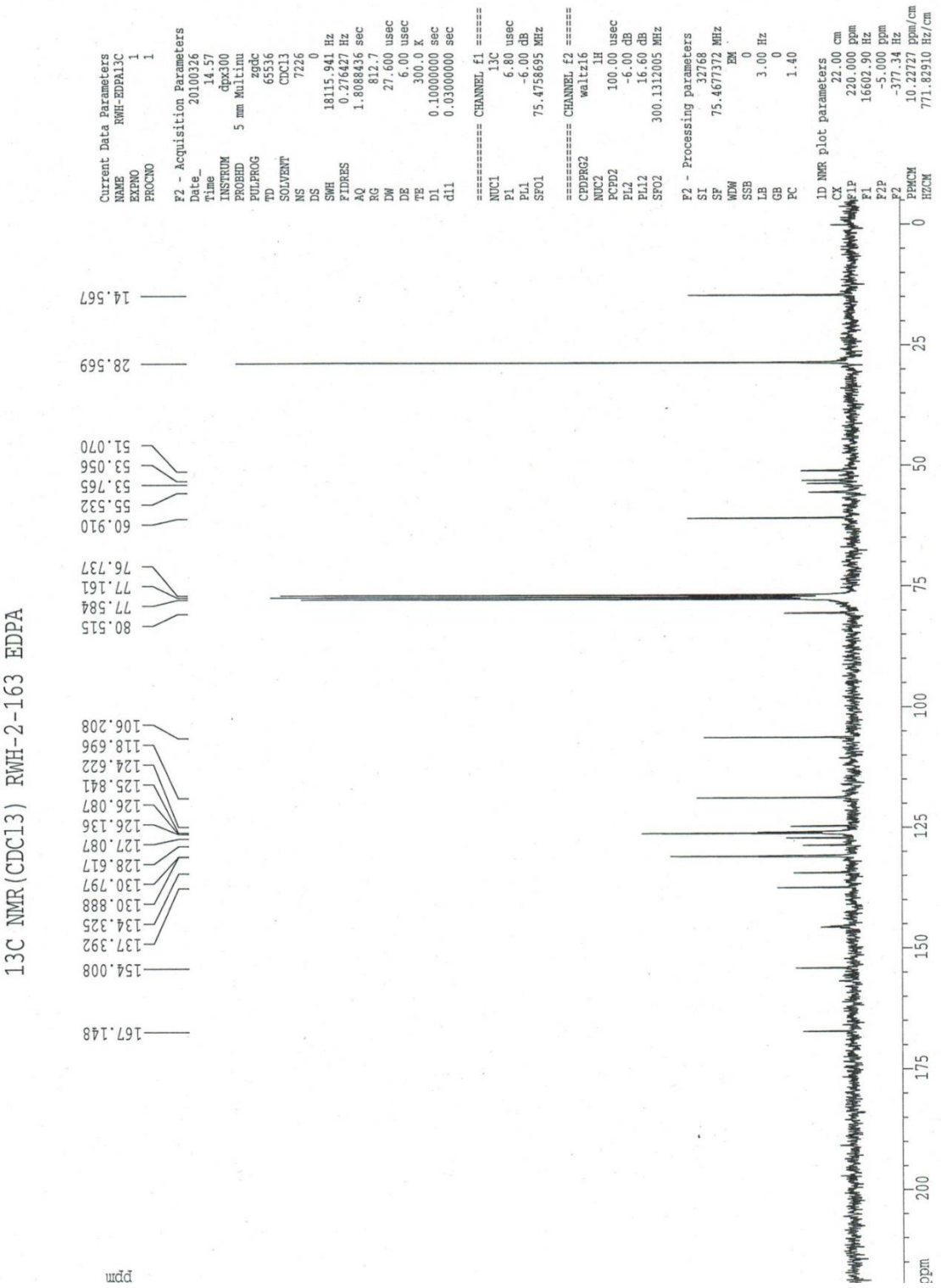
alib. method : using 'K Factors'

Element Name	Element %	Ret.Time	Area	BC	Area ratio	K factor
itrogen	6.7996	1.09	318612	FU	17.569540	.285272E+07
arbon	67.4477	1.41	5597861	TL	1.000000	.535241E+07
ydrogen	6.1159	3.44	1397467	CR	4.005720	.147704E+08

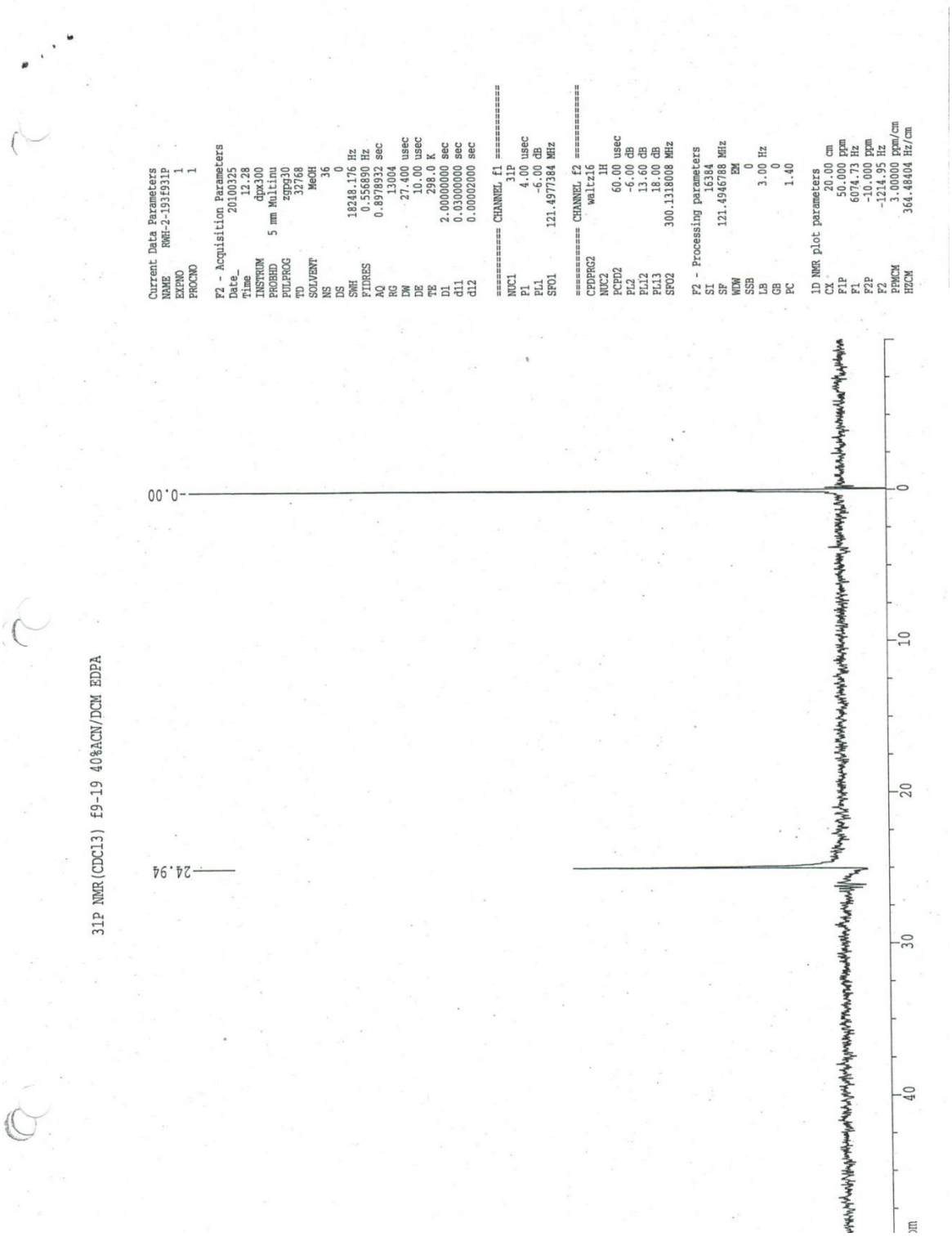
^{1}H NMR *Diethyl 6,6'-(((1R,1'S)-(2,5-bis((tert-butoxycarbonyl)amino)-1,4-phenylene)bis((dimethoxyphosphoryl)methylene))bis(azanediyl))bis(2-naphthoate)* (**16**)



^{13}C NMR *Diethyl 6,6'-(((1R,1'S)-(2,5-bis((tert-butoxycarbonyl)amino)-1,4-phenylene)bis((dimethoxyphosphoryl)methylene))bis(azanediyl))bis(2-naphthoate)* (**16**)



^{31}P NMR *Diethyl 6,6'-(((1R,1'S)-(2,5-bis((tert-butoxycarbonyl)amino)-1,4-phenylene)bis((dimethoxyphosphoryl)methylene))bis(azanediyl))bis(2-naphthoate)* (**16**)



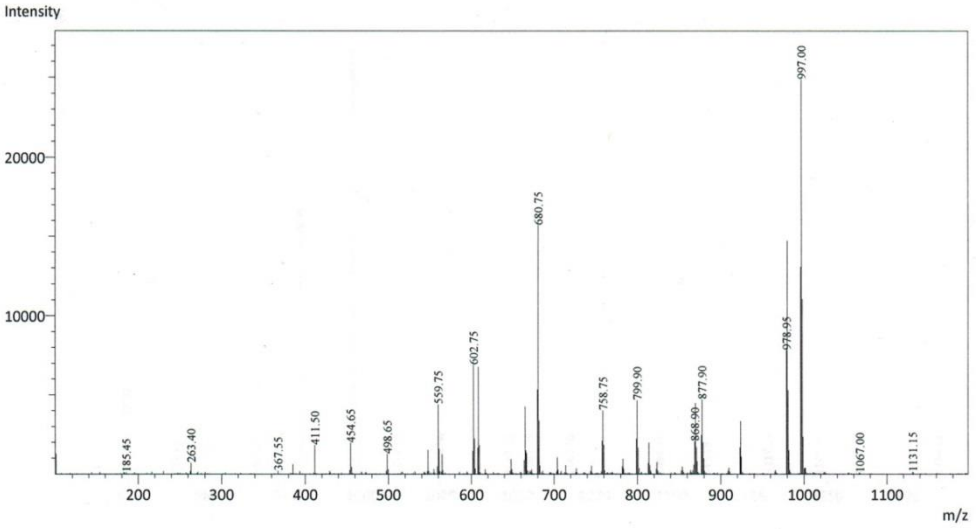
ESI-MS *Diethyl 6,6'-(((1R,1'S)-(2,5-bis((tert-butoxycarbonyl)amino)-1,4-phenylene)bis((dimethoxyphosphoryl)methylene))bis(azanediyl))bis(2-naphthoate)* (**16**)

Shimadzu LCMS-2020 Data Report

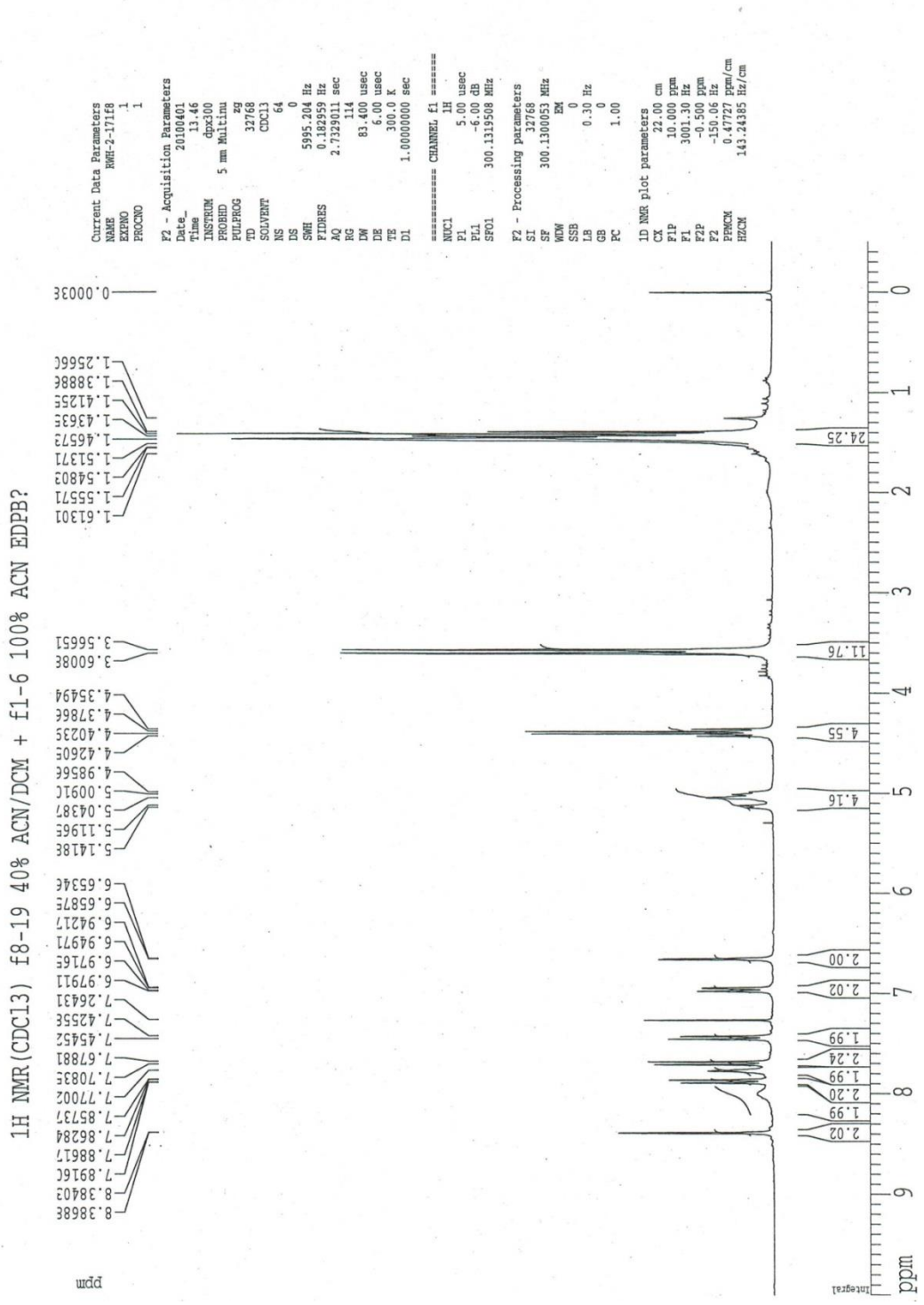
Mass Spectrum for Sample
RWH-4-84 01.lcd

Operator: Mark Wang

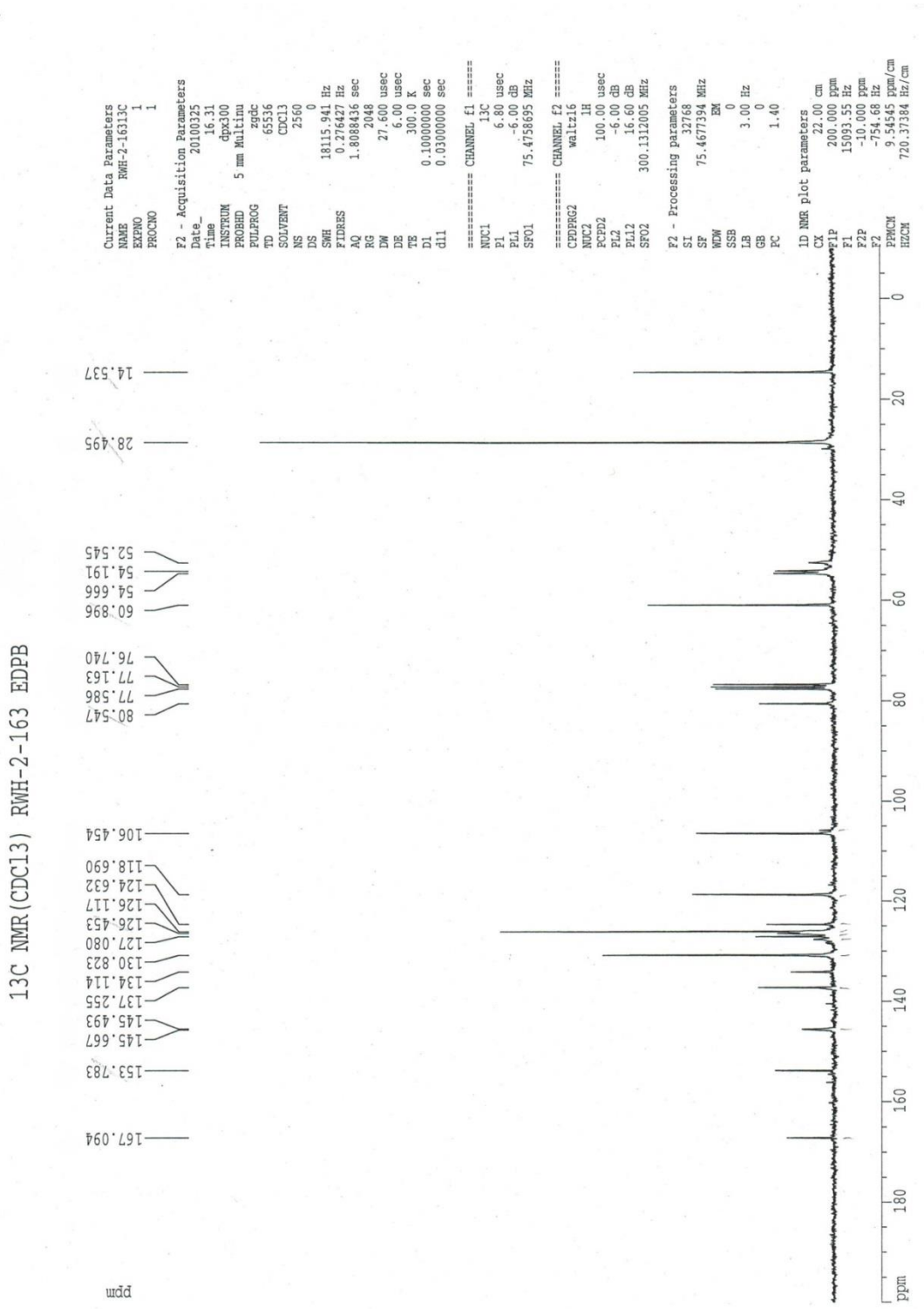
Data Filename: C:\LabSolutions\Data\Schwabacher Alan\RWH-4-84 01.lcd
Spetrum Mode: Averaged
Retention Time: ----
Interface Type (ESI, APCI, DUIS): DUIS
Aquisition Mode: (Scan, SIM, Profife): Scan
Polarity: +



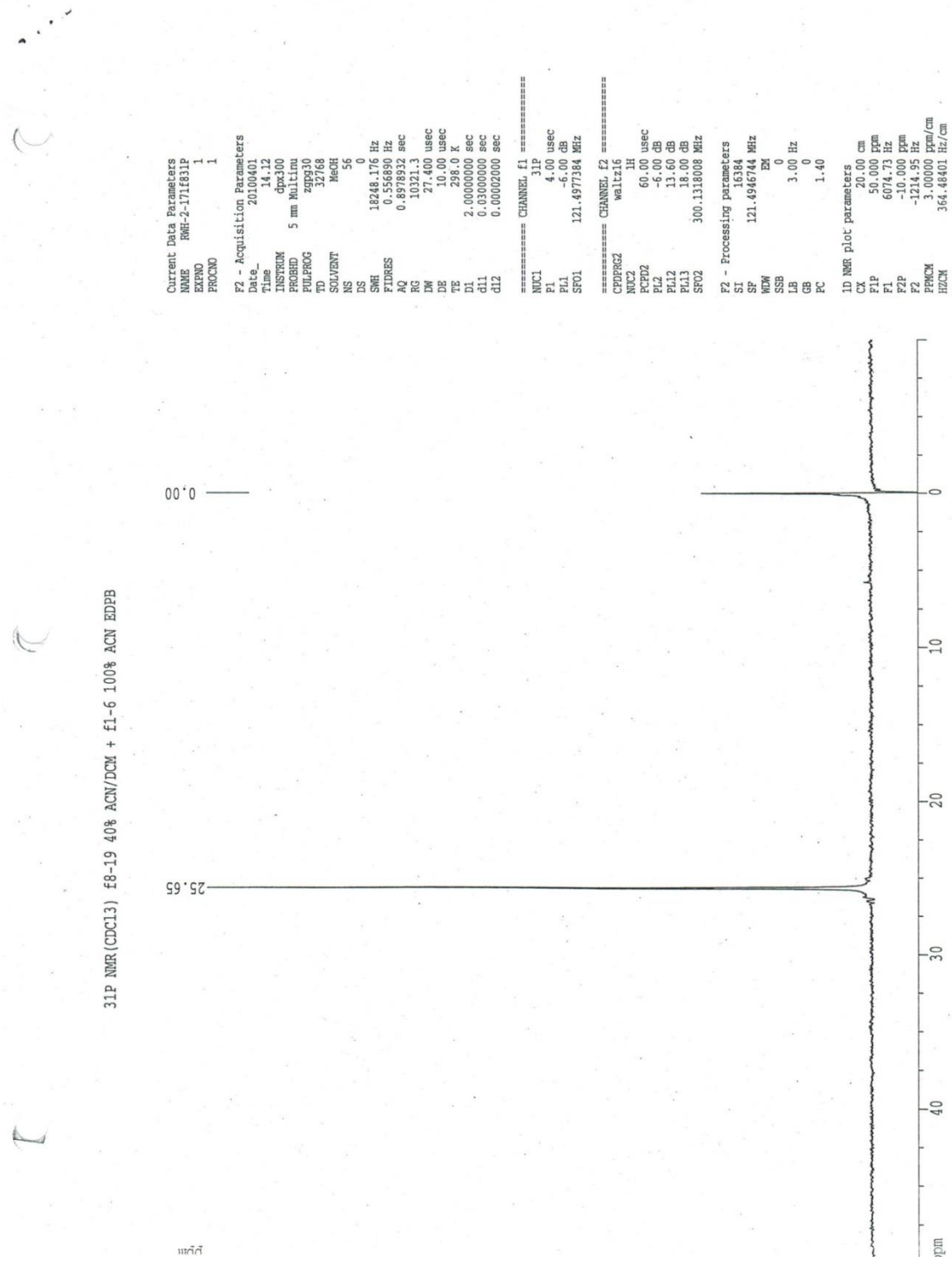
^{1}H NMR *Diethyl 6,6'-(((1S,1'S)-(2,5-bis((tert-butoxycarbonyl)amino)-1,4-phenylene)bis((dimethoxyphosphoryl)methylene))bis(azanediyl))bis(2-naphthoate)* (**17**)



^{13}C NMR *Diethyl 6,6'-(((1S,1'S)-(2,5-bis((tert-butoxycarbonyl)amino)-1,4-phenylene)bis((dimethoxyphosphoryl)methylene))bis(azanediyl))bis(2-naphthoate)* (**17**)



^{31}P NMR *Diethyl 6,6'-(((1S,1'S)-(2,5-bis((tert-butoxycarbonyl)amino)-1,4-phenylene)bis((dimethoxyphosphoryl)methylene))bis(azanediyl))bis(2-naphthoate)* (**17**)



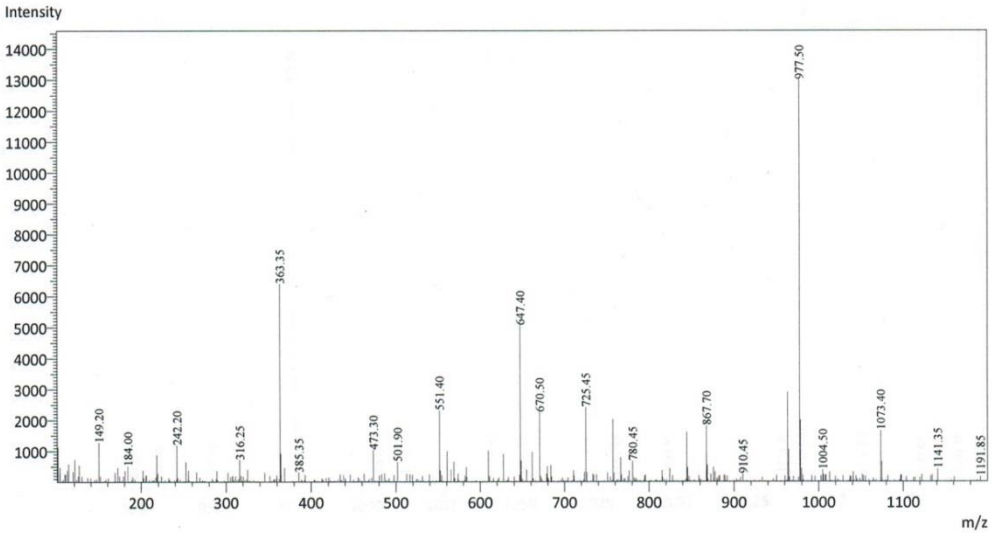
ESI-MS *Diethyl 6,6'-(((1S,1'S)-(2,5-bis((tert-butoxycarbonyl)amino)-1,4-phenylene)bis((dimethoxyphosphoryl)methylene))bis(azanediyl))bis(2-naphthoate)* (**17**)

Shimadzu LCMS-2020 Data Report

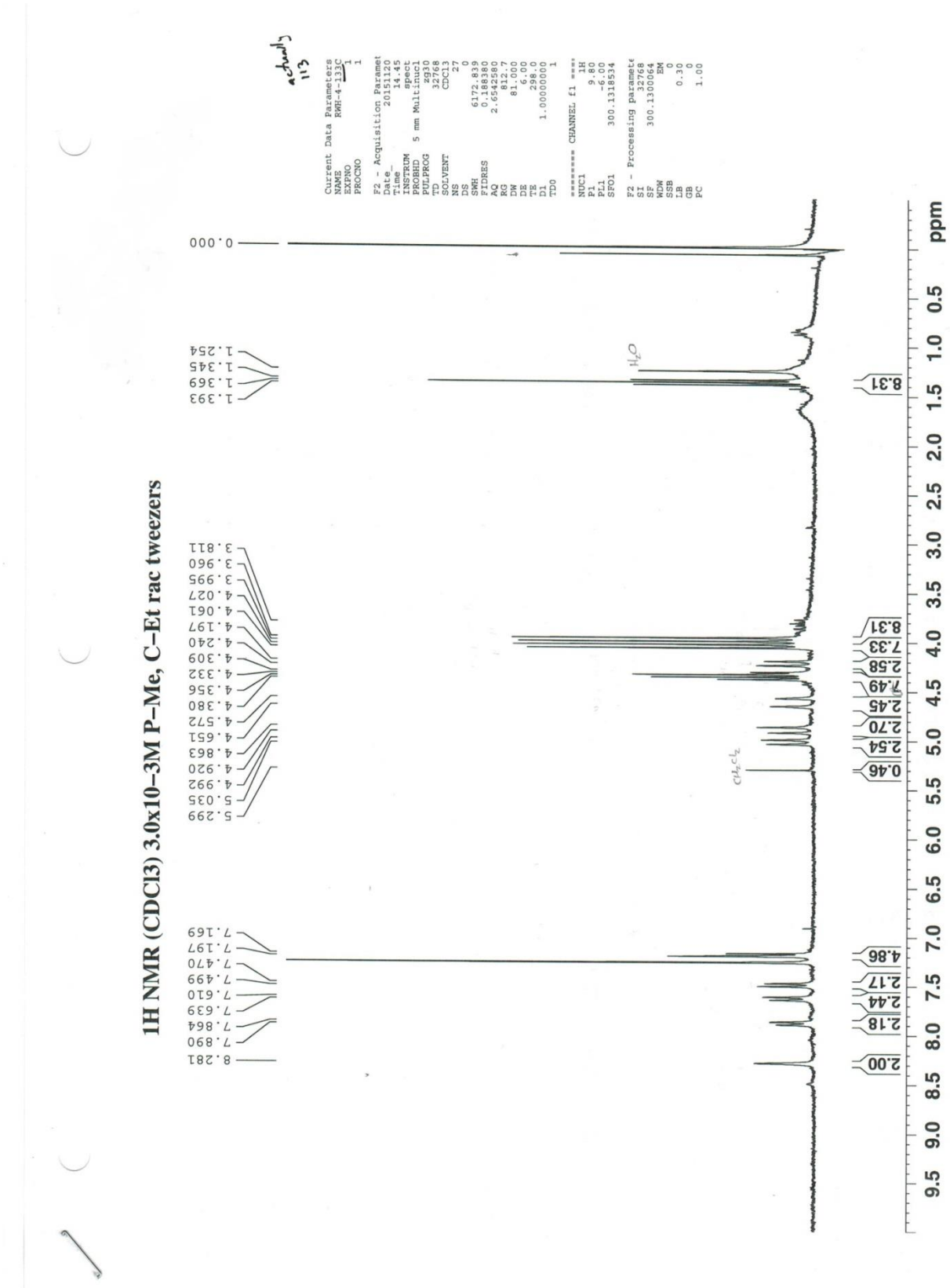
Mass Spectrum for Sample
RWH-4-84 01.lcd

Operator: Mark Wang

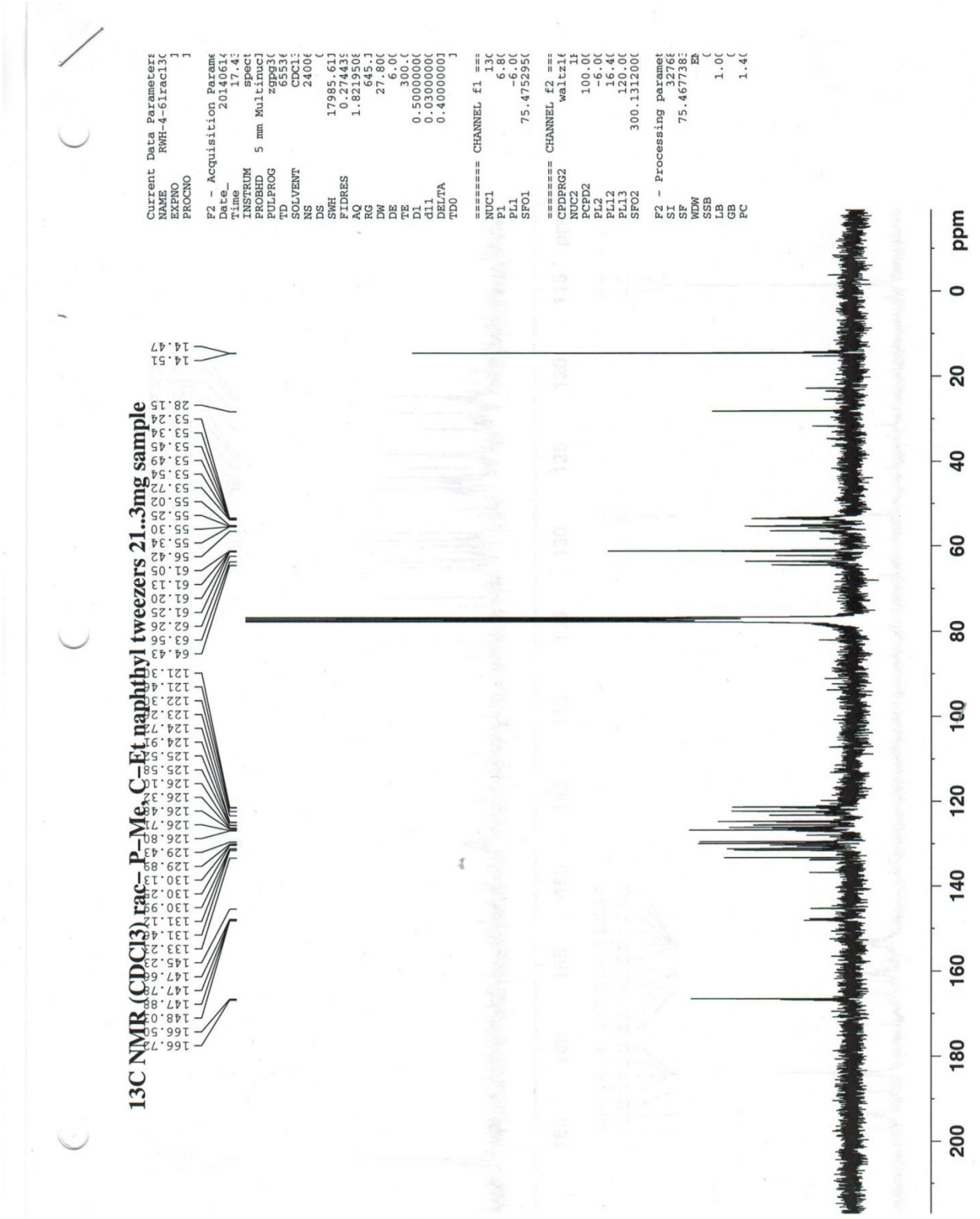
Data Filename: C:\LabSolutions\Data\Schwabacher Alan\RWH-4-84 01.lcd
Spetrum Mode: Averaged
Retention Time: ----
Interface Type (ESI, APCI, DUIS): DUIS
Aquisition Mode: (Scan, SIM, Profife): Scan
Polarity: -



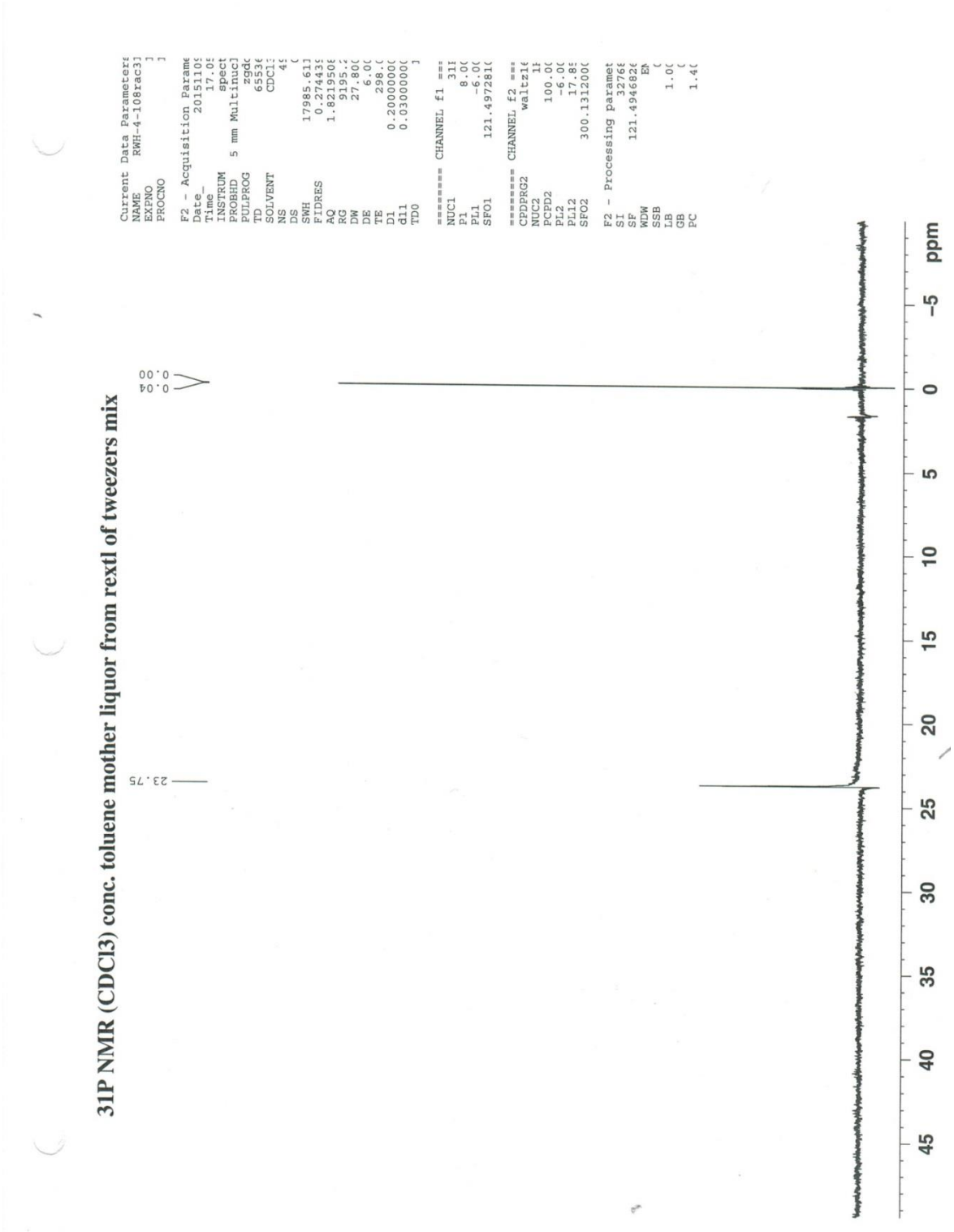
^{1}H NMR *C-Me, P-Me rac-tweezers* (**18**)



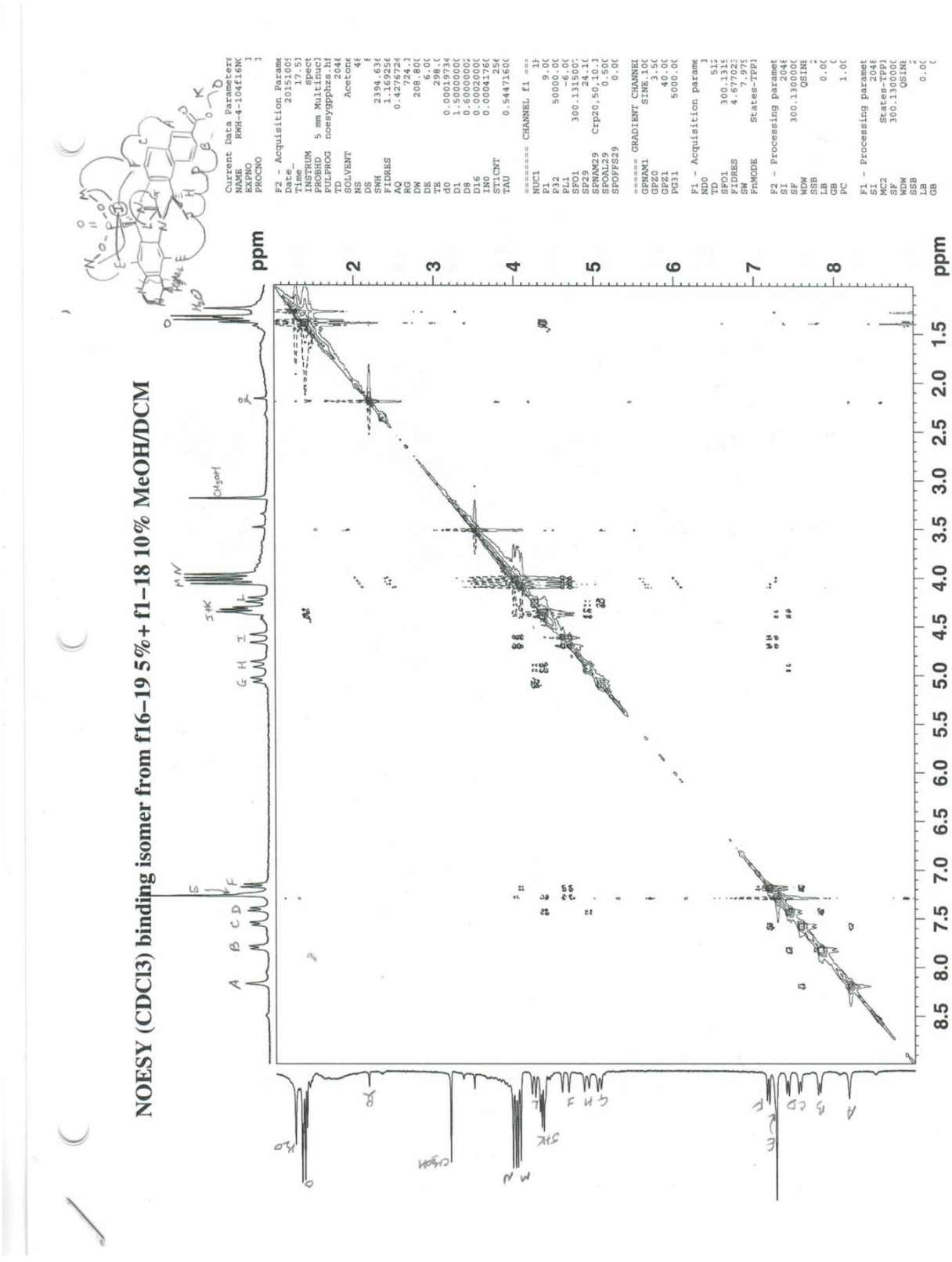
^{13}C NMR *C-Me, P-Me rac-tweezers* (**18**)



^{31}P NMR *C-Me, P-Me rac-tweezers* (**18**)



COSY *C-Me, P-Me rac-tweezers* (**18**)



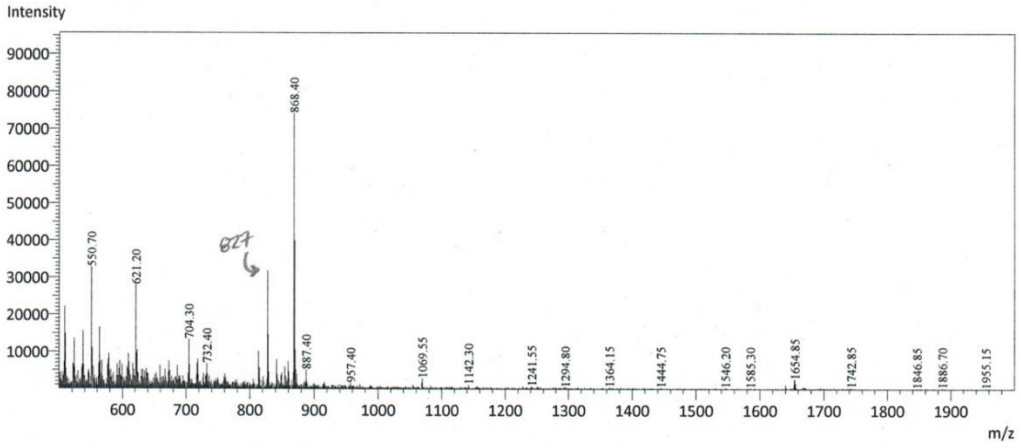
ESI-MS *C-Me, P-Me rac-tweezers* (**18**)

Shimadzu LCMS-2020 Data Report

Mass Spectrum for Sample
RWH-4-108rac.lcd

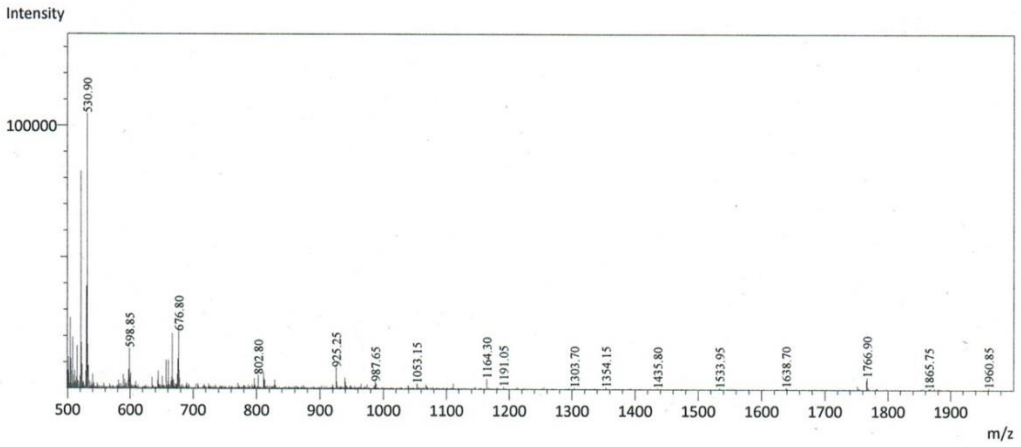
Operator:Robert Hoppe

Data Filename: C:\LabSolutions\Data\Schwabacher Alan\RWH-4-108rac.lcd
Spetrum Mode: Averaged
Retention Time: ----
Interface Type (ESI, APCI, DUIS): DUIS
Aquisition Mode: (Scan, SIM, Profife): Scan
Polarity: +
H2O/0.1% HCOOH, CH3CN/0.1% HCOOH

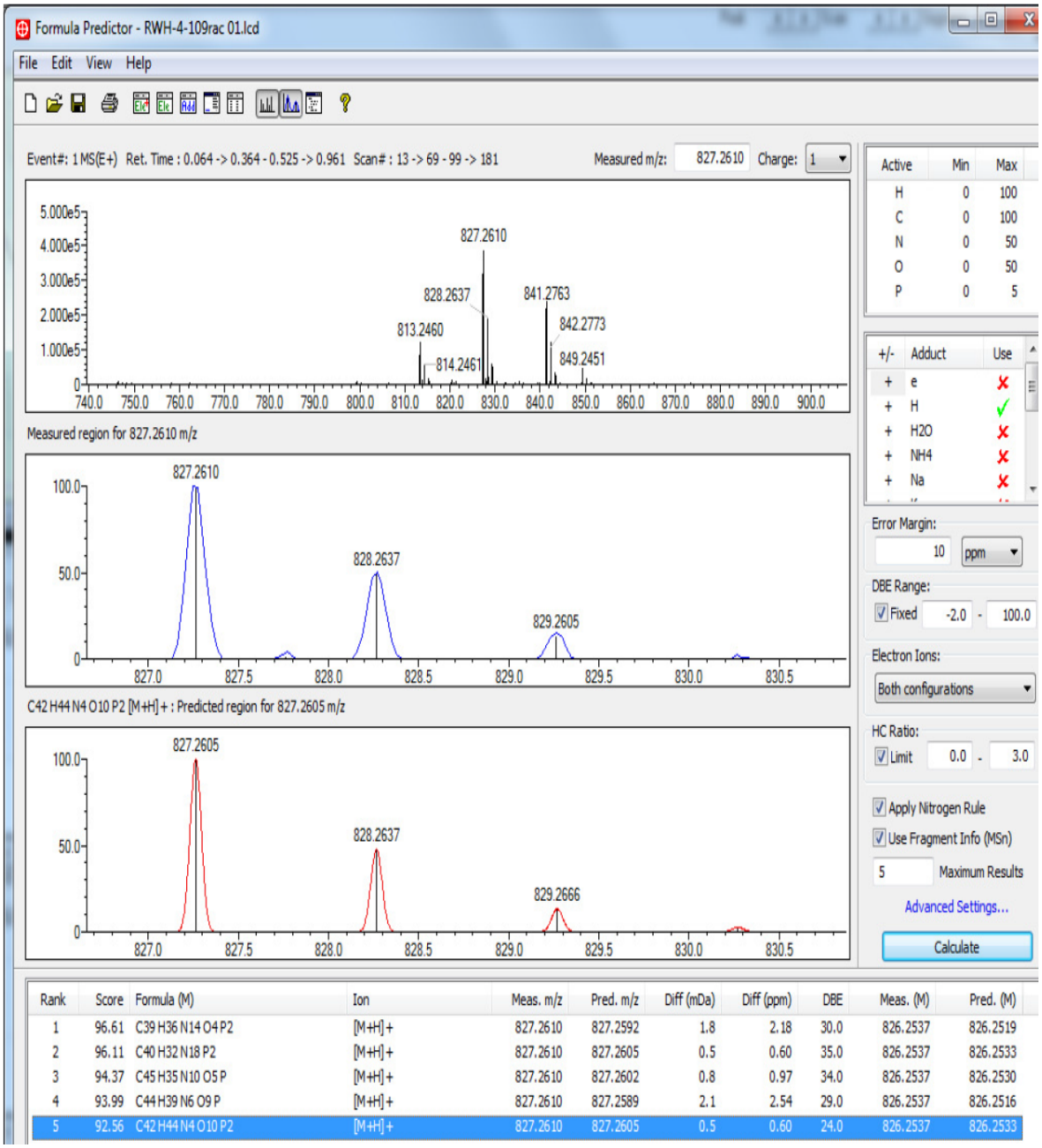


Operator:Robert Hoppe

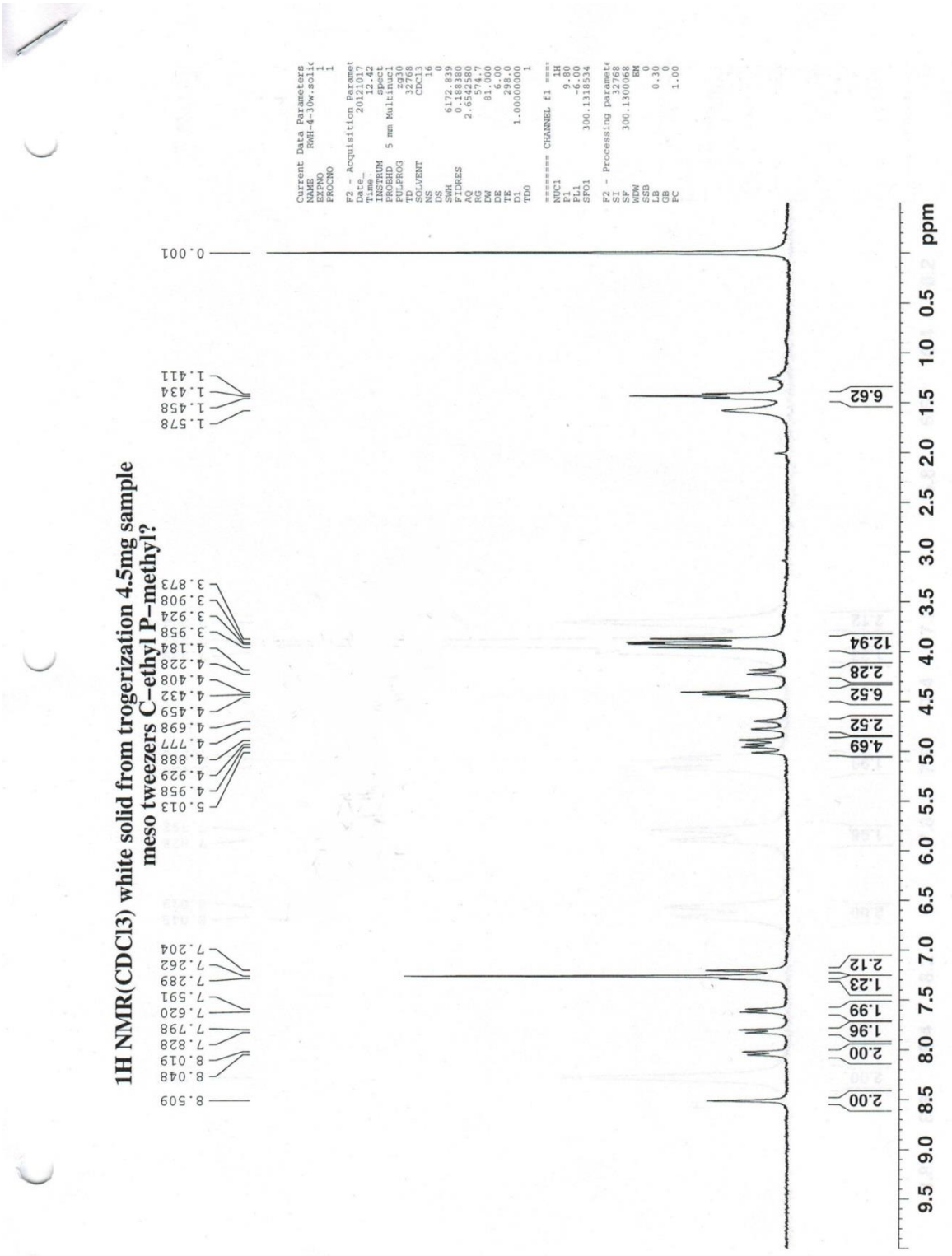
Data Filename: C:\LabSolutions\Data\Schwabacher Alan\RWH-4-108rac.lcd
Spetrum Mode: Averaged
Retention Time: ----
Interface Type (ESI, APCI, DUIS): DUIS
Aquisition Mode: (Scan, SIM, Profife): Scan
Polarity: -
H2O/0.1% HCOOH, CH3CN/0.1% HCOOH



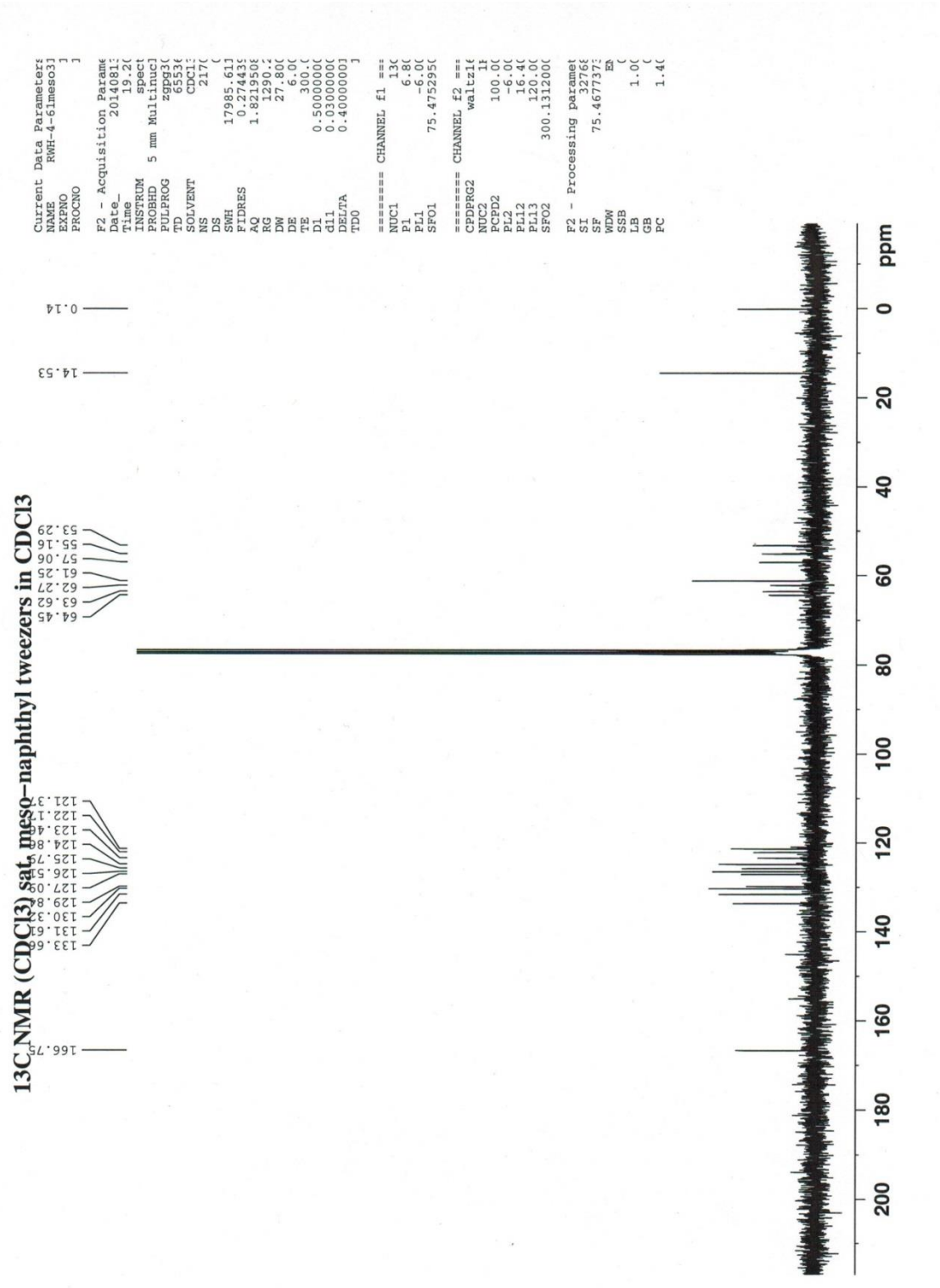
HRMS *C-Me, P-Me rac-tweezers* (**18**)



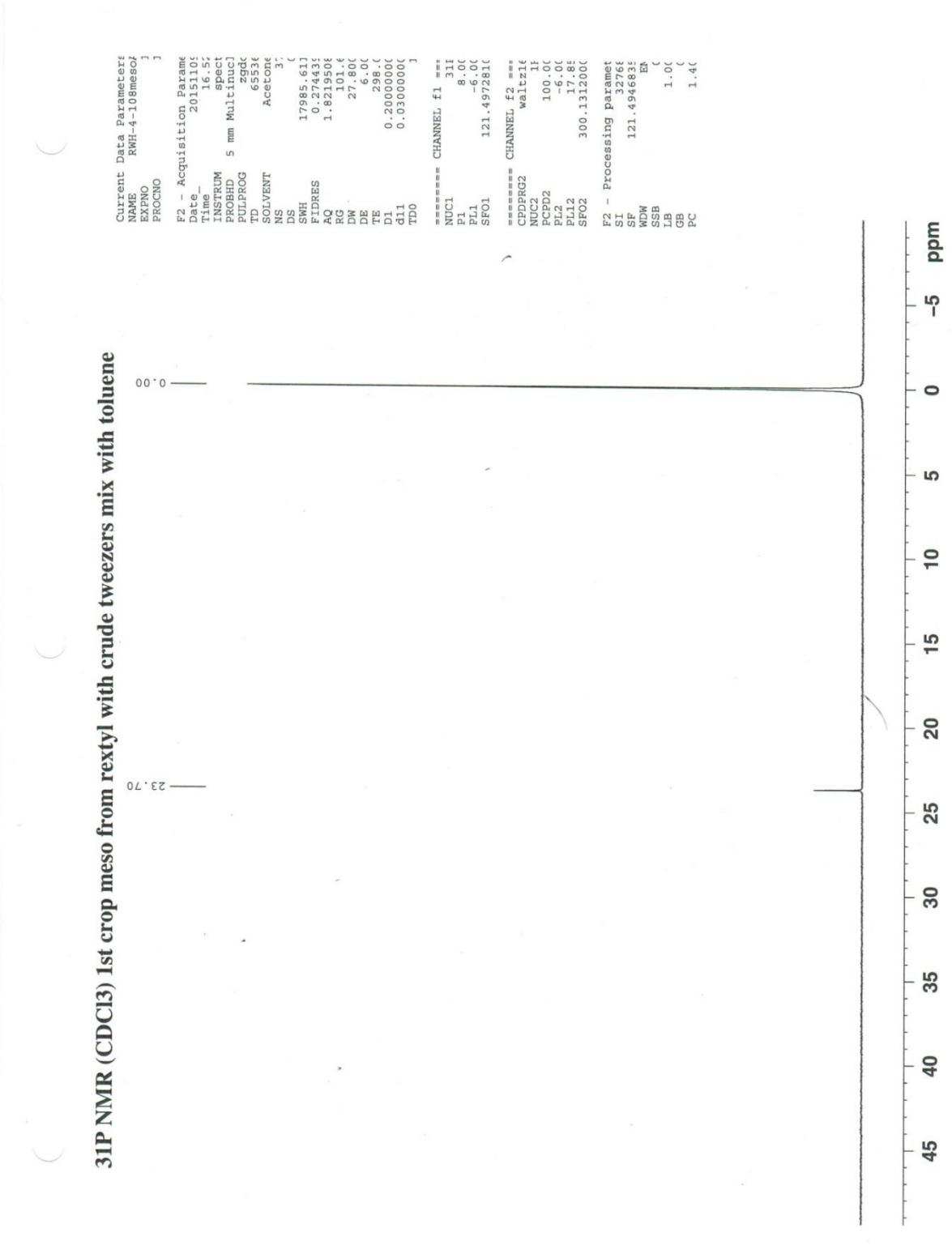
^{1}H NMR *C-Me, P-Me meso-isomer* (**19**)



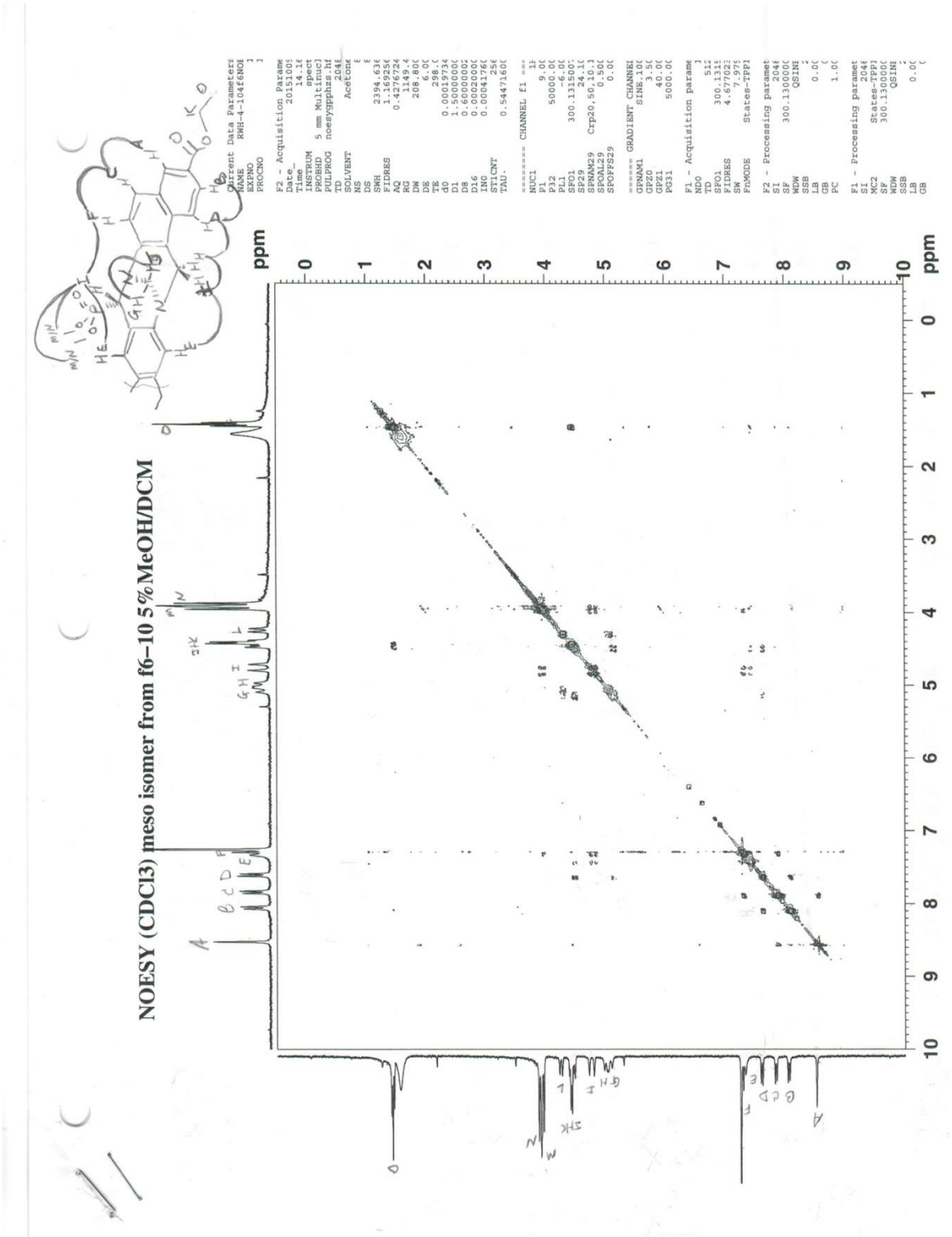
^{13}C NMR *C-Me, P-Me meso-isomer* (**19**)



^{31}P NMR *C-Me, P-Me meso-isomer* (**19**)



COSY *C-Me, P-Me meso-isomer* (**19**)



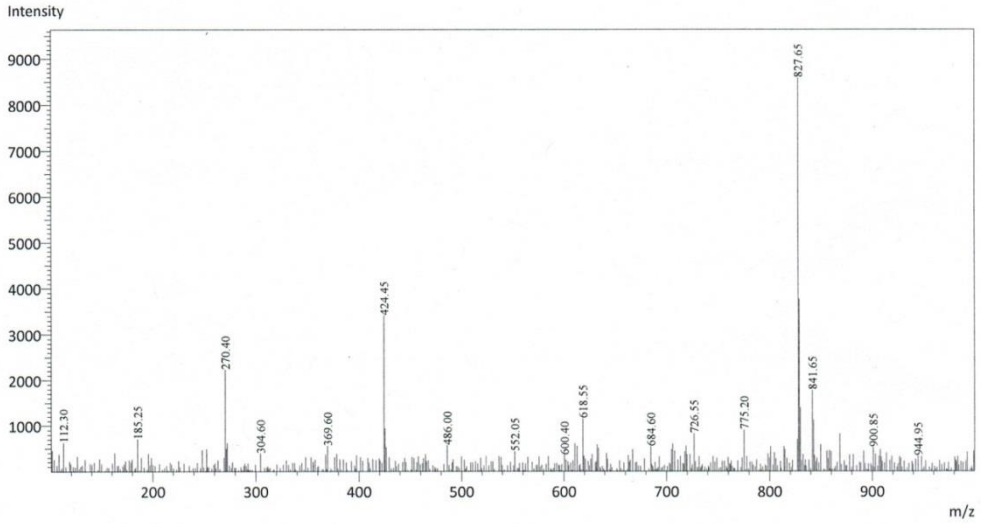
ESI-MS *C-Me, P-Me meso-isomer* (**19**)

Shimadzu LCMS-2020 Data Report

Mass Spectrum for Sample
RWH-4-30 01.lcd

Opeator: Mark Wang

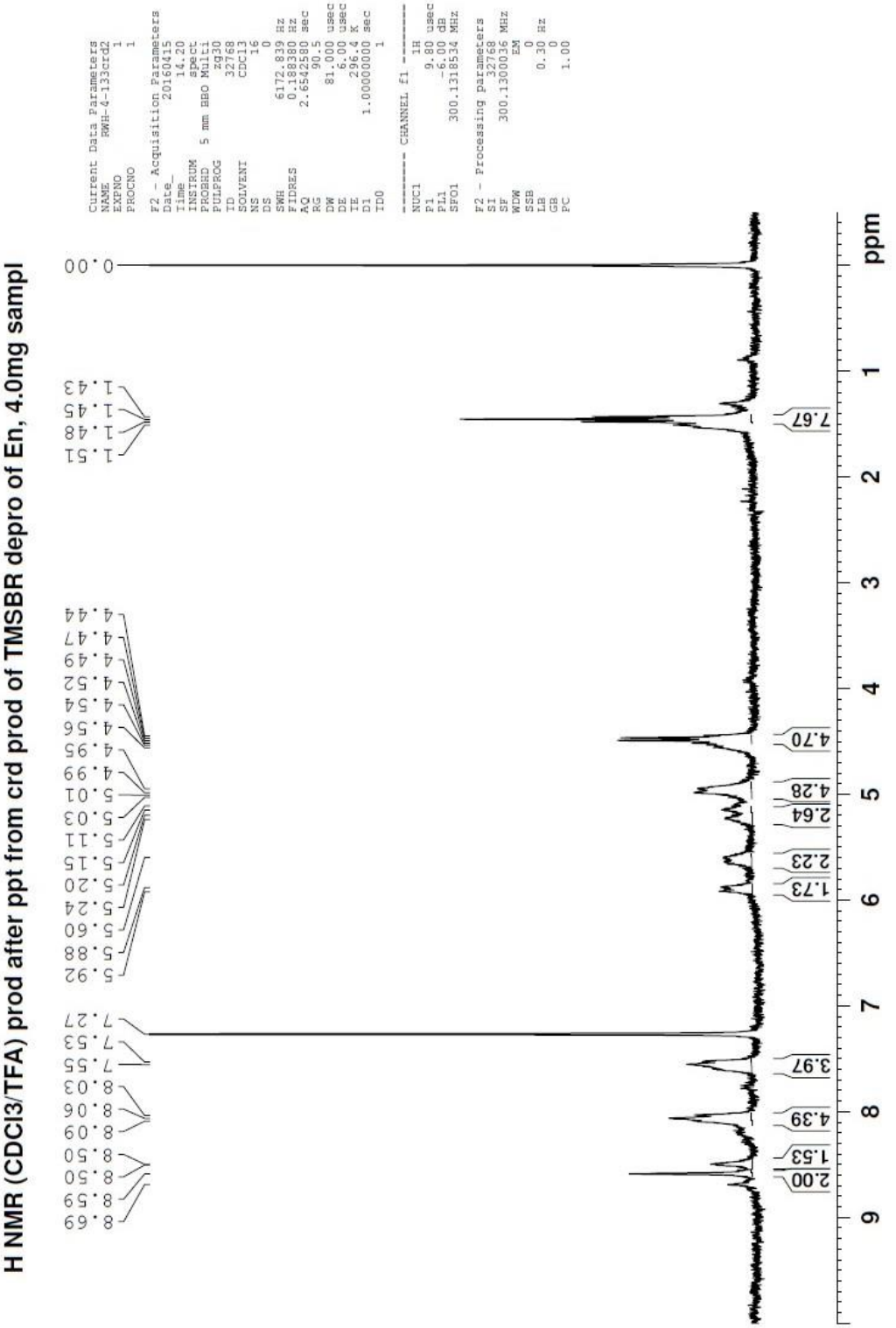
Data Filename: C:\LabSolutions\Data\Schwabacher Alan\RWH-4-30 01.lcd
Spetrum Mode: Averaged
Retention Time: ----
Interface Type (ESI, APCI, DUIS): DUIS
Aquisition Mode: (Scan, SIM, Profife): Scan
Polarity: +



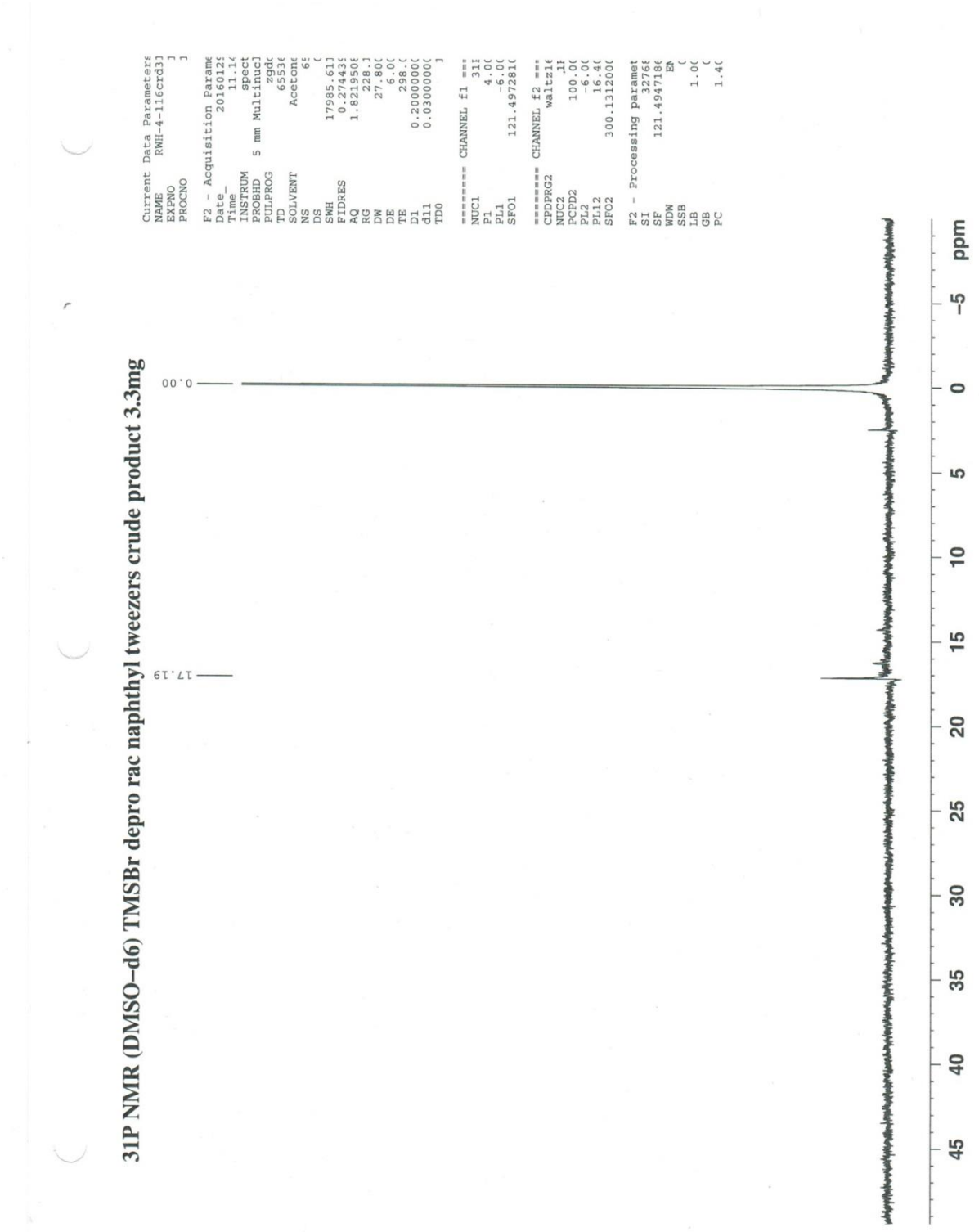
HRMS *C-Me, P-Me meso-isomer* (**19**)



^{1}H NMR <u>*rac*- carbethoxy *tetra acid tweezers*</u> (**23**)



^{31}P NMR <u>*rac*- carbethoxy *tetra acid tweezers*</u> (**23**)



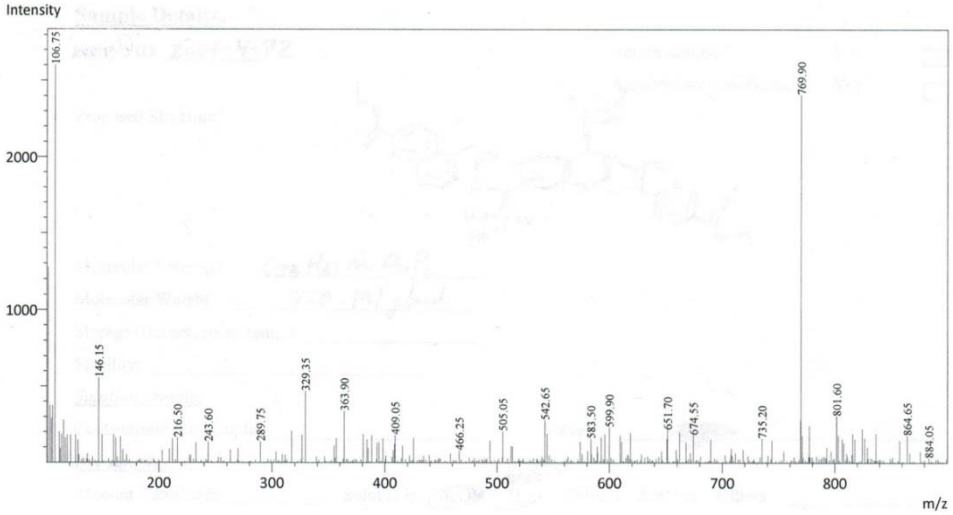
ESI-MS *rac*- carbethoxy *tetra acid tweezers* (**23**)

Shimadzu LCMS-2020 Data Report

Mass Spectrum for Sample
RWH-4-72 01.lcd

Operator: Mark Wang

Data Filename: C:\LabSolutions\Data\Schwabacher Alan\RWH-4-72 01.lcd
Spetrum Mode: Averaged
Retention Time: ----
Interface Type (ESI, APCI, DUIS): DUIS
Aquisition Mode: (Scan, SIM, Profife): Scan
Polarity: -

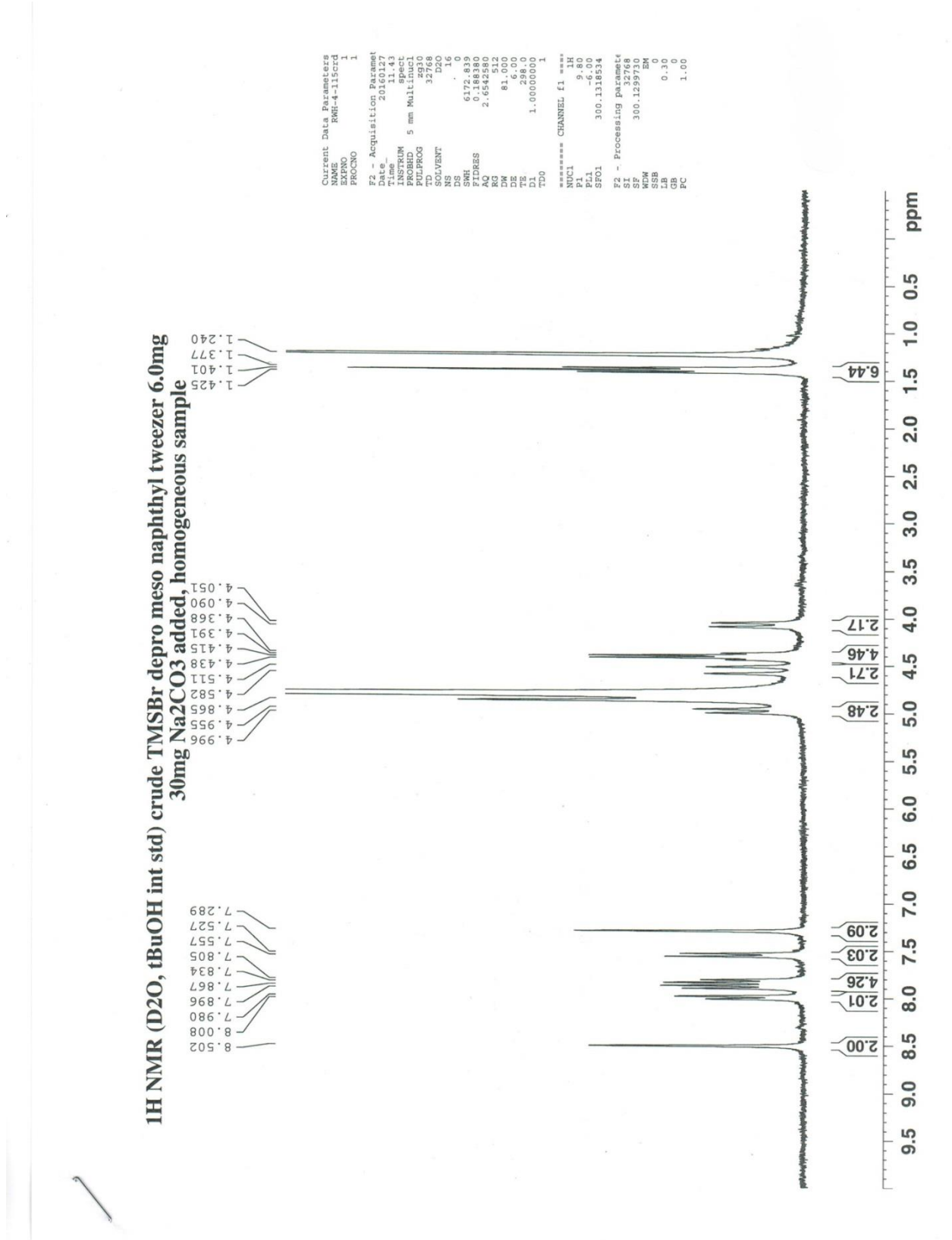


HRMS *rac*- carbethoxy *tetra acid tweezers* (**23**)

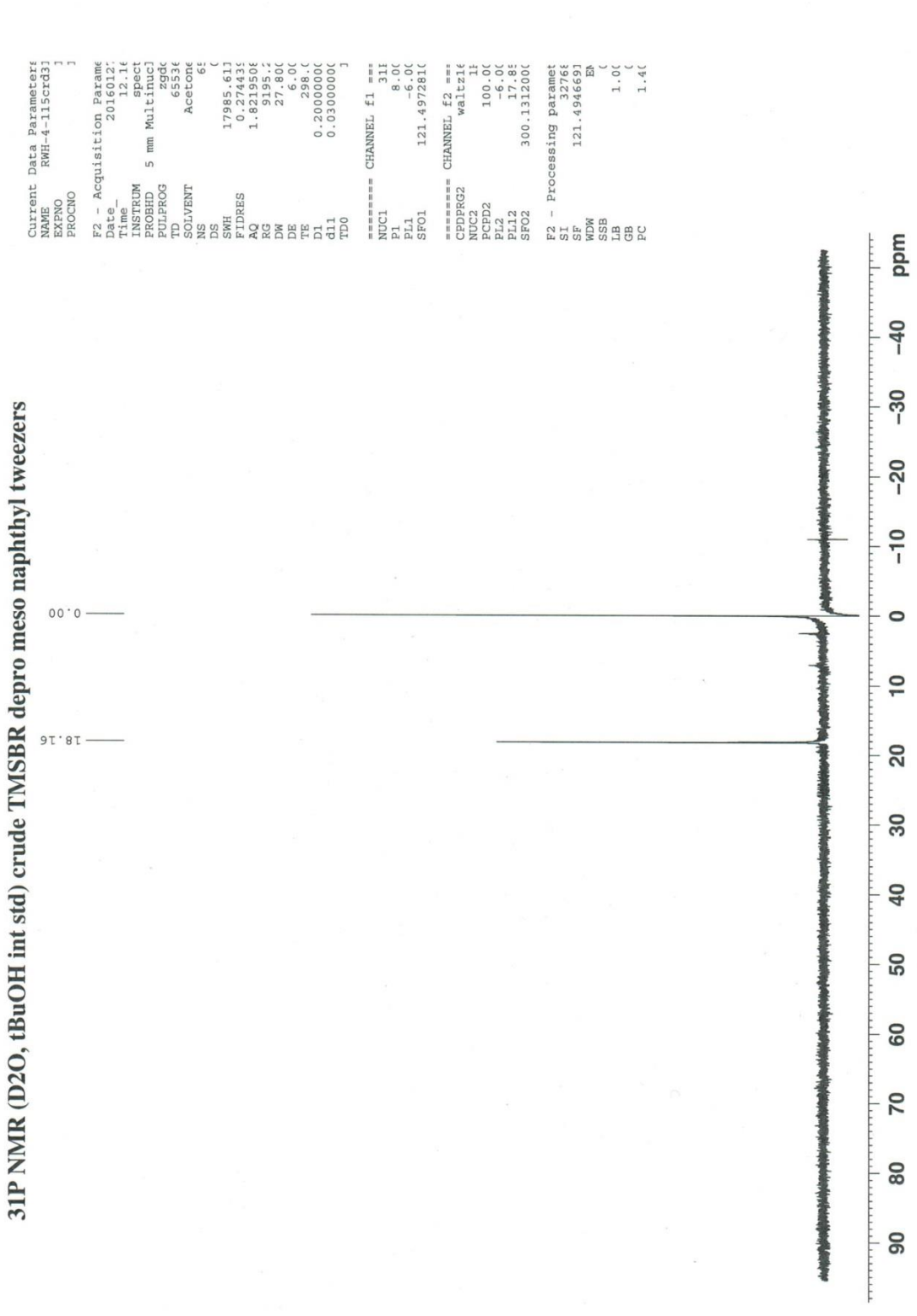


Rank	Score	Formula (M)	Ion	Meas. m/z	Pred. m/z	Diff (mDa)	Diff (ppm)	DBE	Meas. (M)
1	38.36	C38 H36 N4 O10 P2	[M+H]+	771.1970	771.1979	-0.9	-1.17	24.0	770.1897
2	28.04	C46 H30 N2 O10	[M+H]+	771.1970	771.1973	-0.3	-0.39	33.0	770.1897
3	25.44	C50 H32 N2 O3 P2	[M+H]+	771.1970	771.1961	0.9	1.17	37.0	770.1897
4	21.50	C58 H26 O3	[M+H]+	771.1970	771.1955	1.5	1.95	46.0	770.1897
5	18.87	C57 H27 N2 P	[M+H]+	771.1970	771.1985	-1.5	-1.95	46.0	770.1897

^{1}H NMR *meso*- carbethoxy *tetra acid isomer* (**24**)



^{31}P NMR <u>*meso*- carbethoxy *tetra acid isomer*</u> (**24**)



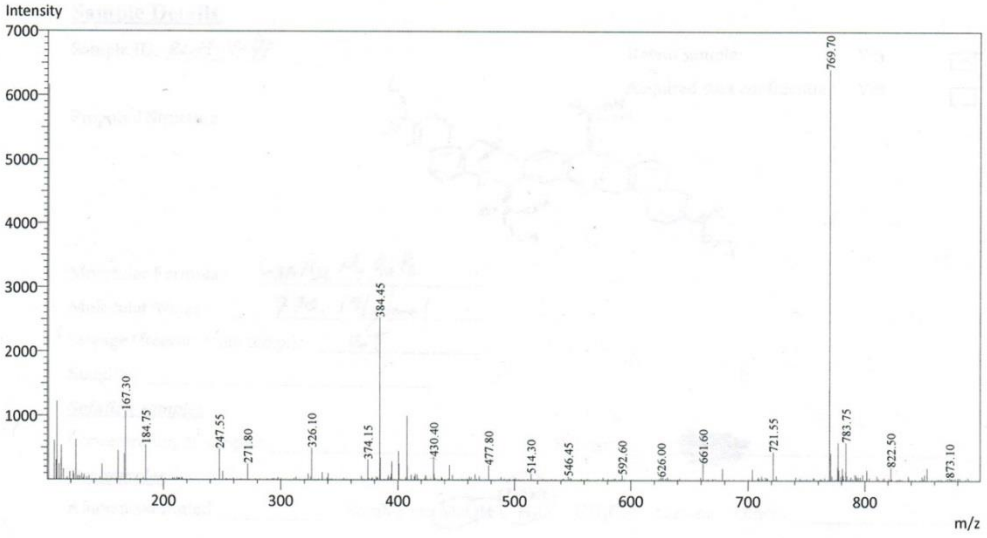
ESI-MS *meso*- carbethoxy *tetra acid isomer* (**24**)

Shimadzu LCMS-2020 Data Report

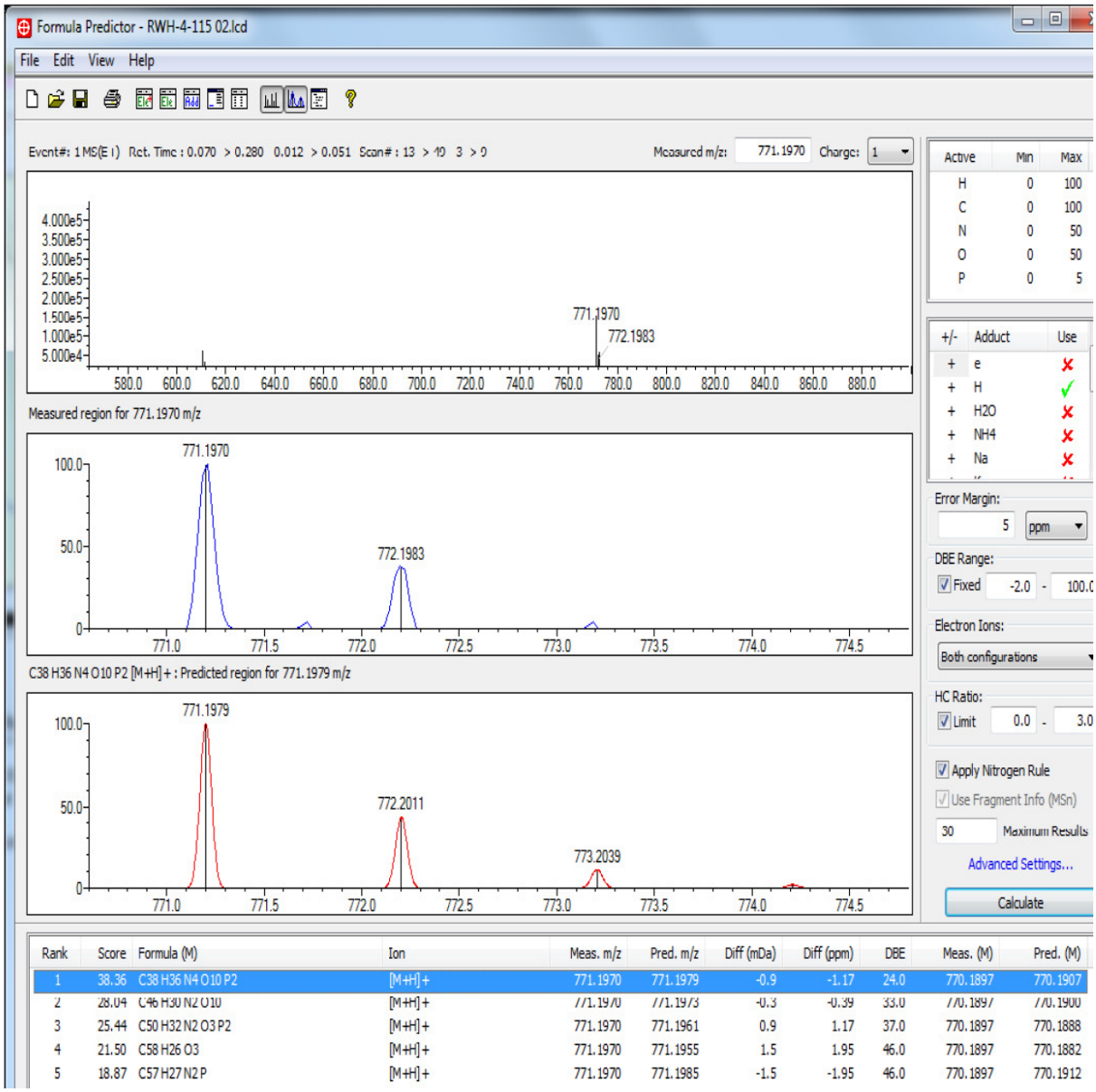
Mass Spectrum for Sample
RWH-4-71 02.lcd

Operator: Mark Wang

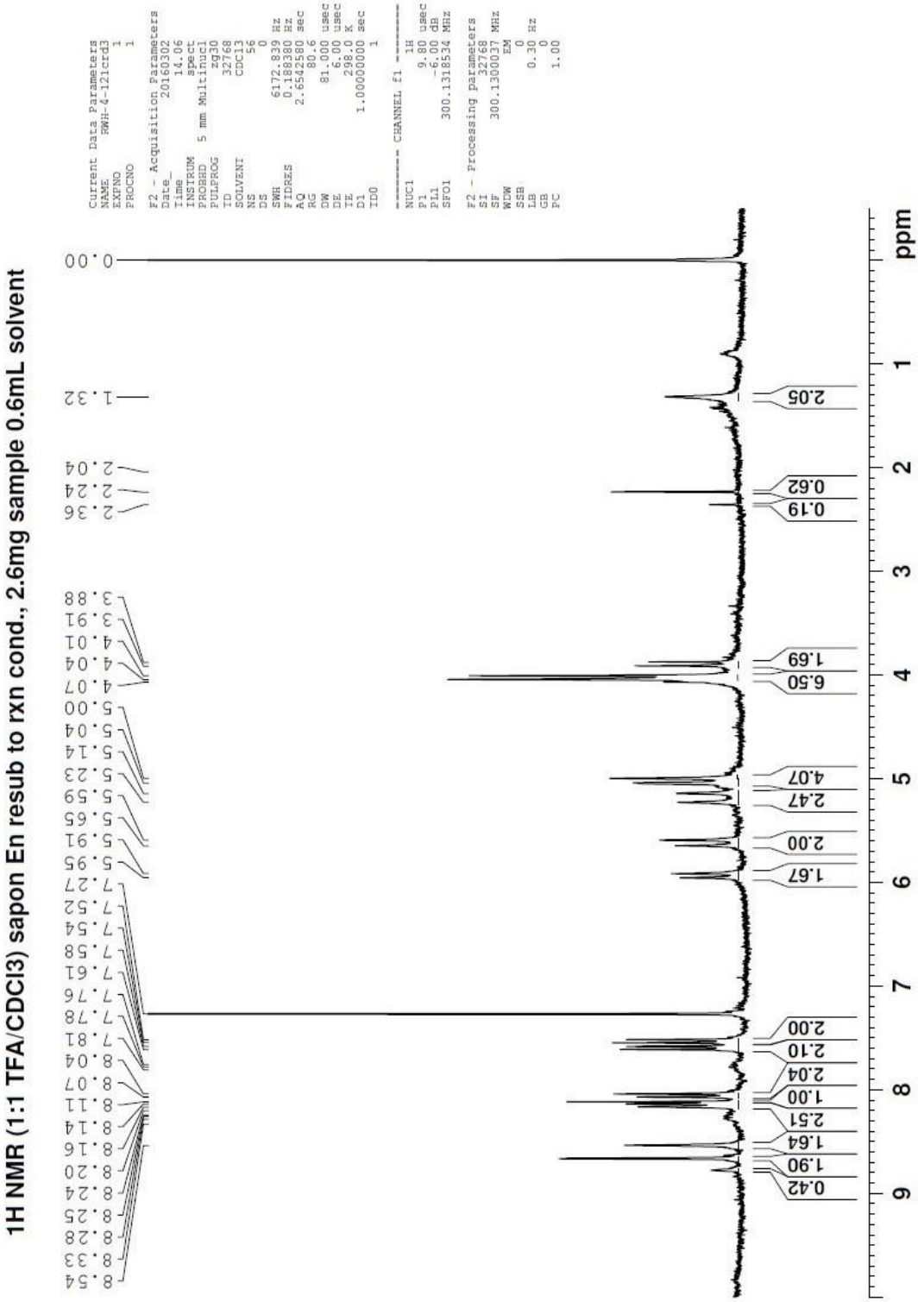
Data Filename: C:\LabSolutions\Data\Schwabacher Alan\RWH-4-71 02.lcd
Spetrum Mode: Averaged
Retention Time: ----
Interface Type (ESI, APCI, DUIS): DUIS
Aquisition Mode: (Scan, SIM, Profife): Scan
Polarity: -



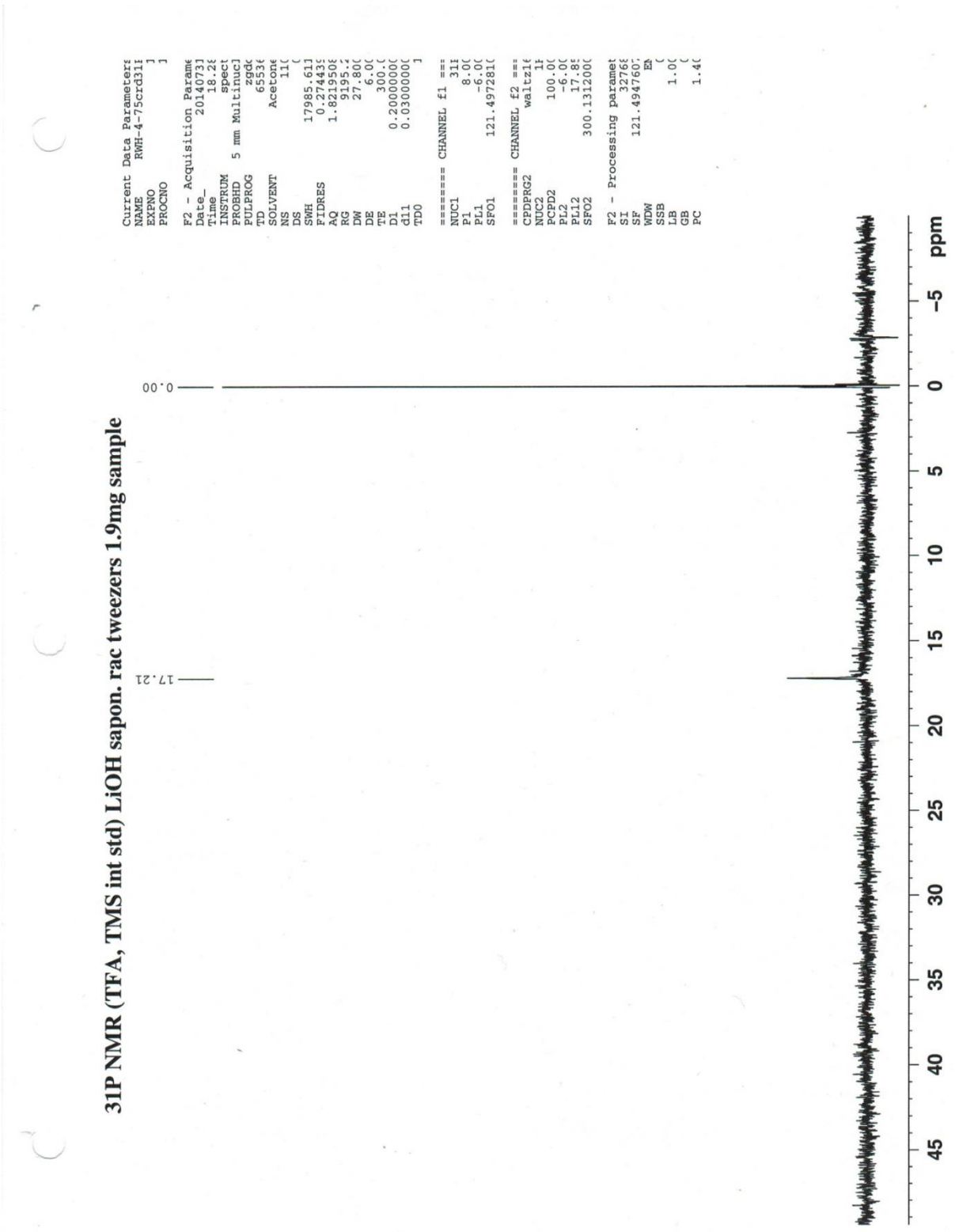
HRMS *meso*- carbethoxy *tetra acid isomer* (**24**)



^{1}H NMR *rac-methylphosphonate tetra anionic tweezers* (**25**)



^{31}P NMR *rac-methylphosphonate tetra anionic tweezers* (**25**)

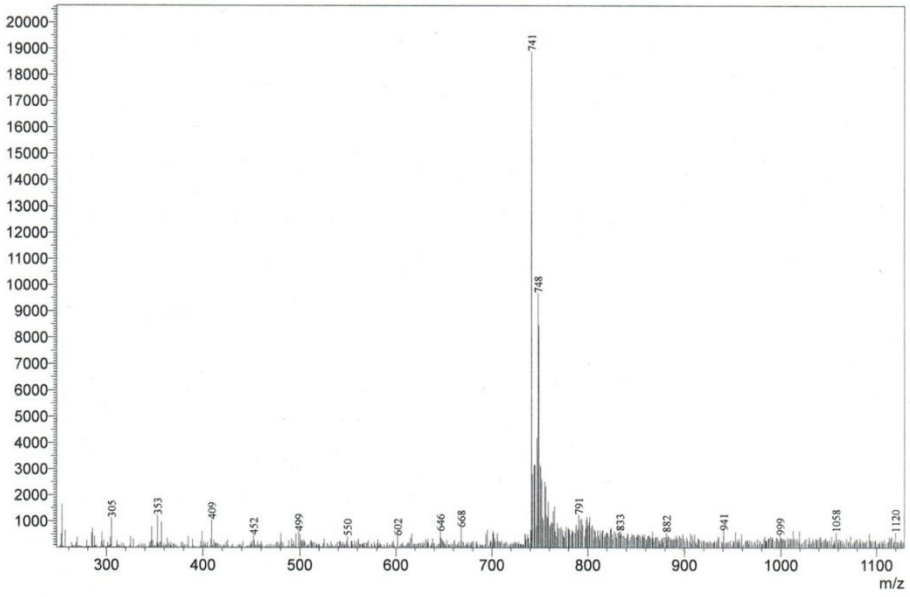


ESI-MS *rac-methylphosphonate tetra anionic tweezers* (**25**)

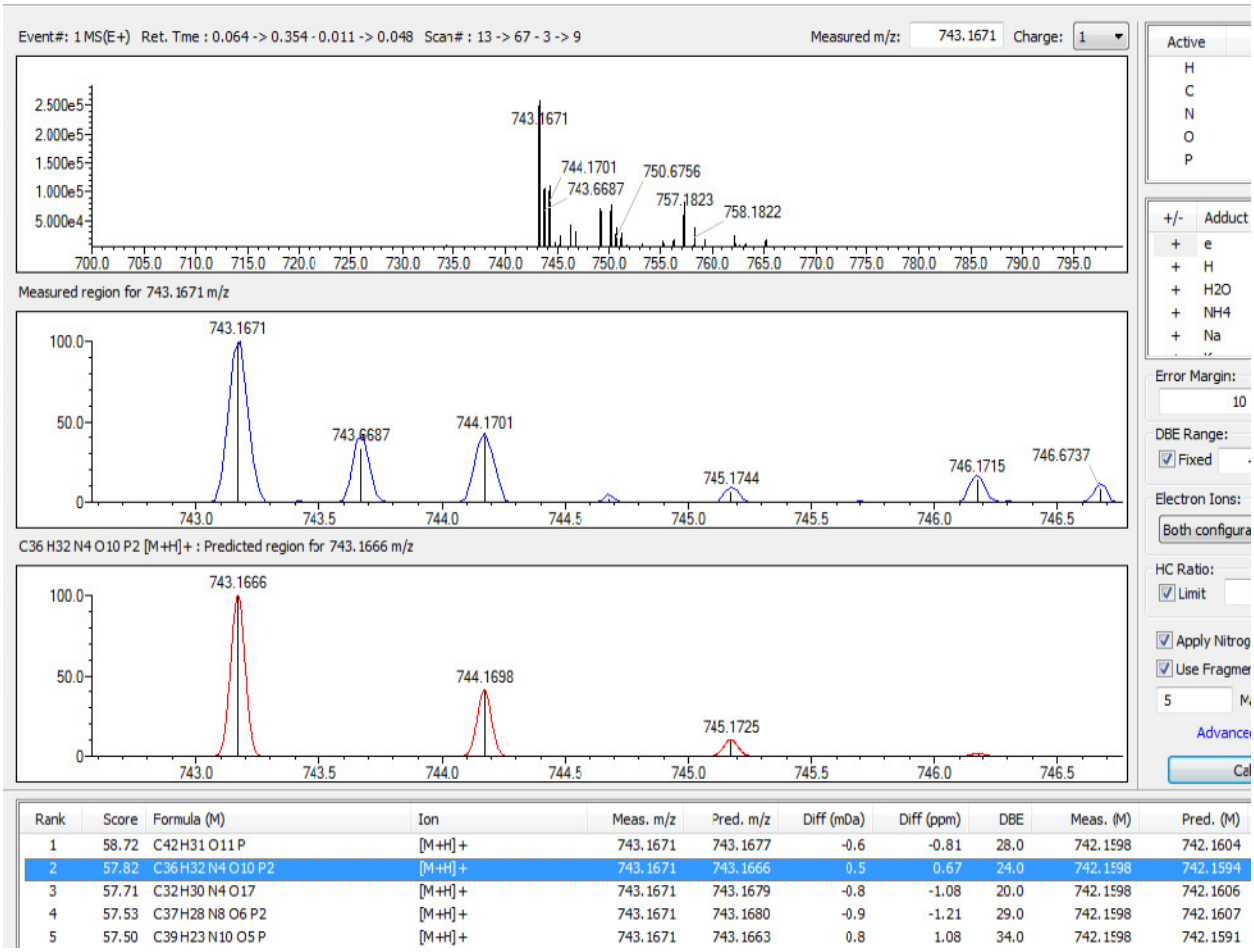
==== Shimadzu LabSolutions Data Report ====

<Spectrum>

Line#:1 R.Time:----(Scan#:----)
MassPeaks:1515
RawMode:Averaged 0.762-1.395(184-336) BasePeak:741(18901)
BG Mode:Averaged 0.012-0.303(4-74) Segment 1 - Event 2

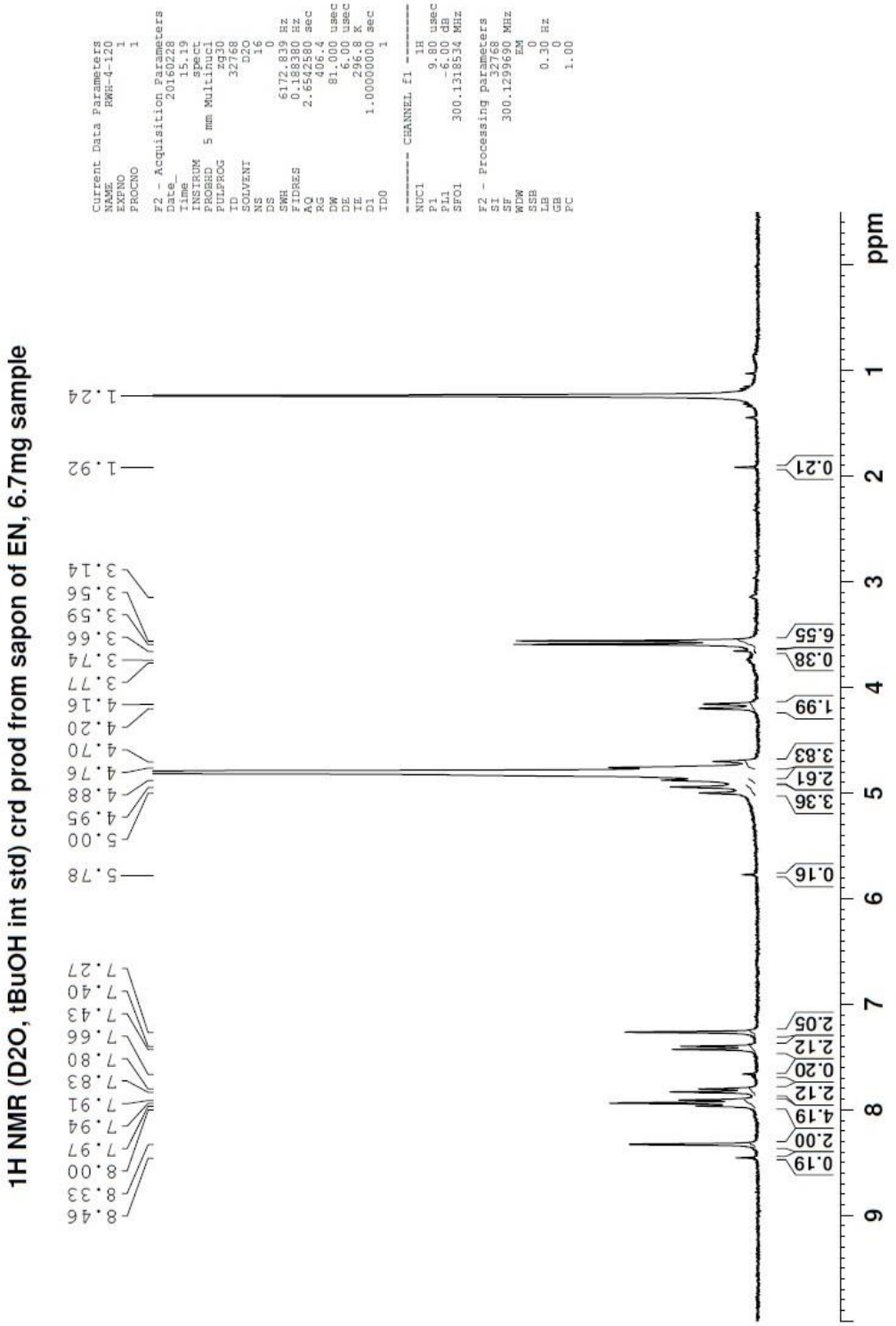


HRMS *rac-methylphosphonate tetra anionic tweezers* (**25**)

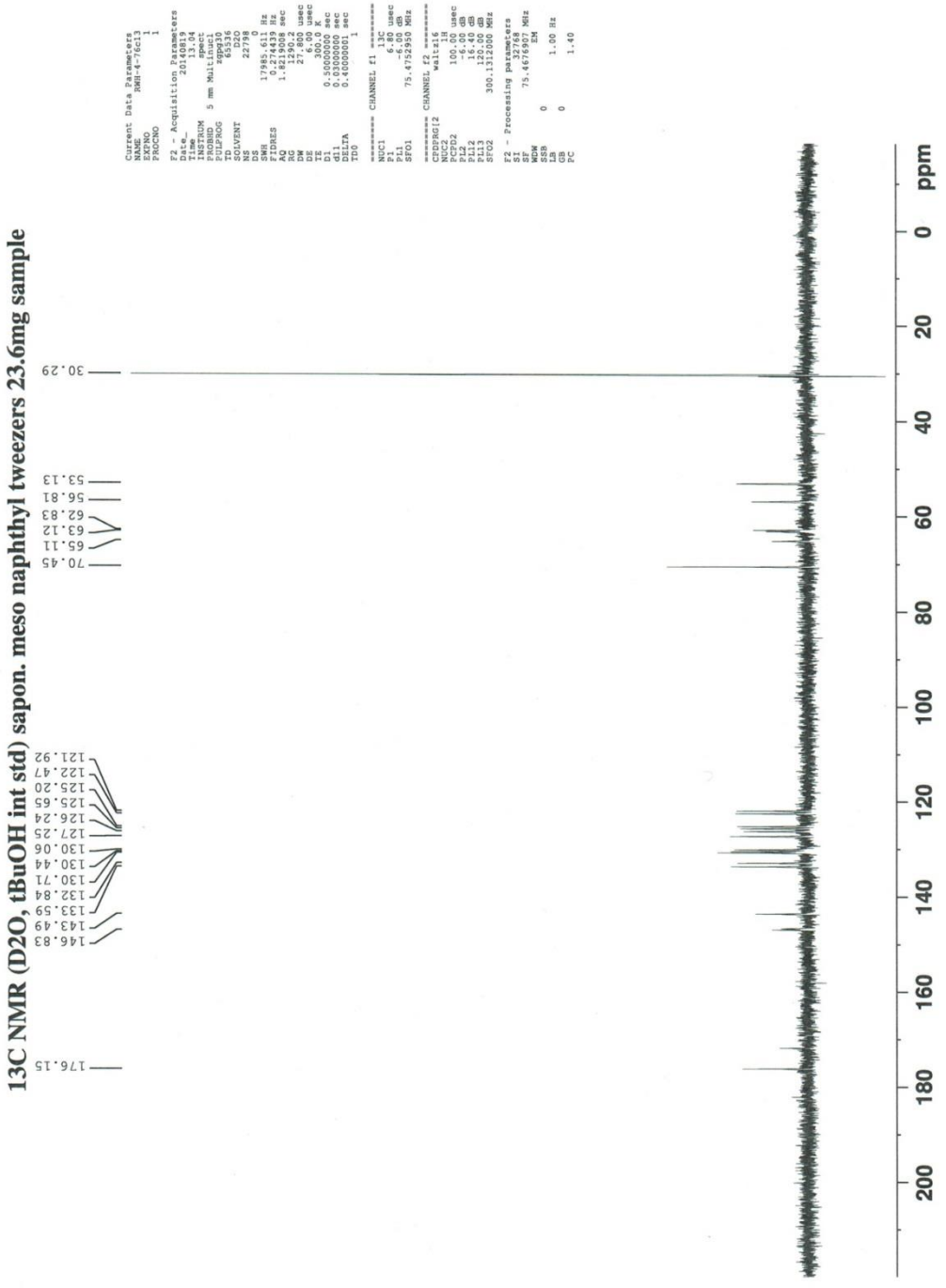


Rank	Score	Formula (M)	Ion	Meas. m/z	Pred. m/z	Diff (mDa)	Diff (ppm)	DBE	Meas. (M)	Pred. (M)
1	58.72	C42 H31 O11 P	[M+H]+	743.1671	743.1677	-0.6	-0.81	28.0	742.1598	742.1604
2	57.82	C36 H32 N4 O10 P2	[M+H]+	743.1671	743.1666	0.5	0.67	24.0	742.1598	742.1594
3	57.71	C32 H30 N4 O17	[M+H]+	743.1671	743.1679	-0.8	-1.08	20.0	742.1598	742.1606
4	57.53	C37 H28 N8 O6 P2	[M+H]+	743.1671	743.1680	-0.9	-1.21	29.0	742.1598	742.1607
5	57.50	C39 H23 N10 O5 P	[M+H]+	743.1671	743.1663	0.8	1.08	34.0	742.1598	742.1591

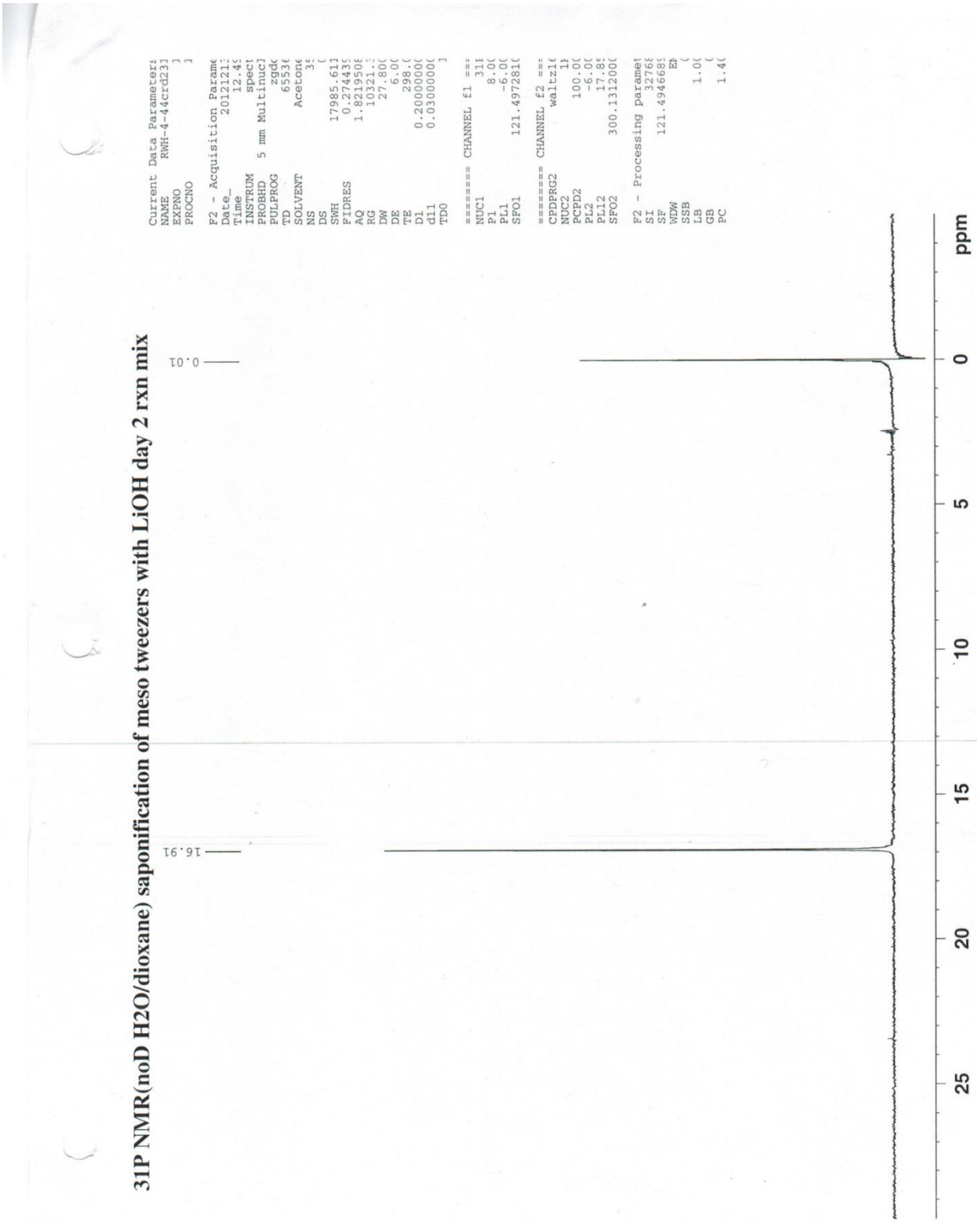
^{1}H NMR *meso-methylphosphonate tetra anionic isomer* (**26**)



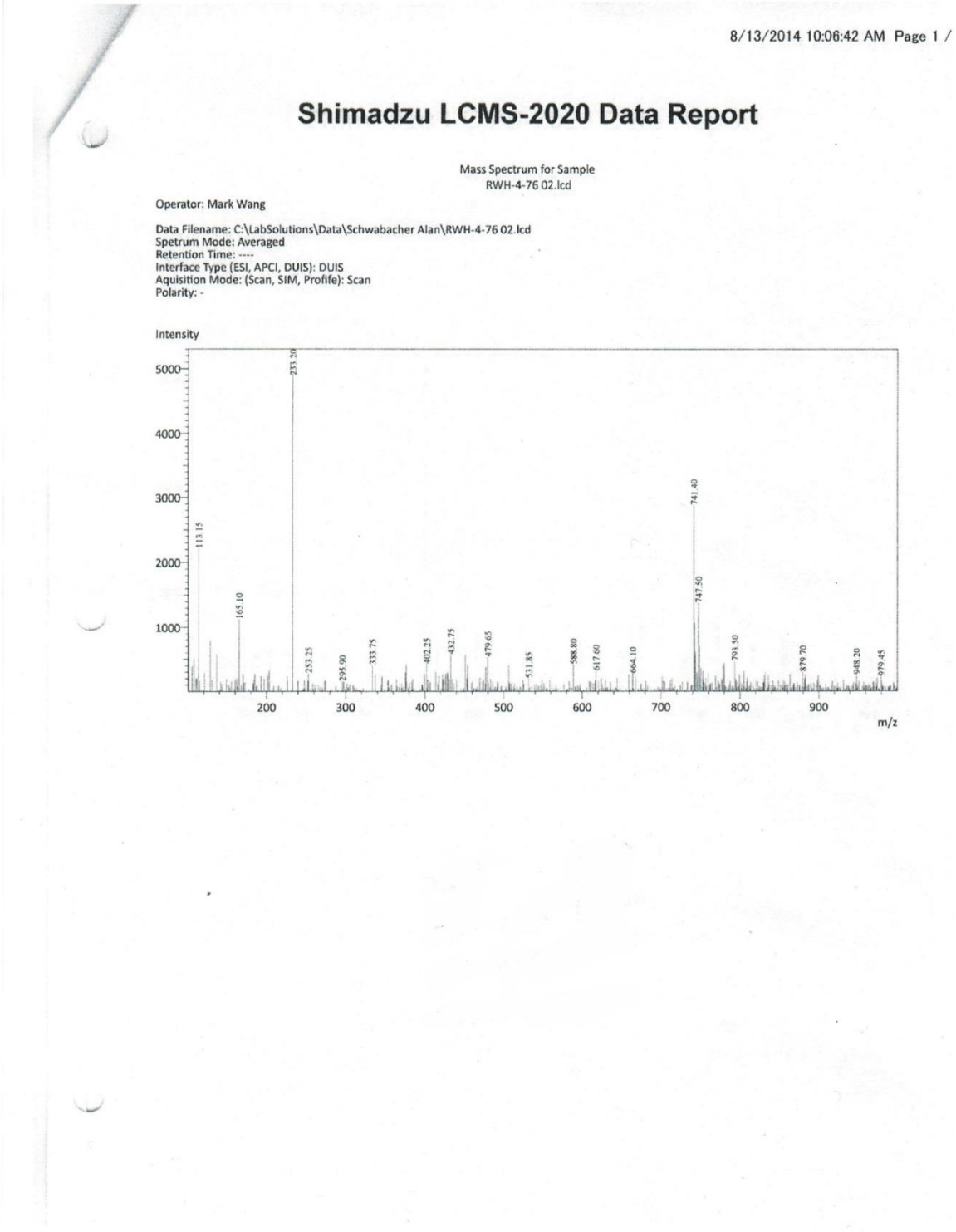
^{13}C NMR *meso-methylphosphonate tetra anionic isomer* (**26**)



^{31}P *meso-methylphosphonate tetra anionic isomer* (**26**)



ESI-MS *meso-methylphosphonate tetra anionic isomer* (**26**)



8/13/2014 10:06:42 AM Page 1 /

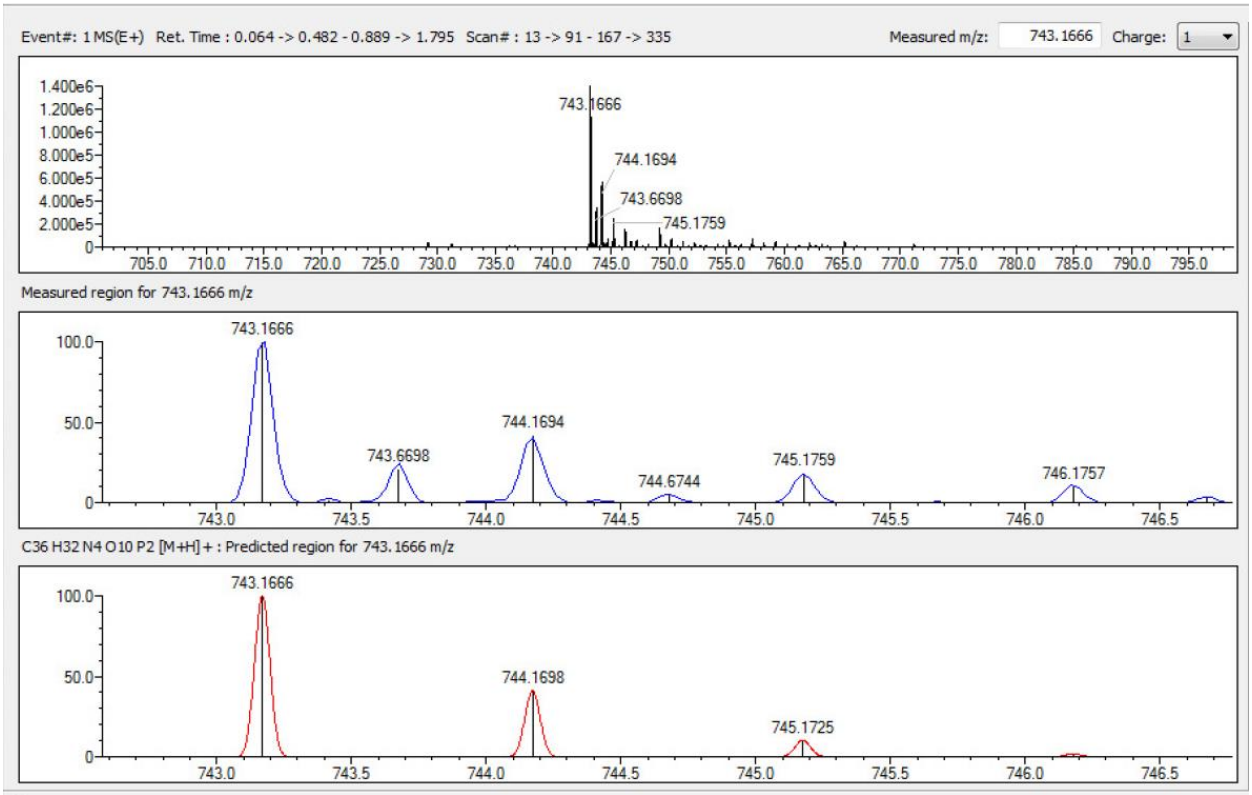
Shimadzu LCMS-2020 Data Report

Mass Spectrum for Sample
RWH-4-76 02.lcd

Operator: Mark Wang

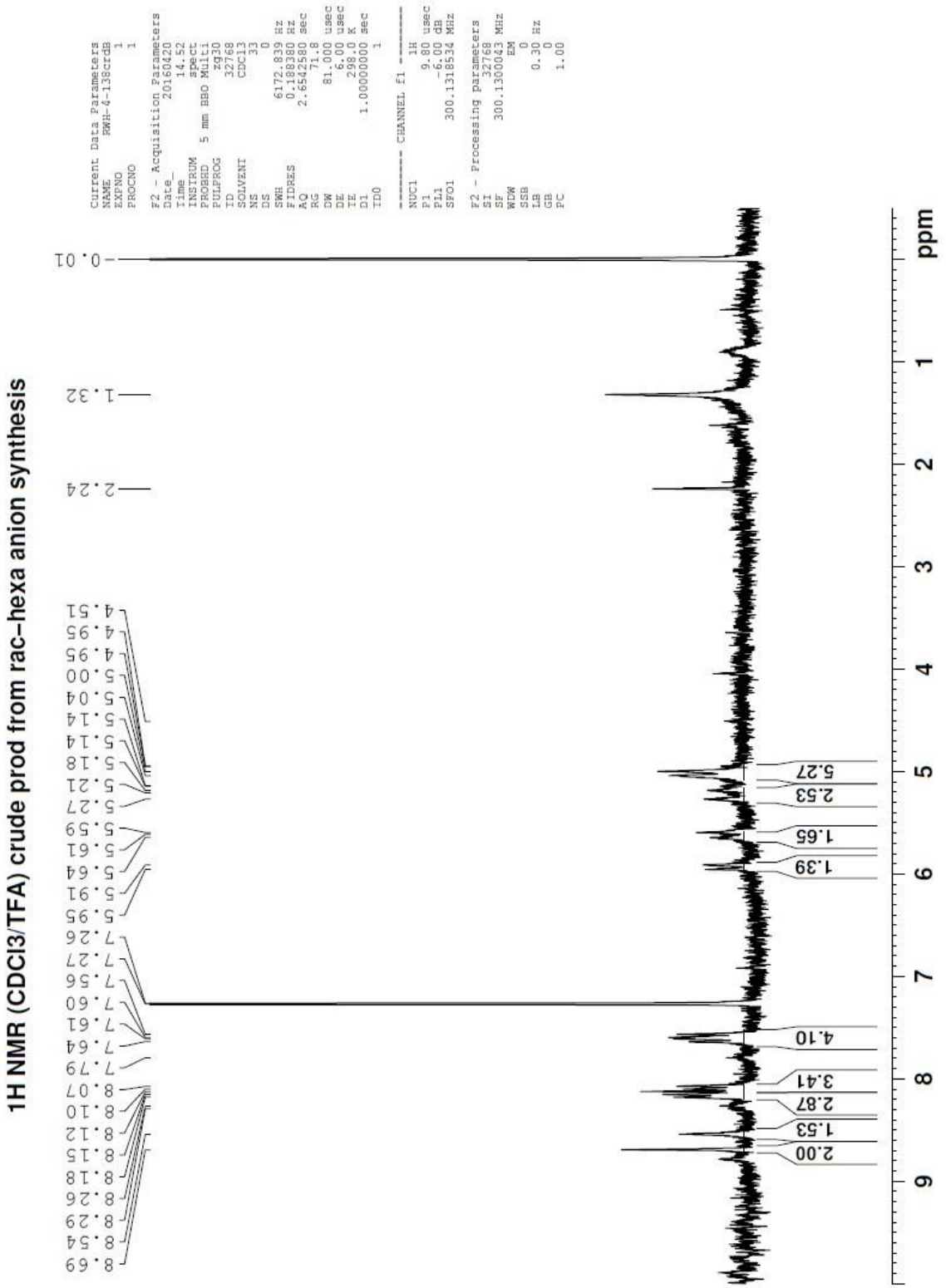
Data Filename: C:\LabSolutions\Data\Schwabacher Alan\RWH-4-76 02.lcd
Spetrum Mode: Averaged
Retention Time: ----
Interface Type (ESI, APCI, DUIS): DUIS
Aquisition Mode: (Scan, SIM, Profife): Scan
Polarity: -

HRMS *meso-methylphosphonate tetra anionic isomer* (**26**)

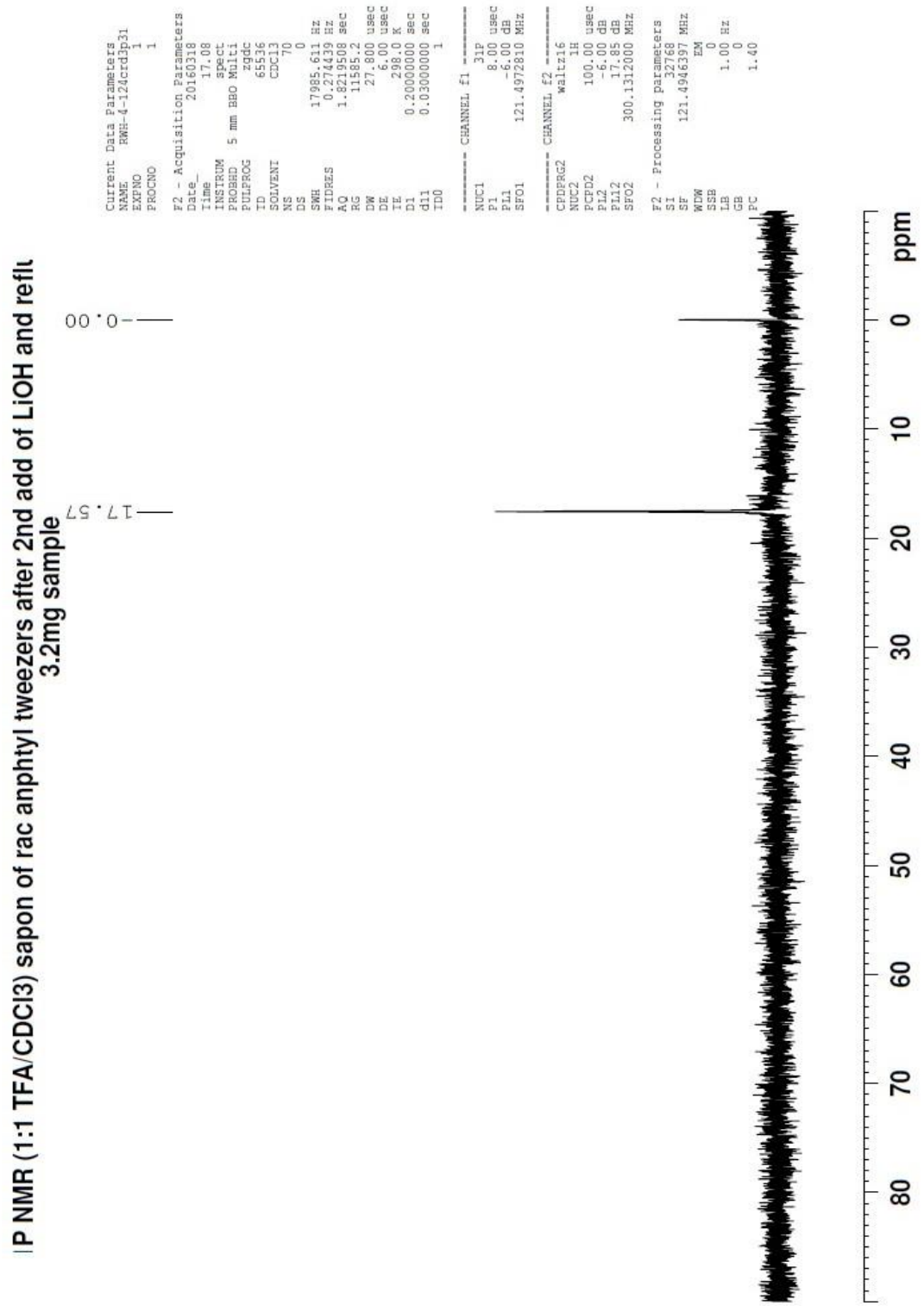


Rank	Score	Formula (M)	Ion	Meas. m/z	Pred. m/z	Diff (mDa)	Diff (ppm)	DBE	Meas. (M)
1	67.63	C42 H31 O11 P	[M+H]+	743.1666	743.1677	-1.1	-1.48	28.0	742.1593
2	67.43	C44 H26 N2 O10	[M+H]+	743.1666	743.1660	0.6	0.81	33.0	742.1593
3	66.89	C36 H32 N4 O10 P2	[M+H]+	743.1666	743.1666	0.0	0.00	24.0	742.1593
4	66.31	C39 H23 N10 O5 P	[M+H]+	743.1666	743.1663	0.3	0.40	34.0	742.1593
5	65.90	C38 H39 N2 O4 P5	[M+H]+	743.1666	743.1671	-0.5	-0.67	23.0	742.1593

^{1}H NMR *rac-hexa anionic tweezers* (**27**)



^{31}P NMR *rac-hexa anionic tweezers* (**27**)



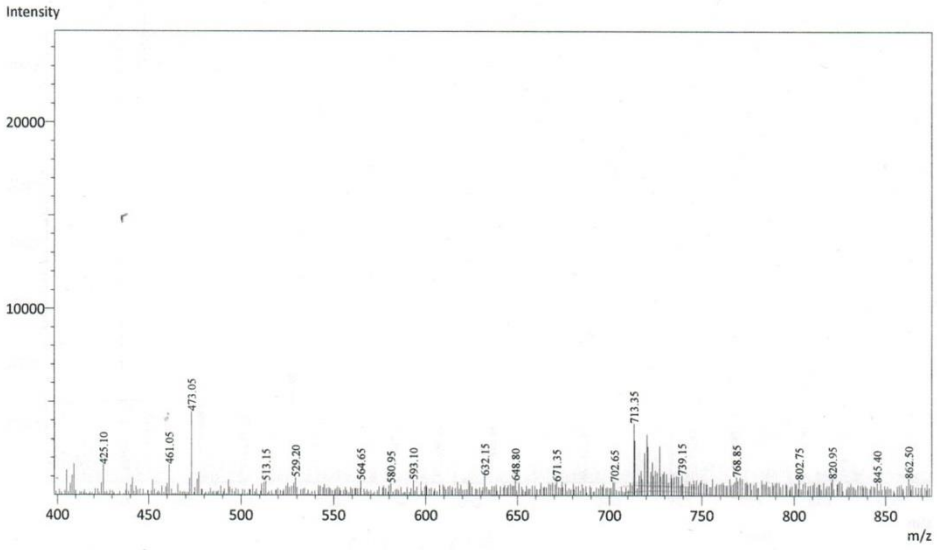
ESI-MS *rac-hexa anionic tweezers* (**27**)

Shimadzu LCMS-2020 Data Report

Mass Spectrum for Sample
RWH-4-127B01.lcd

Operator:Robert Hoppe

Data Filename: C:\LabSolutions\Data\Schwabacher Alan\RWH-4-127B01.lcd
Spetrum Mode: Averaged
Retention Time: ----
Interface Type (ESI, APCI, DUIS): DUIS
Aquisition Mode: (Scan, SIM, Profife): Scan
Polarity: -
H2O/0.1% HCOOH, CH3CN/0.1% HCOOH



HRMS NMR *rac-hexa anionic tweezers* (**27**)

Formula Predictor Report - RWH-4-127.lcd

Data File: C:\LabSolutions\Data\Training 20160307\RWH-4-127.lcd

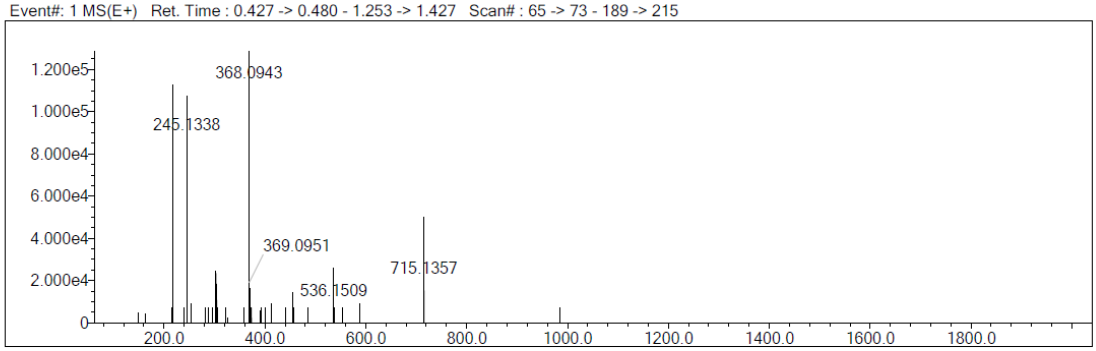
Elmt	Val.	Min	Max	Elmt	Val.	Min	Max	Use Adduct
H	1	0	40	O	2	0	15	H
C	4	0	40	P	3	0	4	
N	3	0	5					

Error Margin (ppm): 5
HC Ratio: unlimited
Max Isotopes: all
MSn Iso RI (%): 75.00

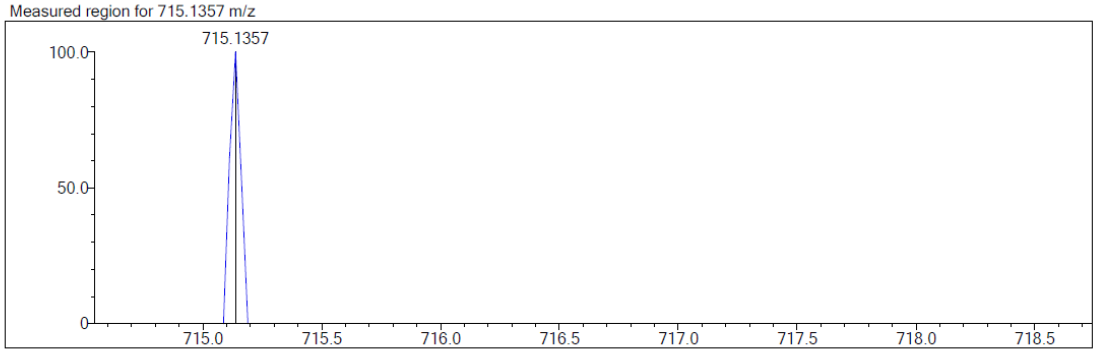
DBE Range: not fixed
Apply N Rule: yes
Isotope RI (%): 1.00
MSn Logic Mode: AND

Electron Ions: both
Use MSn Info: yes
Isotope Res: 10000
Max Results: 50

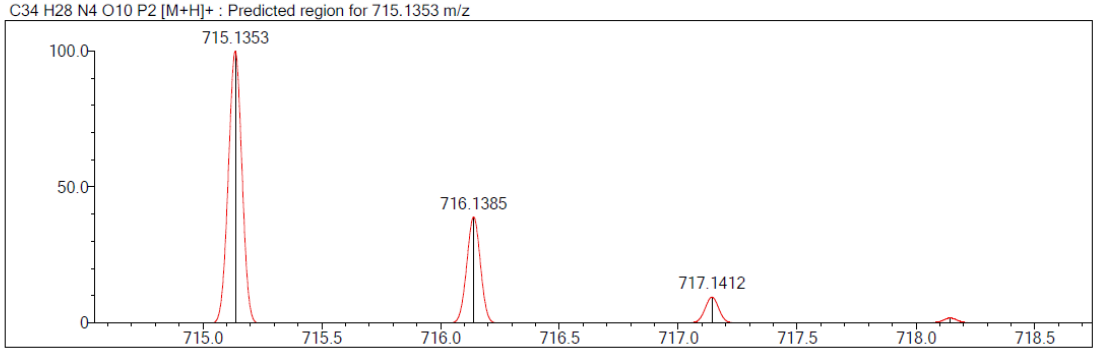
Event#: 1 MS(E+) Ret. Time : 0.427 -> 0.480 - 1.253 -> 1.427 Scan# : 65 -> 73 - 189 -> 215



Measured region for 715.1357 m/z

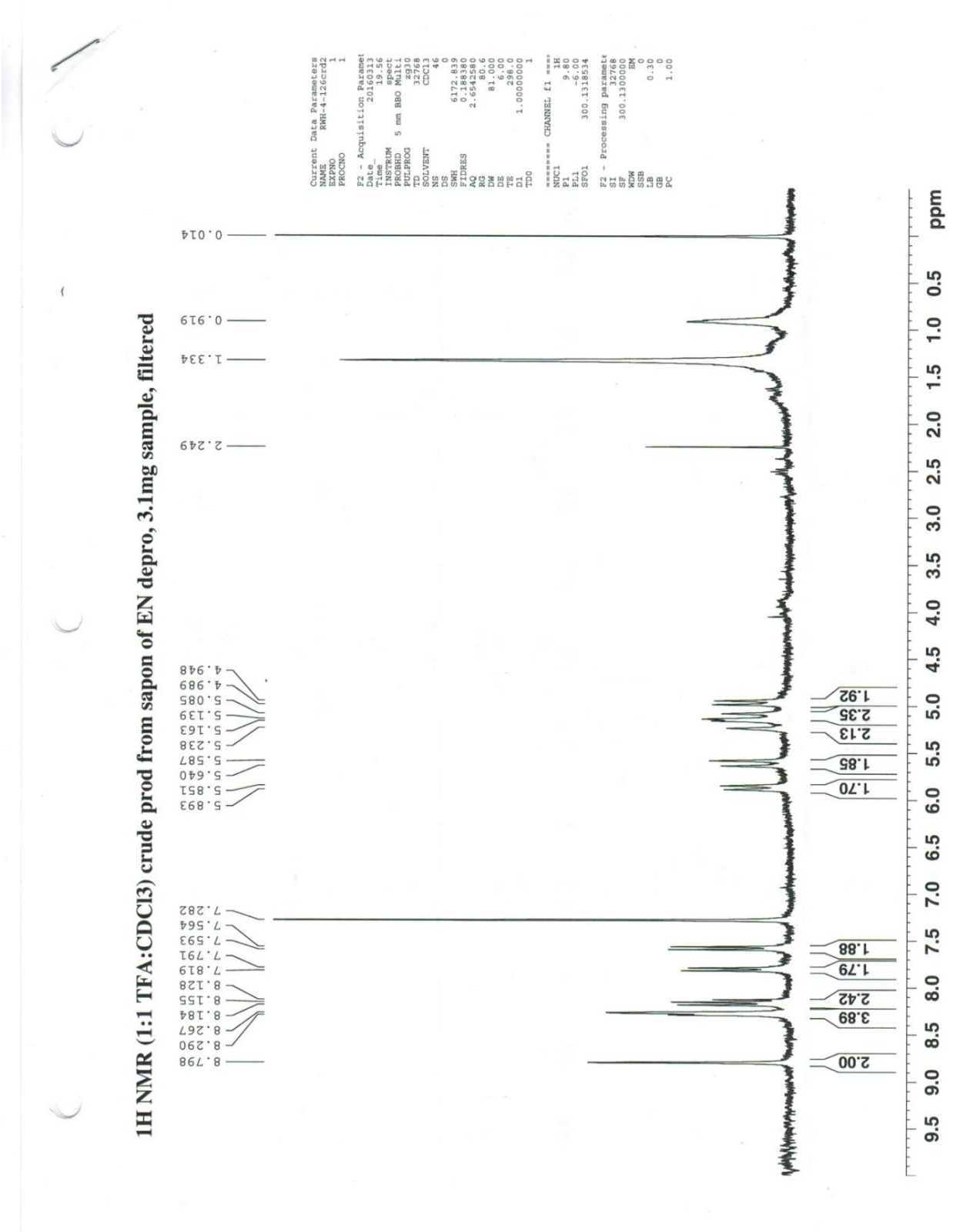


C34 H28 N4 O10 P2 [M+H]+ : Predicted region for 715.1353 m/z

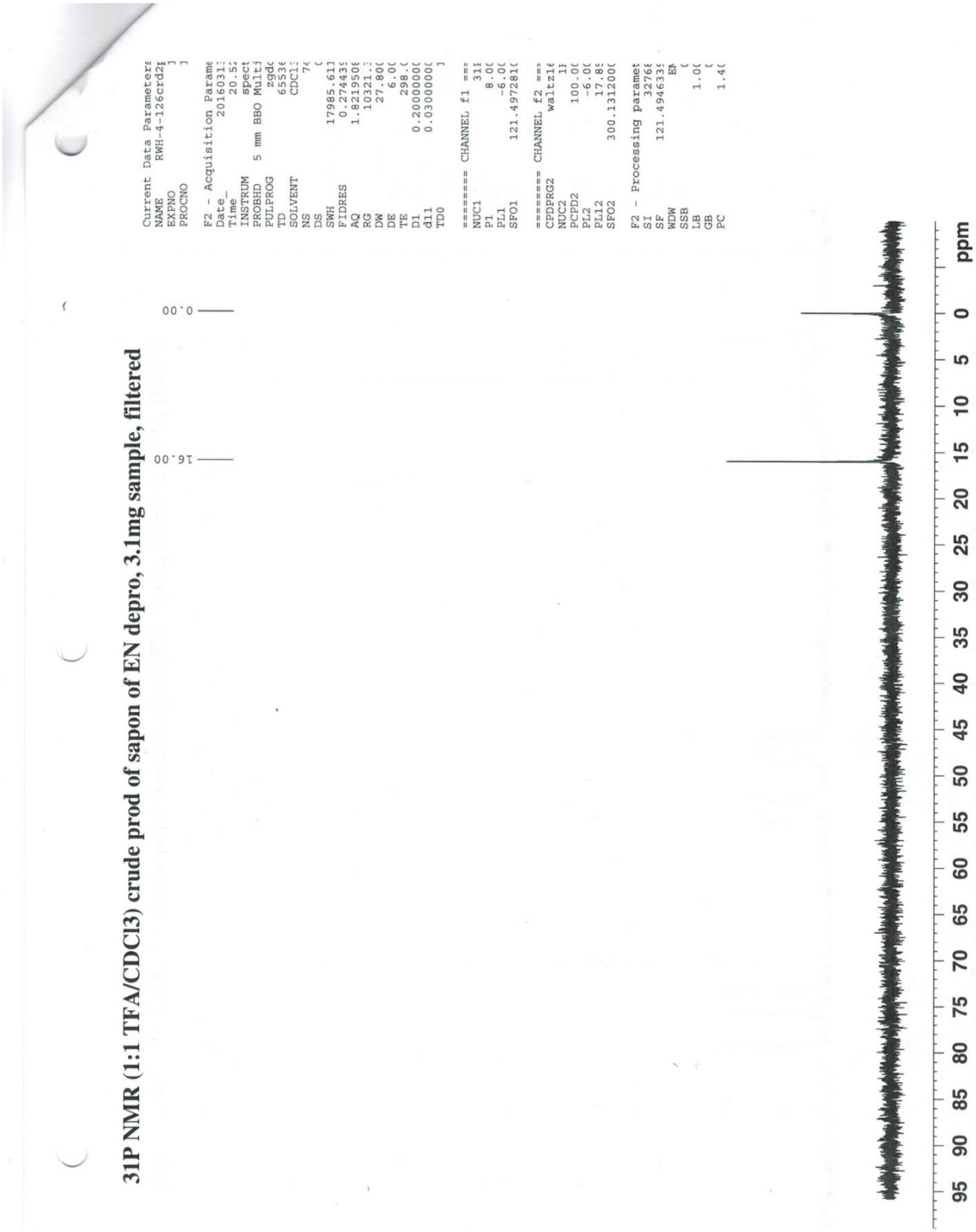


Rank	Score	Formula (M)	Ion	Meas. m/z	Pred. m/z	Df. (mDa)	Df. (ppm)	DBE	Meas. (M)	Pred. (M)	Iso
1	0.00	C34 H28 N4 O10 P2	[M+H]+	715.1357	715.1353	0.4	0.56	24.0	714.1284	714.1281	0.00

^{1}H NMR *meso-hexa anionic isomer* (**28**)



^{31}P NMR *meso-hexa anionic isomer* (**28**)



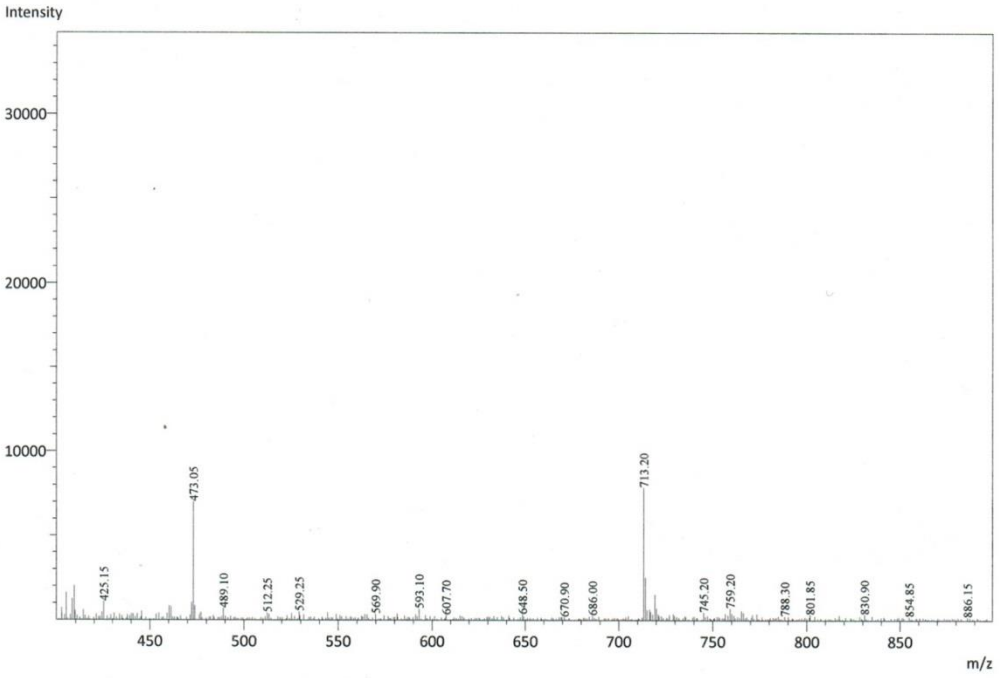
ESI-MS *meso-hexa anionic isomer* (**28**)

Shimadzu LCMS-2020 Data Report

Mass Spectrum for Sample
RWH-4-126.lcd

Operator:Robert Hoppe

Data Filename: C:\LabSolutions\Data\Schwabacher Alan\RWH-4-126.lcd
Spetrum Mode: Averaged
Retention Time: ----
Interface Type (ESI, APCI, DUIS): DUIS
Aquisition Mode: (Scan, SIM, Profife): Scan
Polarity: -
H2O/0.1% HCOOH, CH3CN/0.1% HCOOH



HRMS *meso-hexa anionic isomer* (**28**)

Formula Predictor Report - RWH-4-126.lcd

Data File: C:\LabSolutions\Data\Training 20160307\RWH-4-126.lcd

Elmt	Val.	Min	Max
H	1	0	50
C	4	0	50
N	3	0	4

Elmt	Val.	Min	Max
O	2	0	10
P	3	0	2

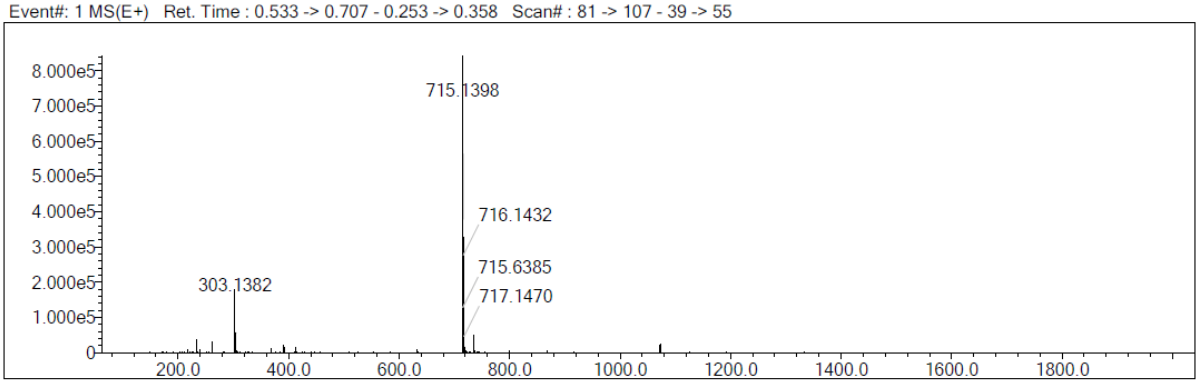
Use Adduct
H

Error Margin (ppm): 25
HC Ratio: unlimited
Max Isotopes: all
MSn Iso RI (%): 75.00

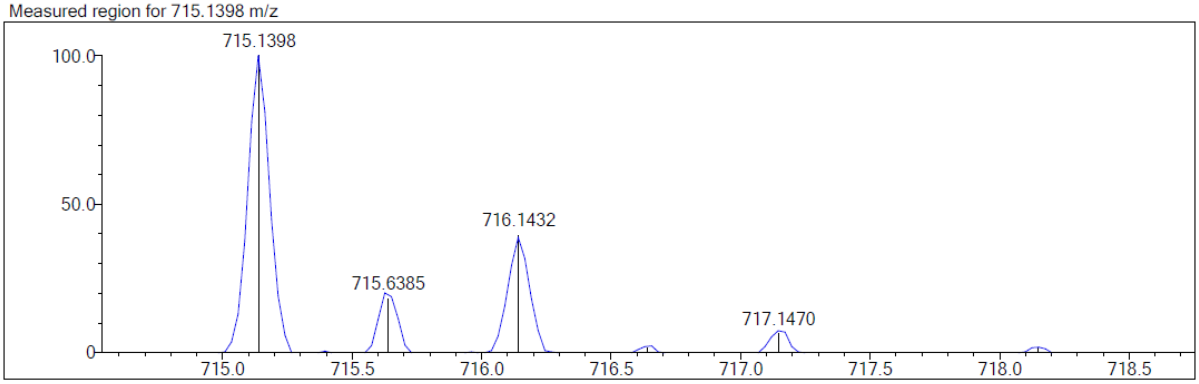
DBE Range: not fixed
Apply N Rule: yes
Isotope RI (%): 1.00
MSn Logic Mode: AND

Electron Ions: both
Use MSn Info: yes
Isotope Res: 10000
Max Results: 50

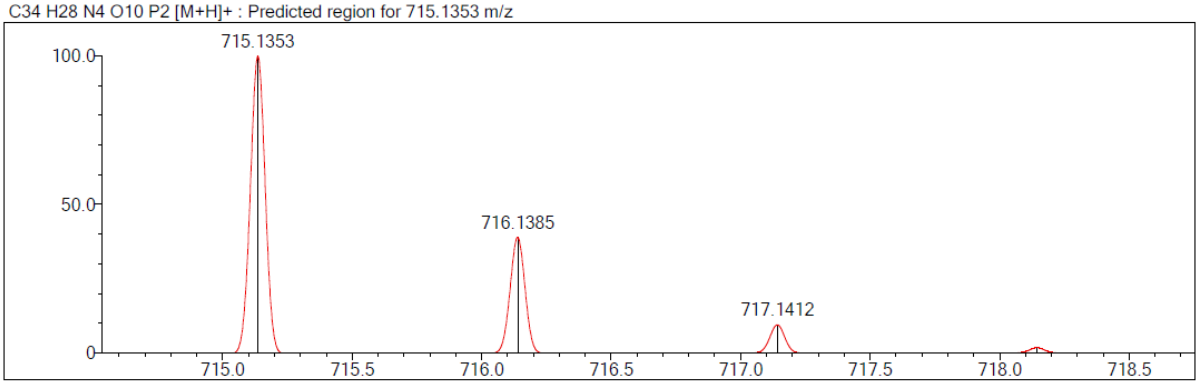
Event#: 1 MS(E+) Ret. Time : 0.533 -> 0.707 - 0.253 -> 0.358 Scan# : 81 -> 107 - 39 -> 55



Measured region for 715.1398 m/z

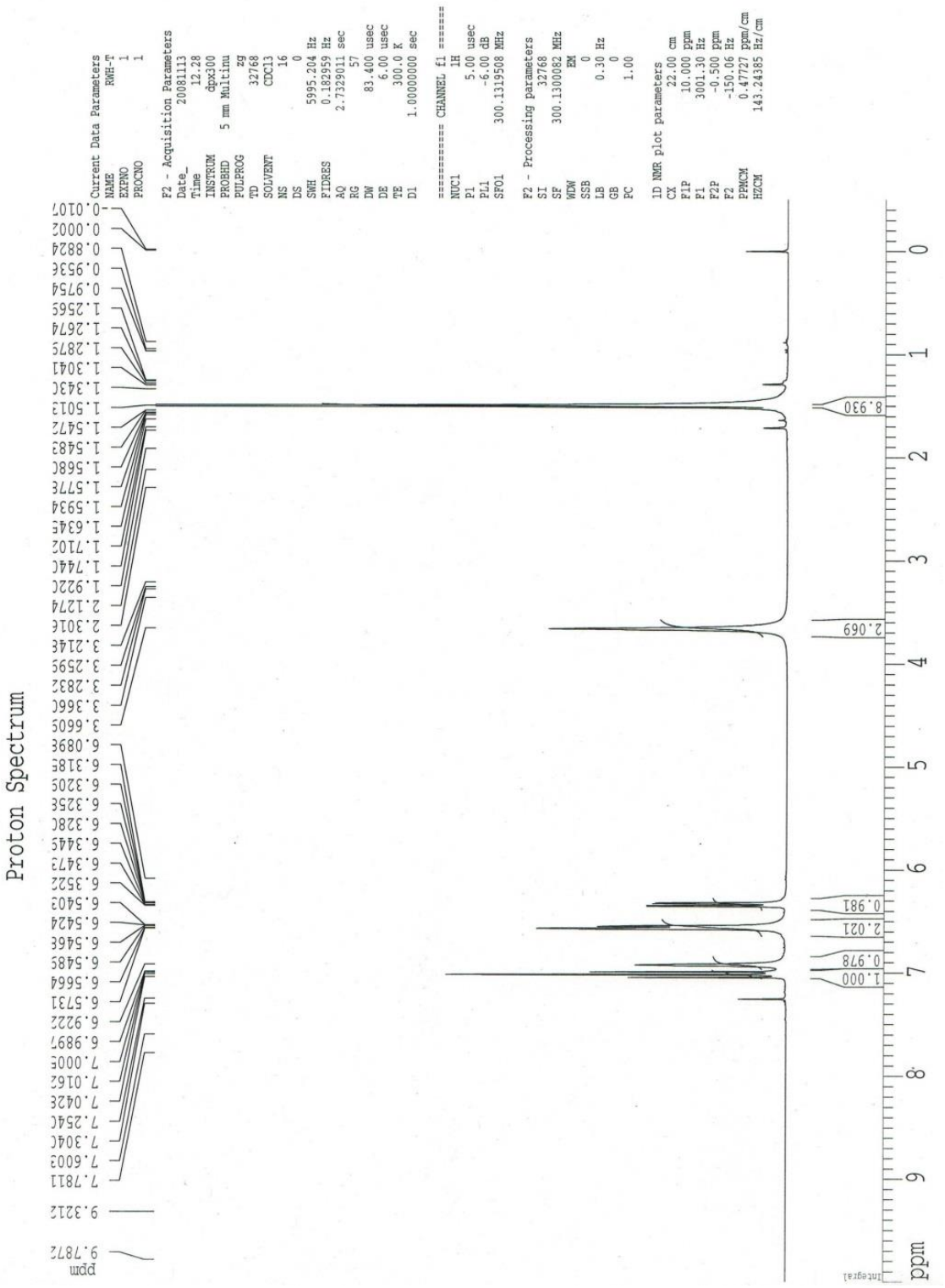


C34 H28 N4 O10 P2 [M+H]+ : Predicted region for 715.1353 m/z

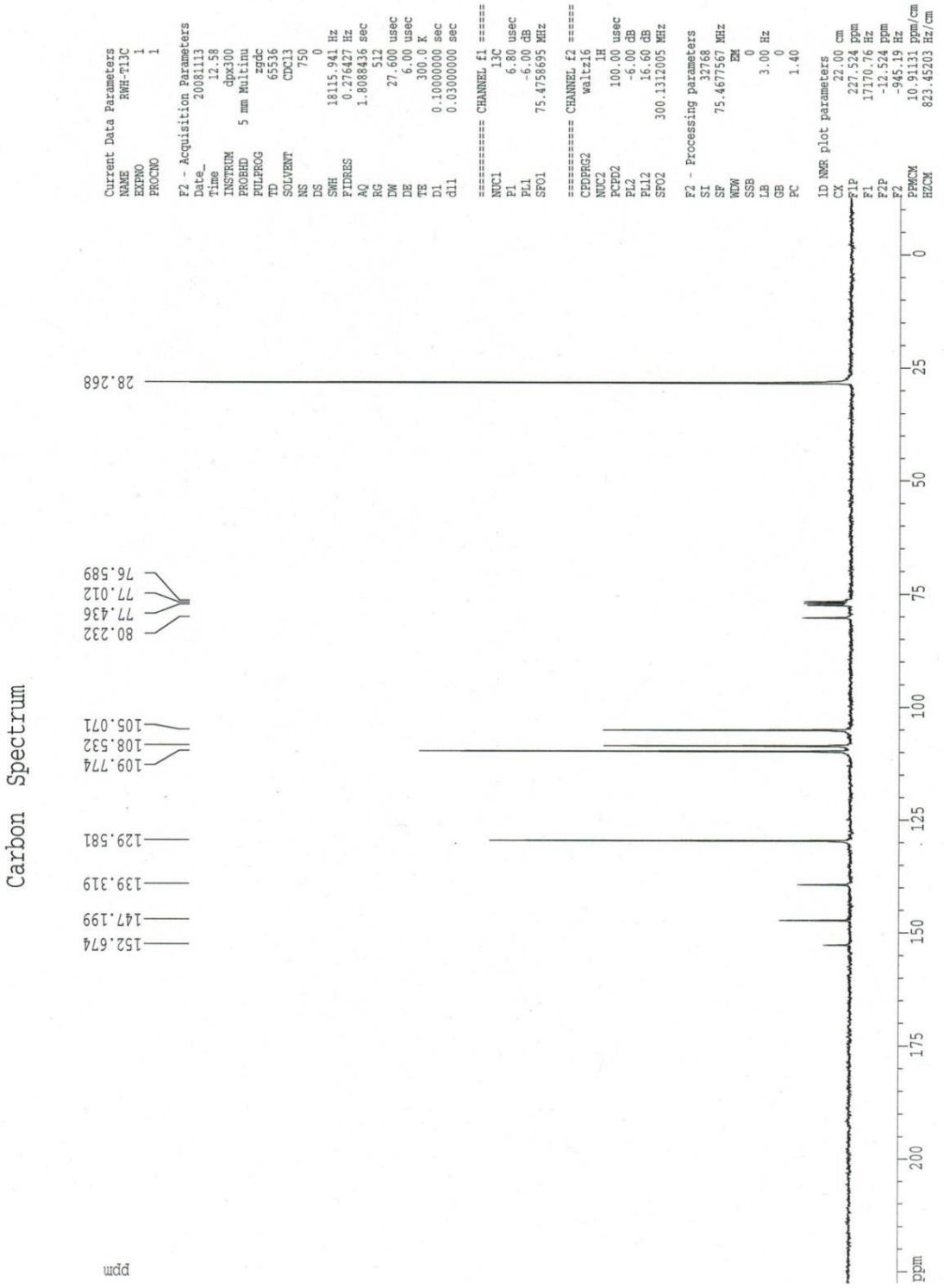


Rank	Score	Formula (M)	Ion	Meas. m/z	Pred. m/z	Df. (mDa)	Df. (ppm)	DBE	Meas. (M)	Pred. (M)	Iso
3	72.38	C34 H28 N4 O10 P2	[M+H]+	715.1398	715.1353	4.5	6.29	24.0	714.1325	714.1281	93.88

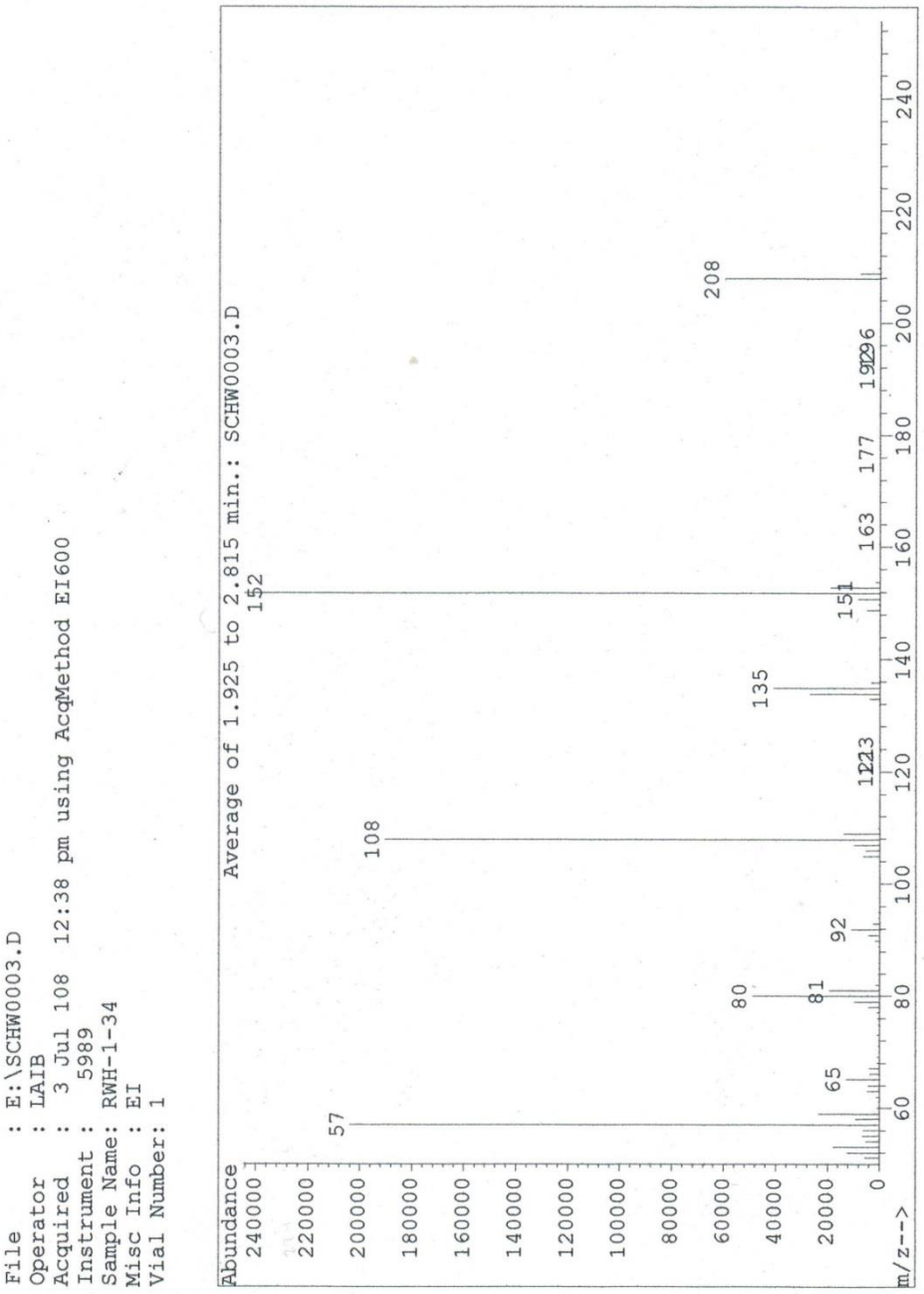
^{1}H NMR *tert*-butyl (3-aminophenyl)carbamate (**29**)



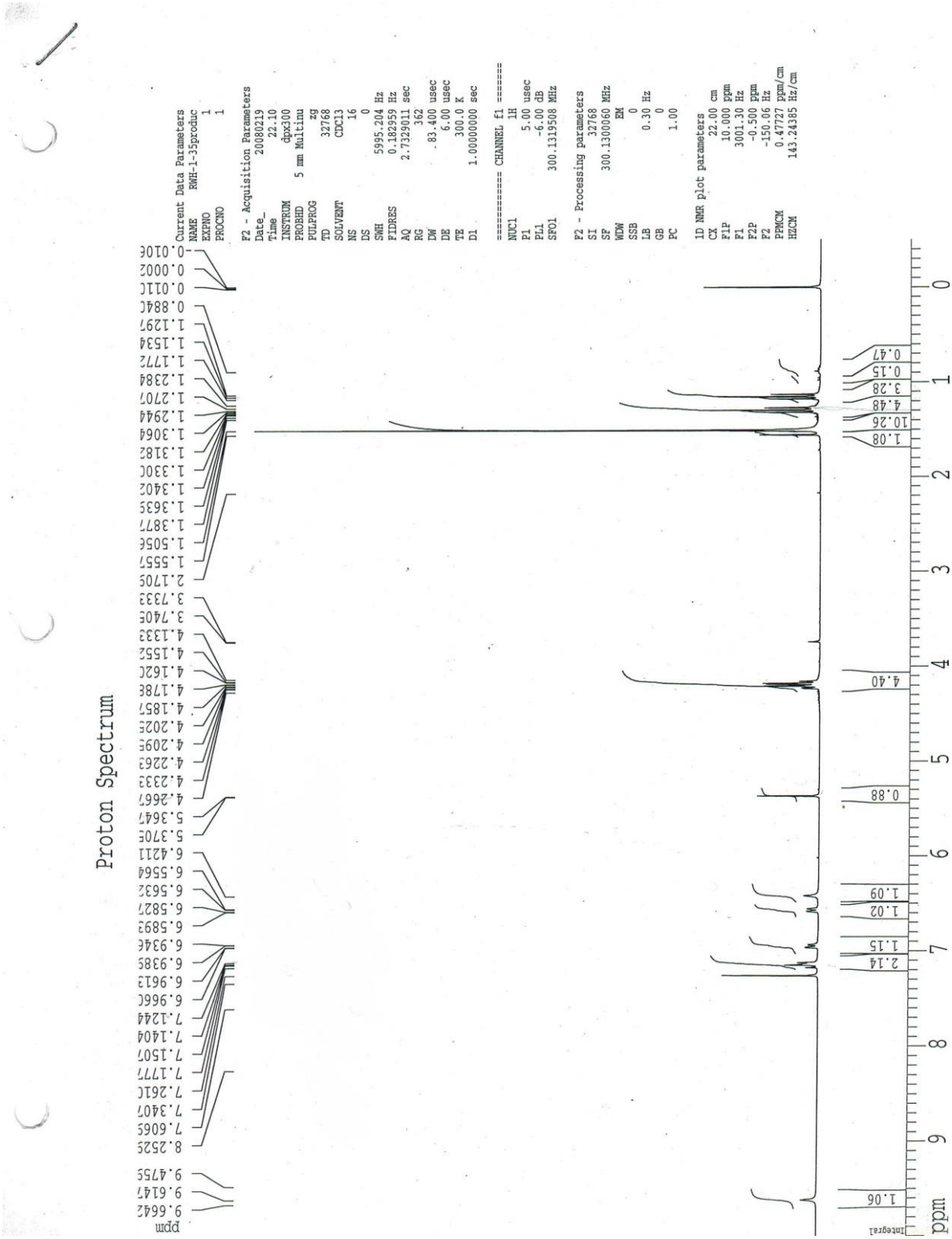
^{13}C NMR <u>*tert*-butyl (3-aminophenyl)carbamate</u> (**29**)



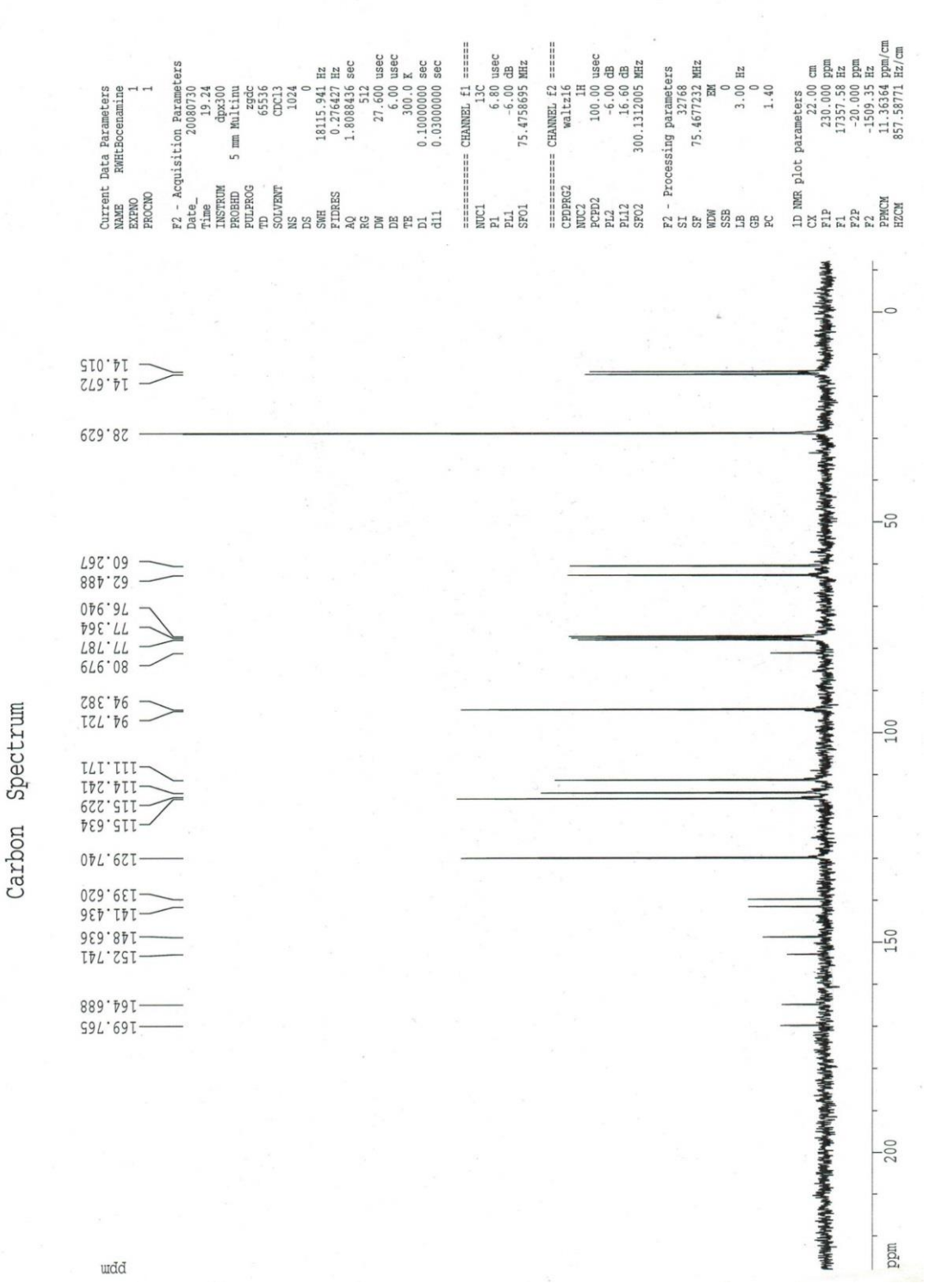
MS (EI, 70eV) <u>*tert*-butyl (3-aminophenyl)carbamate</u> (**29**)



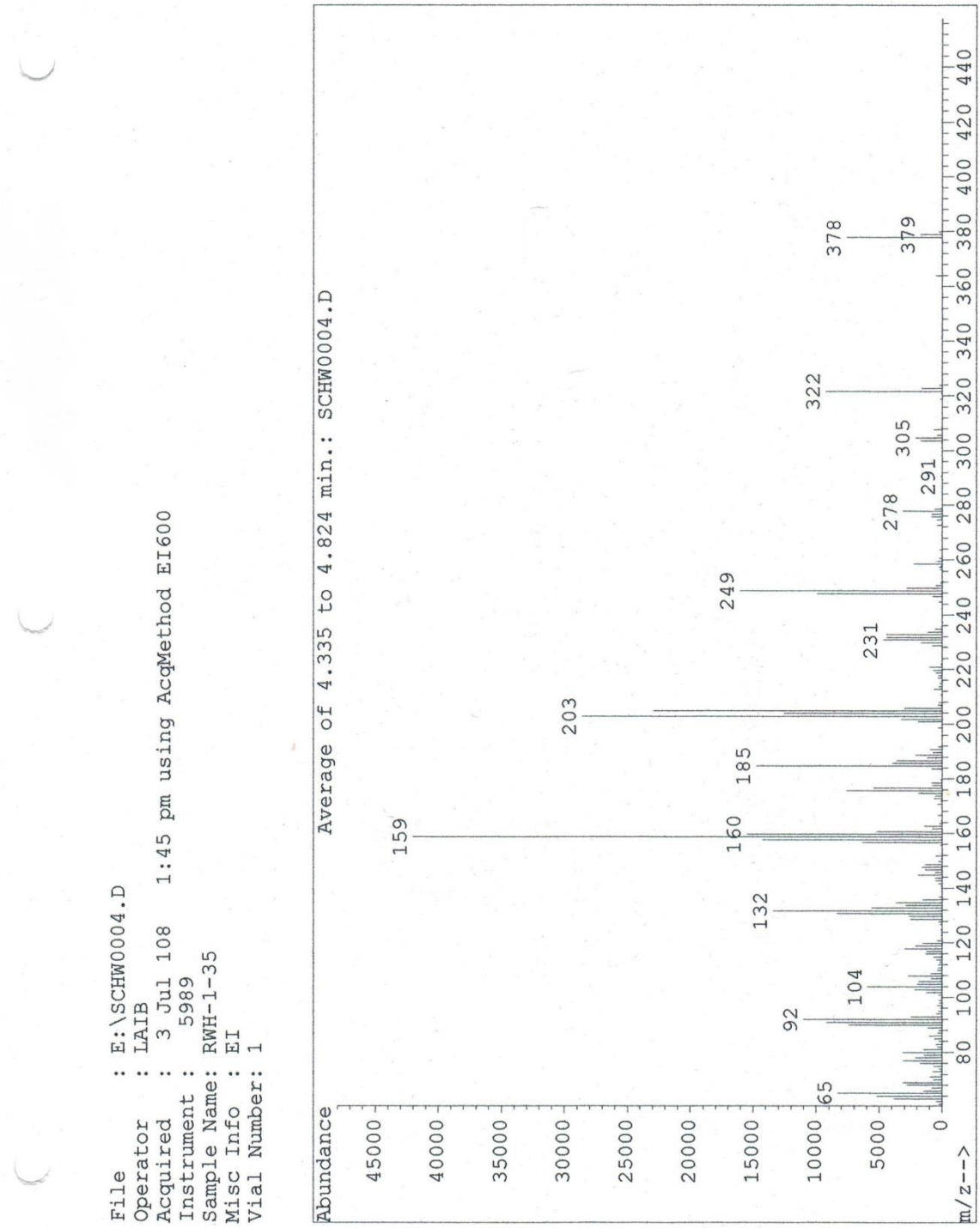
^{1}H NMR *2-(3-tert-Butoxycarbonylamino-phenylamino)-but-2-enedioic acid diethyl ester* (**30**)



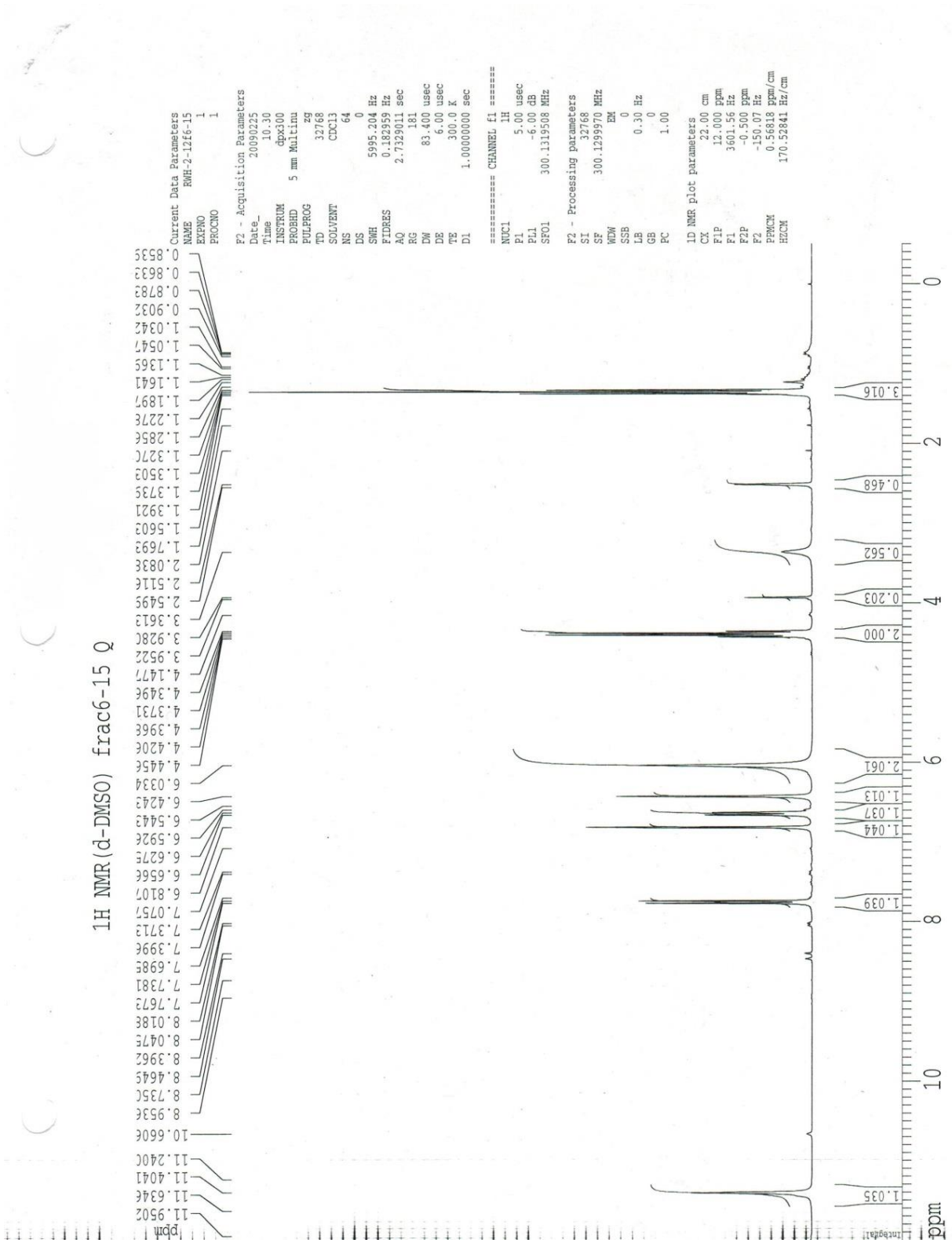
^{13}C NMR *2-(3-tert-Butoxycarbonylamino-phenylamino)-but-2-enedioic acid diethyl ester* (**30**)



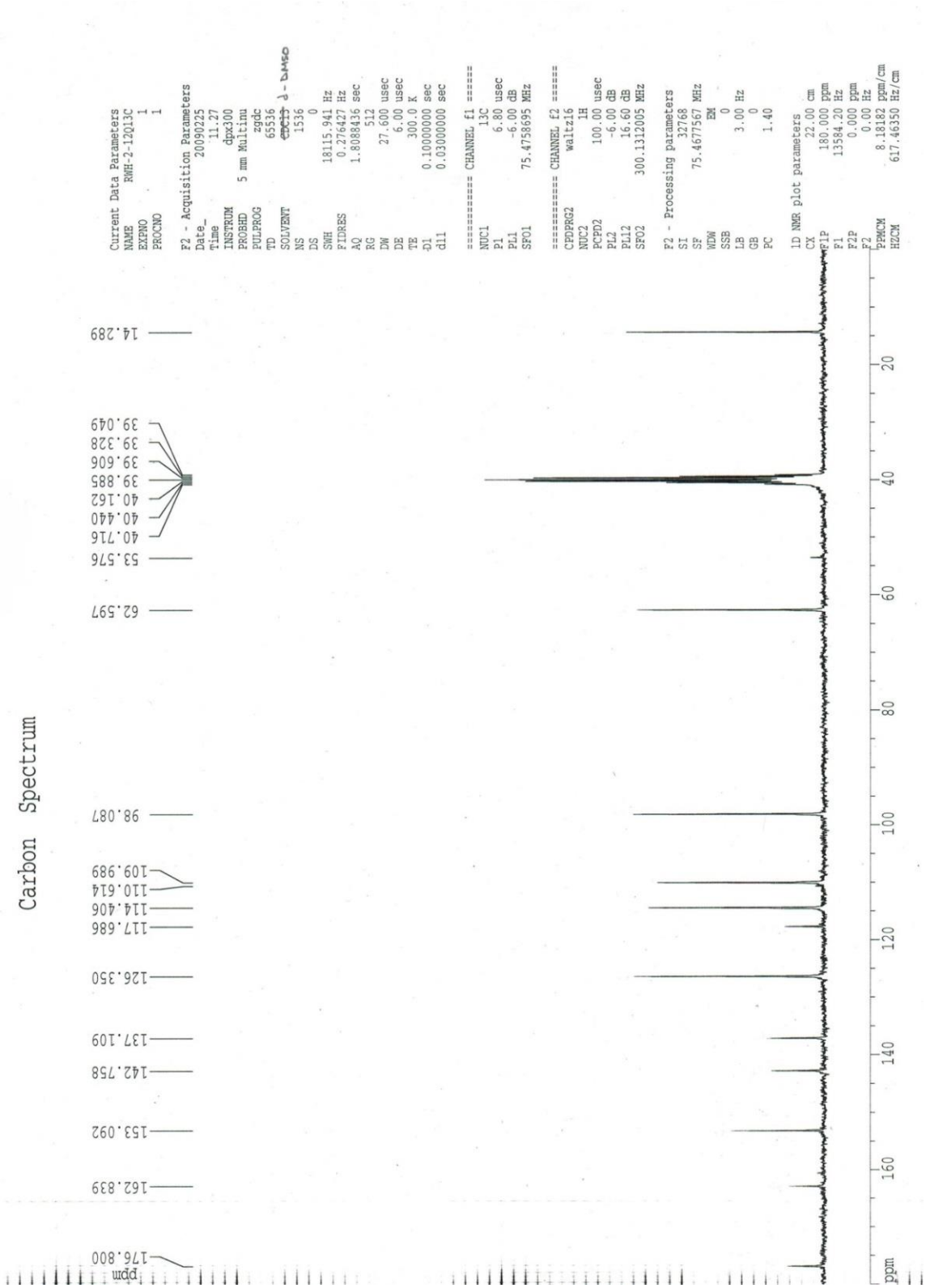
MS (70eV) <u>*2-(3-tert-Butoxycarbonylamino-phenylamino)-but-2-enedioic acid diethyl ester*</u> (**30**)



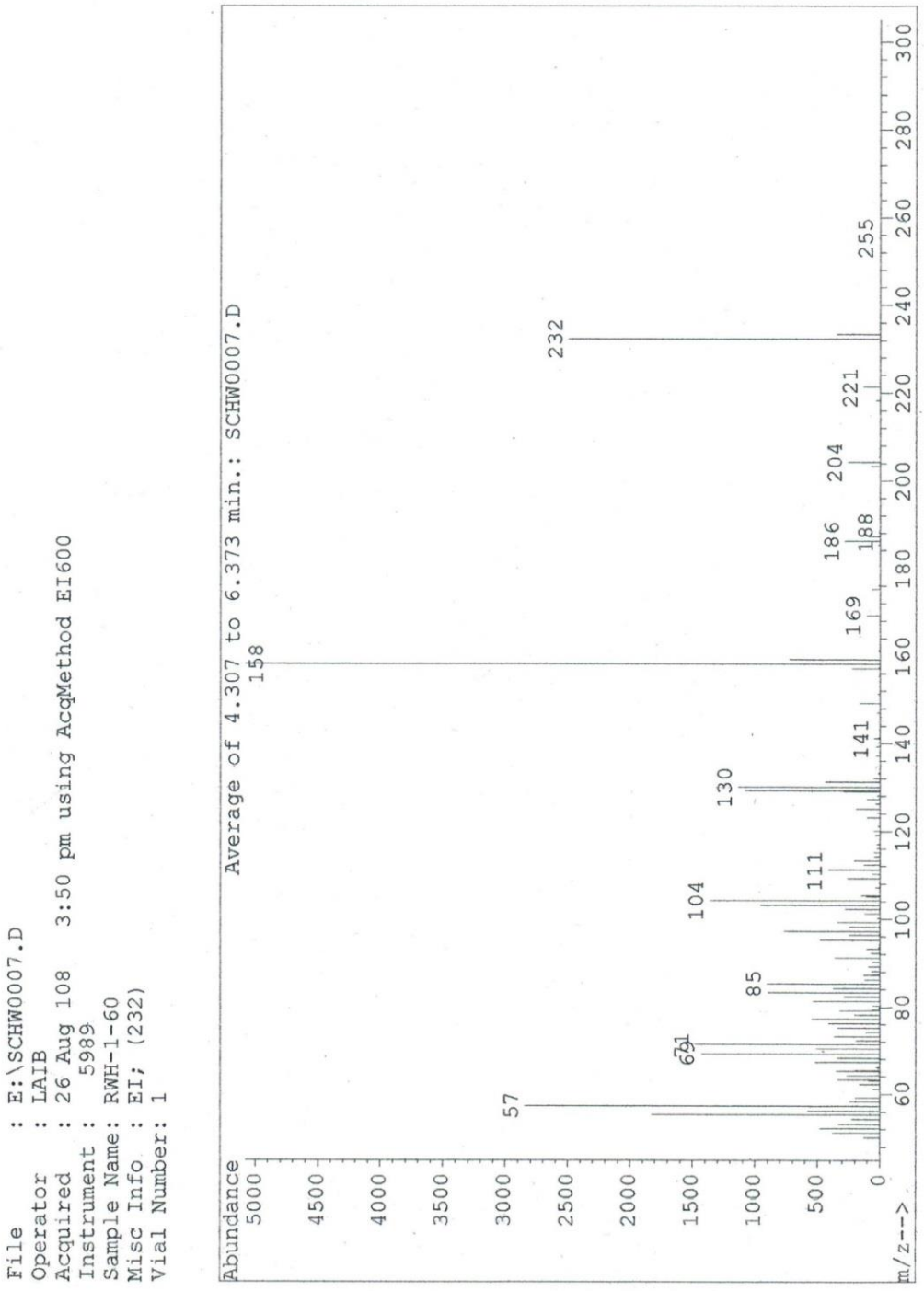
[1]H NMR *7-Amino-4-oxo-1,4-dihydro-quinoline-2-carboxylic acid ethyl ester* (**31**)



^{13}C NMR *7-Amino-4-oxo-1,4-dihydro-quinoline-2-carboxylic acid ethyl ester* (**31**)



MS (EI, 70eV) *7-Amino-4-oxo-1,4-dihydro-quinoline-2-carboxylic acid ethyl ester* (**31**)



MS (ESI, + ion) *7-Amino-4-oxo-1,4-dihydro-quinoline-2-carboxylic acid ethyl ester* (**31**)

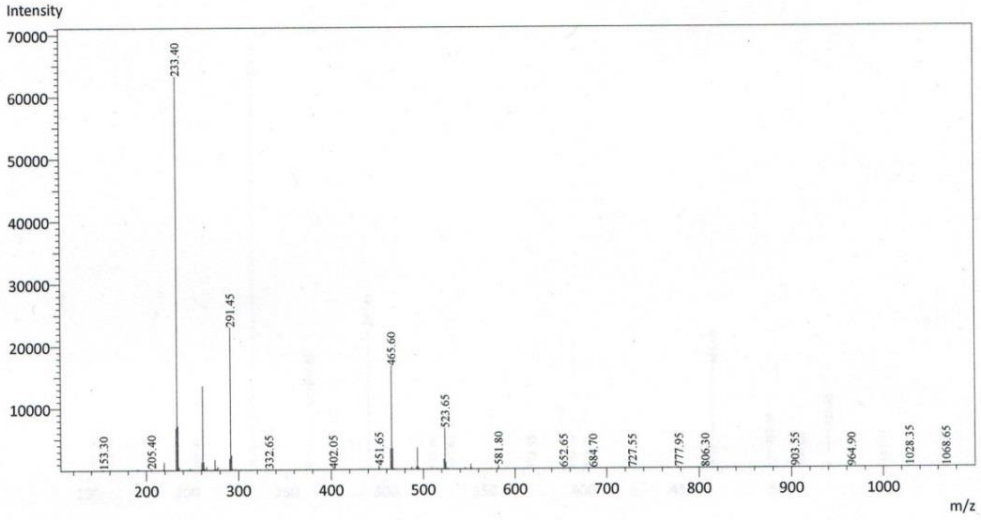
8/14/2014 11:52:49 AM Page 1 / 1

Shimadzu LCMS-2020 Data Report

Mass Spectrum for Sample
RWH-4-83.lcd

Operator: Mark Wang

Data Filename: C:\LabSolutions\Data\Schwabacher Alan\RWH-4-83.lcd
Spetrum Mode: Averaged
Retention Time: ----
Interface Type (ESI, APCI, DUIS): DUIS
Aquisition Mode: (Scan, SIM, Profife): Scan
Polarity: +

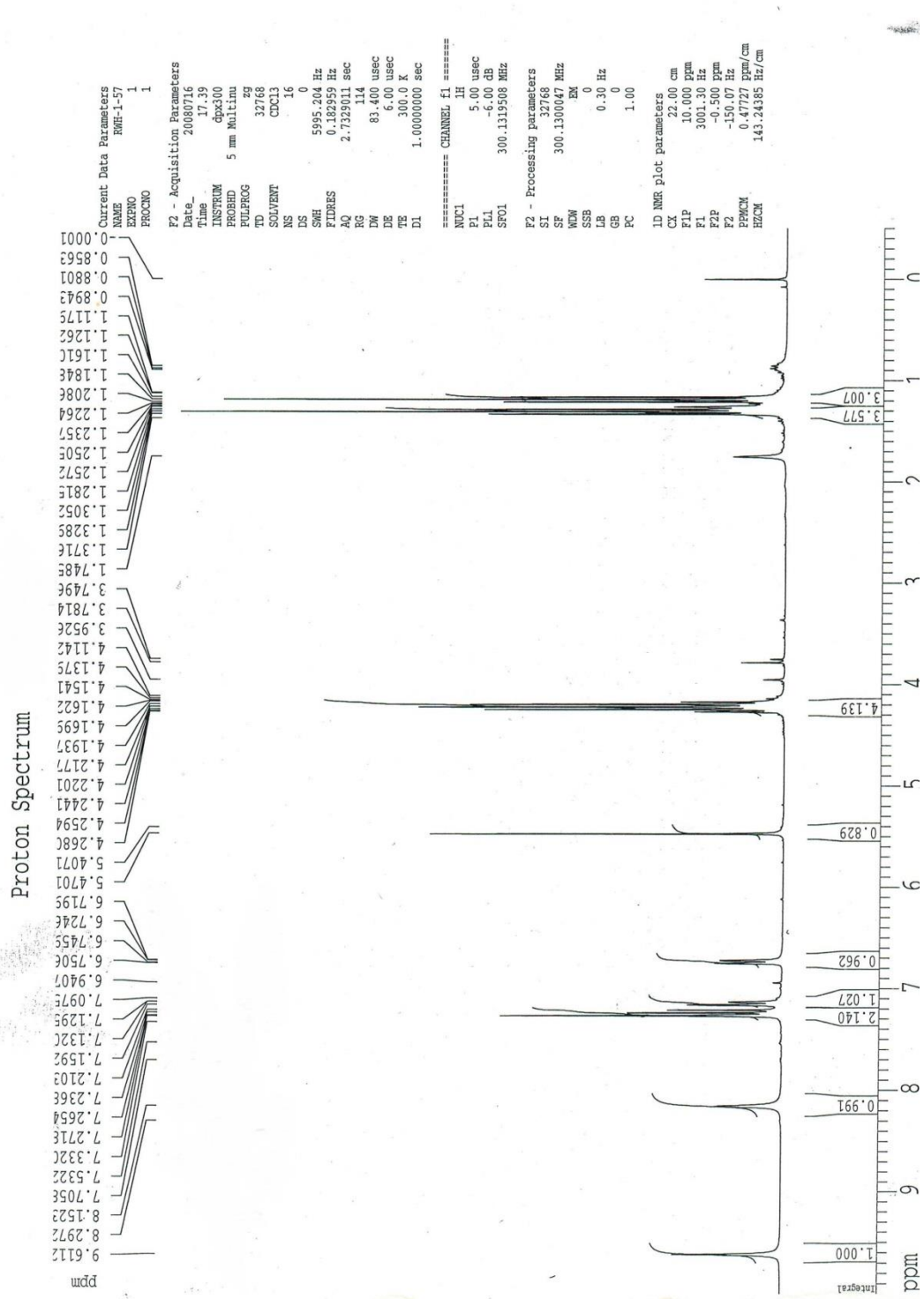


233 = M + M^+

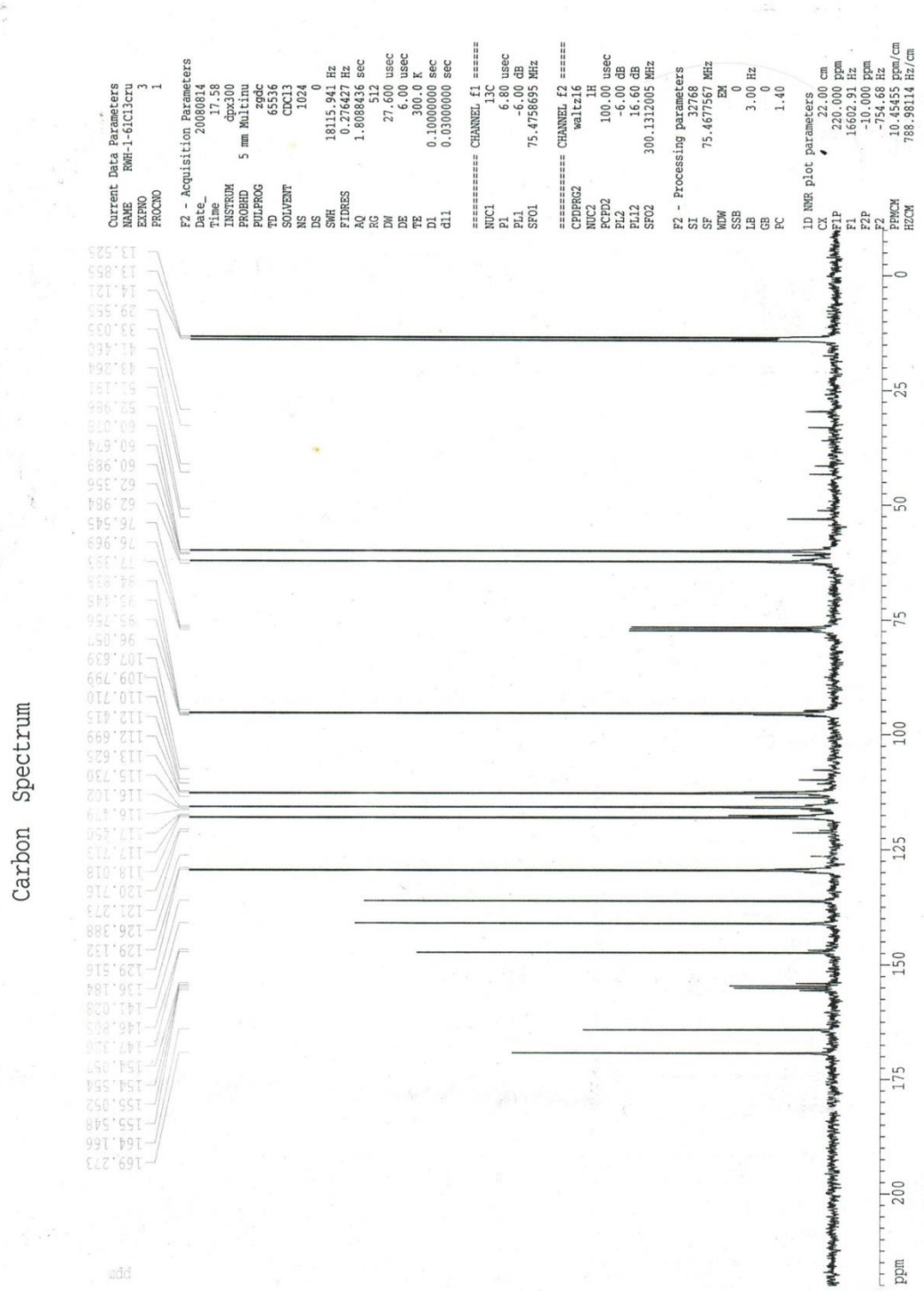
291 = M + 59

465 = 2M + M^+

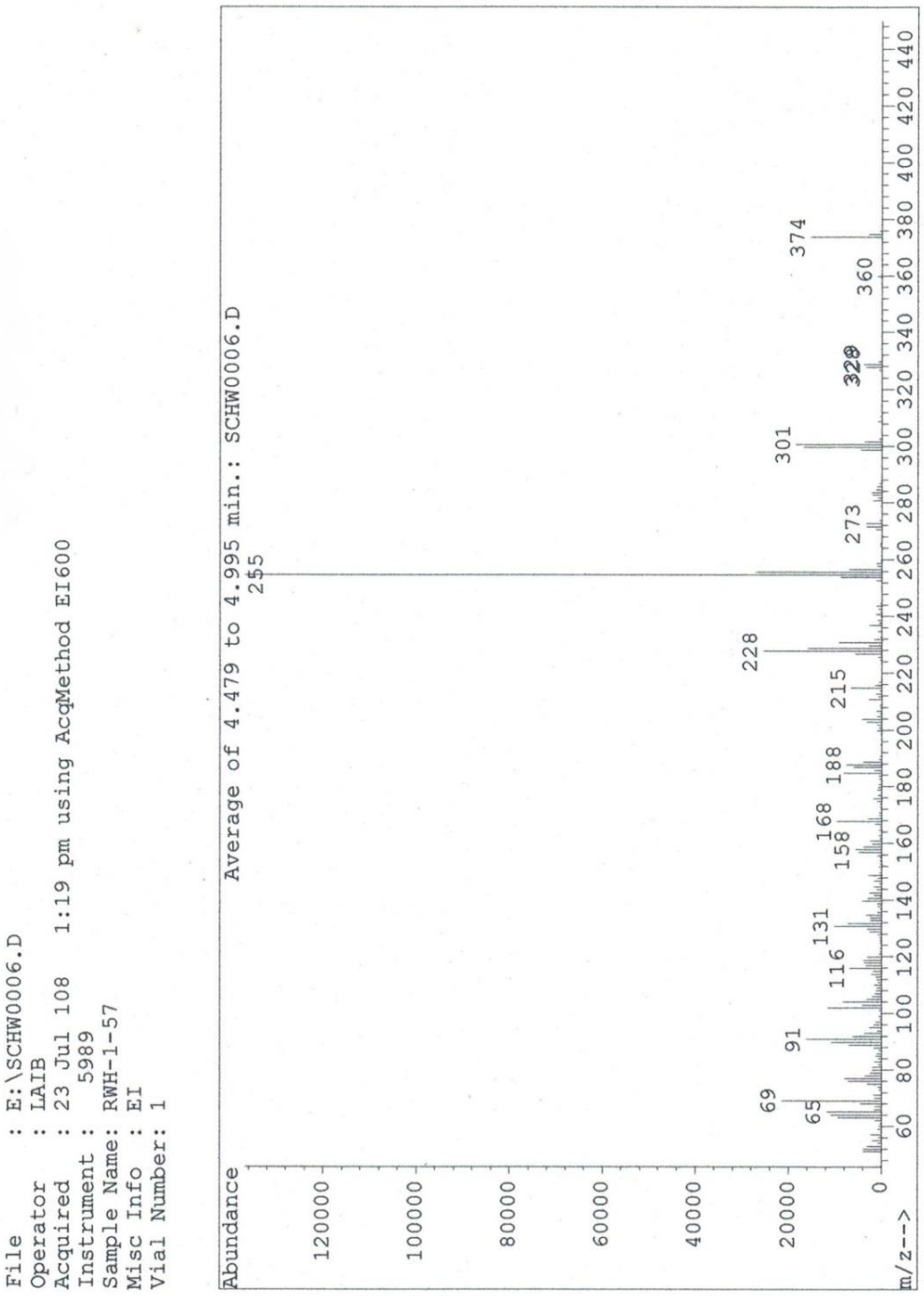
^{1}H NMR *Diethyl 2-((3-(2,2,2-trifluoroacetamido)phenyl)amino)fumarate* (**34**)



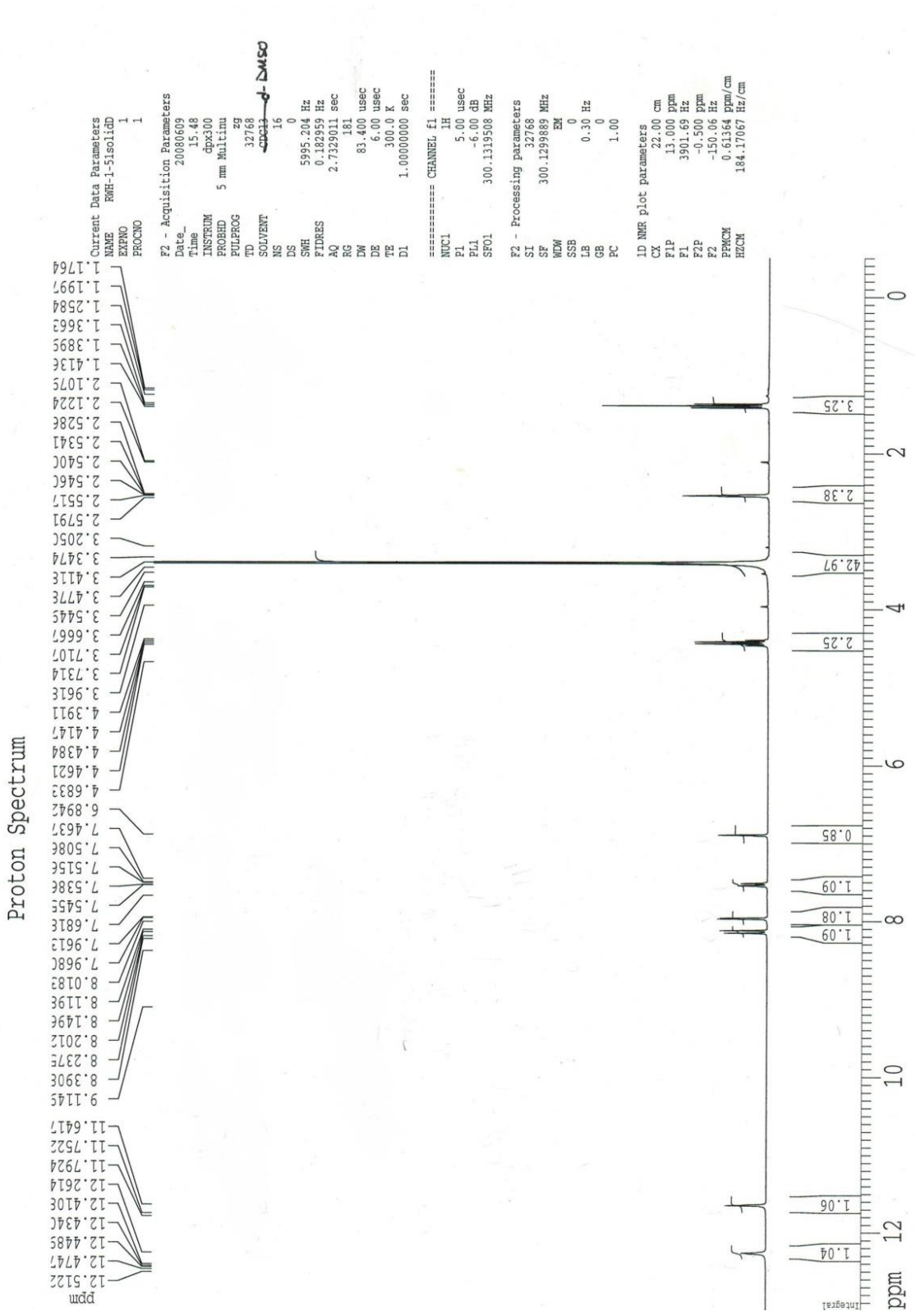
^{13}C NMR *Diethyl 2-((3-(2,2,2-trifluoroacetamido)phenyl)amino)fumarate* (**34**)



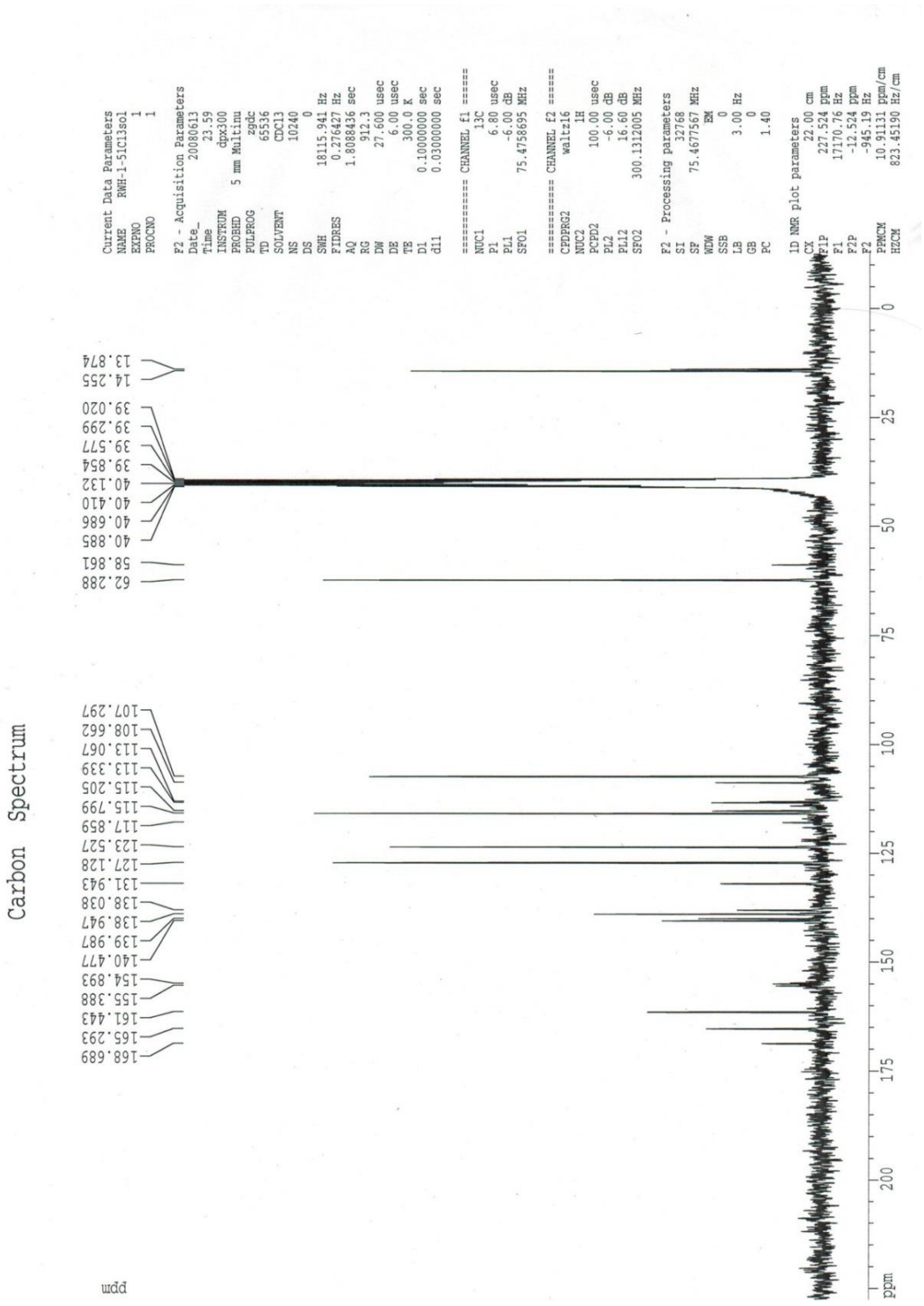
MS (EI, 70eV) *Diethyl 2-((3-(2,2,2-trifluoroacetamido)phenyl)amino)fumarate* (**34**)



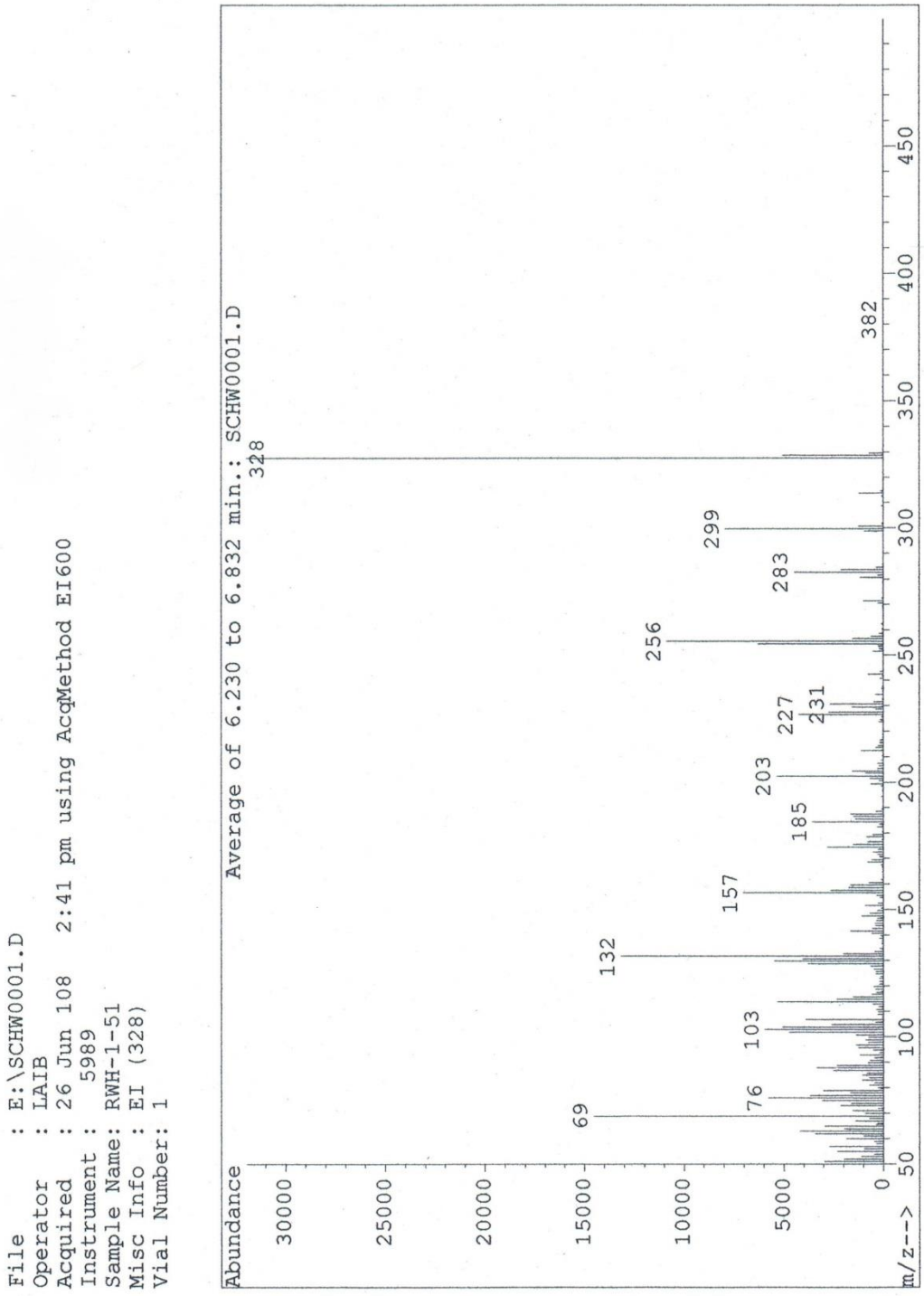
^{1}H NMR *Ethyl 4-oxo-7-(2,2,2-trifluoroacetamido)-1,4-dihydroquinoline-2-carboxylate* (**35**)



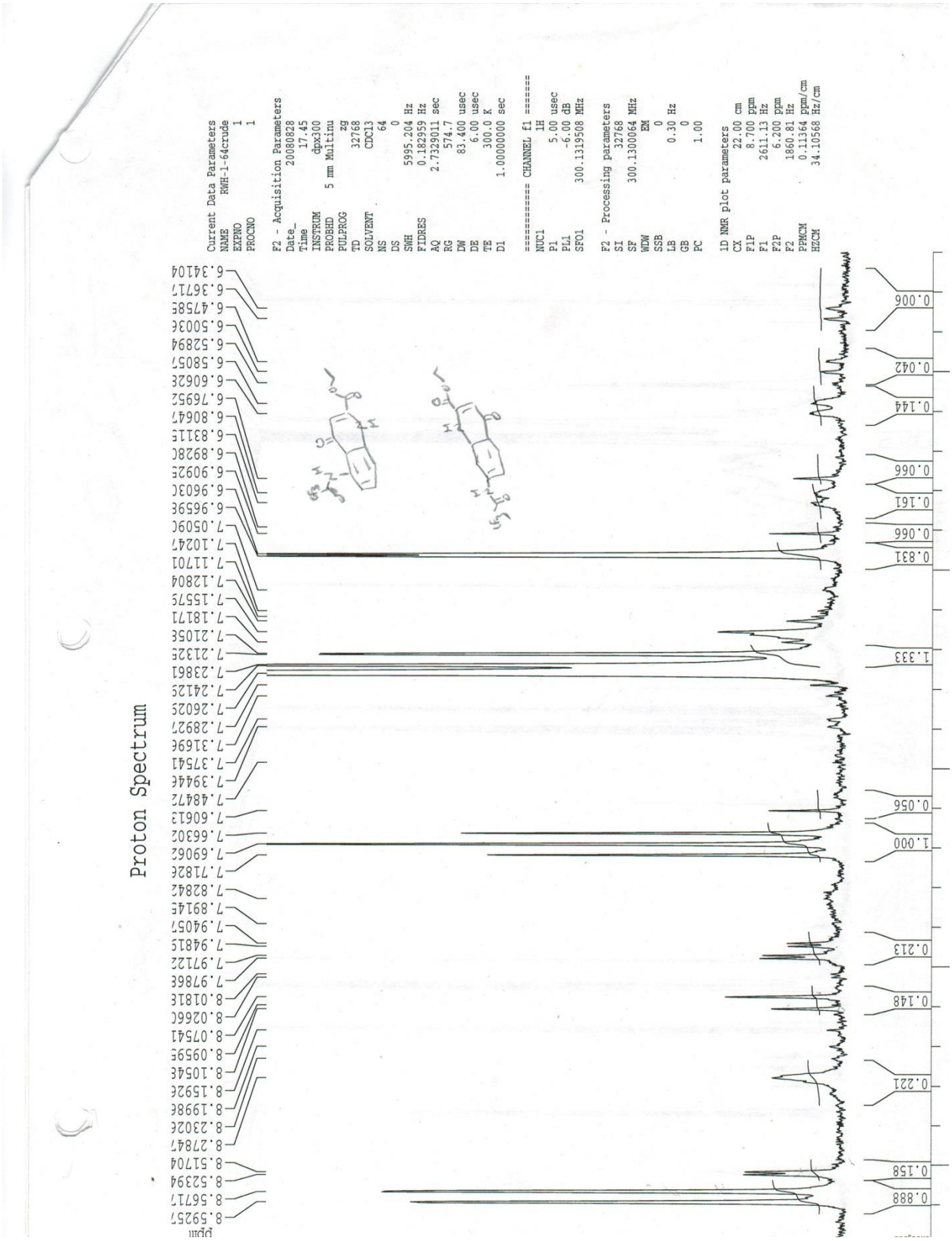
^{13}C NMR *Ethyl 4-oxo-7-(2,2,2-trifluoroacetamido)-1,4-dihydroquinoline-2-carboxylate* (**35**)



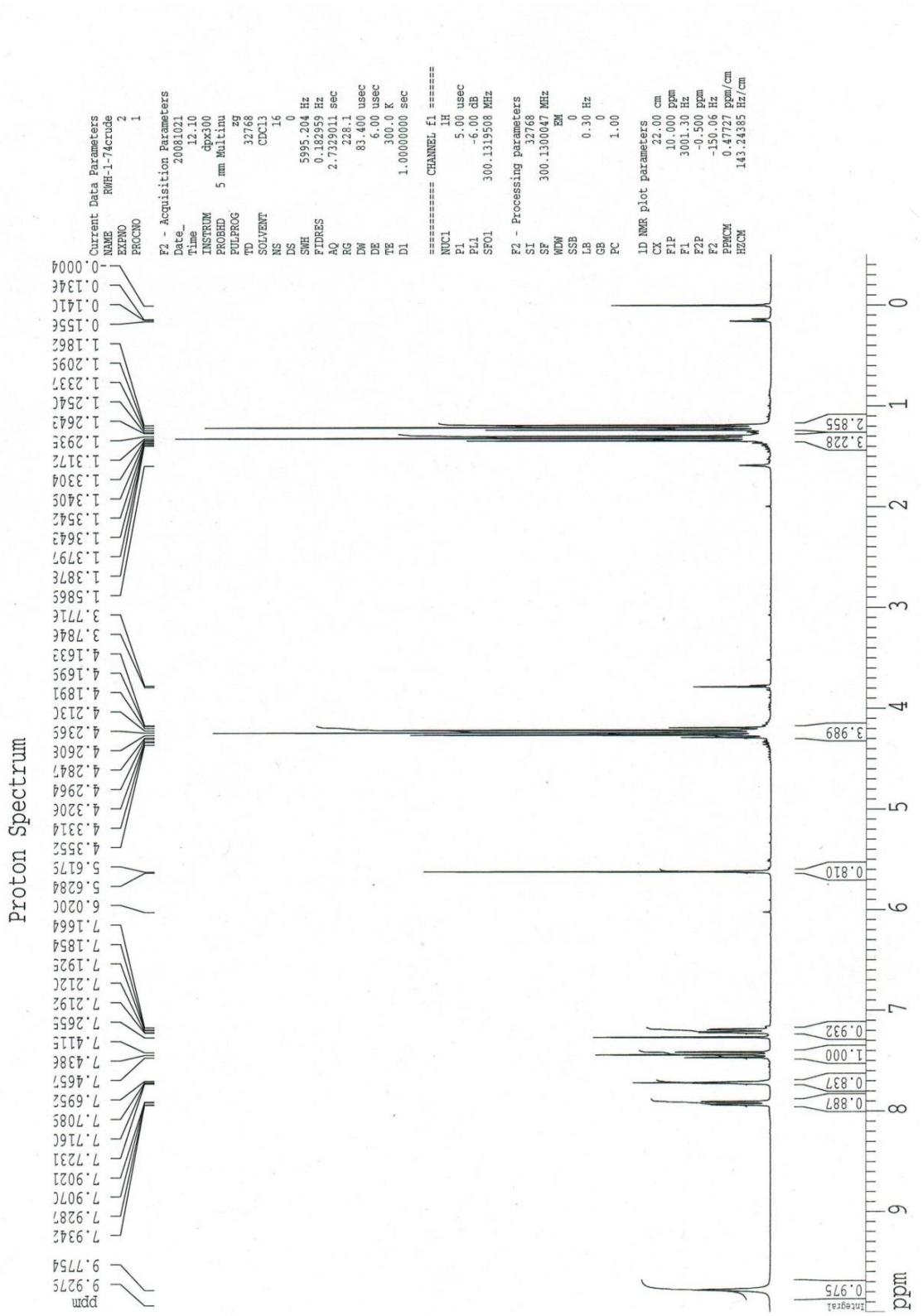
MS (EI, 70eV) *Ethyl 4-oxo-7-(2,2,2-trifluoroacetamido)-1,4-dihydroquinoline-2-carboxylate* (**35**)



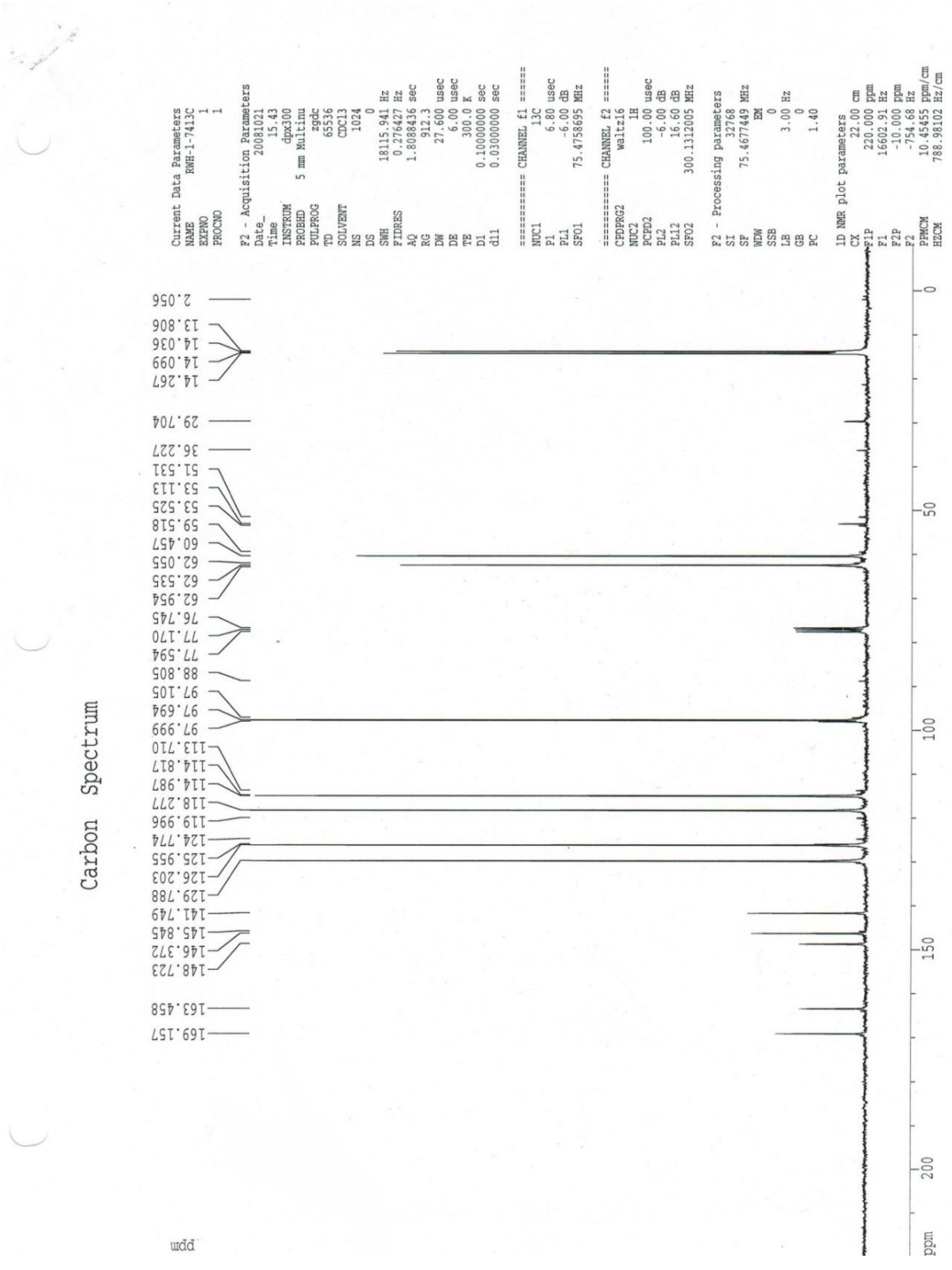
^{1}H NMR *Ethyl 4-oxo-5-(2,2,2-trifluoroacetamido)-1,4-dihydroquinoline-2-carboxylate* (**36**)



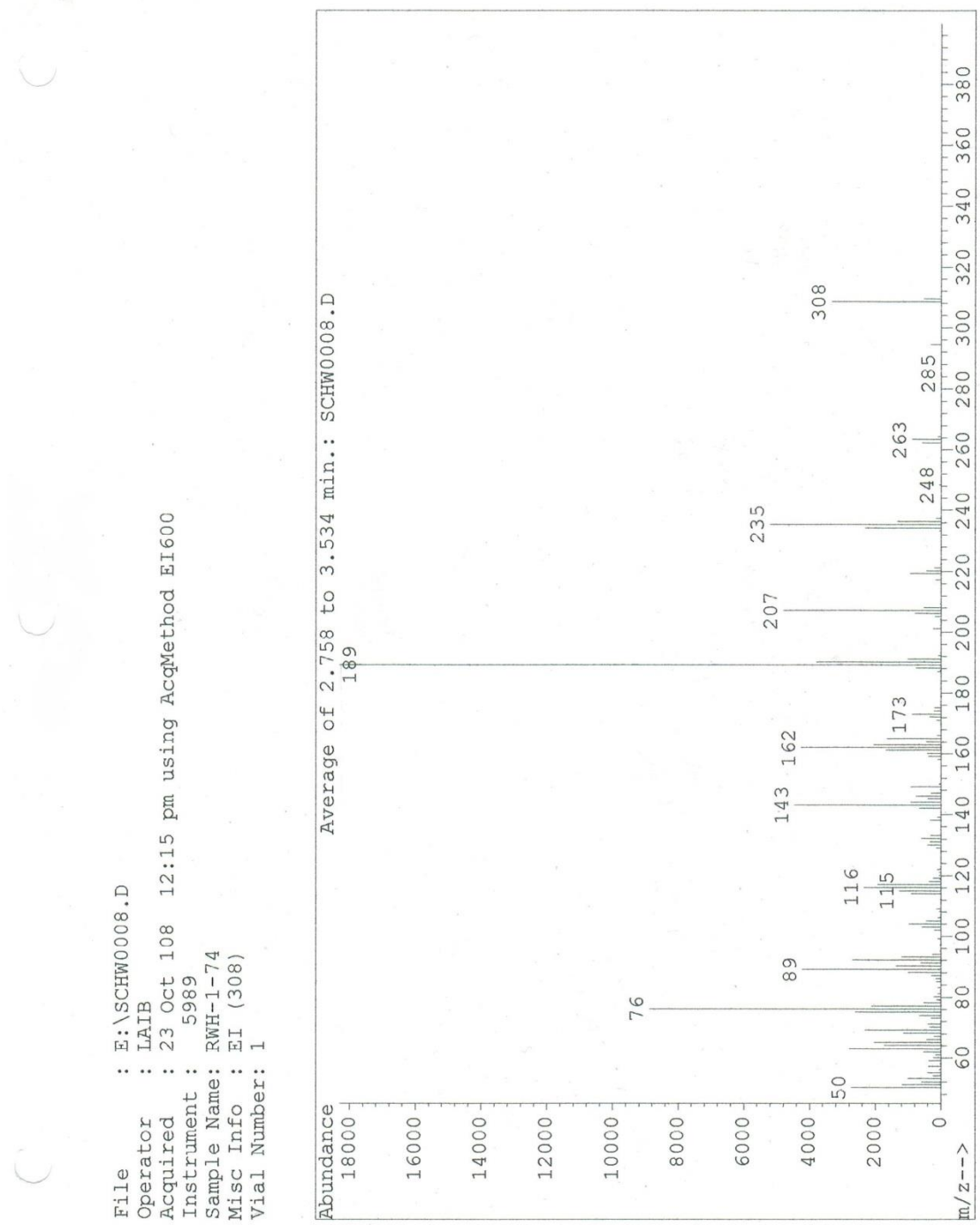
^{1}H NMR *Diethyl 2-((3-nitrophenyl)amino)fumarate* (**37**)



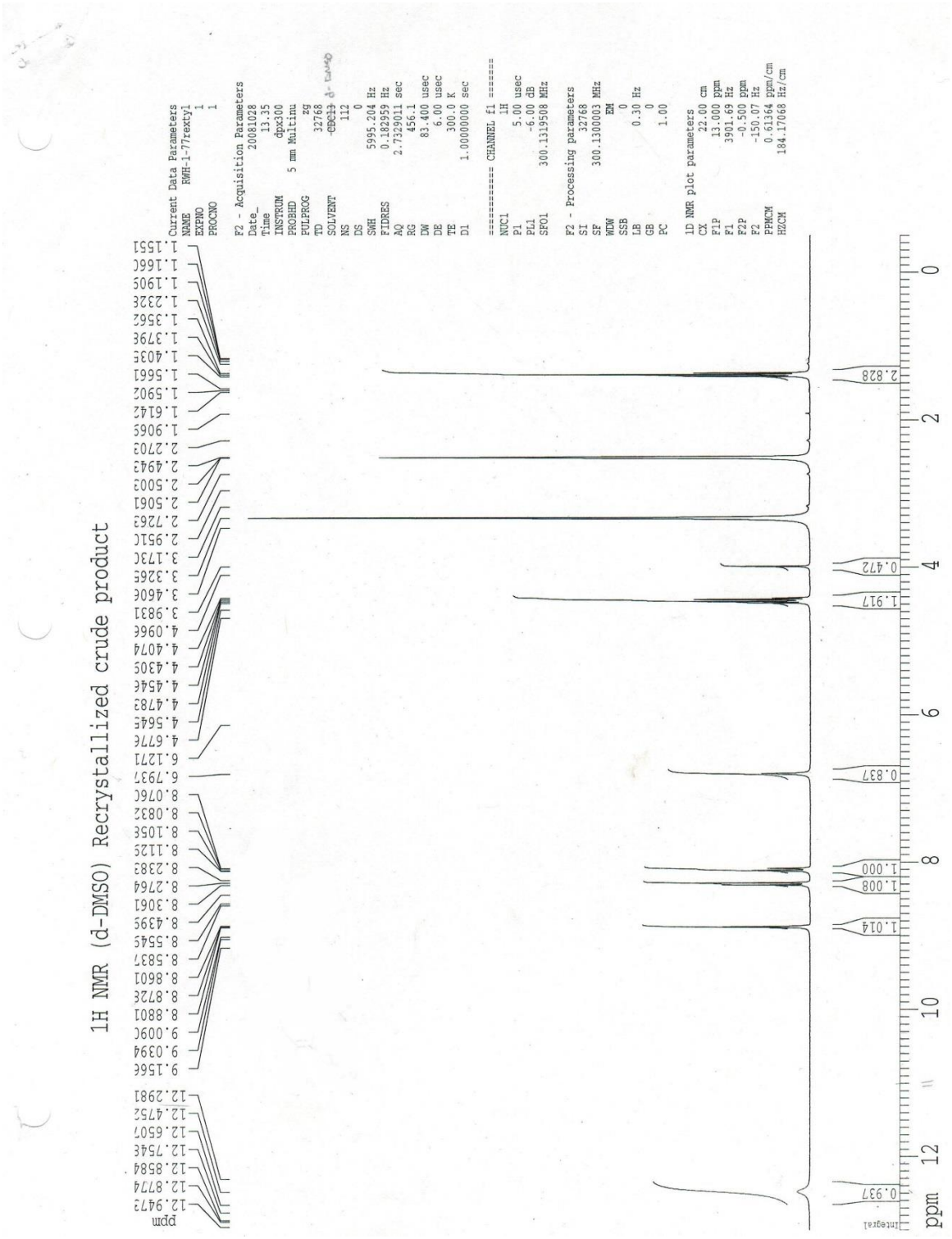
^{13}C NMR <u>*Diethyl 2-((3-nitrophenyl)amino)fumarate*</u> (**37**)



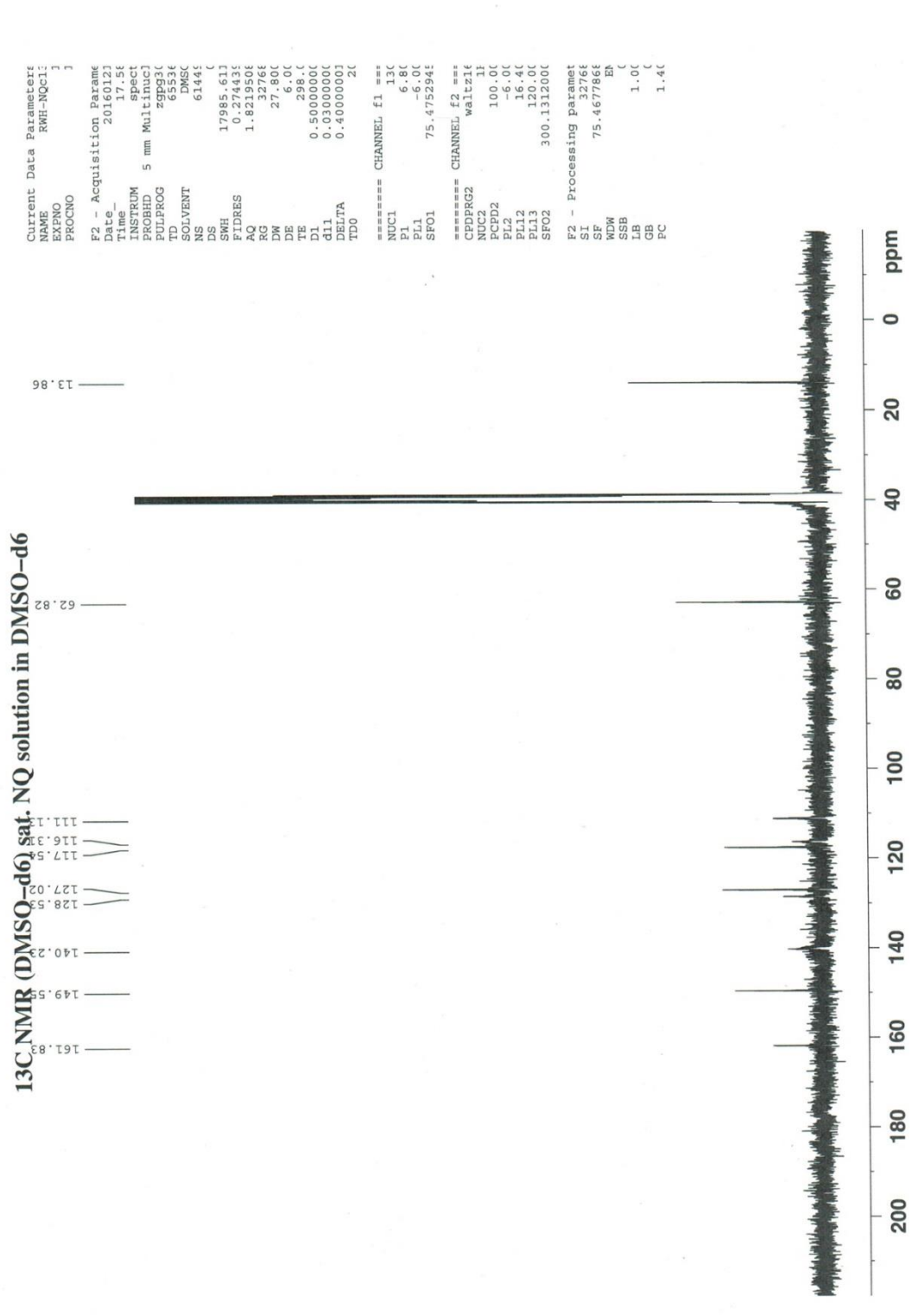
MS (EI, 70eV) *Diethyl 2-((3-nitrophenyl)amino)fumarate* (**37**)



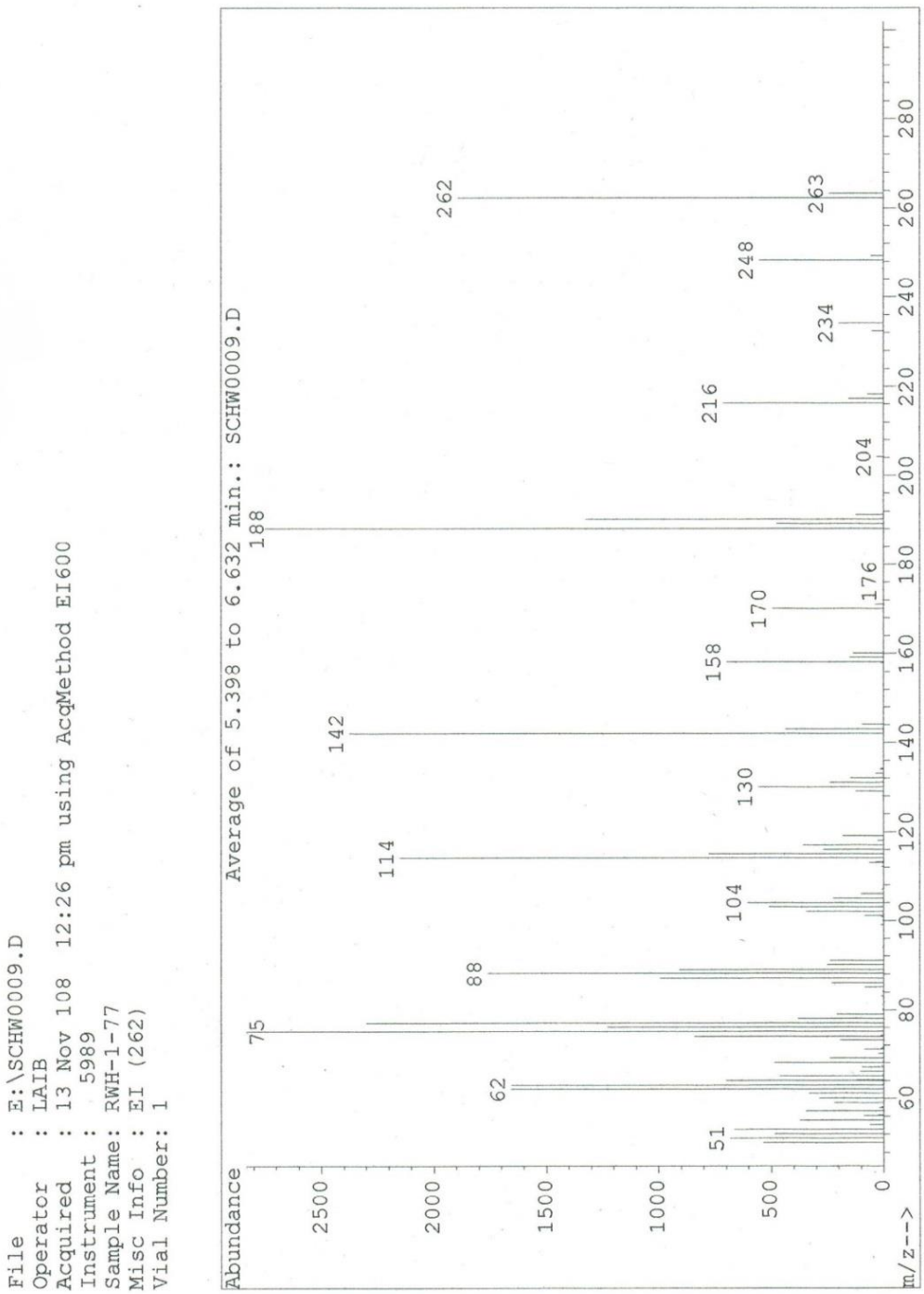
^{1}H NMR *Ethyl 7-nitro-4-oxo-1,4-dihydroquinoline-2-carboxylate* (**38**)



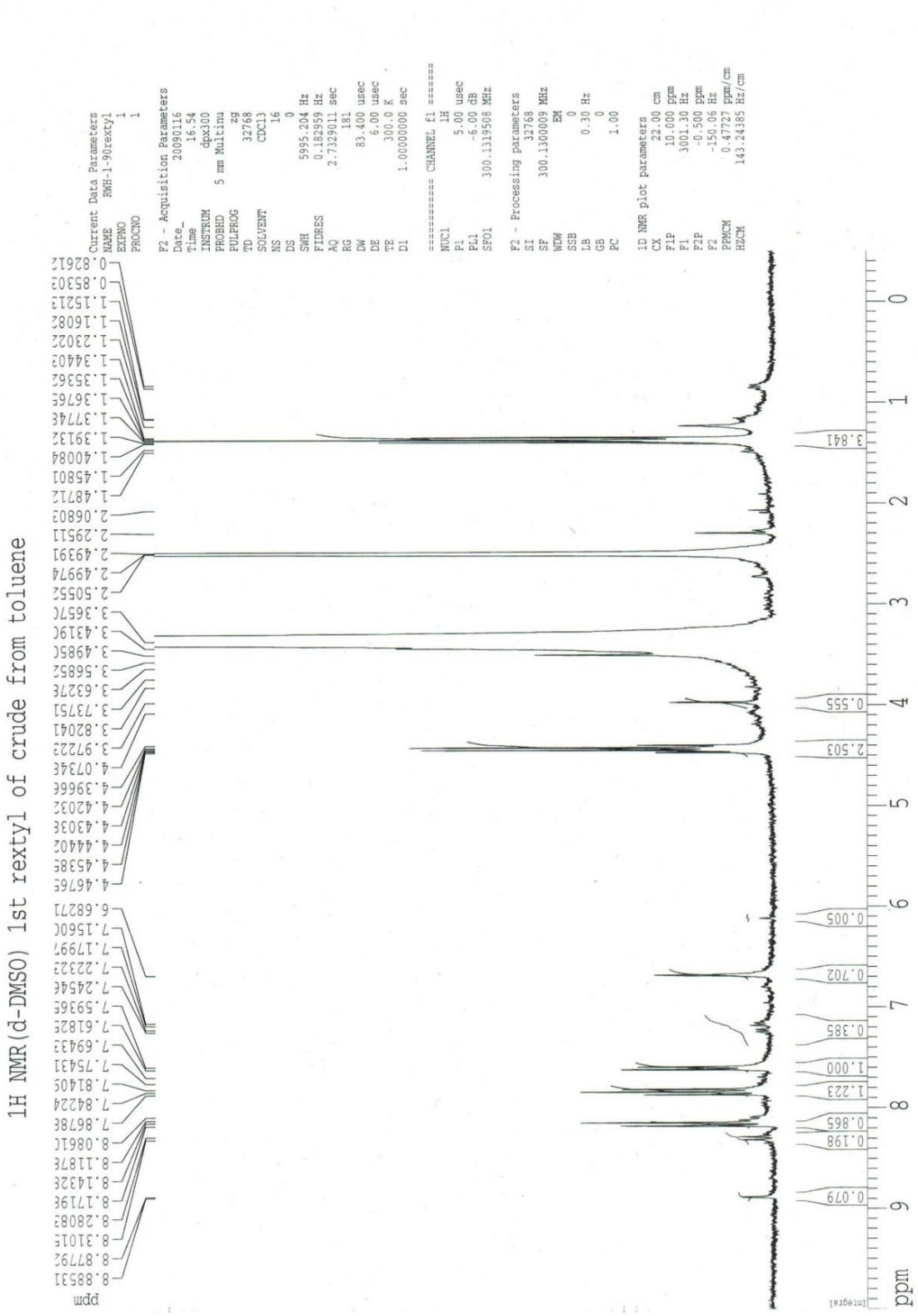
^{13}C NMR *Ethyl 7-nitro-4-oxo-1,4-dihydroquinoline-2-carboxylate* (**38**)



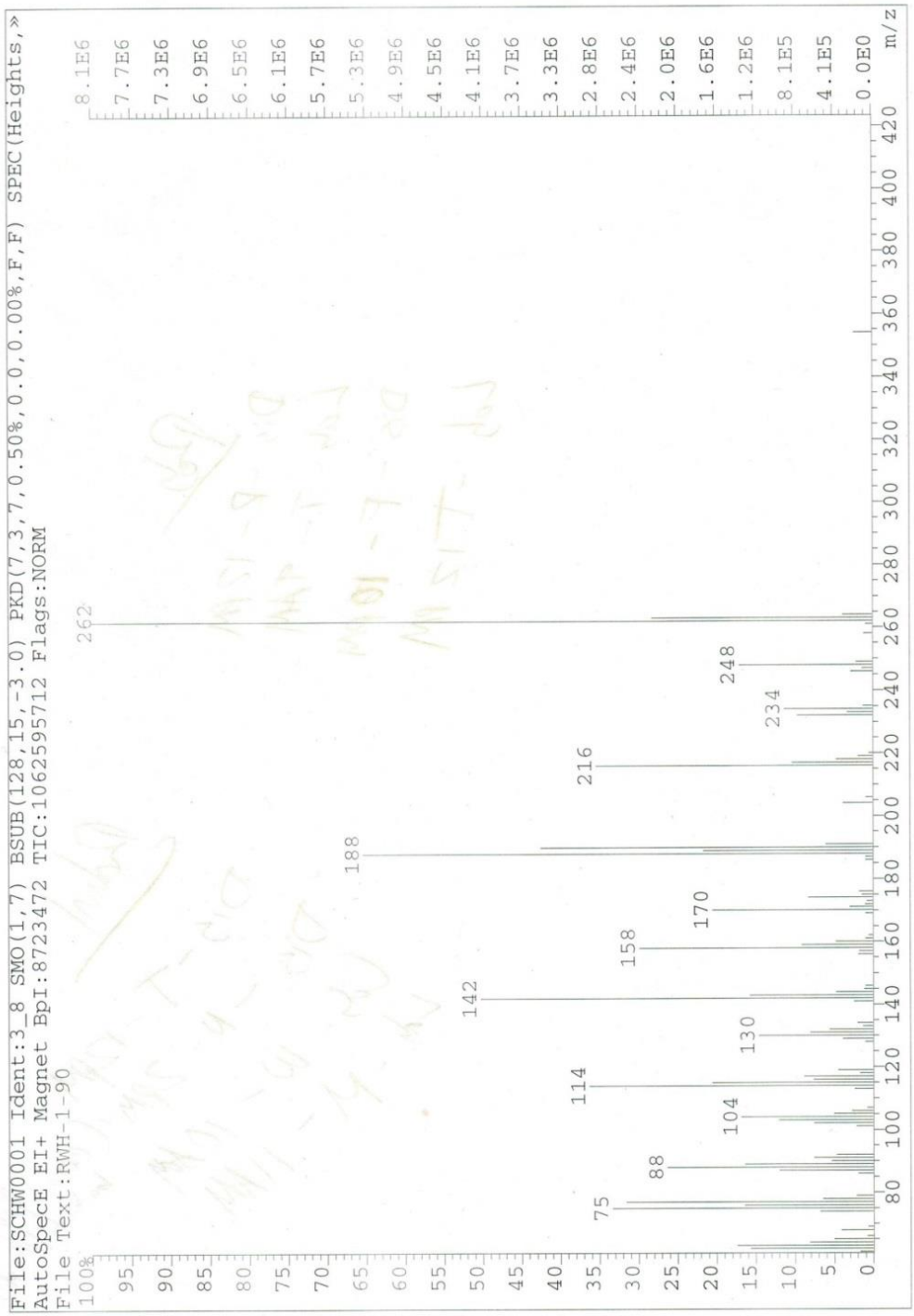
MS (EI, 70eV) <u>*Ethyl 7-nitro-4-oxo-1,4-dihydroquinoline-2-carboxylate*</u> (**38**)



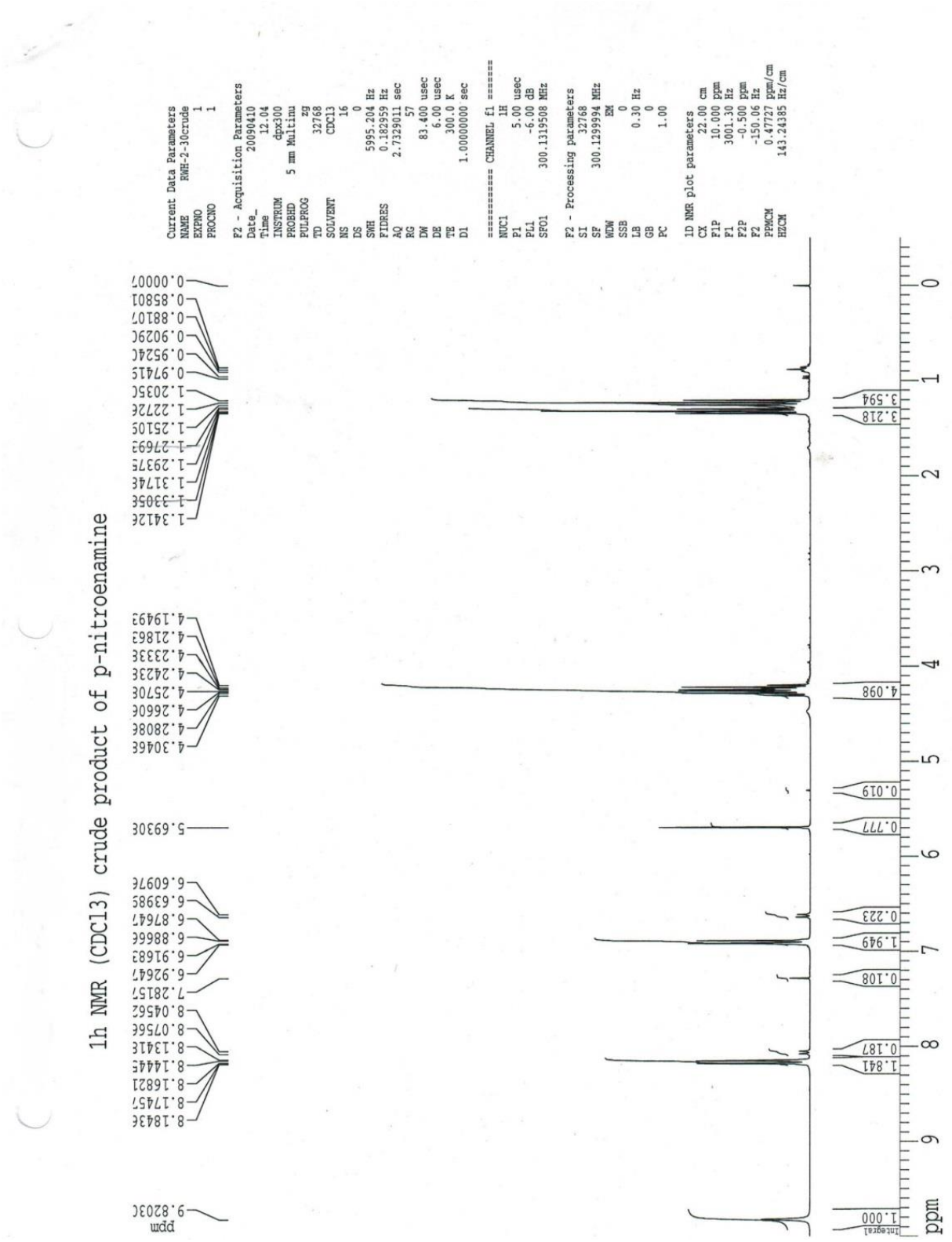
^{1}H NMR *Ethyl 5-nitro-4-oxo-1,4-dihydroquinoline-2-carboxylate* (**39**)



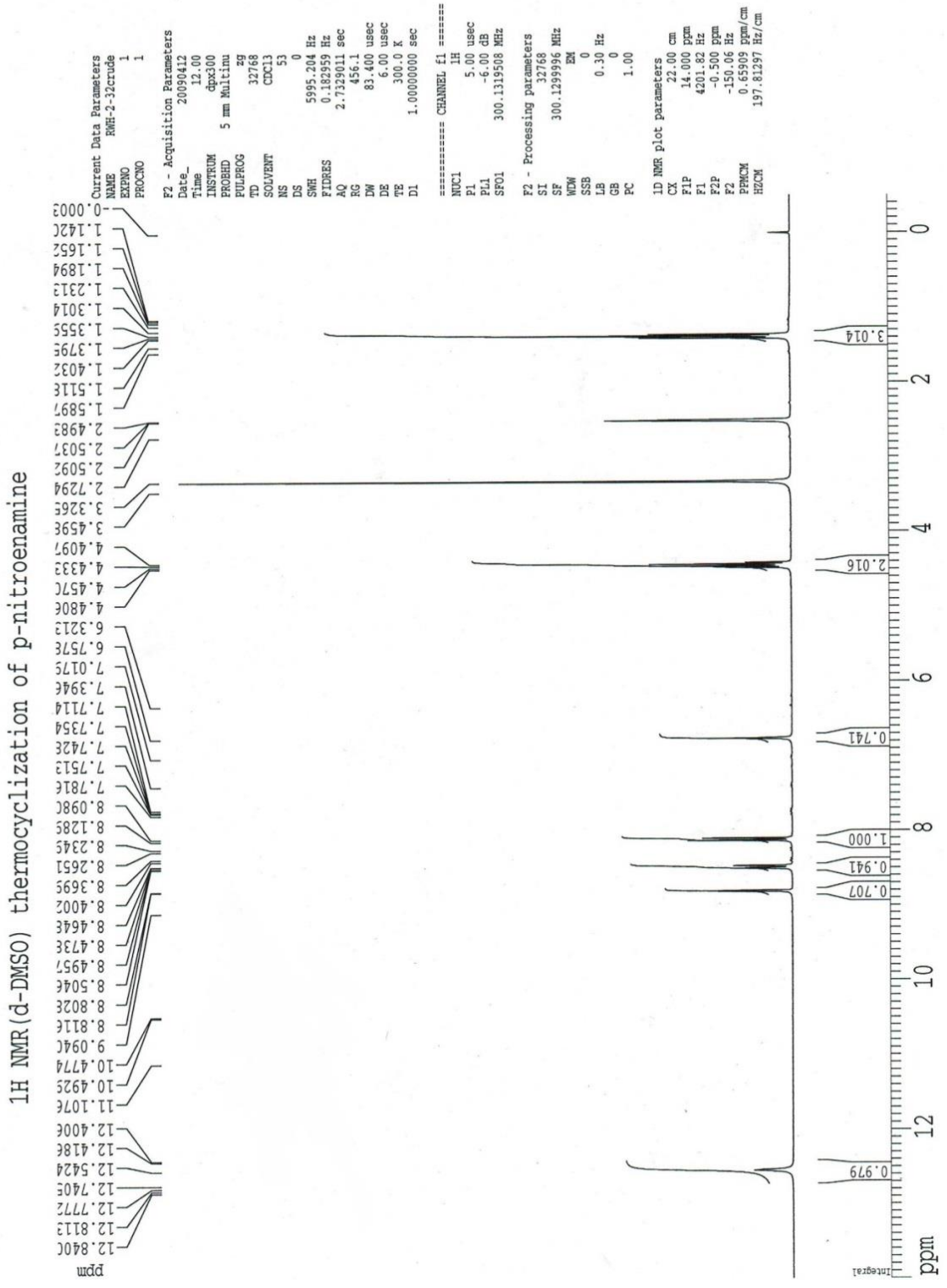
MS (EI, 70eV) *Ethyl 5-nitro-4-oxo-1,4-dihydroquinoline-2-carboxylate* (**39**)



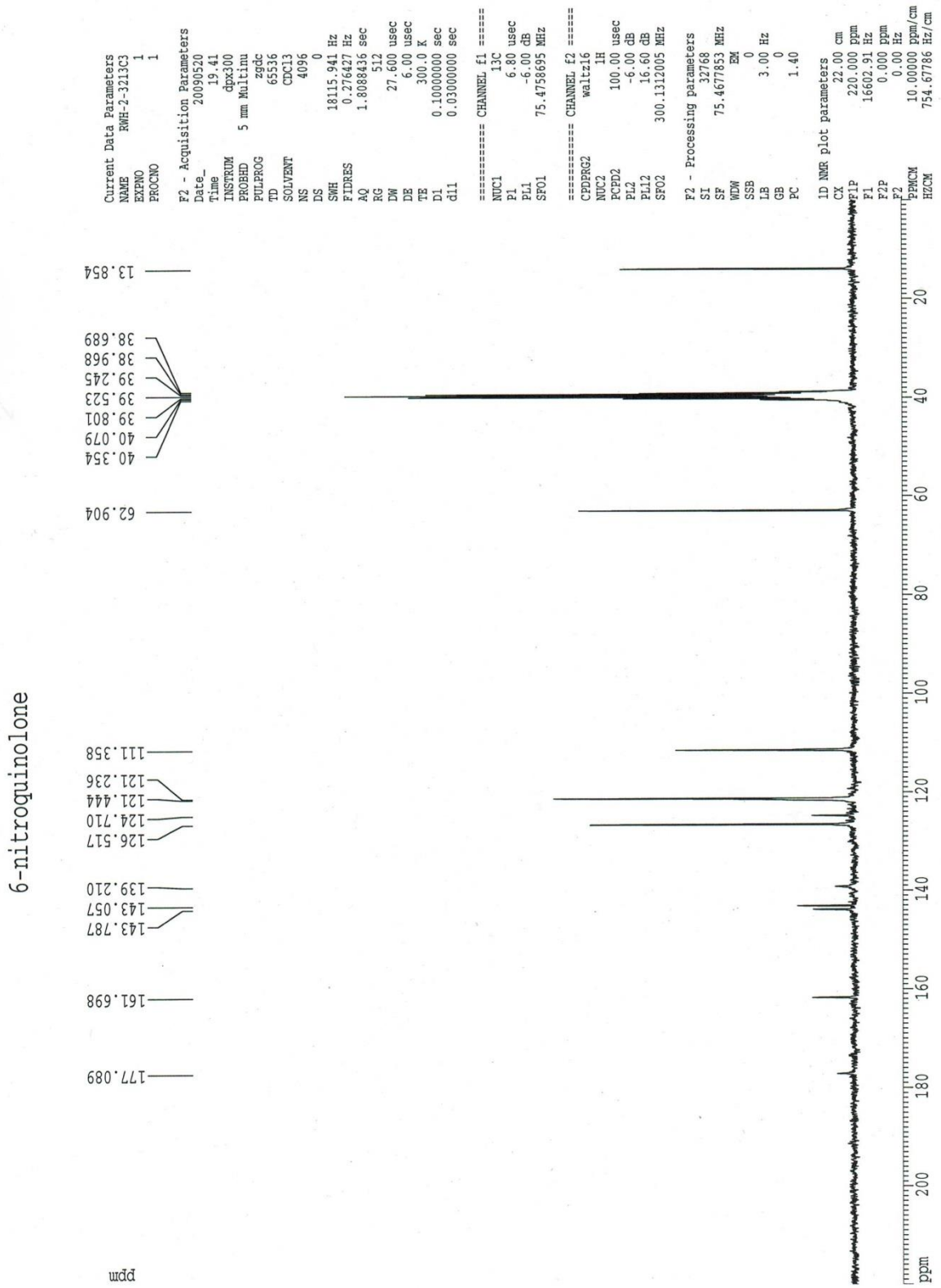
[1]H NMR *Diethyl 2-((4-nitrophenyl)amino)fumarate* (**40**)



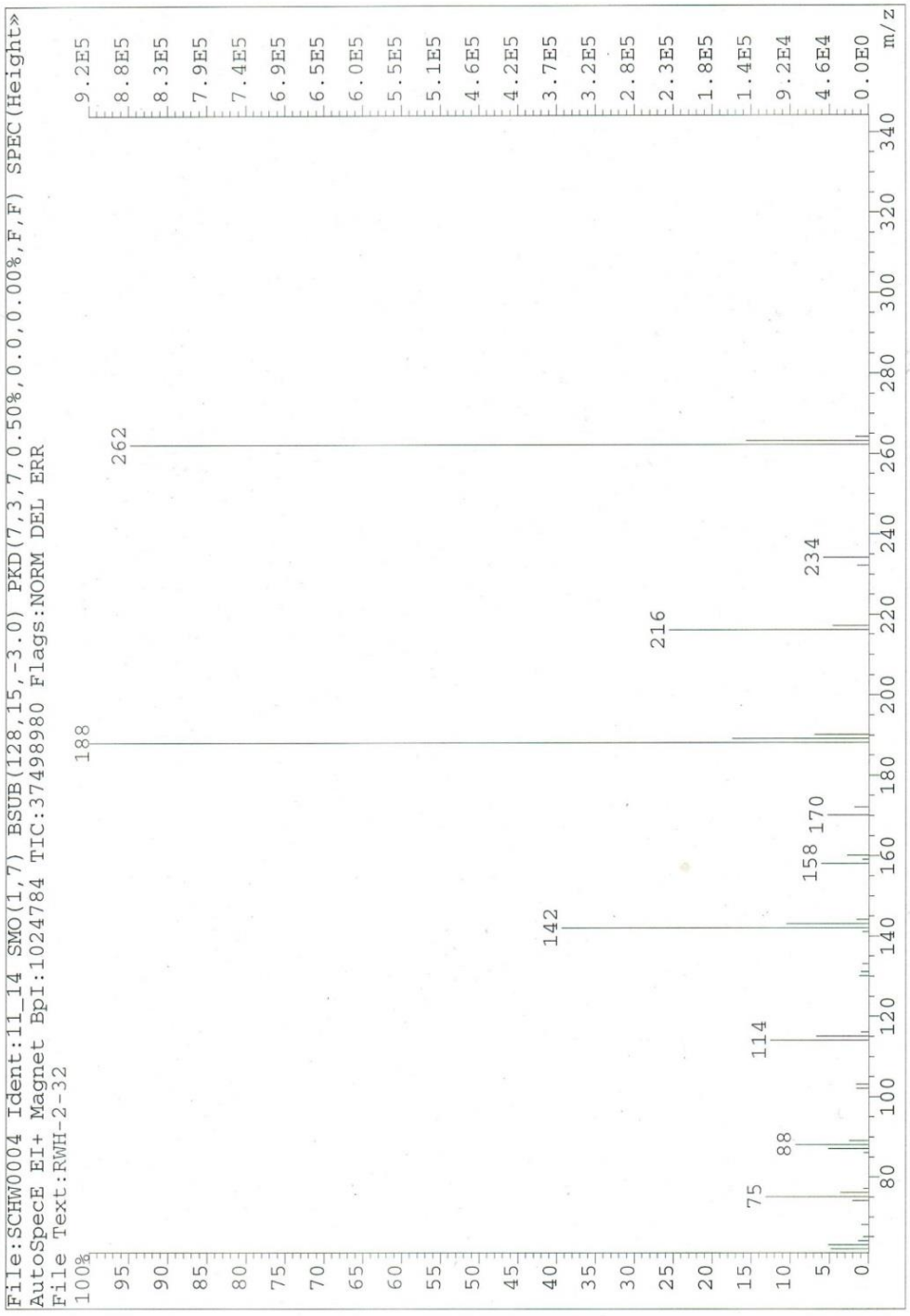
^{1}H NMR *Ethyl 6-nitro-4-oxo-1,4-dihydroquinoline-2-carboxylate* (**41**)



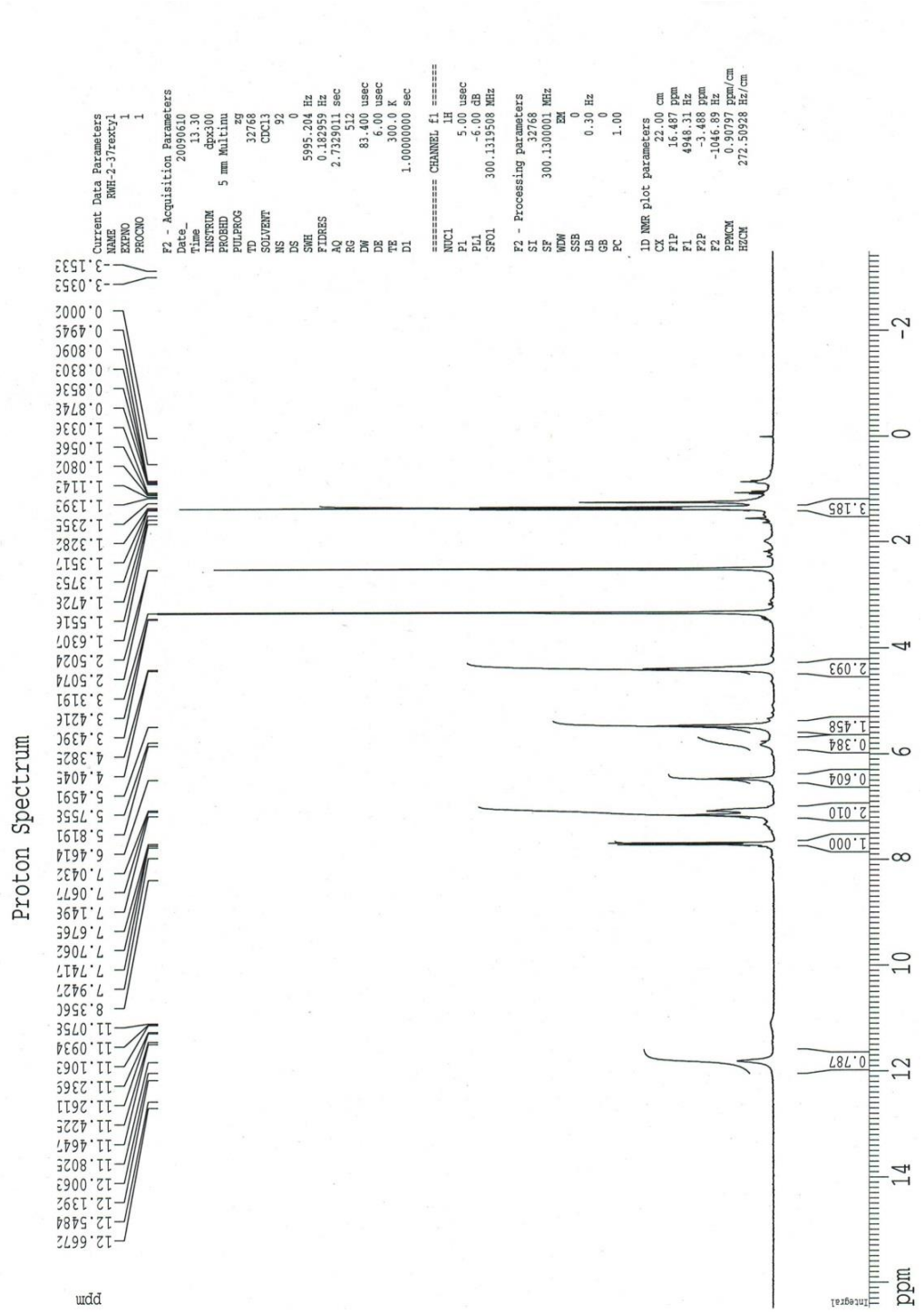
^{13}C NMR *Ethyl 6-nitro-4-oxo-1,4-dihydroquinoline-2-carboxylate* (**41**)



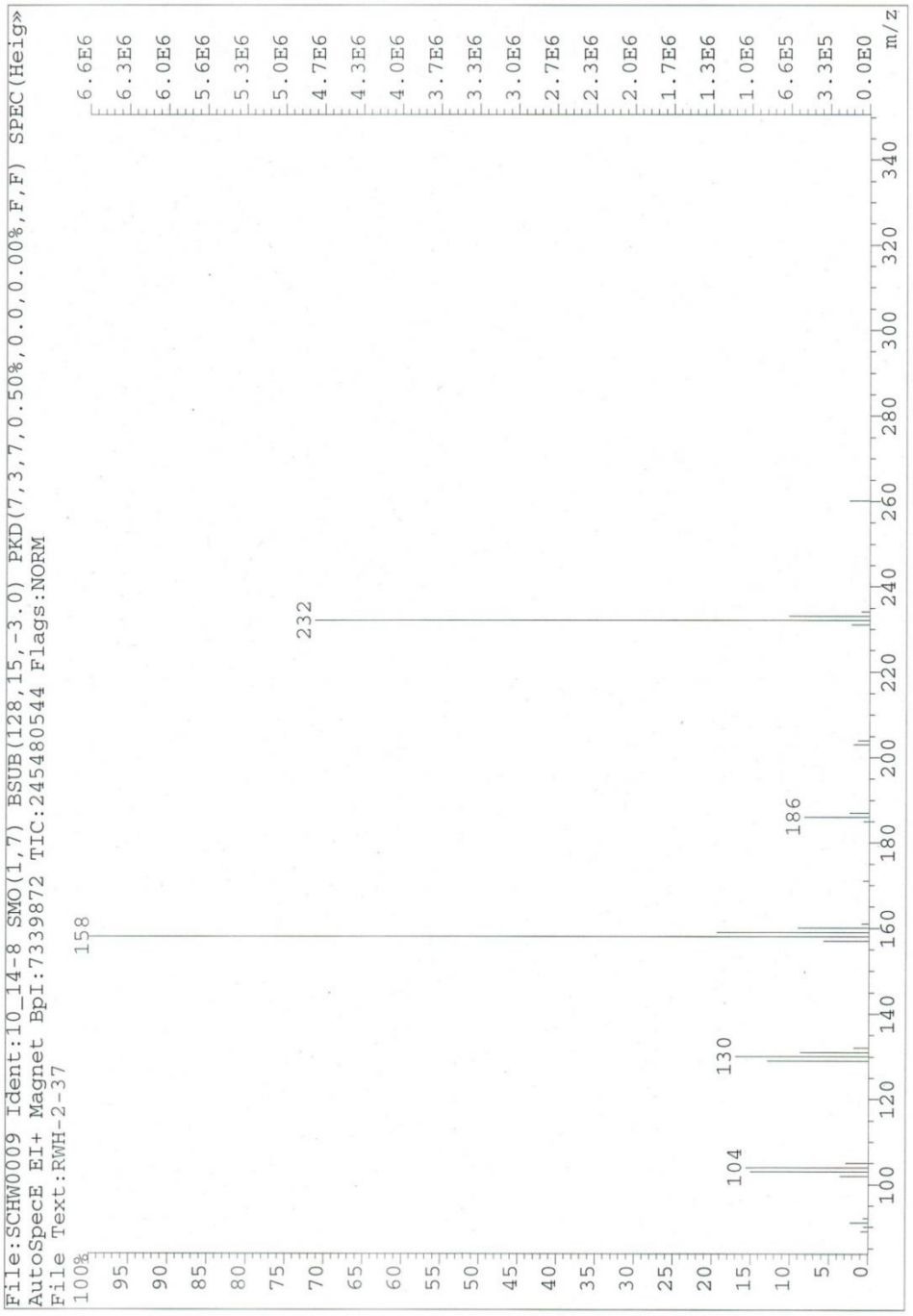
MS (EI, 70eV) *Ethyl 6-nitro-4-oxo-1,4-dihydroquinoline-2-carboxylate* (**41**)



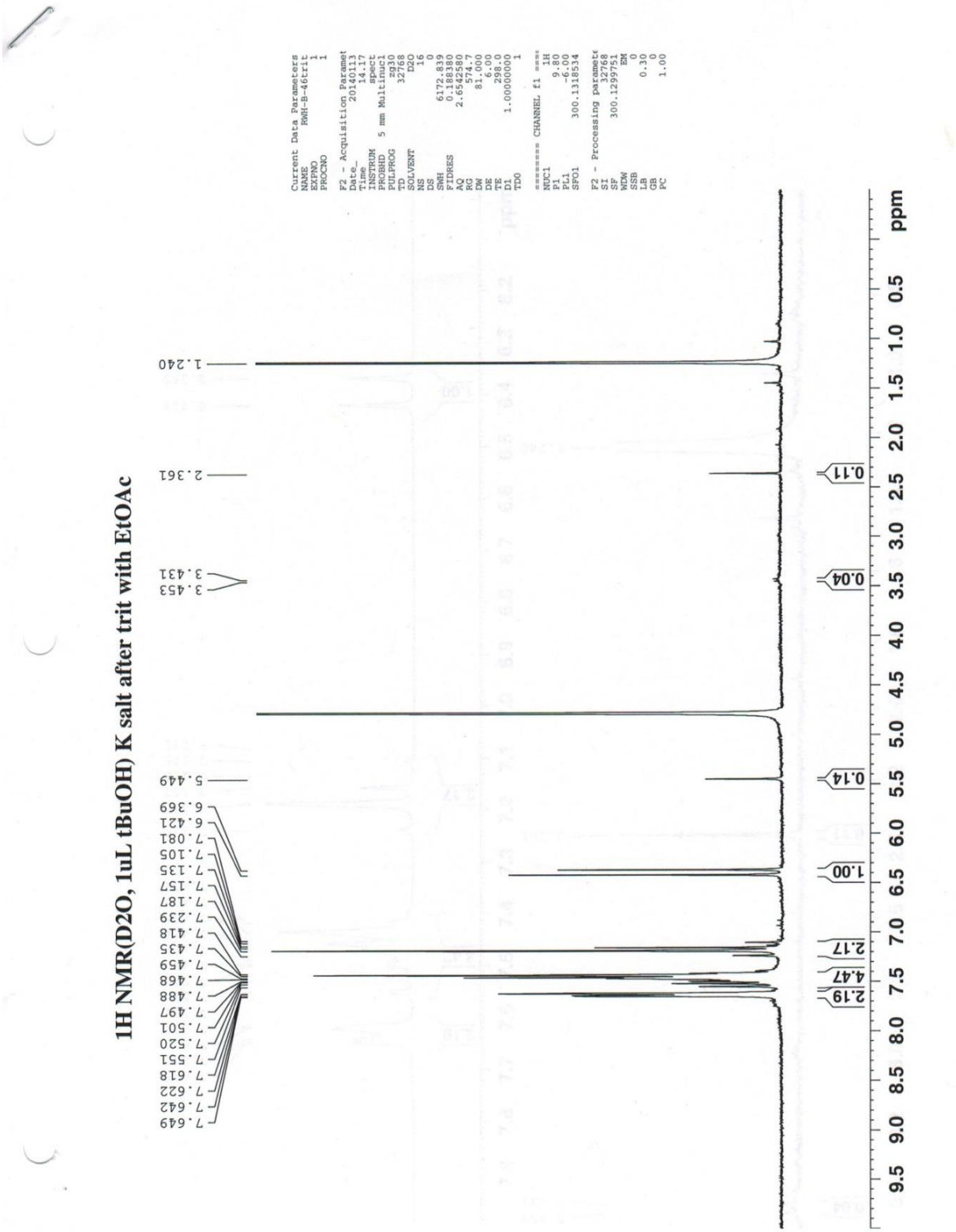
^{1}H NMR *Ethyl 6-amino-4-oxo-1,4-dihydroquinoline-2-carboxylate* (**42**)



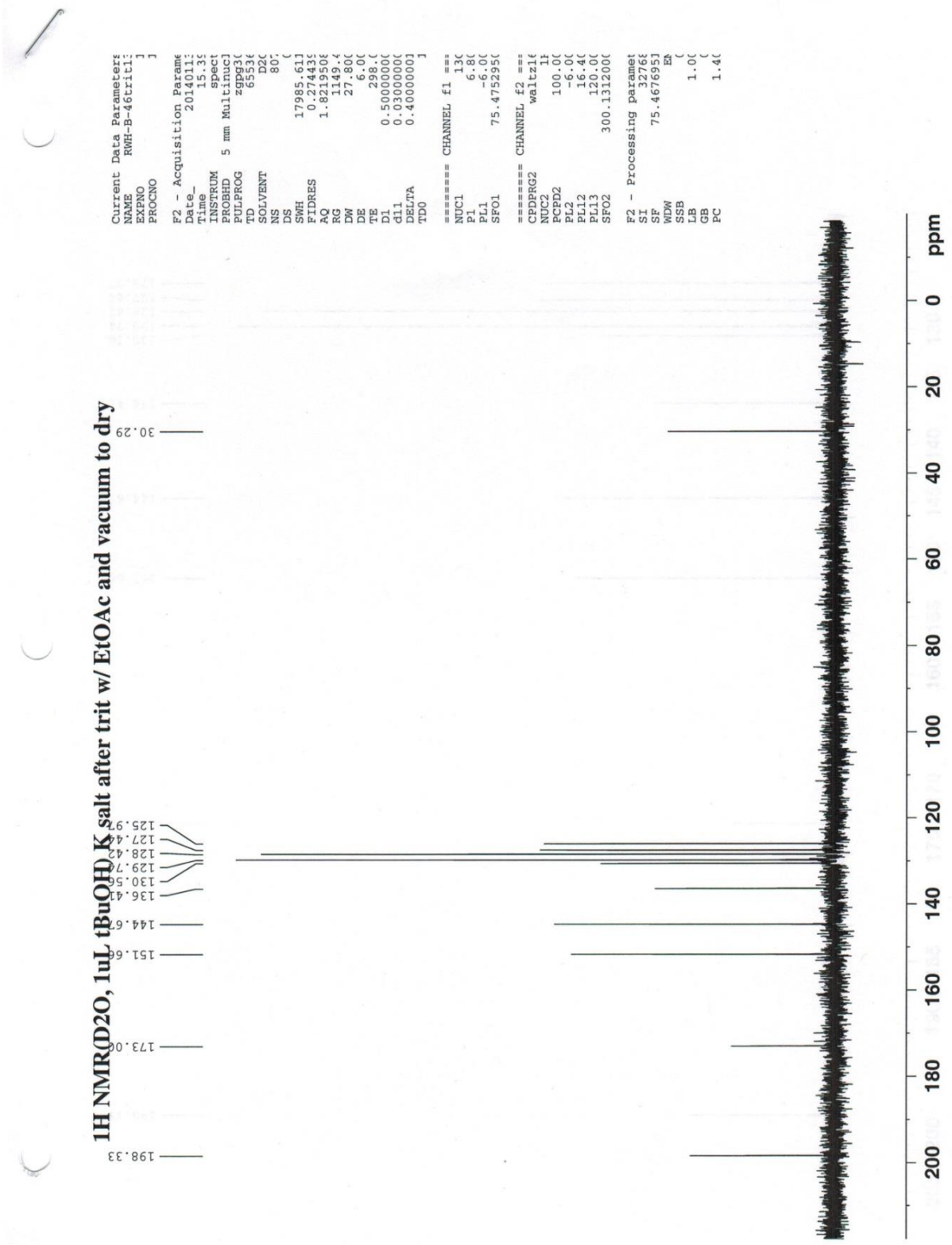
MS (EI, 70eV) *Ethyl 6-amino-4-oxo-1,4-dihydroquinoline-2-carboxylate* (**42**)



^{1}H NMR *Potassium (3E,5E)-2-oxo-6-phenylhexa-3,5-dienoate* (**45**)



^{13}C NMR *Potassium (3E,5E)-2-oxo-6-phenylhexa-3,5-dienoate* (**45**)



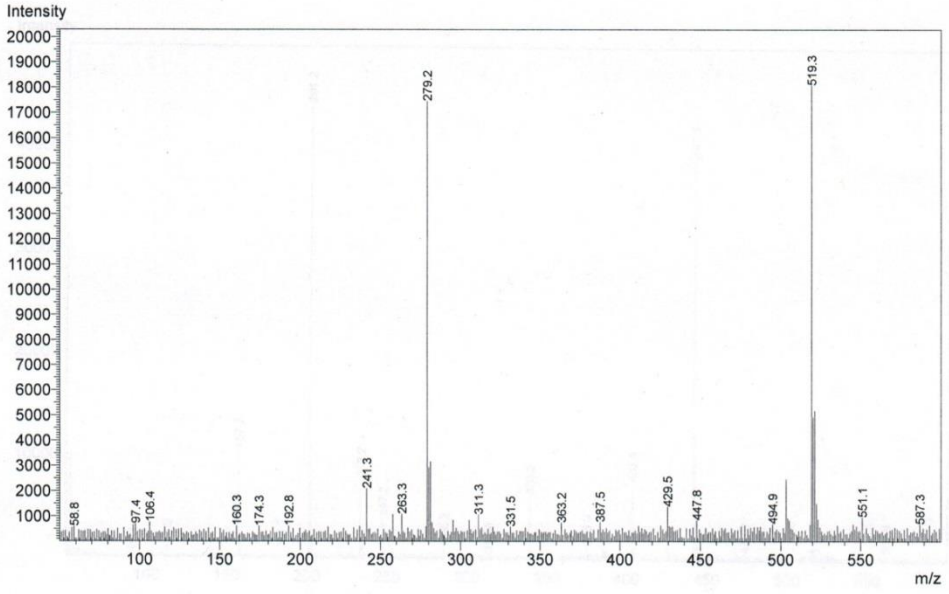
ESI-MS *Potassium (3E,5E)-2-oxo-6-phenylhexa-3,5-dienoate* (**45**)

Shimadzu LCMS-2020 Data Report

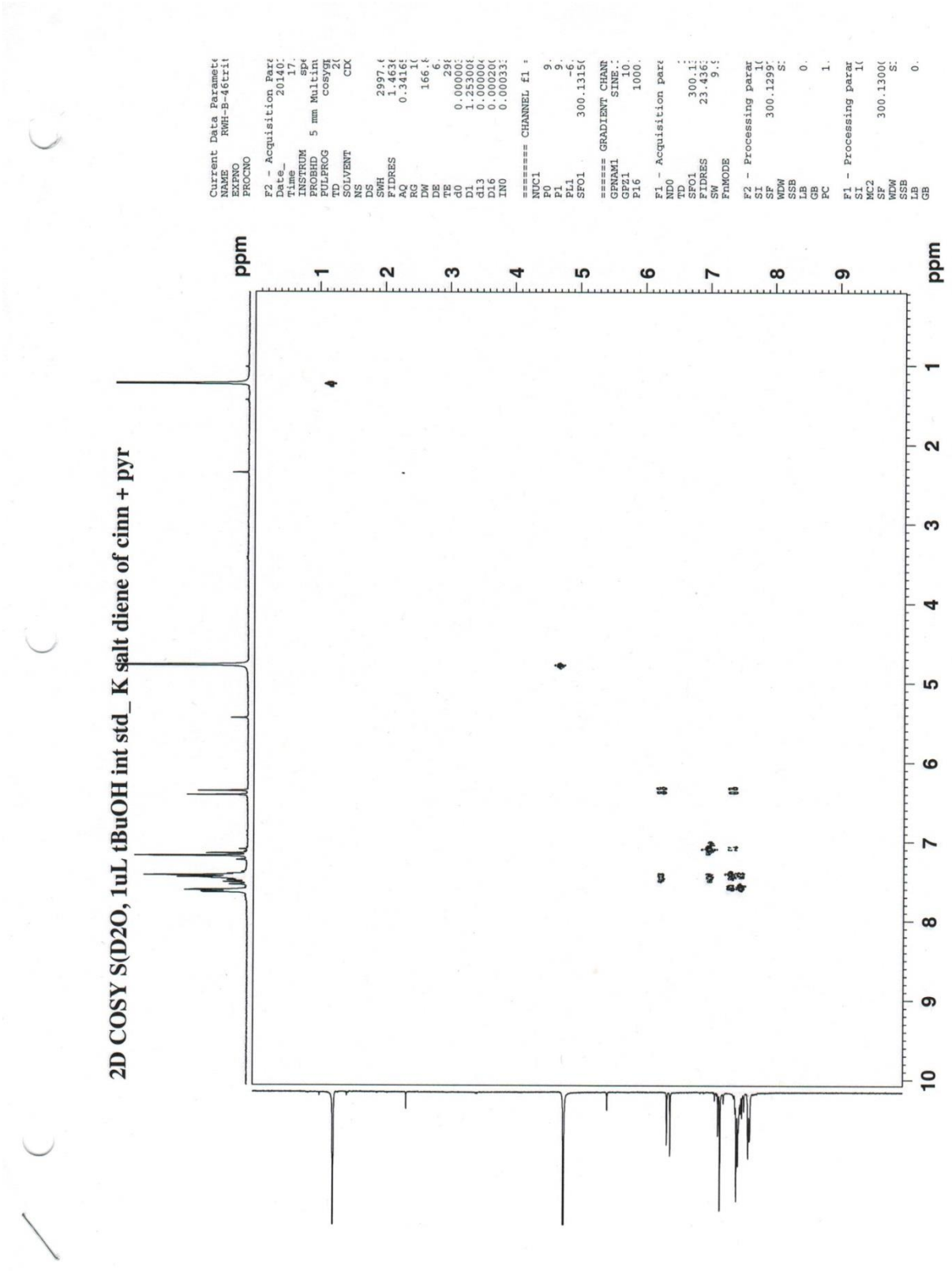
Mass Spectrum for Sample:
RWH-B-42xtyl

Operator: Mark Wang

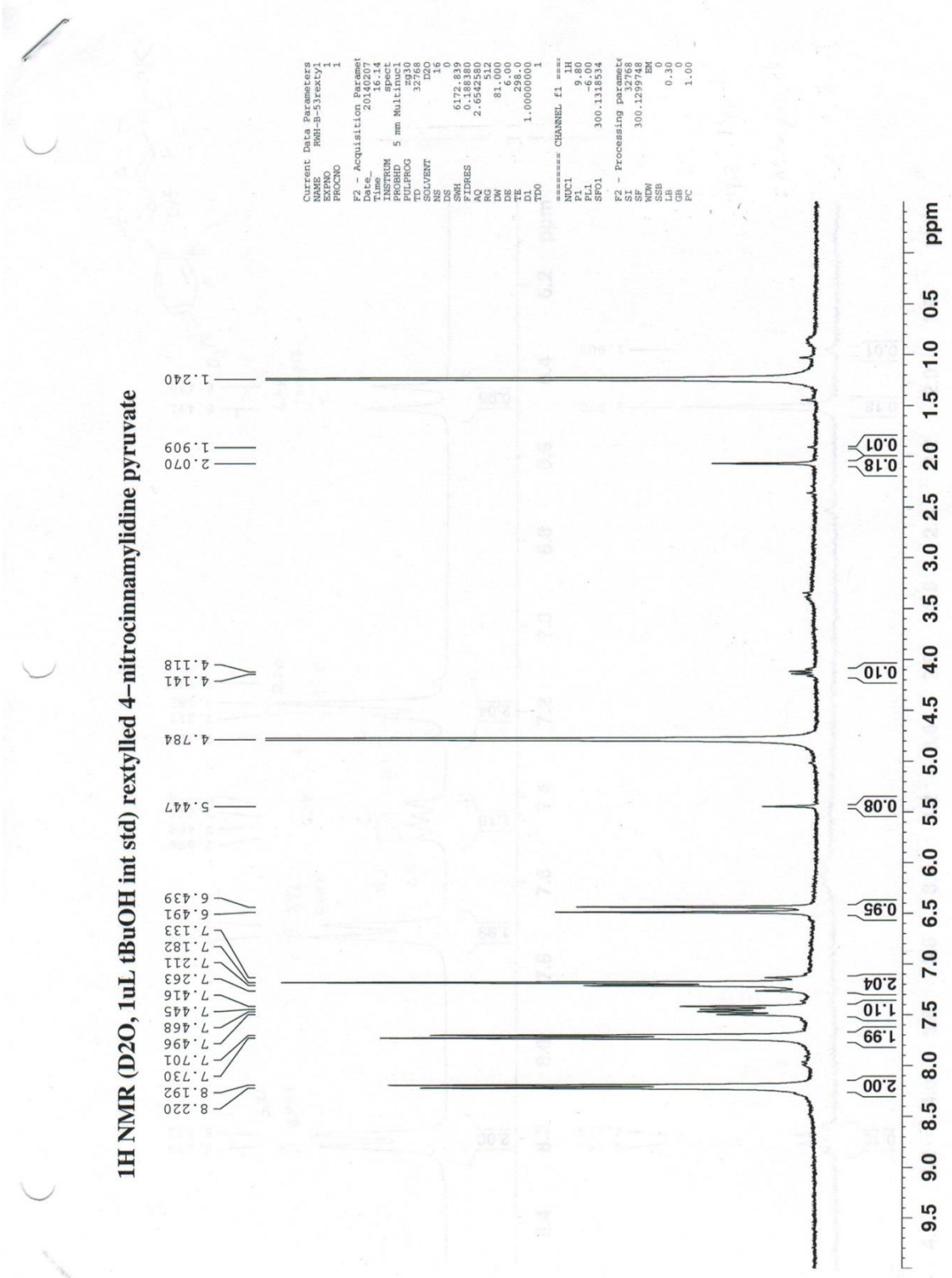
Data filename: C:\LabSolutions\Data\Schwabacher Alan\RWH-B-42xtyl.lcd
Spectrum Mode: Single
Retention Time: 0.100 min.
Interface Type (ESI, APCI, DUIS): DUIS
Aquisition Mode (Scan, SIM, Profile): Scan
Polarity (+,-): +



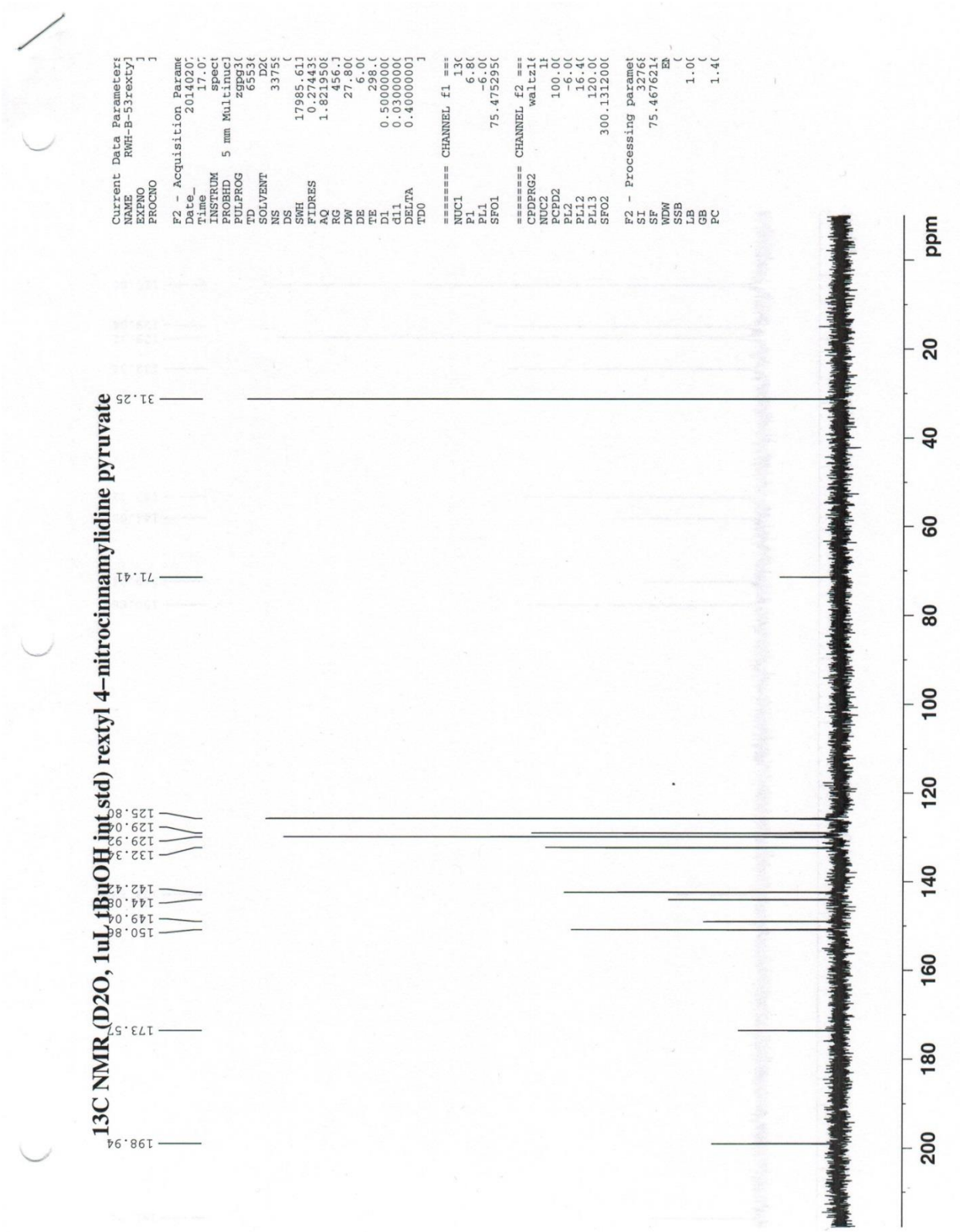
COSY *Potassium (3E,5E)-2-oxo-6-phenylhexa-3,5-dienoate* (**45**)



^{1}H NMR *Potassium (3E,5E)-6-(4-nitrophenyl)-2-oxohexa-3,5-dienoate* (**46**)



^{13}C NMR *Potassium (3E,5E)-6-(4-nitrophenyl)-2-oxohexa-3,5-dienoate* (**46**)



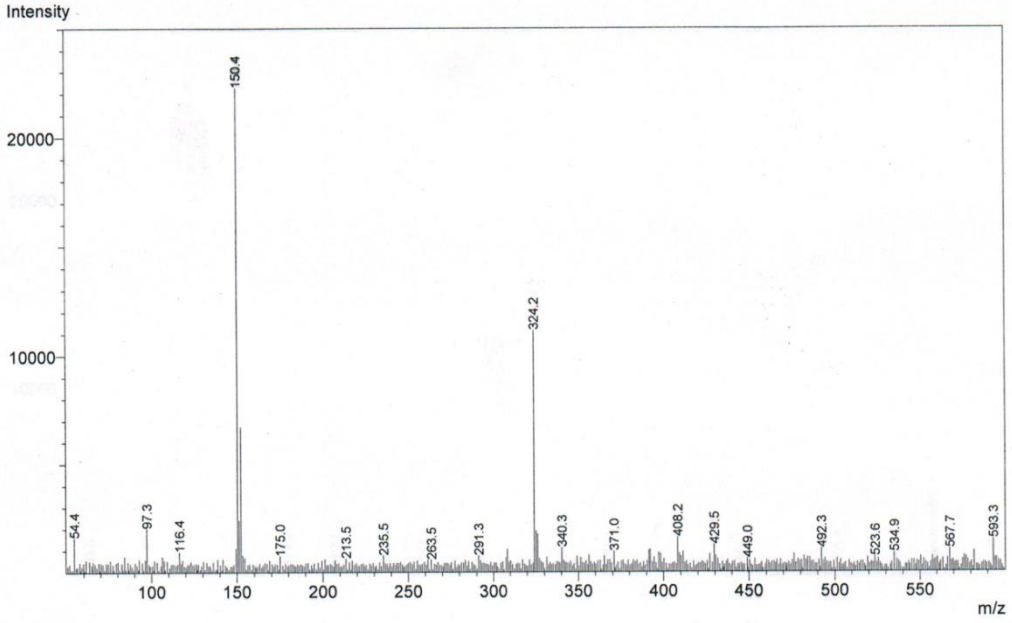
ESI-MS *Potassium (3E,5E)-6-(4-nitrophenyl)-2-oxohexa-3,5-dienoate* (**46**)

Shimadzu LCMS-2020 Data Report

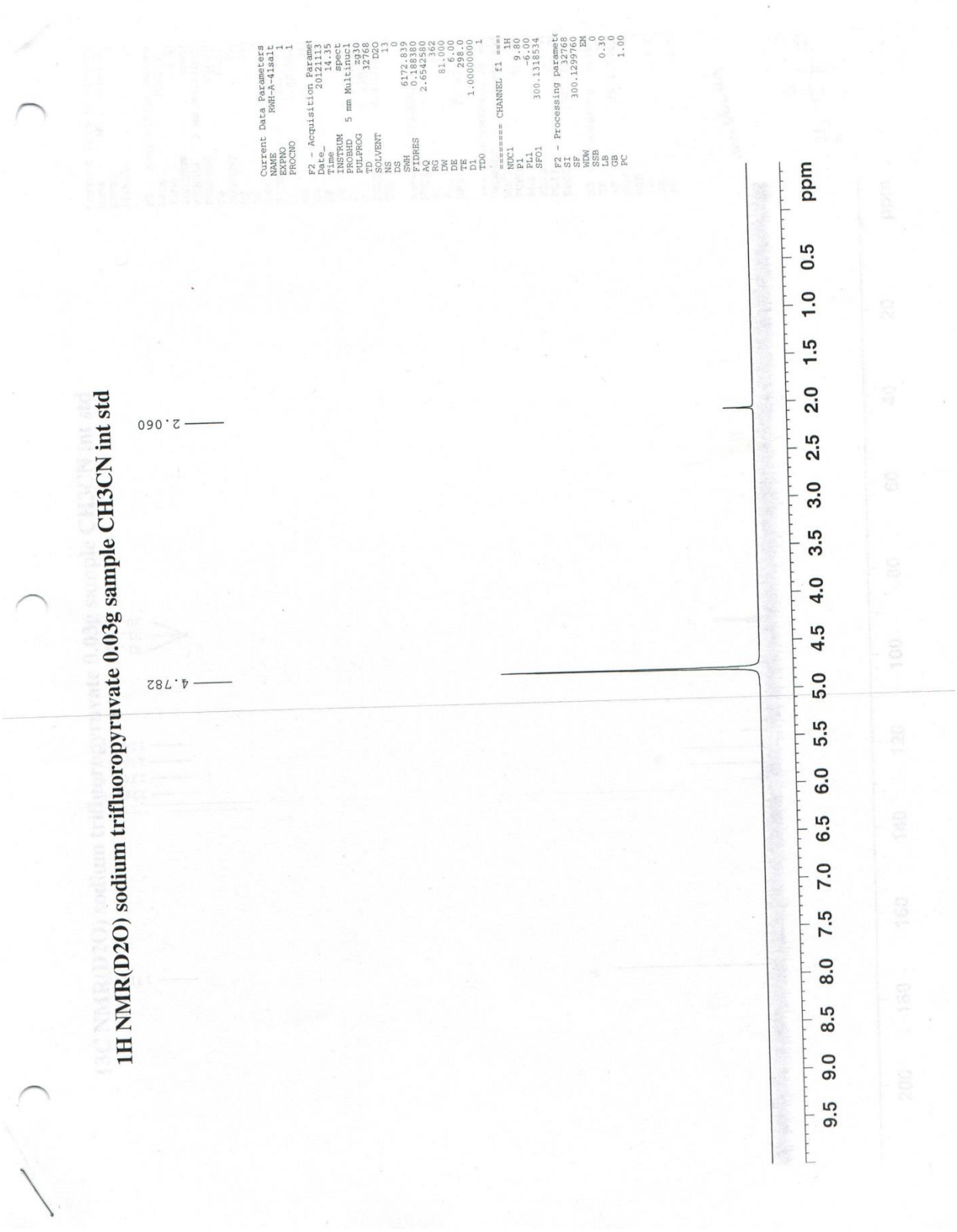
Mass Spectrum for Sample:
RWH-B-53xtyl

Operator: Mark Wang

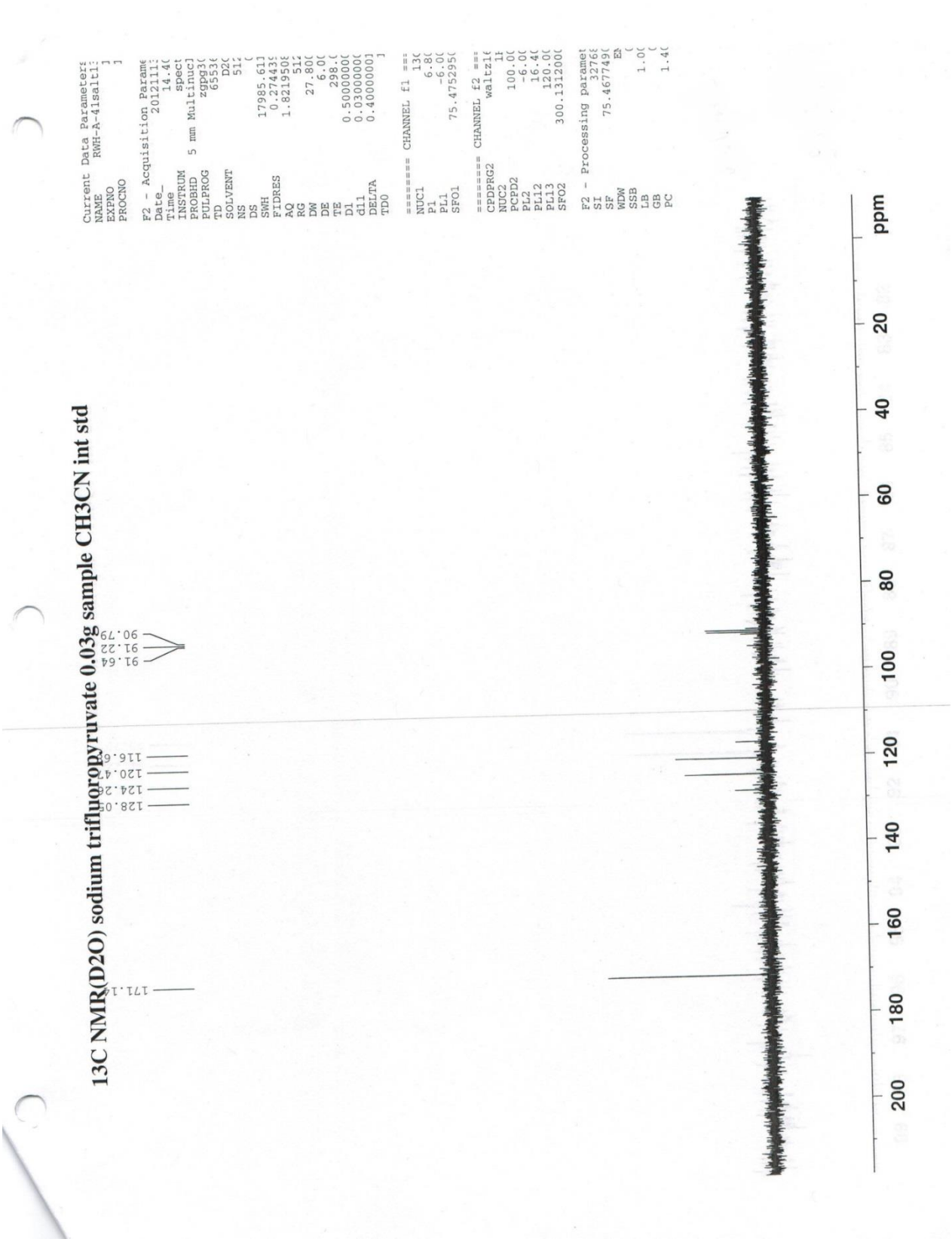
Data filename: C:\LabSolutions\Data\Schwabacher Alan\RWH-B-53xtyl.lcd
Spectrum Mode: Single
Retention Time: 0.100 min.
Interface Type (ESI, APCI, DUIS): DUIS
Aquisition Mode (Scan, SIM, Profile): Scan
Polarity (+,-): +



^{1}H NMR *Sodium trifluoropyruvate* (**47**)



^{13}C NMR *Sodium trifluoropyruvate* (**47**)



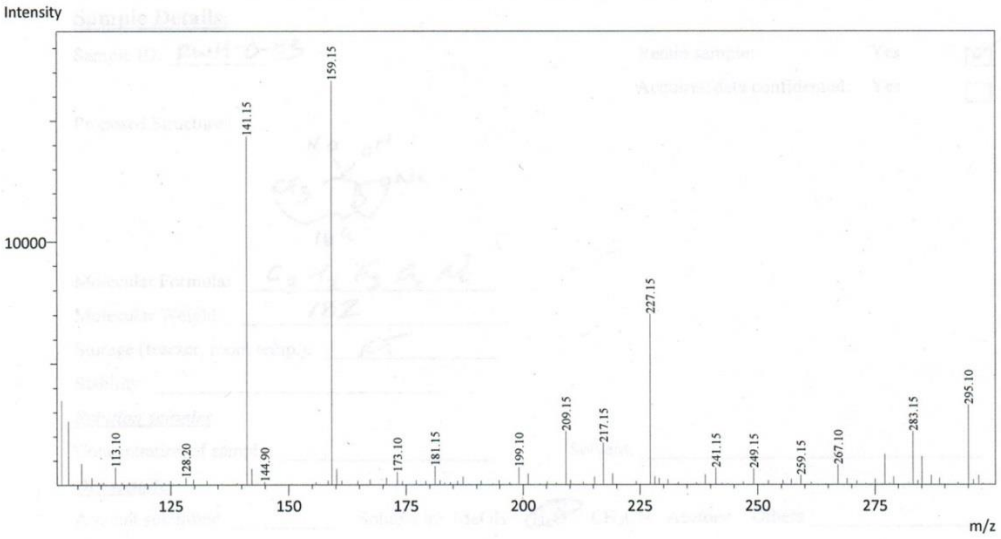
ESI-MS *Sodium trifluoropyruvate* (**47**)

Shimadzu LCMS-2020 Data Report

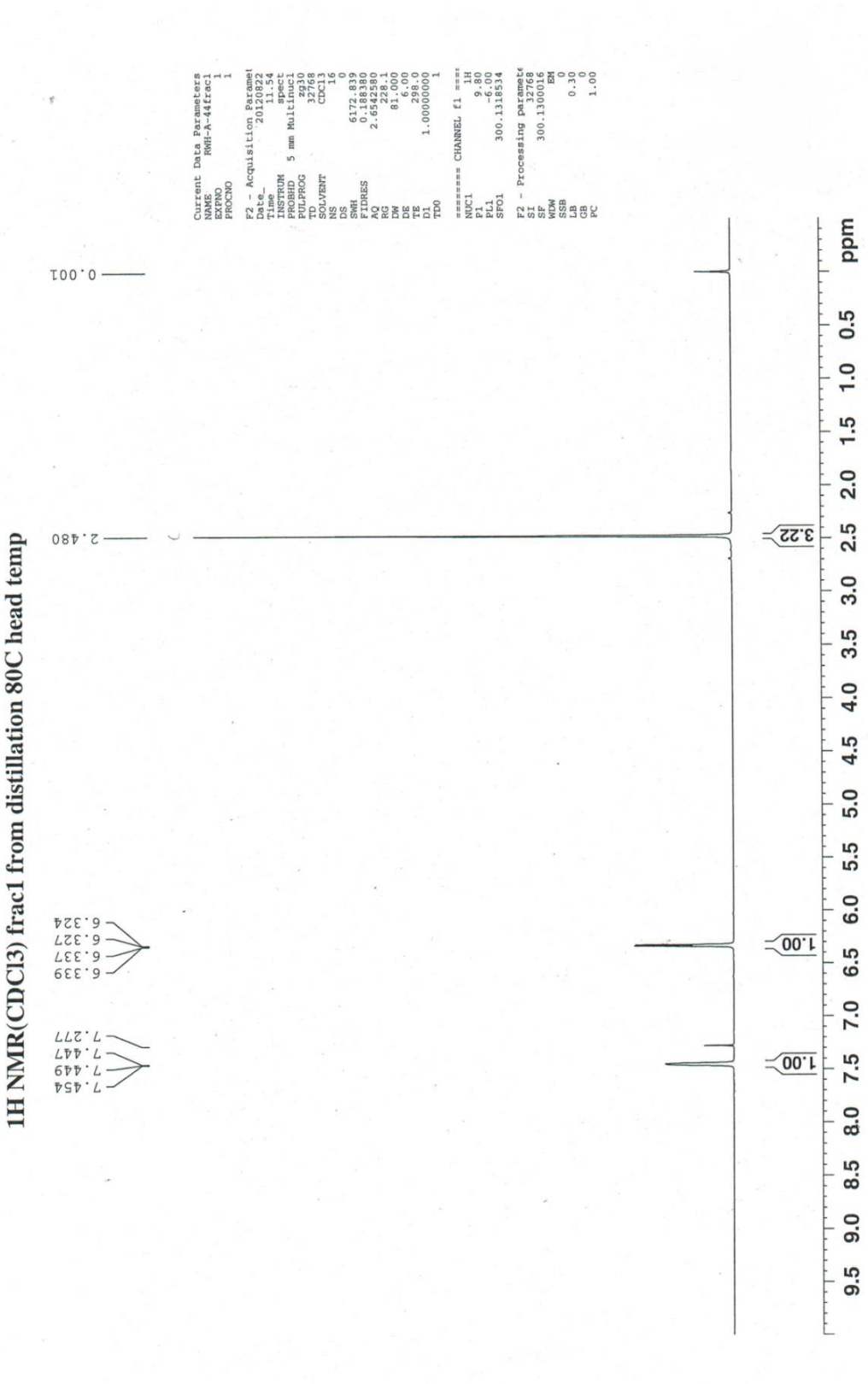
Mass Spectrum for Sample
RWH-B-43.lcd

Operator: Mark Wang

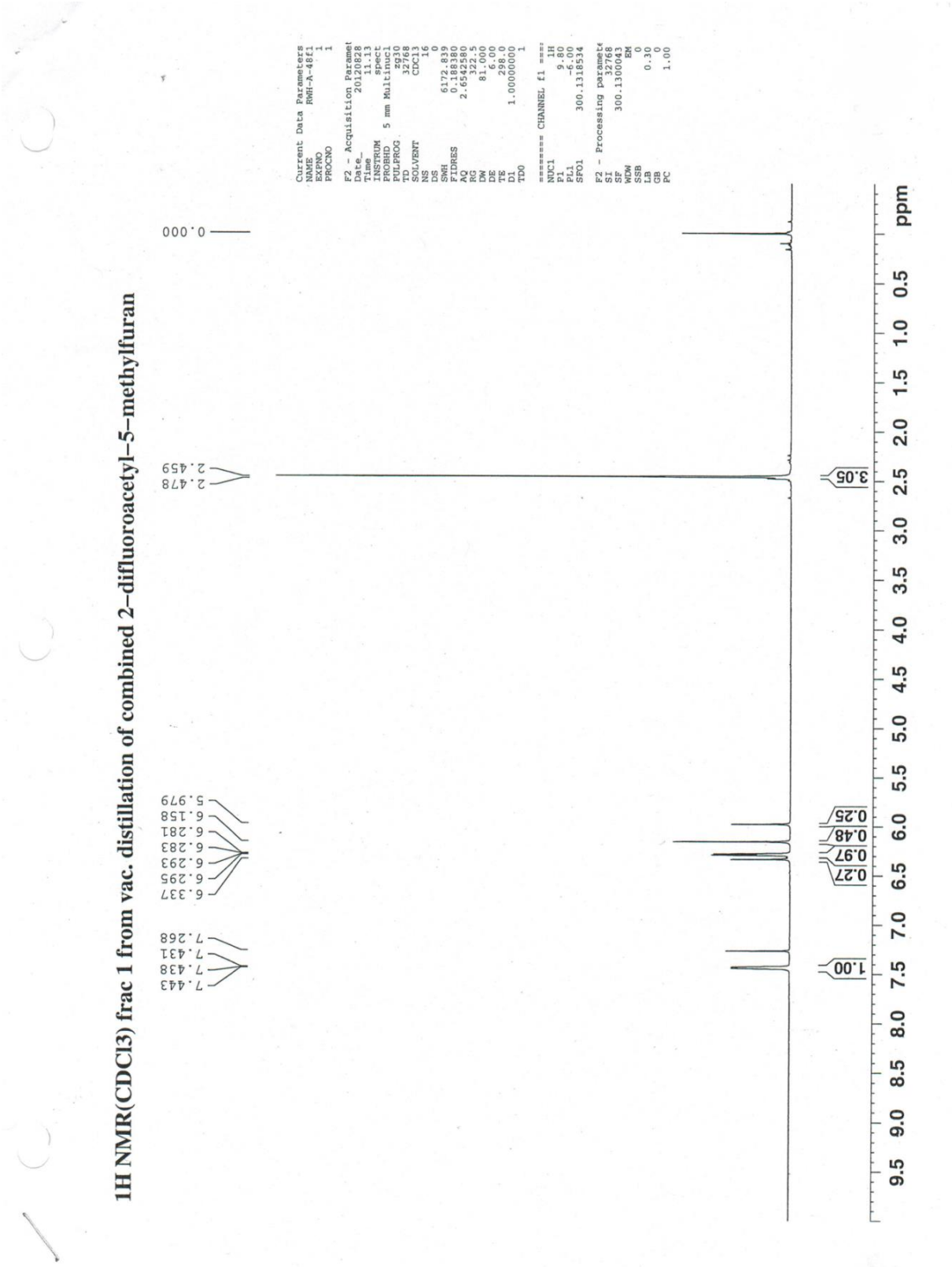
Data Filename: C:\LabSolutions\Data\Schwabacher Alan\RWH-B-43.lcd
Spetrum Mode: Averaged
Retention Time: ----
Interface Type (ESI, APCI, DUIS): DUIS
Aquisition Mode: (Scan, SIM, Profife): Scan
Polarity: -



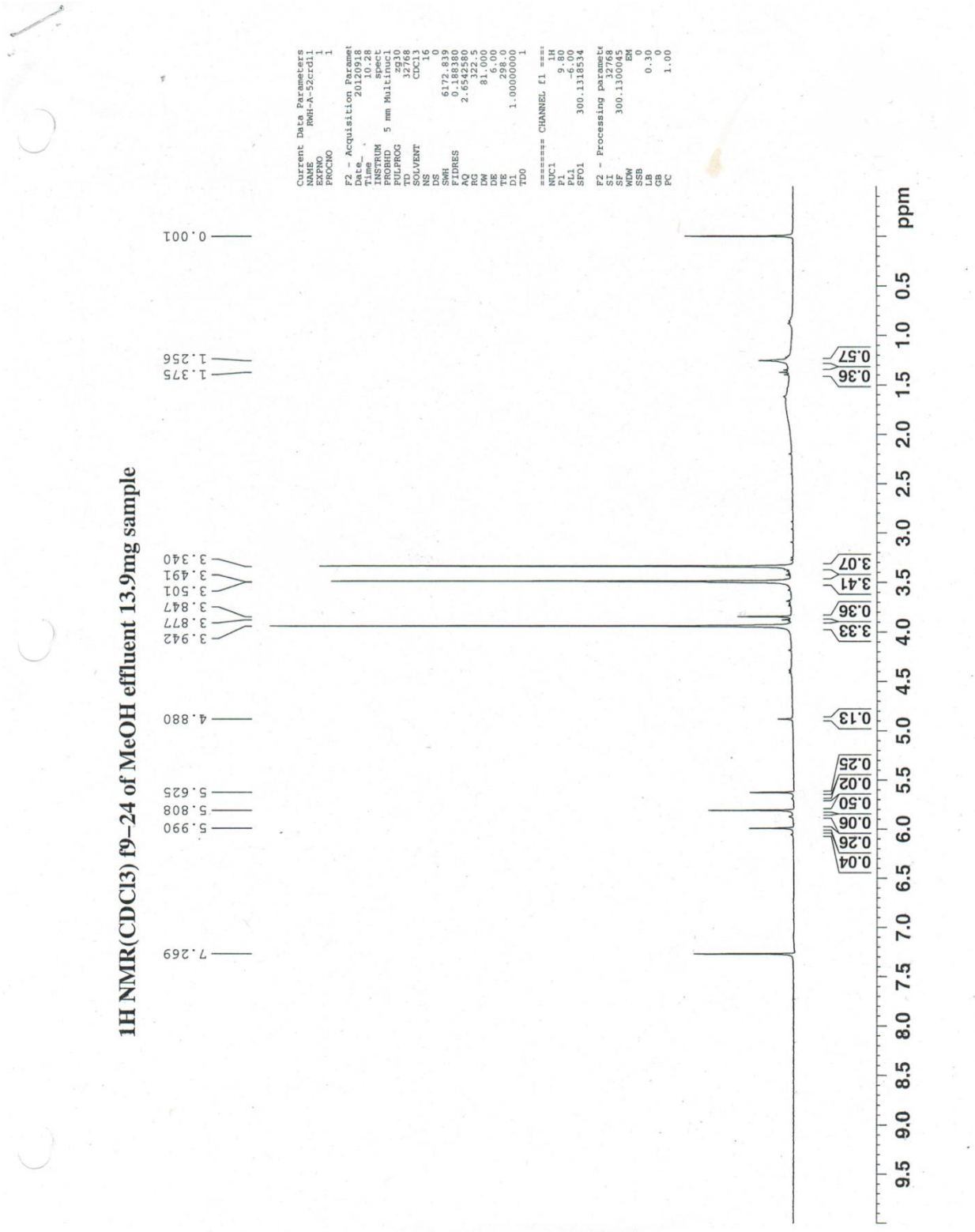
^{1}H NMR *5-methyl-2-(2,2,2-trifluoroacetyl)furan* (**50**)



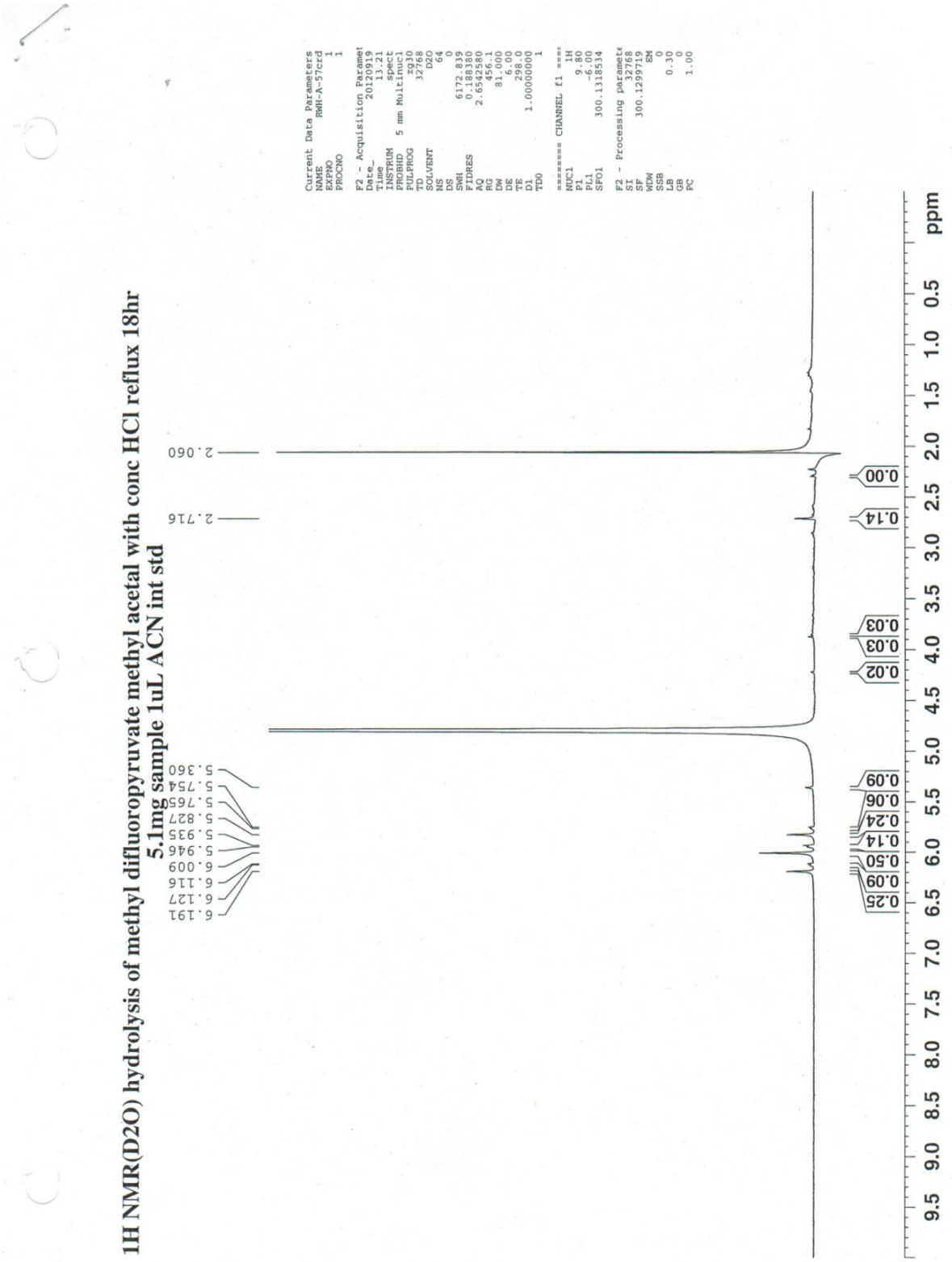
^{1}H NMR *5-methyl-2-(2,2-difluoroacetyl)furan* (**51**)



^{1}H NMR *Methyl difluoropyruvate methyl hemiacetal* (**52**)



^{1}H NMR *Sodium difluoropyruvate hydrate* (**53**)



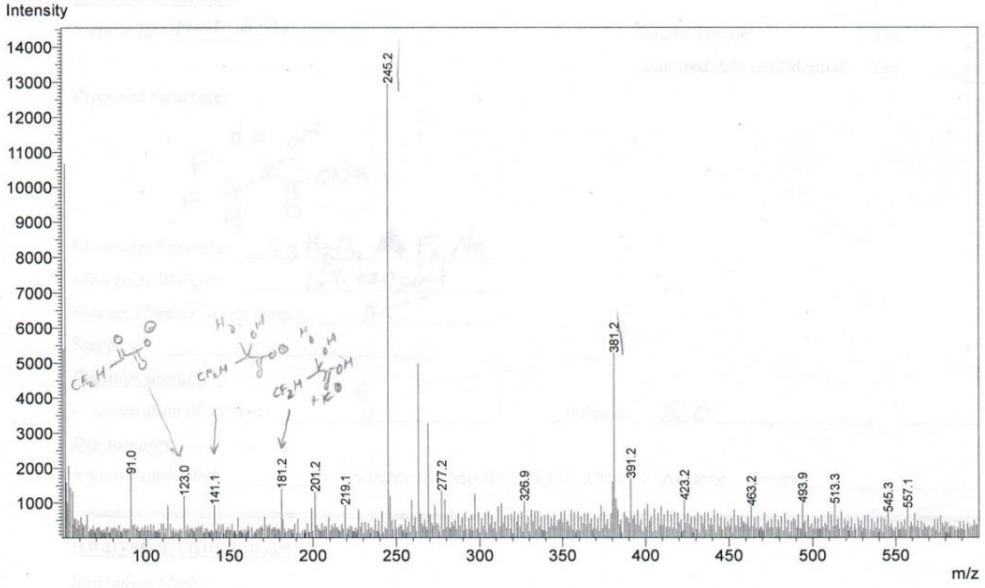
MS *Sodium difluoropyruvate hydrate* (**53**)

Shimadzu LCMS-2020 Data Report

Mass Spectrum for Sample:
RHW-B-21-1

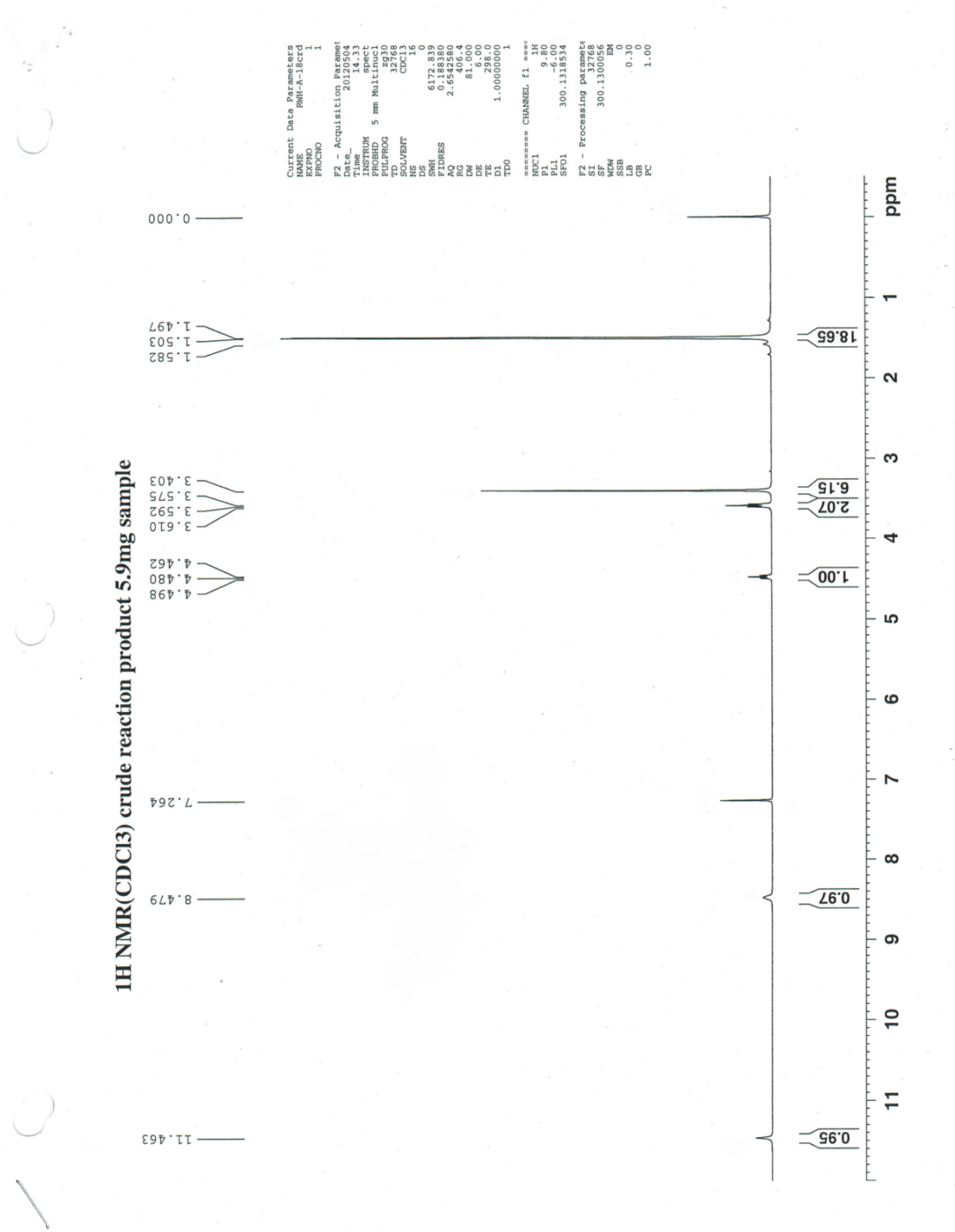
Operator: Mark Wang

Data filename: C:\LabSolutions\Data\Schwabacher Alan\RHW-B-21-1.lcd
Spectrum Mode: Single
Retention Time: 0.150 min.
Interface Type (ESI, APCI, DUIS): DUIS
Aquisition Mode (Scan, SIM, Profile): Scan
Polarity (+,-): -

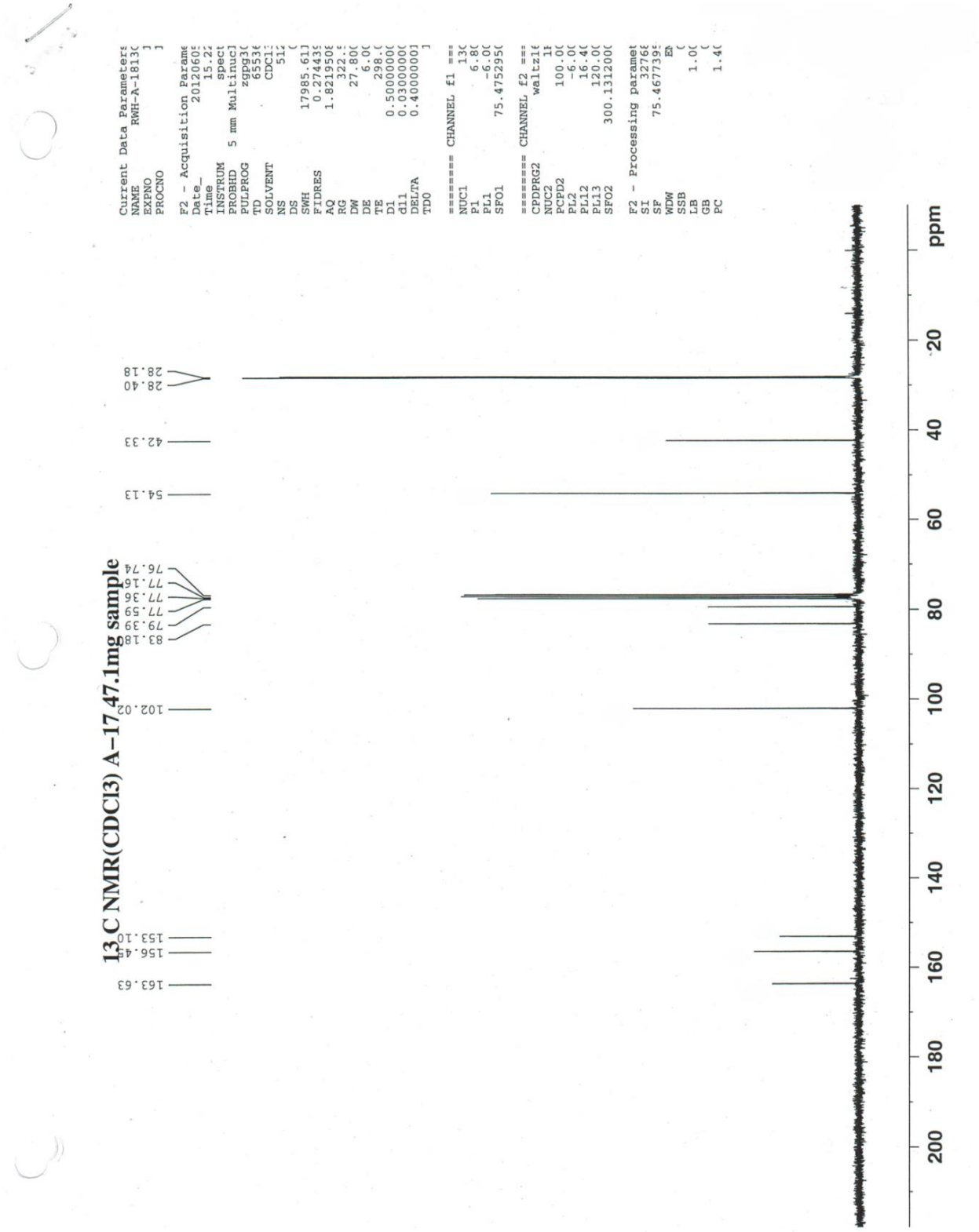


M+. M⁻ = 247

^{1}H NMR *N,N'-Di-Boc-N"-(2,2-dimethoxy-ethyl)-guanidine* (**54**)



^{13}C NMR *N,N'-Di-Boc-N"-(2,2-dimethoxy-ethyl)-guanidine* (**54**)



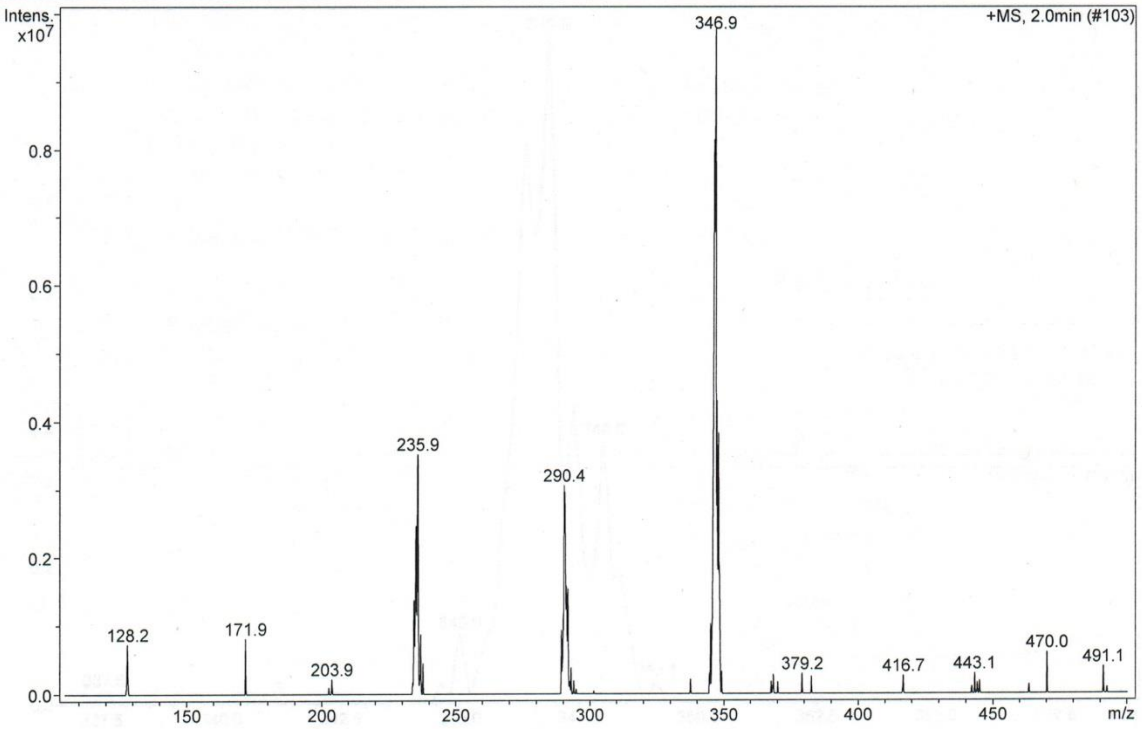
MS *N,N'-Di-Boc-N"-(2,2-dimethoxy-ethyl)-guanidine* (**54**)

Display Report - All Windows Selected Analy

Analysis Name: 06112201.d
Method: Copy of MARK02.M
Sample Na RWH-A-18
Analysis Inf

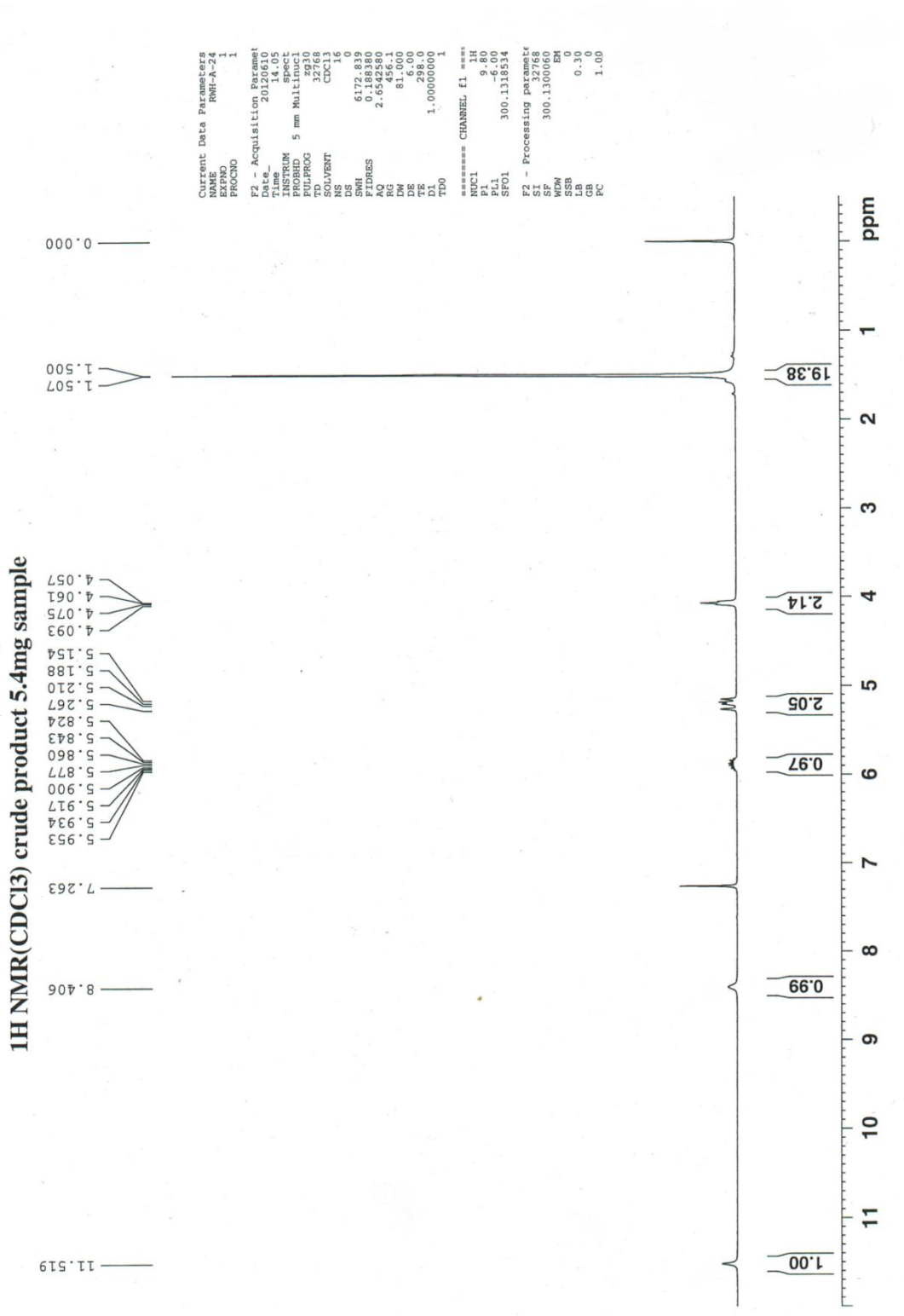
Instrume LC-MSD-Trap-SL
Operator: Mark Wang

Print Date: 06/12/12 14:21:47
Acq. Date 06/12/12 14:17:35

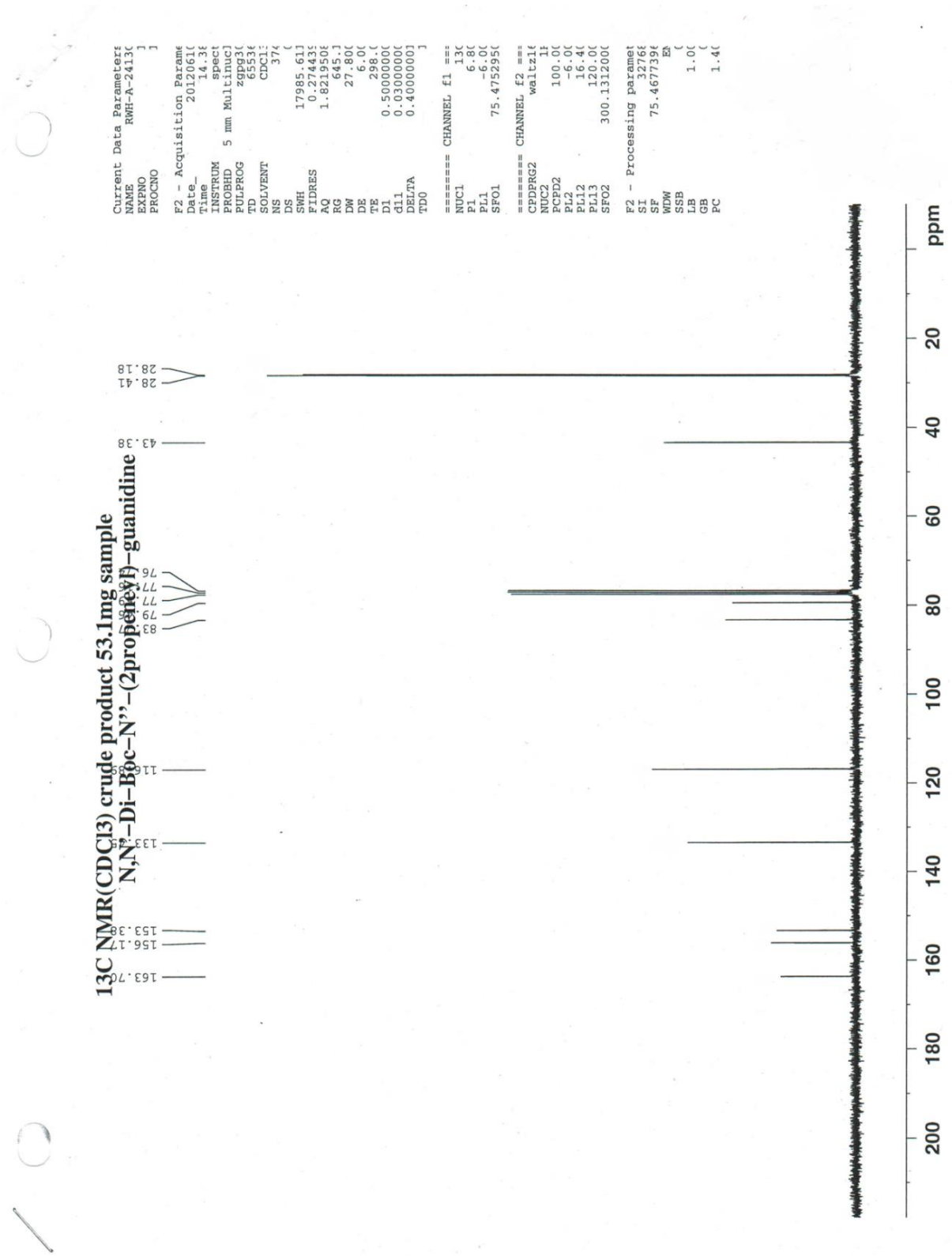


Agilent Technologies

^{1}H NMR *N-Allyl-N',N''-Di-Boc-guanidine* (**55**)



^{13}C NMR *N-Allyl-N',N''-Di-Boc-guanidine* (**55**)



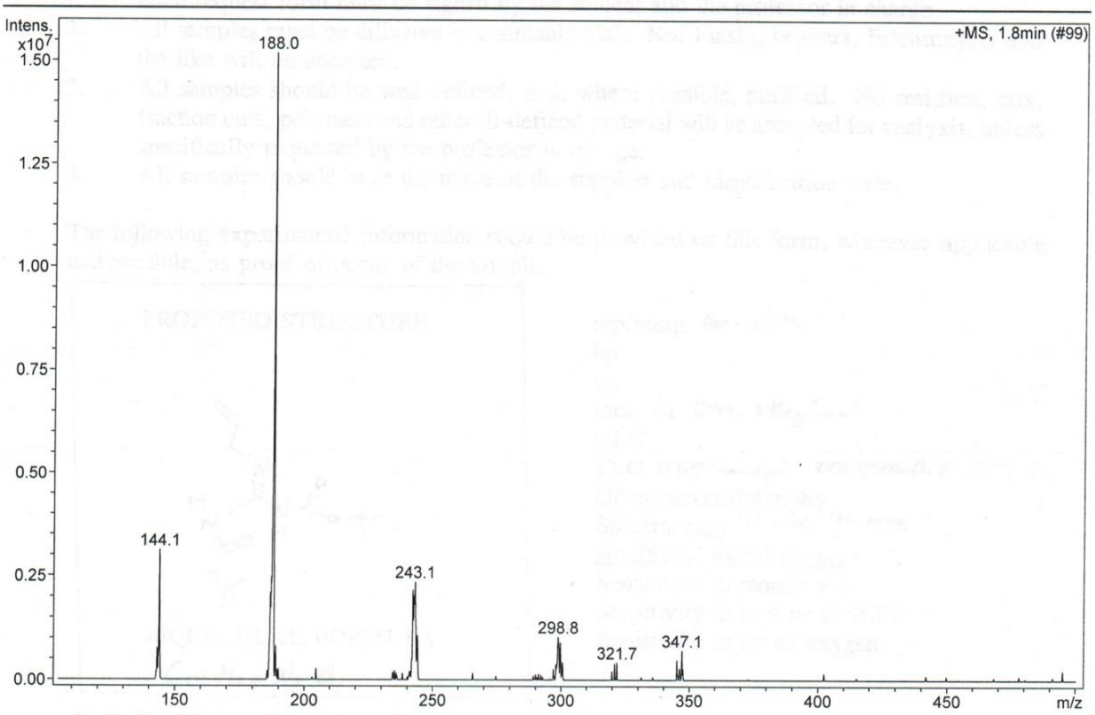
MS *N-Allyl-N',N''-Di-Boc-guanidine* (**55**)

Display Report - All Windows Selected Analy

Analysis Name: 06121203.D
Method: Copy of MARK02.M
Sample Na RWH-A-24
Analysis Inf

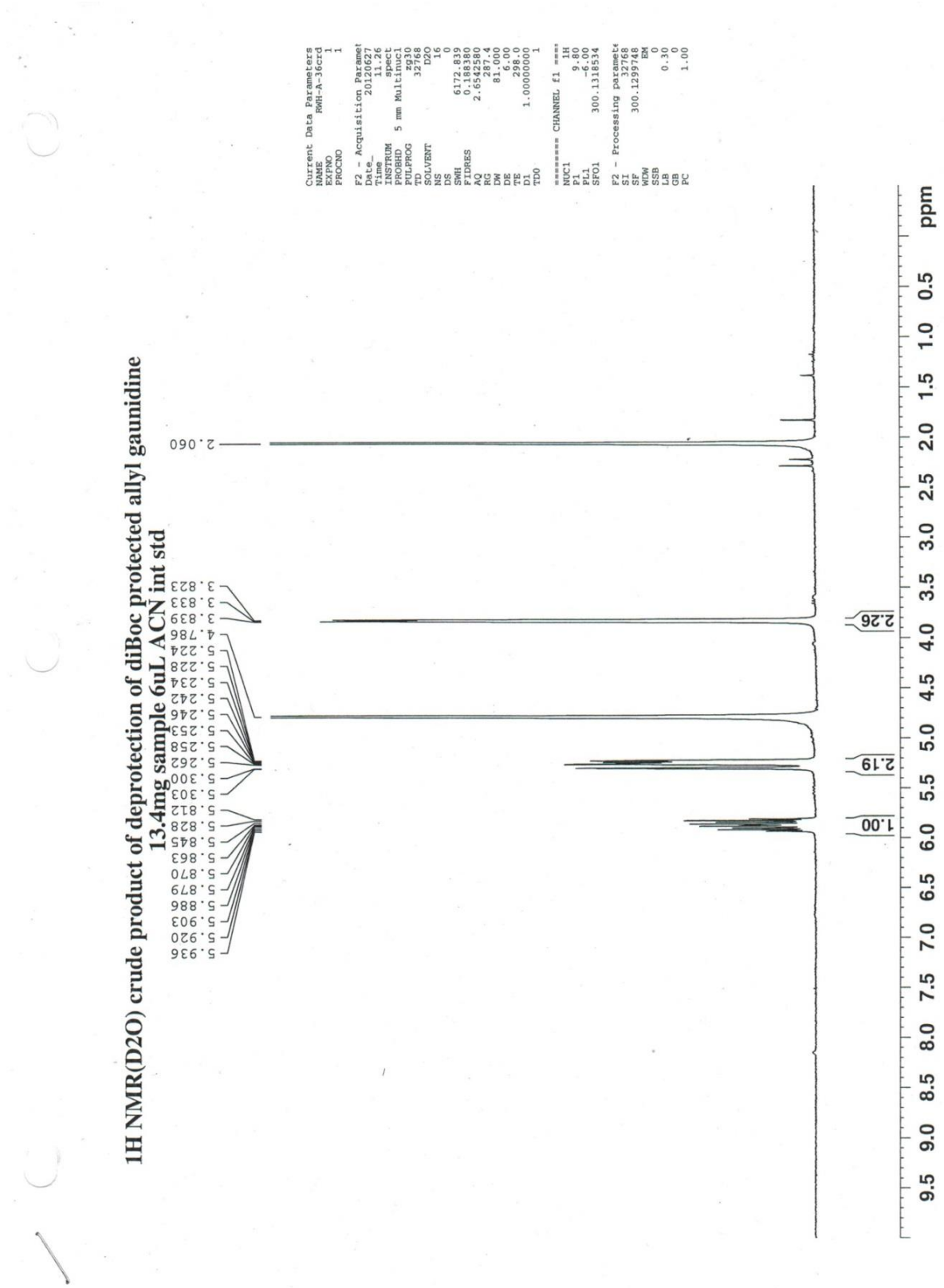
Instrume LC-MSD-Trap-SL
Operator: Mark Wang

Print Date: 06/12/12 14:38:44
Acq. Date 06/12/12 14:34:41

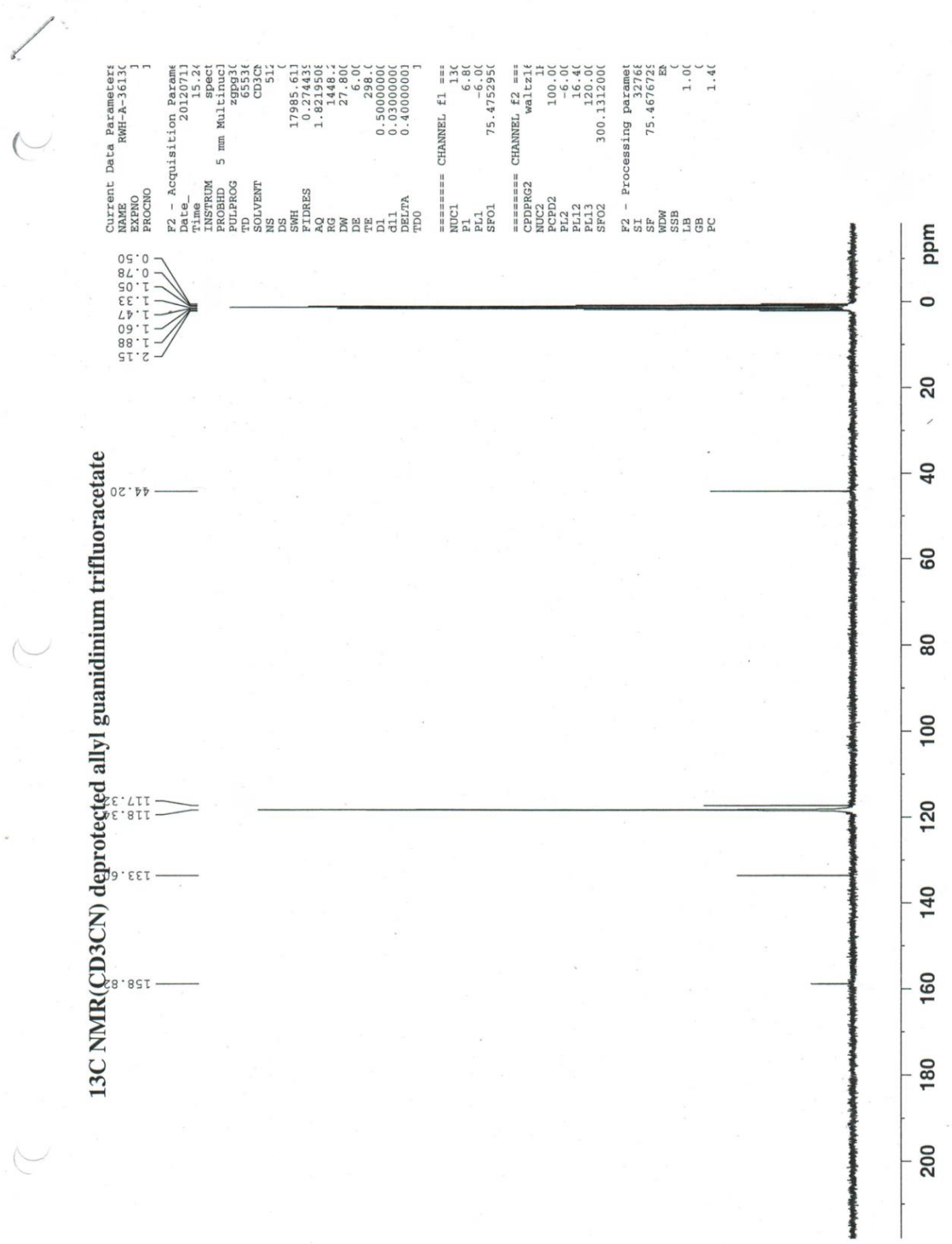


Agilent Technologies

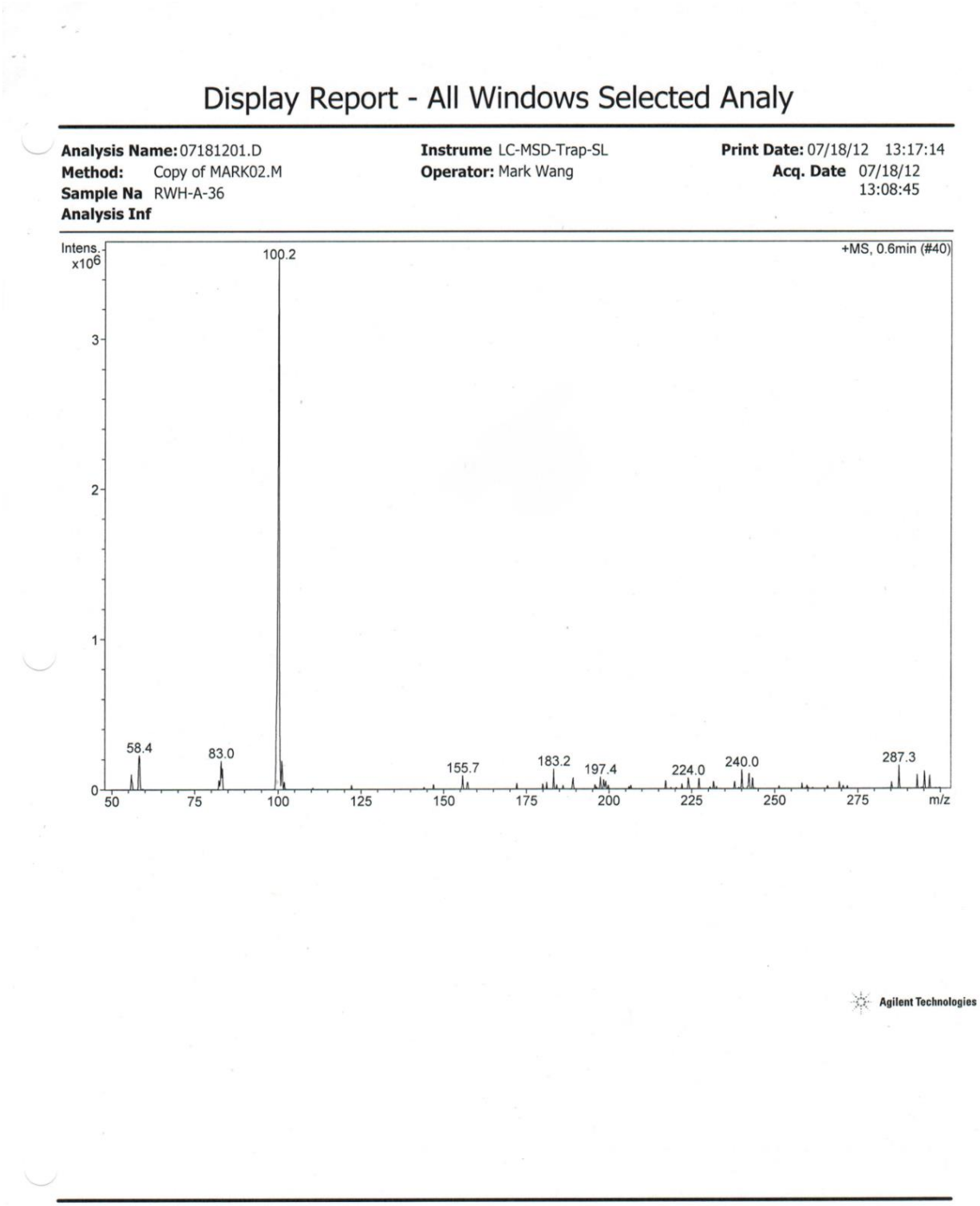
^{1}H NMR *N-allyl guanidinium trifluoracetate* (**57**)



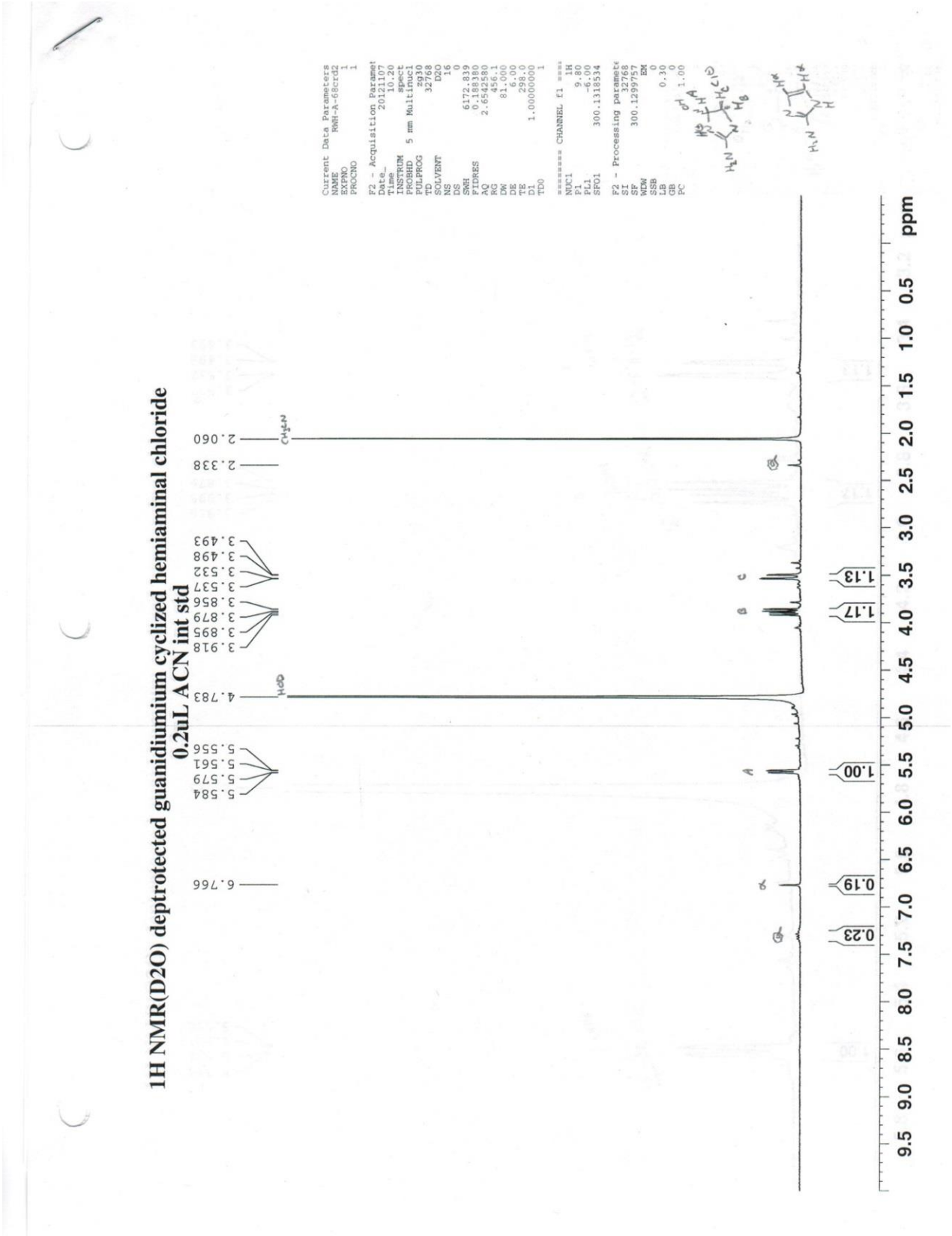
^{13}C NMR *N-allyl guanidinium trifluoracetate* (**57**)



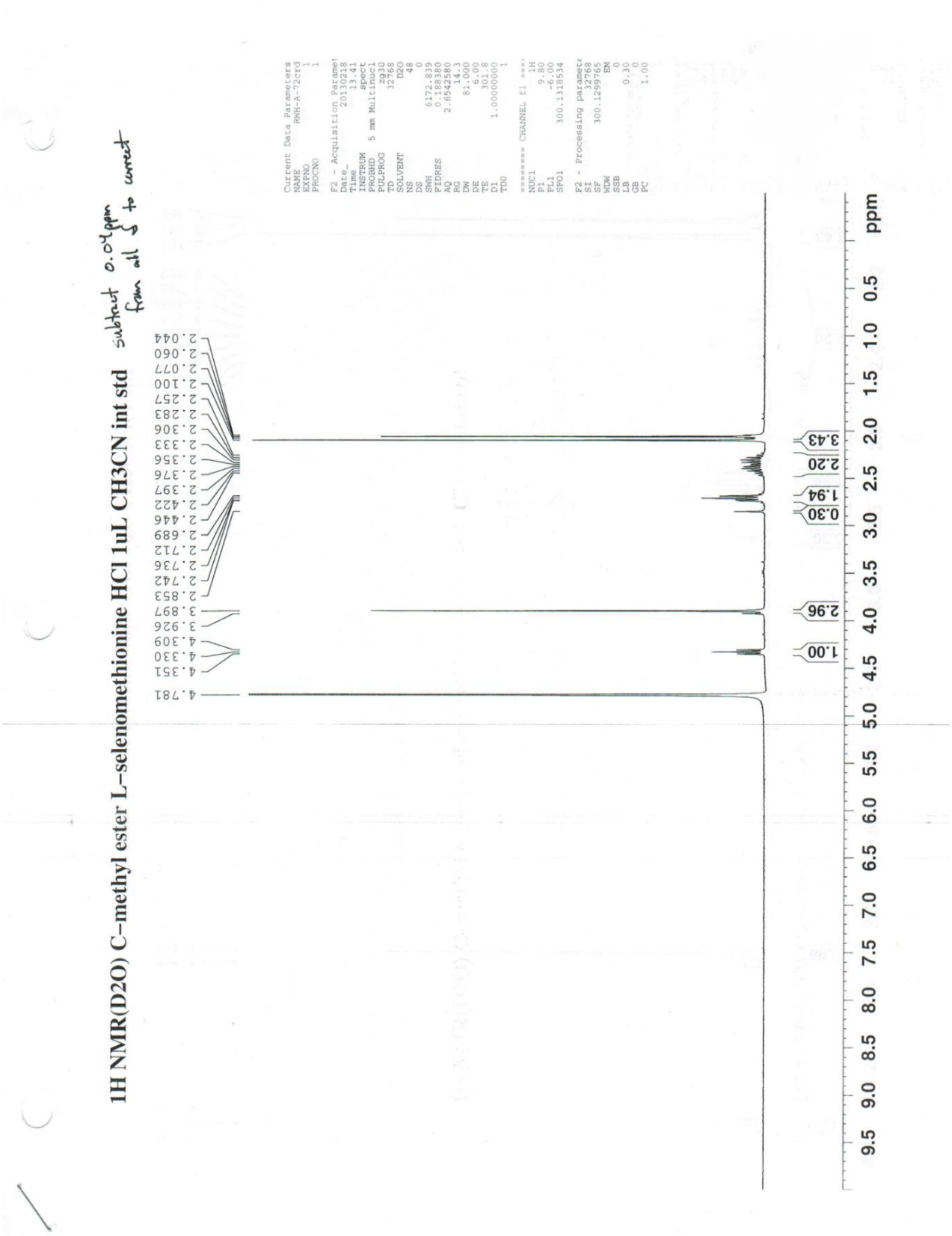
MS *N-allyl guanidinium trifluoracetate* (**57**)



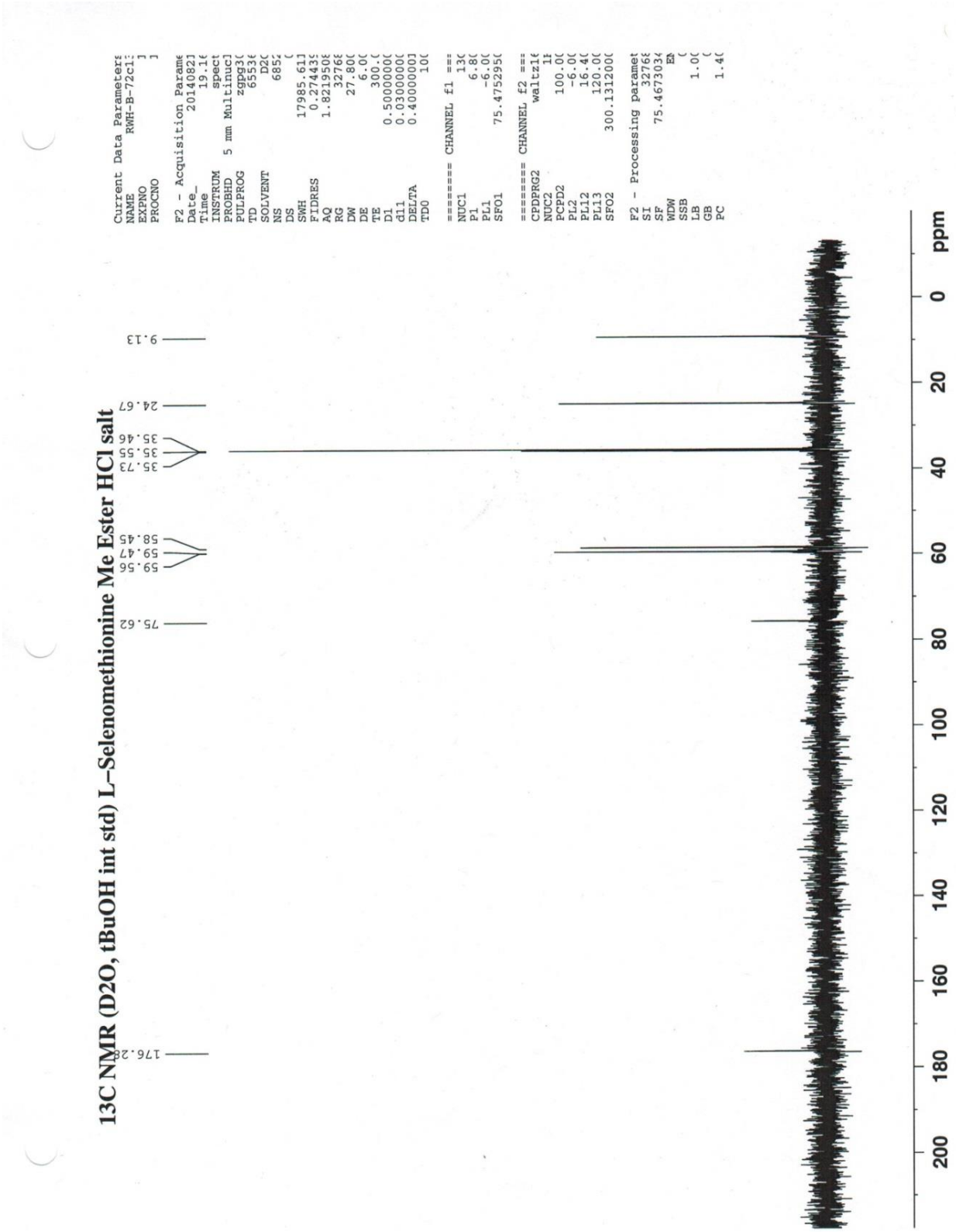
[1] H NMR *2-Amino-5-hydroxy-4,5-dihydro-3H-imidazolium chloride* (**58**)



^{1}H NMR *L-Selenomethionine methyl ester hydrochloride* (**62**)



^{13}C NMR *L-Selenomethionine methyl ester hydrochloride* (**62**)



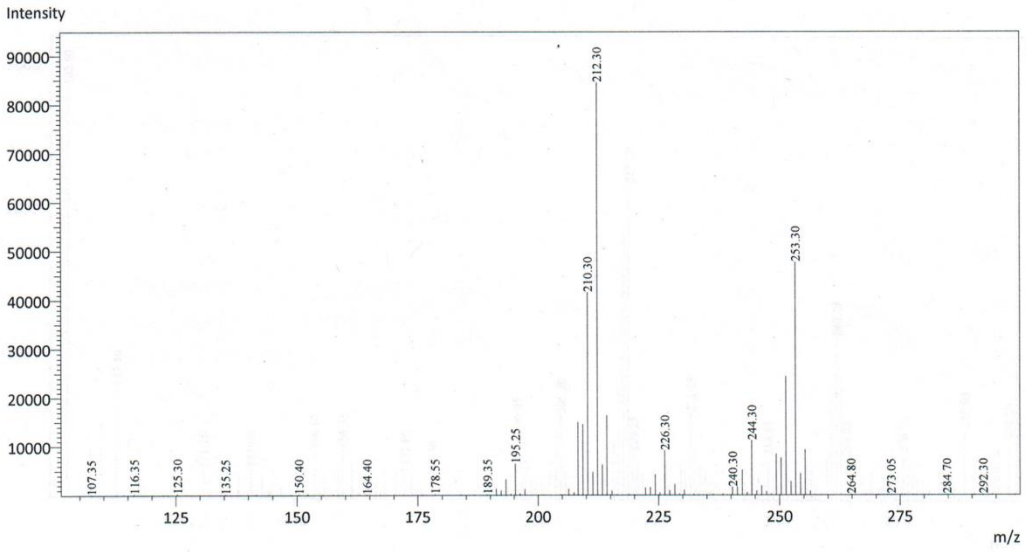
ESI-MS *L-Selenomethionine methyl ester hydrochloride* (**62**)

Shimadzu LCMS-2020 Data Report

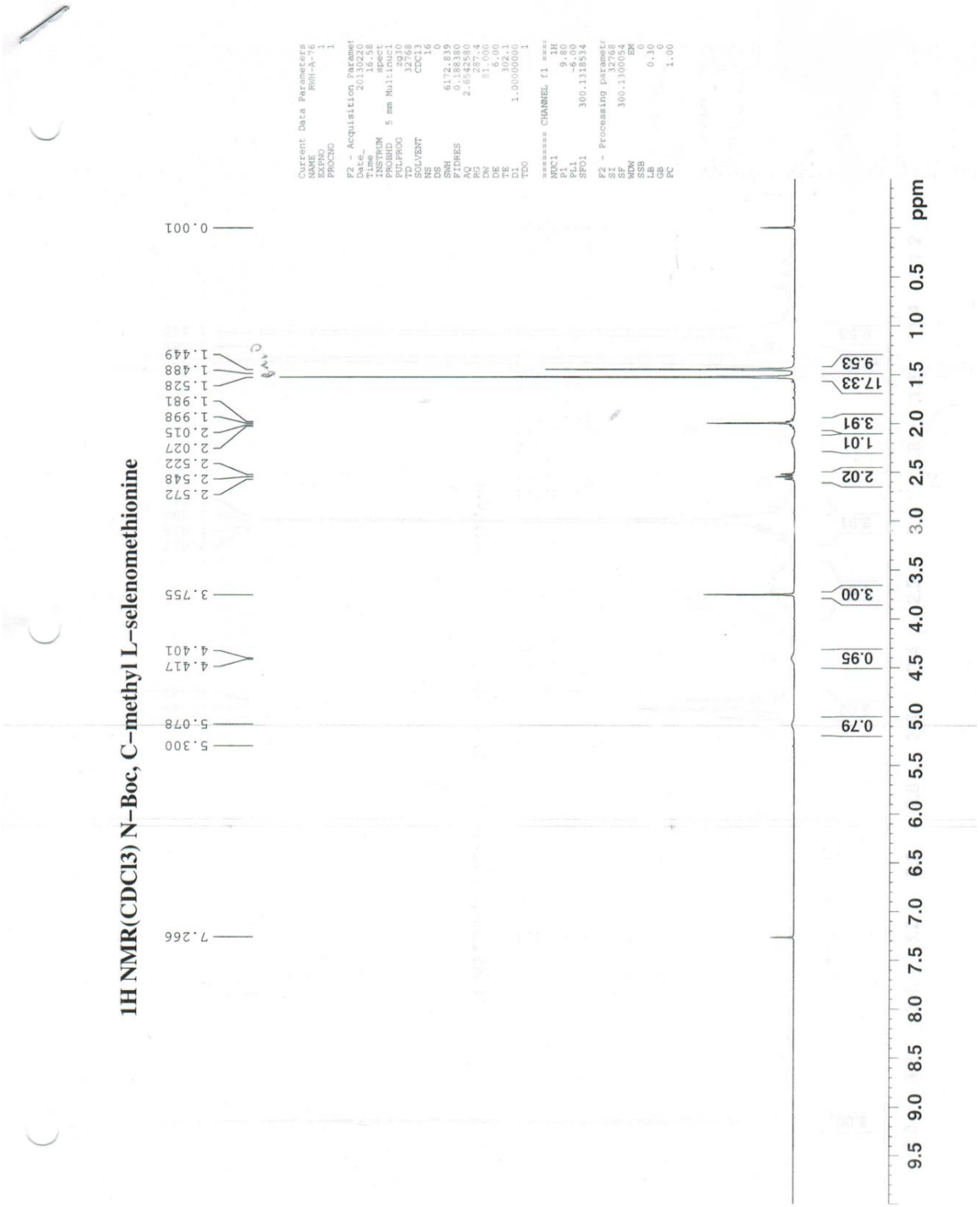
Mass Spectrum for Sample
RWH-A-72 01.lcd

Operator: Mark Wang

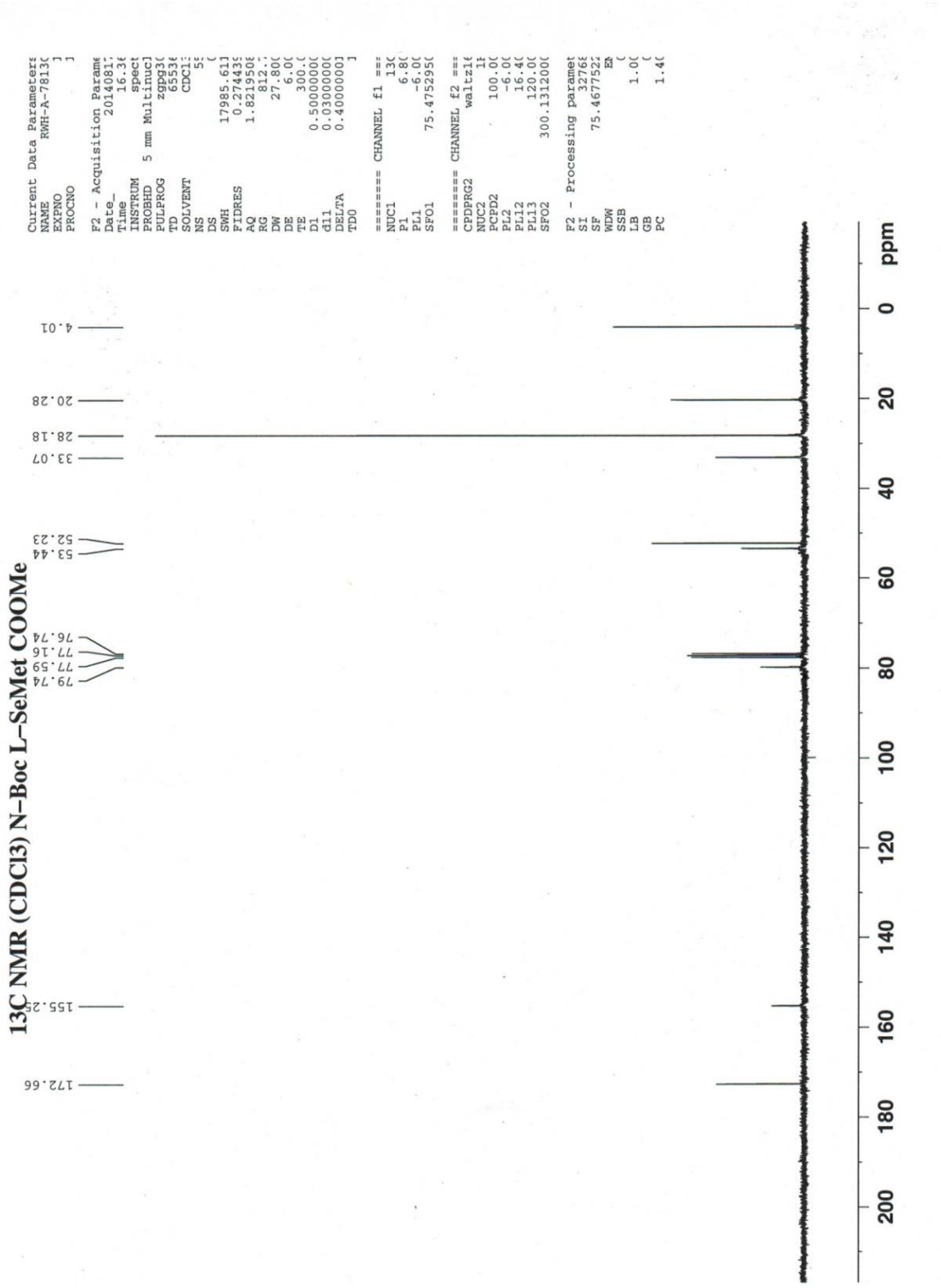
Data Filename: C:\LabSolutions\Data\Schwabacher Alan\RWH-A-72 01.lcd
Spetrum Mode: Averaged
Retention Time: ----
Interface Type (ESI, APCI, DUIS): DUIS
Aquisition Mode: (Scan, SIM, Profife): Scan
Polarity: +



^{1}H NMR *N-Boc-L-Selenomethionine methyl ester* (**63**)



^{13}C NMR *N-Boc-L-Selenomethionine methyl ester* (**63**)



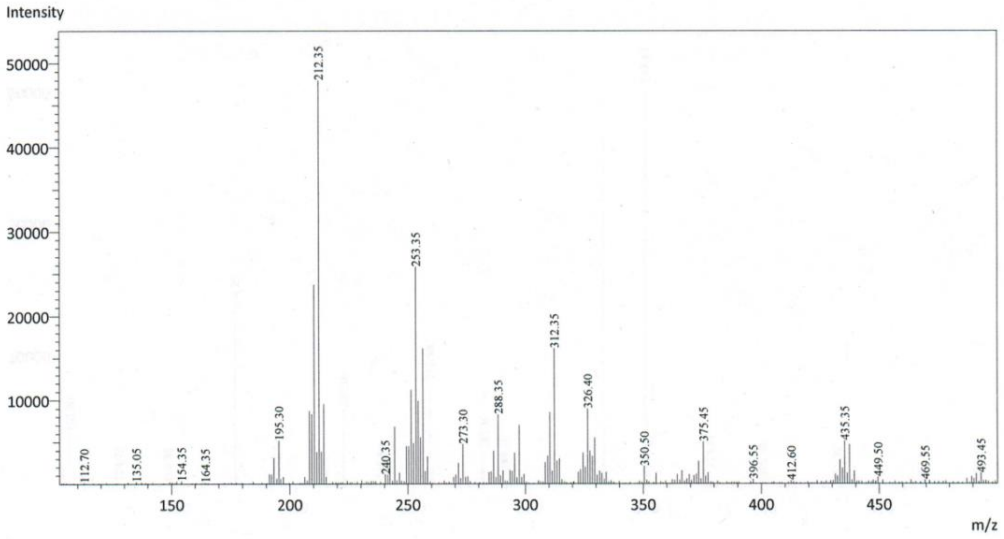
MS *N-Boc-L-Selenomethionine methyl ester* (**63**)

Shimadzu LCMS-2020 Data Report

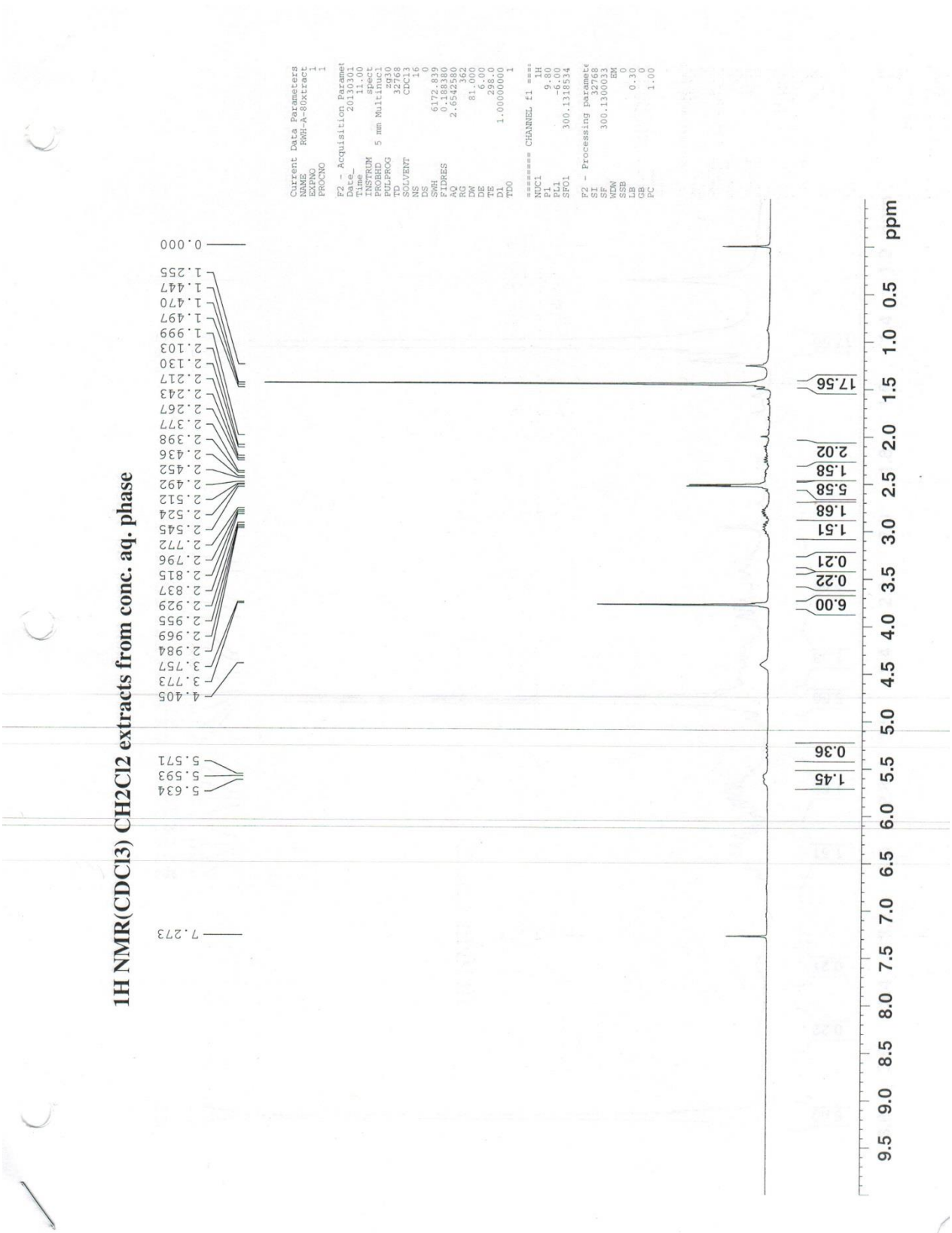
Mass Spectrum for Sample
RWH-A-78 02.lcd

Operator: Mark Wang

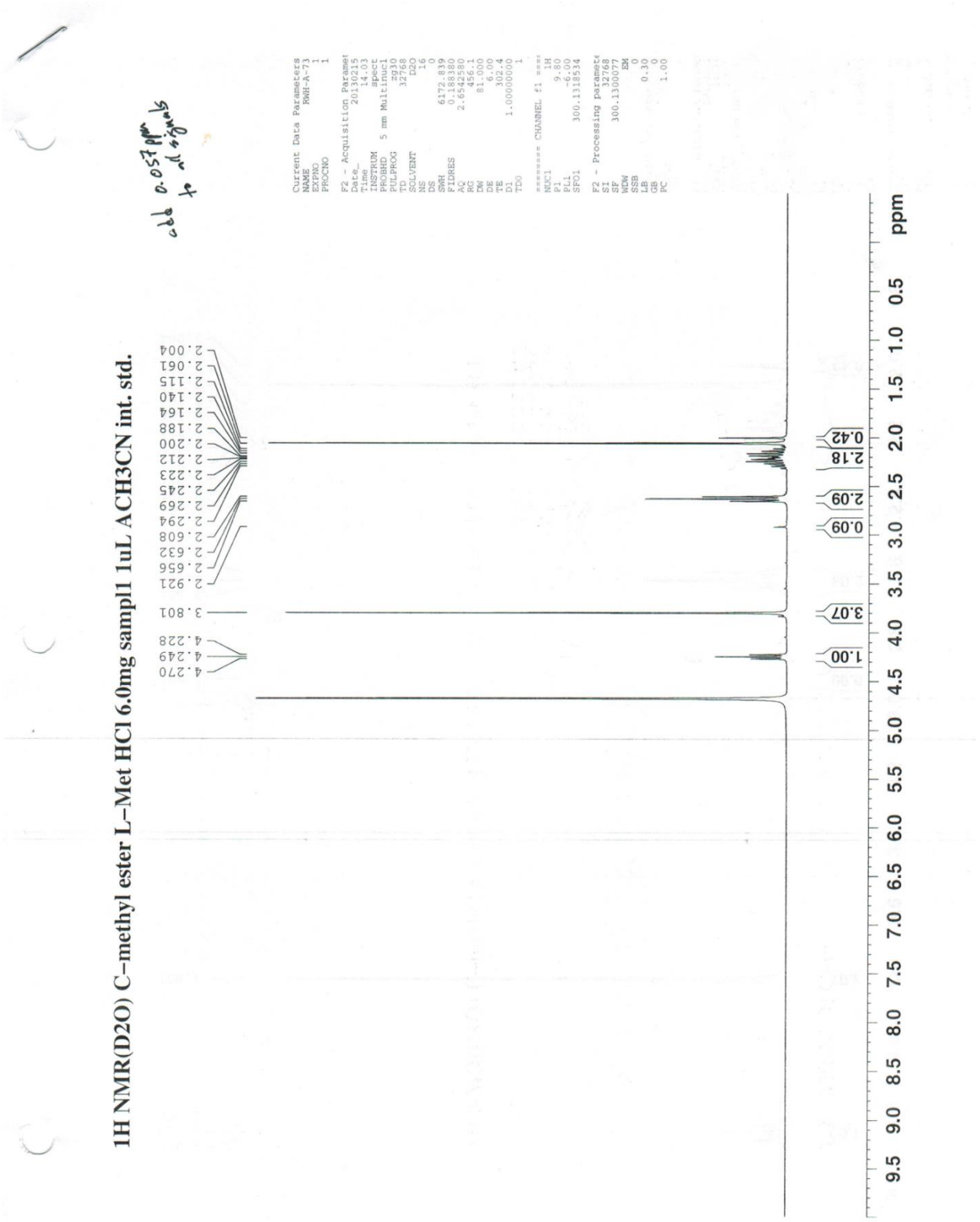
Data Filename: C:\LabSolutions\Data\Schwabacher Alan\RWH-A-78 02.lcd
Spetrum Mode: Averaged
Retention Time: ----
Interface Type (ESI, APCI, DUIS): DUIS
Aquisition Mode: (Scan, SIM, Profife): Scan
Polarity: +



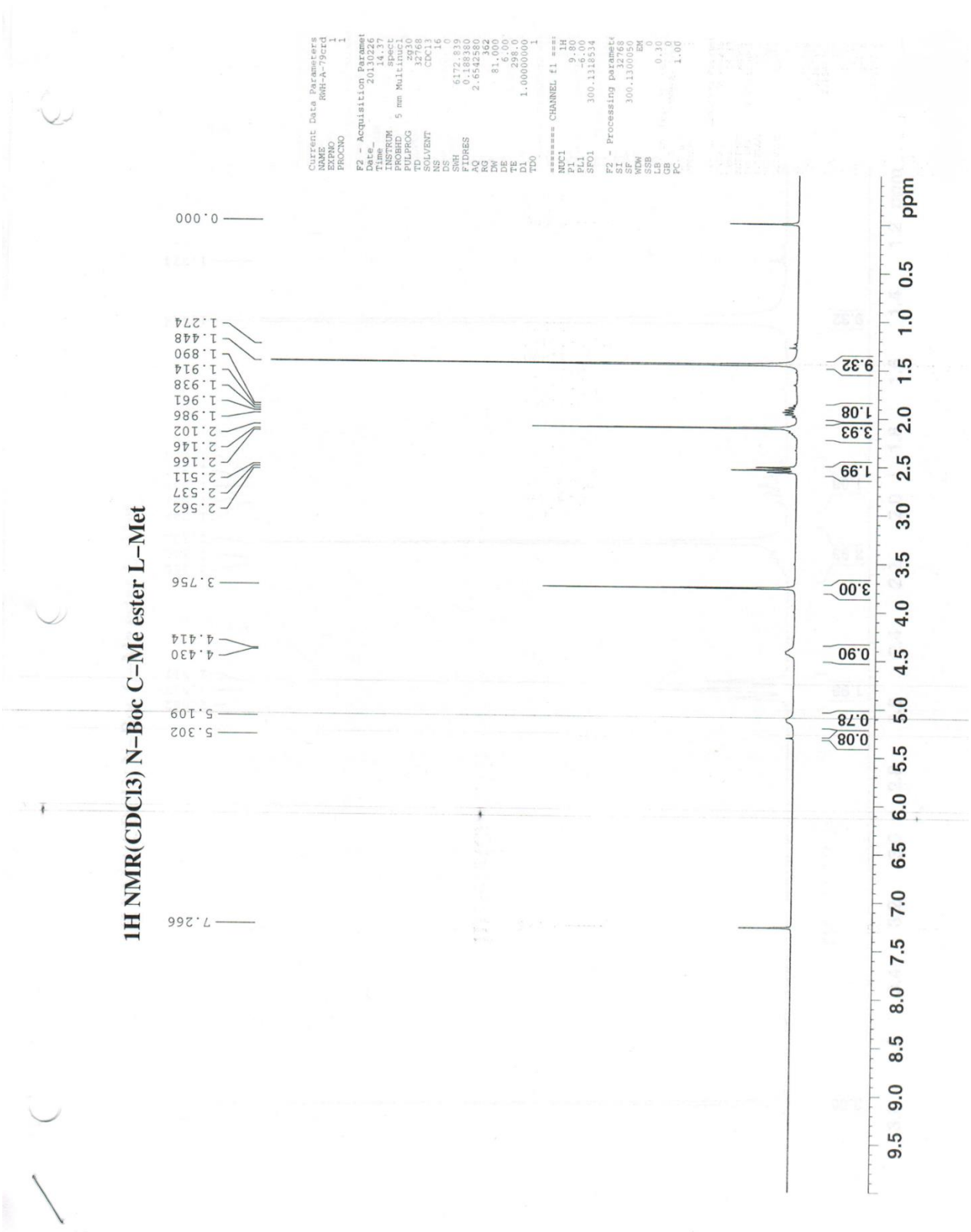
^{1}H NMR *N-Boc-L-Selenomethionine oxide methyl ester* (**64**)



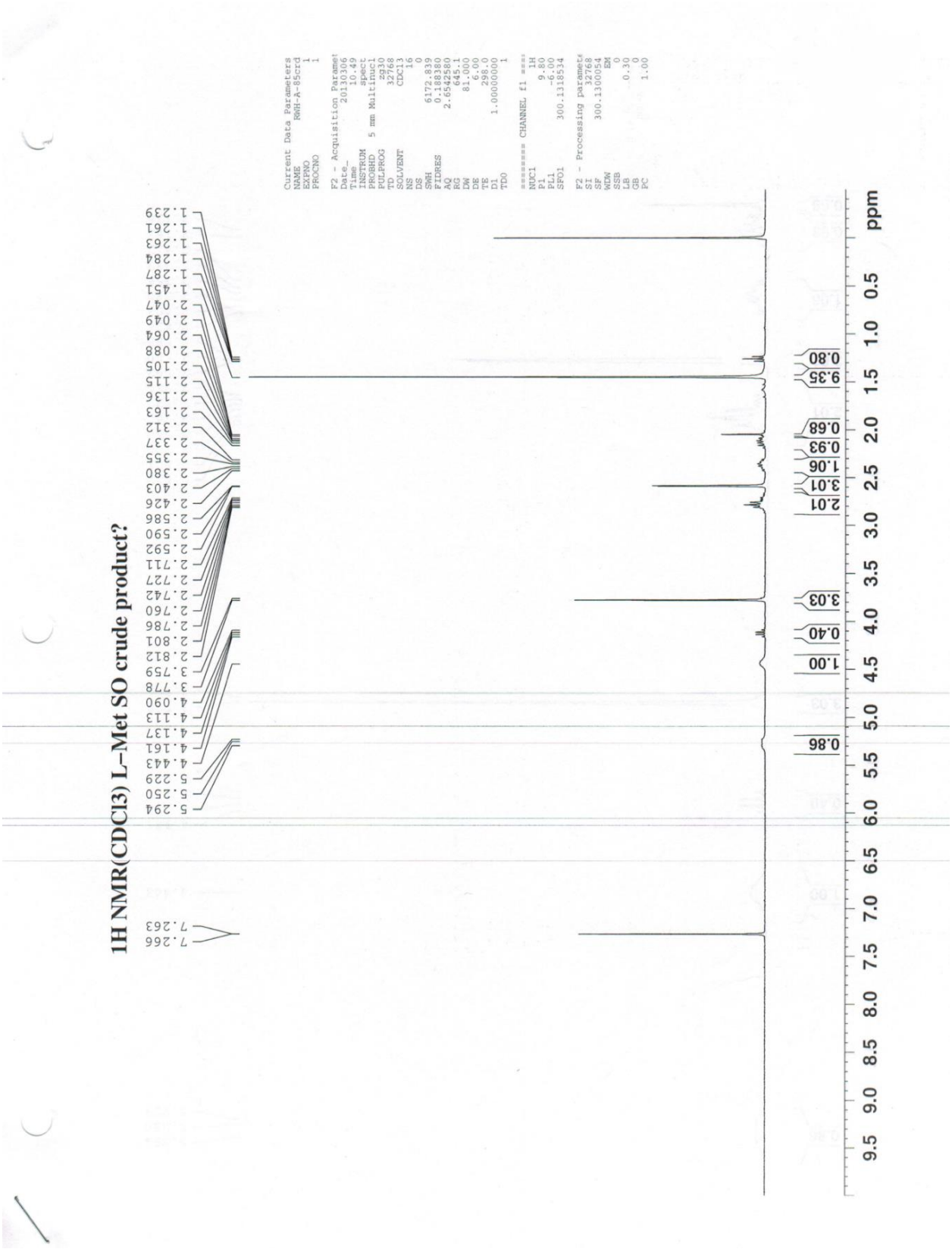
^{1}H NMR *L-Methionine methyl ester hydrochloride* (**66**)



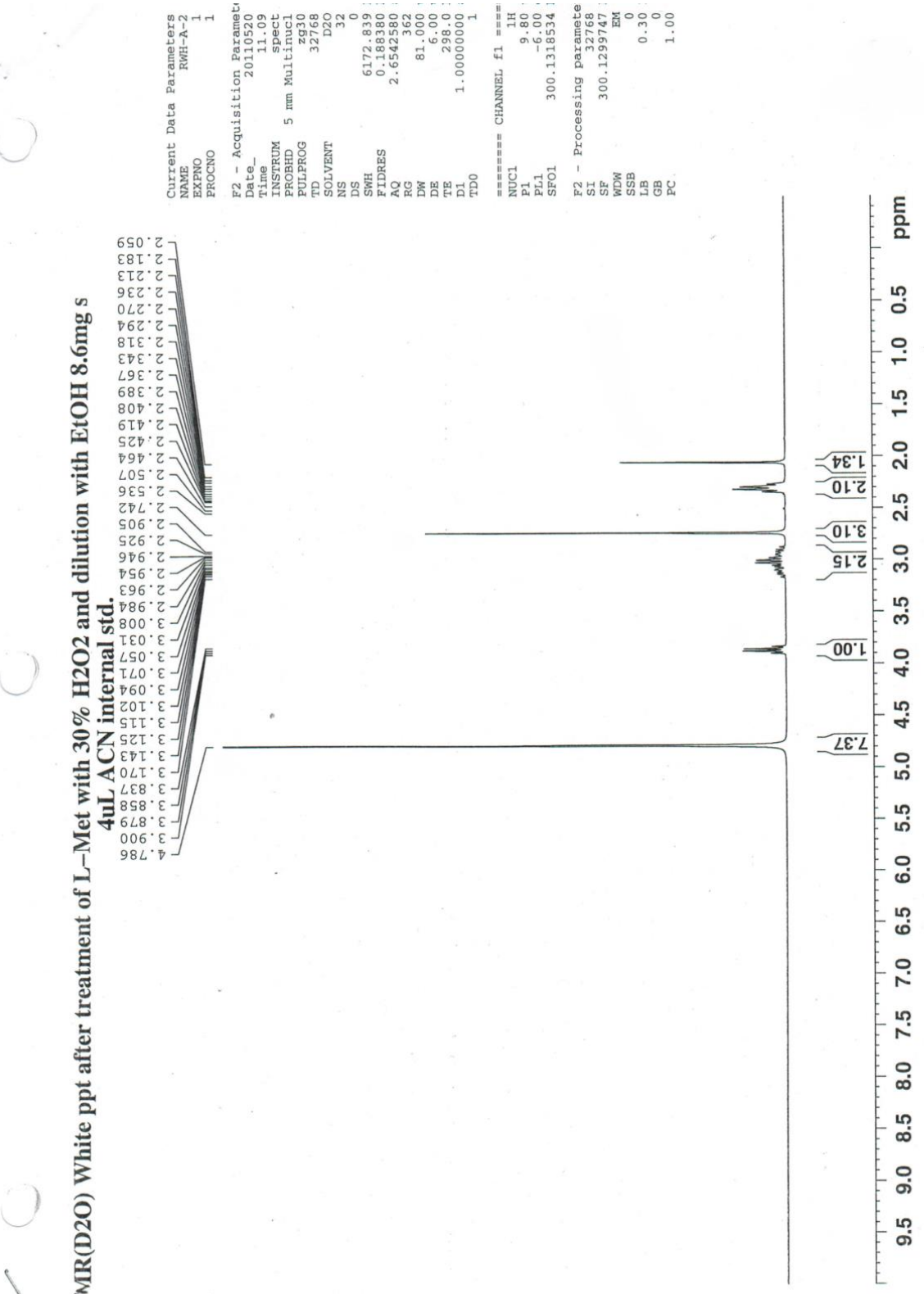
^{1}H NMR *N-Boc-L-Methionine methyl ester* (**67**)



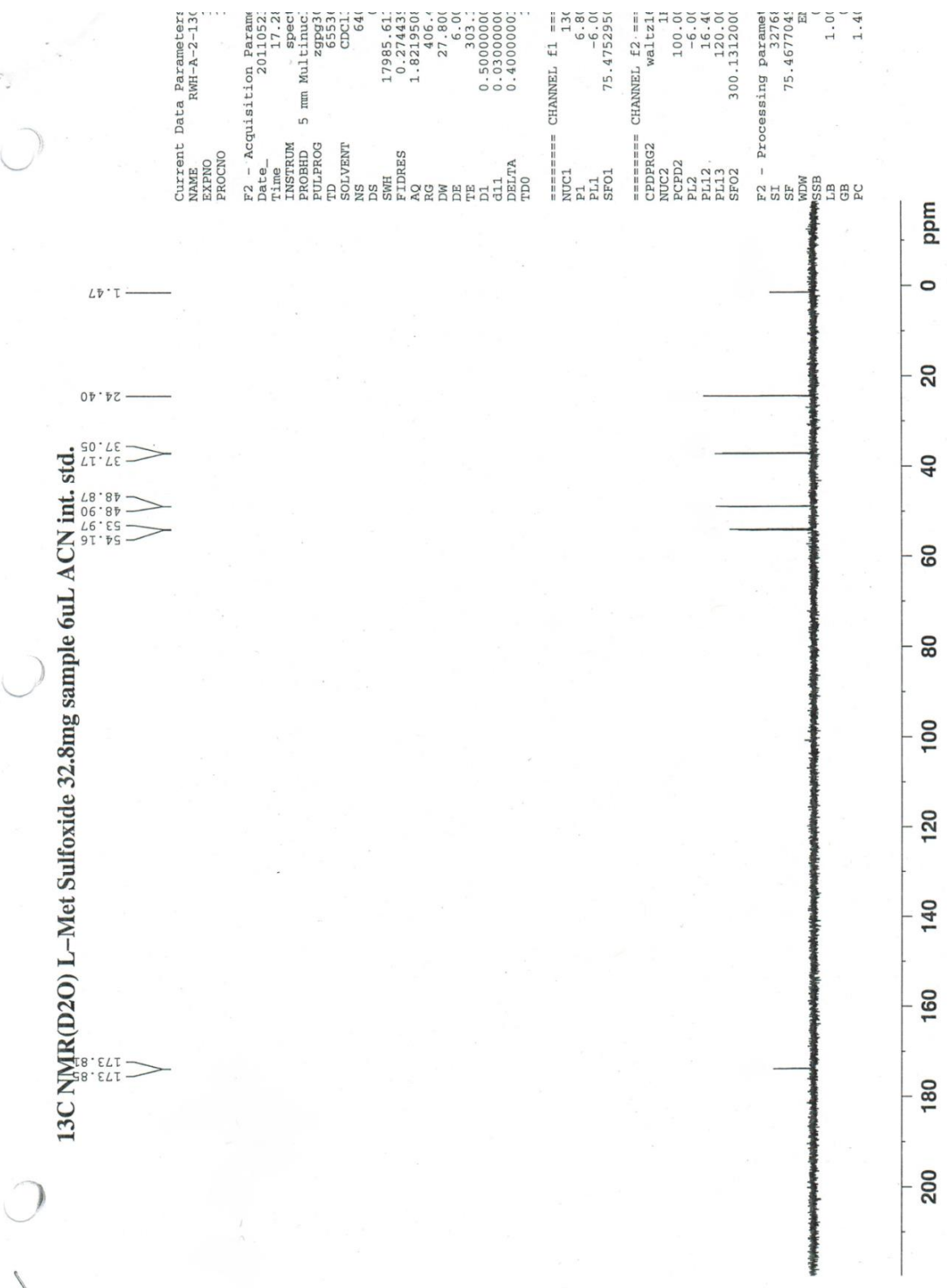
[1]H NMR *N-Boc-L-Methionine sulfoxide methyl ester* (**68**)



^{1}H NMR *L-Methionine sulfoxide* (**70**)



^{13}C NMR *L-Methionine sulfoxide* (**70**)



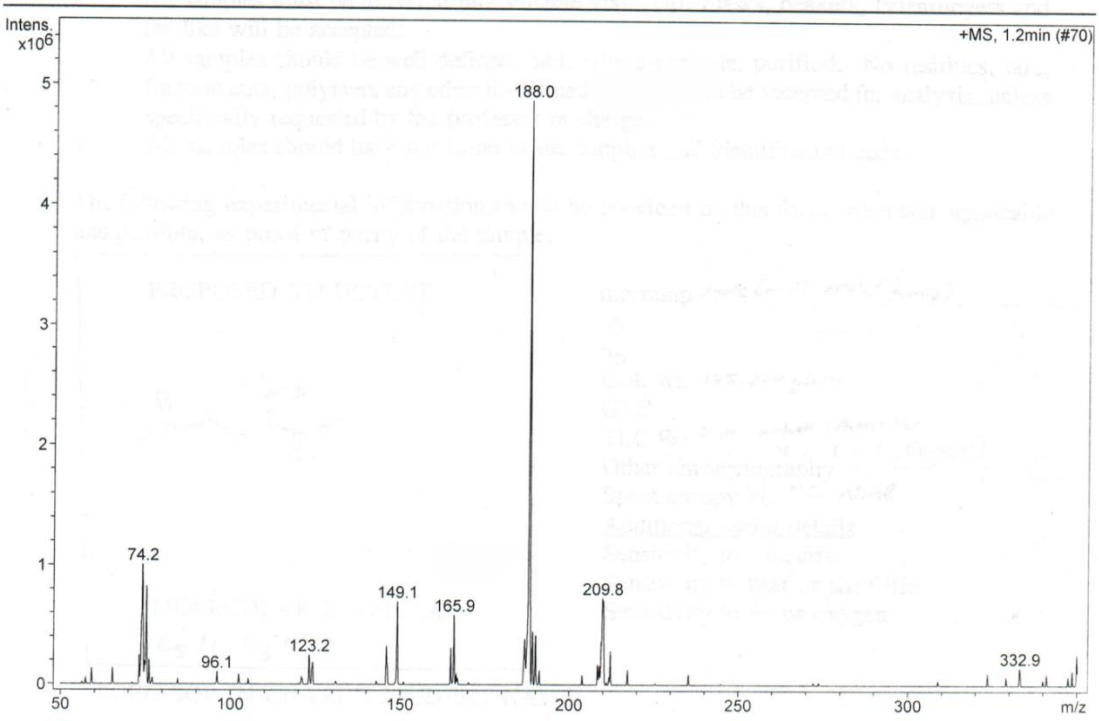
MS *L-Methionine sulfoxide* (**70**)

Display Report - All Windows Selected Analy

Analysis Name: 06141109.d
Method: Copy of Mark01.MS
Sample Na RWH-A-2
Analysis Inf Sample RWH-A-2 in Water, ESI positive mode

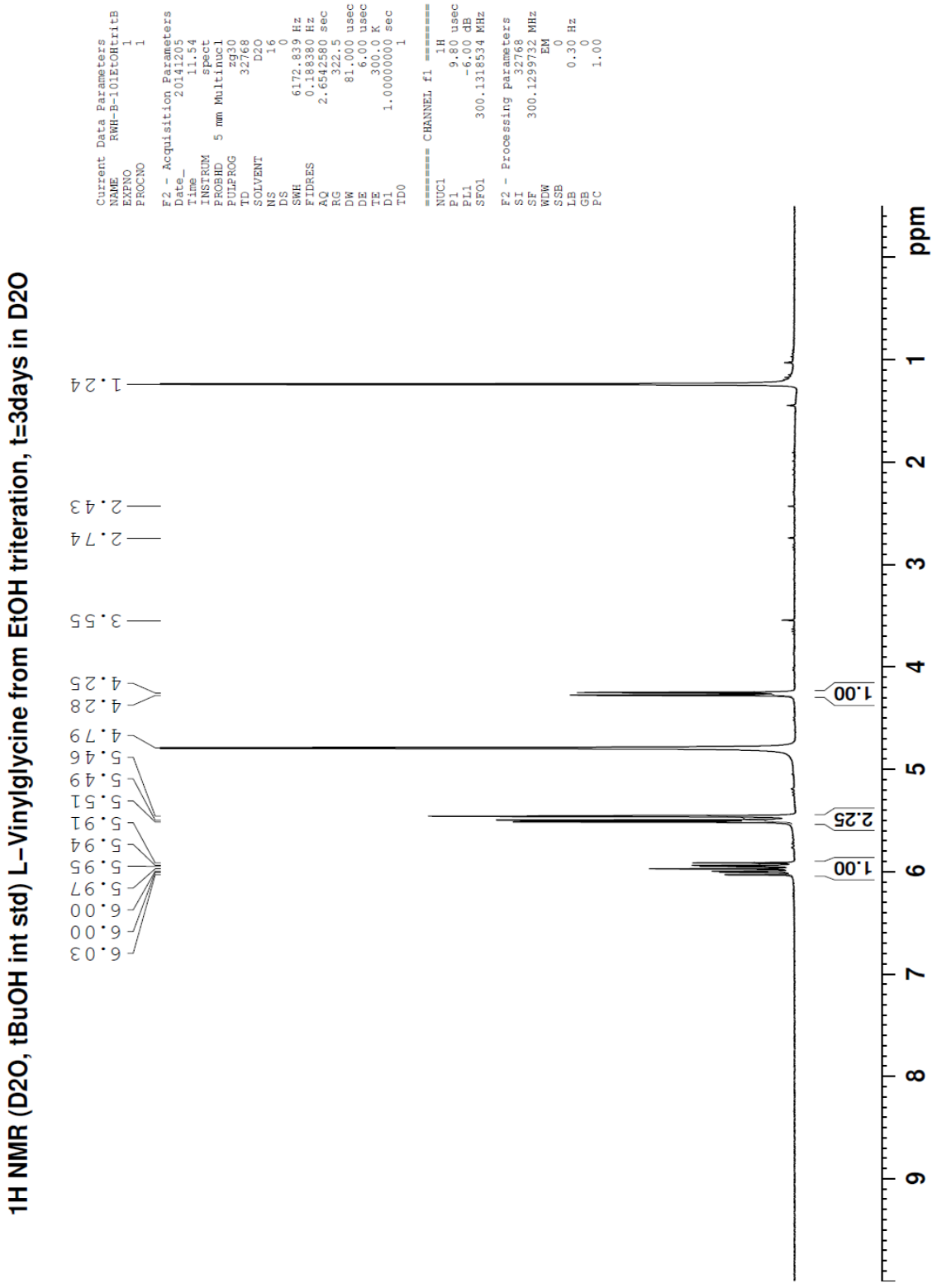
Instrume LC-MSD-Trap-SL
Operator: Mark Wang

Print Date: 06/14/11 12:06:12
Acq. Date 06/14/11 12:02:54

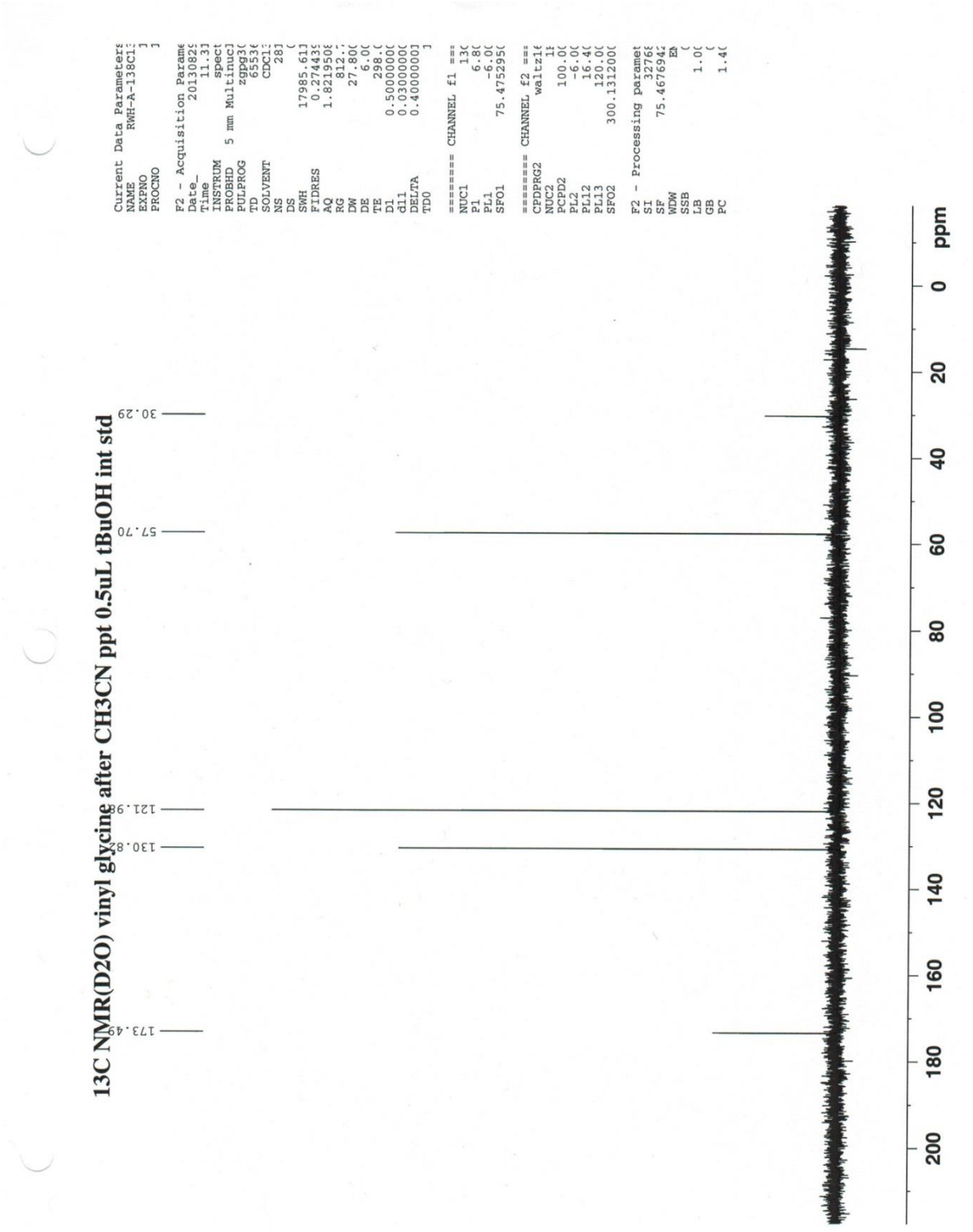


Agilent Technologies

^{1}H NMR *L-Vinylglycine* (**71**)



^{13}C NMR *L-Vinylglycine* (**71**)



ESI-MS *L-Vinylglycine* (**71**)

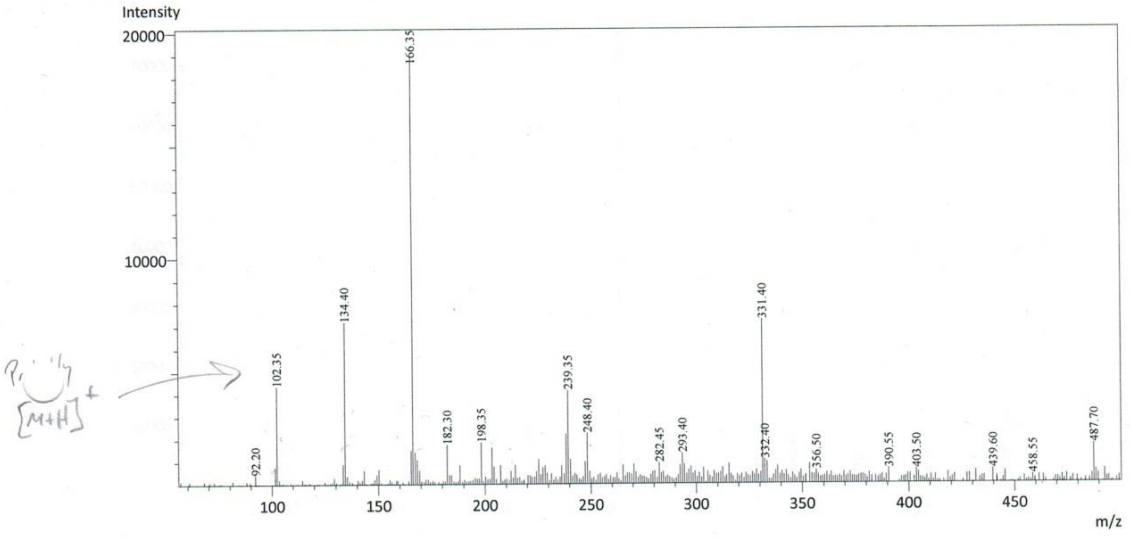
7/24/2014 4:35:22 PM Page 1 / 1

Shimadzu LCMS-2020 Data Report

Mass Spectrum for Sample
RWH-B-83A_03.lcd

Operator: Margaret Guthrie

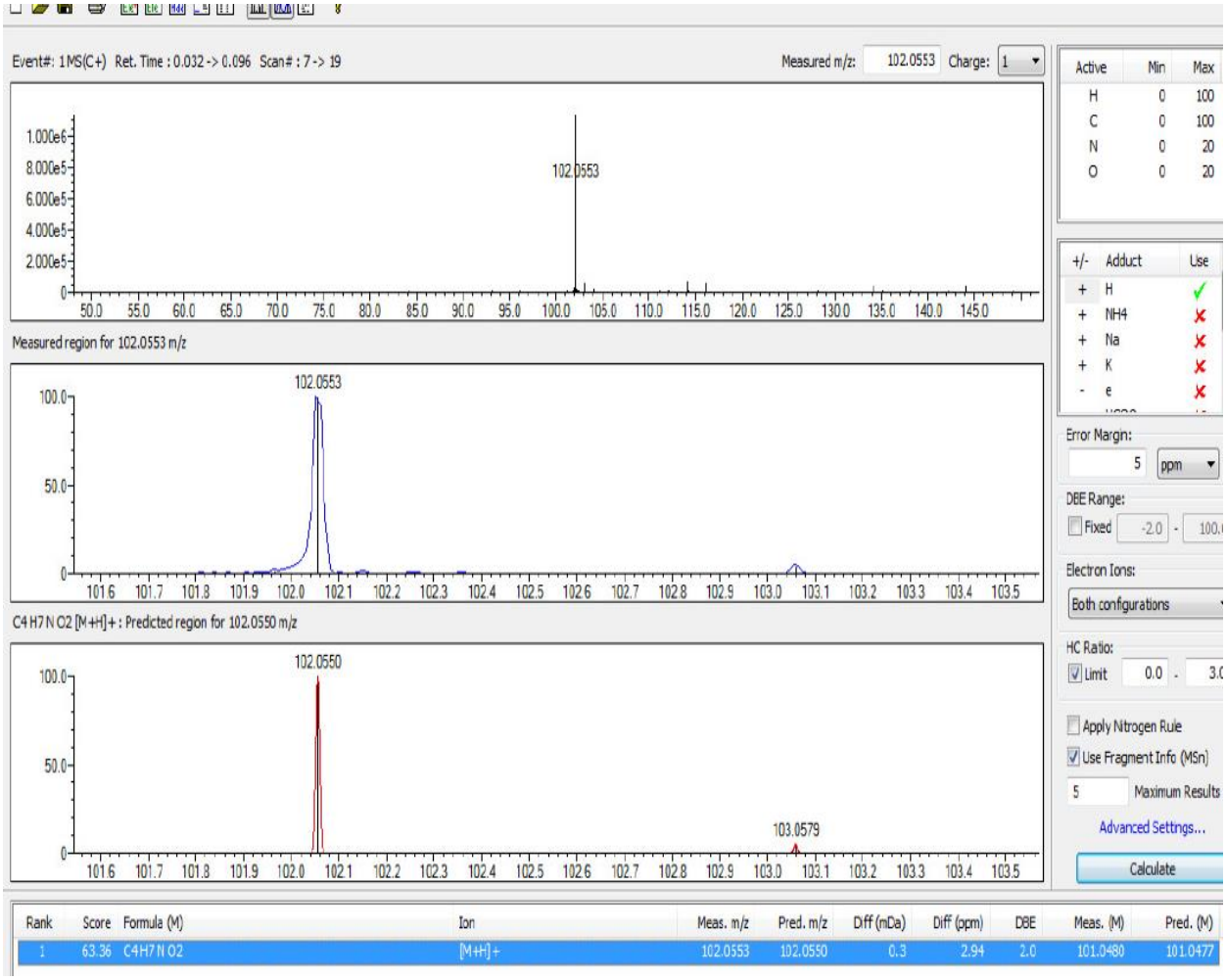
Data Filename: C:\LabSolutions\Data\Guthrie, Margaret\RWH-B-83A_03.lcd
Spetrum Mode: Averaged
Retention Time: ----
Interface Type (ESI, APCI, DUIS): DUIS
Aquisition Mode: (Scan, SIM, Profife): Scan
Polarity: +



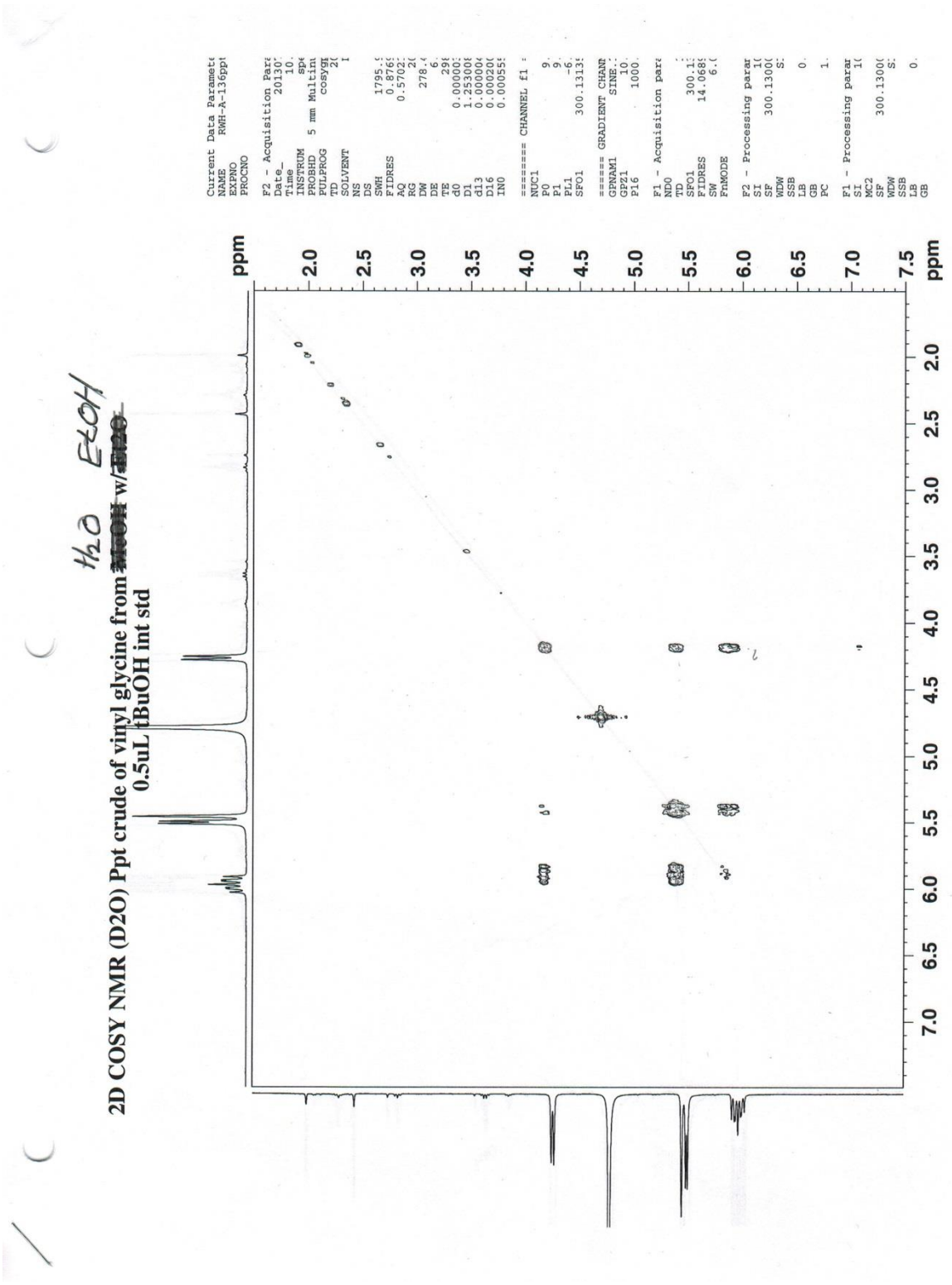
90% MeOH
10% H_2O

No modifiers

HRMS (IT-TOF) *L-Vinylglycine* (**71**)

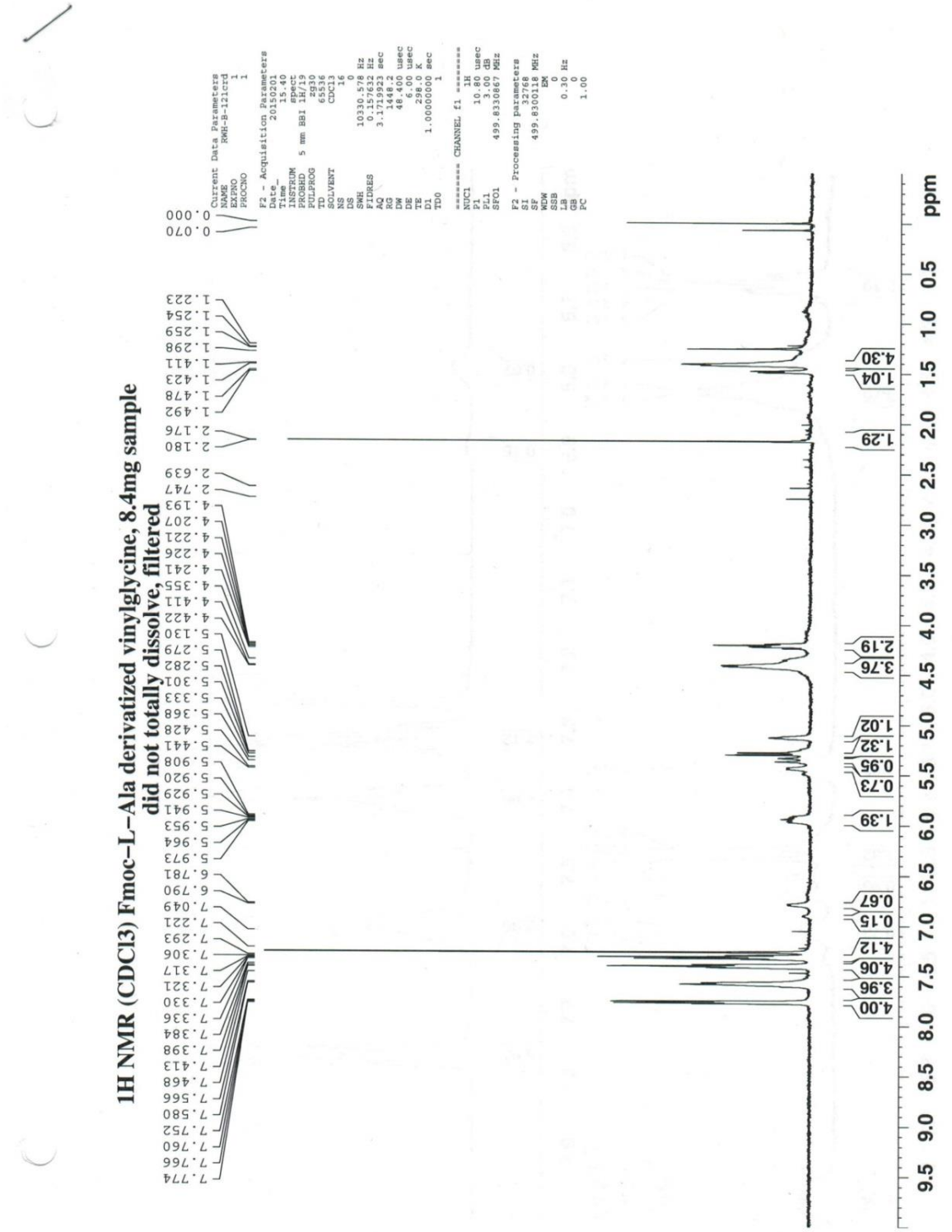


COSY *L-Vinylglycine* (**71**)



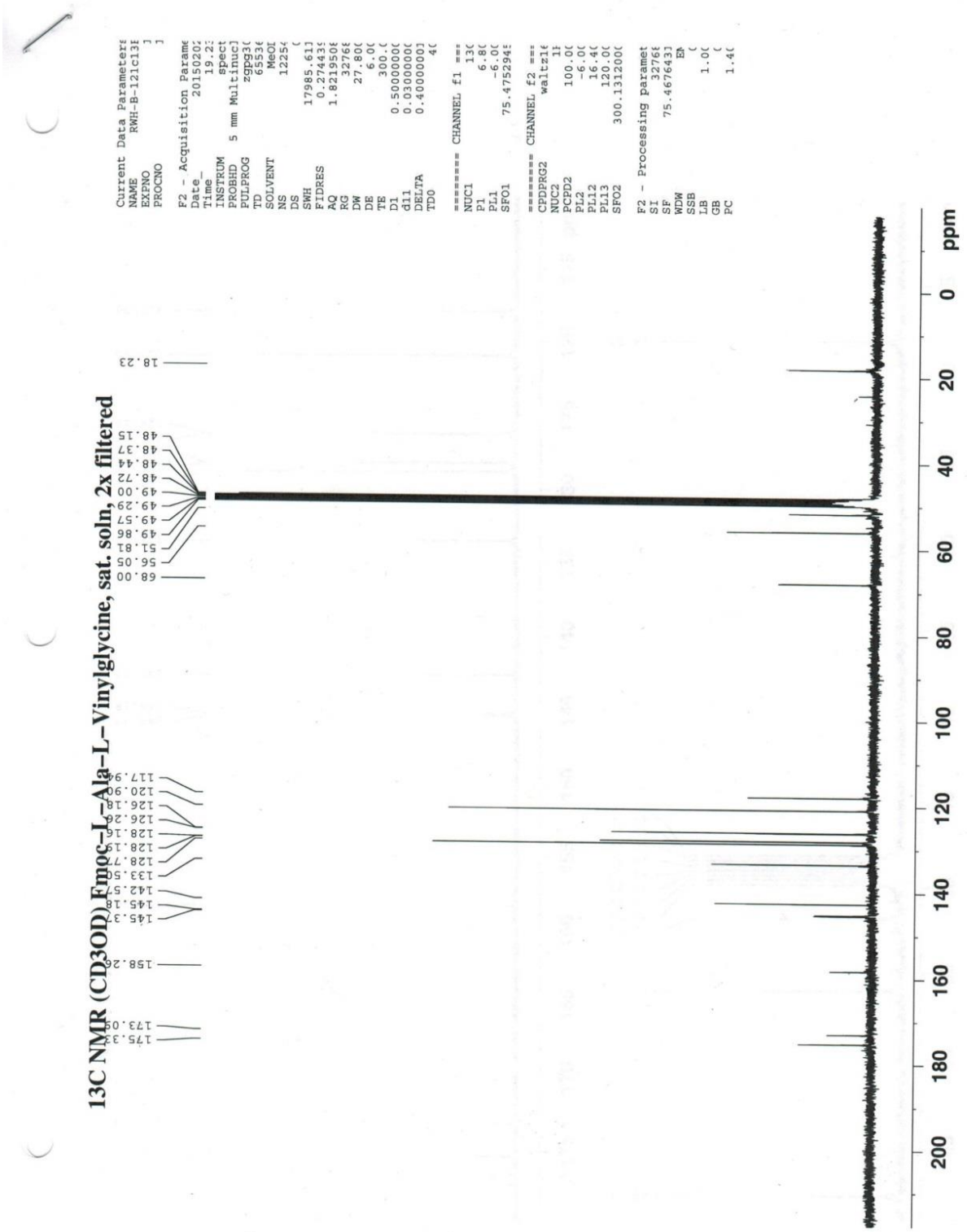
^{1}H NMR

(S)-2-((R)-2-((((9H-fluoren-9-yl)methoxy)carbonyl)amino)propanamido)but-3-enoic acid (**72**)



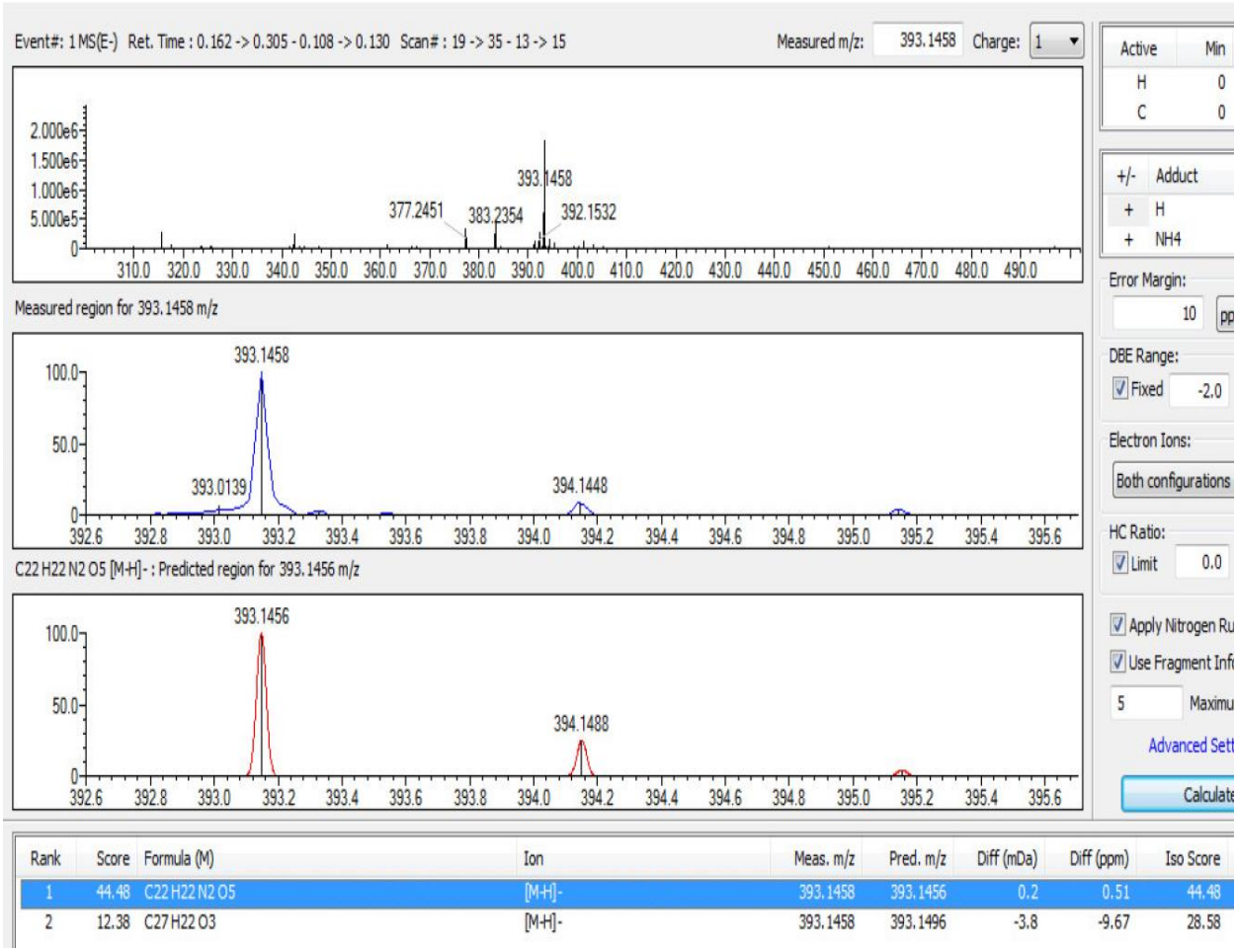
^{13}C NMR

(S)-2-((R)-2-((((9H-fluoren-9-yl)methoxy)carbonyl)amino)propanamido)but-3-enoic acid (**72**)

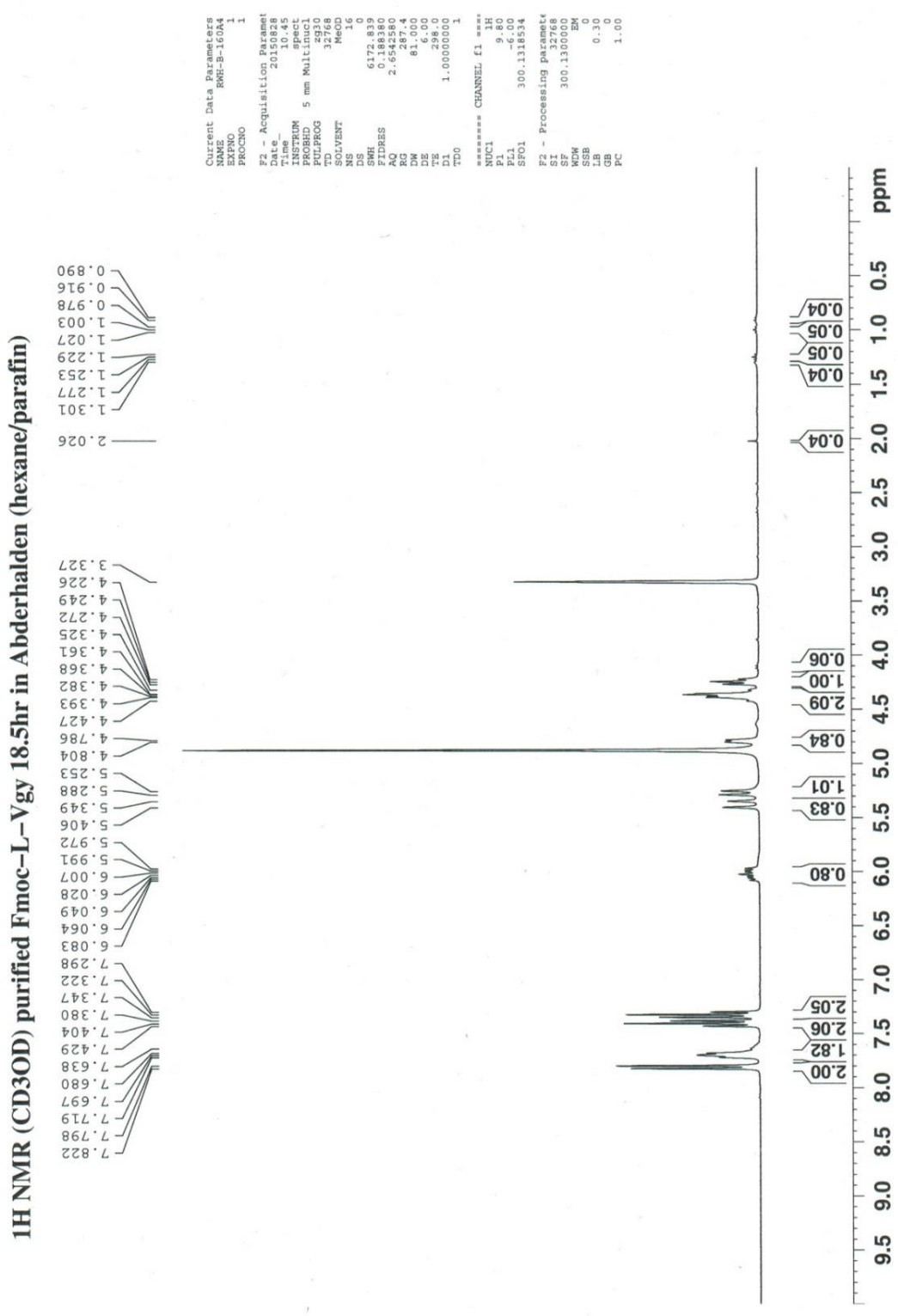


HRMS (IT-TOF)

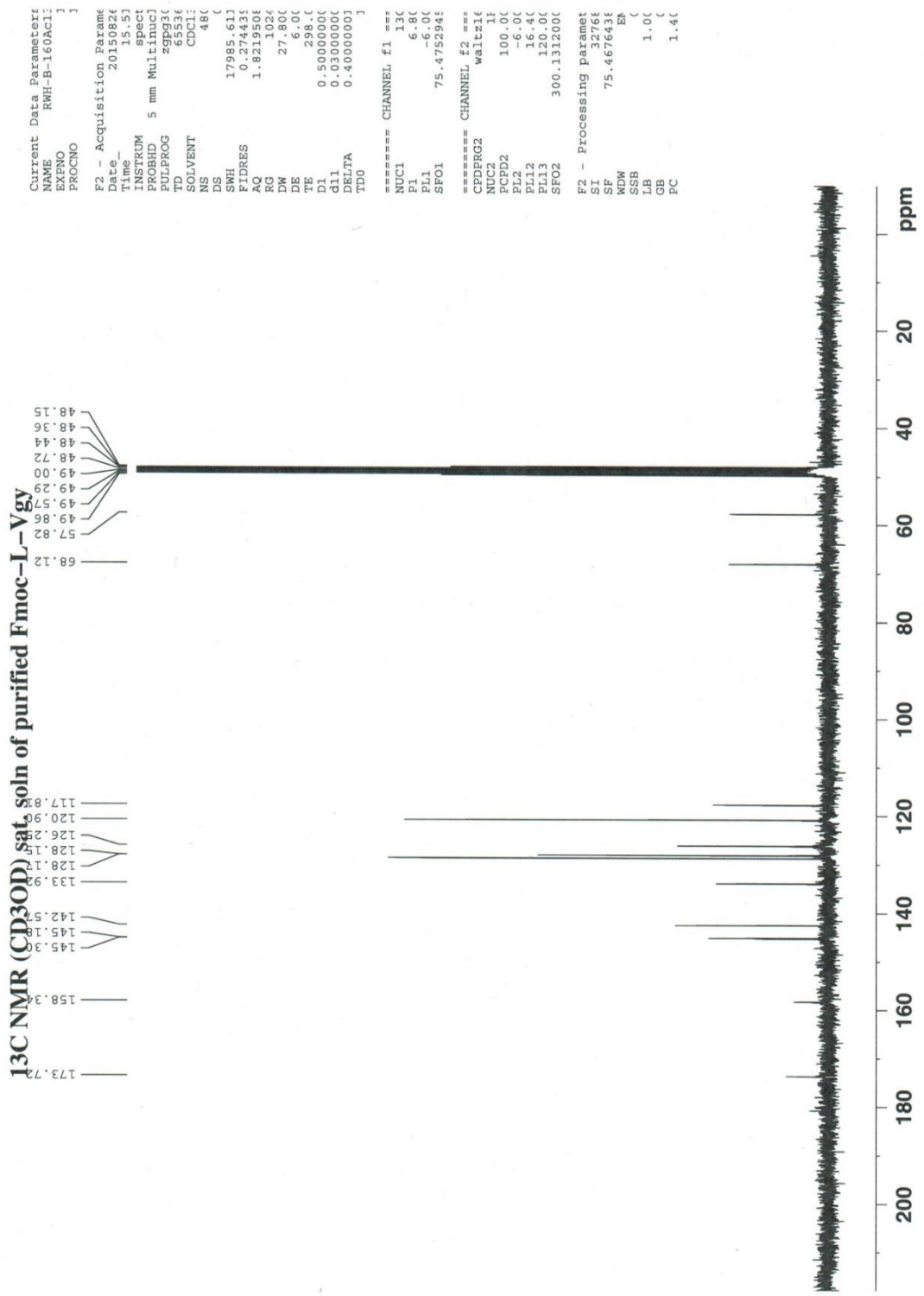
(S)-2-((R)-2-((((9H-fluoren-9-yl)methoxy)carbonyl)amino)propanamido)but-3-enoic acid (**72**)



^{1}H NMR *(S)-2-((((9H-fluoren-9-yl)methoxy)carbonyl)amino)but-3-enoic acid* (**73**)



^{13}C NMR *(S)-2-((((9H-fluoren-9-yl)methoxy)carbonyl)amino)but-3-enoic acid* (**73**)



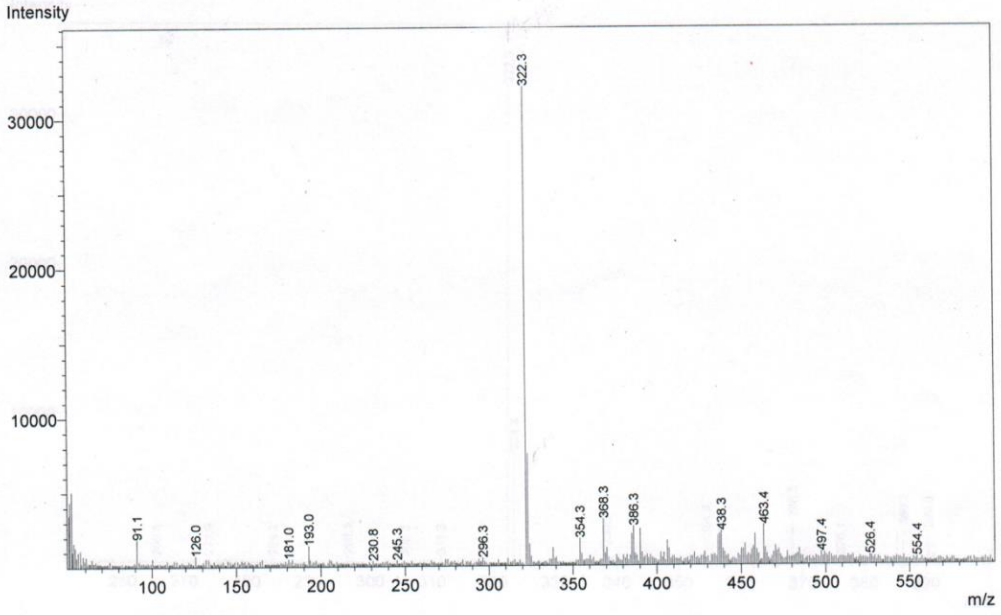
ESI-MS *(S)-2-((((9H-fluoren-9-yl)methoxy)carbonyl)amino)but-3-enoic acid* (**73**)

Shimadzu LCMS-2020 Data Report

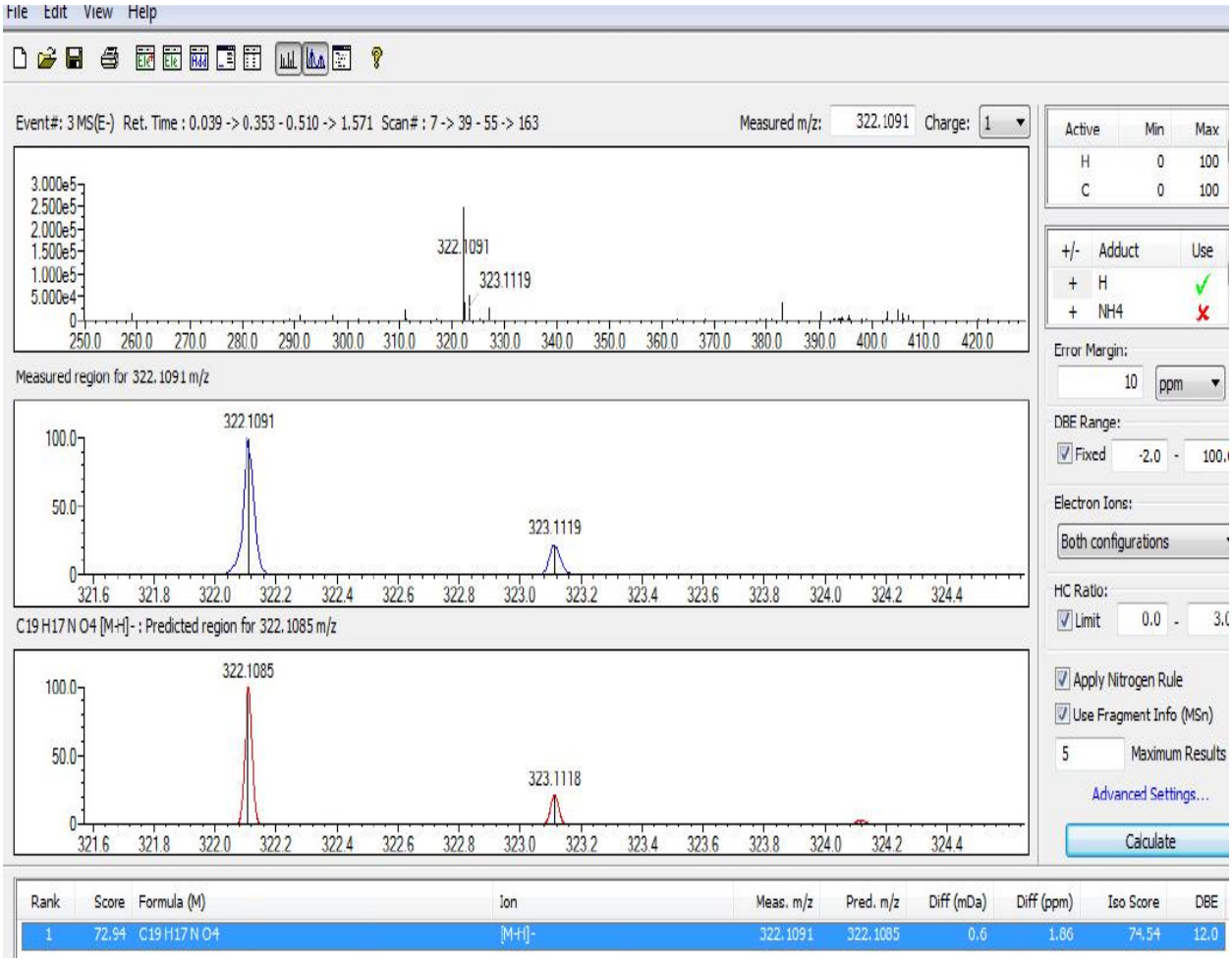
Mass Spectrum for Sample:
RWH-B-33

Operator: Mark Wang

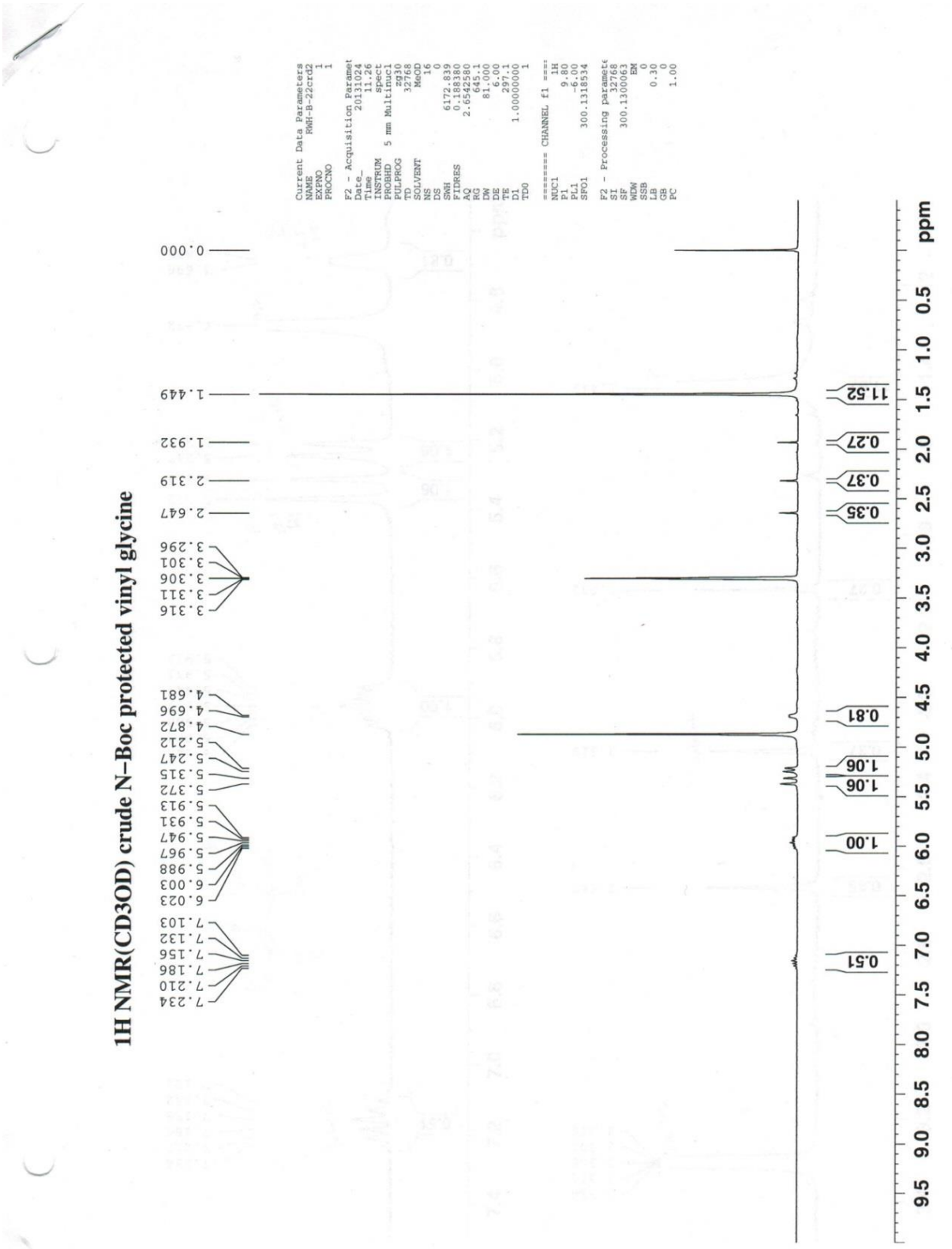
Data filename: C:\LabSolutions\Data\Schwabacher Alan\RWH-B-33.lcd
Spectrum Mode: Single
Retention Time: 0.150 min.
Interface Type (ESI, APCI, DUIS): DUIS
Aquisition Mode (Scan, SIM, Profile): Scan
Polarity (+,-): -



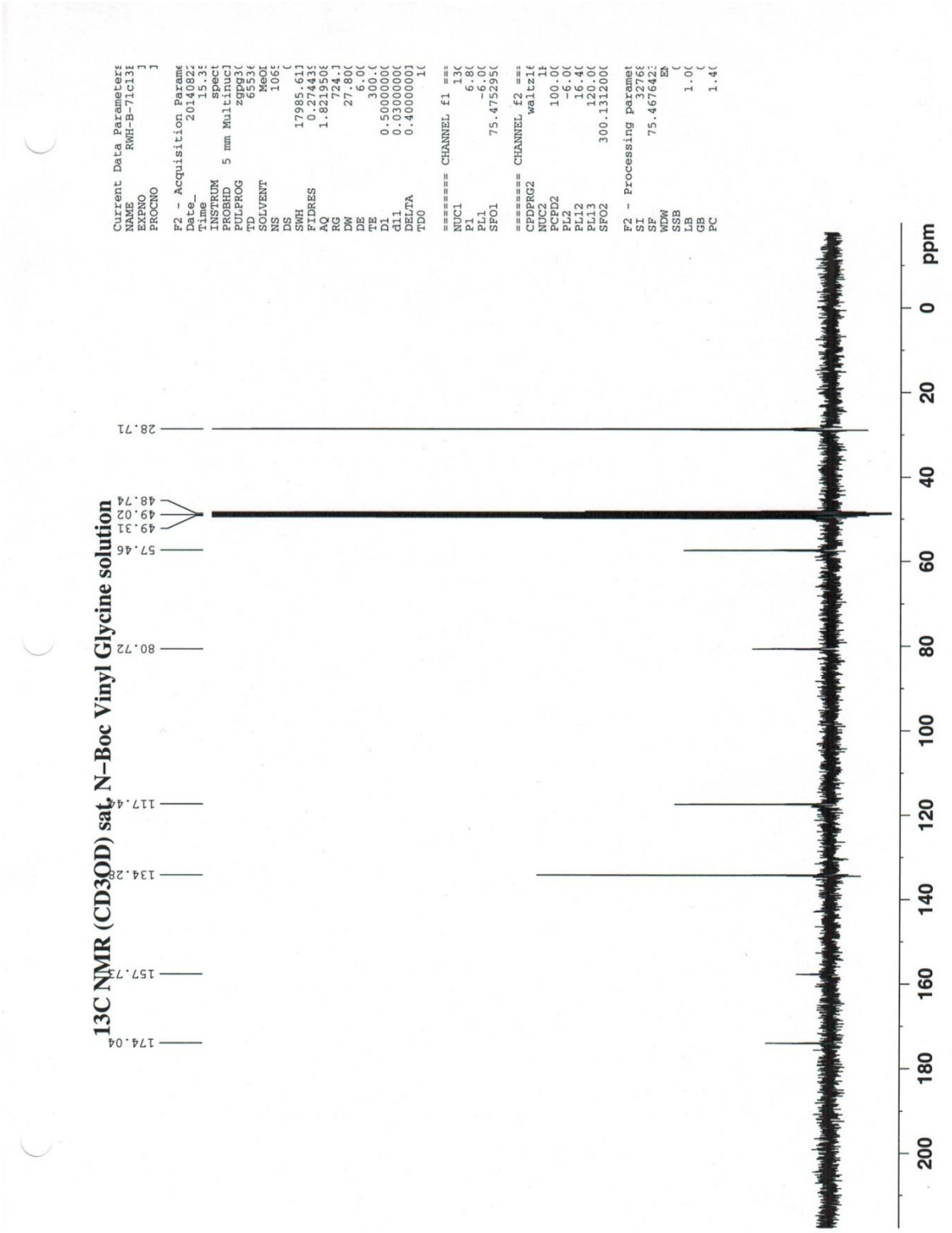
HRMS (IT-TOF) *(S)-2-((((9H-fluoren-9-yl)methoxy)carbonyl)amino)but-3-enoic acid* (**73**)



^{1}H NMR *(S)-2-((tert-butoxycarbonyl)amino)but-3-enoic acid* (**74**)



^{13}C NMR *(S)-2-((tert-butoxycarbonyl)amino)but-3-enoic acid* (**74**)



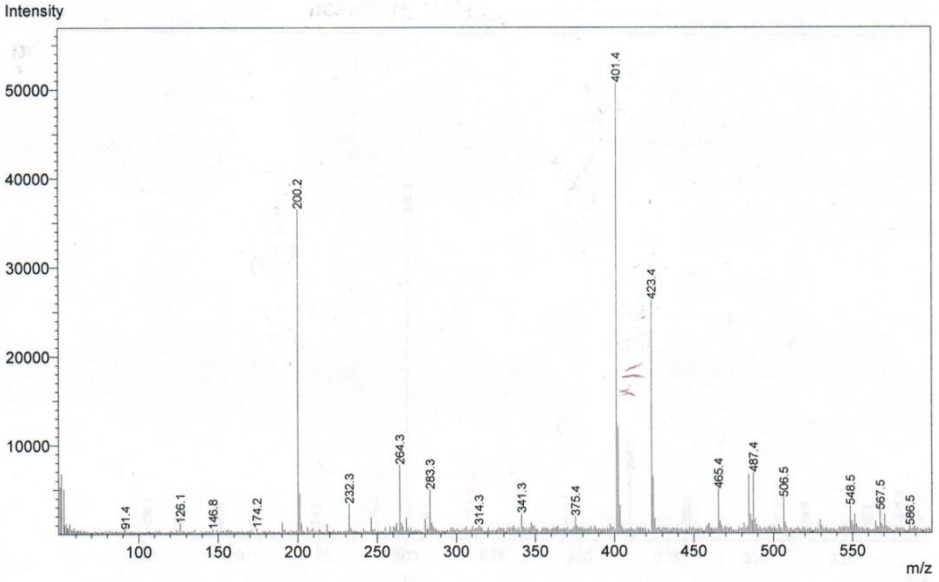
ESI-MS *(S)-2-((tert-butoxycarbonyl)amino)but-3-enoic acid* (**74**)

Shimadzu LCMS-2020 Data Report

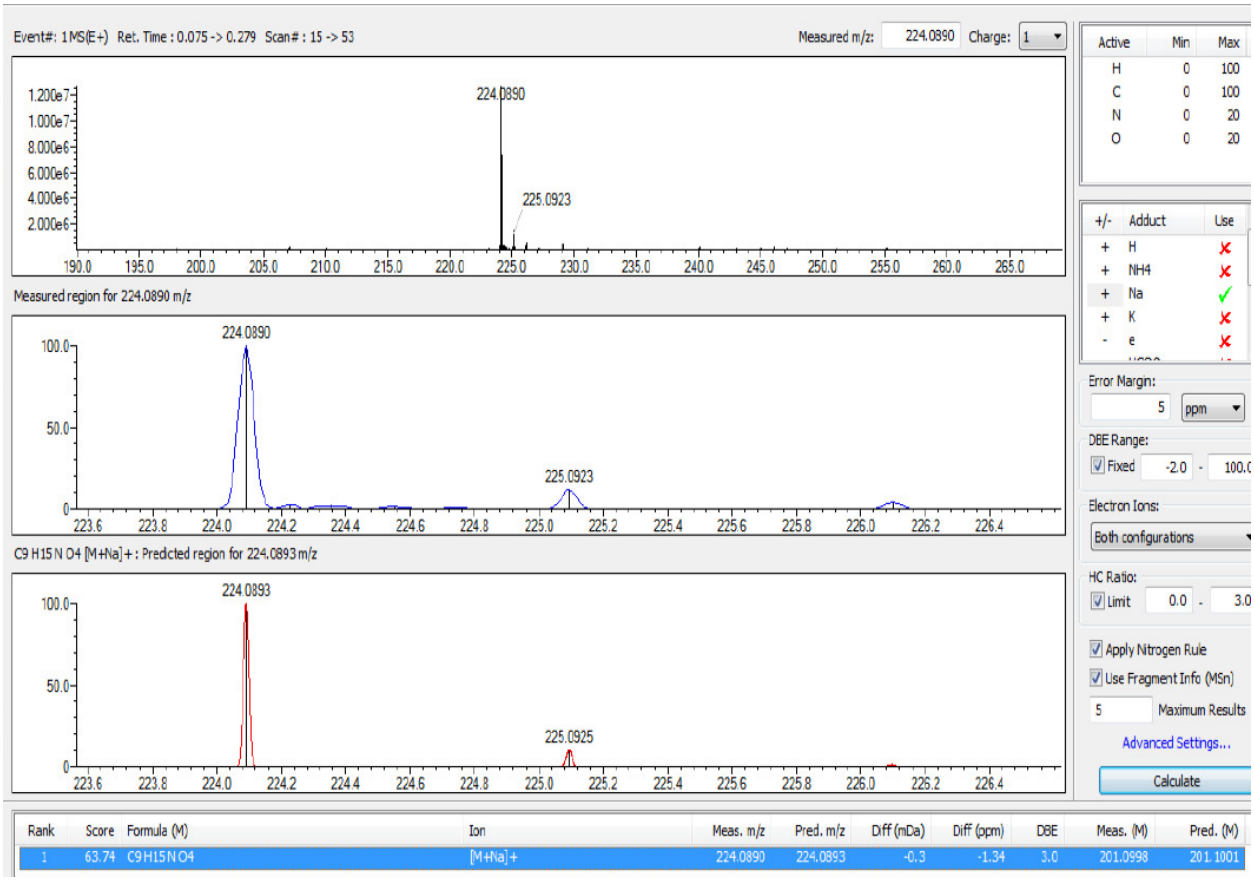
Mass Spectrum for Sample:
RWH-B-22

Operator: Mark Wang

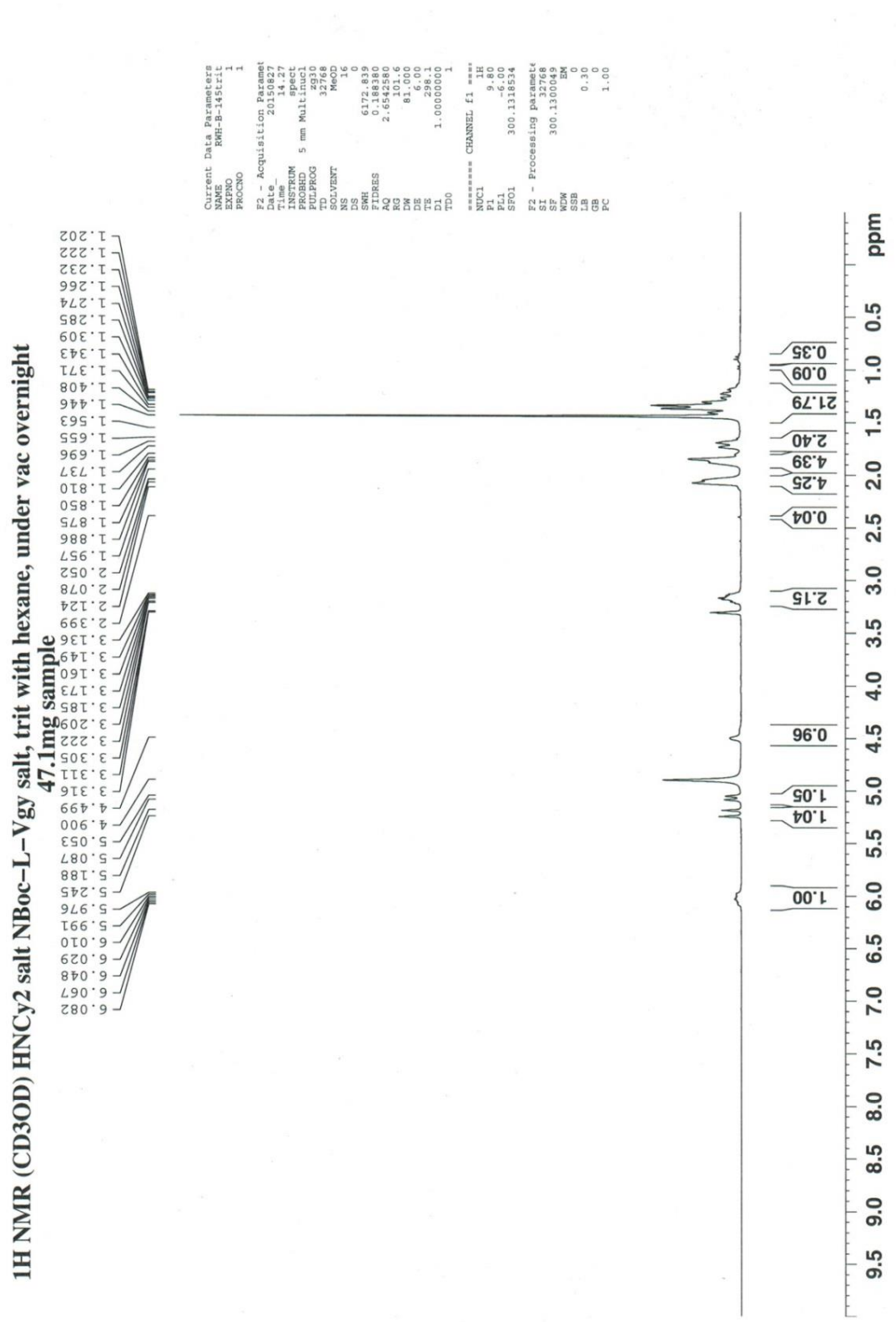
Data filename: C:\LabSolutions\Data\Schwabacher Alan\RWH-B-22.lcd
Spectrum Mode: Single
Retention Time: 0.150 min.
Interface Type (ESI, APCI, DUIS): DUIS
Aquisition Mode (Scan, SIM, Profile): Scan
Polarity (+,-): -



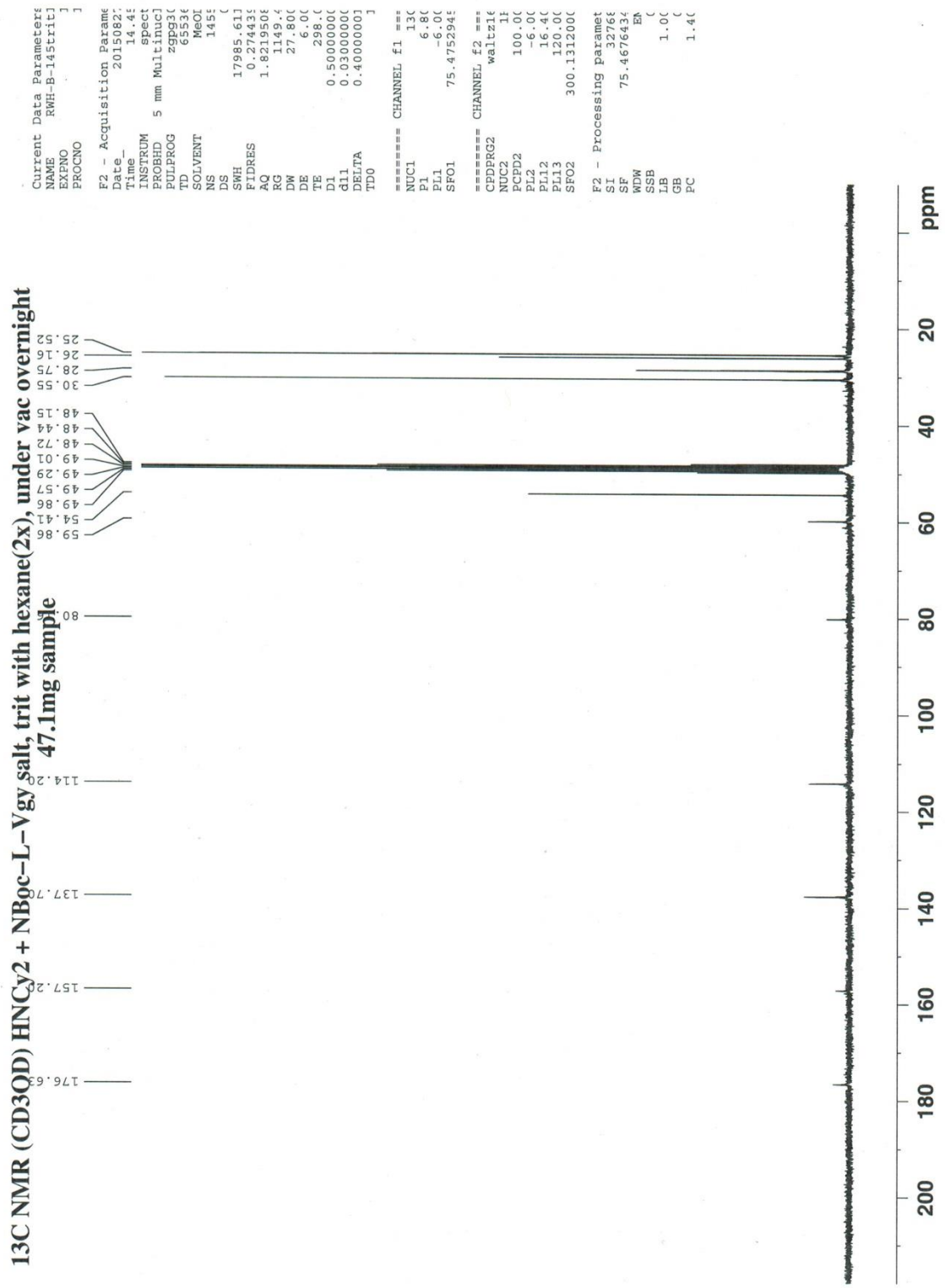
HRMS (IT-TOF) *(S)-2-((tert-butoxycarbonyl)amino)but-3-enoic acid* (**74**)



^{1}H NMR *Dicyclohexyl ammonium 2-((tert-butoxycarbonyl)amino)but-3-enoate* (**75**)



^{13}C NMR *Dicyclohexyl ammonium 2-((tert-butoxycarbonyl)amino)but-3-enoate* (**75**)



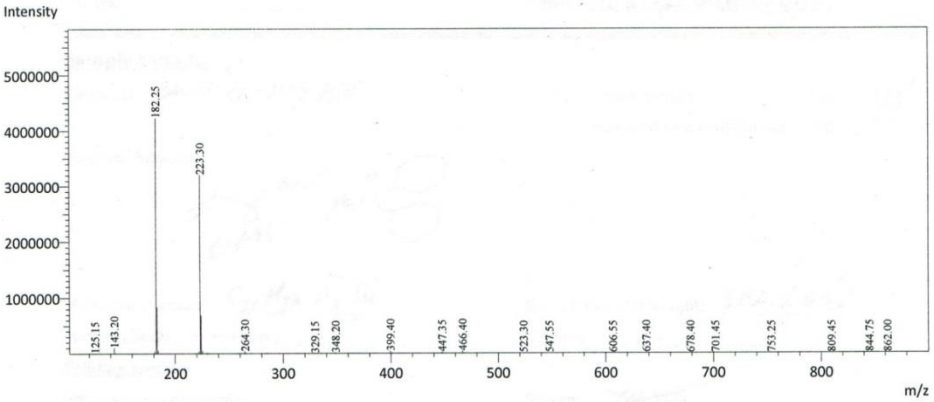
ESI-MS *Dicyclohexyl ammonium 2-((tert-butoxycarbonyl)amino)but-3-enoate* (**75**)

Shimadzu LCMS-2020 Data Report

Mass Spectrum for Sample
RWH-B-145(repeat).lcd

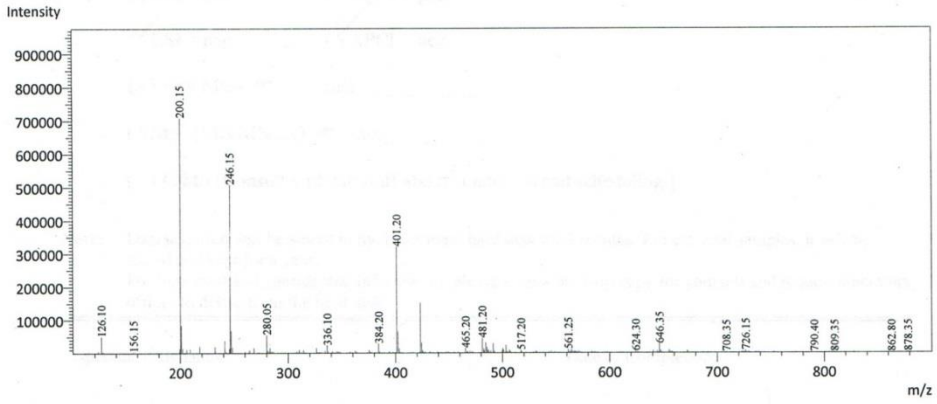
Operator:Tyler Fenske

Data Filename: C:\LabSolutions\Data\Schwabacher Alan\RWH-B-145(repeat).lcd
Spetrum Mode: Averaged
Retention Time: ----
Interface Type (ESI, APCI, DUIS): DUIS
Aquisition Mode: (Scan, SIM, Profife): Scan
Polarity: +
H2O/0.1% HCOOH, CH3CN/0.1% HCOOH

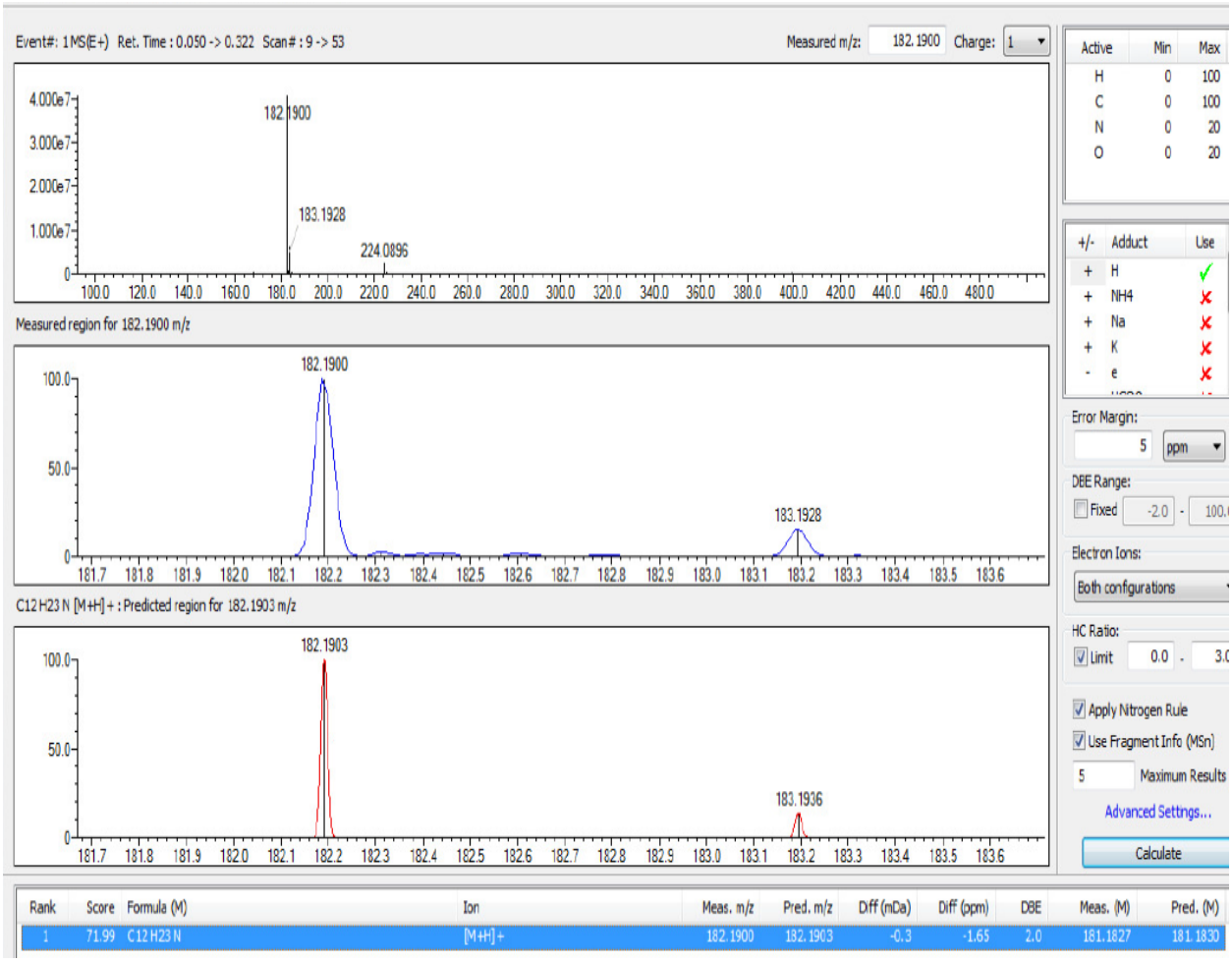


Operator:Tyler Fenske

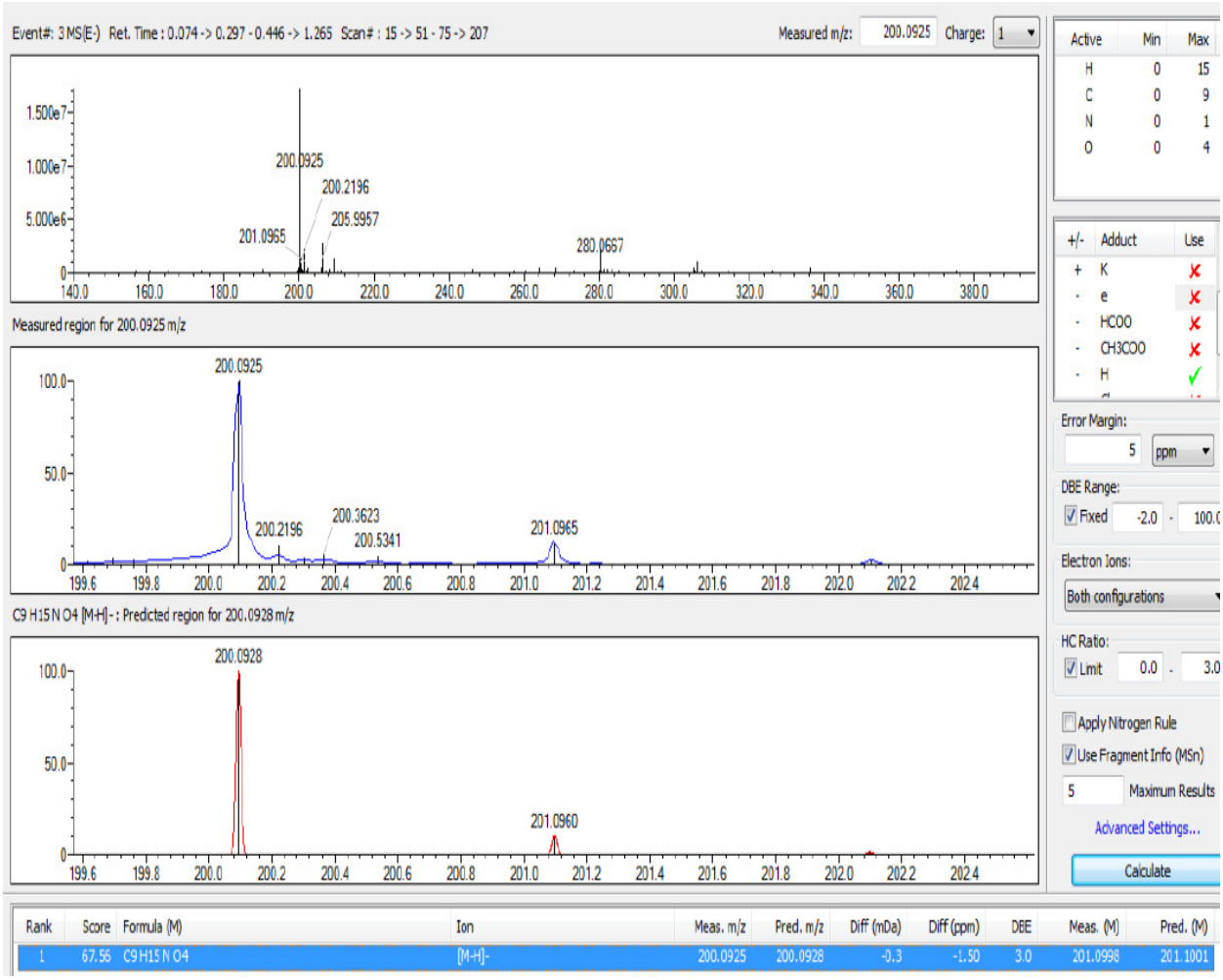
Data Filename: C:\LabSolutions\Data\Schwabacher Alan\RWH-B-145(repeat).lcd
Spetrum Mode: Averaged
Retention Time: ----
Interface Type (ESI, APCI, DUIS): DUIS
Aquisition Mode: (Scan, SIM, Profife): Scan
Polarity: -
H2O/0.1% HCOOH, CH3CN/0.1% HCOOH



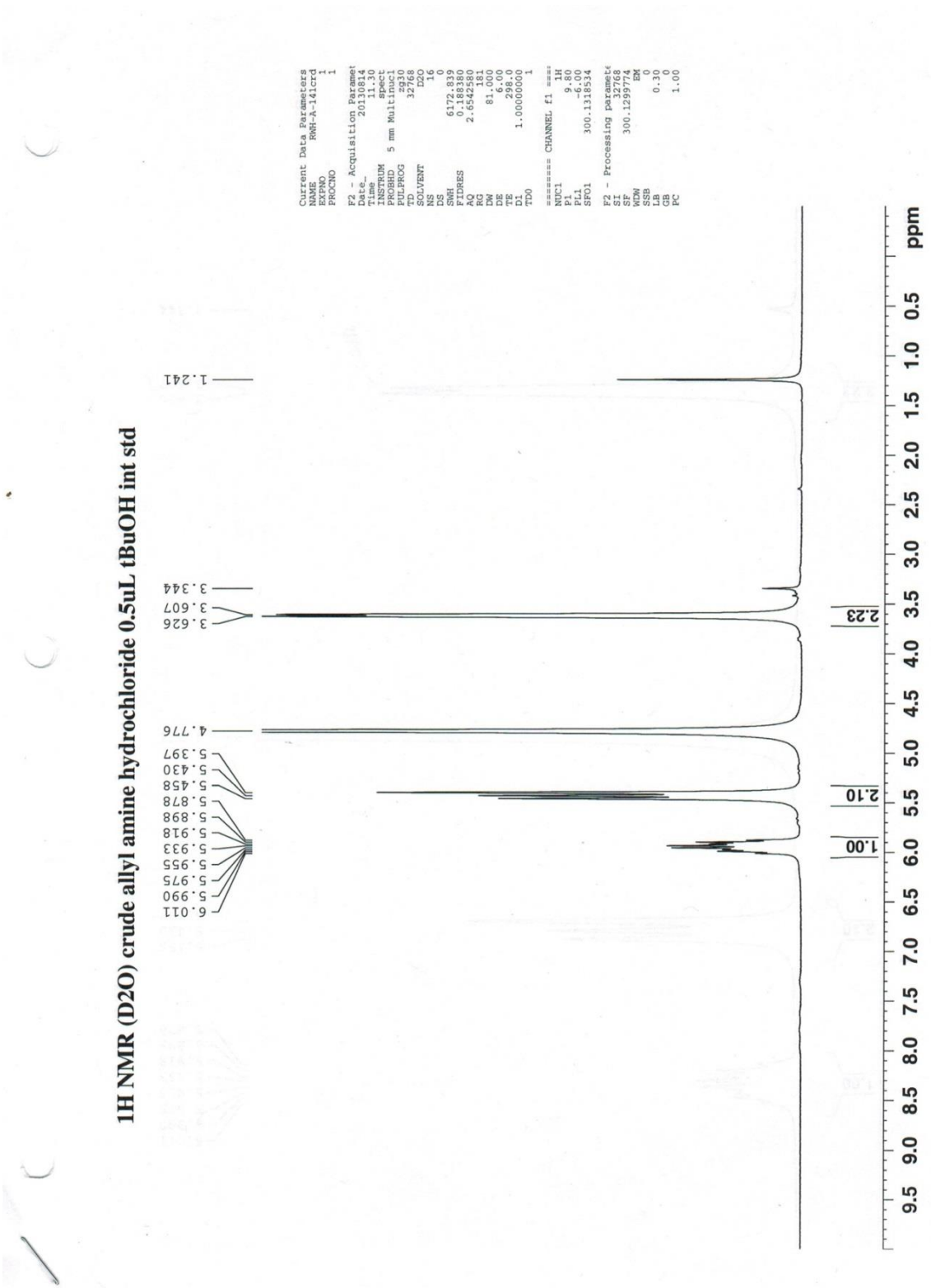
HRMS (IT-TOF, + ion) *Dicyclohexyl ammonium 2-((tert-butoxycarbonyl)amino)but-3-enoate* (**75**)



HRMS (IT-TOF, -ion) *Dicyclohexyl ammonium 2-((tert-butoxycarbonyl)amino)but-3-enoate* (**75**)



^{1}H NMR *Allylammonium chloride* (**76**)



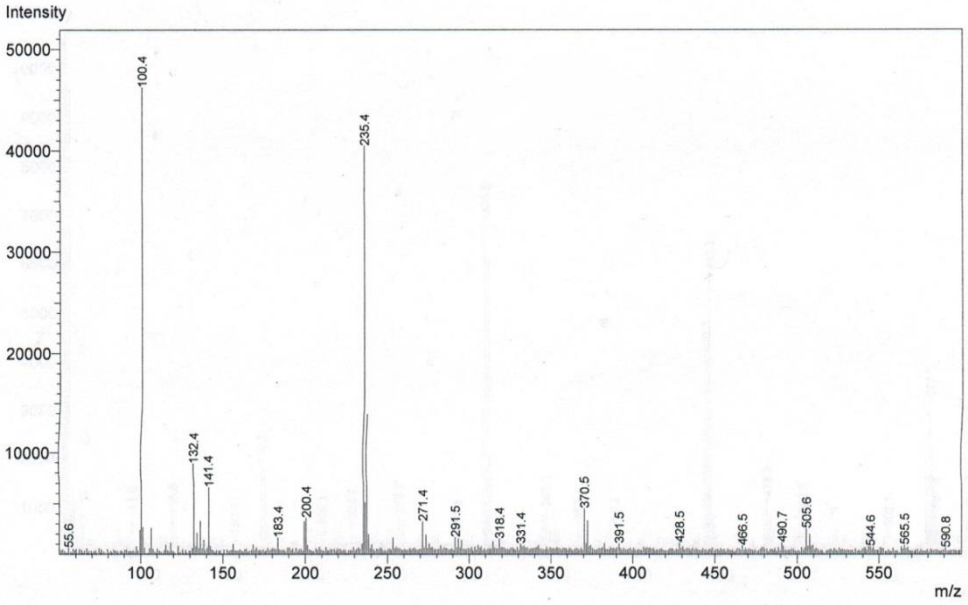
ESI-MS *Allylammonium chloride* (**76**)

Shimadzu LCMS-2020 Data Report

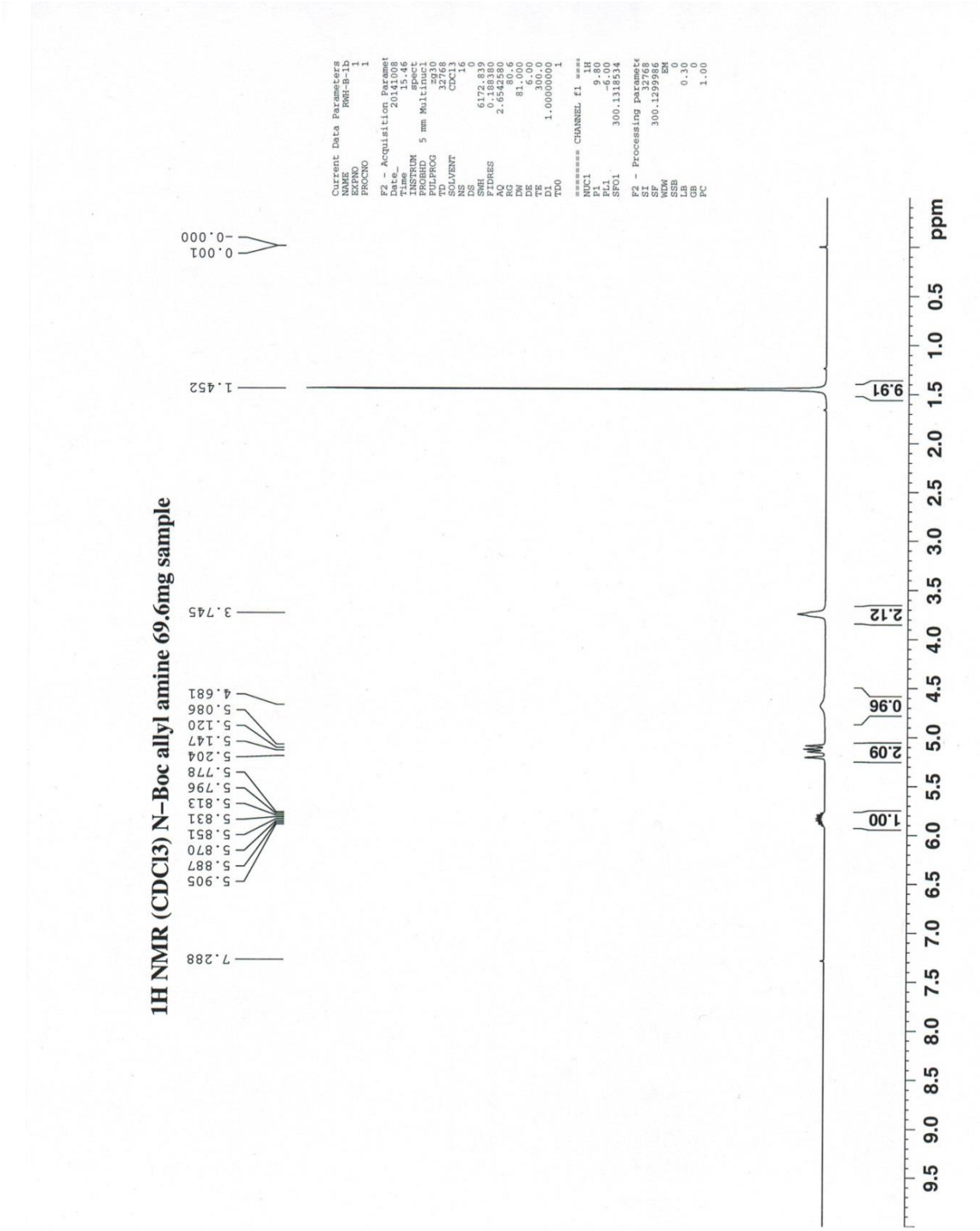
Mass Spectrum for Sample:
RWH-B-2B

Operator: Mark Wang

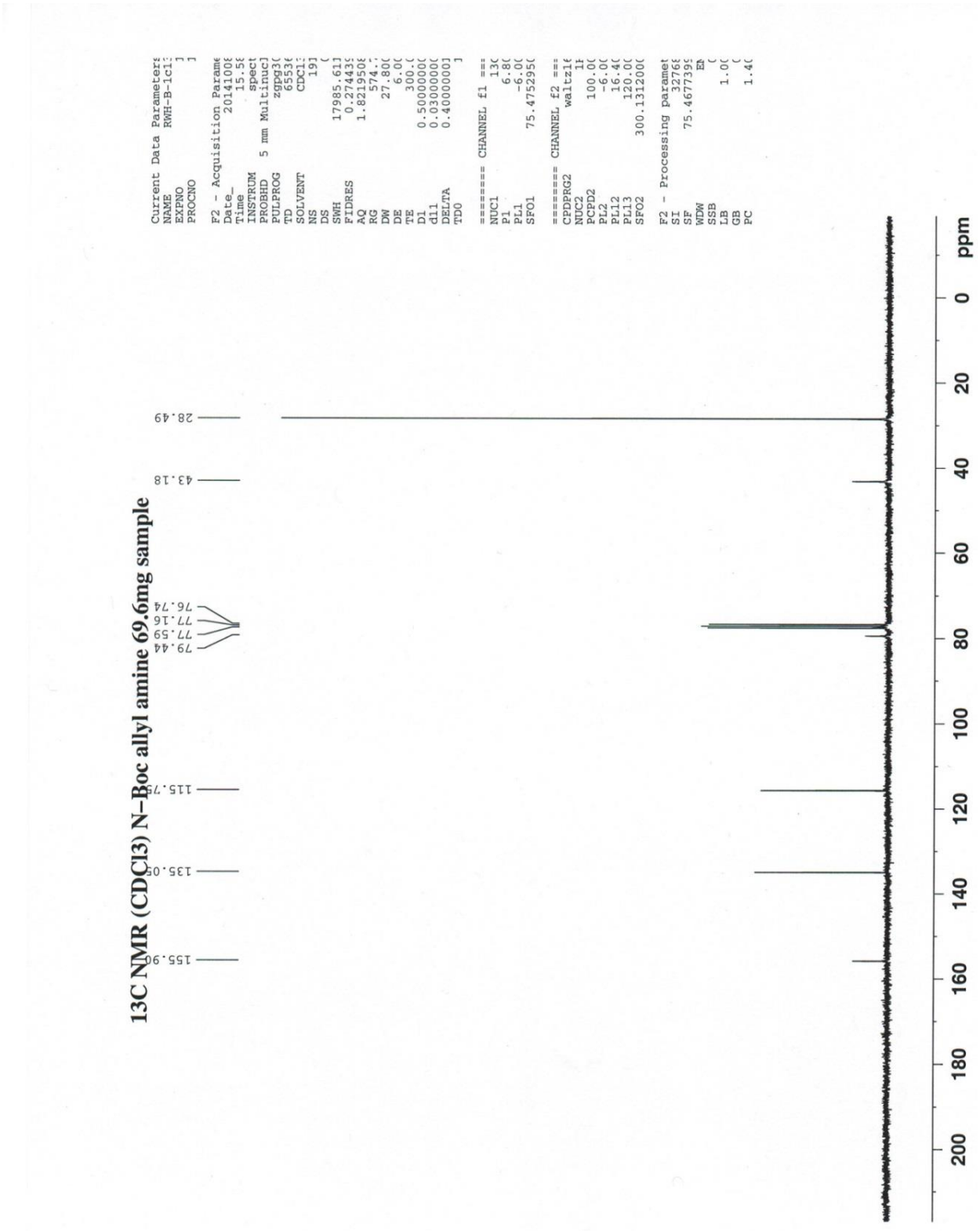
Data filename: C:\LabSolutions\Data\Schwabacher Alan\RWH-B-2B.lcd
Spectrum Mode: Single
Retention Time: 0.133 min.
Interface Type (ESI, APCI, DUIS): DUIS
Aquisition Mode (Scan, SIM, Profile): Scan
Polarity (+,-): +



^{1}H NMR *tert-butyl allylcarbamate* (**78**)



^{13}C NMR *tert-butyl allylcarbamate* (**78**)



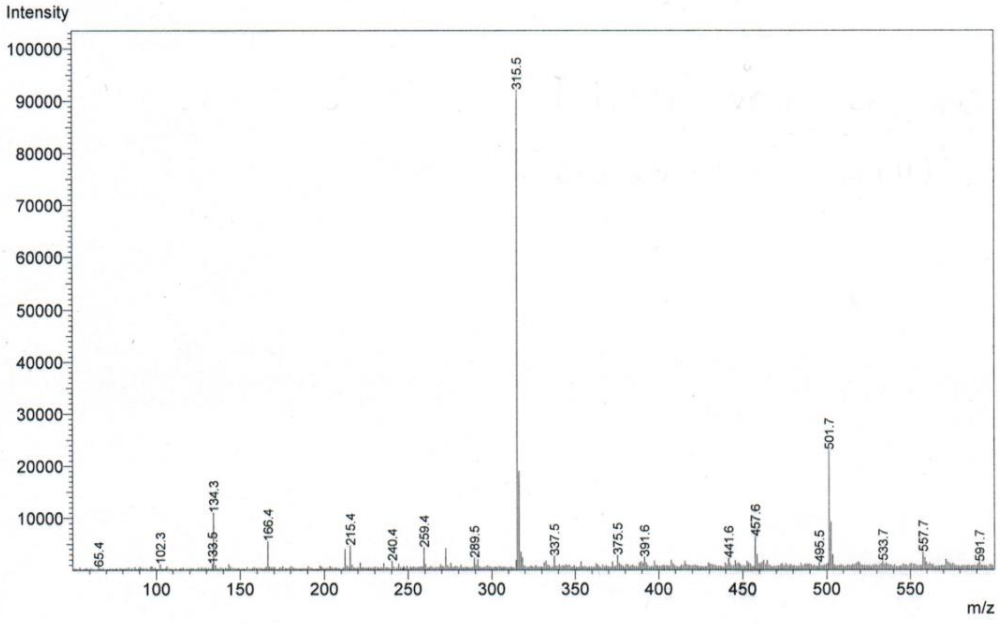
ESI-MS *tert-butyl allylcarbamate* (**78**)

Shimadzu LCMS-2020 Data Report

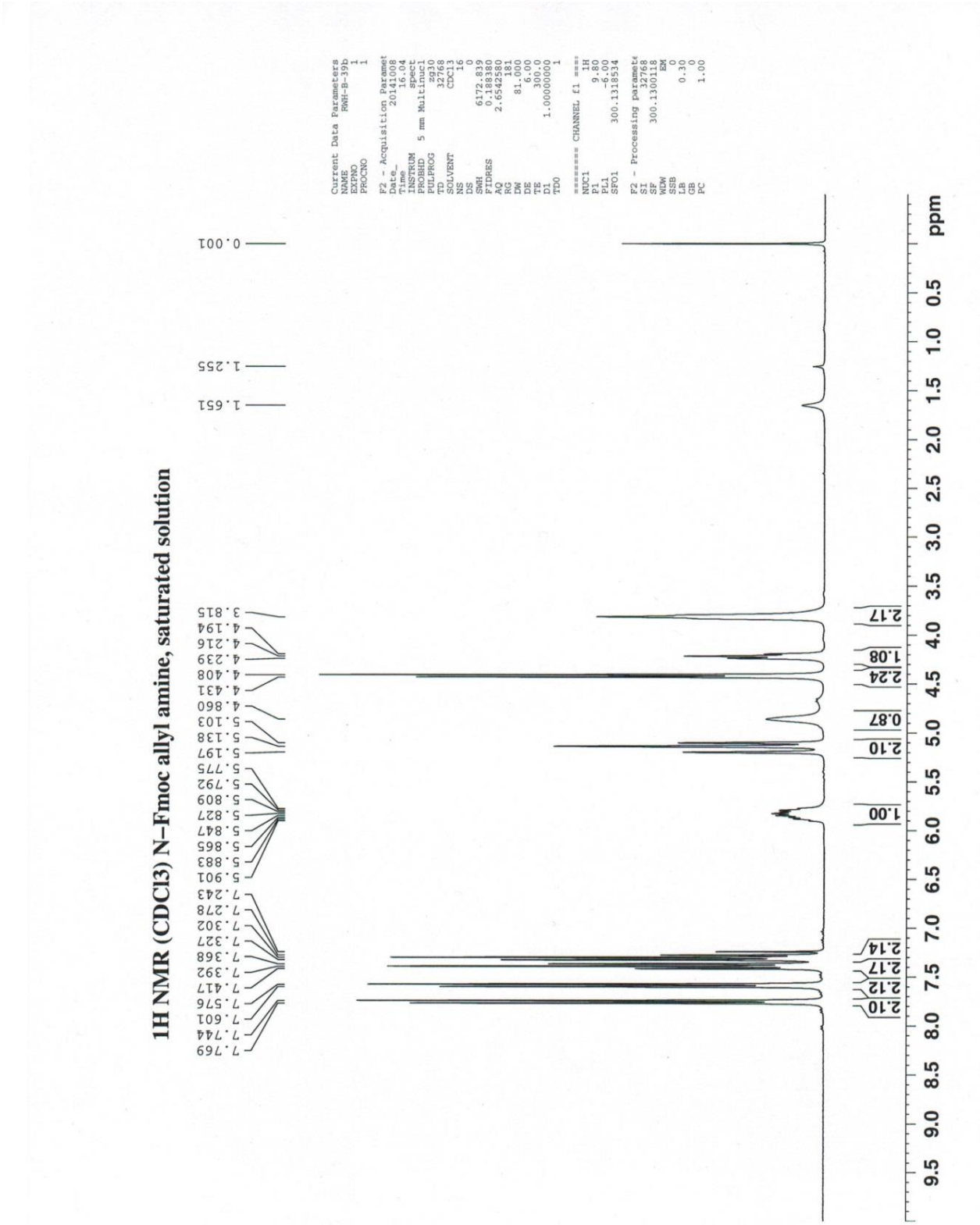
Mass Spectrum for Sample:
RWH-B-1

Operator: Mark Wang

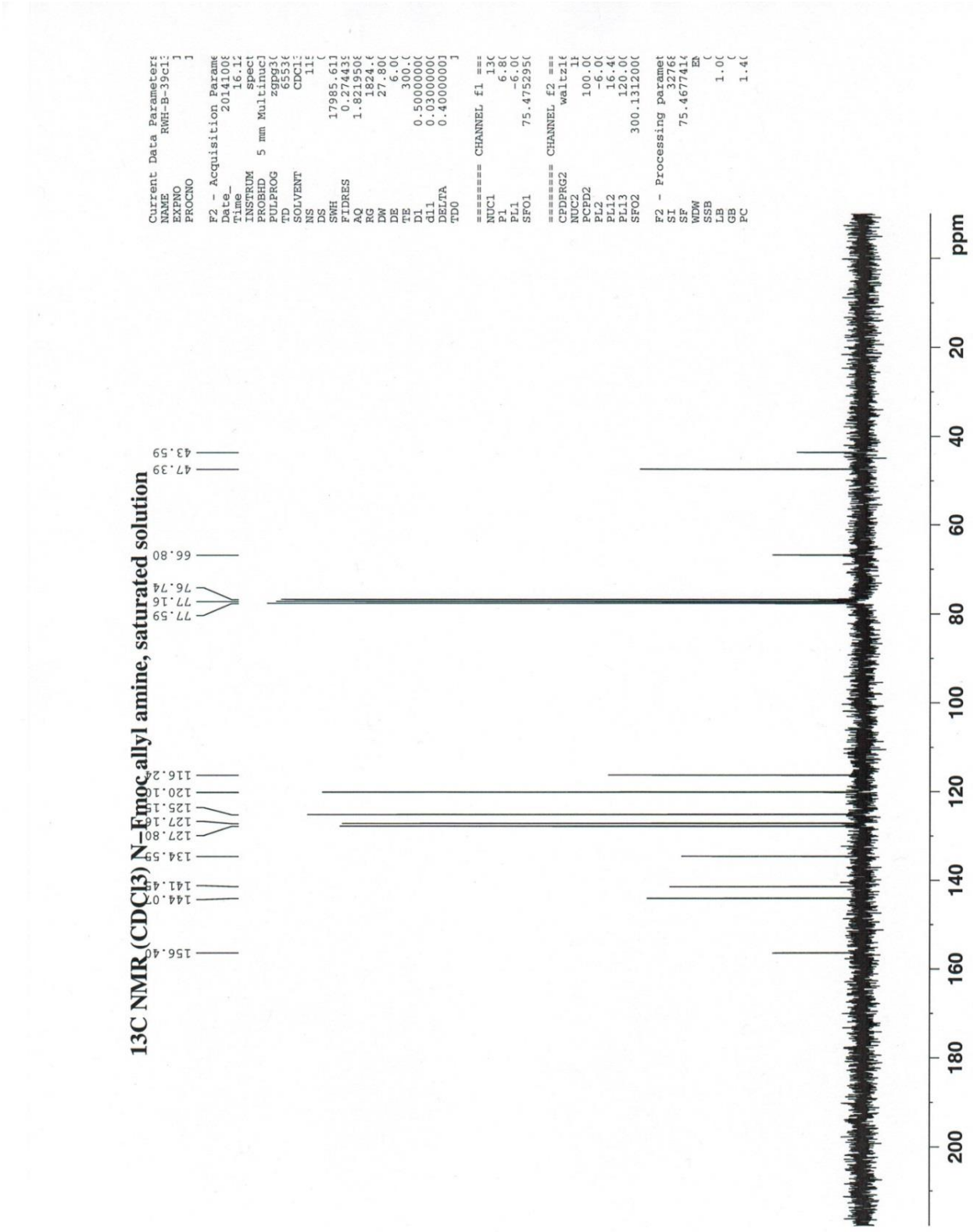
Data filename: C:\LabSolutions\Data\Schwabacher Alan\RWH-B-1.lcd
Spectrum Mode: Single
Retention Time: 0.133 min.
Interface Type (ESI, APCI, DUIS): DUIS
Aquisition Mode (Scan, SIM, Profile): Scan
Polarity (+,-): +



^{1}H NMR *(9H-fluoren-9-yl)methyl allylcarbamate* (**79**)



^{13}C NMR *(9H-fluoren-9-yl)methyl allylcarbamate* (**79**)



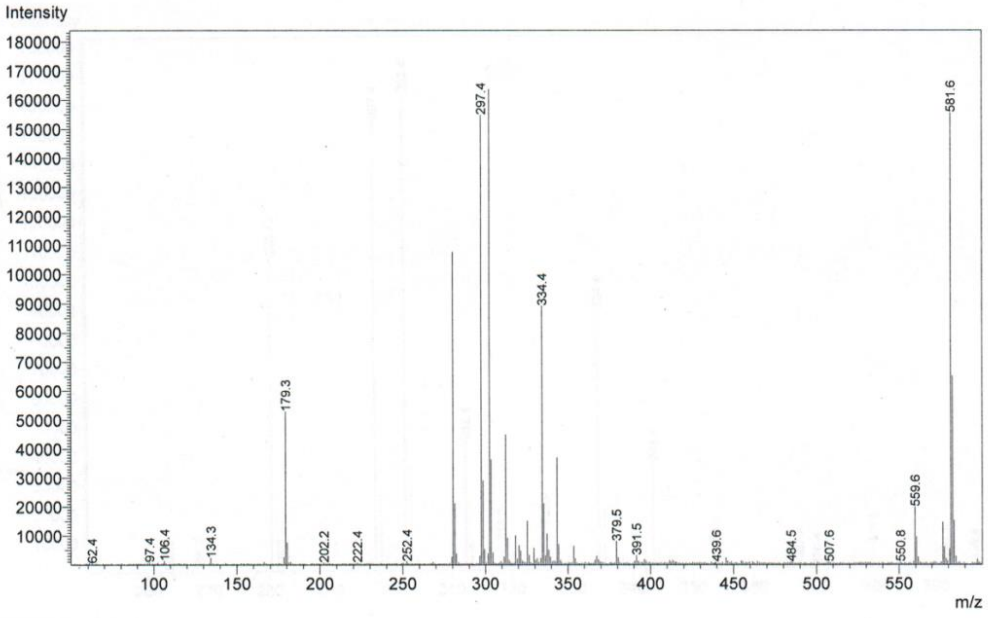
ESI-MS *(9H-fluoren-9-yl)methyl allylcarbamate* (**79**)

Shimadzu LCMS-2020 Data Report

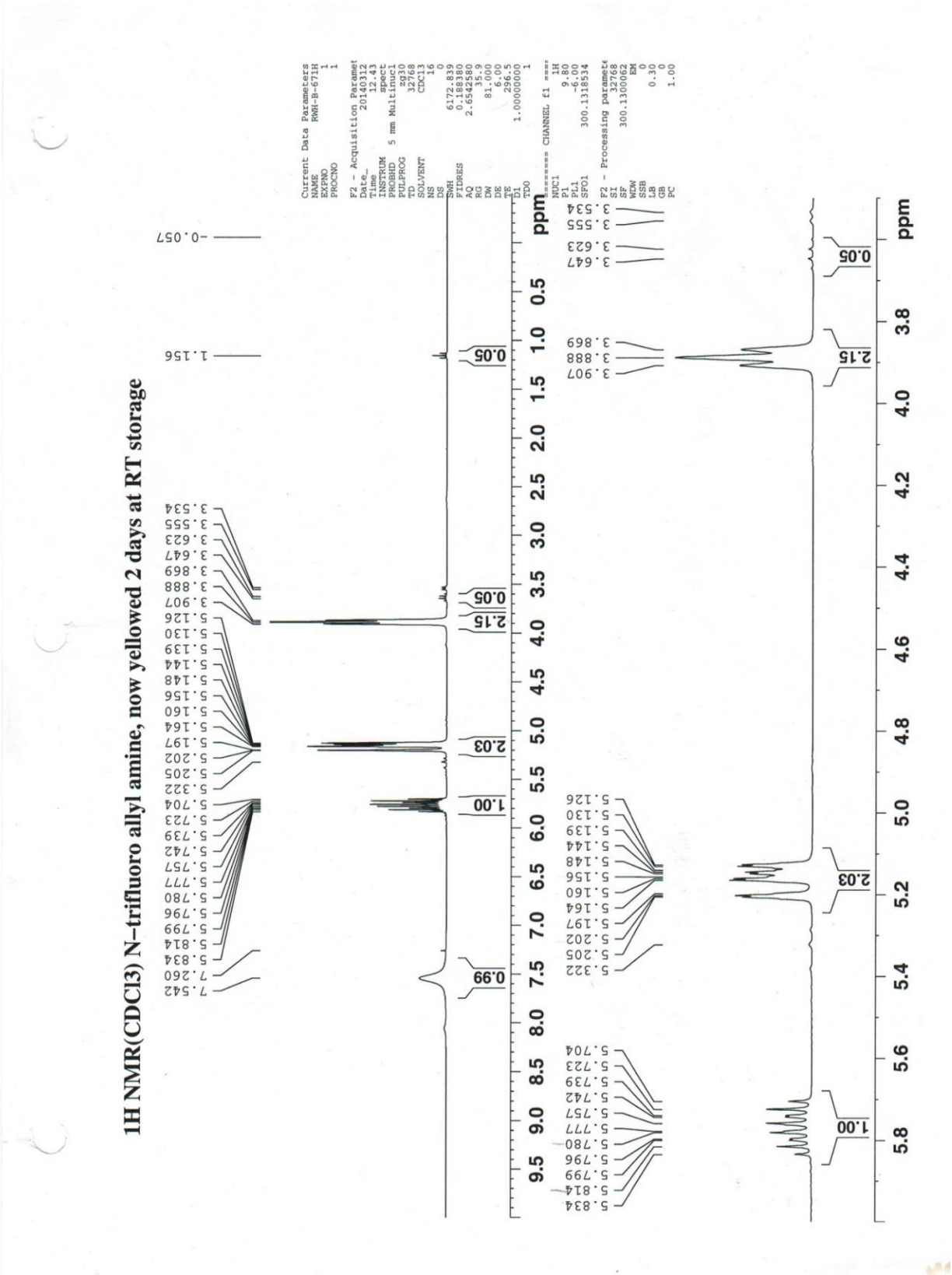
Mass Spectrum for Sample:
RWH-B-37

Operator: Mark Wang

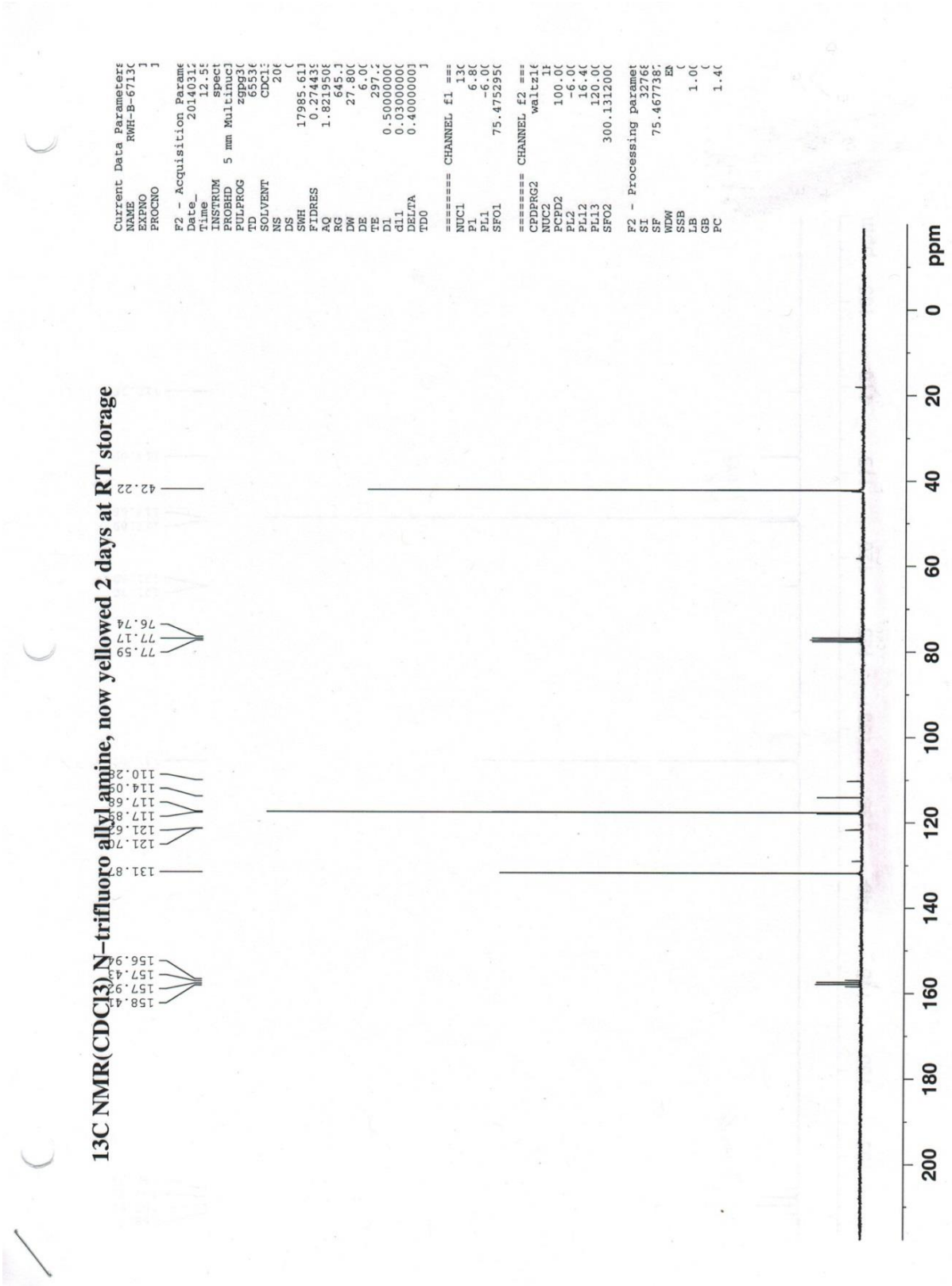
Data filename: C:\LabSolutions\Data\Schwabacher Alan\RWH-B-37.lcd
Spectrum Mode: Single
Retention Time: 0.200 min.
Interface Type (ESI, APCI, DUIS): DUIS
Aquisition Mode (Scan, SIM, Profile): Scan
Polarity (+,-): +



^{1}H NMR *N-allyl-2,2,2-trifluoroacetamide* (**80**)



^{13}C NMR *N-allyl-2,2,2-trifluoroacetamide* (**80**)



ESI-MS *N-allyl-2,2,2-trifluoroacetamide* (**80**)

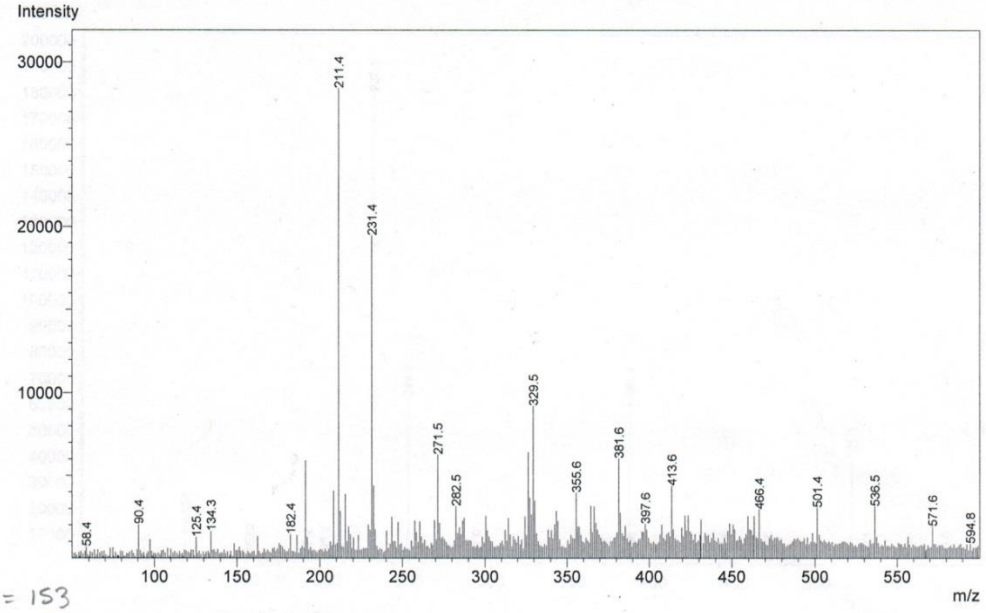
3/11/2014 2:59:19 PM Page 1 / 1

Shimadzu LCMS-2020 Data Report

Mass Spectrum for Sample:
RWH-B-67

Operator: Mark Wang

Data filename: C:\LabSolutions\Data\Schwabacher Alan\RWH-B-67.lcd
Spectrum Mode: Single
Retention Time: 0.100 min.
Interface Type (ESI, APCI, DUIS): DUIS
Aquisition Mode (Scan, SIM, Profile): Scan
Polarity (+,-): +



M = 153

2M = 306

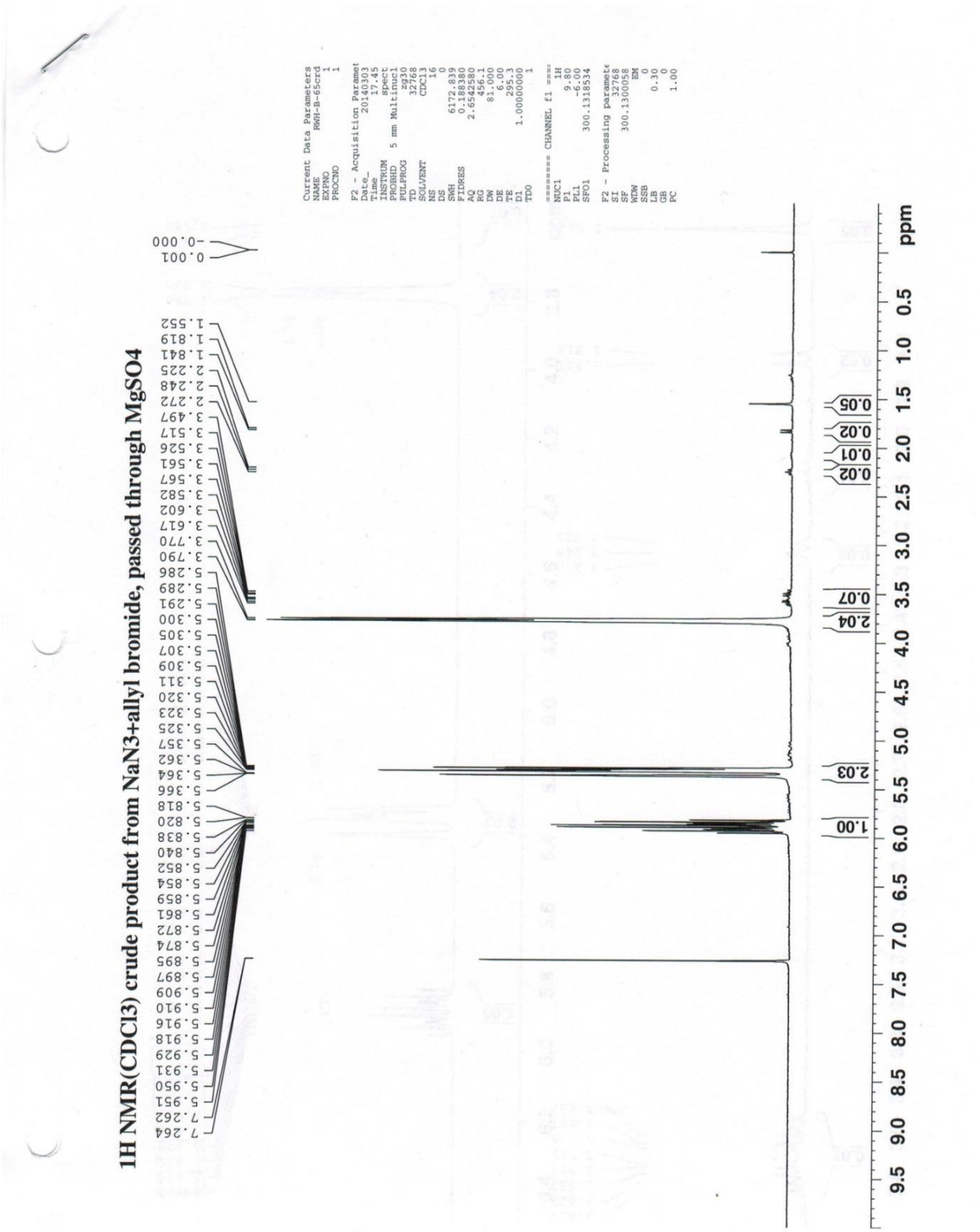
2M + Na^+ = 306 + 23 = 329

211 − 153 = 58

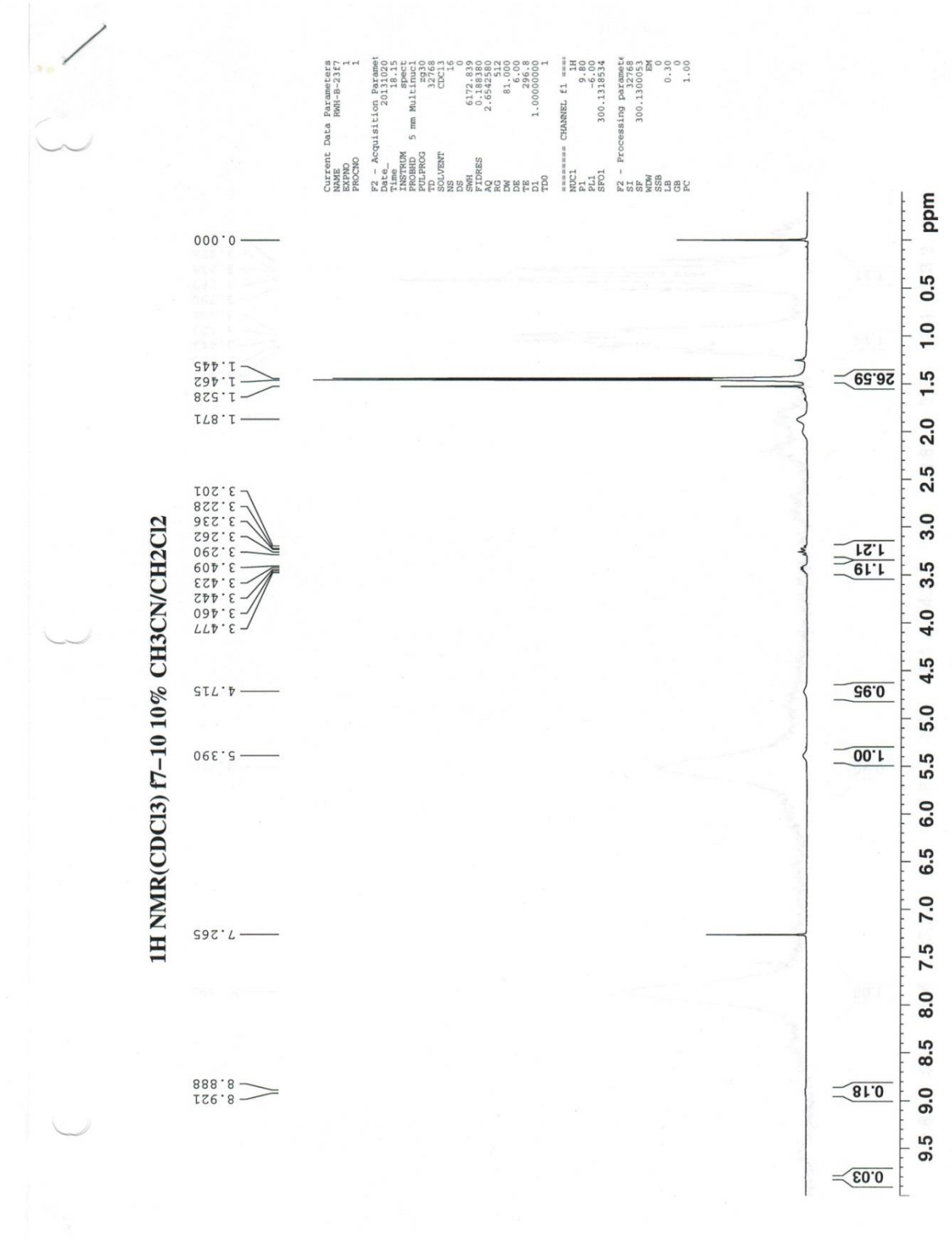
231 − 153 = 78

271 − 153 = 118

^{1}H NMR *3-azidoprop-1-ene* (**81**)



^{1}H NMR *(Z)-di-tert.-butyl but-2-ene-1,4-diyldicarbamate* (**82**)



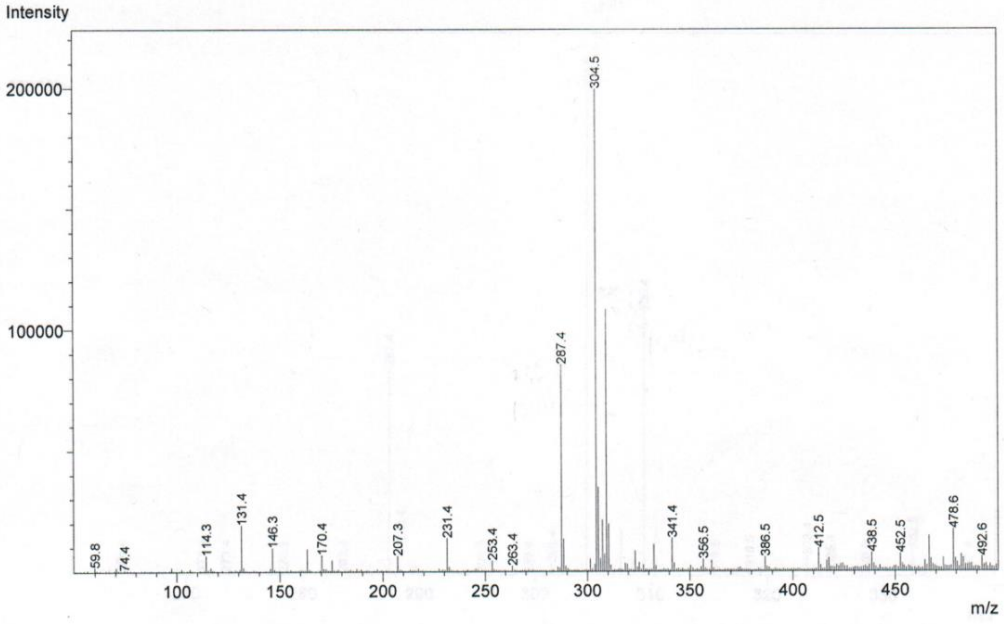
ESI-MS *(Z)-di-tert.-butyl but-2-ene-1,4-diyldicarbamate* (**82**)

Shimadzu LCMS-2020 Data Report

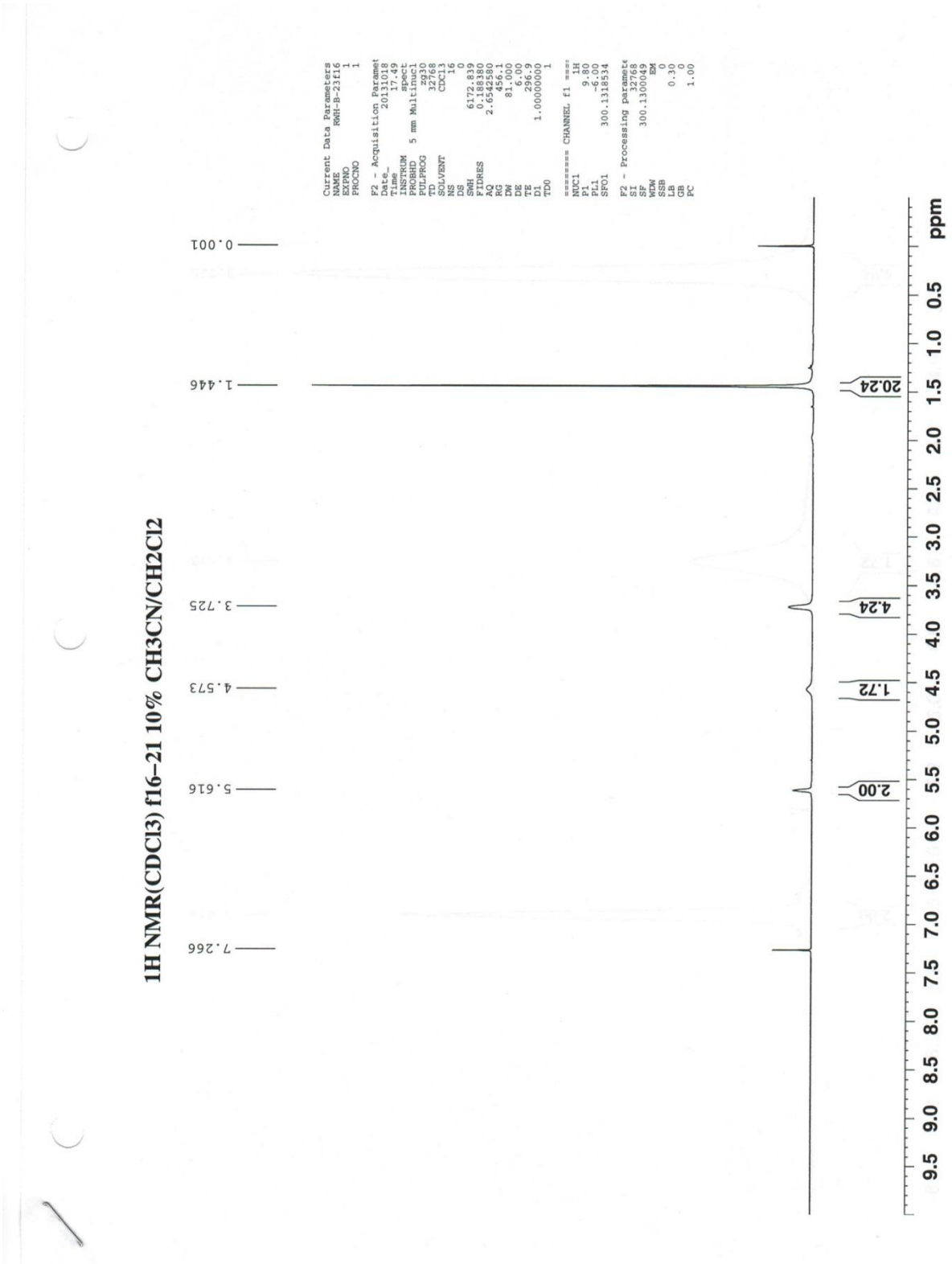
Mass Spectrum for Sample:
RWH-B23f7

Operator: Mark Wang

Data filename: C:\LabSolutions\Data\Schwabacher Alan\RWH-B23f7.lcd
Spectrum Mode: Single
Retention Time: 0.133 min.
Interface Type (ESI, APCI, DUIS): DUIS
Aquisition Mode (Scan, SIM, Profile): Scan
Polarity (+,-): +



^{1}H NMR *(E)-di-tert.-butyl but-2-ene-1,4-diyldicarbamate* (**83**)



ESI-MS *(E)-di-tert.-butyl but-2-ene-1,4-diyldicarbamate* (**83**)

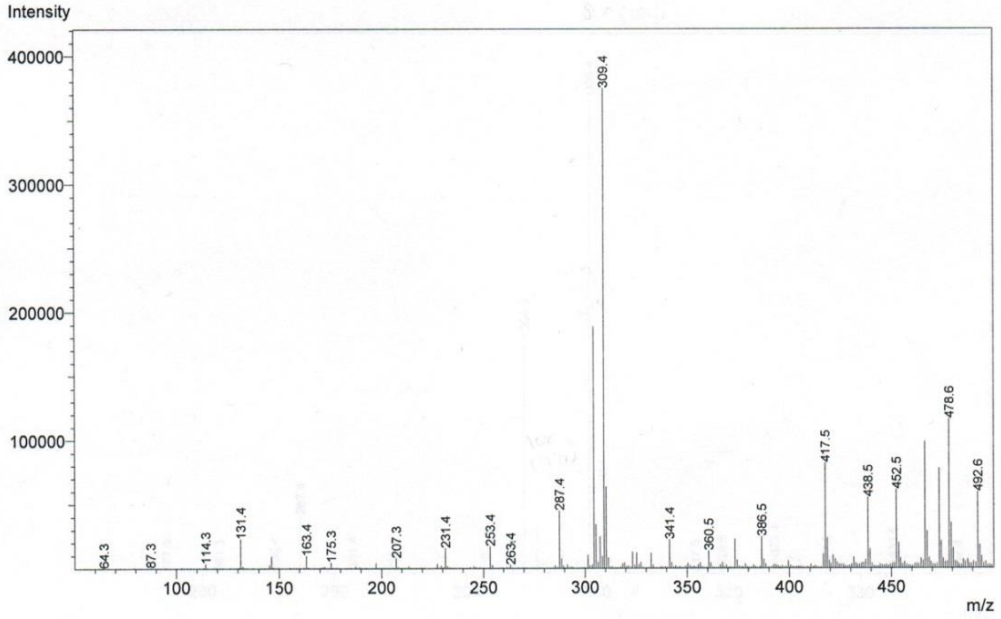
10/21/2013 2:16:20 PM Page 1 / 1

Shimadzu LCMS-2020 Data Report

Mass Spectrum for Sample:
RWH-B23f16-1

Operator: Mark Wang

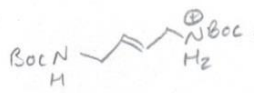
Data filename: C:\LabSolutions\Data\Schwabacher Alan\RWH-B23f16-1.lcd
Spectrum Mode: Single
Retention Time: 0.133 min.
Interface Type (ESI, APCI, DUIS): DUIS
Aquisition Mode (Scan, SIM, Profile): Scan
Polarity (+,-): +



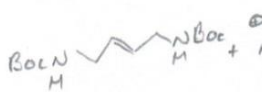


= 286 = M

304/305 = M+17 / M+18
50%

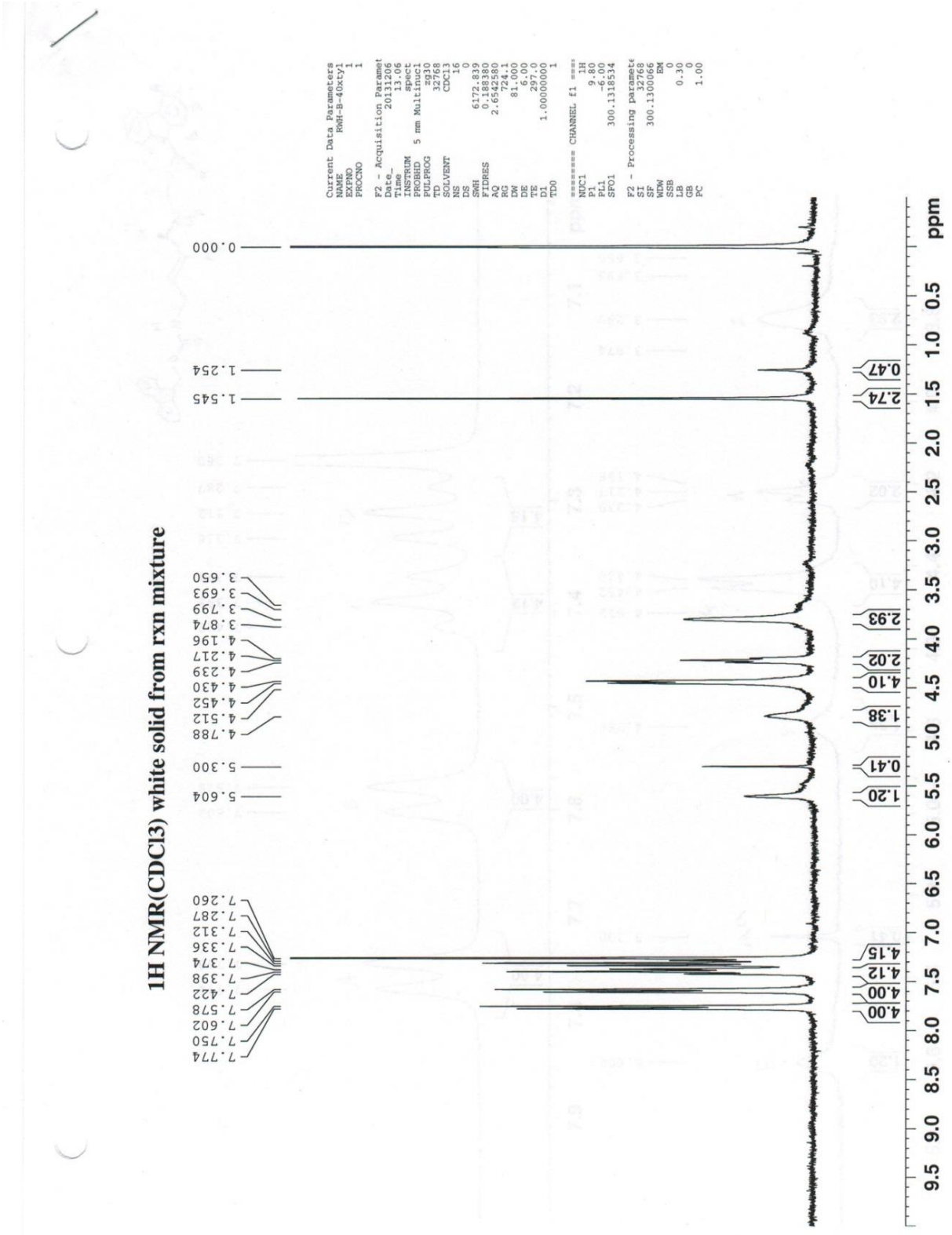


= 287 = M+H⊕
12%



= 309 = M+Na⊕
100%

^{1}H NMR *(E)-bis((9H-fluoren-9-yl)methyl) but-2-ene-1,4-diyldicarbamate* (**84**)



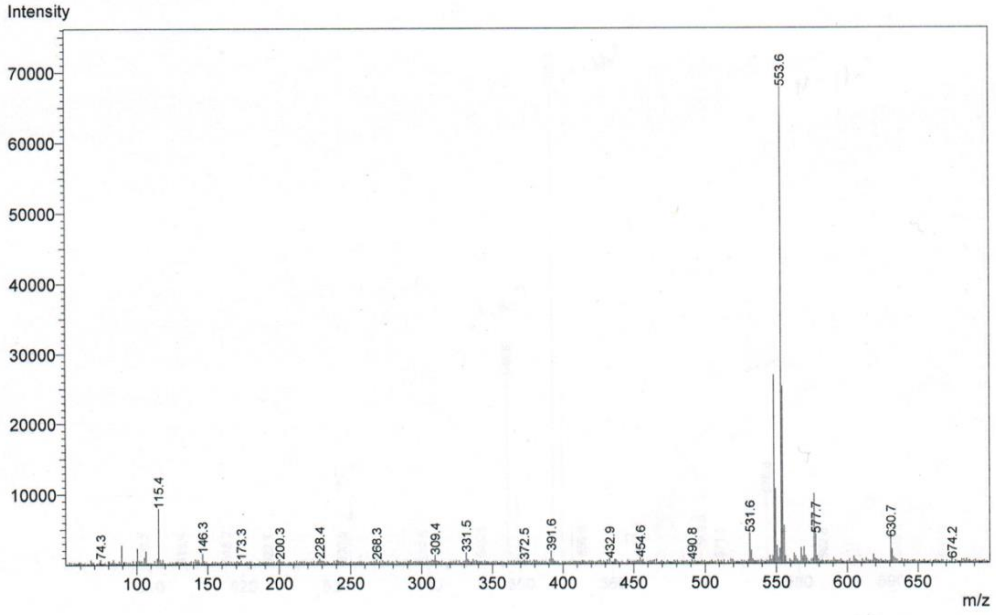
ESI-MS *(E)-bis((9H-fluoren-9-yl)methyl) but-2-ene-1,4-diyldicarbamate* (**84**)

Shimadzu LCMS-2020 Data Report

Mass Spectrum for Sample:
RWH-B-40

Operator: Mark Wang

Data filename: C:\LabSolutions\Data\Schwabacher Alan\RWH-B-40-1.lcd
Spectrum Mode: Single
Retention Time: 0.133 min.
Interface Type (ESI, APCI, DUIS): DUIS
Aquisition Mode (Scan, SIM, Profile): Scan
Polarity (+,-): +



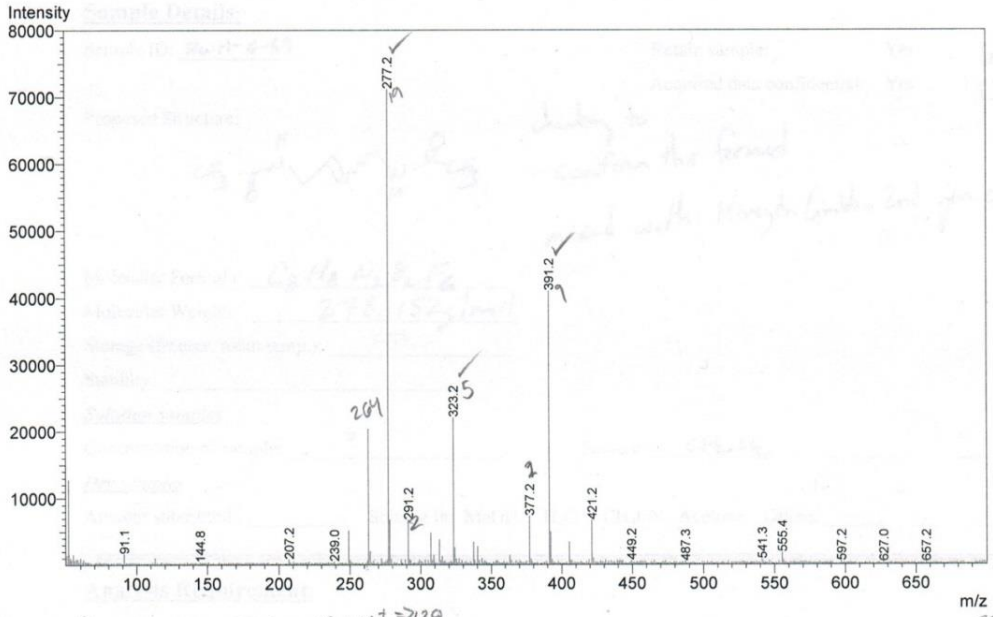
ESI-MS *(E/Z)-N,N'-(but-2-ene-1,4-diyl)bis(2,2,2-trifluoroacetamide)* (**85**)

Shimadzu LCMS-2020 Data Report

Mass Spectrum for Sample:
RWH-B-69

Operator: Mark Wang

Data filename: C:\LabSolutions\Data\Hossain, Mahmun\RWH-B-69.lcd
Spectrum Mode: Single
Retention Time: 0.150 min.
Interface Type (ESI, APCI, DUIS): DUIS
Aquisition Mode (Scan, SIM, Profile): Scan
Polarity (+,-): -



278 = M

276 = M-2H+ = 138

277 = M - H+, 100%.

323 = M + HCOO⊖, 26%.

391 = M + CF3COO⊖, 47%.

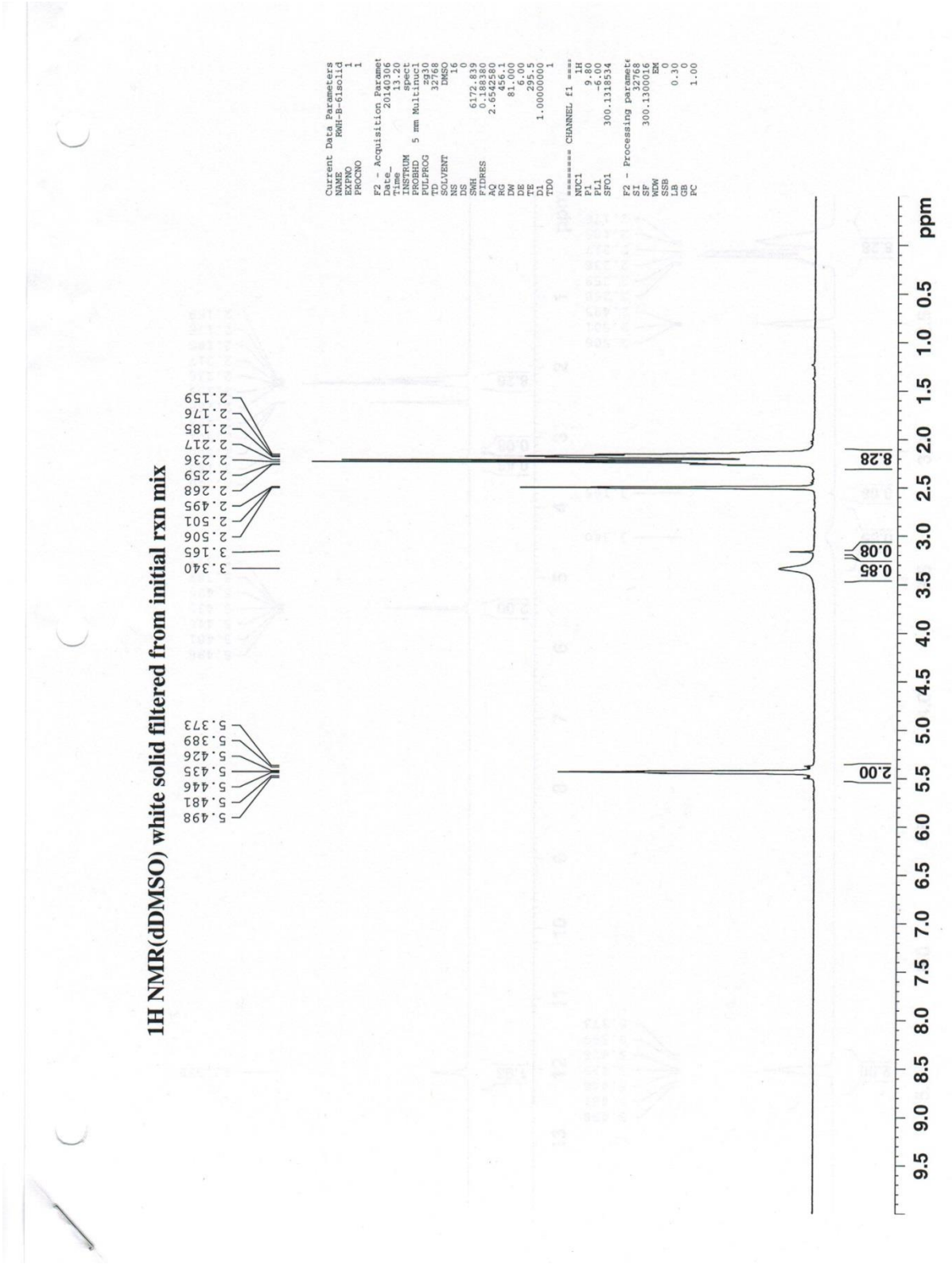
323 − 278 = 45

391 − 278 = 113

421 − 278 = 143

monomer = 153

^{1}H NMR *(E)-oct-4-enedioic acid* (**86**)



ESI-MS *(E)-oct-4-enedioic acid* (**86**)

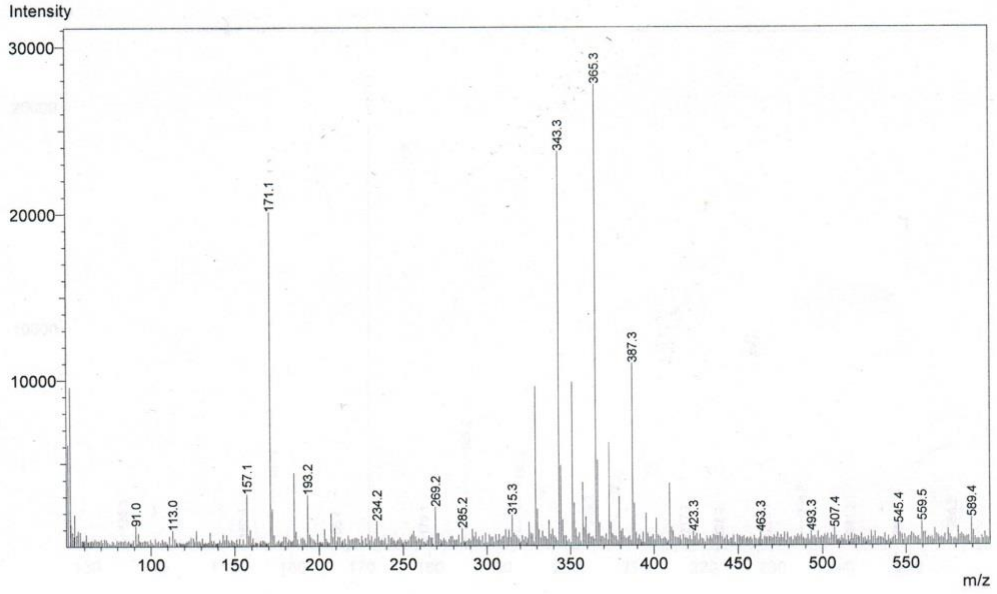
3/3/2014 12:49:12 PM Page 1 / 1

Shimadzu LCMS-2020 Data Report

Mass Spectrum for Sample:
RWH-B-59

Operator: Mark Wang

Data filename: C:\LabSolutions\Data\Schwabacher Alan\RWH-B-59.lcd
Spectrum Mode: Single
Retention Time: 0.150 min.
Interface Type (ESI, APCI, DUIS): DUIS
Aquisition Mode (Scan, SIM, Profile): Scan
Polarity (+,-): -



171 = M - H+
72%

343 = M + M-
86%

365 = 2M- + Na+
100%

2M- = 342

387 - 2M- = 45

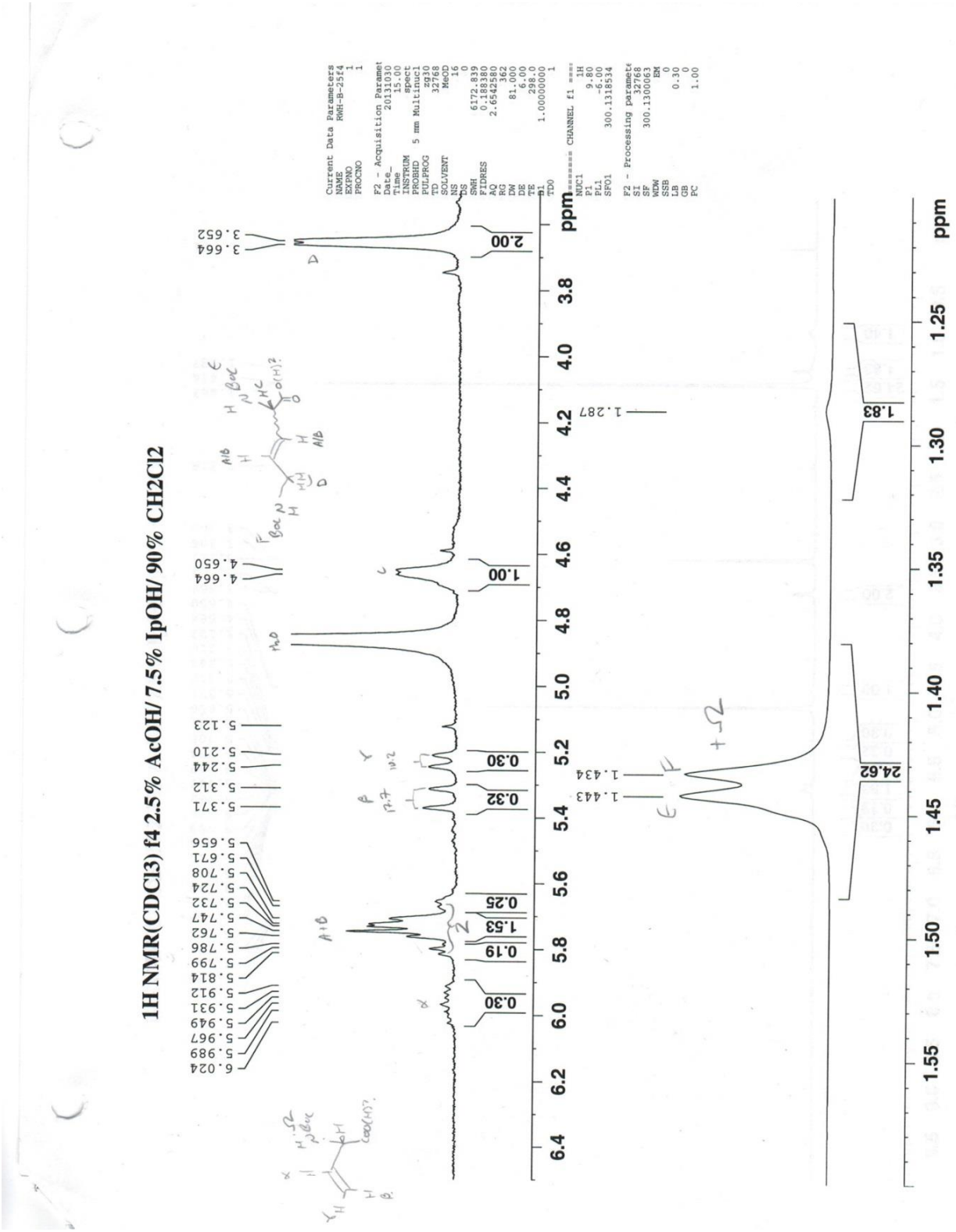
387 - M - M- = 44

$CO_2 = 44$

44 = 

$C_3H_8 = 44$

^{1}H NMR *(S,E)-2,5-bis((tert-butoxycarbonyl)amino)hept-3-enoic acid* (**87**)



ESI-MS *(S,E)-2,5-bis((tert-butoxycarbonyl)amino)hept-3-enoic acid* (**87**)

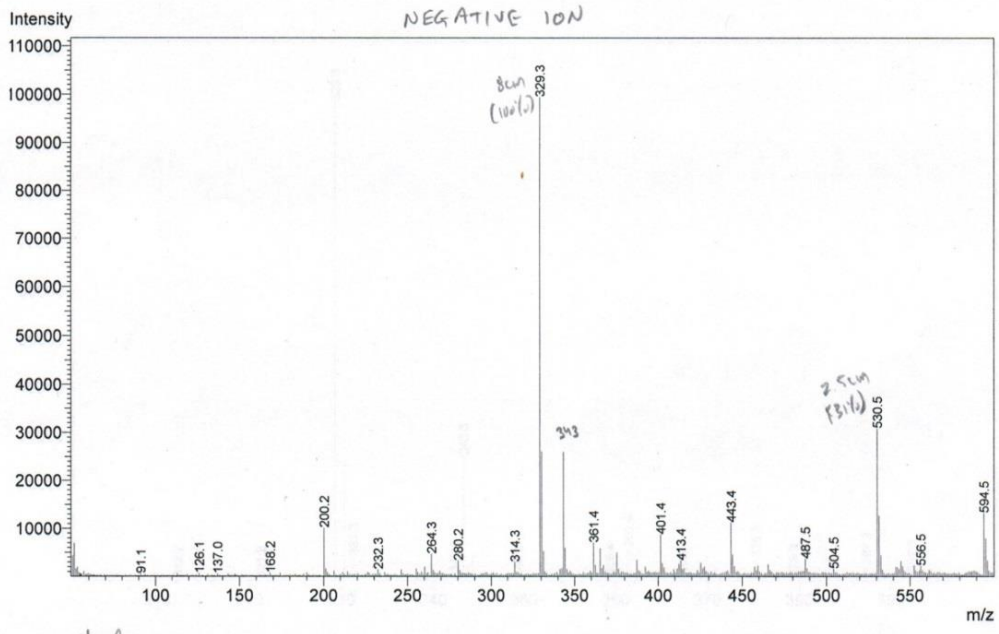
10/28/2013 3:45:37 PM Page 1 / 1

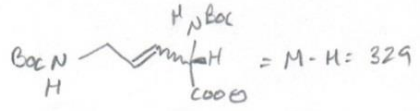
Shimadzu LCMS-2020 Data Report

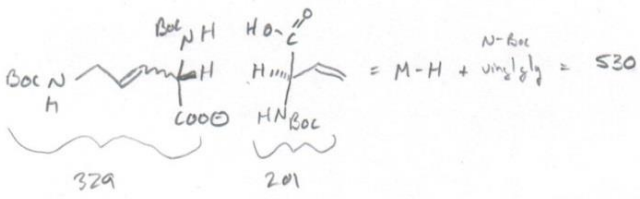
Mass Spectrum for Sample:
RWH-B-25

Operator: Mark Wang

Data filename: C:\LabSolutions\Data\Schwabacher Alan\RWH-B-25.lcd
Spectrum Mode: Single
Retention Time: 0.116 min.
Interface Type (ESI, APCI, DUIS): DUIS
Aquisition Mode (Scan, SIM, Profile): Scan
Polarity (+,-): -







ESI-MS

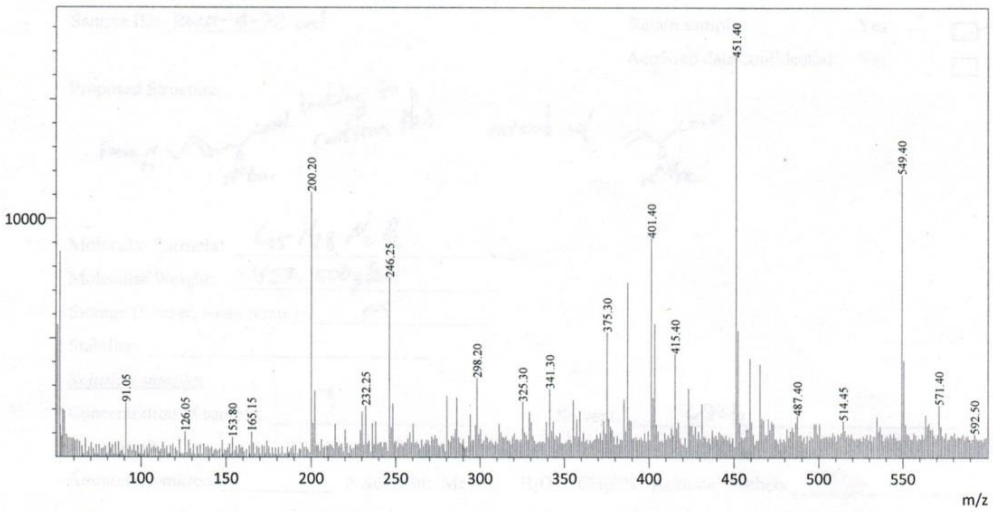
(S,E)-5-((((9H-fluoren-9-yl)methoxy)carbonyl)amino)-2-((tert-butoxycarbonyl)amino)pent-3-enoic acid (**88**)

Shimadzu LCMS-2020 Data Report

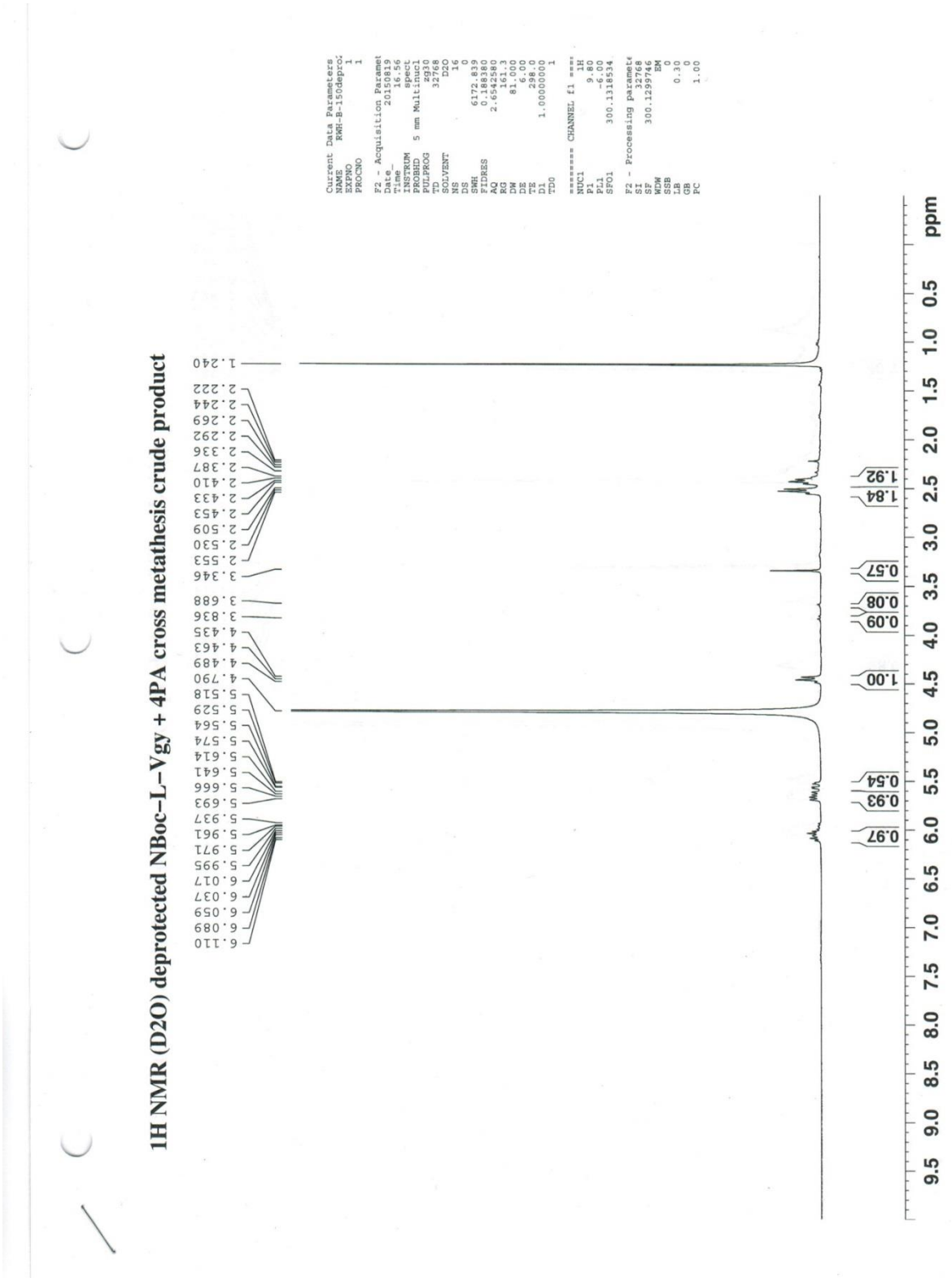
Mass Spectrum for Sample
RWH-B-72 cld.lcd

Opeator: Mark Wang

Data Filename: C:\LabSolutions\Data\Schwabacher Alan\RWH-B-72 cld.lcd
Spetrum Mode: Single
Retention Time: 0.150
Interface Type (ESI, APCI, DUIS): DUIS
Aquisition Mode: (Scan, SIM, Profife): Scan
Polarity: -



^{1}H NMR *(S,E)-2-((tert-butoxycarbonyl)amino)hept-3-enoic acid* (**89**)



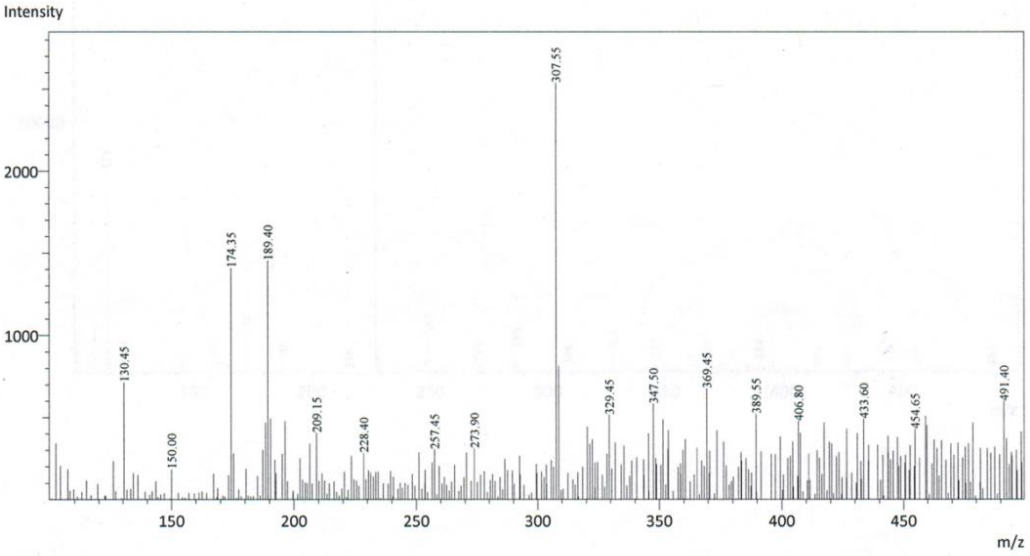
ESI-MS *(S,E)-2-((tert-butoxycarbonyl)amino)hept-3-enoic acid* (**89**)

Shimadzu LCMS-2020 Data Report

Mass Spectrum for Sample
RWH-B-74 depro 01.lcd

Operator: Mark Wang

Data Filename: C:\LabSolutions\Data\Schwabacher Alan\RWH-B-74 depro 01.lcd
Spetrum Mode: Averaged
Retention Time: ----
Interface Type (ESI, APCI, DUIS): DUIS
Aquisition Mode: (Scan, SIM, Profife): Scan
Polarity: +



XI. CURRICULUM VITAE

Robert W. Hoppe

Highlights

- Experience in developing, optimizing and scaling up organic synthetic procedures
- Extensive experience in characterization of molecular structure and behavior using NMR, MS, HPLC, and fluorescence spectroscopy
- Directed research of multiple undergraduates emphasizing fundamental synthetic technique, prudent record keeping, and spectroscopic analysis
- Managing daily laboratory operations including chemical purchasing, organization and storage, and maintenance and repair of equipment

Education

- Dissertation Title: "Molecular Recognition in Water: Rigid Synthetic Receptors and Enzymatic Mechanistic Probes"
  Adviser: Professor Alan W. Schwabacher

- BS, Chemistry, University of Wisconsin-Oshkosh, Oshkosh WI, 2006
  Adviser: Professor Brant L. Kedrowski

Research Experience

2007-Present Graduate Assistant, University of Wisconin-Milwaukee
Adviser: Professor Alan W. Schwabacher

- Synthesis and characterization of a water soluble artificial molecular receptor
- Dramatic simplification of thermal reactions: L-Vinylglycine synthesis
- Small molecule synthesis for catalytic and kinetic characterization of enzymes
- Identification of a novel synthesis of diaryl amines in optimization of a large scale synthesis
- Quinolone heterocycles synthesis and correlating factors in regioselectivity in formation

2004-2006 Undergraduate Research Assistant, University of Wisconsin Oshkosh
Adviser: Brant L. Kedrowski

- Studied natural product synthesis

Teaching Experience

General Chemistry (5 terms), Survey of Biochemistry (4 terms), Organic Chemistry (4 terms), Advanced Organic Laboratory (5 terms)

Affiliations

- American Chemical Society

Publications

- Mueller, L.; Hoppe, R.; Ochsenwald, J.; Berndt, R.; Severin, G.; Schwabacher, A. W.; Silvaggi, N. "Sbi00515, a Protein of Unknown Function from *Streptomyces bingchenggensis*, Highlights the Functional Versatility of the Acetoacetate Decarboxylase Scaffold" *Biochemistry*, 2015, 54 (25), 3978-3988
- Burroughs, A. M.; Hoppe, R.; Goebel, N.; Sayyed, B.; Voegtline, T.; Schwabacher, A. W.; Zabriskie, T. M.; Silvaggi, N. "Structural and Functional Characterization of MppR, an Enduracididine Biosynthetic Enzyme from *Streptomyces hygroscopicus*: Functional Diversity in the Acetoacetate Decarboxylase-like Superfamily" *Biochemistry*, 2013, 52 (26), 4492-4506
- Kedrowski, B.; Hoppe, R. " A Concise Synthesis of (±)-Cacalol" J. Org. Chem., 2008, 73 (13), 5177-5179

References

Professor Alan W. Schwabacher, Dept. of Chemistry & Biochemistry, Univ. of Wisconsin-Milwaukee, Milwaukee WI 414-229-4410 awschwab@uwm.edu

Professor Nicholas Silvaggi, Dept. of Chemistry & Biochemistry, Univ. of Wisconsin-Milwaukee, Milwaukee WI 414-229-2647 silvaggi@uwm.edu

Professor Anja Blecking, Dept. of Chemistry & Biochemistry, Univ. of Wisconsin- Milwaukee, Milwaukee WI 414-229-2974 blecking@uwm.edu